

Pertanika Journal of  
**TROPICAL**  
**AGRICULTURAL SCIENCE**

**JITAS**

**VOL. 48 (1) JAN. 2025**



A scientific journal published by Universiti Putra Malaysia Press

# ***PERTANIKA* JOURNAL OF TROPICAL AGRICULTURAL SCIENCE**

## **About the Journal**

### ***Overview***

*Pertanika* Journal of Tropical Agricultural Science is an official journal of Universiti Putra Malaysia. It is an open-access online scientific journal. It publishes the scientific outputs. It neither accepts nor commissions third party content.

Recognised internationally as the leading peer-reviewed interdisciplinary journal devoted to the publication of original papers, it serves as a forum for practical approaches to improving quality in issues pertaining to tropical agriculture and its related fields.

*Pertanika* Journal of Tropical Agricultural Science currently publishes 6 issues per year (*January, February, May, June, August, and November*). It is considered for publication of original articles as per its scope. The journal publishes in **English** and it is open for submission by authors from all over the world.

The journal is available world-wide.

### ***Aims and scope***

*Pertanika* Journal of Tropical Agricultural Science aims to provide a forum for high quality research related to tropical agricultural research. Areas relevant to the scope of the journal include agricultural biotechnology, biochemistry, biology, ecology, fisheries, forestry, food sciences, genetics, microbiology, pathology and management, physiology, plant and animal sciences, production of plants and animals of economic importance, and veterinary medicine.

### ***History***

*Pertanika* was founded in 1978. Currently, as an interdisciplinary journal of agriculture, the revamped journal, *Pertanika* Journal of Tropical Agricultural Science now focuses on tropical agricultural research and its related fields.

### ***Vision***

To publish journals of international repute.

### ***Mission***

Our goal is to bring the highest quality research to the widest possible audience.

### ***Quality***

We aim for excellence, sustained by a responsible and professional approach to journal publishing. Submissions are guaranteed to receive a decision within 90 days. The elapsed time from submission to publication for the articles averages 180 days. We are working towards decreasing the processing time with the help of our editors and the reviewers.

### ***Abstracting and indexing of Pertanika***

*Pertanika* Journal of Tropical Agricultural Science is now over 47 years old; this accumulated knowledge has resulted in *Pertanika* Journal of Tropical Agricultural Science being abstracted and indexed in Journal Citation Reports (JCR-Clarivate), SCOPUS (Elsevier), BIOSIS, National Agricultural Science (NAL), Google Scholar, MyCite and ISC.

### ***Citing journal articles***

The abbreviation for *Pertanika* Journal of Tropical Agricultural Science is *Pertanika J. Trop. Agric. Sci.*

### ***Publication policy***

*Pertanika* policy prohibits an author from submitting the same manuscript for concurrent consideration by two or more publications. It prohibits as well publication of any manuscript that has already been published either in whole or substantial part elsewhere. It also does not permit publication of manuscript that has been published in full in proceedings.

### ***Code of Ethics***

The *Pertanika* journals and Universiti Putra Malaysia take seriously the responsibility of all its journal publications to reflect the highest publication ethics. Thus, all journals and journal editors are expected to abide by the journal's codes of ethics. Refer to *Pertanika's Code of Ethics* for full details, available on the official website of *Pertanika*.

### ***Originality***

The author must ensure that when a manuscript is submitted to *Pertanika*, the manuscript must be an original work. The author should check the manuscript for any possible plagiarism using any program such as Turn-It-In or any other software before submitting the manuscripts to the *Pertanika* Editorial Office, Journal Division.

All submitted manuscripts must be in the journal's acceptable **similarity index range**:  
 $\leq 20\%$  – *PASS*;  $> 20\%$  – *REJECT*.

### ***International Standard Serial Number (ISSN)***

An ISSN is an 8-digit code used to identify periodicals such as journals of all kinds and on all media—print and electronic. All *Pertanika* journals have an e-ISSN.

*Pertanika* Journal of Tropical Agricultural Science: e-ISSN 2231-8542 (Online).

### ***Lag time***

A decision on acceptance or rejection of a manuscript is expected within 90 days (average). The elapsed time from submission to publication for the articles averages 180 days.

### ***Authorship***

Authors are not permitted to add or remove any names from the authorship provided at the time of initial submission without the consent of the journal's Chief Executive Editor.

### ***Manuscript preparation***

For manuscript preparation, authors may refer to *Pertanika's INSTRUCTION TO AUTHORS*, available on the official website of *Pertanika*.

### ***Editorial process***

Authors who complete any submission are notified with an acknowledgement containing a manuscript ID on receipt of a manuscript, and upon the editorial decision regarding publication.

*Pertanika* follows a double-blind peer review process. Manuscripts deemed suitable for publication are sent to reviewers. Authors are encouraged to suggest names of at least 3 potential reviewers at the time of submission of their manuscripts to *Pertanika*, but the editors will make the final selection and are not, however, bound by these suggestions.

Notification of the editorial decision is usually provided within 90 days from the receipt of manuscript. Publication of solicited manuscripts is not guaranteed. In most cases, manuscripts are accepted conditionally, pending an author's revision of the material.

### ***The journal's peer review***

In the peer review process, 2 or 3 referees independently evaluate the scientific quality of the submitted manuscripts. At least 2 referee reports are required to help make a decision.

Peer reviewers are experts chosen by journal editors to provide written assessment of the **strengths** and **weaknesses** of written research, with the aim of improving the reporting of research and identifying the most appropriate and highest quality material for the journal.

### ***Operating and review process***

What happens to a manuscript once it is submitted to *Pertanika*? Typically, there are 7 steps to the editorial review process:

1. The journal's Chief Executive Editor and the Editor-in-Chief examine the paper to determine whether it is relevance to journal needs in terms of novelty, impact, design, procedure, language as well as presentation and allow it to proceed to the reviewing process. If not appropriate, the manuscript is rejected outright and the author is informed.
2. The Chief Executive Editor sends the article-identifying information having been removed, to 2 or 3 reviewers. They are specialists in the subject matter of the article. The Chief Executive Editor requests that they complete the review within 3 weeks.

Comments to authors are about the appropriateness and adequacy of the theoretical or conceptual framework, literature review, method, results and discussion, and conclusions. Reviewers often include suggestions for strengthening of the manuscript. Comments to the editor are in the nature of the significance of the work and its potential contribution to the research field.

3. The Editor-in-Chief examines the review reports and decides whether to accept or reject the manuscript, invite the authors to revise and resubmit the manuscript, or seek additional review reports. In rare instances, the manuscript is accepted with almost no revision. Almost without exception, reviewers' comments (to the authors) are forwarded to the authors. If a revision is indicated, the editor provides guidelines to the authors for attending to the reviewers' suggestions and perhaps additional advice about revising the manuscript.
4. The authors decide whether and how to address the reviewers' comments and criticisms and the editor's concerns. The authors return a revised version of the paper to the Chief Executive Editor along with specific information describing how they have answered the concerns of the reviewers and the editor, usually in a tabular form. The authors may also submit a rebuttal if there is a need especially when the authors disagree with certain comments provided by reviewers.
5. The Chief Executive Editor sends the revised manuscript out for re-review. Typically, at least 1 of the original reviewers will be asked to examine the article.
6. When the reviewers have completed their work, the Editor-in-Chief examines their comments and decides whether the manuscript is ready to be published, needs another round of revisions, or should be rejected. If the decision is to accept, the Chief Executive Editor is notified.
7. The Chief Executive Editor reserves the final right to accept or reject any material for publication, if the processing of a particular manuscript is deemed not to be in compliance with the S.O.P. of *Pertanika*. An acceptance notification is sent to all the authors.

The editorial office ensures that the manuscript adheres to the correct style (in-text citations, the reference list, and tables are typical areas of concern, clarity, and grammar). The authors are asked to respond to any minor queries by the editorial office. Following these corrections, page proofs are mailed to the corresponding authors for their final approval. At this point, **only essential changes are accepted**. Finally, the manuscript appears in the pages of the journal and is posted on-line.

Pertanika Journal of

# **TROPICAL AGRICULTURAL SCIENCE**

**Vol. 48 (1) Jan. 2025**



A scientific journal published by Universiti Putra Malaysia Press



## EDITOR-IN-CHIEF

## CHIEF EXECUTIVE EDITOR

## UNIVERSITY PUBLICATIONS COMMITTEE

## CHAIRMAN Zamberi Sekawi

## EDITORIAL STAFF

### Journal Officers:

Ellyianur Puteri Zainal  
Kanagamalar Silvarajoo  
Siti Zuhaila Abd Wahid

### Editorial Assistants:

Siti Juridah Mat Arip  
Zulinaardawati Kamarudin

### English Editor:

Norhanizah Ismail

## PRODUCTION STAFF

### Pre-press Officers:

Ku Ida Mastura Ku Baharom  
Nur Farrah Dila Ismail

## WEBMASTER

### IT Officer:

Kiran Raj Kaneswaran

## EDITORIAL OFFICE

### JOURNAL DIVISION

Putra Science Park  
1<sup>st</sup> Floor, IDEA Tower II  
UPM-MTDC Technology Centre  
Universiti Putra Malaysia  
43400 Serdang, Selangor Malaysia.

### Gen Enquiry

Tel. No: +603 9769 1622 | 1616

E-mail:

[executive\\_editor.pertanika@upm.edu.my](mailto:executive_editor.pertanika@upm.edu.my)

URL: [www.journals-jd.upm.edu.my](http://www.journals-jd.upm.edu.my)

## PUBLISHER

### UPM PRESS

Universiti Putra Malaysia  
43400 UPM, Serdang, Selangor, Malaysia.  
Tel: +603 9769 8851

E-mail: [penerbit@putra.upm.edu.my](mailto:penerbit@putra.upm.edu.my)

URL: <http://penerbit.upm.edu.my>



**PENERBIT**  
**UPM**  
UNIVERSITI PUTRA MALAYSIA  
**PRESS**



**PERTANIKA**  
JOURNALS

## ASSOCIATE EDITOR 2023-2025

**Ahmed Osumanu Haruna**  
*Soil Fertility and Management, Plant and Soil Interaction, Wastes Management*  
Universiti Islam Sultan Sharif Ali, Brunei

**Noureddine Benkeblia**  
*Postharvest Physiology and Biochemistry of Horticultural Crops*  
University of the West Indies, Jamaica

## EDITORIAL BOARD 2024-2026

**Abd. Razak Alimon**  
*Animal Production, Animal Nutrition*  
Universitas Gadjah Mada, Indonesia

**Kadambot H. M. Siddique**  
*Crop and Environment Physiology, Germplasm Enhancement*  
University of Western Australia, Australia

**Norhasnida Zawawi**  
*Biochemistry, Food Science, Food Chemistry, Antioxidant Activity, Food Analysis*  
Universiti Putra Malaysia, Malaysia

**Alan Dargantes**  
*Veterinary Epidemiology and Surveillance, Disease Diagnostics and Therapeutics, Disease Ecology*  
Central Mindanao University, Philippines

**Kayindra Nath Tiwari**  
*Plant Biotechnology, Natural Products*  
Banaras Hindu University, India

**Saw Leng Guan**  
*Botany and Conservation, Plant Ecology*  
Curator of Penang Botanic Gardens, Malaysia

**Amin Ismail**  
*Food Biochemistry*  
Universiti Putra Malaysia, Malaysia

**Khanitta Somtrakoon**  
*Bioremediation, Phytoremediation, Environmental Microbiology*  
Mahasarakham University, Thailand

**Shamshuddin Jusop**  
*Soil Science, Soil Mineralogy*  
Universiti Putra Malaysia, Malaysia

**Azamal Husen**  
*Plant Stress Physiology, Nanoparticles, Plant Propagation, Tree Improvement, Medical Plants*  
Wolaita Sodo University, Ethiopia

**Lai Oi Ming**  
*Esterification, Lipase, Fatty Acids, Transesterification*  
Universiti Putra Malaysia, Malaysia

**Sivakumar Sukumaran**  
*Plant Breeding, Molecular Breeding, Quantitative Genetics*  
University of Queensland, Australia

**Chye Fook Yee**  
*Food Science and Nutrition, Food Microbiology, Food Biotechnology*  
Universiti Putra Malaysia, Malaysia

**Md. Tanvir Rahman**  
*Antimicrobial Resistance/AMR, Virulence and Pathogenesis, Vaccine, Microbial Ecology, Zoonoses, Food Hygiene and Public Health*  
Bangladesh Agricultural University, Bangladesh

**Tan Wen Siang**  
*Molecular Biology, Virology, Protein Chemistry*  
Universiti Putra Malaysia, Malaysia

**Faez Firdaus Jesse Abdullah**  
*Ruminant Medicine*  
Universiti Putra Malaysia, Malaysia

**Mohammad Noor Amal Azmal**  
*Fish Disease Diagnosis, Fish Disease Epidemiology, Development of Fish Vaccines*  
Universiti Putra Malaysia, Malaysia

**Tati Suryati Syamsudin**  
*Ecology, Entomology, Invertebrate, Fruit Fly management*  
Institut Teknologi Bandung, Indonesia

**Faridah Abas**  
*Bioactive Compounds, Natural Products Chemistry, Metabolomics, LCMS, Functional Food*  
Universiti Putra Malaysia, Malaysia

**Mohd Effendy Abdul Wahid**  
*Immunology, Pathology, Bacteriology, Vaccine*  
Universiti Malaysia Terengganu, Malaysia

**Vincenzo Tufarelli**  
*Animal Science, Animal Nutrition, Poultry Science*  
University of Bari 'Aldo Moro', Italy

**Indika Herath**  
*Soil Science, Environmental Impact, Crop Water Use, Water Footprint, Carbon Footprint*  
Wayamba University of Sri Lanka, Sri Lanka

**Najiah Musa**  
*Bacteriology, Biopharmaceuticals, Disease of Aquatic Organisms*  
Universiti Malaysia Terengganu, Malaysia

**Zora Singh**  
*Horticulture, Production Technology and Post-handling of Fruit Crops*  
Edith Cowan University, Australia

## INTERNATIONAL ADVISORY BOARD 2024-2027

**Banpot Napompeth**  
*Entomology*  
Kasetsart University, Thailand

**Graham Matthews**  
*Pest Management*  
Imperial College London, UK

## ABSTRACTING AND INDEXING OF PERTANIKA JOURNALS

The journal is indexed in Journal Citation Reports (JCR-Clarivate), SCOPUS (Elsevier), BIOSIS, National Agricultural Science (NAL), Google Scholar, MyCite and ISC.





**Pertanika Journal of Tropical Agricultural Science**  
**Vol. 48 (1) Jan. 2025**

**Contents**

Foreword <i>Chief Executive Editor</i>	i
Principal Component Analysis of Physicochemical Parameters and Microstructure Characteristics of Wampee Fruit Affected by Storage Temperatures <i>Hai Wang, Feilong Yin, Shurou Chen, Ting Wei, Ziyi Qin, Jing Li, Xia Li, Xinhong Dong and Hock Eng Khoo</i>	1
Morphological Sex Determination of East Asian Barn Swallows ( <i>Hirundo rustica</i> ) in Tropical Wintering Region <i>Nor Adibah Ismail, Ummi Nur Syafiqah Daud, Noor Fatimah Najihah Arazmi, Nurfatim Batrisyia Md Ali, Shukor Md Nor and Mohammad Saiful Mansor</i>	19
A Comprehensive Method to Generating and Identifying Transgenic Tobacco Lines with a Single Transgene Integration Locus for Functional Analysis <i>Mohamad Shafek Hilman, Omar Nawawi, Mohd Farhan Azhari, Tianqi Bai, Cuixian Zhang, Mohd Puad Abdullah, Mat Yunus Abdul Masani and Chong Yu Lok Yusuf</i>	31
Microalgae as Potential Antioxidants: Assessment of Antioxidant Capacities in Microalgae from Selected Regions of Peninsular Malaysia <i>Noor Amanina Awang, Malinna Jusoh, Nor Faizura Said, Norhayati Yusuf, Mohd Nizam Lani and Fauziah Tufail Ahmad</i>	59
Low-sodium Chaya Leaf Seasoning Powder with Potassium Chloride Substitution: Nutritional, Antioxidant, and Microbial Quality Assessment <i>Theeraphol Senphan, Kotchaporn Puangtong, Benyapa Namdamrassiri, Chodsana Sriket, Md. Sazedul Hoque, Supatra Karnjanapratum and Patcharaporn Narkthewan</i>	77
Nanoemulsion and Topical Cream for Delivery of Tocotrienol-rich fraction, Ascorbyl Tetraisopalmitate, and Carotenes: Formulation and <i>in vitro</i> Release <i>Yee-Lin Gan, Chin Ping Tan, Cheah Yoke Kqueen, Hidayah Ariffin, Helmi Wasoh and Oi Ming Lai</i>	91

Sequential Cropping Productivity Evaluation of Corn, Mung Bean, and Sweet Potato Intercrop under Coconut Field in Zamboanga del Sur, Philippines <i>Nelmie Bendanillo Pongao-Ponio and Ma. Stella M. Paulican</i>	117
<i>Review Article</i>	
Prevailing Knowledge on Aquaculture of Abalone in Southeast Asia: A Review <i>Nur-Syahirah Mamat, Yuzine Esa, Hidayah Manan, Nur Leena W. S. Wong, Julia D. Sigwart, Siti-Azizah Mohd Nor, Nazia Abdul Kadar, Hon Jung Liew, Jalilah Mohamad, Suhairi Mazelan, Khor Waiho and Aziz Arshad</i>	137
Identifying Collagenase (MMP-1, -8, -13) Expression and Correlation with Periodontitis Progression Using the Rat Model <i>Fazle Khuda, Badiyah Baharin, Nur Najmi Mohamad Anuar, Putri Ayu Jayusman, Mariati Abdul Rahman and Nurul Shaqinah Nasruddin</i>	159
Floristic Composition and Diversity of Plants Across Three Vegetation Zones of Gashaka Gumti National Park, Northeastern Nigeria <i>Salihu Abba Hammanjoda, Rosimah Nulit, Chee Kong Yap, Umaru Buba Nformi, George Nodza, Abdulwakil Olawale Saba, Edward Entalai Besi and Rusea Go</i>	175
Effects of Temperature on Growth and Biochemical Composition of Arctic <i>Pseudanabaena</i> sp. and Tropical <i>Synechococcus</i> sp. <i>Nurul Farhanah Azlee, Azmir Hamidi, Zoya Khan, Faradina Merican, Jerzy Smykla, Siti Aisyah Alias and Wan Maznah Wan Omar</i>	201
Heavy Metals Assessment in Selected Leafy Vegetables from Selangor, Malaysia <i>Sian Nee See, Mohd Sabri Pak Dek, Maimunah Sanny, Radhiah Shukri and Nurul Shazini Ramli</i>	215
<i>Review Article</i>	
Effects of Different Extraction Methods on Yield, Polyunsaturated Fatty Acids, Antioxidants, and Stability Improvement of Chia Seed Oil: A Review <i>Izzreen Ishak, Ranil Coorey, Maaruf Abd Ghani, Chin Ping Tan, Nazamid Saari and Norhayati Hussain</i>	237

Dietary Administration of Karonda ( <i>Carissa carandas</i> ) on the Growth, Digestive Enzymes, Skin Mucosal Immunity, and Pigmentation in Siamese Fighting Fish ( <i>Betta splendens</i> ) <i>Kotchaporn Ponsin, Janeeya Khunchalee and Phukphon Munglue</i>	259
<i>In silico</i> Study of Neoagaro-Oligosaccharides (NAOs) Anti-Inflammatory Activity: Molecular Docking with iNOS and COX-2 Proteins <i>Pinki Anggrahini Puspitasari, Visi Endah Pratitis, Syahputra Wibowo, Nastiti Wijayanti and Fajar Sofyantoro</i>	279
Determination of the Pathogenicity of the Variant UPM 1432/2019 IBDV in SPF Chicken Eggs and Chicken Fibroblast Cell Line <i>Ali Youssif Mansour, Abdul Rahman Omar, Mohd Hair Bejo, Noorjahan Banu Alitheen and Nurulfiza Mat Isa</i>	295
Antioxidant Properties and Storage Stability of Spray-dried <i>Melastoma malabathricum</i> L. Fruit Extract for Natural Colorant <i>Nurul Syazwani Zahari, Siti Fatimah Sabran, Norhaidah Mohd Asrah, Mohd Fadzelly Abu Bakar, Furzani Pa'ee, Norhayati Muhammad, Fazleen Izzany Abu Bakar and Mohd Khairil Said</i>	307



# Foreword

Welcome to the first issue of 2025 for the *Pertanika Journal of Tropical Agricultural Science (PJTAS)*!

PJTAS is an open-access journal for studies in Tropical Agricultural Science published by Universiti Putra Malaysia Press. It is independently owned and managed by the university for the benefit of the world-wide science community.

This issue contains 17 articles: two review articles; and the rest are regular articles. The authors of these articles come from different countries namely Australia, Bangladesh, China, Germany, Indonesia, Malaysia, Nigeria, Northern Ireland, Philippines, Poland and Thailand.

The regular article entitled “Morphological Sex Determination of East Asian Barn Swallows (*Hirundo rustica*) in Tropical Wintering Region” determines the best morphological parameters for sexing East Asian Barn Swallows (*Hirundo rustica*) in Bentong, Pahang, Malaysia. Tail fork depth (the difference between the outermost and innermost tail feathers, T6-T1) and the length of the outermost tail feather (6th rectrix, T6) were identified as the best predictors. Using these variables, sex determination achieved an accuracy of 89.47% for females and 96.3% for males, providing a reliable and convenient method for field-based sex determination in this population. Further details of this study are found on page 19.

A selected article entitled “Sequential Cropping Productivity Evaluation of Corn, Mung Bean, and Sweet Potato Intercrop under Coconut Field in Zamboanga del Sur, Philippines” assessed the effects of eight cropping patterns on the agronomic performance, yield, and profitability of corn, mung bean, and sweet potato under coconut ground in Zamboanga del Sur, Philippines. Results showed that cropping patterns influenced key growth parameters and yields of the crops. The CP6 pattern (sweet potato followed by corn) had the highest total yield and a 98% return on investment, making it the recommended cropping pattern for coconut-based farming systems in the area. The detailed information of this article is available on page 117.

A study by Sian Nee See and team entitled “Heavy Metals Assessment in Selected Leafy Vegetables from Selangor, Malaysia” analyzed heavy metal concentrations (Al, Cd, Cr, Cu, Fe, and Pb) in leafy vegetables (cabbage, mustard, spinach, and pak choi)

from Selangor wholesale wet markets using inductively coupled plasma–optical emission spectrometry. Results showed that Al and Fe concentrations were within permissible limits, with spinach containing the highest Al level (41.37 mg/kg). The mean Fe levels in cabbage, mustard, spinach, and pak choi were  $6.30 \pm 5.78$ ,  $4.12 \pm 1.84$ ,  $13.59 \pm 4.73$ , and  $4.14 \pm 0.31$  mg/kg, respectively. Cd, Cr, Cu, and Pb were not detected in any samples. Full information on this study is presented on page 215.

We anticipate that you will find the evidence presented in this issue to be intriguing, thought-provoking and useful in reaching new milestones in your own research. Please recommend the journal to your colleagues and students to make this endeavour meaningful.

All the papers published in this edition underwent Pertanika’s stringent peer-review process involving a minimum of two reviewers comprising internal as well as external referees. This was to ensure that the quality of the papers justified the high ranking of the journal, which is renowned as a heavily-cited journal not only by authors and researchers in Malaysia but by those in other countries around the world as well.

We would also like to express our gratitude to all the contributors, namely the authors, reviewers, Editor-in-Chief and Editorial Board Members of PJTAS, who have made this issue possible.

PJTAS is currently accepting manuscripts for upcoming issues based on original qualitative or quantitative research that opens new areas of inquiry and investigation.

**Chief Executive Editor**

[executive\\_editor.pertanika@upm.edu.my](mailto:executive_editor.pertanika@upm.edu.my)

## Principal Component Analysis of Physicochemical Parameters and Microstructure Characteristics of Wampee Fruit Affected by Storage Temperatures

Hai Wang<sup>1</sup>, Feilong Yin<sup>2</sup>, Shurou Chen<sup>1</sup>, Ting Wei<sup>1</sup>, Ziyi Qin<sup>1</sup>, Jing Li<sup>1,3</sup>, Xia Li<sup>1,3</sup>, Xinhong Dong<sup>1,3\*</sup> and Hock Eng Khoo<sup>1,3</sup>

<sup>1</sup>Guangxi Key Laboratory of Electrochemical and Magneto-chemical Functional Materials, College of Chemistry and Bioengineering, Guilin University of Technology, Guilin 541006, China

<sup>2</sup>College of Food and Biological Engineering, Guangxi Key Laboratory of Health Care Food Science and Technology, Hezhou University, Hezhou 542800, China

<sup>3</sup>South Asia Branch of National Engineering Research Center of Dairy Health for Maternal and Child Health, Guilin University of Technology, Guilin 541006, China

### ABSTRACT

This study investigates the positive effect of two storage temperatures on physicochemical characteristics, texture and structure of wampee fruits. The fruits were treated by storing them at low (10°C) and room temperature (25°C) for eight days. The results showed that the low-temperature (10°C) treatment compared to the room temperature storage could reduce fruit decay rate and weight loss, inhibit O<sub>2</sub><sup>-</sup> production rate, maintain higher total soluble solids, and slower increment in total flavonoids and phenolics. Principal component analysis (PCA) and partial least squares regression analysis further showed that weight loss was positively correlated with the content of total phenolics and flavonoids. The changes in the physiological indicators of the fruits were notably affected by storage temperature, especially in the early storage stages. Texture properties analysis indicated that the hardness and chewiness of the fruit at the low temperature (10°C) were significantly better

than that at 25°C. Fruit colour values (L\*, C\* and h angle) of fruits at 10°C were also remarkably higher than that at 25°C. All the results suggested that low-temperature storage was a convenient and effective method to maintain the quality of the wampee and extend its shelf life compared to room temperature.

**Keywords:** Antioxidant, cold storage, oxygen radical, preservation, subtropical fruit

### ARTICLE INFO

#### Article history:

Received: 16 January 2024

Accepted: 11 July 2024

Published: 28 January 2025

DOI: <https://doi.org/10.47836/pjtas.48.1.01>

#### E-mail addresses:

wanghai990601@163.com (Hai Wang)

Yfeilong1994@163.com (Feilong Yin)

chenshurou0604@163.com (Shurou Chen)

tingwei925@163.com (Ting Wei)

h2oqzy@163.com (Ziyi Qin)

2017002@glut.edu.cn (Jing Li)

biology754@163.com (Xia Li)

dongxhok@126.com (Xinhong Dong)

2020153@glut.edu.cn (Hock Eng Khoo)

\*Corresponding author

## INTRODUCTION

The fruit of *Clausena lansium* (Lour.) Skeels, also known as Chinese wampee (CW), is a tropical and subtropical evergreen fruit of the Rutaceae family in southern China. The wampee ripens from May to July, and the humid subtropical climate accelerates its decay. It will become brown overnight and lose edible value and commercial quality after 2–3 days (Zeng et al., 2020). The short shelf-life of wampee could be due to the fruit softening and peel browning. The increased fruit respiration rate during the warm ambient accelerates fruit ripening. The fruit's shelf life can be prolonged using several preservation techniques and storage conditions to solve this postharvest issue. These preservation techniques are modified atmosphere packaging, ethylene, oxalic acid,  $\gamma$ -aminobutyric acid, ultrasound and melatonin treatments. Low-temperature storage has been used as an effective way to keep fruits among many preservation technologies for fruits and vegetables.

The low fruit quality during room temperature storage is attributed to an increased atmospheric temperature (Mphaphuli et al., 2020). Sanchez et al. (2021) investigated the quality and shelf-life of Malaysian sweet potatoes, including moisture content (MC), soluble solids content (SSC), colour values and textural properties during different storage temperatures. Low-temperature storage of ripe pepper significantly inhibited the lipoxygenase activity, of which the low temperature inhibited ethylene production and delayed fruit senescence (Maalekuu et al., 2006). The enzymatic activities of several enzymes involved in the browning reaction are temperature-dependent. Therefore, low-temperature storage is used as an effective method for the postharvest preservation of fruits. Cai et al. (2010) found that too low temperature would cause cold damage to peach fruit, and the flesh would also have a leather-like texture or structure, affecting the fruit taste. Fruit texture is another important indicator of a fruit's quality besides its appearance and physiological quality.

The literature reported significant correlations between texture parameters and storage quality in bananas and dates (Granados et al., 2014; Singh et al., 2013). Appropriate storage temperatures maintain the fruit quality. No previous study on texture analysis of wampee fruit has been published; a study compared the biochemical parameters of wampee stored at different storage temperatures. The results showed that the storage temperature of 8°C–10°C and 23°C–25°C did not significantly affect the biochemical parameters (total soluble solid, titratable acid and vitamin C content) of the matured post harvested wampee fruit during the 14 days of storage (Meng et al., 2021). The study also reported that the fruit samples stored at room temperature 23°C–25°C had lower peel lightness and hue (h) angle values. Their respiration rate was higher at room temperature. Another study also determined the browning index of wampee fruit stored at 4°C for 12 days (Zeng et al., 2020). Moreover, ethanol fumigation effectively reduced wampee peel browning and increased the antioxidant status of the peel during the storage of the fruit at 8°C for 12 days



(Shao et al., 2020). Therefore, we considered 10°C and 25°C as the storage temperatures of the wampee.

These studies did not determine the other physicochemical properties and perform a microstructure analysis of the wampee fruit peel, and no previous report on the comprehensive postharvest quality of wampee stored at different temperatures, especially all related physicochemical and biochemical characteristics, texture parameters and microstructure evaluation of the fruit peels. Thus, the primary objective of this study was to determine the influences of two storage temperatures and duration on the biochemical, physicochemical and texture parameters of wampee.

## **MATERIALS AND METHODS**

### **Sample Preparation and Treatments**

Wampee was harvested at a commercial maturity stage from a plantation in Guilin, China. They had uniform shapes with good appearances, hard fruit texture and milky white pulp. The fruits were slightly ripened, with a mildly sour taste. A fully ripened wampee has a sweet taste with a citrus flavour. The harvested fruits had a maturity point of 8 out of 10 points and features like a light-yellow hue, round shape and similar sizes. All fruit samples were without disease or mechanical damage. Moreover, no peel browning was observed for all fruits.

All fruit samples (500 fruits) were divided into two groups, where 250 fruits from each group were packed into a foam box (lined with paper scraps to prevent the fruit from squeezing and scraping each other) and stored at 10°C and 25°C. A random sample of 50 fruits was respectively selected to determine the fruit quality values at 0, 2, 4, 6 and 8 days. The temperature selection was because 10°C is a more cost-effective storage temperature than the other lower temperatures. The literature also showed that a storage temperature higher than 10°C for wampee had significantly higher respiration rates (Meng et al., 2021). The fruit sample was also pre-treated with liquid nitrogen and stored at -80°C before further analyses.

### **Decay Incidence, Weight Loss, pH and Total Soluble Solids**

Wampee fruits were considered to decay if they had the characteristics of rot, visible fungal growth, or bacterial damage. The decay incidence was expressed as the percentage of diseased fruits to the total number of fruits (%). Weight loss rate of CW samples was calculated according to the method described by Singh et al. (2013). The pH values of the wampee samples were determined using a pH meter. In brief, the fruits stored at different temperatures were selected randomly, blended and filtered. The filtrates were measured for their pH value using a pH meter (INESA Scientific Instrument Co., Ltd., China).

Total soluble solid (TSS) of CW samples was measured by a handheld Boehmometer (LICHEN-BX Instrument Technology Co., Ltd., China). A random fruit sample was

pounded and filtered. A drop of clear liquid was obtained and measured on the prism of a handheld refractometer. The unit was determined as a Brix value (Xu et al., 2023). All analyses were performed based on three experimental replications.

### **Total Flavonoids, Total Phenolics and Vitamin C**

Total phenolic content (TPC) was determined using a slightly modified method (Ghasemnezhad et al., 2011). Before TPC analysis, the methanolic extracts of wampee samples were centrifuged for 10 min at  $1,127 \times g$  (centrifugal force). The supernatant was subjected to determine TPC and total flavonoid content (TFC). In brief, 0.1 ml of the supernatant, 0.9 ml of distilled water and 0.4 ml of Folin reagent were mixed and reacted for 3 min at  $25^\circ\text{C}$  and then added with 1.0 ml of saturated sodium bicarbonate solution and left for 1 h at  $25^\circ\text{C}$ . The absorbance at 760 nm was determined, and the TPC was expressed as gallic acid equivalent. The aluminium chloride colourimetric assay was used to measure the TFC of the wampee sample (Karadeniz et al., 2005). TFC was expressed as rutin equivalent.

The vitamin C (VC) content was determined by referring to the method described previously with slight modification (Suntornsuk et al., 2002). A 3.0 g wampee sample was weighed, added with 2% hydrochloric acid solution, pulverised, filtered, and then transferred to a 100 ml volumetric flask. The filtrate (5.0 ml) was added with 0.5 ml of 10 g/L potassium iodide solution, 2.0 ml of 5 g/L starch solution and 2.5 ml of distilled water in a conical flask. The mixture was homogenised and titrated with potassium iodate solution. The amount of iodate solution (ml) used was recorded. For blank, 5.0 ml of 2% hydrochloric acid solution was used. All these analyses were performed based on three experimental replications.

### **Hydrogen Peroxide Level and $\text{O}_2^-$ Production Rate**

Hydrogen peroxide/peroxidase assay kit (Suzhou Keming Biotechnology Co. Ltd., China) was applied to determine the hydrogen peroxide ( $\text{H}_2\text{O}_2$ ) level (Cao et al., 2020). A 2.0 g wampee sample was weighed and added with 10 ml of the precooled acetone (Chengdu Kelong Chemical Co., Ltd., China) at  $-20^\circ\text{C}$ . The mixture was agitated for 30 s, incubated in an ice water bath for 10 min and then centrifugated at  $4^\circ\text{C}$   $1,127 \times g$  for 20 min. In triplicate measurements, the supernatant was collected and measured using an  $\text{H}_2\text{O}_2$  detection kit supplied by the Nanjing Jiancheng Bioengineering Research Institute Co., Ltd. (Jiangsu, China).

The  $\text{O}_2^-$  production rate was determined using the method described by Wang et al. (2015) with a slight modification. After weighing 2.0 g of the lyophilised sample, 10 ml of extraction buffer (50 mM, pH 7.8 in phosphate buffer) was added, mixed and agitated for 30 s. The mixture was kept in an ice bath for 10 min, followed by centrifugation at  $1,127 \times g$  for 30 min ( $4^\circ\text{C}$ ). The supernatant (1 ml) was added with 1 ml of phosphate

buffer (0.05 mol/L, pH 7.8) and 1 ml of 1 mM hydroxylamine hydrochloride of pH 3.2 (Thermo Scientific, Rockford, USA), shaken well, and kept at 25°C for 1 h. A 1 ml 17 mM p-aminobenzene sulfonic acid solution of pH 2.5 (Runfeng Synthetic Technology Co., Ltd., China) pre-dissolved in boiling water and 1 ml of 7 mM  $\alpha$ -naphthylamine solution of pH 7.1 (Macklin Biochemical Technology Co., Ltd., China) (prepared using 75% aqueous acetic acid solution as solvent) were pipetted into the reacting sample solution and then mixed well. The absorbance was measured at 530 nm in triplicate measurements.

### Colour Attributes and Texture Profile Analysis

Colour attributes such as lightness ( $L^*$ ), red-green ( $a^*$ ), yellow blue ( $b^*$ ), chroma ( $C^*$ ) and h angle of the fruit peel were determined using a fully automatic colourimeter (Ma et al., 2021). An analytical sample of 30 fruits was measured for  $L^*$ ,  $a^*$ ,  $b^*$ ,  $C^*$  and h values. A three-point measurement (front, side and back) of the fruit was performed for each fruit. A single experimental replication was considered for analysing all colour attributes of each fruit.

The texture profile of wampee samples was determined using the method described by Požrl et al. (2010) with slight modification. The texture parameters were hardness, springiness, chewiness, cohesiveness, resilience and stringiness. The mode set was texture profile analysis (TPA). An analytical sample of 30 fruits was analysed for each texture parameter with a single measurement.

### Microstructure Measurement

The microstructure of the wampee peels was measured using a scanning electron microscope (SEM). The samples (five pieces of the peel) were soaked into a solution of 2% (Wuhan Kangdeli Chemical Co., Ltd., China). The peels were then rinsed three times with the corresponding phosphate buffer for 15 min and dehydrated in ethanolic solutions of 50%, 70%, 80% and 90% at 15 min each (Qin et al., 2022). The ethanol was purchased from Fuyu Chemical Company (China). The samples were freeze-dried before the electron microscope scanning. All SEM analyses were done based on three sample replications.

### Statistical Analysis

All data were presented as means  $\pm$  standard errors of different sample replicates. The data for biochemical characteristics, colour attributes and textural parameters were statistically analysed using Statistical Package for Social Sciences (SPSS) version 25.0 software. The significant differences between the two variables were analysed using a one-way analysis of variance (ANOVA) coupled with Duncan's multiple range test. The PCA was also determined using SPSS software for selected biochemical and physicochemical parameters of wampee peels, with a significance value set at  $p < 0.05$ .

## RESULTS

### Decay Incidence, Weight Loss, pH and Total Soluble Solids

Table 1 shows the quality parameters of wampee samples stored at two temperatures (10°C and 25°C). The results showed that the TSS values of the fruit samples decreased with the increasing storage duration. The decreasing rate of the fruit samples stored at 10°C was significantly lower than those kept at 25°C ( $p < 0.05$ ). In contrast, the fruit samples stored at 10°C had better brightness and smoothness of the surface than those at 25°C throughout the storage period. In this study, the weight loss rate of wampee samples kept at 10°C was significantly lower than the fruit samples stored at 25°C ( $p < 0.05$ ).

As shown in Table 1, the fruit samples kept at 10°C had a lower peel decaying rate than those stored at 25°C. On day eight, the peel decaying rate of the fruit samples kept at 25°C was four times higher than that of 10°C. The wampee samples stored at the low temperature had better fruit quality than those at 25°C. TSS of the wampee samples kept at 10°C was significantly higher than the room temperature storage. The TSS of the fruit samples that were stored at 25°C had a decreasing trend. The reduction was significantly higher than the low-temperature storage starting from day two ( $p < 0.05$ ). The acidity trend (based on pH value) of the fruit samples stored at 10°C remained relatively constant during storage. However, the acidity of the fruits in the 25°C group was significantly ( $p < 0.05$ ) reduced on day eight.

### Total Flavonoids, Total Phenolics and Vitamin C

The TPC and TFC of wampee samples stored at 10°C and 25°C had an increasing trend. The TPC of the low-temperature storage samples had a slower increment than those kept at 25°C (Table 1). The results also showed that the TFC content of the fruit samples was significantly increased after four days of storage at 25°C ( $p < 0.05$ ). Similar to the reported TPC values, the TFC of the fruit samples stored at 10°C had a slower increment. On the other hand, the VC of the fruit samples kept at both temperatures decreased from day 0 until day 6. The VC values of these fruit samples significantly increased to over four times higher on day 8 than on day 6. The fruit samples stored at 10°C had a higher increase in VC than those at 25°C.

### Hydrogen Peroxide Content and $O_2^-$ Production Rate

The  $H_2O_2$  accumulation in the wampee samples kept at both storage temperatures showed an increasing trend with the extended storage times (Table 1). Starting from day 4, the fruit samples refrigerated at 10°C had a significantly slower increment in the level of  $H_2O_2$  than the samples stored at 25°C ( $p < 0.05$ ). The increasing  $O_2^-$  production trend in both fruit samples was unlike the  $H_2O_2$  level. The wampee samples stored at room temperature showed increasing levels of  $O_2^-$ , but the  $O_2^-$  values of the fruit samples kept at 10°C fluctuated. The baseline value was higher than those determined in the samples stored at room temperature for two days.

Table 1  
Changes in fruit quality and biochemical indexes

Parameters	Day 0		Day 2		Day 4		Day 6		Day 8									
	10°C	25°C	10°C	25°C	10°C	25°C	10°C	25°C	10°C	25°C								
Weight loss (%)	0.00	0.39	f	1.68	d	0.72	ef	2.55	c	1.05	e	3.92	b	1.75	d	5.46	a	
Decay rate (%)	0.00	a	0.00	16.67	c	3.33	ab	46.67	d	10.00	bc	60.00	e	13.33	c	83.33	f	
pH	3.18	a	3.36	bc	3.36	bc	3.39	bc	3.39	cd	3.33	b	3.41	d	3.33	b	3.51	e
TSS (Brix)	16.30	d	16.70	b	15.77	f	17.47	ab	15.80	f	16.53	c	15.77	f	16.00	e	14.53	g
TPC (g/kg)	59.57	e	58.41	e	63.07	d	63.88	d	67.16	c	60.14	e	77.65	b	59.44	e	88.08	a
TFC (g/kg)	0.06	e	0.09	d	0.11	cd	0.11	cd	0.13	c	0.12	cd	0.16	b	0.18	b	0.25	a
Vitamin C (mg/kg)	4.42	h	3.85	g	2.68	d	3.25	f	2.60	d	3.09	e	1.19	b	16.62	c	5.08	a
H <sub>2</sub> O <sub>2</sub> (mmol/kg FW)	0.89	e	1.20	d	1.22	d	1.33	d	1.43	c	1.41	c	1.57	b	1.58	b	1.70	a
O <sub>2</sub> <sup>-</sup> production rate (mmol/min/kg FW)	0.28	d	0.37	cd	0.15	e	0.57	ab	0.26	d	0.45	bc	0.67	a	0.38	cd	0.69	a

Note. Data are presented as mean values of three sample replicates. Different superscript lowercase letters (<sup>a-e</sup>) denote a significant difference ( $p < 0.05$ ). TSS=Total soluble solids; TFC=Total flavonoid content; TPC=Total phenolic content; FW=Fresh weight

### Principal Component Analysis

As shown in Figure 1a, the variations explained by the first (PC1) and second (PC2) principal components were 76.8% and 10.5%, respectively. The results showed that overall responses to the 10°C treatment were more closely associated with each other than those in the 25°C fruit, regardless of storage duration. PC1 can discern the differences in quality parameters of the wampee treated with the two storage temperatures.

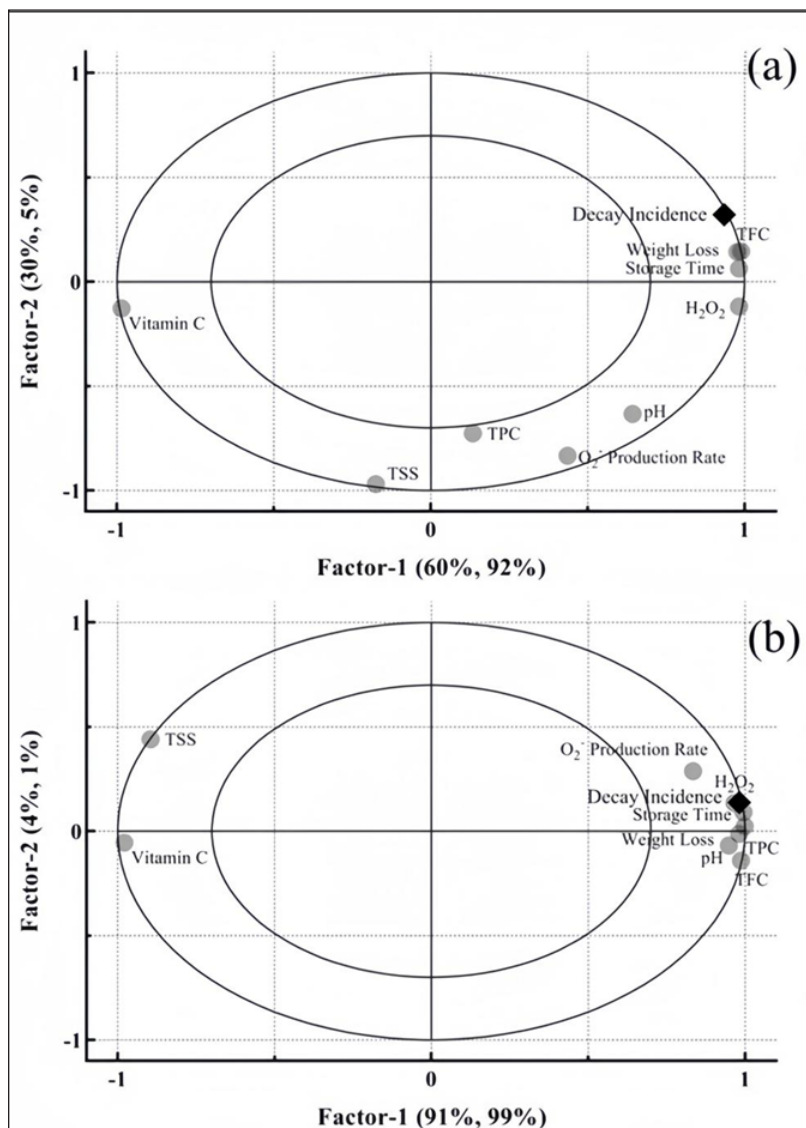


Figure 1. Loadings and scores of principal component analysis for Wampee samples. (a) Biplot of the biochemical indicators and (b) loading and score plots. These plots showing components 1 and 2 are explained by 90% of the total variation

Six indicators (decay rate, weight loss, TPC, TFC, pH values and  $\text{H}_2\text{O}_2$  level) of the wampee samples contributed the most to the PC1 score, while TSS and  $\text{O}_2^-$  production rate were explained by PC2 (Figure 1b). PC1 distinguished the differences in the variables between the wampee samples kept at day 6 and day 8 for both temperatures. This indicates that changes in weight loss, TPC, TFC, pH values and  $\text{H}_2\text{O}_2$  levels in the sample have arisen from storage at  $25^\circ\text{C}$ . The differences in these quality parameters for the samples between day 2 and day 4 of storage were better distinguished in PC2. It shows that the changes in TSS and  $\text{O}_2^-$  production rate of the samples on day 2 versus day 4 were due to the low-temperature storage.

### Partial Least Squares Regression Analysis

The decay incidence of the wampee samples was selected as the dependent variable (Y). The other indicators were independent variables (X). The partial least squares regression (PLSR) model was also developed (Figure 2). Most X and Y variables lie between  $R^2 = 50\%$  and  $100\%$  confidence ellipses, indicating that the model has a higher confidence. TFC, weight loss, storage time,  $\text{H}_2\text{O}_2$  and VC content were the variables with significant effects on the decay incidence under low-temperature storage. As a comparison, four new factors (TSS, TPC, pH and  $\text{O}_2^-$  production rate) affected the wampee decay incidence under room temperature storage.

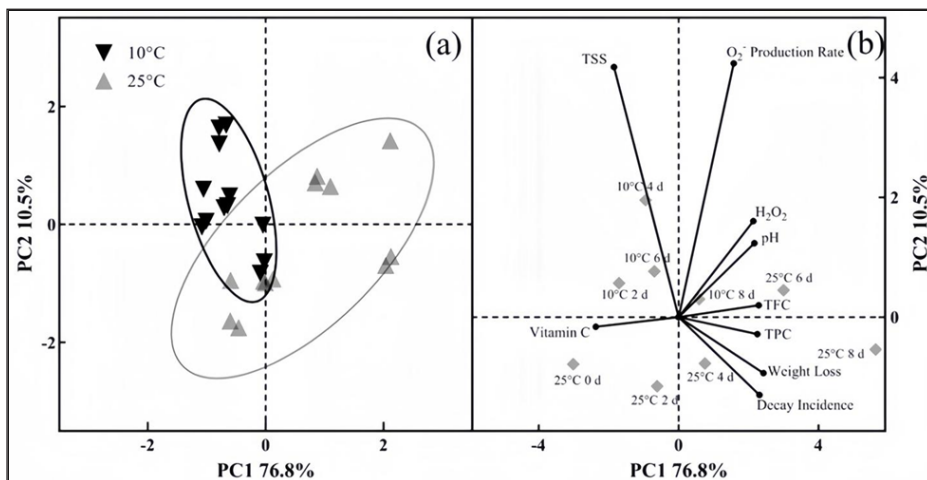


Figure 2. Partial least squares regression biplots for the correlation between decay incidence and postharvest physiology of (a) low-temperature storage and (b) room-temperature storage

### Colour Attributes

The colour attributes of the wampee peel stored for 2, 4, 6 and 8 days are presented in Table 2. The values of all colour attributes of the fruit sample kept at  $25^\circ\text{C}$  for eight days

were significantly lower than 10°C ( $p<0.05$ ), except for a\* value. No significant change in the a\* value was observed between the samples kept at two different temperatures for eight days ( $p>0.05$ ). The trend of C\* values of the samples stored at 10°C was similar to that of L\* values. However, a significant variation was reported for the C\* value of the peel sample kept at 25°C, with a significantly elevated C\* value on day 2 and reduced after day 4 ( $p<0.05$ ). The changes in the h value of the samples kept at 10°C were similar to that of 25°C. However, Table 2 shows a significant decrease ( $p<0.05$ ) in b\* values under the low-temperature storage.

Table 2  
*Lightness, chroma and hue of wampee samples stored at different temperatures*

Appearance	Storage temperatures (°C)	
	25	10
Lightness (L*)		
2	36.27±1.01 <sup>bc</sup>	40.52±0.65 <sup>a</sup>
4	35.73±0.75 <sup>cd</sup>	35.72±0.48 <sup>cd</sup>
6	33.43±0.49 <sup>de</sup>	36.75±0.44 <sup>bc</sup>
8	31.33±0.59 <sup>e</sup>	38.23±0.44 <sup>ab</sup>
Red-green (a*)		
2	15.34±0.46 <sup>c</sup>	15.71±0.60 <sup>c</sup>
4	16.67±0.36 <sup>bc</sup>	18.65±0.41 <sup>a</sup>
6	17.56±0.29 <sup>ab</sup>	17.31±0.31 <sup>ab</sup>
8	16.40±0.29 <sup>bc</sup>	16.71±0.35 <sup>bc</sup>
Yellow blue (b*)		
2	25.29±0.88 <sup>cd</sup>	30.36±0.47 <sup>a</sup>
4	26.33±0.59 <sup>c</sup>	26.51±0.38 <sup>bc</sup>
6	23.74±0.44 <sup>de</sup>	27.01±0.36 <sup>bc</sup>
8	22.09±0.41 <sup>e</sup>	28.32±0.35 <sup>b</sup>
Chroma (C*)		
2	29.76±0.79 <sup>c</sup>	34.39±0.30 <sup>a</sup>
4	31.54±0.49 <sup>b</sup>	32.83±0.20 <sup>ab</sup>
6	29.60±0.48 <sup>c</sup>	32.30±0.26 <sup>b</sup>
8	27.62±0.44 <sup>d</sup>	33.11±0.26 <sup>ab</sup>
Hue (h)		
2	58.26±1.17 <sup>b</sup>	62.56±1.17 <sup>a</sup>
4	56.90±0.88 <sup>bc</sup>	54.69±0.92 <sup>cd</sup>
6	53.35±0.41 <sup>d</sup>	57.13±0.70 <sup>bc</sup>
8	53.23±0.52 <sup>d</sup>	59.31±0.72 <sup>ab</sup>

Note. Data are presented as mean ± standard error (n=30, sample replicate). Different superscript lowercase letters (<sup>a-e</sup>) denote a significant difference ( $p<0.05$ )



## Texture Characteristic

Table 3 presents the TPA data of wampee samples stored at 10°C and 25°C. No significant changes in TPA values were observed between the sample variables ( $p>0.05$ ). The hardness value of the samples stored at 10°C increased gradually with increasing storage duration, and it dropped after six days of storage. However, the springiness and resilience under room temperature storage decreased significantly ( $p<0.05$ ). The stringiness values of the fruit samples kept at 10°C were slightly reduced with increasing storage times of up to six days, whereas the fruit samples stored at 25°C for six to eight days had a significant increase in stringiness values ( $p<0.05$ ).

Table 3

*Texture characteristics of wampee samples stored at different temperatures*

Days	Hardness	Springiness	Chewiness	Cohesiveness	Resilience	Stringiness
10 °C						
2	257±21 <sup>c</sup>	0.86±0.01 <sup>a</sup>	184±15 <sup>bc</sup>	0.83±0.01 <sup>a</sup>	0.84±0.02 <sup>a</sup>	0.28±0.03 <sup>b</sup>
4	330±32 <sup>bc</sup>	0.87±0.01 <sup>a</sup>	234±22 <sup>a</sup>	0.82±0.01 <sup>a</sup>	0.84±0.02 <sup>a</sup>	0.23±0.03 <sup>b</sup>
6	431±28 <sup>a</sup>	0.88±0.01 <sup>a</sup>	305±23 <sup>ab</sup>	0.81±0.01 <sup>ab</sup>	0.83±0.02 <sup>a</sup>	0.18±0.04 <sup>b</sup>
8	391±26 <sup>ab</sup>	0.85±0.01 <sup>ab</sup>	266±17 <sup>bc</sup>	0.80±0.01 <sup>abc</sup>	0.79±0.01 <sup>ab</sup>	0.43±0.11 <sup>ab</sup>
25 °C						
2	325±32 <sup>bc</sup>	0.86±0.01 <sup>ab</sup>	221±20 <sup>bc</sup>	0.80±0.02 <sup>abc</sup>	0.85±0.03 <sup>a</sup>	0.30±0.05 <sup>b</sup>
4	310±45 <sup>bc</sup>	0.79±0.02 <sup>c</sup>	178±24 <sup>c</sup>	0.75±0.02 <sup>bc</sup>	0.71±0.03 <sup>c</sup>	0.29±0.07 <sup>b</sup>
6	267±27 <sup>c</sup>	0.82±0.02 <sup>bc</sup>	165±21 <sup>c</sup>	0.74±0.04 <sup>c</sup>	0.75±0.04 <sup>bc</sup>	0.60±0.10 <sup>a</sup>
8	275±37 <sup>c</sup>	0.82±0.02 <sup>bc</sup>	173±26 <sup>c</sup>	0.76±0.02 <sup>bc</sup>	0.71±0.03 <sup>c</sup>	0.69±0.12 <sup>a</sup>

*Note.* Data are presented as mean ± standard error (n=30, sample replicate). Different superscript lowercase letters (<sup>a-c</sup>) denote a significant difference ( $p<0.05$ )

## Microstructures of Wampee Peel

Figure 3a depicts the exocarp microstructures of wampee samples stored at 10°C and 25°C. Notable changes were observed in the microstructures during the storage of wampee samples. The result showed that the exocarp surface of the fruit was lined with a uniform, dense and waxy layer; the stomata were evenly distributed on the surface; and villi of different lengths were observed. At the top layer of the fruit, more villi were clustered, usually 2–5 villi in each cluster.

On the contrary, the villi were solitary on the surface. The increasing storage time caused a gradual fall off of the hypha and waxy layer, and the stomata gradually changed from smooth round edges to irregular ellipses Figure 3a [a–e]. As shown in Figure 3a [h], some wedge-shaped damage to the waxy layer is observed. Figure 3a [i] shows that rod-shaped and granular pathogenic infections appeared around the base of the epidermal villi of the samples stored at 25°C for up to six days. In contrast, the fruit samples kept at 10°C

had intact and waxy surfaces, flake cracks were not seen, and the texture remained intact with fewer fractures and no pathogenic infection.

Figure 3b shows the endocuticle structures of wampee samples stored at 10°C [k–o] and 25°C [p–t]. It can be seen from Figure 3b that many cavities formed between the parenchyma and vascular bundle on the lining of the outer epidermis and the outer epidermis. The parenchyma gradually shrunk and curled with the increase in storage time, resulting in the deepening of the longitudinal depth of the cavities, which is presented in Figure 3b [o and r]. On the contrary, the low-temperature storage could maintain better tissue denseness and orderliness than those kept at 25°C. It indicates that the low temperature maintains the structure of wampee peels.

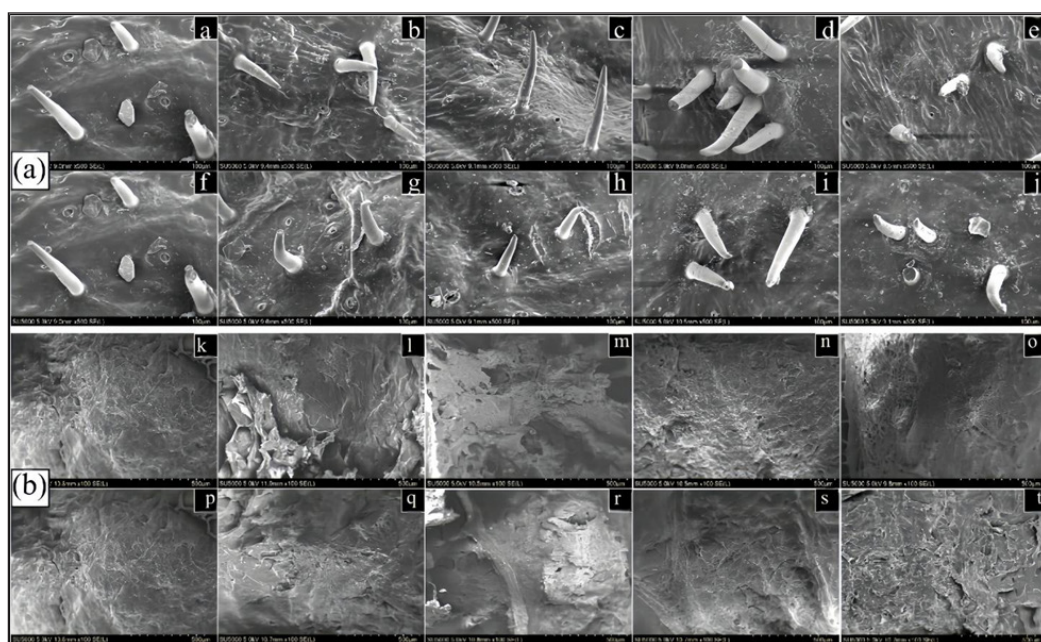


Figure 3. Microstructure of wampee peel samples during storage at 10°C and 25°C for eight days. (a) peel surface, scale bar of 100 µm; (b) inner peel, scale bar of 500 µm

## DISCUSSION

Temperature controls various physiological changes during fruit storage. Our work showed that the surface of the matured wampee stored at 10°C was brighter and had fewer black spots. The results are consistent with the findings reported in the literature that the fruit samples stored at 25°C had a significantly higher decay rate than that of the other two lower temperatures (6°C and 10°C) (Hong et al., 2013). A storage temperature below 9°C could cause chilling injuries to mandarin oranges and develop off-flavours (Morales et al., 2020). The weight loss rate is also consistent with the previous report (Požrl et al., 2010).

The positive finding could be that fruit respiration is the most active at 25°C. The results also showed that the fruit samples stored at room temperature had a significantly lower fruit quality starting from day 4 of storage than those refrigerated at a low temperature.

Storing matured and ripe wampee samples at 25°C could maintain their freshness for up to three days. The reason was that decreased storage temperature reduced the respiration rate of fruit. Storing the fruits at 25°C increases the ripening process. The quality rating of the fruit samples is closely related to the peel decay rate. The decay process of frozen fruits is faster than that of those kept in the chiller, probably because the inner membrane of the frozen peel is disrupted, which releases polyphenol oxidase and leads to peel decay. TSS of the wampee samples stored at 10°C was significantly higher than the room temperature storage. It indicates that 10°C inhibited sugar metabolism inside the cell wall of the wampee. This finding is consistent with a previous report that low-temperature storage reduced the loss of TSS in Chinese bayberries stored for up to 14 days (Yang et al., 2007). The main reason for the decrease in TSS was the increased carbohydrate metabolism.

In this study, the VC content of the wampee samples stored at room temperature for up to six days showed a decreasing trend, but the low-temperature storage inhibited the VC loss in fruit samples during the 8-day storage. Citrus fruit typically has a higher acidity than many other fruits. Due to wampee being a citrus fruit, the low pH value is attributed to VC and phenolic acid content. The ripe wampee has a higher pH because the ripened fruit has low acidity. Also, low-temperature storage reduced the ripening process. Carmona et al. (2017) found that higher temperatures increased gene expression of the flavonoid pathway in blood orange. However, the low-temperature storage did not affect total phenolics and VC in the red raspberries (Mullen et al., 2002). High-temperature storage induced oxidative stress on the fruit. The high level of H<sub>2</sub>O<sub>2</sub> in the fruit tissue denotes increased oxidative stress. Li et al. (2017) speculated that the reduced accumulation of these oxidative products during the prolonged storage period was possibly due to the antioxidative activity in the fruit pulp. The positive correlations between total phenolic content, O<sub>2</sub><sup>-</sup> production rate and decay incidence at higher temperatures were due to the accelerated degradation of phenolic compounds.

The results of this study showed that the brightness of wampee peels reduced during storage at ambient temperature, the colour saturation decreased, and the peel brightness faded. This could be observed from the wampee peel, where the peel colour changed from bright golden yellow to matte brown. However, the low-temperature storage was favourable in maintaining the brightness and colour tone of the fresh wampee. The low temperature also maintained the fruit's pleasant appearance, quality and shelf life.

This finding is consistent with a previous report that the low-temperature storage preserved the freshness, colour and appearance of the Chinese bayberry fruit at the prolonged storage duration (Yang et al., 2007). The report from Carmona et al. (2017)

also confirmed that a higher temperature promoted the accumulation of flavonoids in the fruit peel, which resulted in a high  $C^*$  value. These colour attributes are closely related to peel browning. The samples stored at 25°C had a higher decay rate and reduced lightness values than those at 10°C. The higher  $L^*$  value denotes a brighter peel. The value of  $C^*$  indicates the saturation of the colour; the higher  $C^*$  value shows a more intense colour. A higher  $h$  value represents a better hue. Usually, the colour of the fruit changed from green to brownish red, while the  $b^*$  value remained stable during the postharvest period (Wang et al., 2020).

The springiness and resilience under room temperature storage decreased, which can be attributed to the fact that the stiffness coefficient of the fruit was affected by temperature (Singh & Reddy, 2006). Higher temperatures stimulated pectinamethylesterase and polygalacturonase responses, leading to fruit hardness decay (da Silva et al., 2021). The TPA data showed that the wampee samples stored at 10°C had better texture characteristics than those at 25°C. It could also maintain a better quality of the fruit.

Dehydration of fruit causes changes in the microstructures of the fruit peel. The weight loss determined for the wampee samples denotes fruit dehydration. The dehydrated capsule membrane of the fruit peel cracked, and the sac structure completely collapsed and deformed. Pathogen infections may also be associated with fruit dehydration, and the respiration, transpiration and metabolism rates were the highest. The energy and water consumed were also the largest (Teixeira et al., 2011). These are related to the loose histiocyte and huge intercellular space between the pedicel. Hence, the organisation structure deformed due to prolonged storage time and water loss.

## CONCLUSION

This study showed that low-temperature storage (10°C) significantly improved the quality of wampee samples, including quality parameters, texture properties and microstructure of wampee peel. It had positive effects against weight reduction and wampee peel browning, inhibited loss of TSS, free fatty acids, phenolic compounds and VC, and reduced accumulation of reactive oxygen species compared with the fruit samples stored at 25°C. The texture and microstructure analysis of the peel samples further confirmed that the low-temperature storage was more effective in maintaining better texture and tissue integrity. Therefore, storage of wampee at 10°C is a more economical and effective method for maintaining the quality of the fruit. It also reduced fruit senescence and peel browning. Extending storage periods and comparing a few different storage temperatures are suggested for future studies to obtain a more effective way of maintaining fruit quality. The physical factors contributing to fruit decay are the alternative recommendations for future research.

## ACKNOWLEDGEMENTS

This study was supported by the National Natural Science Foundation of China [Grant No. 31760472] and Guangxi Key Laboratory of Electrochemical and Magnetochemical Functional Materials, Guilin University of Technology [Grant No. EMFM20211108].

## REFERENCES

- Cai, Y., Yu, M., Xing, H., Di, H., Pei, J., Xu, F., & Zheng, Y. (2010). Effects of low temperature conditioning on chilling injury and quality of cold-stored juicy peach fruit. *Transactions of the Chinese Society of Agricultural Engineering*, 26(6), 334-338. <https://doi.org/10.3969/j.issn.1002-6819.2010.06.058>
- Cao, J., Kang, C., Chen, Y., Karim, N., Wang, Y., & Sun, C. (2020). Physiochemical changes in *Citrus reticulata* cv. Shatangju fruit during vesicle collapse. *Postharvest Biology and Technology*, 165, 111180. <https://doi.org/10.1016/j.postharvbio.2020.111180>
- Carmona, L., Alquézar, B., Marques, V. V., & Peña, L. (2017). Anthocyanin biosynthesis and accumulation in blood oranges during postharvest storage at different low temperatures. *Food Chemistry*, 237, 7-14. <https://doi.org/10.1016/j.foodchem.2017.05.076>
- da Silva, E. P., de Freitas, F. A., Carvalho, E. E. N., Junior, L. C. C., de Freitas, M. S. L., Calderaro, F. L., Damiani, C., & de Barros Vilas Boas, E. V. (2021). Effect of storage temperature on the quality of marolo fruit (*Annona crassiflora* Mart) “in natura”. *Research, Society and Development*, 10(6), e4110615446. <https://doi.org/10.33448/rsd-v10i6.15446>
- Ghasemnezhad, M., Sherafati, M., & Payvast, G. A. (2011). Variation in phenolic compounds, ascorbic acid and antioxidant activity of five coloured bell pepper (*Capsicum annuum*) fruits at two different harvest times. *Journal of Functional Foods*, 3(1), 44-49. <https://doi.org/10.1016/j.jff.2011.02.002>
- Granados, C., Acevedo, D., Cabeza, A., & Lozano, A. (2014). Texture profile analysis in bananas Pelipita, Hartón and Topocho. *Información Tecnológica*, 25(5), 35-40. <https://doi.org/10.4067/S0718-07642014000500006>
- Hong, K., Xu, H., Wang, J., Zhang, L., Hu, H., Jia, Z., Gu, H., He, Q., & Gong, D. (2013). Quality changes and internal browning developments of summer pineapple fruit during storage at different temperatures. *Scientia Horticulturae*, 151, 68-74. <https://doi.org/10.1016/j.scienta.2012.12.016>
- Karadeniz, F., Burdurlu, H. S., Koca, N., & Soyer, Y. (2005). Antioxidant activity of selected fruits and vegetables grown in Turkey. *Turkish Journal of Agriculture and Forestry*, 29(4), 297-303.
- Li, X., Li, M., Han, C., Jin, P., & Zheng, Y. (2017). Increased temperature elicits higher phenolic accumulation in fresh-cut pitaya fruit. *Postharvest Biology and Technology*, 129, 90-96. <https://doi.org/10.1016/j.postharvbio.2017.03.014>
- Ma, J., Zhou, Z., Li, K., Li, K., Liu, L., Zhang, W., Xu, J., Tu, X., Du, L., & Zhang, H. (2021). Novel edible coating based on shellac and tannic acid for prolonging postharvest shelf life and improving overall quality of mango. *Food Chemistry*, 354, 129510. <https://doi.org/10.1016/j.foodchem.2021.129510>
- Maalekuu, K., Elkind, Y., Leikin-Frenkel, A., Lurie, S., & Fallik, E. (2006). The relationship between water loss, lipid content, membrane integrity and LOX activity in ripe pepper fruit after storage. *Postharvest Biology and Technology*, 42(3), 248-255. <https://doi.org/10.1016/j.postharvbio.2006.06.012>

- Meng, X. C., Huang, Z. P., Fan, C., & Lu, Y. S. (2021). Effects of storage temperature on the preservation period and quality of seedless wampee fruit. *Journal of Food Safety and Quality*, 12(21), 8530-8535. <https://doi.org/10.19812/j.cnki.jfsq11-5956/ts.2021.21.033>
- Morales, J., Bermejo, A., Besada, C., Navarro, P., Gil, R., Hernando, I., & Salvador, A. (2020). Physicochemical changes and chilling injury disorders in 'Tango' mandarins stored at low temperatures. *Journal of the Science of Food and Agriculture*, 100(6), 2750-2760. <https://doi.org/10.1002/jsfa.10307>
- Mphaphuli, T., Slabbert, R. M., & Sivakumar, D. (2020). Storage temperature and time changes of phenolic compounds and antioxidant properties of Natal plum (*Carissa macrocarpa*). *Food Bioscience*, 38, 100772. <https://doi.org/10.1016/j.fbio.2020.100772>
- Mullen, W., Stewart, A. J., Lean, M. E., Gardner, P., Duthie, G. G., & Crozier, A. (2002). Effect of freezing and storage on the phenolics, ellagitannins, flavonoids, and antioxidant capacity of red raspberries. *Journal of Agricultural and Food Chemistry*, 50(18), 5197-5201. <https://doi.org/10.1021/jf020141f>
- Požrl, T., Žnidarčič, D., Kopjar, M., Hribar, J., & Simčič, M. (2010). Change of textural properties of tomatoes due to storage and storage temperatures. *Journal of Food Agriculture and Environment*, 8(2), 292-296. <https://doi.org/10.1234/4.2010.1655>
- Qin, Z., Pan, J., Li, J., Sun, J., Khoo, H. E., & Dong, X. (2022). Effects of 1-methylcyclopropene and abscisic acid treatments on texture properties and microstructures of postharvest tangerine (*Citrus reticulata* cv. Orah). *Journal of Food Processing and Preservation*, 46(7), e16633. <https://doi.org/10.1111/jfpp.16633>
- Sanchez, P. D. C., Hashim, N., Shamsudin, R., & Nor, M. Z. M. (2021). Effects of different storage temperatures on the quality and shelf life of Malaysian sweet potato (*Ipomoea Batatas* L.) varieties. *Food Packaging and Shelf Life*, 28, 100642. <https://doi.org/10.1016/j.fpsl.2021.100642>
- Shao, Y., Jiang, Z., Zeng, J., Li, W., & Dong, Y. (2020). Effect of ethanol fumigation on pericarp browning associated with phenol metabolism, storage quality, and antioxidant systems of wampee fruit during cold storage. *Food Science & Nutrition*, 8(7), 3380-3388. <https://doi.org/10.1002/fsn3.1617>
- Singh, K. K., & Reddy, B. S. (2006). Post-harvest physico-mechanical properties of orange peel and fruit. *Journal of Food Engineering*, 73(2), 112-120. <https://doi.org/10.1016/j.jfoodeng.2005.01.010>
- Singh, V., Guizani, N., Al-Alawi, A., Claereboudt, M., & Rahman, M. S. (2013). Instrumental texture profile analysis (TPA) of date fruits as a function of its physico-chemical properties. *Industrial Crops and Products*, 50, 866-873. <https://doi.org/10.1016/j.indcrop.2013.08.039>
- Suntornsuk, L., Gritsanapun, W., Nilkamhank, S., & Paochom, A. (2002). Quantitation of vitamin C content in herbal juice using direct titration. *Journal of Pharmaceutical and Biomedical Analysis*, 28(5), 849-855. [https://doi.org/10.1016/S0731-7085\(01\)00661-6](https://doi.org/10.1016/S0731-7085(01)00661-6)
- Teixeira, G. H., Durigan, J. F., Santos, L. O., Hojo, E. T., & Cunha Junior, L. C. (2011). Changes in the quality of jaboticaba fruit (*Myrciaria jaboticaba* (Vell) Berg. cv. Sabará) stored under different oxygen concentrations. *Journal of the Science of Food and Agriculture*, 91(15), 2844-2849. <https://doi.org/10.1002/jsfa.4530>
- Wang, J., You, Y., Chen, W., Xu, Q., Wang, J., Liu, Y., Song, L., & Wu, J. (2015). Optimal hypobaric treatment delays ripening of honey peach fruit via increasing endogenous energy status and enhancing antioxidant

- defence systems during storage. *Postharvest Biology and Technology*, *101*, 1-9. <https://doi.org/10.1016/j.postharvbio.2014.11.004>
- Wang, Q., Wei, Y., Chen, X., Xu, W., Wang, N., Xu, F., Wang, H., & Shao, X. (2020). Postharvest strategy combining maturity and storage temperature for 1-MCP-treated peach fruit. *Journal of Food Processing and Preservation*, *44*(4), e14388. <https://doi.org/10.1111/jfpp.14388>
- Xu, H., Qiao, P., Pan, J., Qin, Z., Li, X., Khoo, H. E., & Dong, X. (2023). CaCl<sub>2</sub> treatment effectively delays postharvest senescence of passion fruit. *Food Chemistry*, *417*, 135786. <https://doi.org/10.1016/j.foodchem.2023.135786>
- Yang, Z., Zheng, Y., Cao, S., Tang, S., Ma, S., & Li, N. A. (2007). Effects of storage temperature on textural properties of Chinese bayberry fruit. *Journal of Texture Studies*, *38*(1), 166-177. <https://doi.org/10.1111/j.1745-4603.2007.00092.x>
- Zeng, J. K., Jiang, Z. T., Li, W., Zhang, L. B., & Shao, Y. Z. (2020). Effects of uv-c irradiation on postharvest quality and antioxidant properties of wampee fruit (*Clausena lansium* (Lour.) skeels) during cold storage. *Fruits*, *75*(1), 36-43. <https://doi.org/10.17660/th2020/75.1.4>





## Morphological Sex Determination of East Asian Barn Swallows (*Hirundo rustica*) in Tropical Wintering Region

Nor Adibah Ismail<sup>1</sup>, Umami Nur Syafiqah Daud<sup>1</sup>, Noor Fatimah Najihah Arazmi<sup>2</sup>, Nurfatin Batrisyia Md Ali<sup>2</sup>, Shukor Md Nor<sup>3</sup> and Mohammad Saiful Mansor<sup>2\*</sup>

<sup>1</sup>Department of Earth Science and Environment, Faculty of Science and Technology, Universiti Kebangsaan Malaysia, 43600 Bangi, Selangor, Malaysia

<sup>2</sup>Department of Biological Sciences and Biotechnology, Universiti Kebangsaan Malaysia, 43600 Bangi, Selangor, Malaysia

<sup>3</sup>50 Jalan 7, Taman Tenaga, Batu 9, Jalan Puchong, 47100 Puchong, Selangor, Malaysia

### ABSTRACT

The Barn Swallow *Hirundo rustica* is a non-breeding, sexually dimorphic, and diurnal migrant that overwinters worldwide, including in Peninsular Malaysia. While numerous studies on Barn Swallows have been conducted, their ecology in wintering sites, particularly tropical regions, remains poorly understood. Notably, little information is available on the morphological sex determination of Barn Swallows, especially for the East Asian Barn Swallow *H. r. gutturalis* population. This population migrates through or winters in the Thai-Malay Peninsula, while breeding occurs from the eastern Himalayas to northeast Russia (Siberia), China, the Korean Peninsula, and Japan. This study aims to determine the best parameters for the morphological sexing of East Asian Barn Swallows and was conducted in Bentong, Pahang, central Peninsular Malaysia. Swallows were captured using a modified scoop net attached to a telescopic pole, and their morphological data were recorded. A total of 46 individual East Asian Barn Swallows (19 females and 27 males) were captured for sex determination. We confirmed the sex and subspecies of sampled individuals

using a molecular approach. We observed that two of the seven measured variables—tail fork depth (the length difference between the outermost and innermost tail feathers; T6-T1) and the length of the outermost tail feather (6th rectrix; T6) were chosen as the best predictors for sex determination. According to the quadratic discriminant functions constructed, approximately 89.47% of females and 96.3% of males were correctly classified using a combination of both chosen predictors. These morphological determination findings represent

### ARTICLE INFO

#### Article history:

Received: 20 March 2024

Accepted: 18 July 2024

Published: 28 January 2025

DOI: <https://doi.org/10.47836/pjtas.48.1.02>

#### E-mail addresses:

nadibahismail@gmail.com (Nor Adibah Ismail)

ummisyafiqah96@gmail.com (Umami Nur Syafiqah Daud)

n.fatihahnajihah@gmail.com (Noor Fatimah Najihah Arazmi)

fatinbatrisyia5@gmail.com (Nurfatin Batrisyia Md Ali)

shukor63@live.com (Shukor Md Nor)

msaifulmansor@gmail.com (Mohammad Saiful Mansor)

\*Corresponding author

baseline knowledge that can help to provide more accurate and convenient Barn Swallow sex determination in the field.

*Keywords:* Discriminant function analysis, molecular sexing, swallows, sexual dimorphism, wintering region

---

## INTRODUCTION

The Barn Swallow *H. rustica* is a widespread species that breeds extensively in human settlements. It is one of 83 species belonging to Hirundinidae, a 39 family of birds composed of swallows and martins (communally recognized as hirundines) (Turner, 2006). In total, there are six subspecies of Barn Swallow: *H. r. savignii*, which breed in North Africa; *H. r. transitiva*, which breeds in the Middle East; *H. r. rustica*, which breeds in Europe; *H. r. tyleri*, which breeds in Siberia and Mongolia; *H. r. erythrogaster* breeds in North America (Ismail et al., 2020); and *H. r. gutturalis*, which pass through or overwinter in the Thai-Malay Peninsula (Mansor et al., 2020) and breed from the eastern Himalayas to northeast Russia (Siberia), China, the Korean Peninsula, and Japan (Dor et al., 2010). In addition, the wintering population of *H. rustica* included the subspecies *saturata* Ridgeway and/or *mandschurica* Meise among a majority of *gutturalis* Scopoli. However, the recovery site of one Malayan-ringed bird at Krashyi Chikoi (its presumed breeding location) confirmed that the subspecies *tyleri* Jerdon was also represented among the population wintering in towns in this part of Pahang State in Peninsular Malaysia (Wells, 2007).

Variability in the degree of sexual dimorphism among bird species is due to differences in their social mating mechanisms (Lande & Arnold, 1985; Owens & Hartley, 1998). Such information could help researchers understand the evolutionary features of a population, such as behavioral adaptation (Kissner et al., 2003; Mansor et al., 2018), gender differential distribution (Cristol et al., 1999), sexual selection (Andersson & Iwasa, 1996), and survival problems linked to unfavorable population dynamics arising from a skewed sex ratio (Donald, 2007; Saino & Møller, 1996). Notably, Barn Swallow sexual dimorphism has previously been measured via many sizes and colour-related characteristics (Kose & Møller, 1999; Perrier, 2002; Safran & McGraw, 2004). One method used to identify the sex of adult swallows involves measuring the length and width of white patches on the five outermost tail feathers (Kose & Møller, 1999). This method also provides a total area estimation of the white patches, resulting in sex identification. Hermosell et al. (2007) suggested that sex determination can be analyzed by a discriminant analysis that uses three morphometric variables of Barn Swallows: the length of the outermost tail feathers, the length of the inner tail feathers and the length of the keel). Wells (2007) also has previously reported that, among 1150 wintering birds previously handled when netted at this or neighboring winter roosts, during several years, two peaks in wing-length measurement, at 114–115 mm and 110–112 mm, and two peaks in tail length at 90–95 mm and 80–85 mm, “are likely to have

been adult male and adult female modes.” Additionally, various additional characteristics, such as tail streamer length and plumage ornaments of various colors (including colouration on the throat, forehead, and ventral regions), are also important parameters in determining Barn Swallow sex (Taylor et al., 2011; Vortman et al., 2011), however, these have not been observed in most studies. Most ecological studies of *H. rustica* have focused on their breeding grounds, while relatively few studies related to their migratory routes and wintering grounds have been performed. Notably, studies on Barn Swallows in Peninsular Malaysia have primarily focused on their population dynamics (Mansor et al., 2020; Medway, 1973), behavior (Ismail et al., 2020), and diet (Mansor et al., 2020). The degree to which genetic and sexual selection influences remains disputed and no relevant studies have been conducted on the East Asian subspecies in this regard. Hence, the present study aims to provide new insights into the morphological characteristics of the East Asian Barn Swallow to assess the reliability of morphological sex determination during the migration period in non-breeding and stopover areas, particularly in Peninsular Malaysia.

## MATERIALS AND METHODS

### Location of Study Area

The study was conducted in Bentong, Pahang (389835 N, 823163 E), central Peninsular Malaysia (Figure 1). Bentong is located opposite the Titiwangsa Range, approximately 80 km northeast of Kuala Lumpur, the capital of Malaysia. Bentong District is approximately 1831 km<sup>2</sup> and borders the states of Negeri Sembilan and Selangor at its southern and western edges, respectively.



Figure 1. The location of Bentong town is in the central region of Peninsular Malaysia. The black dot indicates the sampling site of the present study

## Sample Collection

Between December 2019 and February 2020, swallows were captured using a modified scoop net attached to a telescopic pole. The capture sessions were performed in the late evening (from 2200 h onwards) when swallows are said to sleep (based on the behavior of tucking their heads into the feathers of their ventral sides) (Medway, 1973). Parameters such as wing and tail length were measured following Nam et al. (2018), while forehead patch color length was measured following Borrás et al. (2000), and the length of the white patch on the outermost tail feather was measured according to Taylor et al. (2011) (Figure 2). All individuals were kept safely in boxes for release in the morning. We also collected feathers from the tertiary section of their wings to extract deoxyribonucleic acid (DNA) from quill roots for individual sexing and subspecies determination based on the protocols of Griffiths et al. (1998) and Lijtmaer et al. (2012), respectively. A commercial extraction kit (G-spin™ Total DNA Extraction Mini Kit, South Korea) was used to aid the DNA extraction process. The primers used for sex determination were the P2 and P8 primers, which amplified two chromobox-helicase-DNA-binding genes (CHD-W and CHD98 Z) (Griffiths et al., 1998). For subspecies identification, we used the ProgND5F and ProgCBR primers 99 (Dor et al., 2010).



Figure 2. Morphological measurements taken from *H. rustica*: a) bill; b) wings; c) outermost tail feather, T6; d) second outermost tail feather, T5; e) innermost tail feather, T1; f) forehead patch; g) white tail patch

## Statistical Analysis

We checked data distributions for normality using the Shapiro-Wilks test before performing the parametric statistical analyses. The one-sample *t*-test was used to compare the gender differences for each variable, except for two parameters—male wing length and female bill length—that did not fit a normal distribution. Thus, the Mann-Whitney U test was performed. Thereafter, the sexual dimorphism index (SDI) was calculated as  $\text{Log}_{10}(\text{mean male size}) - \text{Log}_{10}(\text{mean female size})$  for each variable (Møller, 1994). The stepwise discriminant function analysis (DFA) chose the best parameters for separating the sexes. The discriminant score of each individual was calculated by a canonical discriminant analysis (Bavoux et al., 2006; Dmitrenok et al., 2007). Jackknife cross-validation methods were used to estimate the proportion of correctly classified individuals based on the quadratic DFA (Dechaume-Moncharmont et al., 2011). All computational analyses were conducted using the JMP Pro 14.0.0 software.

## RESULTS

The molecular sexing method successfully confirmed the subspecies of *H. rustica*. It differentiated male and female individuals by presenting a typical pattern of bands, with females showing two bands and males showing one band. A total of 46 individuals of *H. rustica* (19 females and 27 males) were captured in the study area. Males tend to be consistently larger than females for most measured parameters, except bill size, which did not display any significant differences among genders. The SDI value for tail streamer length (0.2246) was highest, followed by tail fork depth (0.1814) and outermost tail feather length (0.1105). However, the tail streamer length variable was excluded as an optimal predictor for sexing since it has a lower correct classification rate for males and females (Table 1). Outermost tail feather length (T6) and tail fork depth (T6-T1) were selected as the best predictors for determining Barn Swallow sex (Figure 3). When parameters were entered singly at a time into the stepwise DFA, high correct classification rates for the outermost tail feather length (female: 78.95%, male: 96.30%) and tail fork depth (female: 84.21%, male: 92.60%) were observed.

However, when combining both parameters simultaneously, the DFA results showed higher correct classification rates of 89.47% for females and 96.3% for males. The computed discriminant function shows the result:  $D = 0.1182 \cdot \text{outermost tail, T6} - 137.0007 \cdot \text{tail fork depth, T6-T1}$ . Low Wilks' lambda values (outermost tail,  $T6 = 0.4491$ ; tail fork depth,  $138 T6-T1 = 0.4888$ ) indicate that the Wilks' lambda has a great discriminatory ability to separate cases into groups (Table 2). Seven morphological characters can aid in sexing *H. rustica*. However, one of these characters (bill length) was excluded due to an insignificant difference between genders, leaving only six characters. Since female swallows were generally found to have slightly shorter tails (T6, T6-T1, T6-143 T5) when compared to males, these characters were selected as the best predictors for sex determination.

Table 1  
The difference in morphological measurements of *H. rustica* by gender

	Female			Male			t (U) <sup>§</sup>	Sexual dimorphism index (SDI)
	N	Mean ± standard deviation (SD)	Range	N	Mean ± standard deviation (SD)	Range		
Wing	19	106.72 ± 4.2167	96.48 - 116	27	109.87 ± 4.2837	95.97 - 116.82	131.00 <sup>§§</sup>	0.01262
Bill	19	7.75 ± 0.6683	6.64 - 8.94	27	7.55 ± 0.6644	6.13 - 9.00	224.00 <sup>§NS</sup>	-0.01111
Outermost tail (T6)	19	64.55 ± 0.2821	43.32 - 77.67	27	83.25 ± 8.6506	65.83 - 100.03	7.3468 <sup>§§§</sup>	0.110509
Tail streamer	19	19.22 ± 5.7149	7.11 - 28.74	27	32.24 ± 7.7885	16.41 - 49.34	6.1992 <sup>§§§</sup>	0.224644
Tail fork depth (T6-T1)	19	30.97 ± 7.0671	12.75 - 40.62	27	47.02 ± 8.4333	29.21 - 65.42	6.7892 <sup>§§§</sup>	0.181403
Forehead patch	19	5.01 ± 1.4952	2.46 - 7.60	27	6.10 ± 0.7230	4.93 - 7.56	3.3089 <sup>§§</sup>	0.085958
Tail white patch	19	15.13 ± 3.5927	5.67 - 22.36	27	19.20 ± 4.9693	9 - 27.85	3.0361 <sup>§§</sup>	0.102954

Note. \*\*:  $p \leq 0.01$ , \*\*\*:  $p \leq 146 \text{ } 0.001$ . NS: not significant; §: Male wing length in males and female bill length in females did not fit a normal distribution, therefore the test was conducted using the Mann-Whitney U statistic

Table 2  
Two important variables from seven morphological measurements of the *H. rustica* based on stepwise discriminant function analysis

Step	Entered variable	F	p>F	Wilks' lambda	Canonical correlation (CC)	p>CC
1	Outermost tail (T6)	53.97	<0.0001	0.4491	0.7422	<0.0001
2	Tail fork depth (T6-T1)	46.02	<0.0001	0.4888	0.7150	<0.0001

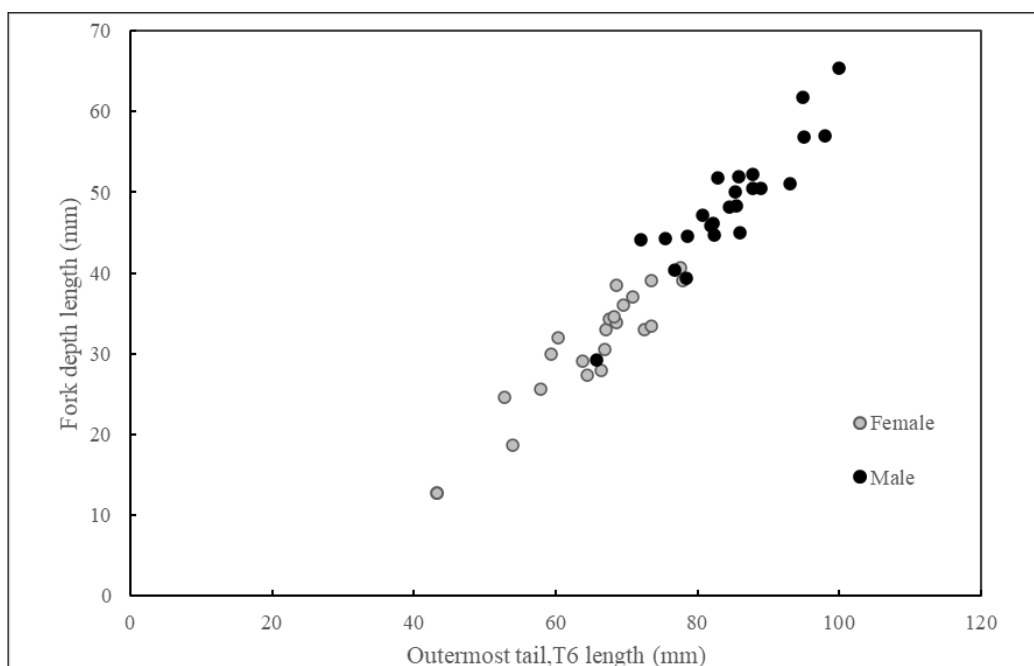


Figure 3. The relationship between tail fork depth length (T6-T1) and outermost tail feather length (T6) for adult male and female Barn Swallows

## DISCUSSION

We found that the rate of correct sex classification in male *H. r. gutturalis* was higher than females, contrary to the trend observed for European Barn Swallow *H. r. rustica* breeding populations (Hermosell et al., 2007). We also found that the tail fork depth (T6-T1) parameter is best paired to the outermost tail feather (T6) for better sex predictors; in contrast, Nam et al. (2018) reported that tail fork depth and tail streamer are better predictors due to their higher F-values, SDI scores, and effect sizes. According to Neuman et al. (2007), males possess more variation in streamer length when compared to females, although some findings reported considerable overlap in this parameter between the sexes (Turner, 2006). Furthermore, Taylor et al. (2011) suggested that swallows cannot be correctly sexed based on tail streamer length alone. Additionally, several other studies combined T6 measurements with other parameters, such as the length of the innermost tail feather and white tail patch length (Hermosell et al., 2007; Taylor et al., 2011). Tail morphology evolution might be revealed through the comparative trials of *H. r. gutturalis*, which possess shorter tail feathers than *H. r. rustica* (Romano et al., 2017; Scordato & Safran, 2014). Several reports of *H. r. rustica* populations have identified the white tail patch as a sexual accessory that functions as a handicap rather than a signal enhancement (Kose et al., 1999; Kose & Møller, 1999); however, with shorter tail feathers than other

subspecies, no significant reproductive benefits were identified in correlational datasets for *H. rustica* (Hasegawa et al., 2010; Hasegawa & Arai, 2013). While the present study revealed that white tail patch length can be used as a criterion for sex determination, it has a lower power of discrimination than T6-T1 and T6.

Moreover, the white tail patch measurement may not be necessary for fieldwork since the measurement of fork depth (T6-T1) alone also predicted sex at a similar level of accuracy. However, Taylor et al. (2011) suggested that white patches should be measured wherever possible since the patch is an easily measurable and meaningful supporting parameter for sex determination and can be measured even in severe cases involving abraded or damaged tails. On the other hand, Taylor et al. (2011) suggested that wing length was the most useful variable for discriminating sex and subspecies. However, according to Nam et al. (2018), wing length shows considerable overlap between the sexes. This indicates that the East Asian population's wing length is not recommended for sex determination in the field. According to Hasegawa and Arai (2013), in Japanese Barn Swallows populations, the length of dark-red plumage patches on the throat is also known as a sexually selected trait. Unfortunately, the present study did not take this into account due to its low discriminant power and some failures in measurement repeatability.

## CONCLUSION

We revealed that external morphometrics seems to be a successful tool for sex determination in *H. rustica*. Moreover, using external morphometries to classify birds is less costly and invasive than gathering laparotomy and blood samples (Montalti et al., 2012). The morphometric approach may also provide valuable knowledge for taxonomic, biological, behavioral, physiological, and evolutionary studies (Mansor & Ramli, 2017). Additionally, DFA proved to be effective for sexing the Barn Swallow and other bird species, such as the Black-crowned night heron (*Nycticorax nycticorax*; Piro et al., 2018) and Chilean flamingo (*Phoenicopterus chilensis*; Montalti et al., 2012). Furthermore, using DFA also proved sufficient for live birds (Montalti et al., 2012). Therefore, the present work could be useful for sexing other bird species. To fully understand the vital role of DFA in sexual dimorphism, sex determination, and its implications on sexually selected traits, future studies on the color and size of plumage—including that of the throat and forehead—are required.

## ACKNOWLEDGMENTS

This work was supported by Universiti Kebangsaan Malaysia Research Fund [GUP-2018-019]. We thank the Department of Wildlife and National Parks for permission to conduct this research.



## REFERENCES

- Andersson, M., & Iwasa, Y. (1996). Sexual selection. *Trends in Ecology and Evolution*, *11*(2), 53-58. [https://doi.org/10.1016/0169-5347\(96\)81042-1](https://doi.org/10.1016/0169-5347(96)81042-1)
- Bavoux, C., Burneleau, G., & Bretagnolle, V. (2006). Gender determination in the Western Marsh Harrier (*Circus aeruginosus*) using morphometrics and discriminant analysis. *Journal of Raptor Research*, *40*(1), 57–64. <https://doi.org/10.3356/0892-1016>
- Borras, A., Pascual, J., & Senar, J. C. (2000). What do different bill measures measure and what is the best method to use in granivorous birds? *Journal of Field Ornithology*, *71*(4), 606–611. <https://doi.org/10.1648/0273-8570-71.4.606>
- Cristol, D. A., Baker, M. B., & Carbone, C. (1999). Differential migration revisited. In V. Nolan, E. D. Ketterson & C. F. Thompson (Eds.), *Current ornithology* (pp. 33-88). Springer Nature. [https://doi.org/10.1007/978-1-4757-4901-4\\_2](https://doi.org/10.1007/978-1-4757-4901-4_2)
- David, R. W. *The birds of the Thai-Malay Peninsula: Passerines*. Helms. <https://www.nhbs.com/the-birds-of-the-thai-malay-peninsula-volume-2-book>
- Dechaume-Moncharmont, F. X., Monceau, K., & Cezilly, F. (2011). Sexing birds using discriminant function analysis: A critical appraisal. *Auk*, *128*(1), 78–86. <https://doi.org/10.1525/auk.2011.10129>
- Dmitrenok, M., Puglisi, L., Demongin, L., Gilbert, G., Polak, M., & Bretagnolle, V. (2007). Geographical variation, sex and age in Great Bittern *Botaurus stellaris* using coloration and morphometrics. *Ibis*, *149*(1), 37–44. <https://doi.org/10.1111/j.1474-919X.2006.00592.x>
- Donald, P. F. (2007). Adult sex ratios in wild bird populations. *Ibis*, *149*(4), 671–692. <https://doi.org/10.1111/J.1474-919X.2007.00724.X>
- Dor, R., Safran, R. J., Sheldon, F. H., Winkler, D. W., & Lovette, I. J. (2010). Molecular phylogenetics and evolution phylogeny of the genus *Hirundo* and the Barn Swallow subspecies complex. *Molecular Phylogenetics and Evolution*, *56*(1), 409–418. <https://doi.org/10.1016/j.ympev.2010.02.008>
- Griffiths, R., Double, M. C., Orr, K., & Dawson, R. J. G. (1998). A DNA test to sex most birds. *Molecular Ecology*, *7*(8), 1071–1075. <https://doi.org/10.1046/j.1365-294x.1998.00389.x>
- Hasegawa, M., & Arai, E. (2013). Divergent tail and throat ornamentation in the barn swallow across the Japanese islands. *Journal of Ethology*, *31*(1), 79–83. <https://doi.org/10.1007/s10164-012-0352-y>
- Hasegawa, M., Arai, E., Watanabe, M., & Nakamura, M. (2010). Mating advantage of multiple male ornaments in the Barn Swallow *Hirundo rustica gutturalis*. *Ornithological Science*, *9*(2), 141–148. <https://doi.org/10.2326/osj.9.141>
- Hermosell, I. G., Balbontín, J., Marzal, A., Reviriego, M., & De Lope, F. (2007). Sex determination in barn swallows *Hirundo rustica* by means of discriminant analysis in two European populations. *Ardeola*, *54*(1), 93–100.
- Ismail, N. A., Al Jufri, A. B. A. K., Daud, U. N. S., Nor, S. M., & Mansor, M. S. (2020). Short communication: Roosting behavior of wintering Barn Swallow (*Hirundo rustica*) in peninsular Malaysia. *Biodiversitas*, *21*(2), 661–665. <https://doi.org/10.13057/BIODIV/D210231>

- Kissner, K. J., Weatherhead, P. J., & Francis, C. M. (2003). Sexual size dimorphism and timing of spring migration in birds. *Journal of Evolutionary Biology*, 16(1), 154–162. <https://doi.org/10.1046/J.1420-9101.2003.00479.X>
- Kose, M., Mänd, R., & Møller, A. P. (1999). Sexual selection for white tail spots in the barn swallow in relation to habitat choice by feather lice. *Animal Behaviour*, 58(6), 1201–1205. <https://doi.org/10.1006/anbe.1999.1249>
- Kose, M., & Møller, A. P. (1999). Sexual selection, feather breakage and parasites: The importance of white spots in the tail of the barn swallow (*Hirundo rustica*). *Behavioral Ecology and Sociobiology*, 45(6), 430–436. <https://doi.org/10.1007/s002650050581>
- Lande, R., & Arnold, S. J. (1985). Evolution of mating preference and sexual dimorphism. *Journal of Theoretical Biology*, 117(4), 651–664. [https://doi.org/10.1016/S0022-5193\(85\)80245-9](https://doi.org/10.1016/S0022-5193(85)80245-9)
- Lijtmaer, D. A., Kerr, K. C. R., Stoeckle, M. Y., & Tubaro, P. L. (2012). DNA barcoding birds: From field collection to data analysis. In W. Kress & D. Erickson (Eds.), *Methods in molecular biology* (pp. 127–152). Springer Nature. [https://doi.org/10.1007/978-1-61779-591-6\\_7](https://doi.org/10.1007/978-1-61779-591-6_7)
- Mansor, M. S., Halim, M. R. A., Abdullah, N. A., Ramli, R., & Cranbrook, E. O. (2020). Barn Swallows *Hirundo rustica* in peninsular malaysia: Urban winter roost counts after 50 years, and dietary segregation from house-farmed swiftlets *Aerodramus* sp. *Raffles Bulletin of Zoology*, 68(6), 238–248. <https://doi.org/10.26107/RBZ-2020-0021>
- Mansor, M. S., Md Nor, S., Ramli, R., & Sah, S. A. M. (2018). Niche shift in three foraging insectivorous birds in lowland Malaysian forest patches. *Behavioural Processes*, 157(3), 73–79. <https://doi.org/10.1016/j.beproc.2018.09.001>
- Mansor, M. S., & Ramli, R. (2017). Niche separation in flycatcher-like species in the lowland rainforests of Malaysia. *Behavioural Processes*, 140(4), 121–126. <https://doi.org/10.1016/j.beproc.2017.04.010>
- Medway, L. (1973). A ringing study of migratory barn swallows in West Malaysia. *Ibis*, 115(1), 60–86. <https://doi.org/10.1111/J.1474-919X.1973.TB02624.X>
- Møller, A. P. (1994). Phenotype-dependent arrival time and its consequences in a migratory bird. *Behavioral Ecology and Sociobiology*, 35(2), 115–122. <https://doi.org/10.1007/BF00171501>
- Montalti, D., Graña, G. M., Maragliano, R. E., & Cassini, G. (2012). The reliability of morphometric discriminant functions in determining the sex of Chilean flamingos *Phoenicopterus chilensis*. *Current Zoology*, 58(6), 851–855. <https://doi.org/10.1093/czoolo/58.6.851>
- Nam, H., Lee, S., Cho, S., Choi, C., Park, S., Bing, G., Park, C., Seo, S., & Kim, Y. (2018). Effectiveness of morphological sex determination in the East Asian barn swallow (*Hirundo rustica gutturalis*) on spring migration. *Zoological Studies*, 57, e43. <https://doi.org/10.6620/ZS.2018.57-43>
- Neuman, C. R., Safran, R. J., & Lovette, I. J. (2007). Male tail streamer length does not predict apparent or genetic reproductive success in North American barn swallows *Hirundo rustica erythrogaster*. *Journal of Avian Biology*, 38(1), 28–36. <https://doi.org/10.1111/J.2007.0908-8857.03713.X>
- Owens, I. P. F., & Hartley, I. R. (1998). Sexual dimorphism in birds: Why are there so many different forms of dimorphism? *Proceedings of the Royal Society B: Biological Sciences*, 265(1394), 397–407. <https://doi.org/10.1098/rspb.1998.0308>

- Perrier, C. (2002). Structural coloration and sexual selection in the Barn Swallow *Hirundo rustica*. *Behavioral Ecology*, 13(6), 728–736. <https://doi.org/10.1093/beheco/13.6.728>
- Piro, A., Fuchs, D. V., & Montalti, D. (2018). Morphometric differences between sexes of two subspecies of Black-crowned Night-Heron (*Nycticorax nycticorax*) using discriminant function analysis. *Waterbirds*, 41(1), 87–92. <https://doi.org/10.1675/063.041.0112>
- Romano, A., Costanzo, A., Rubolini, D., Saino, N., & Møller, A. P. (2017). Geographical and seasonal variation in the intensity of sexual selection in the Barn Swallow *Hirundo rustica*: A meta-analysis. *Biological Reviews*, 92(3), 1582–1600. <https://doi.org/10.1111/brv.12297>
- Safran, R. J., & McGraw, K. J. (2004). Plumage coloration, not length or symmetry of tail-streamers, is a sexually selected trait in North American Barn Swallows. *Behavioral Ecology*, 15(3), 455–461. <https://doi.org/10.1093/beheco/15.3.455>
- Saino, N., & Møller, A. P. (1996). Sexual ornamentation and immunocompetence in the Barn Swallow. *Behavioral Ecology*, 7(2), 227–232. <https://doi.org/10.1093/beheco/7.2.227>
- Scordato, E. S. C., & Safran, R. J. (2014). Geographic variation in sexual selection and implications for speciation in the Barn Swallow. *Avian Research*, 5(8), 1–13. <https://doi.org/10.1186/s40657-014-0008-4>
- Taylor, P., Duijns, S., Dijk, J. G. B. Van, K. R. H. S., & Mateman, A. C. (2011). An additional field method to sex adult barn swallows during the non-breeding season in Zambia: White spot length in the outer tail feather. *Ostrich: Journal of African Ornithology*, 82(9), 37–41. <https://doi.org/10.2989/00306525.2011.603467>
- Turner, A. K. (2006). *The barn swallow*. T. & A. D. Poyser. [https://books.google.com/books/about/The\\_Barn\\_Swallow.html?id=jsxXFkHXKXAC](https://books.google.com/books/about/The_Barn_Swallow.html?id=jsxXFkHXKXAC)
- Vortman, Y., Lotem, A., Dor, R., Lovette, I. J., & Safran, R. J. (2011). The sexual signals of the East-Mediterranean barn swallow: A different swallow tale. *Behavioral Ecology*, 22(6), 1344–1352. <https://doi.org/10.1093/beheco/arr139>



# A Comprehensive Method to Generating and Identifying Transgenic Tobacco Lines with a Single Transgene Integration Locus for Functional Analysis

Mohamad Shafek Hilman<sup>1</sup>, Omar Nawawi<sup>1</sup>, Mohd Farhan Azhari<sup>1</sup>, Tianqi Bai<sup>2</sup>, Cuixian Zhang<sup>2</sup>, Mohd Puad Abdullah<sup>3</sup>, Mat Yunus Abdul Masani<sup>4</sup> and Chong Yu Lok Yusuf<sup>1,2\*</sup>

<sup>1</sup>Laboratory of Plant Genetic and Cell Biology, Faculty of Plantation and Agrotechnology, Universiti Teknologi MARA, Jasin Campus, 77300 Merlimau, Melaka, Malaysia

<sup>2</sup>Institute of Tropical and Subtropical Cash Crops, Yunnan Academy of Agricultural Sciences, Baoshan 675800, China

<sup>3</sup>Department of Cell and Molecular Biology, Faculty of Biotechnology and Biomolecular Sciences, Universiti Putra Malaysia, 43400 UPM, Serdang, Selangor, Malaysia

<sup>4</sup>Malaysian Palm Oil Board (MPOB), No. 6, Persiaran Institusi, Bandar Baru Bangi, 43000 Kajang, Selangor, Malaysia

## ABSTRACT

Tobacco is a popular model plant used for studying gene function. The generation of transgenic tobacco is tremendously essential in functional genomics. The generated transgenic plants must undergo careful selection and analysis before being used. However, most published protocols for generating transgenic tobacco for functional genomics are not comprehensive and involve sophisticated equipment. This study demonstrates an efficient and comprehensive method for developing and selecting transgenic tobacco lines without involving sophisticated equipment. Transgene was delivered into the genome of a tobacco plant via *Agrobacterium tumefaciens*.

Polymerase Chain Reaction (PCR) was performed to verify the integration of transgenes in the putative primary transformants. Reverse Transcription-Polymerase Chain Reaction (RT-PCR) examined transgene expressions. The number of transgene integration loci (TIL) was determined by transgene segregation analysis. PCR results revealed that  $\approx 97\%$  of the primary transformants were positive. The transgene was highly expressed in the transgenic plants. Segregation analysis showed that 47.6%–66.7% of the transgenic plants contained a single TIL, and the T1 and T2 progenies inherited the transgene. Homozygous transgenic lines with

## ARTICLE INFO

### Article history:

Received: 02 April 2024

Accepted: 23 July 2024

Published: 28 January 2025

DOI: <https://doi.org/10.47836/pjtas.48.1.03>

### E-mail addresses:

shafekhilmman676@gmail.com (Mohamad Shafek Hilman)

nawawiomar97@gmail.com (Omar Nawawi)

farhanazhari13@yahoo.com (Mohd Farhan Azhari)

tianqib@163.com (Tianqi Bai)

zhangcuixian1570@126.com (Cuixian Zhang)

puad@upm.edu.my (Mohd Puad Abdullah)

masani@mpob.gov.my (Mat Yunus Abdul Masani)

yusufchong@uitm.edu.my (Chong Yu Lok Yusuf)

\* Corresponding author

a single TIL were successfully developed by using our method. This manuscript encompasses detailed guidance on genetic transformation, molecular analysis, seed production, and transgene segregation analysis. It serves as a guideline for the researchers to produce transgenic tobacco lines that can be used for functional analysis. The procedures described here can be conducted in standard laboratories as they require no high-end equipment. This comprehensive and efficient method for generating transgenic tobacco will foster functional genomics.

*Keywords:* *Agrobacterium*, functional analysis, transgene integration locus, transgenic tobacco

---

## INTRODUCTION

Plant genome databases provide tremendous sequence information for genetic study and plant breeding programs. Many plants of economic importance have their genomes completely sequenced (Guo et al., 2021; Robbins et al., 2023; Wang et al., 2023). A genome consists of genes encoding specific proteins and the intergenic regions (promoter and terminator) regulating gene expression. Without functionally characterizing individual genes in the genome, the genome sequence alone has little impact on any breeding program. Functional characterization aims to disclose the functions of particular genes by studying the coding sequences and their regulatory regions. Such a study often involves transgenic analysis in model plants. Having a plant genome database in which the individual genes are well-characterized would facilitate the breeding program for that plant.

Although *in silico* analyses, including phylogenetic analysis and protein modeling, have been used to predict gene function, further functional analysis is still necessary to elucidate the gene function accurately (Hu et al., 2023; Kiyak & Mutlu, 2023; Liu et al., 2020). Generally, a functional analysis could be performed through a gain- or loss-of-function approach. In the gain-of-function approach, a gene-of-interest (GOI) is overexpressed, whereas in the loss-of-function approach, a GOI is repressed. The consequences of this overexpression or repression are evaluated in the host plant. Heterologous expression of a GOI in model plants such as *Arabidopsis* or tobacco plants has been the most popular approach to functional gene analysis (Kim & Huh, 2019; Wang et al., 2021; Yao et al., 2020). This approach is frequently employed on genes from plant species that show poor *in vitro* regeneration capacity or when an efficient transformation method has not been established. Generating stable transformants allows detailed analysis and characterization of the transgenic plants, providing a better understanding of the transgene's role.

When generating a transgenic plant, the expression level of transgene is one of the major concerns. Transgene silencing associated with integrating transgene at multiple loci has been reported by Rajeevkumar et al. (2015). Previous studies showed that the particle bombardment method always results in transgenic plants carrying a high copy number of transgenes compared to the *Agrobacterium*-mediated method (Hwang et al., 2017; Jackson et al., 2013). Apart from that, a varying extent of genome damage was reported in the

transgenic rice and maize plants transformed by the particle bombardment method (Liu et al., 2019). Even though recent studies showed that transgenic lines with a low copy number of transgenes could be generated via the particle bombardment method by reducing the quantity of Deoxyribonucleic Acid (DNA) used during DNA/gold coating (Ismagul et al., 2018; Jackson et al., 2013), the *Agrobacterium*-mediated transformation method remains preferable due to its simplicity and affordability. As a result, the *Agrobacterium*-mediated transformation method has become the most popular method of plant genetic transformation since it was introduced in the 1980s (Fraley et al., 1983).

Tobacco (*Nicotiana tabacum*) is one of the popular model plants used in functional genomics due to its desirable transformation and regeneration efficiency (Niedbala et al., 2021). Compared with *Arabidopsis thaliana*, tobacco has a real stem and produces a more significant amount of plant biomass for experimental purposes. Owing to its showy and conspicuous flowers, the introduction of a transgene(s) from one transgenic line to another through cross-pollination can be efficiently conducted in tobacco (Zhang et al., 2020). It is also worth noting that the tobacco plant is self-fertile and generates many seeds after flowering, enabling the development of a homozygote line for comprehensive genetic analyses (Lewis et al., 2020; Schmidt et al., 2020). Apart from producing stable transformants, tobacco is also a popular choice of host plant for transient expression analysis through agroinfiltration (Duxbury et al., 2020; Shokouhifar et al., 2019). Due to its fascinating characteristics, tobacco has been used to study the genes from dicot and monocot species (Alexander et al., 2021; Boyidi et al., 2021; Fan et al., 2021; Wang et al., 2021).

Generating transgenic tobacco plants for functional analysis is a lengthy and complicated procedure. It encompasses the *in vitro* regeneration of transformants from the transformed cells and molecular analyses to verify the integration and functionality of transgene in the transgenic lines generated. In most cases, individual transgenic lines with a single transgene integration locus (TIL) are preferable for functional analysis to avoid a transgene silencing phenomenon caused by the insertion of transgenes at multiple loci (Rajeevkumar et al., 2015; Tang et al., 2007). The selection of transgenic lines that fulfill the criteria for functional analysis is time-consuming as it always involves the study of transgene inheritance in several generations. In certain studies, homozygous transgenic lines were generated for experimental purposes to offset the effects caused by the genetic variability within a heterogeneous population (Aleem et al., 2022; Dutta et al., 2023; Xie et al., 2024). Therefore, the researchers engaging in transgenic study need a detailed and comprehensive method for generating and identifying transgenic tobacco lines that comply with the requirements of functional analysis. Our method describes the complete procedures for the *Agrobacterium*-mediated transformation of tobacco plants and the steps involved in generating and identifying transgenic plants, fulfilling the criteria for functional analysis.

## METHODS

To demonstrate the practicality of this method in generating transgenic tobacco plants with a single TIL, two GOI, namely *EgCAD1* reported by Yusuf et al. (2022) and  $\beta$ -glucuronidase (GUS), were used. The steps involved in the method are outlined in Figure 1.

### Section 1: Construction of Transformation Vector

A PCR mixture to amplify the GOI using high-fidelity DNA polymerase was prepared on ice. A total of 10  $\mu$ L of 5X Q5 reaction buffer, 1  $\mu$ L of 10 mM dNTPs, 2.5  $\mu$ L of 10  $\mu$ M forward primer, 2.5  $\mu$ L of 10  $\mu$ M reverse primer, 1  $\mu$ L of template DNA (10 ng/ $\mu$ L plasmid containing the GOI), 0.5  $\mu$ L of Q5 High-Fidelity DNA Polymerase (NEB, USA) and 32.5  $\mu$ L of water were added into a 0.2 ml thin-wall PCR tube. In this study, the *EgCAD1* gene was amplified using CAD1-F (5'-CAC CAT GGC TGG TGC CGG ATC-3') and CAD1-R (5'-TCA GAG TTT GCT GCG AGC CAC A-3') primers. While the GUS gene was amplified using GUS-F (5'-CAC CAT GTT ACG TCC TGT AGA AAC CCC AA-3') and GUS-R (5'-TCA TTG TTT GCC TCC CTG CTG CGG T-3') primers. The PCR was performed using the following thermocycling profile: to 98°C (30 s), 98°C (10 s), and 72°C (1 min) for 30 cycles; 72°C (2 min). Per the manufacturer's instructions, the PCR product was purified using the Monarch® DNA Gel Extraction Kit (NEB, USA). The transformation vectors were developed using the Gateway cloning method described by Yusuf, Abdullah, et al. (2018).

Firstly, to generate the entry clones, the gel-purified PCR products were cloned into the pENTR/D-TOPO vector using the pENTR™ Directional TOPO® Cloning Kits (Life Technologies, USA) according to the manufacturer's instructions. To transfer the GOI from the entry clone to a destination vector (pMDC32), LR recombination was performed using LR Clonase™ II enzyme mix (Life Technologies, USA). The

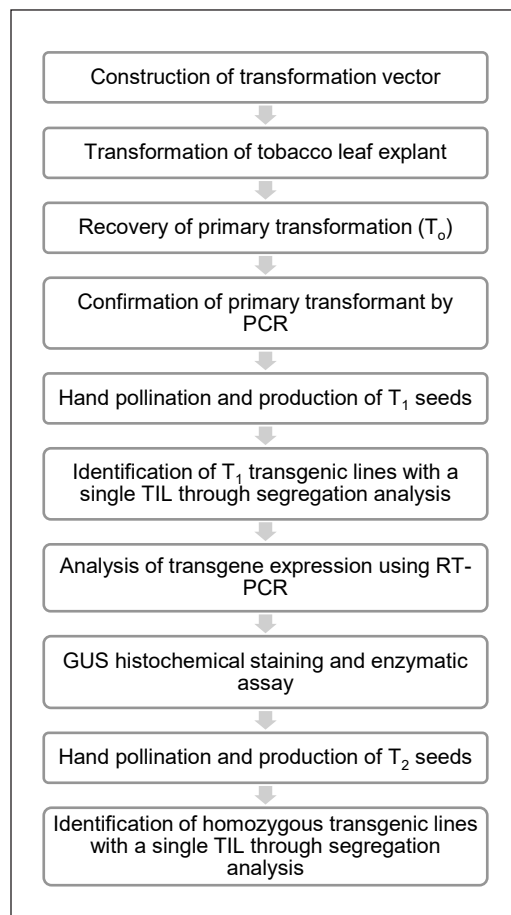


Figure 1. Flow chart outlining the procedures involved in generating and identifying transgenic tobacco lines with a single transgene integration locus



expression cassettes developed in this study are illustrated in Supplementary Figure 1. The sequence of the insert DNA was verified by sequencing.

**Important Note.** To ensure error-free amplification of GOI, high-fidelity DNA polymerase is highly recommended.

## Section 2: Transformation of *Agrobacterium* Through the Electroporation Method

The electrocompetent cells of *A. tumefaciens* Strain LBA4404 were thawed on ice for about 5 min. Approximately 50 ng of plasmid DNA was added into 100  $\mu$ L of the competent cells and mixed by gently tapping the tube. The mixture (competent cells and DNA) was transferred to a pre-cooled electroporation cuvette (gap width: 1 mm), and the electroporation was performed at 2400 V using Electroporator 2510 (Eppendorf, Germany). One milliliter of Luria-Bertani (LB) broth (Miller) was immediately added to the cuvette after the pulse, and the *Agrobacterium* cell suspension was transferred to a 15 ml Falcon tube. The *Agrobacterium* cell suspension was agitated at 250 rpm in an incubator shaker at 28°C under dark conditions for 2 h. Then, 200  $\mu$ L of the *Agrobacterium* cell suspension was spread on an LB agar (1.5% w/v) plate (90 mm  $\times$  15 mm disposable Petri dish) supplemented with 50  $\mu$ g/ml kanamycin, 25  $\mu$ g/ml rifampicin, and 100  $\mu$ g/ml streptomycin. The plate was incubated at 28°C under dark conditions for three days. A single colony was picked using a toothpick and transferred to a 50 ml Falcon tube containing 5 ml of LB broth with the above antibiotics. The bacterial culture was incubated at 28°C overnight under dark conditions using an incubator shaker run at 250 rpm. The next day, 500  $\mu$ L of the bacterial culture was transferred to a 1.5 ml microcentrifuge tube, and the same volume of glycerol was added to prepare a glycerol stock. The glycerol stock was stored at -80 °C.

**Important Note.** *Agrobacterium* strains, such as AGL1 and GV3101, may be used for tobacco transformation. However, our studies have shown that LBA4404 showed satisfactory results. Furthermore, Niedbala et al. (2021) reported that LBA4404 produced the highest transformation efficiency in tobacco plants. Apart from the electroporation method, plasmid DNA also can be introduced into *Agrobacterium* cells through the freeze-thaw method. However, a reduced transformation efficiency will be obtained, and the method requires liquid nitrogen.

## Section 3: Preparation of Plant Materials

About 20–30 tobacco (*Nicotiana tabacum* cv. SR1) seeds were transferred into a 1.5 ml microcentrifuge tube and soaked with distilled water for 2 h. The seeds floating on the water surface were removed, and the water was carefully decanted. Seed surface sterilization was performed in a laminar airflow; 1 ml of 0.5% (v/v) sodium hypochlorite solution was added to the seeds and mixed well by inverting the tube for 10 min. The sodium hypochlorite

solution was decanted carefully. The seeds were rinsed with 1 ml of sterile distilled water for 1 min. The sterile distilled water was decanted, and the washing step was repeated twice. Using a 1 ml pipette tip, about 20–25 sterilized seeds were transferred and distributed evenly on a germination medium. The Petri dish was sealed with a parafilm strip and kept at 4°C under dark conditions for three days. Then, the Petri dish containing the tobacco seeds was moved to a growth chamber, and the seedlings were allowed to grow at 25°C under 16 h light/8 h dark conditions for four weeks.

**Important Note.** All solid tissue culture media were prepared using a 90 mm × 15 mm disposable Petri dish unless specified otherwise. The composition of the culture media used in this protocol is listed in Supplementary Table 1. Incubating the surface-sterilized tobacco seeds at 4°C for three days is optional. However, performing this step would allow uniform germination of the tobacco seeds.

#### Section 4: Preparation of Bacterial Cultures

An inoculating loop was used to streak the glycerol stock of *Agrobacterium* cells carrying the desired construct on an LB agar supplemented with 50 µg/ml kanamycin, 25 µg/ml rifampicin, and 100 µg/ml streptomycin four days before plant transformation. A single colony was picked using a toothpick and transferred into a 100 ml conical flask containing 10 ml of LB broth with antibiotics specified above. The bacterial culture grew at 28°C overnight under dark conditions in an incubator shaker at an agitation speed of 250 rpm. The next day, 5 ml of the overnight bacterial culture was transferred to a 500 ml conical flask containing 50 ml LB broth supplemented with the same antibiotics.

**Important Note.** The volume of bacterial culture can be upscaled or downscaled, depending on the number of leaf discs to be transformed. However, the value of OD<sub>600</sub> should be maintained between 0.8 and 1.0, as this is the optimum concentration of *Agrobacterium* to achieve a high transformation efficiency.

#### Section 5: Plant Transformation and Establishment of Transgenic Plant

In a laminar airflow, the leaves of four-week-old tobacco plants prepared in Section 3 were punched with a sterile paper puncher or cork borer to produce leaf discs of 0.6 cm in diameter. About 50 leaf discs were collected in a 90 mm × 15 mm disposable Petri dish containing a piece of sterile filter paper moistened with 1 ml of sterile distilled water. Subsequently, the inoculation medium prepared earlier was poured into the Petri dish, and the leaf discs were soaked for 30 min with gentle shaking every 3 min. The inoculation medium was drained off, and the leaf discs were blot-dried on sterile tissue paper before being placed on a co-cultivation medium with the abaxial side facing upward. The co-cultivation was performed at 28°C for one to two days under dark conditions. The growth of *Agrobacterium* was observed during this period. The co-cultivation time may vary with

the *Agrobacterium* strain used. The leaf discs were transferred to a regeneration medium 1 when the growth of *Agrobacterium* at the edge of the leaf discs was visible. The leaf discs were subcultured to a fresh regeneration medium once every two weeks or once the *Agrobacterium*'s growth was visible. After one month of culturing on regeneration medium 1 (when the adventitious shoots were about 0.3–0.5 cm in height and forming a multiple shoot cluster), multiple shoot clusters were transferred to regeneration medium 2 for shoot elongation. When the regenerated shoots were about 1–1.5 cm in height, only one shoot from each multiple-shoot cluster was excised and transferred to a rooting medium. The plantlets were acclimatized when the roots were about 1–2 cm.

**Important Note.** All the tissue culture steps described in this section should be performed under sterile conditions in a laminar airflow. The composition of the culture media used in this method is listed in Supplementary Table 1. A co-cultivation period longer than two days should be avoided, as this will result in the overgrowth of *Agrobacterium* and pose a problem in eliminating it during shoot regeneration.

### Section 6: Acclimatization of Transgenic Plantlet

The plantlets from the culture jar were carefully removed, and the roots were washed with tap water to remove the culture medium. The plantlets were transferred to a 16 oz disposable plastic cup filled with a potting mix for gardening purposes, and each plantlet was immediately covered with another plastic cup to create and maintain high air humidity. The plantlets were cultivated in a growth room at 24°C under a 16 h photoperiod. After two weeks (when the leaf and root development was noticeable), the cover (plastic cup) was slightly opened to reduce the air humidity. Then, gradually increase the opening day by day to allow a gradual reduction of air humidity. Finally, the cover was removed after one week when no wilting was observed.

**Important Note.** Ensure the culture medium is completely removed from the roots. Nutrients and sugar in the tissue culture medium will encourage the growth of bacteria and fungi in the soil, killing the plantlets. The young roots are very vulnerable; avoid breaking them when washing them. A sudden or too early cover removal will cause the plantlets to wilt and die. Plantlet acclimatization is recommended in a disposable plastic cup, as the transparent plastic material will allow root growth to be observed easily.

### Section 7: Verification of Transgenic Plant

About 100 mg of leaf tissues from a putative transgenic plant were collected in a 1.5 ml microcentrifuge tube. The tube and a disposable pestle were dipped in liquid nitrogen for 10 s, and the sample was immediately ground into a fine powder using the pre-cooled disposable pestle. According to the manufacturer's protocol, the sample's genomic DNA (gDNA) was extracted using the GF-1 Plant DNA Extraction Kit (Vivantis, Malaysia).

The gDNA sample was quantified using an ultraviolet (UV) spectrophotometer (Thermo Scientific, USA) to obtain the A<sub>260</sub>, A<sub>280</sub>, and A<sub>230</sub> values. A DNA sample with A<sub>260</sub>/A<sub>280</sub> and A<sub>260</sub>/A<sub>230</sub> ratios  $\geq 1.8$  is considered pure. A PCR mixture (20  $\mu$ L final volume) was set up for each transgenic line tube to detect the transgene (*EgCAD1* or GUS in this case) by adding 2  $\mu$ L of 10X DreamTaq Green Buffer, 2  $\mu$ L of 2 mM dNTPs, 1  $\mu$ L of 10  $\mu$ M forward primer and 1  $\mu$ L of 10  $\mu$ M reverse primer, 1  $\mu$ L of gDNA (50 ng/ $\mu$ L), 0.1  $\mu$ L of DreamTaq Green DNA Polymerase (Thermo Scientific, USA) and 12.9  $\mu$ L H<sub>2</sub>O into a 0.2 ml thin-wall PCR. The primer pairs used to develop the transformation constructs (refer to Section 1) were utilized to verify the transgenic plants. The PCR mixture was set up on ice, and a positive control reaction was set up in parallel. Plasmid DNA (the transformation vectors developed in Section 1) was used as a template for the positive control reaction. The PCR was performed using the following thermocycling profile: 3 min at 95°C (1 cycle); 30 s at 95°C, 30 s at 63°C (for *EgCAD1*) or 66°C (for GUS), 30 s at 72°C (35 cycles); 5 min at 72°C (1 cycle). The PCR products (5  $\mu$ L) were analyzed on a 1.2% Tris-acetate-EDTA (TAE) agarose gel. DNA ladder was loaded next to the samples. The agarose gel was viewed using a gel documentation system or UV transilluminator when the gel electrophoresis was completed.

**Important Note.** To ensure that the transformants are not carrying a truncated GOI, PCR primers that amplify the entire sequence of GOI (instead of a partial sequence) were used to verify the transgenic plants. If a detailed gel electrophoresis protocol is required, please refer to Lee et al. (2012).

## Section 8: Seed Production

The PCR-positive transgenic plants (T<sub>0</sub> generation) were cultivated in a growth room at 24°C under a 16 h photoperiod until the plants bloom. The plants were watered daily, and one teaspoon of fertilizer rich in phosphorus and potassium was applied to each plant every three weeks (fertilizer with an N:P:K ratio of 8:16:24 or similar will do). Flower buds were bagged with a pollination bag when they were about to bloom. The pollination bag was removed on the second day after blooming, and the flowers were self-pollinated by transferring pollen to the stigma using a cotton bud to maximize the number of seeds produced. After hand-pollination, the flowers were bagged again to prevent cross-pollination. The pollination bag was removed when seed pod development was noticeable. The seeds were harvested when the seed pods turned brown. The seeds were kept in a 1.5 ml microcentrifuge tube and stored in a chiller until used for transgene segregation analysis.

**Important Note.** Seeds can be produced in tobacco plants without hand-pollination. However, fewer seeds will be obtained due to the absence of pollinating agents. The best time to perform hand pollination is the second day after blooming, as all anthers have dehisced at this time.

## Section 9: Analysis of the Number of Transgene Integration Loci

The number of TIL of a transgenic line was determined by analyzing the transgene inheritance pattern. According to Mendel's law of inheritance, transformants harboring one, two, and three TIL are expected to have their transgenes segregated in their progenies with a segregation ratio (transgenic:non-transgenic) of 3:1, 15:1, and 63:1, respectively (Tizaoui & Kchouk, 2012). Segregation of hygromycin resistance genes among individuals was analyzed in the T<sub>1</sub> generation. Approximately 120 seeds (T<sub>1</sub> generation) collected from a transgenic line were prepared in a 1.5 ml microcentrifuge tube. Surface sterilization was performed as described in Section 3, and the seeds were evenly distributed on a screening medium containing 50 mg/L hygromycin. The Petri dish was stored in a 4°C chiller under dark conditions for three days and then moved to a growth chamber at 25°C under a 16 h light photoperiod for the seeds to germinate. The Petri dish was kept under dark conditions for two days after seed germination and then returned to normal growth conditions. The numbers of hygromycin-resistant (hyg<sup>r</sup>) and hygromycin-sensitive (hyg<sup>s</sup>) seedlings were determined based on hypocotyl length. A seedling with a longer hypocotyl was regarded as hygromycin-resistant (hyg<sup>r</sup>), while a seedling with a shorter hypocotyl was regarded as hygromycin-sensitive (hyg<sup>s</sup>). The data obtained was analyzed with the Chi-square ( $\chi^2$ ) test using the formula as follows:

$$\chi^2 = \frac{(\text{observed } \text{hyg}^r - \text{expected } \text{hyg}^r)^2}{\text{expected } \text{hyg}^r} + \frac{(\text{observed } \text{hyg}^s - \text{expected } \text{hyg}^s)^2}{\text{expected } \text{hyg}^s}$$

The transgenic lines were hypothesized to have a Mendelian segregation ratio of 3:1, 15:1, or 63:1 (hyg<sup>r</sup>:hyg<sup>s</sup>), and the hypothesis was accepted when the value of  $\chi^2 \leq 3.841$ .

**Important Note.** The selective agent may vary with the transformation construct used. Storing the germinating seeds in the dark for two days reduced the time needed to distinguish hyg<sup>r</sup> seedlings from hyg<sup>s</sup> ones based on their phenotypes. The Chi-square analysis can be easily performed using our prepared spreadsheets (<http://surl.li/uhzmm>). The southern blot method can also determine the number of transgene integration loci in a transgenic line. However, special equipment is required and involves lengthy procedures, limiting usage.

## Section 10: Analysis of Transgene Expression

A semi-quantitative RT-PCR was performed to analyze the transgene expression, which was the most economical and easiest method available. In our study, the transgene expression was analyzed in four-week-old CAD1-OE1, CAD1-OE6, CAD1-OE24, GUS-OE1, and GUS-OE3 plants by using the method described by Yusuf, Abu Seman, et al. (2018) with minor modifications. Approximately 100 mg of young leaf sample was collected and homogenized as described in Section 7. According to the manufacturer's instructions, the total RNA from the leaf tissues was extracted using the GF-1 Total RNA Extraction Kit

(Vivantis, Malaysia). The total RNA sample was quantified using a UV spectrophotometer (Thermo Scientific, USA), and the  $A_{260}$ ,  $A_{280}$ , and  $A_{230}$  values were obtained. An RNA sample with  $A_{260}/A_{280}$  and  $A_{260}/A_{230}$  ratios  $\geq 2.0$  is considered a pure RNA sample. Based on the manufacturer's protocol, cDNA was synthesized from 1  $\mu\text{g}$  of total RNA using the Viva cDNA Synthesis Kit (Vivantis, Malaysia). The cDNA was diluted with 40  $\mu\text{L}$  (two volumes) of nuclease-free water, and the diluted cDNA sample was stored at  $-20^\circ\text{C}$ . The PCR mixture was set up as described in Section 7 to amplify the transgene from 1  $\mu\text{L}$  of cDNA sample instead of gDNA. NtEF-F (5'-TCC CCA TCT CTG GTT TTG AAG-3') and NtEF-R (5'-CAG GCT TGA GGA CAC CAG TT-3') primers were used to amplify the *Elongation factor 1- $\alpha$*  (*NtEF-1 $\alpha$* ) gene (accession number: AF120093) which acts as the internal control of gene expression analysis. PCR was performed using the following thermocycling profile: 3 min at  $95^\circ\text{C}$  (1 cycle); 20 s at  $95^\circ\text{C}$ , 25 s at  $63^\circ\text{C}$  (for *EgCAD1*) or  $66^\circ\text{C}$  (for GUS) or  $55^\circ\text{C}$  (for *NtEF-1 $\alpha$* ), 60 s at  $72^\circ\text{C}$  (32 cycles); 5 min at  $72^\circ\text{C}$  (1 cycle). The PCR products were analyzed through gel electrophoresis as described in Section 7.

**Important Note.** DNA-free total RNA samples can be obtained using the GF-1 Total RNA Extraction Kit (Vivantis, Malaysia) as a DNase treatment step included in the protocol. If a conventional method or other RNA extraction kits are used for RNA extraction, an additional DNase treatment step should be conducted to remove contaminating gDNA before cDNA synthesis. If an accurate quantification of transgene expression levels is required, quantitative PCR (real-time PCR) might be used.

### Section 11: GUS Histochemical Staining

The protocol developed by Jefferson et al. (1987) with minor modifications was applied to examine the GUS expression in this study. The tobacco seedlings were collected in a 1.5 ml microcentrifuge tube. One milliliter of 90% (v/v) acetone (Sigma-Aldrich, USA) was added, and the sample was incubated at room temperature for 20 min. The 90% acetone was discarded, and the sample was washed with 1 ml prechilled staining buffer [50 mM sodium phosphate buffer (pH 7.2, Sigma-Aldrich, USA)], 0.2% (v/v) Triton X-100 (Sigma-Aldrich, USA), 2 mM potassium ferrocyanide (Sigma-Aldrich, USA), and 2 mM potassium ferricyanide (Sigma-Aldrich, USA)]. The staining buffer was discarded, and 1 ml prechilled staining solution [50 mM sodium phosphate buffer (pH 7.2), 0.2% (v/v) Triton X-100, 2 mM potassium ferrocyanide, 2 mM potassium ferricyanide and 2 mM X-Gluc] was added to the sample. Then, the sample was placed on ice in a vacuum desiccator connected to a vacuum pump, and the vacuum infiltration was performed at 700 mmHg for 15 min. The vacuum was slowly released, and the sample was incubated overnight at  $37^\circ\text{C}$ . The next day, the sample was successively treated with 1 ml of 20%, 35%, and 50% ethanol (Nacalai Tesque, Japan) for 30 min each at room temperature. The tube was gently inverted several times every 5 min. After that, the 50% ethanol was decanted, and the sample was treated with 1 ml of FAA

fixative (50% ethanol, 10% glacial acetic acid, and 5% formaldehyde) at room temperature for one hour. Lastly, the FAA fixative was replaced with 1 ml of 70% ethanol (Nacalai Tesque, Japan). A photograph of the stained sample was taken using a digital camera.

**Important Note.** Potassium ferrocyanide, potassium ferricyanide, and X-Gluc must be stored in dark conditions as they are light-sensitive. If a transgenic seedling is required for other purposes, use a detached organ from the seedling instead of the whole seedling for histochemical staining of GUS activity, as this assay is destructive to plant tissue. The sample can be stored at 4°C if not photographed immediately.

## Section 12: GUS Enzymatic Assay

The leaf tissues of the transgenic tobacco plant overexpressing the GUS gene were ground using a mortar and pestle to form a fine powder in the presence of liquid nitrogen. Approximately 0.5 g of fine powder was transferred to a 15 ml Falcon tube containing 4 ml pre-cooled GUS extraction buffer [50 mM sodium phosphate (pH 7.0), 10 mM 2-mercaptoethanol (Sigma-Aldrich, USA), 10 mM Na<sub>2</sub>EDTA (Sigma-Aldrich, USA), 0.1 % sarkosyl (Sigma-Aldrich, USA) and 0.1% (v/v) Triton X-100 (Sigma-Aldrich, USA)] and mixed by vortexing for 1 min. The sample was centrifuged at 4°C, 10,000 x g for 45 min. Then, 2 ml of the supernatant was transferred to a 2 ml microcentrifuge tube, and the centrifugation step was repeated. Subsequently, 1.5 ml of the supernatant (crude protein sample) was transferred to a new 1.5 ml microcentrifuge tube. The concentration of the crude protein sample was determined using the Easy Protein Quantitative Kit (TransGen Biotech, China) according to the manufacturer's protocol. A 1.5 ml microcentrifuge tube containing 800 µL of GUS assay buffer [50 mM sodium phosphate (pH 7.0, Sigma-Aldrich, USA), 1 mM Ethylenediaminetetraacetic acid (EDTA, Sigma-Aldrich, USA), 5 mM Dithiothreitol (DTT, Thermo Scientific, USA), and 1.25 mM *p*-Nitrophenyl-β-D-glucuronide (PNPG, Sigma-Aldrich, USA)] was prewarm at 37°C for 5 min. A total of 200 µL of crude protein sample was added to the pre-warmed GUS assay buffer. The reaction buffer was vortexed shortly and incubated at 37°C for 30 min (or up to several hours). The development of a yellow color was observed during the incubation period, indicating the formation of *p*-nitrophenol (product). When the yellow color was visible, 100 µL of the reaction mixture was transferred to a 1.5 ml microcentrifuge tube containing 800 µL of 0.4 M Na<sub>2</sub>CO<sub>3</sub> (stop solution), and the reaction time was recorded. The absorbance of the sample was measured at 405 nm using a UV spectrophotometer (Thermo Scientific, USA) against a stopped blank reaction. The rate of reaction (nanomoles product/ min/ mg protein) was calculated using the formula as follows:

$$\text{Rate of reaction} = \frac{\text{OD}_{405}}{\text{Time (min)} \times \text{Protein concentration} \left(\frac{\text{mg}}{\text{ml}}\right) \times 0.02 \text{ ml} \times 0.02}$$

Where 0.02 is a value derived from the molar extinction coefficient of *p*-nitrophenol. An absorbance of 0.02 is equivalent to 1 nmol of *p*-nitrophenol formed under the conditions used in this method.

**Important Note.** The GUS enzymatic assay was performed in triplicates. The assay allows quantitative determination of GUS activity in the transgenic lines obtained. The incubation period varies according to the promoter used. A strong constitutive promoter, such as the CaMV 35S promoter, may require a shorter time to produce a detectable product. When an uncharacterized promoter is used, it is recommended to perform the enzymatic assay with several different reaction times to ensure the reaction rate is measured in the linear phase of the enzymatic reaction.

### Section 13: Production and Identification of Homozygous Line

Surface sterilization on T<sub>1</sub> seeds derived from the selected transgenic lines containing a single TIL was performed, as mentioned in Section 3. The seeds were cultivated on a screening medium containing 50 mg/L hygromycin under conditions specified in Section 9. Six hyg<sup>r</sup> seedlings (T<sub>1</sub>) from each transgenic line were randomly selected and transferred to the soil. The plants were grown until they set seeds (T<sub>2</sub>) for transgene segregation analysis following the steps in Section 8. About 50 seeds (T<sub>2</sub>) derived from a specific transgenic line (T<sub>1</sub>) were surface sterilized and cultivated on a screening medium. The T<sub>2</sub> seedlings' phenotype was observed and recorded one week after seed germination. The T<sub>1</sub> individuals producing hyg<sup>r</sup> and hyg<sup>s</sup> progenies (T<sub>2</sub> generation) are regarded as hemizygotes, while those producing only hyg<sup>r</sup> seedlings are considered homozygotes. The concept of transgene inheritance in transgenic lines with a single TIL was illustrated in Figure 2.

**Important Note.** Precautions should be taken to avoid cross-pollination between the T<sub>1</sub> plants, even though they are derived from the same origin (T<sub>0</sub>), because the T<sub>1</sub> population consists of homozygous and hemizygous individuals. The probability of obtaining a homozygous individual among the hyg<sup>r</sup> individuals in the T<sub>1</sub> generation is 1/3 (0.33). One could cultivate more than six hyg<sup>r</sup> plants derived from a selected transgenic line for zygosity determination to increase the possibility of obtaining a homozygous individual. However, it is not necessary to determine the zygosity of all T<sub>1</sub> individuals at once. The transgene segregation analysis can be stopped once a homozygous individual is identified.

## RESULTS

### Transformation and Regeneration of Transgenic Plants

The *Agrobacterium*-infected leaf discs expanded and curled after being cultured on a regeneration medium 1 for one week (Figure 3a). The emergence of adventitious shoots at the edges of the leaf discs was visible in the second week (about 11 days after co-cultivation) (Figure 3b). Next, the regenerated shoots developed into a multiple-shoot cluster in 10



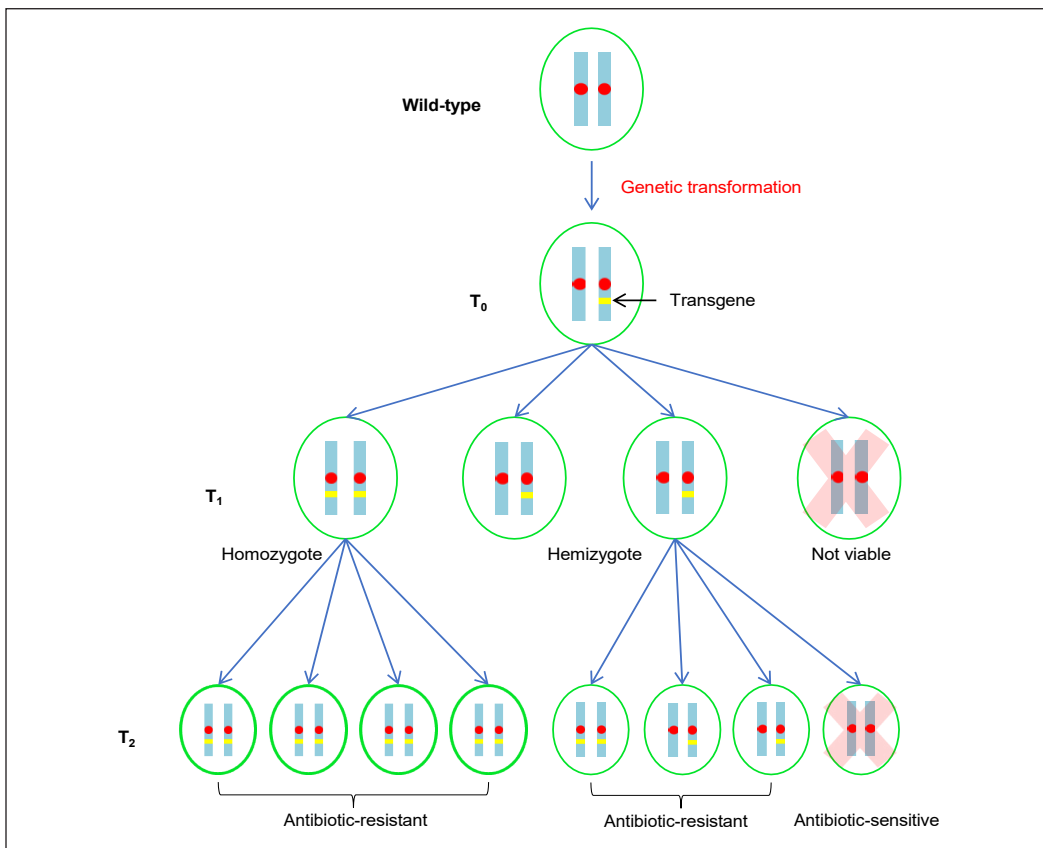
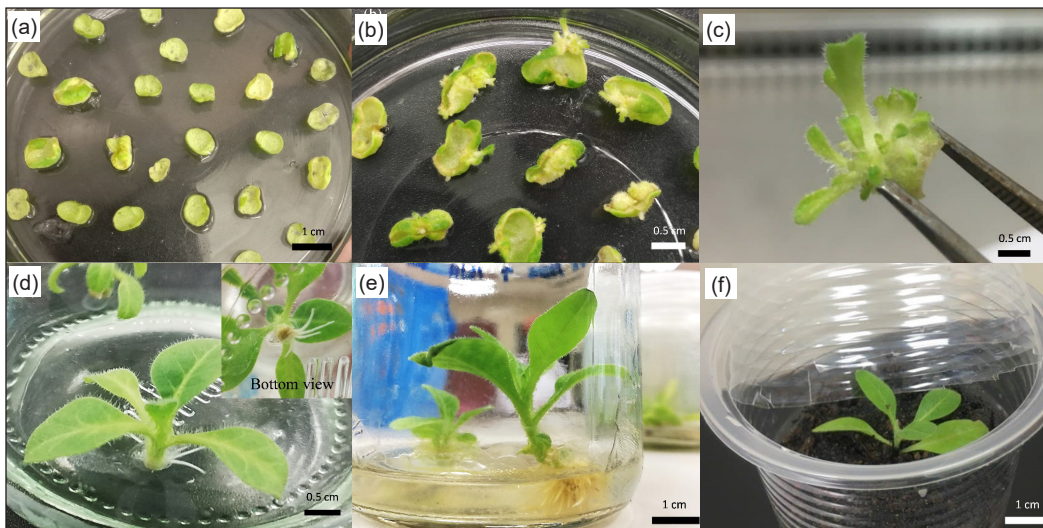


Figure 2. Diagrammatic representation of the inheritance of a transgene in the transgenic plant carrying the transgene at a single locus. The green circle represents the cell nucleus, the blue bars represent the homologous chromosomes, the red dot indicates the centromere, and the yellow line denotes the transgene. Only a single pair of homologous chromosomes is shown

days (Figure 3c), where each cluster consisted of 2–5 shoots. The shoots started to produce roots 7–10 days after being transferred to a rooting medium (Figure 3d). Figure 3e shows a transgenic plantlet ready for acclimatization. Putative transformants carrying the *EgCAD1* gene were designated CAD1-OE lines, while the GUS gene-containing lines were designated GUS-OE lines. A total of 22 putative CAD1-OE plants and nine putative GUS-OE plants were successfully obtained after acclimatization (Figure 3f).

### Verification of Transgenic Plants by PCR

PCR analysis was performed on the putative CAD1-OE and GUS-OE plants to verify transgene incorporation. PCR results showed that a band (approximately 1 kb) corresponding to the *EgCAD1* gene was amplified from the genome of all the CAD1-OE lines except for line 25 (Supplementary Figure 2a). The result indicated that all the transgenic plants



**Figure 3.** Different stages in the generation of putative primary transformants: (a) *Agrobacterium*-infected leaf discs cultured on regeneration medium 1; (b) Adventitious shoots regenerated from leaf discs; (c) Multiple-shoots cluster developed from transformed cells; (d) Roots produced from regenerated shoots; (e) Putative primary transformants; and (f) Acclimatized  $T_0$  transgenic plants

carried the *EgCAD1* gene except line 25. On the other hand, all the GUS-OE plants analyzed contained the GUS gene (Supplementary Figure 2b). Altogether, 21 and nine primary transformants ( $T_0$  generation) carrying the *EgCAD1* and GUS genes, respectively, were successfully generated. By using our established protocol, a transformation efficiency of 30% was obtained in this study.

### Identification of Transgenic Lines with a Single Transgene Integration Locus

To avoid the phenomenon of transgene silencing caused by multiple TIL, transgenic lines with a single TIL were identified. The number of TIL in the primary transformants generated was determined by studying the inheritance of selectable marker genes in  $T_1$  progeny. The hygromycin-resistant ( $hyg^r$ ) seedlings can be distinguished from the hygromycin-sensitive ( $hyg^s$ ) seedlings based on their distinctive phenotypes as early as five days after seed germination. The  $hyg^r$  seedlings possessed a longer hypocotyl compared to the  $hyg^s$  seedlings after being cultured on a screening medium for two days under dark conditions (Figure 4a and 4b). After three weeks, the  $hyg^r$  seedlings thrived on the screening medium and displayed visible root growth, expanded cotyledon, and the development of true leaves. In contrast, the growth of  $hyg^s$  seedlings was retarded (Figures 4c and 4d).

Among the CAD1-OE lines produced, 10 lines (47.6%) yielded a  $hyg^r$  to  $hyg^s$  ratio that fits the Mendelian ratio of 3:1 (Table 1), indicating that these transgenic lines contain



Figure 4. Phenotypes of hygromycin-resistant ( $hyg^r$ ) and hygromycin-sensitive ( $hyg^s$ ) seedlings. The seedlings were observed for one week (a & b) and three weeks (c & d) after germination. The CAD1-OE seedlings (a & c) displayed similar phenotypes to the GUS-OE seedlings (b & d). The GUS-OE seedlings (b & d, right panel) turned blue after being subjected to GUS staining

a single TIL. Besides, the hygromycin resistance gene segregated in the  $T_1$  progenies of seven transgenic lines (33.3%) in a segregation ratio ( $hyg^r:hyg^s$ ) that fits the Mendelian ratio of 15:1, reflecting that there are two TIL present in these transgenic lines. In addition, three CAD1-OE lines (14.3%) carried three TIL, judging by their segregation ratios that fit the Mendelian ratio of 63:1. Another CAD1-OE line (4.8%) exhibited an aberrant transgene inheritance pattern by producing only  $hyg^r$  seedlings in the  $T_1$  generation.

Contrary to CAD1-OE lines, no GUS-OE plants with distorted segregation ratios were generated in this study. Indeed, the GUS-OE lines only displayed a  $hyg^r$  to  $hyg^s$  ratio that fits the Mendelian ratios of 3:1 or 15:1 (refer to Table 1), showing that 66.7% of the population contain a single TIL, and the rest possess two. Details of segregation analysis performed on the transgenic lines generated in this study are shown in Table 1. The results indicate that the *EgCAD1* and GUS genes (individually) were stably integrated into the tobacco genome and transmitted to the progeny.

### Analysis of Transgene Expression

The *EgCAD1* or GUS gene transcript was detected using semi-quantitative RT-PCR in selected transgenic lines containing a single TIL to validate the transgene expression in the transgenic plants. Figure 5 shows an intense band corresponding to the *EgCAD1* or GUS

Table 1

*Analysis of the segregation of hygromycin resistance gene in the T<sub>1</sub> progeny of primary transformants*

Transgenic plant	Line	Germinated seedlings	Hyg <sup>r</sup>	Hyg <sup>s</sup>	Observed ratio (hyg <sup>r</sup> :hyg <sup>s</sup> )	Expected ratio (hyg <sup>r</sup> :hyg <sup>s</sup> )	$\chi^2$	No. of transgenic loci
CAD1-OE	1	192	143	49	2.9:1	3:1	0.028	1
	2	124	91	33	2.8:1		0.172	
	3	122	95	27	3.5:1		0.536	
	6	116	88	28	3.1:1		0.046	
	8	202	157	45	3.5:1		0.799	
	14	230	169	61	2.8:1		0.284	
	21	147	103	44	2.3:1		1.907	
	24	145	110	35	3.1:1		0.057	
	31	165	129	36	3.6:1		0.891	
	32	131	91	40	2.3:1		2.140	
	7	119	112	7	16.0:1	15:1	0.027	2
	10	189	179	10	17.9:1		0.297	
	20	180	167	13	12.8:1		0.290	
	26	116	109	7	15.6:1		0.009	
	27	97	91	6	15.2:1		0.001	
	28	107	100	7	14.3:1		0.016	
	30	120	114	6	19.0:1		0.320	
	5	131	129	2	64.5:1	63:1	0.001	
	18	80	78	2	39.0:1		0.457	
29	132	128	4	32.0:1		1.849		
	17	73	73	0	73.0:0	-	ND	Unknown
GUS-OE	1	234	176	58	3.0:1	3:1	0.006	1
	3	181	134	47	2.9:1		0.090	
	4	165	120	45	2.7:1		0.455	
	5	109	85	24	3.5:1		0.517	
	7	102	72	30	2.4:1		1.059	
	8	113	83	30	2.8:1		0.145	
	2	142	136	6	22.7:1	15:1	0.993	2
	6	106	96	10	9.6:1		1.834	
	9	78	72	6	12.0:1		0.277	

*Note.* ND = Not determined; Hyg<sup>r</sup> = Hygromycin-resistant; Hyg<sup>s</sup> = Hygromycin-sensitive

gene produced by RT-PCR from the cDNA samples of transgenic plants but not from that of wild-type plants. The RT-PCR result reflects that the T<sub>1</sub> progenies inherited the *EgCAD1* or GUS gene, and the transgene was actively transcribed in the transgenic plants analyzed. Apart from the gene expression analysis, the expression of GUS was also confirmed by histochemical staining (Figure 4b & 4d) and enzymatic assay (Data not shown).

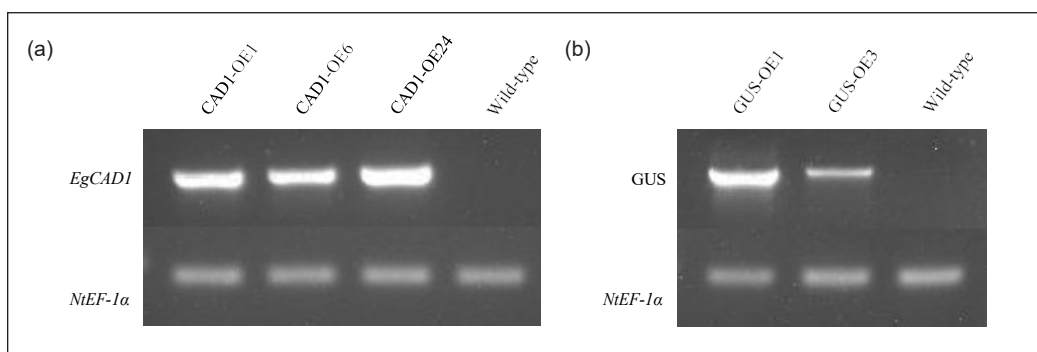


Figure 5. Analysis of RT-PCR products by agarose gel electrophoresis. The expressions of *EgCAD1* (a) and *GUS* (b) genes were examined in the leaf tissue of four-week-old transgenic plants using semi-quantitative RT-PCR. Wild-type tobacco plants were used as the negative control. The tobacco Elongation factor 1- $\alpha$  (*NtEF-1 $\alpha$* ) gene serves as the internal control for the analysis

### Identification of Homozygous Line

The  $T_1$  generation consists of homozygous and hemizygous individuals (Figure 2), but they are visually indistinguishable. Therefore, homozygous individuals were identified by studying the inheritance of the selectable marker gene in  $T_2$  progenies. As anticipated, the hemizygous individual produced both  $hyg^r$  and  $hyg^s$  progenies in a 3:1 ratio, while the homozygous individual produced only  $hyg^r$  progenies. The  $hyg^r$  and  $hyg^s$  seedlings were easily distinguishable by the length of their hypocotyls, with the former displaying a longer hypocotyl compared to the latter after being cultured under dark conditions. The present study successfully developed homozygous plants for the CAD1-OE1, CAD1-OE6, CAD1-OE24, GUS-OE1, and GUS-OE3 transgenic lines. These homozygous plants carry the transgene of interest at a single TIL.

### DISCUSSION

Genetic engineering has become a powerful tool in functional genomics as it allows the direct introduction of foreign DNA into the genome of a species. Plant genetic transformation is commonly performed through the *Agrobacterium*-mediated transformation method owing to the ability of *Agrobacterium* to transfer a portion of its DNA to the host plant genome. Nevertheless, some plant species are recalcitrant to *Agrobacterium*-mediated transformation as the transformation efficiencies are relatively low (Kumar et al., 2021; Masters et al., 2020; Sharma et al., 2020). This problem greatly impedes the progress of functional genomics in plant species that are not amenable to *Agrobacterium*-mediated transformation. Hence, performing a functional study using a model plant can be a strategy to circumvent the bottleneck. This article provides a complete and comprehensive guide to generating and identifying transgenic tobacco lines with a single TIL. This article also provides a guideline for developing a homozygous transgenic plant from selected transgenic lines. Using the

method presented in this manuscript, transgenic tobacco plants carrying the intended GOI were successfully produced. It is worth mentioning that more than 50% of the transgenic tobacco plants generated contained a single TIL (Table 1). Furthermore, homozygous lines were developed from selected transgenic lines. The procedures outlined in our method do not require high-end and sophisticated equipment. Hence, they can be performed in most laboratories at minimal cost. The transgenic tobacco plants produced are appropriate for functional analysis to dissect the roles of a genetic element in plants. Undoubtedly, this method will foster functional genomics.

### **Tobacco as a Model Plant**

The choice of a model plant is of great importance in dissecting the role of a plant gene. Several model plants, such as *Arabidopsis*, petunia, and tobacco, have been used in functional studies (Naing et al., 2022; Shingote et al., 2020; Sun et al., 2021). Being a dicotyledonous plant does not limit the tobacco plant from being used in the functional study of a gene from monocots. The use of dicotyledonous model plants to study a gene from monocots is not uncommon. Previously, transgenic tobacco plants carrying a gene from wheat, maize, rice, and sugarcane had been reported (Li et al., 2018; Miftahudin et al., 2021; Su et al., 2020). Tobacco is a popular model plant due to its efficient and straightforward transformation protocol. Transgenic tobacco plants can be produced by the leaf disc transformation method, which involves co-culturing tobacco leaf disc explants with *Agrobacterium*, followed by a shoot regeneration on a cytokinin-rich medium (Gallois & Marinho, 1995). Alternatively, stable transgenic lines can be regenerated from tobacco leaf tissues infiltrated with *Agrobacterium* (Sparkes et al., 2006). Apart from the direct organogenesis pathway commonly used to obtain transgenic plants, Pathi et al. (2013) also reported the recovery of transgenic tobacco plants through direct somatic embryogenesis.

### **Regeneration of Escape**

The emergence of escapes in genetic transformation works is a common phenomenon, as it has also been reported in other studies (Hayta et al., 2019; Maggini et al., 2021; Miguel et al., 2020). The escaped plant (CAD1-OE25) recovered in this study could be an untransformed plant that escaped the selection procedure, or it has incorporated a truncated T-DNA that only contains the selectable marker gene that renders it resistant to hygromycin. It is also possible that this escape is a chimera that contains both transformed and untransformed cells. Factors affecting the regeneration of escapes in genetic transformation works include the transformation construct used (Hayta et al., 2019), the dose of selective agent (Hu et al., 2016; Li et al., 2013), and the number of subcultures during shoot regeneration (Li et al., 2009). A double selection system that combines selectable markers and fluorescence protein genes could improve selection efficiency.

## Inheritance of Transgene

The transgenic plants produced must undergo a series of molecular analyses before being used in the functional study. Transgene silencing tends to occur in transgenic plants with multiple TIL (Rajeevkumar et al., 2015; Tang et al., 2007). Hence, obtaining a transgenic plant with a single TIL is essential before characterization. The number of transgenic loci in a transgenic line is determined by studying transgene segregation in the offspring generation. Segregation analysis is a simple, reliable, and cost-effective method to determine the number of transgenic loci in transgenic plants. Besides, segregation analysis also helps to illustrate the inheritance of the transgene by the  $T_1$ ,  $T_2$ , and subsequent generations, confirming stable integration of a transgene in the primary transformant ( $T_0$  generation). Unfortunately, the use of this method is limited to plant species that produce a large number of seeds, as many seeds (suggested around 120 seeds) are required in a segregation analysis to obtain a reliable result. For model plant species that produce a lot of seeds (like tobacco, tomato, *Arabidopsis*, and *Brachypodium*), there is no problem with conducting a segregation analysis to determine the number of transgenic loci. Unfortunately, segregation analysis is not feasible for plant species that produce fewer seeds or do not produce seeds (such as orchids, bananas, sugarcane, and cassava). In this regard, Southern blot analysis can determine the number of transgenic loci in transgenic plants. However, it is more tedious and technically challenging compared to segregation analysis. Furthermore, it requires special equipment (Gebbie, 2014). This is why segregation analysis determines the number of transgenic loci in this manuscript. Apart from Mendelian inheritance, non-Mendelian transgene inheritance has also been reported in transgenic rapeseed and wheat plants (Miroshnichenko et al., 2018; Raldugina et al., 2021). Factors leading to the non-Mendelian inheritance of transgene were reviewed by Yin et al. (2004).

The difference in the transgene expression level observed among different transgenic lines (Figure 5) is likely a result of the transgene position effect. The integration position of a transgene within the genome significantly influences its expression level. Transgenes inserted into regions with active chromatin and high transcriptional activity, such as euchromatin, typically exhibit higher expression levels (Kohli et al., 2006). In contrast, insertion into heterochromatin or regions with dense, inactive chromatin can lead to gene silencing or reduced expression due to positional effects and the influence of surrounding regulatory elements (Nguyen & Bosco, 2015). The local genomic context, including enhancers, repressors, and other regulatory sequences, can either enhance or impede transgene expression (Henikoff, 2000). Therefore, multiple transgenic lines should be produced when generating transgenic plants to obtain transgenic lines with high transgene expression levels.

## Challenges in Producing Transgenic Plant

Production of transgenic lines that are usable for functional study is a challenging task. To achieve the goal, in-depth knowledge of genetic engineering and tissue culture is required. Since the *in vitro* culture step is the predominant part of the process, skillful personnel with good aseptic techniques are indispensable to prevent contamination of the cultures. One of the major concerns in *Agrobacterium*-mediated transformation is the elimination of *Agrobacterium* from explants after the inoculation step. It is usually achieved by adding antibiotics to the culture medium coupled with frequent subculture to suppress bacterial growth. Antibiotics such as cefotaxime, carbenicillin, and timentin have been widely used to get rid of *Agrobacterium* contamination in plant transformation (Cano et al., 2021; Haider et al., 2020; Kumar et al., 2019). Previously, several studies have shown that the antibiotics used to eliminate *Agrobacterium* displayed different levels of effectiveness (Teixeira da Silva & Fukai, 2001; Grzebelus & Skop, 2014; Priya et al., 2012). Apart from inhibiting *Agrobacterium* growth, several studies found that some of these selective agents also confer adverse effects on the growth and development of plant tissue when exceeding the optimal amount (Haider et al., 2020; Ma et al., 2015; Song et al., 2020). Hence, the selection of antibiotic(s) and the quantity used in *Agrobacterium*-mediated transformation must be considered carefully.

## CONCLUSION

The production of transgenic plants is vital for functional analysis to dissect the roles of a gene. When producing a transgenic plant for functional analysis, the transgene must be stably integrated into the plant genome and expressed in transgenic plants. Hence, the transgenic plants produced must undergo a strict selection process before being used in functional analysis. It ensures that the selected transgenic plants fulfill all the criteria needed for functional analysis. A complete guide to generating and identifying transgenic tobacco lines for functional analysis is presented in this article. This method successfully produced and identified transgenic lines that comply with the requirements of functional analysis. More than 50% of the transgenic tobacco plants generated contained a single TIL. The transgene was stably integrated into the genome of primary transformants ( $T_0$ ) and passed down to the  $T_1$  and  $T_2$  progenies. In addition, it was also confirmed that the transgenes were abundantly expressed in the selected transgenic lines. It is worth mentioning that no high-end equipment is required in this method, permitting its application in many laboratories. Therefore, this method can be a standard guideline for researchers to produce transgenic tobacco (and other model plants that produce plenty of seeds) plants for functional analysis.



## ACKNOWLEDGMENTS

The authors express their sincere gratitude to the staff of the Laboratory of Plant Genetic and Cell Biology, especially Natasha Afzan Tamby Husin, Roslan Ghaffar, Dahyudeen Dahlan, and Mohd Saidi Awang, for their generous assistance in establishing the facilities for the cultivation of transgenic plants. This work was supported by the Fundamental Research Grant Scheme (Reference Code: FRGS/1/2022/STG01/UITM/02/13) from the Malaysian Ministry of Higher Education (MOHE).

## REFERENCES

- Aleem, M., Riaz, A., Raza, Q., Aleem, M., Aslam, M., Kong, K., Atif, R. M., Kashif, M., Bhat, J. A., & Zhao, T. (2022). Genome-wide characterization and functional analysis of class III peroxidase gene family in soybean reveal regulatory roles of *GsPOD40* in drought tolerance. *Genomics*, *114*(1), 45-60. <https://doi.org/10.1016/j.ygeno.2021.11.016>
- Alexander, A., Singh, V. K., & Mishra, A. (2021). Overexpression of differentially expressed *AhCytb6* gene during plant-microbe interaction improves tolerance to N<sub>2</sub> deficit and salt stress in transgenic tobacco. *Scientific Reports*, *11*(1), 13435. <https://doi.org/10.1038/s41598-021-92424-4>
- Boyidi, P., Trishla, V. S., Botta, H. K., Yadav, D., & Kirti, P. B. (2021). Heterologous expression of rice annexin *OsANN5* potentiates abiotic stress tolerance in transgenic tobacco through ROS amelioration. *Plant Stress*, *2*, 100022. <https://doi.org/10.1016/j.stress.2021.100022>
- Cano, V., Martinez, M. T., Couselo, J. L., Varas, E., Vieitez, F. J., & Corredoira, E. (2021). Efficient transformation of somatic embryos and regeneration of cork oak plantlets with a gene (*CsTL1*) encoding a chestnut thaumatin-like protein. *International Journal of Molecular Science*, *22*(4), 1757. <https://doi.org/10.3390/ijms22041757>
- Dutta, T. K., Vashisth, N., Ray, S., Phani, V., Chinnusamy, V., & Sirohi, A. (2023). Functional analysis of a susceptibility gene (*HIPP27*) in the *Arabidopsis thaliana-Meloidogyne incognita* pathosystem by using a genome editing strategy. *BMC Plant Biology*, *23*(1), 390. <https://doi.org/10.1186/s12870-023-04401-w>
- Duxbury, Z., Wang, S., MacKenzie, C. I., Tenthorey, J. L., Zhang, X., Huh, S. U., Hu, L., Hill, L., Ngou, P. M., Ding, P., Chen, J., Ma, Y., Guo, H., Castel, B., Moschou, P. N., Bernoux, M., Dodds, P. N., Vances, R. E., & Jones, J. D. G. (2020). Induced proximity of a TIR signaling domain on a plant-mammalian NLR chimera activates defense in plants. *Proceedings of the National Academy of Sciences of the United States of America*, *117*(31), 18832-18839. <https://doi.org/10.1073/pnas.2001185117>
- Fan, Y., Peng, J., Wu, J., Zhou, P., He, R., Allan, A. C., & Zeng, L. (2021). NtbHLH1, a JAF13-like bHLH, interacts with NtMYB6 to enhance proanthocyanidin accumulation in Chinese Narcissus. *BMC Plant Biology*, *21*(1), 275. <https://doi.org/10.1186/s12870-021-03050-1>
- Fraley, R. T., Rogers, S. G., Horsch, R. B., Sanders, P. R., Flick, J. S., Adams, S. P., Bittner, M. L., Brand, L. A., Fink, C. L., Fry, J. S., Galluppi, G. R., Goldberg, S. B., Hoffmann, N. L., & Woo, S. C. (1983). Expression of bacterial genes in plant cells. *Proceedings of the National Academy of Sciences of the United States of America*, *80*(15), 4803-4807. <https://doi.org/10.1073/pnas.80.15.4803>

- Gallois, P., & Marinho, P. (1995). Leaf disk transformation using *Agrobacterium tumefaciens*-expression of heterologous genes in tobacco. In H. Jone (Ed.), *Methods in molecular biology* (pp. 39-48). Springer Nature. <https://doi.org/10.1385/0-89603-321-X:39>
- Gebbie, L. (2014). Genomic southern blot analysis. In R. Henry & A. Furtado (Eds.), *Cereal genomics: Methods and protocol* (pp. 159-177). Humana Press. [https://doi.org/10.1007/978-1-62703-715-0\\_14](https://doi.org/10.1007/978-1-62703-715-0_14)
- Grzebelus, E., & Skop, L. (2014). Effect of  $\beta$ -lactam antibiotics on plant regeneration in carrot protoplast cultures. *In Vitro Cellular & Developmental Biology – Plant*, 50(5), 568-575. <https://doi.org/10.1007/s11627-014-9626-0>
- Guo, X., Fang, D., Sahu, S. K., Yang, S., Guang, X., Folk, R., Smith, S. A., Chanderbali, A. S., Chen, S., Liu, M., Yang, T., Zhang, S., Liu, X., Xu, X., Soltis, P. S., Soltis, D. E., & Liu, H. (2021). *Chloranthus* genome provides insights into the early diversification of angiosperms. *Nature Communications*, 12(1), 6930. [10.1038/s41467-021-26922-4](https://doi.org/10.1038/s41467-021-26922-4)
- Haider, S., Gao, Y., & Gao, Y. (2020). Standardized genetic transformation protocol for Chrysanthemum cv. 'Jinba' with TERMINAL FLOWER 1 Homolog *CmTFL1a*. *Genes*, 11(8), 860. <https://doi.org/10.3390/genes11080860>
- Hayta, S., Smedley, M. A., Demir, S. U., Blundell, R., Hinchliffe, A., Atkinson, N., & Harwood, W. A. (2019). An efficient and reproducible *Agrobacterium*-mediated transformation method for hexaploid wheat (*Triticum aestivum* L.). *Plant Methods*, 15(1), 121. <https://doi.org/10.1186/s13007-019-0503-z>
- Henikoff, S. (2000). Heterochromatin function in complex genomes. *Biochimica et Biophysica Acta (BBA) - Reviews on Cancer*, 1470(1), O1-O8. [https://doi.org/10.1016/S0304-419X\(99\)00034-7](https://doi.org/10.1016/S0304-419X(99)00034-7)
- Hu, L., Lu, J., Chiang, H., Wu, H., Edge, A. S., & Shi, F. (2016). Diphtheria toxin-induced cell death triggers Wnt-dependent hair cell regeneration in neonatal mice. *Journal of Neuroscience*, 36(36), 9479-9489. <https://doi.org/10.1523/JNEUROSCI.2447-15.2016>
- Hu, M., Xie, M., Cui, X., Huang, J., Cheng, X., Liu, L., Yan, S., Liu, S., & Tong, C. (2023). Characterization and potential function analysis of the *SRS* gene family in *Brassica napus*. *Genes*, 14(7), 1421. <https://doi.org/10.3390/genes14071421>
- Hwang, H. H., Yu, M., & Lai, E. M. (2017). *Agrobacterium*-mediated plant transformation: Biology and applications. *The Arabidopsis Book*, 2017(15). <https://doi.org/10.1199/tab.0186>
- Ismagul, A., Yang, N., Maltseva, E., Iskakova, G., Mazonka, I., Skiba, Y., Bi, H., Eliby, S., Jatayev, S., Shavrukov, Y., Borisjuk, N., & Langridge, P. (2018). A biolistic method for high-throughput production of transgenic wheat plants with single gene insertions. *BMC Plant Biology*, 18(1), 135. <https://doi.org/10.1186/s12870-018-1326-1>
- Jackson, M. A., Anderson, D. J., & Birch, R. G. (2013). Comparison of *Agrobacterium* and particle bombardment using whole plasmid or minimal cassette for production of high-expressing, low-copy transgenic plants. *Transgenic Research*, 22(1), 143-151. <https://doi.org/10.1007/s11248-012-9639-6>
- Jefferson, R. A., Kavanagh, T. A., & Bevan, M. W. (1987). GUS fusions: Beta-glucuronidase as a sensitive and versatile gene fusion marker in higher plants. *The EMBO Journal*, 6(13), 3901-3907. <https://doi.org/10.1002/j.1460-2075.1987.tb02730.x>

- Kim, Y. H., & Huh, G. H. (2019). Overexpression of *cinnamyl alcohol dehydrogenase* gene from sweetpotato enhances oxidative stress tolerance in transgenic *Arabidopsis*. *In Vitro Cellular & Developmental Biology – Plant*, 55(2), 172-179. <https://doi.org/10.1007/s11627-018-09951-5>
- Kiyak, A., & Mutlu, A. G. (2023). Molecular cloning, characterization and expression profile of *FLOWERING LOCUS T (FT)* gene from *Prunus armeniaca* L. *South African Journal of Botany*, 155, 330-339. <https://doi.org/10.1016/j.sajb.2023.02.026>
- Kohli, A., Melendi, P. G., Abranches, R., Capell, T., Stoger, E., & Christou, P. (2006). The quest to understand the basis and mechanisms that control expression of introduced transgenes in crop plants. *Plant Signaling & Behavior*, 1(4), 185-195. <https://doi.org/10.4161/psb.1.4.3195>
- Kumar, A., Sainger, M., Jaiwal, R., Chaudhary, D., & Jaiwal, P. K. (2021). Tissue culture- and selection-independent *Agrobacterium tumefaciens*-Mediated transformation of a recalcitrant grain legume, cowpea (*Vigna unguiculata* L. Walp). *Molecular Biotechnology*, 63(8), 710-718. <https://doi.org/10.1007/s12033-021-00333-8>
- Kumar, R., Mamrutha, H. M., Kaur, A., Venkatesh, K., Sharma, D., & Singh, G. P. (2019). Optimization of *Agrobacterium*-mediated transformation in spring bread wheat using mature and immature embryos. *Molecular Biology Reports*, 46(2), 1845-1853. <https://doi.org/10.1007/s11033-019-04637-6>
- Lee, P. Y., Costumbrado, J., Hsu, C. Y., & Kim, Y. H. (2012). Agarose gel electrophoresis for the separation of DNA fragments. *Journal of Visualized Experiments*, 62, 3829. <https://doi.org/10.3791/3923>
- Lewis, R. S., Drake-Stowe, K. E., Heim, C., Steede, T., Smith, W., & Dewey, R. E. (2020). Genetic and agronomic analysis of tobacco genotypes exhibiting reduced nicotine accumulation due to induced mutations in *Berberine Bridge Like (BBL)* Genes. *Frontiers in Plant Science*, 11, 368. <https://doi.org/10.3389/fpls.2020.00368>
- Li, B., Xie, C., & Qiu, H. (2009). Production of selectable marker-free transgenic tobacco plants using a non-selection approach: Chimerism or escape, transgene inheritance, and efficiency. *Plant Cell Reports*, 28(3), 373-386. <https://doi.org/10.1007/s00299-008-0640-8>
- Li, Q., Wang, W., Wang, W., Zhang, G., Liu, Y., Wang, Y., & Wang, W. (2018). Wheat f-box protein gene *TaFBA1* is involved in plant tolerance to heat stress. *Frontiers in Plant Science*, 9(521), 1242. <https://doi.org/10.3389/fpls.2018.00521>
- Li, X., Fan, J., Gruber, J., Guan, R., Frentsen, M., & Zhu, L. H. (2013). Efficient selection and evaluation of transgenic lines of *Crambe abyssinica*. *Frontiers in Plant Science*, 4, 162. <https://doi.org/10.3389/fpls.2013.00162>
- Liu, J., Nannas, N. J., Fu, F. f., Shi, J., Aspinwall, B., Parrott, W. A., & Dawe, R. K. (2019). Genome-scale sequence disruption following biolistic transformation in rice and maize. *The Plant Cell*, 31(2), 368-383. <https://doi.org/10.1105/tpc.18.00613>
- Liu, Y., Wang, P., Yan, S., Liu, X., Lu, L., Chen, X., Lu, Y., Hao, Z., Shi, J., & Chen, J. (2020). Molecular cloning and functional characterization of the *DELLA* gene family in *Liriodendron* hybrids. *Forests*, 11(12), 1363. <https://doi.org/10.3390/f11121363>
- Ma, J., Liu, T., & Qiu, D. (2015). Optimization of *Agrobacterium*-mediated transformation conditions for tomato (*Solanum lycopersicum* L.). *Plant Omics*, 8(6), 529-536.

- Maggini, V., Bettini, P., Firenzuoli, F., & Bogani, P. (2021). An efficient method for the genetic transformation of *Acmella oleracea* L. (*Spilanthes acmella* Linn.) with *Agrobacterium tumefaciens*. *Plants*, *10*(2), 198. <https://doi.org/10.3390/plants10020198>
- Masters, A., Kang, M., McCaw, M., Zobrist, J. D., Gordon Kamm, W., Jones, T., & Wang, K. (2020). *Agrobacterium*-mediated immature embryo transformation of recalcitrant maize inbred lines using morphogenic genes. *Journal of Visualized Experiments*, (156), e60782. <https://doi.org/10.3791/60782>
- Miftahudin, M., Roslim, D. I., Fendiyanto, M. H., Satrio, R. D., Zulkifli, A., Umaiyah, E. I., Chikmawati, T., Sulistyarningsih, Y. C., Suharsono, S., Hartana, A., Nguyen, H. T., & Gustafson, J. P. (2021). *OsGERLP*: A novel aluminum tolerance rice gene isolated from a local cultivar in Indonesia. *Plant Physiology and Biochemistry*, *162*, 86-99. <https://doi.org/10.1016/j.plaphy.2021.02.019>
- Miguel, S., Michel, C., Biteau, F., Hehn, A., & Bourgaud, F. (2020). In vitro plant regeneration and *Agrobacterium*-mediated genetic transformation of a carnivorous plant, *Nepenthes mirabilis*. *Scientific Reports*, *10*(1), 17482. <https://doi.org/10.1038/s41598-020-74108-7>
- Miroshnichenko, D., Ashin, D., Pushin, A., & Dolgov, S. (2018). Genetic transformation of einkorn (*Triticum monococcum* L. ssp. *monococcum* L.), a diploid cultivated wheat species. *BMC Biotechnology*, *18*(1), 68. <https://doi.org/10.1186/s12896-018-0477-3>
- Naing, A. H., Xu, J., & Kim, C. K. (2022). Editing of 1-aminocyclopropane-1-carboxylate oxidase genes negatively affects petunia seed germination. *Plant Cell Reports*, *41*(1), 209-220. <https://doi.org/10.1007/s00299-021-02802-5>
- Nguyen, H. Q., & Bosco, G. (2015). Gene positioning effects on expression in eukaryotes. *Annual Review of Genetics*, *49*, 627-646. <https://doi.org/10.1146/annurev-genet-112414-055008>
- Niedbala, G., Niazian, M., & Sabbatini, P. (2021). Modeling *Agrobacterium*-mediated gene transformation of Tobacco (*Nicotiana tabacum*)-A model plant for gene transformation studies. *Frontiers in Plant Science*, *12*, 695110. <https://doi.org/10.3389/fpls.2021.695110>
- Pathi, K. M., Tula, S., & Tuteja, N. (2013). High frequency regeneration via direct somatic embryogenesis and efficient *Agrobacterium*- mediated genetic transformation of tobacco. *Plant Signaling & Behavior*, *8*(6), e24354. <https://doi.org/10.4161/psb.24354>
- Priya, A. M., Pandian, S. K., & Manikandan, R. (2012). The effect of different antibiotics on the elimination of *Agrobacterium* and high frequency *Agrobacterium*-mediated transformation of indica rice (*Oryza sativa* L.). *Czech Journal of Genetics and Plant Breeding*, *48*, 120-130. <https://doi.org/10.17221/77/2011-CJGPB>
- Rajeevkumar, S., Anunanthini, P., & Ramalingam, S. (2015). Epigenetic silencing in transgenic plants. *Frontiers in Plant Science*, *6*(693). <https://doi.org/10.3389/fpls.2015.00693>
- Raldugina, G. N., Hoang, T. Z., Ngoc, H. B., & Karpichev, I. V. (2021). An increased proportion of transgenic plants in the progeny of rapeseed (*Brassica napus* L.) transformants. *Vavilovskii Zhurnal Genetiki i Seleksii*, *25*(2), 147-156. <https://doi.org/10.18699/VJ21.018>
- Robbins, M. D., Bushman, B. S., Huff, D. R., Benson, C. W., Warnke, S. E., Maughan, C. A., Jellen, E. N., Johnson, P. G., & Maughan, P. J. (2023). Chromosome-scale genome assembly and annotation of allotetraploid annual bluegrass (*Poa annua* L.). *Genome Biology and Evolution*, *15*(1), evac180. <https://doi.org/10.1093/gbe/evac180>

- Schmidt, F. J., Zimmermann, M. M., Wiedmann, D. R., Lichtenauer, S., Grundmann, L., Muth, J., Twyman, R. M., Prüfer, D., & Noll, G. A. (2020). The major floral promoter NtFT5 in tobacco (*Nicotiana tabacum*) is a promising target for crop improvement. *Frontier in Plant Science*, *10*, 1666. <https://doi.org/10.3389/fpls.2019.01666>
- Sharma, R., Liang, Y., Lee, M. Y., Pidatala, V. R., Mortimer, J. C., & Scheller, H. V. (2020). *Agrobacterium*-mediated transient transformation of sorghum leaves for accelerating functional genomics and genome editing studies. *BMC Research Notes*, *13*(1), 116. <https://doi.org/10.1186/s13104-020-04968-9>
- Shingote, P. R., Kawar, P. G., Pagariya, M. C., Muley, A. B., & Babu, K. H. (2020). Isolation and functional validation of stress tolerant *EaMYB18* gene and its comparative physio-biochemical analysis with transgenic tobacco plants overexpressing *SoMYB18* and *SsMYB18*. *3 Biotech*, *10*(5), 225. <https://doi.org/10.1007/s13205-020-02197-2>
- Shokouhifar, F., Bahrabadi, M., Bagheri, A., & Mamarabadi, M. (2019). Transient expression analysis of synthetic promoters containing F and D *cis*-acting elements in response to *Ascochyta rabiei* and two plant defense hormones. *AMB Express*, *9*(1), 195. <https://doi.org/10.1186/s13568-019-0919-x>
- Song, Y., Bai, X., Dong, S., Yang, Y., Dong, H., Wang, N., Zhang, H., & Li, S. (2020). Stable and efficient *Agrobacterium*-mediated genetic transformation of larch using embryogenic callus. *Frontier in Plant Science*, *11*, 584492. <https://doi.org/10.3389/fpls.2020.584492>
- Sparkes, I. A., Runions, J., Kearns, A., & Hawes, C. (2006). Rapid, transient expression of fluorescent fusion proteins in tobacco plants and generation of stably transformed plants. *Nature Protocols*, *1*(4), 2019-2025. <https://doi.org/10.1038/nprot.2006.286>
- Su, W., Ren, Y., Wang, D., Su, Y., Feng, J., Zhang, C., Tang, H., Xu, L., Muhammad, K., & Que, Y. (2020). The alcohol dehydrogenase gene family in sugarcane and its involvement in cold stress regulation. *BMC Genomics*, *21*(1), 521. <https://doi.org/10.1186/s12864-020-06929-9>
- Sun, L. J., Zhao, X. Y., Ren, J., Yan, S. P., Zhao, X. Y., & Song, X. S. (2021). Overexpression of *Cerasus humilis* *ChAOX2* improves the tolerance of Arabidopsis to salt stress. *3 Biotech*, *11*(7), 316. [10.1007/s13205-021-02871-z](https://doi.org/10.1007/s13205-021-02871-z)
- Tang, W., Newton, R. J., & Weidner, D. A. (2007). Genetic transformation and gene silencing mediated by multiple copies of a transgene in eastern white pine. *Journal of Experimental Botany*, *58*(3), 545-554. <https://doi.org/10.1093/jxb/erl228>
- Teixeira da Silva, J. A., & Fukai, S. (2001). The impact of carbenicillin, cefotaxime and vancomycin on chrysanthemum and tobacco TCL morphogenesis and *Agrobacterium* growth. *Journal of Applied Horticulture*, *03*(01), 3-12. <https://doi.org/10.37855/jah.2001.v03i01.01>
- Tizaoui, K., & Kchouk, M. E. (2012). Genetic approaches for studying transgene inheritance and genetic recombination in three successive generations of transformed tobacco. *Genetic Molecular Biology*, *35*(3), 640-649. <https://doi.org/10.1590/S1415-47572012000400015>
- Wang, M., Ren, T., Huang, R., Li, Y., Zhang, C., & Xu, Z. (2021). Overexpression of an *Apocynum venetum* flavonols synthetase gene confers salinity stress tolerance to transgenic tobacco plants. *Plant Physiology and Biochemistry*, *162*, 667-676. <https://doi.org/10.1016/j.plaphy.2021.03.034>

- Wang, Z. F., Rouard, M., Droc, G., Heslop-Harrison, P., & Ge, X.-J. (2023). Genome assembly of *Musa beccarii* shows extensive chromosomal rearrangements and genome expansion during evolution of Musaceae genomes. *GigaScience*, *12*, giad005. <https://doi.org/10.1093/gigascience/giad005>
- Xie, X., Lin, M., Xiao, G., Wang, Q., & Li, Z. (2024). Identification and characterization of the *AREB/ABF* gene family in three orchid species and functional analysis of *DcaABI5* in *Arabidopsis*. *Plants*, *13*(6), 774. <https://doi.org/10.3390/plants13060774>
- Yao, W., Zhang, D., Zhou, B., Wang, J., Li, R., & Jiang, T. (2020). Over-expression of poplar *NAC15* gene enhances wood formation in transgenic tobacco. *BMC Plant Biology*, *20*(1), 12. <https://doi.org/10.1186/s12870-019-2191-2>
- Yin, Z., Plader, W., & Malepszy, S. (2004). Transgene inheritance in plants. *Journal of Applied Genetics*, *45*(2), 127-144.
- Yusuf, C. Y. L., Abdullah, J. O., Shaharuddin, N. A., Abu Seman, I., & Abdullah, M. P. (2018). Characterization of promoter of *EgPAL1*, a novel *PAL* gene from the oil palm *Elaeis guineensis* Jacq. *Plant Cell Reports*, *37*(2), 265-278. <https://doi.org/10.1007/s00299-017-2228-7>
- Yusuf, C. Y. L., Abu Seman, I., Ab Shukor, N. A., Mohd Nor, M. N., & Abdullah, M. P. (2018). Cloning and analysis of the *Eg4CL1* gene and its promoter from oil palm (*Elaeis guineensis* Jacq.). *Sains Malaysiana*, *47*(8), 1709-1723. <https://doi.org/10.17576/jsm-2018-4708-10>
- Yusuf, C. Y. L., Nabilah, N. S., Taufik, N., Seman, I. A., & Abdullah, M. P. (2022). Genome-wide analysis of the *CAD* gene family reveals two *bona fide* *CAD* genes in oil palm. *3 Biotech*, *12*(7), 149. <https://doi.org/10.1007/s13205-022-03208-0>
- Zhang, Z., Conner, J., Guo, Y., & Ozias-Akins, P. (2020). Haploidy in tobacco induced by *PsASGR-BBML* transgenes via parthenogenesis. *Genes*, *11*(9), 1072. <https://doi.org/10.3390/genes11091072>

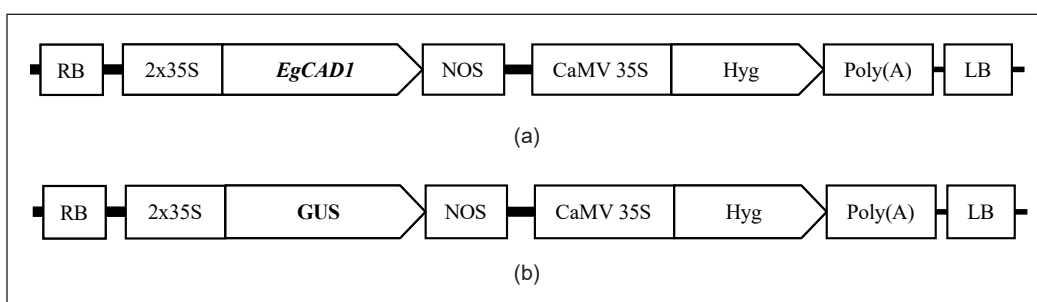
## APPENDIX

Supplementary Table 1

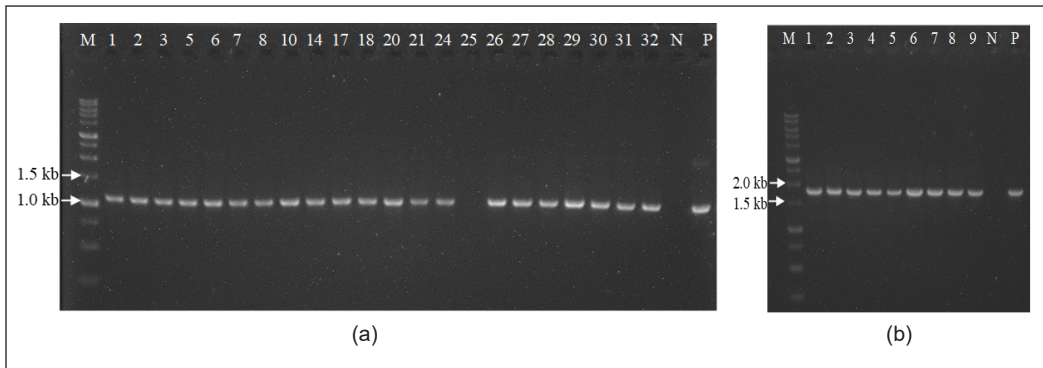
Composition of tissue culture media used to produce transgenic plants

No.	Medium	Nutrient	Sucrose (g/L)	Gelrite (g/L)	Hormone	Antibiotic
1	Germination medium	Half-strength MS & vitamins	15	2.5	-	-
2	Inoculation medium	MS & vitamins	30	-	-	-
3	Co-cultivation medium	MS & vitamins	30	2.5	2.0 mg/L 6-Benzylaminopurine (BAP) + 0.1 mg/L Naphthaleneacetic acid (NAA)	-
4	Regeneration medium 1	MS & vitamins	30	2.5	2.0 mg/L BAP + 0.1 mg/L NAA	50 mg/L hygromycin + 250 mg/L timentin
5	Regeneration medium 2	MS & vitamins	30	2.5	0.5 mg/L BAP	50 mg/L hygromycin + 250 mg/L timentin
6	Rooting medium	MS & vitamins	30	2.5	0.1 mg/L NAA	50 mg/L hygromycin + 250 mg/L timentin
7	Screening medium	Half-strength MS & vitamins	15	2.5	-	50 mg/L hygromycin

Note. MS = Murashige & Skoog (1962) basal salt mixture including original vitamins (Duchefa Biochemie, Netherlands). The pH of all media was adjusted to 5.7-5.8 before autoclave



Supplementary Figure 1. Schematic representation of the T-DNA region of the constructs used in the present study. (a) pMDC32-*EgCAD1* (b) pMDC32-GUS. RB=right border; 2x35S=dual 35S promoter; *EgCAD1*=*Elaeis guineensis* Cinnamyl Alcohol Dehydrogenase 1 gene; GUS= $\beta$ -Glucuronidase gene; NOS=nopaline synthase terminator; CaMV 35S=CaMV 35S promoter; Hyg=hygromycin B resistance gene; Poly(A)=CaMV poly(A) signal; LB=left border



*Supplementary Figure 2.* PCR analysis of putative primary transformants ( $T_0$  generation). (a) PCR products of *EgCAD1* gene (1075 bp) amplified from CAD1-OE transgenic lines. (b) PCR products of GUS gene (1816 bp) amplified from GUS-OE transgenic lines. Numbers above the well represent the individual transgenic lines. M=1kb DNA ladder (1st BASE, Malaysia); N=negative control (wild-type tobacco); P=positive control (pMDC32 plasmid containing *EgCAD1* or GUS gene)



## Microalgae as Potential Antioxidants: Assessment of Antioxidant Capacities in Microalgae from Selected Regions of Peninsular Malaysia

Noor Amanina Awang<sup>1</sup>, Malinna Jusoh<sup>2</sup>, Nor Faizura Said<sup>2</sup>, Norhayati Yusuf<sup>2</sup>, Mohd Nizam Lani<sup>1,3</sup> and Fauziah Tufail Ahmad<sup>1,3\*</sup>

<sup>1</sup>Faculty of Fisheries and Food Science, Universiti Malaysia Terengganu, 21030 Kuala Nerus, Terengganu, Malaysia

<sup>2</sup>Faculty of Science and Marine Environment, Universiti Malaysia Terengganu, 21030 Kuala Nerus, Terengganu, Malaysia

<sup>3</sup>Institute of Climate Adaptation and Marine Biotechnology, Universiti Malaysia Terengganu, 21030 Kuala Nerus, Terengganu, Malaysia

### ABSTRACT

Antioxidants play critical roles in cellular defence mechanisms in both enzymatic and non-enzymatic forms within the intracellular and extracellular environments. While microalgae are recognised as a rich source of antioxidants, limited information is available on species native to Peninsular Malaysia that contain high antioxidant capacity for future applications. This study aimed to assess the antioxidant capacity of both enzymatic and non-enzymatic antioxidants in microalgae, particularly those cultivated locally in Malaysia, which are still scarce. Nineteen microalgae species collected from Kedah, Pahang, Terengganu and Johor were used in this study. Algal samples were cultured and harvested during the early stationary phase and then subjected

to antioxidant assays. Enzymatic antioxidants were assessed using catalase, ascorbate peroxidase and superoxide dismutase (SOD) assays. Non-enzymatic antioxidants were evaluated through the quantification of ascorbate,  $\alpha$ -tocopherol, and carotenoids. The findings reveal significant interspecies variation of microalgae in the types and quantities of antioxidants. Notably, *Neochloris conjuncta* and *Mychonastes ovahimbae* exhibited the highest levels of enzymatic antioxidants ( $p < 0.05$ ) and SOD. *Hematococcus* sp. had the highest concentration of ascorbic acid, while *Chlorella vulgaris* from Terengganu contained

### ARTICLE INFO

#### Article history:

Received: 07 February 2024

Accepted: 05 June 2024

Published: 28 January 2025

DOI: <https://doi.org/10.47836/pjtas.48.1.04>

#### E-mail addresses:

nooramanina.nina@yahoo.com (Noor Amanina Awang)

malinna@umt.edu.my (Malinna Jusoh)

faizurasaid@gmail.com (Nor Faizura Said)

yatiyusuf@umt.edu.my (Norhayati Yusuf)

nizamlani@umt.edu.my (Mohd Nizam Lani)

fauziah.tufail@umt.edu.my (Fauziah Tufail Ahmad)

\* Corresponding author

the most  $\alpha$ -tocopherol, both with statistical significance ( $p < 0.05$ ). The data suggest that *Chlorella vulgaris* from Terengganu possesses considerable potential as a renewable source of antioxidants for diverse industrial applications, including food ingredients.

*Keywords:* Ascorbate,  $\alpha$ -tocopherol, carotenoids, catalase, enzymatic, microalgae, non-enzymatic

---

## INTRODUCTION

Microalgae, a varied collection of photosynthetic microorganisms, has been recognised as a potential source of compounds with numerous applications. Due to their ability to combat oxidative stress, a physiological state associated with a variety of chronic diseases, aging, and cellular degeneration, antioxidants have become a focal point of interest in the scientific community. Biosynthesised by organisms and having bioactive properties, these compounds are of particular interest.

Numerous recent studies have highlighted the remarkable antioxidant capabilities of microalgae, indicating that these microscopic organisms may possess the same or even greater antioxidant qualities than traditionally recognised sources such as fruits and vegetables (Alwi, Ismail, Hatta, Buyong, & Mohamad, 2015; Alwi, Ismail, Hatta, Buyong, Jamil, et al., 2015; Hawksworth, 2020; Hossain et al., 2020; Le et al., 2017; Noor et al., 2007). The synergistic presence of carotenoids, tocopherols, phenolic compounds, and other bioactive chemicals positions microalgae as a potential goldmine for antioxidant research. Frequently, the capacity of these organisms to produce these chemicals exceeds that of terrestrial plants, possibly because of their evolutionary adaptations that thrive in harsh environments. Microalgae are gaining increasing attention due to their extensive ecological range, diverse characteristics, and minimal land requirement. These organisms have remarkable survival and growth rates, permitting them to thrive in a variety of demanding environments, including those typically regarded as unsuitable for numerous plant species (Darvehei et al., 2018). This characteristic enhances their efficacy in biotechnological applications, particularly when land availability is limited.

Carotenoids, a prominent class of bioactive substances abundant in microalgae, have recently received significant attention owing to their wide variety of health benefits. The 40-carbon chained lipophilic compounds are commonly found in microalgae inhabiting marine and freshwater environments. Based on their chemical composition, carotenoids can be classified into two categories: carotenes, which consist solely of hydrocarbons, and xanthophylls, which are distinguished by the presence of oxygenated functional groups (Lietz et al., 2012). Higher plants and microalgae can produce a variety of xanthophylls, including violaxanthin, antheraxanthin, zeaxanthin, neoxanthin, and lutein. However, certain xanthophylls, such as loroxanthin, astaxanthin, canthaxanthin, diatoxanthin, diadinoxanthin, and fucoxanthin, are generated exclusively by certain organisms, including

green microalgae, diatoms, and brown algae (Ahmed, 2015). Multiple scientific studies (Ali et al., 2014) have shown that microalgae possess significant antioxidant potential primarily due to the potent activity of these carotenoids.

Peninsular Malaysia is recognised as a centre for marine research due to its advantageous geographical location and abundant marine biodiversity. While Peninsular Malaysia is known for its abundant microalgal species, there is a significant research gap concerning the antioxidant properties of these species within the region. This gap presents a critical opportunity to explore and understand the factors influencing antioxidant capacities in microalgae, ultimately guiding the selection of species and regions for future product development. Addressing this gap is crucial for unlocking the untapped potential of microalgae as valuable sources of antioxidants and natural sources, which could have far-reaching implications for various industries and contribute to the sustainable utilisation of Peninsular Malaysia's rich aquatic biodiversity. Thus, this study aims to examine the relatively unexplored area of the antioxidant properties of microalgae. By shedding light on this overlooked aspect, the research seeks to elucidate the potential of microalgae as a natural and safe source of antioxidants and highlight the vast diversity of unexploited microalgal species in the region. The findings of this study are expected to contribute significantly to our understanding of the antioxidant capacities of microalgae and inform future research and product development.

In this study, 19 species of microalgae was used to determine the antioxidant properties includes *Chlorella* sp., different strains of *Chlorella vulgaris* (a, b, c, and d), *Neochloris conjuncta*, *Nephrochlamys ovahimbae*, *Mychonastes ovahimbae*, *Desmodesmus brasiliensis*, *Desmodesmus abundans*, *Nannochloropsis oceanica* (strains a and b), *Dicloster acuatius*, *Navicula pelliculosa*, *Tetraselmis chui*, *Isochrysis galbana*, *Botryosphaerella sudetica*, and *Hematococcus* sp. Their distribution and uniqueness additionally guide the selection of microalgae for this study. An overview of the geographical spread of microalgae species discussed across the Association of Southeast Asian Nations (ASEAN) countries is shown in Figure 1.

In addition to the visual representation in Figure 1, Table 1 provides a detailed summary of the species of microalgae, their distribution, and unique characteristics. This table offers a comprehensive overview of the data presented in this study. Based on the data presented in Table 1, the distribution patterns of microalgae across different regions may offer insights into why only certain species were identified in our study. Due to their proximity to the coast, the coastal or littoral zones of Peninsular Malaysia serve as essential microalgal reservoirs in addition to the terrestrial environments. These locations serve as abundant reservoirs and offer unique environmental conditions that can influence microalgal adaptation and interactions. The pH of bark, particularly in terrestrial environments, resembles the complex metabolic processes utilised by microalgae (Alwi, Ismail, Hatta,

Buyong, & Mohamad, et al., 2015; Alwi, Ismail, Hatta, Buyong, Jamil, et al., 2015). The involvement of these pathways in the production of antioxidants suggests that coastal areas have a great deal of potential as microalgal sources. In this investigation, enzymatic antioxidants was determined using assays for catalase, ascorbate peroxidase (APX), and SOD. Simultaneously, non-enzymatic antioxidants were evaluated by quantifying  $\alpha$ -tocopherol, ascorbic acid, and carotenoids. Our objective is to elucidate the potential of these enzymatic and non-enzymatic antioxidants across a spectrum of industries.

Given the rising global demand for natural antioxidants and the acknowledged biodiversity of Peninsular Malaysia, it is crucial to investigate the antioxidant capabilities of its native microalgae species. This study seeks to address the existing knowledge gap by concentrating on the untapped potential of Peninsular Malaysian microalgae as valuable antioxidant sources. In addition, it aims to elucidate the significance of these microalgae in the broader fields of health, nutrition, and ecological balance.



Figure 1. Global distribution of microalgae species across ASEAN countries

Table 1  
Distribution and uniqueness of microalgae species to ASEAN countries

Microalgae	Potential ASEAN distribution	Uniqueness
<i>Chlorella</i> sp. and <i>C. vulgaris</i>	Thailand, Malaysia, Indonesia, and the Philippines have all reported the presence of <i>Chlorella</i> species due to their vast freshwater resources.	As one of the most researched microalgae, its potential in biofuel, nutrition, and wastewater treatment is globally recognised. Its presence in ASEAN countries can contribute to local biotechnological developments.

Table 1 (continue)

Microalgae	Potential ASEAN distribution	Uniqueness
<i>Neochloris conjuncta</i>	Limited data exist, but freshwater bodies in countries like Malaysia or Indonesia might host this species.	It is not widely discussed in ASEAN literature, which can signify a potential new area of research.
<i>Desmodesmus brasiliensis</i> and <i>Desmodesmus abundans</i>	The " <i>brasiliensis</i> " suggests a Brazilian origin, but these species can be found in various freshwater habitats, potentially including countries like Vietnam, Thailand, or the Philippines.	Their resilience to environmental stressors might have implications for bioremediation efforts in the region.
<i>Nannochloropsis oceanica</i> *	Coastal countries like the Philippines, Indonesia, and Malaysia might host marine species like <i>Nannochloropsis</i> sp.	They are known for their high lipid content, making them prime candidates for biofuel research.
<i>Navicula pelliculosa</i> *	Both marine and freshwater habitats across ASEAN countries, potentially Thailand, Vietnam, and the Philippines.	As a diatom, its silica cell wall offers unique biotechnological applications.
<i>Tetraselmis chui</i> *	Marine environments, potentially in countries with vast coastlines, like the Philippines and Indonesia.	Popular in aquaculture, ASEAN, being a hub for aquaculture, can benefit from its cultivation.
<i>Nephrochlamys ovahimbae</i>	The specific ASEAN distribution is not clear from the last update. However, considering the diversity of freshwater habitats in countries like Laos, Cambodia, or Myanmar, it is conceivable they may host this or related species.	As it is not a commonly discussed microalgae in global literature, its presence and potential benefits in the ASEAN region could be an uncharted research area.
<i>Mychonastes ovahimbae</i>	The specific ASEAN distribution for this species is not clear. Freshwater habitats across countries, especially Indonesia and Malaysia, with their numerous lakes and ponds, might be places to explore.	Its rarity in common literature could make it an interesting candidate for detailed research in the ASEAN context.
<i>Dicloster acuatus</i>	It is likely in freshwater systems of countries like Vietnam, Thailand, or the Philippines.	Any unique metabolic or ecological properties discovered could affect regional biotechnological applications.
<i>Isochrysis galbana</i> *	It is a marine microalga, so coastal countries such as Indonesia, the Philippines, and Malaysia might be hosting this species with their vast marine ecosystems.	It is known for its nutritional value, especially in aquaculture, a major industry in many ASEAN countries.
<i>Botryosphaerella sudetica</i>	Freshwater habitats in countries with tropical climates, such as Malaysia, Thailand, and Indonesia, might be probable areas.	Detailed research on this species in the ASEAN context can shed light on any region-specific properties or benefits.
<i>Hematococcus</i> sp.*	Given the variety of this genus, it is conceivable that they can be found in both freshwater and marine environments in countries like Malaysia, Indonesia, and the Philippines.	<i>Hematococcus</i> is known for producing astaxanthin, a powerful antioxidant. Its cultivation and exploration in the ASEAN region can offer insights into the natural sources of this compound.

Note. \*Samples were collected from coastal areas within the respective ASEAN countries. The focus on coastal regions reflects the specific scope of this study and its relevance to understanding microalgae distribution in coastal environments

## MATERIALS AND METHODS

### Microalgae Cultivation

Freshly collected microalgae samples, including *C. vulgaris*, *N. conjuncta*, *N. ovahimbae*, *M. ovahimbae*, *D. brasiliensis*, *D. abundans*, *N. oceanica*, *D. acuatus*, *N. pelliculosa*, *T. chui*, *I. galbana*, *B. sudetica*, and *Hematococcus* sp, were cultured and maintained at the SATREPS-COSMOS Laboratory, Universiti Malaysia Terengganu. The microalgae cells were cultured in three replicates of conical flasks, with a concentration of  $1 \times 10^5$  cells/ml, using Bold's Basal Media (Sigma, Germany) (Kanz & Bold, 1969). Throughout the study, the cultures were exposed to continuous light-emitting diode lamps (2,000 lux) at  $24 \pm 2^\circ\text{C}$ .

### Microalgae Harvesting

Cultures were harvested during the early stationary growth phase, specifically on day 13, as described by Zakaria et al. (2020). A Beckman Coulter Allegra X-30R Centrifuge (Germany) was used to harvest the microalgal cultures. The cultures were centrifugated at  $11180 \times g$  for 10 min at  $4^\circ\text{C}$ . The pellets were subsequently used for phytochemical and antioxidant activity analyses.

### Enzymatic Antioxidant Assays

Using a method adapted from Price et al. (1994), the specific activity of SOD was analysed. 0.1 g of freshly collected samples underwent homogenisation in 2 ml of 0.1 M phosphate buffer (pH 7.0, Bioenno Tech, USA) with the use of a pre-chilled mortar and pestle and then centrifuged at  $10,000 \times g$  (Hettich Universal 32R, Germany) at  $4^\circ\text{C}$  for 10 min (Beauchamp & Fridovich, 1971). To 1.0 ml of buffer solution containing 50 mM phosphate buffer (Bioenno Tech, USA) with 0.1 mM ethylenediaminetetraacetic acid (EDTA, pH 7.8, GBiosciences, USA), 0.1 mM nitro blue tetrazolium (NBT, Sigma-Aldrich, USA), 0.048 mM xanthine oxidase (Sigma-Aldrich, U.S.A), and 0.05 mM xanthine (Sigma-Aldrich, U.S.A), 100 L of unprocessed extract was added. At 560 nm, the SOD activity was analysed spectrophotometrically (Shimadzu UV-1601, Japan). The amount of SOD needed to reduce the rate of NBT reduction by 50% is defined as one unit, and the specific activity of SOD was calculated as units/mg protein.

To calculate units of SOD activity in assayed fraction:

The rate of  $\Delta\text{Abs } 560$  increased from 2.5-5.5 min = Rate B

Initial rate of  $\Delta\text{Abs } 560$  from 0-2.0 min = Rate A

$$\therefore \% \text{ Decline in } A_{560} \text{ increase} = \frac{A - B}{A} \times 100\%$$

$$\begin{aligned} \therefore \text{Units of SOD activity /mg protein} &= \frac{\% \text{ Decline in A560 increae}}{50\% \times \text{mg protein}} \\ &= \text{Unit SOD/mg protein} \end{aligned}$$

### ***Catalase Activity Test (CAT) Assay***

CAT-specific activity was assessed using the procedure by Claiborne (1985). About 0.15 g of the sample was homogenised with 1.0 ml of 50 mM phosphate buffer (pH 7.4), cleaned in a pre-chilled mortar, and pestled. Following this, the homogenate underwent centrifugation (Eppendorf 5840R, Switzerland) at  $11180 \times g$  at  $4^{\circ}\text{C}$  for 10 min. The mixture contained 3.0 ml of 19 mM hydrogen peroxide ( $\text{H}_2\text{O}_2$ ) (Fisher Scientific, USA) in 50 mM phosphate buffer (pH 7.0, Bioenno Tech, USA) and 100  $\mu\text{l}$  of the extract. The change in absorbance rate was observed at 240 nm using a spectrophotometer (Shimadzu UV-1800, Japan). CAT-specific activity was determined in  $\mu\text{mol}$  of  $\text{H}_2\text{O}_2$  consumed per min per mg of protein.

### ***APX Assay***

APX-specific activity was evaluated using the method outlined by Nakano and Asada (1981). Approximately 0.15 g of sample was homogenised using a pre-chilled mortar and pestle with 1.0 ml of 1 mM of ascorbic acid (Scharlau, Spain) in a 100 mM phosphate buffer (pH 7.0; Bioenno Tech, U.S.A) at  $0-4^{\circ}\text{C}$ . This homogenate was centrifuged (Eppendorf 5840R, Switzerland) at  $11180 \times g$  at  $4^{\circ}\text{C}$  for 10 min. The reaction mixture contained 1.5 ml of 100 mM phosphate buffer (pH 7.0, Bioenno Tech, USA), 0.5 ml of 3 mM ascorbic acid (Scharlau, Spain, 0.1 ml of 3 mM EDTA (GBioscience, U.S.A), 0.3 ml of distilled water, and 0.2 ml of 1.5 mM  $\text{H}_2\text{O}_2$  was added into 200  $\mu\text{l}$  of the enzyme extract. The absorbance rate of the reaction mixture was measured at 290 nm using the spectrophotometer (Shimadzu UV-1800, Japan).

## **Non-enzymatic Antioxidant Assays**

### ***$\alpha$ -tocopherol Assay***

The extraction of  $\alpha$ -tocopherol was done following the protocol developed by Hodges et al. (1996). This procedure was conducted under subdued lighting and on an ice bed. Fresh microalgae samples weighing 0.15 g were homogenised in a mixture containing 1.5 ml acetone (Emsure, Germany) and fine sand. Subsequently, the homogenate was mixed with 0.5 ml hexane (Emsure, Germany), vortexed for 30 s, and centrifuged at  $11180 \times g$  for 10 min. The supernatant was then carefully decanted, and the extraction process was repeated twice. The assay formulation was prepared in alignment with the guidelines provided by Kanno and Yamauchi (1997). Subsequently, 0.5 ml of the hexane-extracts were combined

with 0.4 ml of 0.1% (w/v) 3-(2-pyridyl)-5,6-diphenyl-1,2,4 triazine, solubilised in ethanol (PDT, Emsure, Germany) and 0.4 ml 0.1% (w/v) ferric chloride (Sigma-Aldrich, U.S.A). The total volume was adjusted to 3.0 ml using absolute ethanol (Emsure, Germany). After gentle agitation, the mixture was allowed to stand for 4 min to facilitate colour development. Then, 0.2 ml of 0.2 M orthophosphoric acid (Sigma-Aldrich, USA) was added and left to stabilise for 30 min at ambient temperature prior to spectrophotometric measurement at 554 nm.

### ***Ascorbic Acid Assay***

All procedures were conducted under subdued light conditions to prevent photodegradation. Fresh samples weighing 0.15 g were ground using a pre-chilled mortar and pestle in 1.0 ml of 10% trichloroacetic acid (TCA, Emsure, Germany) under ice-cold conditions (Jagota & Dani, 1982). The mixture was centrifuged at  $3044 \times g$  for 10 min at 4°C using an Eppendorf 5840R (Switzerland) centrifuge. After that, 300 µl of the supernatant was diluted with 1,700 µl of distilled water and treated with 200 µl of 10% Folin reagent (Sigma-Aldrich, USA). The mixture was softly agitated and allowed to stand on the bench in subdued light for 10 min prior to the absorbance reading at 760 nm. Following the same procedure described above, 300 µl ascorbic acid was introduced into the solution, and the quantity of ascorbic acid in the sample was determined using the standard curve.

### ***Carotenoids Assay***

The carotenoid amounts were quantified using the Lichtenthaler method (1987). Samples were processed under dim light conditions and on a cold bed of ice to ensure sample integrity. Fresh leaf tissue samples weighing 0.02 g were homogenised with 3.0 ml of 80% (v/v) acetone (Emsure, Germany) The mixture was centrifuged at  $11180 \times g$  for 10 min. Subsequently, the absorbances of the collected supernatant were assessed at three distinct wavelengths: 663.2, 646.8, and 470 nm.

## **RESULTS AND DISCUSSION**

### **Enzymatic Antioxidant Assay**

Results of the concentration of enzymatic antioxidant capacity (CAT, APX, and SOD) towards 19 species of microalgae collected along the Peninsular Malaysia coastal area were shown as follows (Figures 2-5).

Figure 2 illustrates that microalgal species from Terengganu exhibit the highest catalase activity compared to those from Kedah, Pahang, and Johor. Notably, *C. vulgaris* (strain c) demonstrated the highest activity, with 1.405 units/mg protein, followed by *N. oceanica* (strain b) and *D. acuatius*. On the contrary, species from Johor, Kedah, and Pahang displayed low CAT activities and were not significantly different ( $p > 0.05$ ).



Figure 3 depicts APX activity varied from 0.025 to 1.078 units/mg protein. The maximum APX activity was assayed from *N. oceanica* (strain a), followed by *C. vulgaris*, and *Hemotococcus* sp. However, the species with the lowest APX activity was *C. vulgaris*, but different strains with 0.025 units/mg protein. *N. oceanica* demonstrated superior enzymatic antioxidant activities, particularly in CAT and APX. However, it lagged in SOD activities (Figure 4). The SOD activity of these microalgae ranged considerably, from 23.985 to 0.375 (units/mg protein), with *N. conjuncta* and *M. ovahimbae* manifesting significantly higher SOD activities compared to the other species examined. In contrast, the SOD activities in the remaining species were considerably lower and significantly different from those two species.

In essence, microalgae, being photosynthetic organisms, generate reactive oxygen species (ROS) through both enzymatic and non-enzymatic pathways. Scientific research has firmly established the detrimental effects on cellular structure and functions due to increased oxidative stress. Antioxidant enzymes such as ascorbate oxidase, peroxidase, catalase, and ascorbate peroxidase serve as cellular detoxifying agents in cells (Hakiman & Maziah, 2009). In this study, highly significant variances in mean squares for CAT, APX, and SOD were observed across species, indicating species-specific enzymatic antioxidant defence mechanisms.

Several factors, such as the microalgae’s aquatic habitat and environmental stressors like metal exposure or pH fluctuations, may contribute to the variations in antioxidant

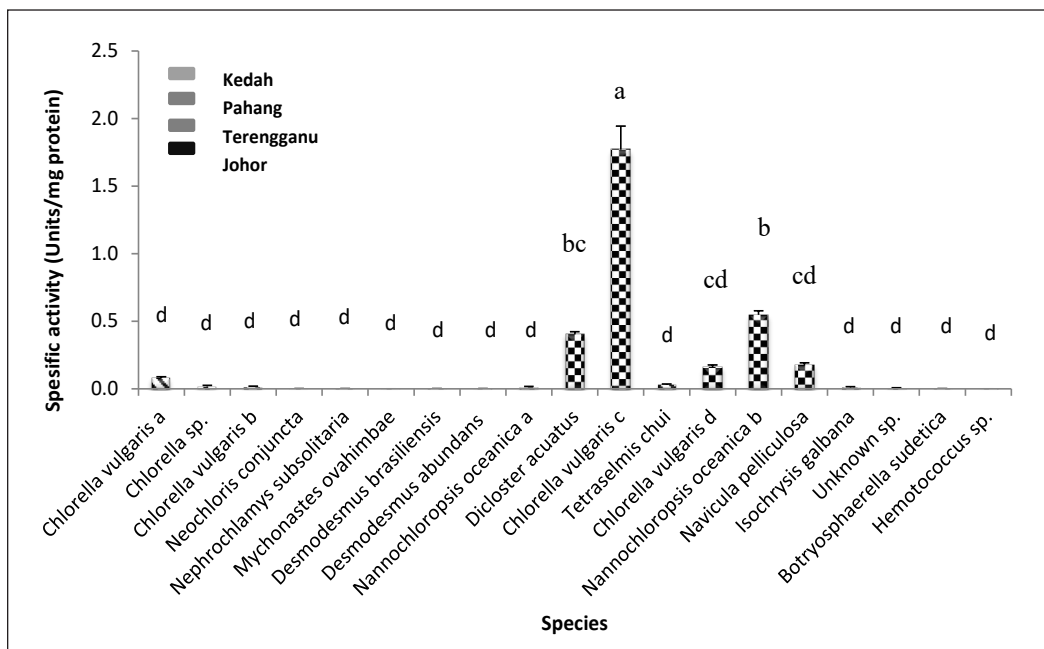


Figure 2. Catalase activity in different species of microalgae collected from selected regions in Peninsular Malaysia

Note. Data are means ± standard errors. Different letters in the graph represent significantly different at  $p < 0.05$

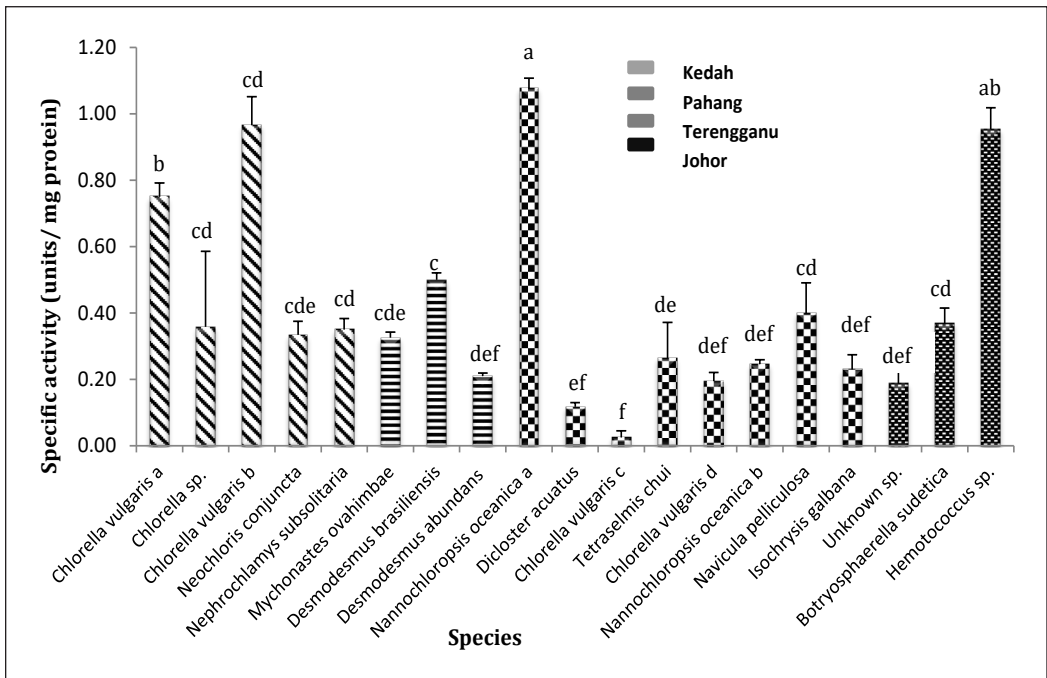


Figure 3. Ascorbate peroxidase (APX) activity in different species of microalgae collected from selected regions in Peninsular Malaysia

Note. Data are means ± standard errors. Different letters in the graph represent significantly different at  $p < 0.05$

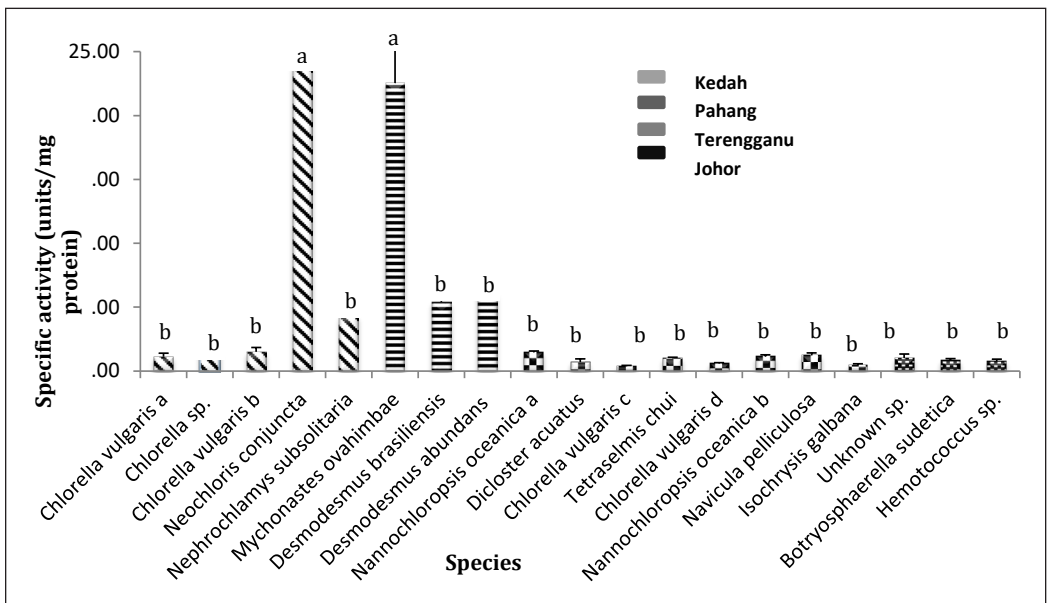


Figure 4. Superoxide dismutase (SOD) activity in different species of microalgae collected from selected regions in Peninsular Malaysia

Note. Data are means ± standard errors. Different letters in the graph represent significantly different at  $p < 0.05$

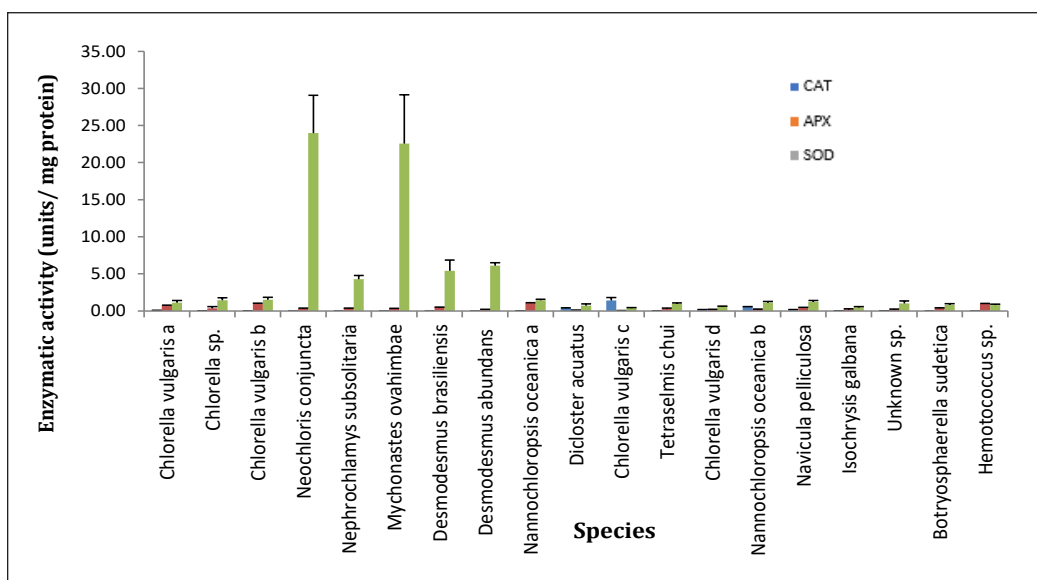


Figure 5. Comparison of enzymatic antioxidant activities (catalase [CAT], ascorbate peroxidase [APX], and superoxide dismutase [SOD]) in different species of microalgae from selected regions in Peninsular Malaysia

enzyme activities (Gauthier et al., 2020). For example, the elevated CAT activity in *C. vulgaris* from Terengganu, a marine environment, may attributed to these environmental variables.

APX is predominantly localised in the chloroplasts and cytoplasm of cells, and it has a greater affinity for  $H_2O_2$  than CAT, making it crucial for ROS detoxification (Gauthier et al., 2020). APX activities of microalgae were the highest in green microalgae such as *N. oceanica* and *C. vulgaris*, which is similar to Hakiman and Maziah (2009), who said APX activities were found to be higher in the leaves extracts than roots and stems extract due to the location of APX in the chloroplast. Green microalgae tend to contain higher chloroplast than brown microalgae or blue-green microalgae. It suggests higher APX activity corresponds to greater antioxidant potential in these green microalgae species. Variation in enzymatic antioxidant activities among different microalgae species indicates that each species uniquely develops its antioxidant mechanisms in response to its surroundings.

SOD is an important antioxidant enzyme found in all subcellular compartments of aerobic organisms that are susceptible to ROS-mediated oxidative damage (Danouche et al., 2020). Elevated SOD activities in *N. conjuncta* and *M. ova-himbae* may reflect their adaptive responses to environmental stress, as suggested by Kumar et al. (2014). Antioxidant enzymes like SOD are important in eliminating ROS generated within microalgae as part of their response to diverse physical and chemical stressors. These two species likely arise from environmental stress conditions. However, compared to other plants like citrus, microalgae produce lower SOD activities (23.99 units/mg

protein) compared to citrus (284.00 units/mg protein) (Arbona et al., 2003). Despite that, microalgae are way more convenient to be cultivated in a very short time. Microalgae, as photosynthesising plant cells, can experience photooxidative damage under extremely high light and oxygen conditions, which require microalgae to produce cells that possess protective, antioxidative mechanisms, and compounds that lead to the production of various antioxidants (Kumar et al., 2014). It necessitates the production of cells that possess protective antioxidative mechanisms and compounds, leading to the generation of various antioxidants. Therefore, higher SOD and APX activities in our microalgae samples imply higher antioxidant activity, indicating that these species can produce significant antioxidant defences under stress conditions.

### Non-enzymatic Antioxidant Assay

Figures 6–9 represent the non-enzymatic antioxidant assay in microalgae species collected from selected places in Peninsular Malaysia.

Our analysis of non-enzymatic antioxidants revealed distinct patterns varying with species. According to Figure 6, the highest ascorbate content was found in a *Hematococcus* sp. collected from Johor, followed by *Nephrochlamys subsolitaria* from Kedah. Meanwhile, *C. vulgaris* from Terengganu was found to be the highest in  $\alpha$ -tocopherol, as per Figure 7, and *N. pelliculosa* exhibited the highest in carotenoid levels, as illustrated in Figure 8. Figure 9 further accentuates that  $\alpha$ -tocopherol predominates as the most abundant antioxidant in most of the analysed microalgae, with *C. vulgaris* containing the highest levels.

Although the samples were derived from various locations, the underlying factors causing the observed differences in antioxidant properties across species remain unclear. The possibility of this explanation is due to abiotic stresses that can induce antioxidant properties in Malaysian indigenous microalgae and cyanobacterium (Azim et al., 2018). These variations could stem from morphological differences between species or be influenced by the environmental conditions in their respective habitats. Previous research suggests that elevated oxidative stress can stimulate antioxidant activity in microalgae (Chokshi et al., 2017). Moreover, microalgae exposed to specific environmental stressors, such as metal contamination, fluctuating pH levels, and nutrient scarcity, tended to exhibit higher ascorbate, carotenoids and  $\alpha$ -tocopherol content (Gauthier et al., 2020).

It is noteworthy that  $\alpha$ -tocopherol, also known as vitamin E, was the predominant antioxidant in our study. It could be attributed to its crucial role in protecting cellular structures from oxidative damage by scavenging free radicals (Szewczyk et al., 2021).

The higher  $\alpha$ -tocopherol content in *C. vulgaris* from Terengganu could respond to specific environmental stressors prevalent in the Terengganu coastal waters, such as high ultraviolet radiation, fluctuating salinity, and temperature variations. Additionally, Terengganu's well-known petroleum extraction activities (offshore drilling) may introduce

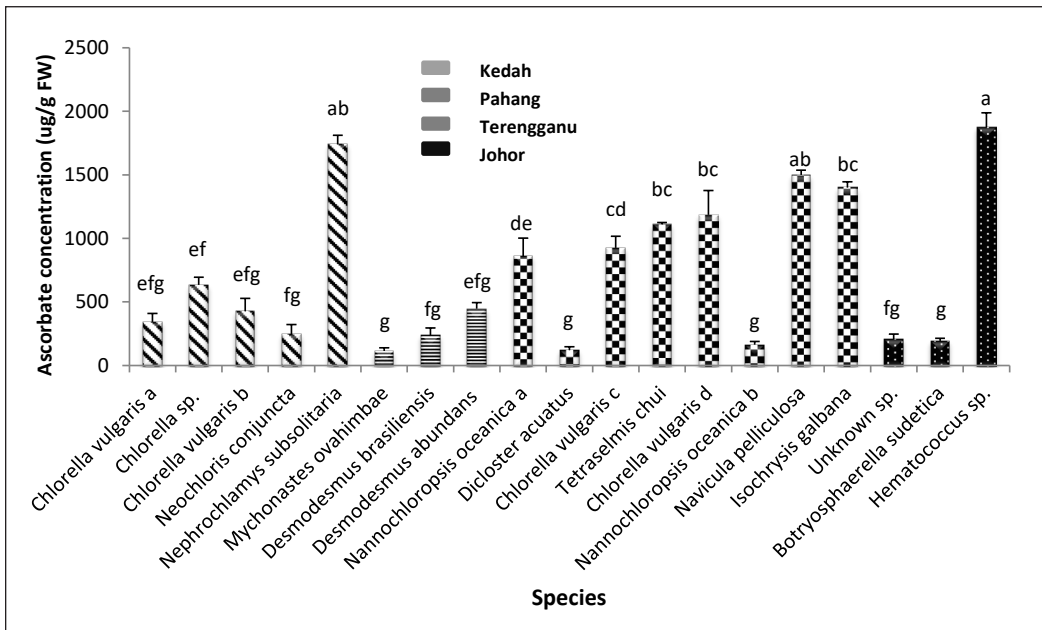


Figure 6. Ascorbate concentration ( $\mu\text{g/g FW}$ ) in different species of microalgae collected from selected regions in Peninsular Malaysia

Note. Data are means  $\pm$  standard errors. Different letters in the graph represent significantly different at  $p < 0.05$

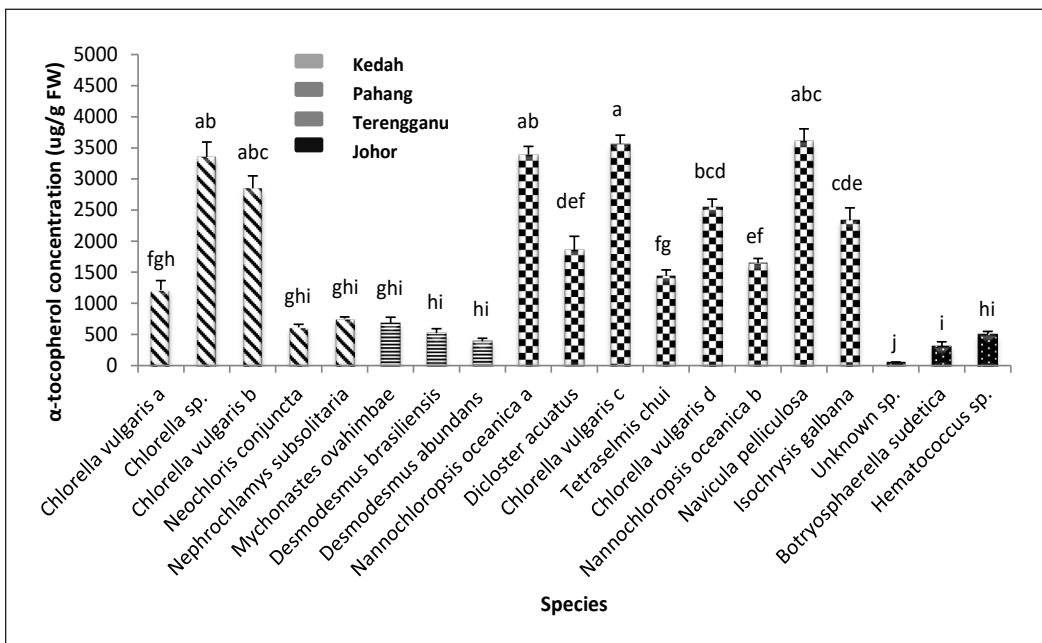


Figure 7.  $\alpha$ -tocopherol concentration ( $\mu\text{g/g FW}$ ) in different species of microalgae collected from selected regions in Peninsular Malaysia

Note. Data are means  $\pm$  standard errors. Different letters in the graph represent significantly different at  $p < 0.05$

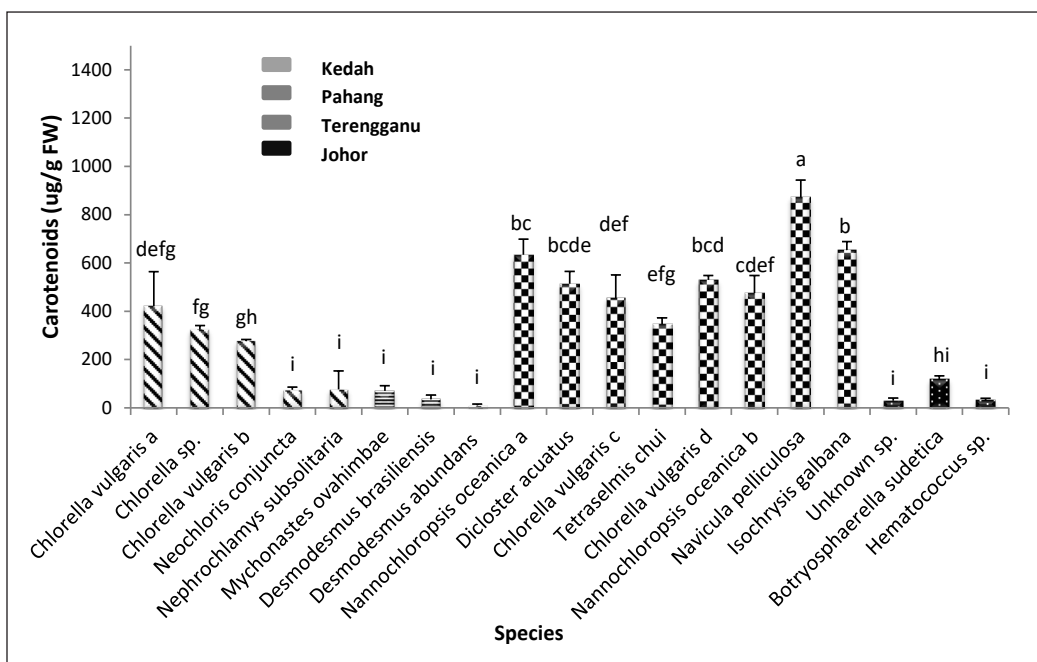


Figure 8. Carotenoids content (ug/g FW) in different species of microalgae collected from selected regions in Peninsular Malaysia

Note. Data are means ± standard errors. Different letters in the graph represent significantly different at  $p < 0.05$

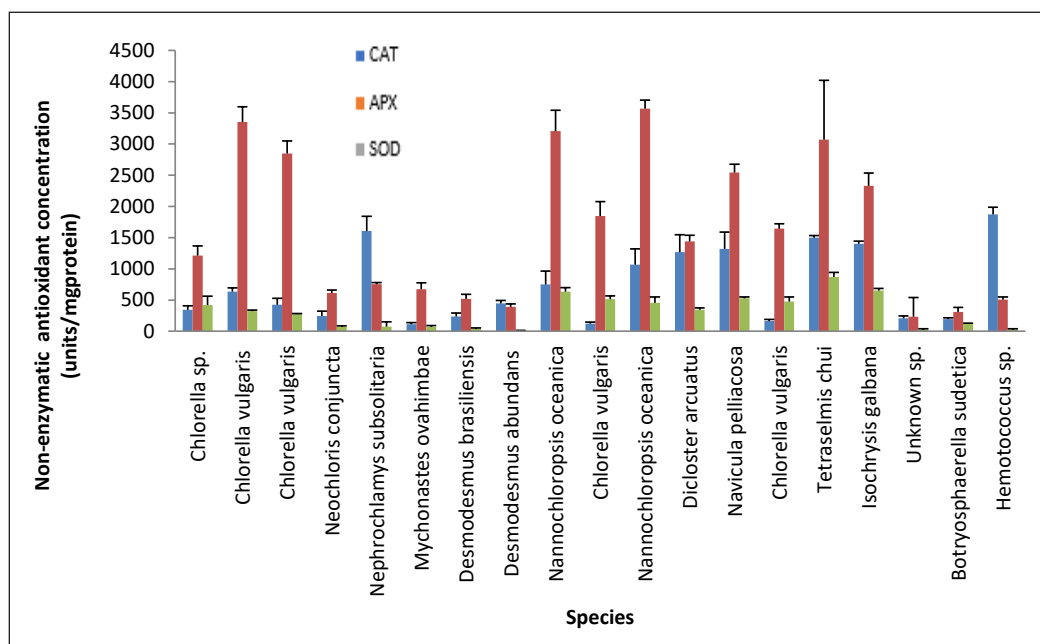


Figure 9. Comparison of non-enzymatic antioxidant (ascorbate,  $\alpha$ -tocopherol, and carotenoids) concentration ( $\mu\text{g/g FW}$ ) in different species of microalgae collected from selected regions in Peninsular Malaysia

metal contaminants and other pollutants into the marine environment, inducing oxidative stress in microalgae and thereby enhancing the synthesis of  $\alpha$ -tocopherol as a protective mechanism (Azim et al., 2018).

Additionally, research has shown that tocopherols can be extracted, purified, or concentrated from higher plant substances, including *Spirulina*, *Dunaliella tertiolecta*, and *Chlorella* sp. (Ogbonna, 2009). Furthermore, the oceanographic conditions in Terengganu, including nutrient availability and water quality, may create a conducive environment for the synthesis of  $\alpha$ -tocopherol in microalgae. The presence of specific nutrients and the overall quality of the water can significantly influence the metabolic pathways involved in antioxidant production (Poot-Delgado & Pkplodkov, 2016; Xiao et al., 2023). Therefore, the abundant  $\alpha$ -tocopherol content in microalgae from Terengganu might reflect an adaptive response to these environmental factors.

Despite these insights, the exact factors contributing to the variations in antioxidant properties among different species of microalgae in Peninsular Malaysia remain speculative. This study unequivocally underscores the potential applications of these microalgae based on their valuable properties.

However, to gain a more comprehensive understanding, it is suggested that the perimeter of the sampling area be expanded with additional parameters such as the physical properties of microalgae, pH changes, metal exposure, weather conditions, water salinity, and nutrient content.

## CONCLUSION

This study successfully screened and identified the antioxidant composition and capacity of various microalgae species collected from the selected coastal areas of Peninsular Malaysia. The findings demonstrate that the antioxidant profiles are species-specific and possibly influenced by their habitat. Specifically, *N. conjuncta* and *M. ovahimbae* exhibited the highest enzymatic antioxidant activities, particularly in SOD concentrations. Additionally, *Hematococcus* sp. showed the highest ascorbic acid content, while *C. vulgaris* from Terengganu was found to have the richest concentration of  $\alpha$ -tocopherol. The results indicate that microalgae from Terengganu, particularly, are abundant in antioxidants, highlighting the potential of this region as a valuable source of natural antioxidants. These findings align with the study's objective to explore and compare the antioxidant capacities of different microalgae species from various regions, providing insights into their potential applications in health and wellness.

Overall, this study underscores the significant diversity of antioxidant compounds in microalgae and their promising potential as natural sources of antioxidants. Future research should focus on the isolation and detailed characterisation of these compounds, as well as the exploration of their bioactivity and possible commercial applications.

## ACKNOWLEDGEMENTS

The authors would like to thank Universiti Malaysia Terengganu for all the facilities and support for the research. This research was supported by the Japan Science and Technology Agency (JST)/ Japan International Cooperation Agency (JICA), Science and Technology Research Partnership for Sustainable Development (SATREPS) through the project for Continuous Operation System for Microalgae Production Optimised for Sustainable Tropical Aquaculture (COSMOS) (Grant Vot. No. JPMJSA1509).

## REFERENCES

- Ahmed, F. (2015). *Induction of carotenoid and phytosterol accumulation in microalgae* [Doctoral thesis, University of Queensland]. UQ eSpace. <https://doi.org/10.14264/uql.2015.808>
- Ali, H. E. A., Shanab, S. M. M., Abo-Aly, M., Shalaby, E., Eldermerdash, U., & Abdullah, M. A. (2014). Screening of microalgae for antioxidant activities, carotenoids and phenolic contents, *Applied Mechanics and Materials*, 625, 156–159. <https://doi.org/10.4028/www.scientific.net/AMM.625.156>
- Alwi, I., Ismail, A., Hatta, S. K. M., Buyong, F., & Mohamad, N. (2015). Bark pH as a factor affecting the density of epiphytic terrestrial algae in Taman Wetland Putrajaya, Malaysia. *Journal of Applied and Physical Sciences*, 1(1), 13-18. <https://doi.org/10.20474/-japs1.1.3>
- Alwi, I., Ismail, A., Hatta, S. K. M., Buyong, F., Jamil, N. M., Sidek, N. J., Wahab, N. A., & Ismail, A. (2015). Bark pH as a factor affecting number of algal density of epiphytic terrestrial algae in Putrajaya, Malaysia. *Proceeding of Global Trends in Academic Research*, 2, 362–371.
- Arbona, V., Flors., V., Jacas, J., García-Agustín, P., & Gómez- Cadenas, A. (2003). Enzymatic and non-enzymatic antioxidant responses of Carrizo citrange, a salt-sensitive citrus rootstock, to different levels of salinity. *Plant and Cell Physiology*, 44(4), 388–394. <https://doi.org/10.1093/pcp/pcg059>
- Azim N., H., Subki, A., & Yusof, Z., N. (2018) Abiotic stresses induce total phenolic, total flavonoid and antioxidant properties in Malaysian indigenous microalgae and cyanobacterium. *Malaysian Journal of Microbiology*, 14(1), 25-33. <https://doi.org/10.21161/MJM.100317>
- Beauchamp, C., & Fridovich, I. (1971). Superoxide dismutase: Improve assays and an assay applicable to acrylamide gels. *Analytical Biochemistry*, 44(1), 276-287. [https://doi.org/10.1016/0003-2697\(71\)90370-8](https://doi.org/10.1016/0003-2697(71)90370-8)
- Chokshi, K., Pancha, I., Ghosh, A., & Mishra, S. (2017) Salinity induced oxidative stress alters the physiological responses and improves the biofuel potential of green microalgae *Acutodesmus dimorphus*. *Bioresource Technology*, 244, 1376-1383. <https://doi.org/10.1016/j.biortech.2017.05.003>
- Claiborne, A. L. (1985). Catalase activity. In R. A. Greenwald (Ed.), *Handbook of method for oxygen radical research* (pp. 283-284). CRC Press.
- Danouche, M., Ghachtouli, N. E., Baouchi, A. E., & Arroussi, H. E. (2020). Heavy metals phycoremediation using tolerant green microalgae: Enzymatic and non-enzymatic antioxidant systems for the management of oxidative stress. *Journal of Environmental Chemical Engineering*, 8(5), 1-11. <https://doi.org/10.1016/j.jece.2020.104460>



- Darvehei, P., Bahri, P. A., & Moheimani, N. R. (2018). Model development for the growth of microalgae: A review. *Renewable and Sustainable Energy Reviews*, *97*, 233–258. <https://doi.org/10.1016/j.rser.2018.08.027>
- Gauthier, M. R., Senhorinho, G. N. A., & Scott, J. A. (2020) Microalgae under environmental stress as a source of antioxidants. *Algal Research*, *52*, 1-10. <https://doi.org/10.1016/j.algal.2020.102104>
- Hakiman, M., & Maziah, M. (2009). Non enzymatic and enzymatic antioxidant activities in aqueous extract of different *Ficus deltoidea* accessions. *Journal of Medicinal Plants Research*, *3*(3), 120–131.
- Hawksworth, D. L. (2020). Books on biodiversity and conservation. *Biodiversity Conversation*, *29*, 3843-3862. <https://doi.org/10.1007/s10531-020-02054-x>
- Hodges, D. M., Andrews, C. J., Johnson, D. A., & Hamilton, R. I. (1996). Antioxidant compound responses to chilling stress in differentially sensitive inbred maize lines. *Physiologia Plantarum*, *98*(4), 685-692. <https://doi.org/10.1034/j.1399-3054.1996.980402.x>
- Hossain, N., Hasan, M. H., Mahlia, T. M. I., Shamsuddin, A. H., & Silitonga, A. S. (2020). Feasibility of microalgae as feedstock for alternative fuel in Malaysia: A review. *Energy Strategy Reviews*, *32*, 100536. <https://doi.org/10.1016/j.esr.2020.100536>
- Jagota, S., & Dani, H. (1982). A new colorimetric technique for the estimation of vitamin C using Folin phenol reagent. *Analytical Biochemistry*, *127*(1), 178-182. [https://doi.org/10.1016/0003-2697\(82\)90162-2](https://doi.org/10.1016/0003-2697(82)90162-2)
- Kanno, C., & Yamauchi, K. (1997). Application of a new iron reagent, 3-(2-Pyridyl)-5,6-diphenyl-1,2,4-triazine, to spectrophotometric determination of tocopherols. *Agricultural and Biological Chemistry*, *41*(3), 593-596. <https://doi.org/10.1080/00021369.1977.10862541>
- Kanz, T., & Bold, H. C. (1969). *Physiological studies, morphological and taxonomical investigation of Nostoc and Anabaena in culture*. University of Texas Press.
- Kumar, R. R., Rao, P. H., Subramanian, V. V., & Sivasubramanian. (2014) Enzymatic and non-enzymatic antioxidant potentials of *Chlorella vulgaris* grown in effluent of a confectionery industry. *Journal of Food Science and Technology*, *51*, 322–328. <https://doi.org/10.1007/s13197-011-0501-2>
- Le, Q. D., Haron, N. A., Tanaka, K., Ishida, A., Sano, Y., Dung, L. V., & Shirai, K. (2017). Quantitative contribution of primary food sources for a mangrove food web in Setiu lagoon from East coast of Peninsular Malaysia, stable isotopic ( $\delta^{13}\text{C}$  and  $\delta^{15}\text{N}$ ) approach. *Regional Studies in Marine Science*, *9*, 174-179. <https://doi.org/10.1016/j.risma.2016.12.013>
- Lichtenthaler, H. K. (1987). Chlorophylls and carotenoids: Pigments of photosynthetic biomembranes. *Methods in enzymology*, *146*, 350-382. [https://doi.org/10.1016/0076-6879\(87\)48036-1](https://doi.org/10.1016/0076-6879(87)48036-1)
- Lietz, G., Oxley, A., Boesch-Saadatmandi, C., & Kobayashi, D. (2012). Importance of  $\beta,\beta$ -carotene 15,15'-monooxygenase 1 (BCMO1) and  $\beta,\beta$ -carotene 9',10'-dioxygenase 2 (BCDO2) in nutrition and health. *Molecular Nutrition and Food Research*, *56*(2), 241-250. <https://doi.org/10.1002/mnfr.201100387>
- Nakano, Y., & Asada, K. (1981). Hydrogen peroxide is scavenged by ascorbate-specific peroxidase in spinach chloroplasts. *Plant and Cell Physiology*, *22*(5), 867-880. <https://doi.org/10.1093/oxfordjournals.pcp.a076232>
- Noor, N. M., Anton, A., & Amin, N. M. (2007). Biodiversity of dinoflagellates in the coastal waters off Malacca, Peninsular Malaysia. *Borneo Science*, *21*(1), 12-18.

- Ogbonna, J. C. (2009). Microbiological production of tocopherols: Current state and prospects. *Applied Microbiology and Biotechnology*, 84, 217- 225. <https://doi.org/10.1007/s00253-009-2104-7>
- Poot-Delgado, C. A., & Pkplodkov, Y. B. (2016). *Microalgae as water quality indicators: An overview*. Nova Science Publishers.
- Price, A. H., Taylor, A., Ripley, S. J., Griffiths, A., & Trewavas, A. J. (1994). Oxidative signals in tobacco increase cytosolic calcium. *The Plant Cell*, 6(9), 1301-1310. <https://doi.org/10.2307/3869827>
- Xiao, X., Li, W., Jin, M., Zhang, L., Qin, L., & Geng, W. (2023). Responses and tolerance mechanisms of microalgae to heavy metal stress: A review. *Marine Environmental Research*, 183, 105805. <https://doi.org/10.1016/j.marenvres.2022.105805>
- Zakaria, M. F., Haris, N., Abd Wahid, M. E., Katayama, T., & Jusoh, M. (2020). Isolation and Nile red screening of indigenous microalgae species Pahang lakes potential lipid source in aquaculture feed. *Malaysian Applied Biology*, 49(4), 149-156. <https://doi.org/10.55230/mabjournal.v49i4.1606>

## Low-sodium Chaya Leaf Seasoning Powder with Potassium Chloride Substitution: Nutritional, Antioxidant, and Microbial Quality Assessment

Theeraphol Senphan<sup>1</sup>, Kotchaporn Puangtong<sup>1</sup>, Benyapa Namdamrassiri<sup>1</sup>, Chodsana Sriket<sup>2\*</sup>, Md. Sazedul Hoque<sup>3</sup>, Supatra Karnjanapratum<sup>4</sup> and Patcharaporn Narkthewan<sup>2</sup>

<sup>1</sup>Program in Food Science and Technology, Faculty of Engineering and Agro-Industry, Maejo University, Sansai, Chiangmai 50290, Thailand

<sup>2</sup>Food Innovation and Management Program, Department of General Science and Liberal Arts, King Mongkut's Institute of Technology Ladkrabang, Prince of Chumphon Campus, Pathiu, Chumphon 86160, Thailand

<sup>3</sup>Department of Fisheries Technology, Faculty of Fisheries, Patuakhali Science and Technology University, Dumki, Patuakhali-860, Bangladesh

<sup>4</sup>Division of Marine Product Technology, Faculty of Agro-Industry, Chiang Mai University, Chiang Mai 50100, Thailand

### ABSTRACT

This study investigates the development of a low-sodium seasoning powder using Chaya (*Cnidoscolus chayamansa*), popularly known as Mexican spinach, by substituting sodium chloride (NaCl) with potassium chloride (KCl) at various ratios. The antioxidant capabilities of dried Chaya leaves, dried at 60°C for five hours, were tested using 2,2-Diphenyl-1-picrylhydrazyl (DPPH), Ferric reducing antioxidant power (FRAP), and 2,2'-azino-bis-(3-ethylbenzothiazoline-6-sulfonic acid (ABTS) techniques, demonstrating excellent free radical scavenging activity and making it suitable for low sodium seasoning compositions. The substitution of 25% KCl was the most favored option, as it effectively balanced flavor and health advantages without causing noticeable changes

in appearance, color, and aroma. This recipe successfully reduced the sodium content to 1171 mg/100 g while maintaining Chaya's original nutritional values, which include 23.57 g/100 g of protein, 4.77 g/100 g of fats, and 54.12 g/100 g of carbohydrates, as well as dietary fibers. Additionally, the formulation demonstrated physicochemical stability, as indicated by an ash content of 14.00 g/100 g, moisture content of 3.51 g/100g, and a total energy of 353.69 kcal/100 g. The safety of this new seasoning is validated by its microbiological quality, which

### ARTICLE INFO

#### Article history:

Received: 08 May 2024

Accepted: 09 July 2024

Published: 28 January 2025

DOI: <https://doi.org/10.47836/pjtas.48.1.05>

#### E-mail addresses:

theeraphol\_s@mju.ac.th (Theeraphol Senphan)

kcp.oangkor@gmail.com (Kotchaporn Puangtong)

kbennerr@gmail.com (Benyapa Namdamrassiri)

chodsana.sr@kmitl.ac.th (Chodsana Sriket)

sazedul.fst@pstu.ac.bd (Sazedul Hoque)

supatra.ka@cmu.ac.th (Supatra Karnjanapratum)

patcharaporn.na@kmitl.ac.th (Patcharaporn Narkthewan)

\* Corresponding author

is indicated by a total bacterial count of  $2.6 \times 10^4$  cfu/g and the absence of mold and yeast. This emphasizes the potential of the seasoning to promote healthy dietary choices by reducing sodium intake without affecting sensory appeal.

*Keywords:* Antioxidant activity, Chaya leaf, KCl, low-sodium seasoning, nutrients

---

## INTRODUCTION

The increasing occurrence of hypertension and cardiovascular diseases (CVDs), significant global health issues, is closely linked to the use of large amounts of dietary sodium. Although much evidence connects salt intake to higher risks of hypertension and CVDs, attempts to address these health concerns through dietary changes encounter substantial obstacles (Kario et al., 2024). In response, the World Health Organization (WHO) has set an ambitious target to lower global salt consumption by 30% by 2025, a strategy intended to mitigate the prevalence of chronic health issues (Rybicka et al., 2022). Despite these clear objectives, developing palatable low-sodium food alternatives remains a formidable challenge, often compromised by the difficulty of maintaining the desirable taste and flavor profiles that consumers demand. Recent efforts have predominantly focused on replacing sodium chloride (NaCl) with other salts, such as potassium chloride (KCl), which can maintain ionic strength and enhance flavors without the adverse health effects of high sodium levels. Research by He et al. (2021) has shown that achieving up to a 30% reduction in sodium without significantly affecting taste perception, establishing a practical threshold for sodium reduction in food products is possible. Furthermore, innovative approaches have explored incorporating natural ingredients with inherent health benefits.

For example, Kingwascharapong et al. (2024) have studied the substitution of sodium with potassium and calcium salts in snack foods, reducing sodium levels and enhancing the mineral contents, which are beneficial for cardiovascular health. Likewise, the utilization of herbal and plant-based ingredients, such as Chaya (*Cnidoscolus chayamansa*), commonly known as Mexican spinach, offers the dual benefits of reducing sodium while enriching the nutritional and antioxidant properties of food products (Loarca-Piña et al., 2010). Despite these advancements, replacing sodium chloride with alternative salts often fails to adequately satisfy health benefits and consumer taste preferences (Kingwascharapong et al., 2024). Moreover, the potential of integrating underexplored natural ingredients with favorable health attributes into seasoning powders remains largely untapped. Chaya, for instance, is highly nutritious but seldom used in culinary product development (Hutasingh et al., 2023). This research aims to bridge these gaps by examining the use of potassium chloride as a substitute for sodium chloride and incorporating Chaya leaves into the formulation of a low-sodium seasoning powder. This study seeks to meet WHO's salt reduction targets and enhance dietary options' palatability

and health benefits, thereby addressing the dual challenge of reducing sodium intake and enriching food products with health-promoting ingredients. Through this approach, the study contributes to the expanding field of food science and public health nutrition, exploring Chaya's potential to broaden the array of ingredients available for creating healthier dietary choices.

## MATERIALS AND METHODS

### Preparation of Chaya Leaf Powders

Fresh Chaya leaf (*C. chayamansa*) samples were collected from Mueang Surat Thani District, Surat Thani Province, and brought to the Food Innovation and Management Laboratory, King Mongkut's Institute of Technology Ladkrabang, Prince of Chumphon Campus, Chumphon Province. The samples were washed with clean water and blanched in boiling water for 2 min. After that, the Chaya samples were dried at 60°C for 5 h. The dried samples were ground using a grinder (MX-T2G National, Japan) and then sieved through an 80-mesh sieve (with a diameter of 0.1 mm) to obtain a uniformly sized powder. The Chaya leaf powder was then packed into plastic bags and vacuum-sealed before being stored in a freezer (-20°C) for no more than two months before the samples were analyzed and used to develop seasoning powder from Chaya leaf powders.

### Antioxidant Activity of Chaya Leaf Powder

#### *Preparation of Ethanolic Chaya Leaf Powder Extract*

Chaya leaf powder (10 g) was mixed with 350 mL of 60% (v/v) ethanol (Lab-Scan, Thailand). The mixture was stirred for 3 h, followed by filtering (Buamard & Benjakul, 2019). The supernatant, referred to as 'Chaya leaf extract,' was placed in an amber bottle, capped tightly and kept in a cold condition during analyses.

#### *Analyses*

***DPPH Radical Scavenging Activity (DPPH-RA).*** The 2,2-Diphenyl-1-picrylhydrazyl (DPPH) activity of an extract from Chaya leaf powder was examined according to the method described by Tagrida and Benjakul (2021). A diluted sample (0.3 ml) was mixed with 2.7 ml of 0.15 mM DPPH in methanol (Lab-Scan, Bangkok, Thailand), shaken and incubated for 60 min at 25°C in the dark. The decrease in optical density (OD) at 517 nm using spectrophotometer (VIS-7235, Rayleigh, Beijing, China) monitored the DPPH reduction.

***ABTS Radical Scavenging Activity (ABTS-RA).*** 2,2'-azino-bis-(3-ethylbenzothiazoline-6-sulfonic) acid (ABTS) radical scavenging activity of extract from Chaya leaf powder was

determined according to the method described by Karnjanapratum and Benjakul (2015). A diluted sample (150  $\mu$ L) was mixed with ABTS solution (2850  $\mu$ L) and incubated for 1 h at room temperature in the dark. Absorbance 734 nm was read with spectrophotometer. Blank was prepared using distilled water instead of a sample.

***Ferric-reducing Antioxidant Power (FRAP).*** The FRAP of an extract from Chaya leaf powder was determined following the method of Benjakul et al. (2012). The sample solution (150  $\mu$ L) was mixed with 2.85 mL of working FRAP reagent, and the mixture was incubated in the dark at room temperature for 30 min. The absorbance at 593 nm was read using spectrophotometer.

### **Production of Chaya Seasoning Powder Using Potassium Chloride (KCl) to Replace Sodium Chloride (NaCl)**

The seasoning powder formula used in the research obtained from the preliminary results of our research team (data not shown) was used as the standard formula (salt; NaCl 22.7 g, sugar 26.6 g, Chaya leaf powder 30.7 g, fish powder 16.0 g, pepper powder 2.0 g, and garlic powder 2.0 g) to study the suitable ratios for substituting KCl for NaCl at replacement levels of 0, 25, 50, 75, and 100 percent, resulting in five experiments (Table 1), each replicated three times, as shown in Table 1. Then, considering the appearance of the produced seasoning powder before and after dissolving it in hot water, sensory evaluation, proximate composition, color values, moisture content, water activity, and pH values of the product were determined. The nutrition values of the best recipe were also determined.

Table 1  
*The percentage of potassium chloride used to replace sodium chloride in Chaya leaf seasoning powder*

Salts (%)	Formulas				
	1	2	3	4	5
NaCl	100	75	50	25	0
KCl	0	25	50	75	100

### ***Sensory Evaluation***

Samples were prepared as soup by boiling 20 g of Chaya leaf seasoning powder in 1 L of boiling water for 3 min. Then, 30 mL of the soup were placed into heat-resistant plastic cups with tight-fitting lids and kept in a temperature-controlled cabinet at 70°C, awaiting sensory evaluation by 60 untrained panelists. The evaluation assessed the sensory characteristics of aroma, taste, saltiness, sweetness, bitterness, and overall liking using a 9-point hedonic scale, with scores ranging from 1 (disliked extremely) to 9 (liked extremely). The sample with the highest acceptance score was selected to test the other parameters.

### ***Proximate Composition Determination***

The amounts of moisture, ash, fat, protein, and dietary fiber in the Chaya leaf seasoning powder samples were analyzed according to the standard methods of Association of Official Analytical Chemists (AOAC) 2011. The carbohydrate content was determined by subtracting the other components in the Chaya leaf powder samples. Sodium content was also determined according to the AOAC 2012.

### ***Color Values Determination***

The color values of the Chaya leaf seasoning powder samples were measured using a colorimeter (HunterLab's Color Flex EZ<sup>®</sup>, USA) and reported in terms of L\* (lightness), a\* (redness/greenness), and b\* (yellowness/blueness). Furthermore, the entire color difference, denoted as  $\Delta E^*$ , was computed utilizing the subsequent equation 1:

$$\Delta E^* = \sqrt{(\Delta L^*)^2 + (\Delta a^*)^2 + (\Delta b^*)^2} \quad [1]$$

Where  $\Delta L^*$ ,  $\Delta a^*$ , and  $\Delta b^*$  denote the disparities between the color characteristics of the specimen and the white reference standard ( $L^* = 93.63$ ,  $a^* = -0.94$ , and  $b^* = 0.40$ ).

### ***Water Activity ( $A_w$ )***

The low-sodium seasoning powder sample from Chaya leaf was analyzed for water activity ( $A_w$ ) using an AquaLab Series 3 water quality meter (USA). A sample of the seasoning powder, weighing approximately 1 g, was placed into the measurement cell of the water activity meter. The sample was evaluated in triplicate and performed at room temperature.

### ***pH Determination***

The pH values of various Chaya leaf seasoning powder formulas were analyzed using a pH meter (Euteon Instruments, Singapore). The powder was dissolved in hot water before analysis.

### ***Nutritional Values and Microbial Quality Determination***

Moisture, protein, total fat, total carbohydrate, ash and sodium content were determined according to the AOAC 2012. Total sugar (Kongkaew et al., 2014), cholesterol content was determined using AOAC Official Method 994.10 (direct saponification-gas chromatographic method), total energy (Calorie calculation), total bacteria was analyzed following AOAC Official Method 966.23 (Aerobic Plate Count at 35°C, 21<sup>st</sup> ed 2019), Mold and Yeast counts were determined according to AOAC Official Method 997.02 (Yeast and Mold Counts in Foods, Dry Rehydratable Film Method, 19<sup>th</sup> ed 2012) were also determined.

## Statistical Analysis

The experiment was conducted in triplicate for each factor studied. The data variance was analyzed using Analysis of Variance (ANOVA) to compare the differences between the factors studied with Duncan's Multiple Range Test. Data analysis was performed using Statistical Package for the Social Sciences (SPSS) statistical software (SPSS 10.0 for Windows, SPSS Inc., Chicago, USA) at a 95% confidence level.

## RESULTS AND DISCUSSION

### Antioxidant Capacity

The antioxidant activities of fresh and dried Chaya leaves at a temperature of 60°C for 5 h, measured by DPPH, FRAP, and ABTS assays, are shown in Table 2. The antioxidant properties in Chaya leaves, which were dried, demonstrated a substantial increase in antioxidant capabilities, particularly as observed through the DPPH, FRAP, and ABTS assays. The DPPH radical scavenging activity of dried leaves increased significantly from  $35.96 \pm 1.29$   $\mu\text{mol}$  Trolox equivalent (TE)/g in fresh specimens to  $654.23 \pm 5.53$   $\mu\text{mol}$  TE/g. Similarly, the ABTS and FRAP values showed a significant increase from  $86.28 \pm 1.11$  and  $29.64 \pm 0.86$   $\mu\text{mol}$  TE/g to  $1465.94 \pm 16.73$  and  $425.77 \pm 6.48$   $\mu\text{mol}$  TE/g, respectively. The significant increase in antioxidant capacity after drying indicates the important function of the drying process in not only concentrating natural bioactive components but also potentially creating new antioxidant substances. The increase in value highlights the importance of incorporating dried Chaya leaves into the diet due to their strong ability to fight oxidative stress. Chaya is an excellent ingredient for health-enhancing food items like low-sodium spice powders. Adding Chaya to these products could reduce sodium consumption and enhance the nutritional composition by adding powerful antioxidant qualities (Carlsen et al., 2010; Pandey & Rizvi, 2009). These findings correspond with previous research, confirming the important role of natural antioxidants in preventing chronic diseases and promoting overall health. Therefore, incorporating dried Chaya leaves into food products and nutraceuticals is a commendable strategy for improving health outcomes by increasing antioxidant intake.

Table 2

*The antioxidant activity of fresh and dried chaya using the DPPH, ABTS<sup>+</sup>, and FRAP assays after exposure to 60°C for 5 h*

Analytical methods	Samples	
	Fresh Chaya leaf	Dried Chaya leaf
DPPH radical scavenging activity ( $\mu\text{mol}$ TE/g sample)	$35.96 \pm 1.29^b$	$654.23 \pm 5.53^a$
ABTS radical scavenging activity ( $\mu\text{mol}$ TE/g sample)	$86.28 \pm 1.11^b$	$1465.94 \pm 16.73^a$
FRAP ( $\mu\text{mol}$ TE/g sample)	$29.64 \pm 0.86^b$	$425.77 \pm 6.48^a$

Note. \* Mean  $\pm$  SD ( $n=3$ ). Different letters in the same row indicate significant differences ( $p<0.05$ )



## Sensory Attributes

The sensory evaluation of the seasoning powders with various levels of KCl substitution is shown in Table 3. The results showed a marked preference for the 25% KCl substitution level, attaining an overall acceptability rating of  $6.25 \pm 0.22$ . The decrease in consumer acceptance at KCl levels above 25% can be attributed to reduced saltiness and some consumers' potential detection of a bitter metallic taste. This dual impact highlights the importance of balancing KCl substitution to maintain flavor and consumer satisfaction. This finding signifies a willingness among consumers to accept moderate sodium reductions if the sensory quality is maintained, suggesting KCl as a feasible NaCl alternative without compromising taste, appearance, aroma, or flavor. Such sensory acceptance is crucial for the success of healthier food options in the market, as Drewnowski and Rehm (2014) highlighted. Additionally, insights from Grimes et al. (2009) and Sarmugam et al. (2013) underscore the influence of consumer awareness and socio-demographic factors on dietary choices, emphasizing the need for educational strategies to enhance acceptance of low-sodium products.

Furthermore, the study reveals the minimal impact of KCl substitution on the sensory attributes of the seasoning powders, indicating that Chaya's distinct qualities, combined with KCl, can effectively maintain or enhance the product's appeal. It aligns with the understanding that comprehensive consumer education and targeted communication strategies, based on accurate salt knowledge and correcting misconceptions, could facilitate broader acceptance of such health-oriented innovations.

Table 3

*Sensory properties of Chaya leaf seasoning powder with a low sodium content that replaces sodium chloride with various potassium chloride recipes*

Likeness scores	Percentage of sodium chloride replaced by potassium chloride				
	Control	25%	50%	75%	100%
Appearance	7.43±1.07 <sup>*a</sup>	7.52±1.06 <sup>a</sup>	7.47±1.03 <sup>a</sup>	7.22±1.90 <sup>a</sup>	7.08±2.04 <sup>a</sup>
Color	7.62±1.02 <sup>a</sup>	7.68±1.20 <sup>a</sup>	7.68±1.00 <sup>a</sup>	7.45±1.71 <sup>a</sup>	7.38±1.85 <sup>a</sup>
Odor	6.67±1.27 <sup>a</sup>	6.95±1.17 <sup>a</sup>	6.77±1.06 <sup>a</sup>	6.60±1.02 <sup>a</sup>	6.57±0.85 <sup>a</sup>
Saltiness	6.95±1.12 <sup>a</sup>	6.83±1.01 <sup>a</sup>	5.57±1.16 <sup>b</sup>	5.47±1.92 <sup>b</sup>	5.17±1.00 <sup>b</sup>
Umami	7.12±1.00 <sup>a</sup>	7.35±0.17 <sup>a</sup>	5.63±1.08 <sup>b</sup>	5.47±1.84 <sup>b</sup>	5.17±1.10 <sup>b</sup>
Overall	6.87±1.10 <sup>a</sup>	6.25±0.22 <sup>a</sup>	5.47±1.00 <sup>b</sup>	5.50±1.72 <sup>b</sup>	5.00±1.07 <sup>b</sup>

*Note.* \*Value mean ± standard deviation ( $n=60$ ). Different superscripts within the same row indicate significant differences ( $p<0.05$ )

## Sodium Reduction

The salt content of seasoning powder from Chaya leaf with various levels of KCl substitution is depicted in Table 4. The findings indicated that the salt level was reduced proportionately to the rise of KCl in the incorporated seasoning ( $p<0.05$ ). A compelling

link between consumer acceptance and the health benefits of reduced sodium intake was previously reported. The sensory evaluation highlighting a preference for the 25% KCl substitution level, with an overall acceptability rating of  $6.25 \pm 0.22$ , demonstrates that moderate sodium reduction is feasible and well-received when the sensory quality of the seasoning powder is preserved. Without compromising taste, appearance, aroma, or flavor, this preference for a lower sodium option mirrors the critical public health need to reduce sodium consumption, as substantial sodium reduction to  $0.30 \pm 0.23$  mg NaCl/g in the 100% KCl substitution sample directly addresses the risks associated with high sodium intake, such as hypertension and cardiovascular diseases (Aburto et al., 2013; He et al., 2021).

The willingness among consumers to embrace such moderate sodium reductions, underscored by the maintained sensory appeal of the KCl-substituted seasoning powder, suggested that KCl served as a practical NaCl substitute. It aligns with Drewnowski and Rehm's (2014) emphasis on the importance of sensory acceptance for the success of healthier food products and is supported by studies exploring the impact of consumer knowledge and socio-demographic factors on dietary choices (Grimes et al., 2009; Sarmugam et al., 2013). The minimal impact of KCl substitution on the sensory attributes of the seasoning powders, particularly when combined with Chaya's unique qualities, not only maintains but potentially enhances the product's appeal, offering a healthier alternative that does not sacrifice flavor for sodium reduction.

This strategic approach to developing low-sodium seasoning options, which balance sensory quality with significant health benefits, contributes to broader public health efforts to mitigate diet-related risks by providing a viable solution for reducing sodium intake. By ensuring the sensory quality of reduced-sodium products, we encourage wider consumer acceptance, supporting the goal of lowering the incidence of hypertension and cardiovascular diseases linked to excessive sodium consumption.

### Chemical Compositions

The chemical component of seasoning powder from Chaya leaves with low sodium that replaced sodium chloride with potassium chloride at a rate of 25% is illustrated in Table 5. The seasoning powder had a high content of carbohydrates ( $42.50\% \pm 1.23\%$ ), protein ( $25.83\% \pm 0.91\%$ ), ash ( $25.16\% \pm 0.39\%$ ) and fiber ( $17.01\% \pm 0.78\%$ ) contents. Including

Table 4  
*The salt content of seasoning powder from Chaya leaves with low sodium that replaces sodium chloride with potassium chloride at various contents*

Potassium chloride (%)	Sodium chloride content (mg NaCl/g sample)
0%	$189.00 \pm 0.02^{*a}$
25%	$141.00 \pm 0.10^b$
50%	$69.00 \pm 0.48^c$
75%	$46.00 \pm 0.16^d$
100%	$0.30 \pm 0.23^c$

Note. \*Values mean  $\pm$  standard deviation ( $n=3$ ). Different superscripts within the same column indicate significant differences ( $p<0.05$ )

Chaya leaf powder in the development of seasoning powders provided a low-sodium alternative and significantly enhanced the nutritional profile of the products. Chaya, known for its superior nutrient density compared to conventional leafy vegetables, is rich in essential minerals like calcium, iron, potassium, and vitamins such as vitamin C and  $\beta$ -carotene, alongside notable levels of protein, fat, ash, carbohydrates, and dietary fiber (Kuti & Kuti, 1999). These findings emphasized the nutritional benefits of incorporating Chaya into seasoning powders. They supported the global initiative to recognize the value of neglected and underutilized species in improving food and nutritional security. This strategic integration of Chaya into food products reaffirms its multifaceted benefits, supporting efforts to diversify diets with underutilized plants for improved health outcomes.

Table 5

*Chemical components of seasoning powder from Chaya leaves with low sodium that replace sodium chloride with potassium chloride at a rate of 25%*

Protein (%)	Lipid (%)	Ash (%)	Carbohydrate (%)	Fiber (%)
25.83 $\pm$ 0.91 <sup>*b</sup>	5.24 $\pm$ 0.30 <sup>d</sup>	25.16 $\pm$ 0.39 <sup>b</sup>	42.50 $\pm$ 1.23 <sup>a</sup>	17.01 $\pm$ 0.78 <sup>c</sup>

*Note.* \*Value mean  $\pm$  standard deviation ( $n=3$ ). Different superscripts within the same row indicate significant differences ( $p<0.05$ )

### Moisture Content, Water Activity ( $A_w$ ), and pH

The moisture content, water activity and pH of the selected formulation (25% KCl substitution) are shown in Table 6. The selected formulation had a moisture content of  $3.4 \pm 0.05\%$ , water activity ( $A_w$ ) of  $0.43 \pm 0.01$ , and pH of  $6.45 \pm 0.1$ , suggesting the enhanced stability and safety for the practical use of the low-sodium seasoning powder in various culinary applications. Recent studies highlight the critical role of these physicochemical properties in food preservation. For instance, low water activity significantly reduces the risk of microbial growth by limiting water availability necessary for microbial metabolism, thus contributing to the product's safety and extended shelf-life (Beuchat, 1983; Erkmen & Bozoglu, 2016). Furthermore, the pH level within this range can effectively suppress the growth of spoilage-causing microorganisms, ensuring the product's longevity (Smith et al., 2010).

Incorporating ingredients like Chaya (*C. chayamansa*) and using KCl as a sodium substitute exemplify innovative approaches to creating nutritious products that meet

Table 6

*Moisture content, water activity ( $A_w$ ) and pH of seasoning powder from Chaya leaves with low sodium that replaces sodium chloride with potassium chloride at a rate of 25%*

Recipe	Moisture (%)	Water activity ( $A_w$ )	pH
25% Substituted	3.4 $\pm$ 0.05 <sup>*</sup>	0.43 $\pm$ 0.01	6.45 $\pm$ 0.1

*Note.* \*Value mean  $\pm$  standard deviation ( $n=3$ )

health-conscious consumers' needs (Ramírez et al., 2021). The seasoning powder's physicochemical stability suggests its utility in the food industry. It provides a viable ingredient for manufacturing products consistent with sodium reduction public health initiatives to address diet-related health concerns, such as hypertension and cardiovascular disease.

### Color Values

The color value of seasoning powder derived from Chaya leaves, which has a reduced sodium content by replacing sodium chloride with potassium chloride at a ratio of 25%, is presented in Table 7. Color analysis revealed minimal changes in the color attributes of the seasoning powder with KCl substitution, maintaining its visual appeal. Preservation of color is crucial for consumer acceptance, as visual cues play a significant role in food choice (Spence et al., 2016). The ability to retain color attributes while reducing sodium content further supports the feasibility of KCl substitution in producing visually appealing, healthier food products.

Table 7

*Color values of seasoning powder from Chaya leaves with low sodium that replaces sodium chloride with potassium chloride at a rate of 25%*

Recipe	Color values			
	L*	a*	b*	ΔE*
25% Substituted	40.89 ± 0.41*	-5.89 ± 0.07	18.95 ± 0.26	5.40 ± 0.17

Note. \*Mean ±, Standard deviation (n=3)

### Nutritional Values and Microbial Quality

The seasoning powder contains a high amount of protein (25.57 g per 100 g) due to fish meat in the Chaya leaf seasoning powder. This combination resulted in a higher protein level than that of many plant-based products on their own, hence improving the nutritional composition of the powder. Inosine from fish protein and glutamate from Chaya leaf work together to improve the umami flavor in foods seasoned with this low-sodium powder, making the sensory experience more enjoyable. The study by Hutasingh et al. (2024) revealed the substantial influence of drying techniques on the aromatic attributes and umami constituents of Chaya leaves. This research establishes the foundation for understanding how these factors contribute to the seasoning powder's high protein content and its ability to enhance umami taste.

The carbohydrate content of 54.12 g/100 g and fat content of 4.77 g/100 g in the low-sodium seasoning powder contribute to its substantial energy source of 353.69 Kcal/100 g. These nutritional values, indicative of a nutritionally dense product, suggest that while

the seasoning powder is nutritious, it should be consumed in moderation within a balanced diet to avoid excessive caloric intake. The presence of fish meat in the seasoning blend, which is known for its high protein and essential amino acids content, further complements the powder's nutritional profile by enhancing the overall taste and mouthfeel of the food products it seasons (Kingwascharapong et al., 2023). Moreover, the incorporation of Chaya leaf not only adds to the product's nutritional value by providing dietary fibers but also enriches it with glutamate, a natural umami-enhancing compound, synergistically working with inosine present in the fish meat to enhance the umami flavor, a key aspect in the acceptability of low-sodium food products (Kingwascharapong et al., 2023).

The study highlights the sodium content as a key aspect, which has been lowered to 1171 mg/100 g. However, it is important to consume it cautiously to adhere to global dietary guidelines for reducing sodium intake. Minimizing the risks connected with high blood pressure and cardiovascular illnesses is crucial. This decrease is crucial, emphasizing the difficulty of balancing taste preferences and health concerns in developing low-sodium food products. The salt content of the powder was significantly reduced to 698.33 mg/100 g, suggesting a possible approach for attaining large sodium reduction without negatively affecting the sensory characteristics. In a study conducted by Kingwascharapong et al. (2023), the researchers examined the replacement of NaCl with alternative salts such as KCl and calcium chloride (CaCl<sub>2</sub>) in smoked green mussel products. The study highlighted the importance of choosing and using sodium substitutes carefully to maintain the quality of the product while reducing its sodium content. This research supports the ongoing efforts to develop healthier food choices.

The low-sodium seasoning powder has a minimal cholesterol content of 2.13 mg/100 g, corresponding to dietary standards that recommend reducing cholesterol intake. This highlights the product's positive impact on heart health. The Chaya leaf reduced sodium seasoning powder is a valuable addition to the food sector due to its unique characteristics and extensive nutritional advantages. It provides a healthier alternative to traditional seasoning solutions. The study conducted by Cicero et al. (2020) examines the effects of commonly used seasonings and cooking fats on arterial stiffness and blood lipid patterns in a sample of individuals from a rural population. The findings of this research highlight the importance of selecting healthier fats to enhance lipid profiles and potentially lower the risk of cardiovascular disease. This seasoning powder suits consumers who want to reduce their sodium and cholesterol intake without affecting taste or quality. It maintains the original nutritional properties of Chaya and guarantees food safety through careful control of microbiological purity.

Furthermore, evaluating the microbial quality of the newly developed low-sodium seasoning powder demonstrates remarkable compliance with food safety regulations, as no mold or yeast was found, and the overall bacterial count was  $2.6 \times 10^4$  cfu/g. This result

indicates adhering to strict manufacturing standards and the product's durability. The lack of mold and yeast, as emphasized in our research, aligns with the results of Odamtten et al. (2018), who investigated the microbiological content and potential toxicity of imported spice powders in the Ghanaian market, emphasizing the significance of ensuring microbial safety in food items. Through rigorous microbiological quality control measures, our low-sodium seasoning powder provides a dependable component for culinary purposes. It is safer for consumers who want to decrease sodium consumption without sacrificing food safety or sensory satisfaction.

## CONCLUSION

Chaya leaf-based seasoning powder effectively reduced sodium levels by replacing NaCl with KCl without compromising taste. A 25% substitution of KCl was found to optimally balance health benefits with consumer satisfaction, significantly reducing the sodium content and demonstrating KCl's efficacy as a sodium substitute. The seasoning powder exhibited a low cholesterol level of 2.13 mg/100g. It maintained a balanced nutrient profile, consisting of 23.57 g/100g protein, 54.12 g/100g carbohydrates, and 4.77 g/100g fats while ensuring excellent microbiological safety. Additionally, the high antioxidant activity of Chaya leaves enhanced the nutritional value of the seasoning powder, suggesting the potential for a longer shelf life. These findings underscore the feasibility of introducing low-sodium seasoning options that do not sacrifice flavor for health, supporting broader public health efforts to reduce dietary sodium intake.

## ACKNOWLEDGEMENTS

The research obtained financial support from King Mongkut's Institute of Technology Ladkrabang under grant No. KREF186620, given to Asst. Prof. Dr. Chodsana Sriket.

## REFERENCES

- Aburto, N. J., Ziolkovska, A., Hooper, L., Elliott, P., Cappuccio, F. P., & Meerpohl, J. J. (2013). Effect of lower sodium intake on health: Systematic review and meta-analyses. *British Medical Journal*, *346*, f1326. <https://doi.org/10.1136/bmj.f1326>
- Benjakul, S., Kittiphattanabawon, P., Sumpavapol, P., & Maqsood, S. (2012). Antioxidant activities of lead (*Leucaena leucocephala*) seed as affected by extraction solvent, prior dechlorophyllisation and drying methods. *Journal of Food Science and Technology*, *49*(6), 785-791. <https://doi.org/10.1007/s13197-012-0846-1>
- Beuchat, L. R. (1983). Influence of water activity on growth, metabolic activities and survival of yeasts and molds. *Journal of Food Protection*, *46*(2), 135-141. <https://doi.org/10.4315/0362-028X-46.2.135>
- Buamard, N., & Benjakul, S. (2019). Effect of ethanolic coconut husk extract and pre-emulsification on properties and stability of surimi gel fortified with seabass oil during refrigerated storage. *LWT - Food Science and Technology*, *108*, 160-167. <https://doi.org/10.1016/j.lwt.2019.03.038>

- Carlsen, M. H., Halvorsen, B. L., Holte, K., Böhn, S. K., Dragland, S., Sampson, L., & Barikmo, I. (2010). The total antioxidant content of more than 3100 foods, beverages, spices, herbs, and supplements used worldwide. *Nutrition Journal*, *9*, 3. <https://doi.org/10.1186/1475-2891-9-3>
- Cicero, A. F. G., Fogacci, F., Grandi, E., Rizzoli, E., Bove, M., D'Addato, S., & Borghi, C. (2020). Prevalent seasoning and cooking fats, arterial stiffness, and blood lipid pattern in a rural population sample: Data from the Brisighella Heart Study. *Nutrients*, *12*(10), 3063. <https://doi.org/10.3390/nu12103063>
- Drewnowski, A., & Rehm, C. D. (2014). Sodium intakes of US children and adults from foods and beverages by location of origin and by specific food source. *Nutrition Journal*, *13*, 41. <https://doi.org/10.1186/1475-2891-13-41>
- Erkmen, O., & Bozoglu, T. F. (Eds.). (2016). *Food preservation by reducing water activity*. Academic Press. <https://doi.org/10.1002/9781119237860.ch30>
- Grimes, C. A., Riddell, L. J., Campbell, K. J., & Nowson, C. A. (2009). Dietary salt intake, sugar-sweetened beverage consumption, and obesity risk. *Pediatrics*, *123*(1), 131-139. <https://doi.org/10.1542/peds.2008-2195>
- He, F. J., Campbell, N. R. C., Woodward, M., & MacGregor, G. A. (2021). Salt reduction to prevent hypertension: The reasons of the controversy. *European Heart Journal*, *42*(25), 2501-2505. <https://doi.org/10.1093/eurheartj/ehab274>
- Hutasingh, N., Chuntakaruk, H., Tubtimrattana, A., Ketngamkum, Y., Pewlong, P., Phaonakrop, N., Roytrakul, S., Rungrotmongkol, T., Paemane, A., Tansrisawad, N., Siripatrawan, U., & Sirikantaramas, S. (2023). Metabolite profiling and identification of novel umami compounds in the chaya leaves of two species using multiplatform metabolomics. *Food Chemistry*, *404*(PartA), 134564. <https://doi.org/10.1016/j.foodchem.2022.134564>
- Hutasingh, N., Tubtimrattana, A., Pongpamorn, P., Pewlong, P., Paemane, A., Tansrisawad, N., Kario, K., Okura, A., Hoshide, S., & Mogi, M. (2024). The WHO Global report 2023 on hypertension warning the emerging hypertension burden in globe and its treatment strategy. *Hypertension Research*, *47*, 1099-1102. <https://doi.org/10.1038/s41440-024-01622-w>
- Karnjanapratum, S., & Benjakul, S. (2015). Characteristics and antioxidative activity of gelatin hydrolysates from unicorn leatherjacket skin as affected by autolysis-assisted process. *Journal of Food Processing and Preservation*, *39*(6), 915-926. <https://doi.org/10.1111/jfpp.12304>
- Kario, K., Hoshide, S., & Mogi, M. (2024). Hypertension treatment up-date on World Hypertension Day 2024: Current status and future prospects in Asia. *Hypertension Research*, *47*, 1763-1765. <https://doi.org/10.1038/s41440-024-01744-1>
- Kingwascharapong, P., Paewpisakul, P., Sripoovieng, W., Sanprasert, S., Pongsetkul, J., Meethong, R., Hunsakul, K., Karnjanapratum, S., Ali, A. M. M., Petsong, K., & Rawdkuen, S. (2024). Development of fish snack (Keropok) with sodium reduction using alternative salts (KCl and CaCl<sub>2</sub>). *Future Foods*, *8*, 100285. <https://doi.org/10.1016/j.fufo.2023.100285>
- Kingwascharapong, P., Sanprasert, S., Hunsakul, K., Pongsetkul, J., Wararam, W., & Rawdkuen, S. (2023). Partial substitution of NaCl with alternative salts (KCl, CaCl<sub>2</sub>, and yeast extract) in smoked green mussel product. *Future Foods*, *8*, 100266. <https://doi.org/10.1016/j.fufo.2023.100266>

- Kongkaew, S., Chaijan, M., & Riebroy, S. (2014). Some characteristics and antioxidant activity of commercial sugars produced in Thailand. *KMITL Science and Technology Journal*, 14(1), 1-9.
- Kuti, J. O., & Kuti, H. O. (1999). Proximate composition and mineral content of two edible species of *Cnidoscolus* (tree spinach). *Plant Foods for Human Nutrition*, 53(3), 275–283. <https://doi.org/10.1023/A:1008081501857>
- Loarca-Piña, G., Mendoza, S., Ramos-Gómez, M., & Reynoso, R. (2010). Antioxidant, antimutagenic, and antidiabetic activities of edible leaves from *Cnidoscolus chayamansa* Mc. Vaugh. *Journal of Food Science*, 75(2), 68-72. <https://doi.org/10.1111/j.1750-3841.2009.01505.x>
- Odamtten, G. T., Nartey, L. K., Kwagyan, W. M., Anyebuno, G., & Baffour, K. V. (2018). Resident microbial load, toxigenic potential and possible quality control measures of six imported seasoning powders on the Ghanaian market. *Journal of Nutritional Health & Food Engineering*, 8(1), 00252. <https://doi.org/10.15406/jnhfe.2018.08.00252>
- Pandey, K. B., & Rizvi, S. I. (2009). Plant polyphenols as dietary antioxidants in human health and disease. *Oxidative Medicine and Cellular Longevity*, 2(5), 270-278. <https://doi.org/10.4161/oxim.2.5.9498>
- Ramírez, R. M. M., Metri, O. J. C., González, D. M., & Baigts, A. D. K. (2021). Use of Chaya (*Cnidoscolous chayamansa*) leaves for nutritional compounds production for human consumption. *Journal of the Mexican Chemical Society*, 65(1), 118-128. <https://doi.org/10.29356/jmcs.v65i1.1433>
- Rybicka, I., Silva, M., Gonçalves, A., Oliveira, H., Marques, A., Fernandes, M.H., Alfaia, C.M., Fraqueza, M.J., & Nunes, M.L. (2022). The development of smoked mackerel with reduced sodium content. *Foods*, 11(3), 349. <https://doi.org/10.3390/foods11030349>.
- Sarmugam, R., Worsley, A., & Wang, W. (2013). An examination of the mediating role of salt knowledge and beliefs on the relationship between socio-demographic factors and discretionary salt use: A cross-sectional study. *International Journal of Behavioral Nutrition and Physical Activity*, 10, 25. <https://doi.org/10.1186/1479-5868-10-25>
- Siripatrawan, U., & Sirikantaramas, S. (2024). Unraveling the effects of drying techniques on chaya leaves: Metabolomics analysis of nonvolatile and volatile metabolites, umami taste, and antioxidant capacity. *Food Chemistry*, 446, 138769. <https://doi.org/10.1016/j.foodchem.2024.138769>
- Smith, J. P., Daifas, D. P., El-Khoury, W., Koukoutsis, J., & El-Khoury, A. (2010). Shelf life and safety concerns of bakery products—A review. *Critical Reviews in Food Science and Nutrition*, 57(2), 237-253. <https://doi.org/10.1080/10408690490263774>
- Spence, C., Okajima, K., Cheok, A. D., Petit, O., & Michel, C. (2016). Eating with our eyes: From visual hunger to digital satiation. *Brain and Cognition*, 110, 53-63. <https://doi.org/10.1016/j.bandc.2015.08.006>
- Tagrida, M., & Benjakul, S. (2021). Betel (*Piper betle* L.) leaf ethanolic extracts dechlorophyllized using different methods: Antioxidant and antibacterial activities and application for shelf-life extension of Nile tilapia (*Oreochromis niloticus*) fillets. *RSC Advances*, 11(25), 17630–17641. <https://doi.org/10.1039/D1RA02464G>



## Nanoemulsion and Topical Cream for Delivery of Tocotrienol-rich fraction, Ascorbyl Tetraisopalmitate, and Carotenes: Formulation and *in vitro* Release

Yee-Lin Gan<sup>1</sup>, Chin Ping Tan<sup>2</sup>, Cheah Yoke Kqueen<sup>3</sup>, Hidayah Ariffin<sup>1,4</sup>, Helmi Wasoh<sup>1</sup> and Oi Ming Lai<sup>1,5,6\*</sup>

<sup>1</sup>Department of Bioprocess Technology, Faculty of Biotechnology and Biomolecular Sciences, Universiti Putra Malaysia, Serdang, Selangor, Malaysia

<sup>2</sup>Department of Food Technology, Faculty of Food Science and Technology, Universiti Putra Malaysia, Serdang, Selangor, Malaysia

<sup>3</sup>Department of Biomedical Sciences, Faculty of Medicine and Health Sciences, Universiti Putra Malaysia, Serdang, Selangor, Malaysia

<sup>4</sup>Laboratory of Biopolymer and Derivatives, Institute of Tropical Forestry and Forest Products, Universiti Putra Malaysia, Serdang, Selangor, Malaysia

<sup>5</sup>International Joint Laboratory on Plant Oils Processing and Safety, UPM-Jinan University China, Institute of Bioscience, Universiti Putra Malaysia, Serdang, Selangor, Malaysia

<sup>6</sup>Natural Product and Medicine Research, Institute of Bioscience, Universiti Putra Malaysia, Serdang, Selangor, Malaysia

### ABSTRACT

Objectives of this study were to encapsulate tocotrienol-rich fraction (TRF), ascorbyl tetraisopalmitate (AT) and carotenes into nanoemulsion, incorporate the formulated nanoemulsion into moisturizer cream, and characterize the formulated nanoemulsion and cream. A stepwise factorial design methodology was used to screen the nanoemulsion's ingredients and preparation parameters. With mean droplet size, polydispersity index (PDI), creaming index (CI) and irritational potential as evaluation criteria, the ideal nanoemulsion formulation comprised deionized water, red palm oil (RPO) and Kolliphor® EL in a ratio of 20.00:6.25:73.75, fabricated using a high-shear mixer at 7000 rpm and 45°C for 10 min

followed by a high-pressure homogenizer at 750 bars for five cycles. The nanoemulsion's mean droplet size and PDI were  $121.5 \pm 1.8$  nm and  $0.178 \pm 0.010$ , respectively. The cream formulation was then screened using a factorial experiment that considered lipid and emulsifier concentrations. The optimal cream formulation contained deionized water, formulated nanoemulsion, petrolatum, mineral oil, glycerol, emulsifying wax and carbomer 940

#### ARTICLE INFO

##### Article history:

Received: 23 April 2024

Accepted: 15 July 2024

Published: 28 January 2025

DOI: <https://doi.org/10.47836/pjtas.48.1.06>

##### E-mail addresses:

yeelingan@gmail.com (Yee- Lin Gan)

tancp@upm.edu.my (Chin Ping Tan)

ykcheah@upm.edu.my (Cheah Yoke Kqueen)

hidayah@upm.edu.my (Hidayah Ariffin)

helmi\_wmi@upm.edu.my (Helmi Wasoh)

omlai@upm.edu.my (Oi Ming Lai)

\* Corresponding author

in a ratio of 66.8:10.0:7.5:7.5:5.0:3.0:0.2, showing the preferred shear-thinning behavior, excellent physical stability and high conclusiveness. The formulated cream exhibited Korsmeyer-Peppas and Weibull release kinetic mechanisms during the *in vitro* release. This study showed that the developed formulations were suitable for the topical delivery system for TRF, AT and carotenes.

*Keywords:* Ascorbyl tetraisopalmitate, atopic dermatitis, carotenes, moisturizer cream, nanoemulsion, tocotrienol-rich fraction

---

## INTRODUCTION

Atopic dermatitis (AD) is a common chronic skin disorder associated with a relapsing-remitting inflammatory condition, persistent pruritus and xerosis. The interaction of epidermal dysfunction and immune dysregulation is a key pathophysiological mechanism of AD (Williamson et al., 2020). Though non-life threatening, AD symptoms have considerably impaired the quality of life of patients and caregivers (Laughter et al., 2021). No curable medicine is available, and current AD management mainly focuses on flare prevention and symptom relief to enable patients to attain satisfying functional life status. It involves the daily application of moisturizer to restore and maintain skin barrier function, thus reducing the number of skin flares during the remitting period (Weber et al., 2015; Zuuren et al., 2017). During the relapsing period, topical corticosteroids or calcineurin inhibitors are twice-daily applied as the first-line treatment. However, concerns have been raised as topical corticosteroids and calcineurin inhibitors are associated with considerable side effects. Concerns regarding the adverse side effects have hindered the application of topical drugs. To minimize topical corticosteroids or calcineurin inhibitors, efforts have been made to discover and incorporate ingredients that possess skin repairment and anti-inflammatory properties into the moisturizer (Hebert et al., 2020).

It is evident that AD patients are characterized by lower levels of antioxidants and increased oxidative stress compared to healthy controls (Amin et al., 2015; Leveque et al., 2003; Sivaranjani et al., 2013). Disrupted antioxidant defense promotes dysregulation of skin homeostasis and immune response, encouraging AD development (Ji & Li, 2016). Thus, reinforcing the antioxidant systems by increasing the skin's antioxidant capacity is a potential drug-sparing strategy for managing AD. Vitamin E, vitamin C, and carotenes are the predominant exogenous antioxidants in the skin. Previous studies reported that vitamin E can improve epidermal function by upregulating the expression of epidermal differentiation enzymes and proteins, increasing ceramide production, and reducing transepidermal water loss (TEWL) (De Pascale et al., 2006; Kato & Takahashi, 2012; Parish et al., 2005). As well, vitamin E reduced inflammatory conditions and ameliorated AD symptoms in sensitized animals and AD patients (Babaye-Nazhad et al., 2013; Hayashi et al., 2012; Jaffary et al., 2015; Javanbakht et al., 2011; Kapun et al., 2014; Tsuduki et al., 2013). Similarly, literature also has demonstrated that vitamin C promoted keratinocyte differentiation,

reduced TEWL, and improved inflammatory status and AD symptoms in sensitized animals (Pasonen-Seppänen et al., 2001; Savini et al., 2002; Parish et al., 2005; Kim et al., 2015; Lee et al., 2017). Meanwhile, findings demonstrated that  $\beta$ -carotene significantly improved the scratching behavior, skin moisture level and inflammatory status in sensitized animals (Hiragun et al., 2016; Kake et al., 2019; Sakai et al., 2011; Sato et al., 2004)

Considering that topical agents are the mainstays for localized AD treatment and the adsorption and biodistribution of exogenous antioxidants following oral administration exhibit isomeric and regional variations that affect the delivery of antioxidants to the targeted skin sites, topical delivery of these antioxidants is thus recommended (Hemrajani et al., 2022; Myriam et al., 2006; Packer et al., 2001). However, the limited solubility and poor skin penetration of antioxidants hinder their practical application when delivered topically, consequently diminishing their efficacy. Many delivery systems have been developed to overcome these issues. Amongst the delivery systems, nanoemulsion emerges as a promising approach. Pertaining to the nano-size droplets (20–200 nm), nanoemulsion can improve solubilities, increase thermodynamic activities, favor partitioning and promote skin penetration of the encapsulated compounds (Hemrajani et al., 2022). However, the rheology characteristics of watery nanoemulsion, which have low viscosity, limit their feasibility in the practical topical application (Chellapa et al., 2015). Fortunately, nanoemulsion can be further incorporated into different formulations, such as creams and gels, to solve the problem.

In light of the information above, the main objectives of this study were to develop an oil-in-water nanoemulsion loaded with vitamin E (tocotrienol-rich fraction [TRF]), vitamin C (AT) and carotenes using high-pressure homogenization by studying the influence of ingredients and preparation process conditions. The nanoemulsion with a small mean droplet size, lowest polydispersity index (PDI), zero creaming index (CI) and lowest irritational potential was subsequently formulated into moisturizer cream by considering the effect of the cream's ingredients. Physical stability, spreadability, rheological behavior, and occlusion factors were used as evaluation parameters for the cream formulation selection. Finally, the behavior of the selected nanoemulsion and moisturizer cream formulations was determined.

## **MATERIALS AND METHODS**

### **Materials**

Rice bran, sunflower, olive, canola and red palm oils were purchased from local markets. TRF, AT and carotenes were procured from Sime Darby Sdn. Bhd. (Selangor, Malaysia), Nikko Chemicals Co. Ltd. (Tokyo, Japan), and Super Vitamins Sdn. Bhd. (Johor, Malaysia), respectively. Tween 80 and Tween 20 were supplied by Thermo Fisher Scientific Inc. (Massachusetts, USA) and Merck KGaA (Darmstadt, Germany), respectively. Kolliphor® EL and Tween 85 were obtained from Sigma-Aldrich Corporation (Missouri, USA). Mineral

oil, petrolatum, emulsifying wax, and carbomer 940 were acquired from Spectrum Chemical Manufacturing Corporation (New Jersey, USA). Glycerol and sodium hydroxide were supplied by Fisher Scientific UK Ltd. (Leicestershire, UK). The water was purified and deionized using the Millipore system (Millipore GmbH, Darmstadt, Germany). All other chemicals and solvents were either in analytical or high-performance liquid chromatography (HPLC) grade.

## **Formulation of Oil-in-Water Nanoemulsion**

### ***Screening of Oils***

For the solubility study of carotenes, an excess amount of carotenes was added to 5 g of oil (rice bran, sunflower, olive, canola and red palm oils) in a tube, blanketed with nitrogen, sonicated for 30 min (Model Powersonic 520, Hwashin Tech Co., Ltd., Seoul, Korea, 40 kHz), then shaken at 150 rpm and 25°C for 72 hr in an orbital shaking incubator (Model LSI-3016A, Daihan Labtech Co., Ltd., Gyeonggi-do, Korea) (Roohinejad et al., 2015). The resulting samples were centrifuged at  $18000 \times g$  for 15 min to remove undissolved carotenes. The supernatant oil fraction was filtered through 0.45  $\mu\text{m}$  polytetrafluoroethylene membrane filters, and the concentration of dissolved carotenes was quantified using HPLC.

To determine the thermal stability of total antioxidants, 5% w/w TRF, 5% w/w AT and 0.5% w/w carotenes were dissolved in each oil type via sonication for 30 min. One gram of the sample was heated at 45°C, 60°C and 75°C in a water bath for 1 h, cooled to room temperature, and the retained number of antioxidants was determined using HPLC. The oil that provides greater thermal stability and higher solubility was selected for subsequent experiments.

### ***Screening of Coarse Emulsion Formation Preparation Process Conditions***

The 20% w/w oil phase (1% w/w TRF, 1% w/w AT and 0.1% w/w carotenes at final concentration) was mixed with 80% w/w aqueous phase (deionized water with 5% w/w Tween 80 at final concentration), using a high-shear mixer (Model L4RT, Silverson Machines, Inc., USA). The processing conditions evaluated were homogenization speed (5000 to 9000 rpm), time (1 min to 10 min) and temperature (30°C to 60°C). The prepared coarse emulsions' mean droplet size, PDI and CI were evaluated. The preparation process conditions producing a coarse emulsion with the lowest mean droplet size, PDI and CI, were used for subsequent experiments.

### ***Screening of Nanoemulsion Formation Preparation Process Conditions***

The coarse emulsions were prepared by mixing 20% w/w oil phase (1% w/w TRF, 1% w/w AT and 0.1% w/w carotenes at final concentration) and the 80% w/w aqueous phase

(5% w/w Tween 80 at final concentration), using a high-shear mixer at 7000 rpm and 45°C for 10 min. The temperature was adjusted during preparation in the incubator. The coarse emulsions were immediately placed into a high-pressure homogenizer (Model Panda PLUS 2000, GEA Niro Soavi, Italy). The processing conditions studied were homogenization pressure (250 to 1250 bar) and cycle (one to eight). The prepared nanoemulsion were examined for their mean droplet size, PDI and CI. The preparation process conditions that can produce nanoemulsion with small droplet size (100–200 nm), PDI <0.200 and zero CI were used for the following experiments.

### ***Screening of Types of Surfactants and Surfactant-to-Oil Ratio***

The non-ionic surfactants studied in this experiment were Tween 85 [Hydrophilic-Lipophilic Balance (HLB):11], Kolliphor® EL (HLB:12–14), Tween 80 (HLB:15) and Tween 20 (HLB:16.7) at the surfactant-to-oil ratio of 1:8, 1.5:8, 2:8, 2.5:8, 3:8, 3.5:8 and 4:8. The coarse emulsions were prepared by mixing 20% w/w oil phase (1% w/w TRF, 1% w/w AT and 0.1% w/w carotenes at final concentration) with aqueous phase that containing the targeted type and concentration of surfactants, using a high-shear mixer at 7000 rpm and 45°C for 10 min. The coarse emulsions were rapidly processed using a high-pressure homogenizer at 750 bars for five cycles. Mean droplet size, PDI, CI and irritation potential were measured for each prepared nanoemulsion. The type of surfactant at a surfactant-to-oil ratio that can produce nanoemulsion with a mean droplet size between 100 to 200 nm, PDI <0.200, zero CI and lowest irritational potential was selected as the best formulation.

### **Evaluation of Coarse Emulsion and Nanoemulsion**

#### ***Mean Droplet Size and PDI Evaluations***

Each sample was diluted 10 times with deionized water to minimize the multiple scattering effects. The mean droplet size and PDI measurements were carried out at  $25 \pm 0.5^\circ\text{C}$  using a dynamic light scattering instrument (Model Zetasizer Nano ZS, Malvern Instruments Ltd., UK), as previously described (Uluata et al., 2016). The mean droplet size is calculated using the photon correlation spectroscopy concept combined with cumulant methods and expressed as the Z-average droplet diameter. The PDI results were determined based on the volume versus droplet diameter profile. The refractive indices of the dispersed and continuous phases employed for the PDI calculation were 1.47 and 1.33, respectively.

#### ***CI Evaluation***

The CI was determined using a previously described method (Uluata et al., 2016). Ten milliliters of each freshly prepared sample were transferred into new tubes and incubated for 24 hr at room temperature. The entire height of the samples ( $H_E$ ) and the height of

the cream layer ( $H_C$ ) were determined using a ruler, and the magnitude of creaming was calculated using Equation 1:

$$CI (\%) = H_C/H_E \times 100\% \quad [1]$$

### ***Irritational Potential Evaluation***

The irritational potential for each surfactant at the concentrations used in nanoemulsion preparation was determined using the erythrocytes cellular model and expressed as hemolysis percentage (Rocha-Filho et al., 2017). Human blood was collected in a vacutainer tube containing ethylenediaminetetraacetic acid, mixed well and centrifuged at  $650 \times g$  for 10 min. The supernatant was discarded, and the erythrocytes were resuspended in phosphate buffer saline (PBS) (pH 7.4). Next, the erythrocytes were washed three times using PBS in a volume ratio 4:1. In each washing step, the buffy coat (precipitated debris and serum proteins) in the upper phase was removed. The erythrocytes were resuspended in PBS to achieve 50% hematocrit in the final wash. Twenty-five microliters of erythrocyte suspension and 975  $\mu\text{L}$  of the sample were then aliquoted into a tube and incubated in a water bath under 100 rpm shaking speed for 30 min at  $37^\circ\text{C}$ . Later, the intact and debris erythrocytes were removed via 10 min centrifugation at  $650 \times g$ . The hemoglobin released into the supernatant was analyzed spectrophotometrically at 540 nm against a corresponding blank sample. The percentage of hemolysis ( $H\%$ ) was calculated based on the released hemoglobin using Equation 2:

$$H (\%) = (A_S - A_{C1}) / (A_{C2} - A_{C1}) \times 100 \quad [2]$$

Where  $A_S$  refers to the absorbance of the sample,  $A_{C1}$  refers to the absorbance of mechanical hemolysis (erythrocytes in a PBS solution; hemolysis happened due to sample preparation), and  $A_{C2}$  refers to the absorbance of 100% hemolysis (erythrocytes in deionized water).

### **Formulation of Moisturizer Creams**

The aqueous phase was prepared by hydrating 0.2% w/w carbomer 940 and dissolving 5% w/w glycerol in deionized water (Table 1). The oil phase consisted of a 5 to 10% w/w mixture of mineral oil and petrolatum (ratio 1:1) and 1 to 5% w/w emulsifying wax mixed homogeneously (Table 1). Both phases were heated to  $70^\circ\text{C}$  using a water bath. The oil phase was then gradually added to the aqueous phase at a stirring speed of 500 rpm until the temperature dropped to  $40^\circ\text{C}$ . Then, 10% w/w of nanoemulsion was added and stirred at 200 rpm for 10 min. The pH value of the mixture was adjusted to 5.5 using 1 M sodium hydroxide to impart the thickening property of carbomer 940. The physically stable and semifluid-formulated cream with shear-thinning rheological behavior and the highest occlusion factor was selected for further analysis.

Table 1  
*Formulation of moisturizer creams*

Formulation	Weight (% w/w)							
	Petrolatum	Mineral oil	Emulsifying wax	Glycerol	Nanoemulsion	Carbomer 940	Sodium Hydroxide	Deionized water
TC01	2.5	2.5	1.0	5.0	10.0	0.2	qs	qs ad to 100
TC02	5.0	5.0	1.0	5.0	10.0	0.2	qs	qs ad to 100
TC03	7.5	7.5	1.0	5.0	10.0	0.2	qs	qs ad to 100
TC04	10.0	10.0	1.0	5.0	10.0	0.2	qs	qs ad to 100
TC05	2.5	2.5	2.0	5.0	10.0	0.2	qs	qs ad to 100
TC06	5.0	5.0	2.0	5.0	10.0	0.2	qs	qs ad to 100
TC07	7.5	7.5	2.0	5.0	10.0	0.2	qs	qs ad to 100
TC08	10.0	10.0	2.0	5.0	10.0	0.2	qs	qs ad to 100
TC09	2.5	2.5	3.0	5.0	10.0	0.2	qs	qs ad to 100
TC10	5.0	5.0	3.0	5.0	10.0	0.2	qs	qs ad to 100
TC11	7.5	7.5	3.0	5.0	10.0	0.2	qs	qs ad to 100
TC12	10.0	10.0	3.0	5.0	10.0	0.2	qs	qs ad to 100
TC13	2.5	2.5	4.0	5.0	10.0	0.2	qs	qs ad to 100
TC14	5.0	5.0	4.0	5.0	10.0	0.2	qs	qs ad to 100
TC15	7.5	7.5	4.0	5.0	10.0	0.2	qs	qs ad to 100
TC16	10.0	10.0	4.0	5.0	10.0	0.2	qs	qs ad to 100
TC17	2.5	2.5	5.0	5.0	10.0	0.2	qs	qs ad to 100
TC18	5.0	5.0	5.0	5.0	10.0	0.2	qs	qs ad to 100
TC19	7.5	7.5	5.0	5.0	10.0	0.2	qs	qs ad to 100
TC20	10.0	10.0	5.0	5.0	10.0	0.2	qs	qs ad to 100

Note. qs = Quantity sufficient; qs ad = Quantity sufficient to make

## Evaluation of Moisturizer Creams

### *Physical Stability and Spreadability Evaluations*

Freshly prepared creams (10g) were stored at 25°C and 40°C for 24 hr and subjected to centrifugation at 3000 rpm for 30 min (Dantas et al., 2016). The macroscopic observation was then performed to determine the presence of physical instability (creaming, cracking, phase inversion, bleeding or oiling off).

The spreadability of creams was determined using the parallel plate method (Oladimeji et al., 2015). Cream samples, prepared 48 hr prior, weighing  $1 \pm 0.01$  g, were positioned at the center of a circular glass plate (diameter: 15 cm). A second glass plate (weighing  $125 \pm 1$  g) was then placed atop the cream. The spreading diameter was measured after 1

min, enabling classification into three categories based on diameter: semistiff cream ( $25 \text{ mm} < \varnothing \leq 50 \text{ mm}$ ), semifluid cream ( $50 \text{ mm} < \varnothing \leq 70 \text{ mm}$ ), and fluid cream ( $\varnothing > 70 \text{ mm}$ ). Semifluid formulations demonstrating physical stability were chosen for subsequent evaluation of rheological behavior and *in vitro* occlusive properties.

### ***Rheological Behaviors Evaluation***

The rheological behaviors of cream were evaluated using a HAAKE RheoStress 6000 rheometer (Thermo Fisher Scientific Inc., USA) equipped with a Peltier system and 35 mm stainless steel serrated parallel plate. About 0.5 g of cream sample was put on the lower plate for each evaluation. The lower plate was slowly raised to the preset trimming gap of 0.55 mm. After removing the excess cream, the lower plate was lifted to the measurement geometry gap of 0.5 mm. The sample was equilibrated at  $25 \pm 0.1^\circ\text{C}$  for 5 min. The flow property of the cream was characterized using the steady-state-flow method. The shear rate over a 0.01 to  $100 \text{ s}^{-1}$  range was programmed in a logarithmic ramp mode in 3 min (Siska et al., 2019). The recorded results were plotted in a graph and fitted into the mathematical model of Power Law to calculate the flow behavior and consistency indices.

### ***In vitro Occlusive Evaluation***

A 50 ml beaker was filled with 20 ml of water, then enclosed with cellulose acetate filter paper ( $0.2 \mu\text{m}$ , Sartorius AG, Goettingen, Germany) (Swarnavalli et al., 2016). A 200mg cream sample was applied and spread evenly on the filter surface. The beaker without cream application on the filter served as a control. All the prepped beakers were incubated at  $32^\circ\text{C}$  and  $50^\circ\text{C}$  at 55% Relative Humidity (RH) for 24 h. The prepped beakers were weighed to determine the water loss through the filter due to evaporation. The occlusion factor for each sample, F, was then calculated using Equation 3:

$$F (\%) = (A - B)/A \times 100\% \quad [3]$$

Where A refers to the water loss without cream applied on the filter (control), and B represents the water loss with the cream applied on the filter.

## **Characterization of the Selected Nanoemulsion and Moisturizer Cream Formulations**

### ***Morphological Study***

The selected nanoemulsion formulation was diluted ten times with deionized water. A drop of diluted sample was deposited on a carbon film-covered 400 mesh copper grid. Excess nanoemulsion was blotted with filter paper from the copper grid to produce a thin-film specimen. The specimen was negatively stained with 1% w/w uranyl acetate, air-dried



and examined under a Jem-2100F field emission electron microscope (Jeol Ltd., Tokyo, Japan), which operated at an accelerating voltage of 200 kV.

Morphology of the selected cream formulation was observed using an optical microscope (Model Olympus CX23, Olympus Corporation, Japan). The cream was applied, spread evenly onto a microscopic glass slide, and viewed under the microscope. The images were taken and processed using the TouPCam camera and TouPView software (TouPTek Photonics Co., Ltd., China).

### *In vitro Release*

*In vitro* release profiles of antioxidants from nanoemulsion and moisturizer cream were investigated and compared to bulk oil using the Franz diffusion method (Jung et al., 2012). 0.45  $\mu\text{m}$  cellulose acetate membrane (diameter: 25 mm) was presoaked in the receiver medium (PBS and ethanol in the ratio 1:1, pH 7.4) for 30 min, then mounted between the donor and receiver compartments of the Franz diffusion cell. The receiver chamber was then filled with receiver medium. The receiver fluid was continuously stirred with a magnetic stirrer at 500 rpm and  $32 \pm 0.5$  °C. After equilibrating for 15 min, 1 g of sample was placed into the donor compartment and covered with parafilm. At predetermined intervals (1, 2, 3, 4, 5, 6, 8 and 12 h), 400  $\mu\text{L}$  of samples were collected from the received chamber, and 400  $\mu\text{L}$  of fresh receiver medium was refilled back. The samples were analyzed using HPLC. The cumulative number of antioxidants released per surface area of the membrane ( $\mu\text{g cm}^{-2}$ ) was calculated using Equation 4 and plotted as a function of time (t):

$$Q = [C_n V + \sum_{i=1}^{n-1} C_i S] / A \quad [4]$$

Where Q refers to the cumulative amount of antioxidants released per surface area of membrane ( $\mu\text{g/cm}^2$ ),  $C_n$  denotes the concentration of antioxidants ( $\mu\text{g/ml}$ ) determined at the nth sampling interval, V is the volume of individual Franz diffusion cell,  $\sum_{i=1}^{n-1} C_i$  refers to the sum of concentrations of antioxidants ( $\mu\text{g/ml}$ ) determined at sampling intervals 1 through n-1, S represents the volume of sampling aliquot (0.4 ml), and A is the surface area of Franz diffusion cell ( $2.27 \text{ cm}^2$ ).

The data were then fitted to the kinetic Equations 5 and 6:

Zero-order model (Salamanca et al., 2018):

$$Q_t = Q_0 + k_0 t \quad [5]$$

Where  $Q_t$  is the percentage of the released antioxidants at time t,  $Q_0$  represents the initial percentage of antioxidants in the receiver compartment (normally zero),  $k_0$  denotes the rate constant of zero-order release kinetics, and t is the sampling time.

First-order model (Bruschi, 2015):

$$\text{Log}Q_t = \text{Log}Q_0 + k_1t/2.303 \quad [6]$$

Where  $Q_t$  is the percentage of antioxidants that remained in the donor compartment at time  $t$ ,  $Q_0$  represents the initial percentage of antioxidants in the donor compartment,  $k_1$  denotes the rate constant of first-order release kinetics, and  $t$  is the sampling time.

Higuchi model (Paarakh et al., 2018), Equation 7:

$$Q_t = k_H t^{1/2} \quad [7]$$

Where  $k_H$  represents the Higuchi dissolution constant, and  $t$  represents the sampling time.

Korsmeyer-Peppas model (Yarce et al., 2016), Equation 8:

$$M_t/M_\infty = k_r t^n \quad [8]$$

Where  $M_t$  is the percentage of the released antioxidants at time  $t$ ,  $M_\infty$  represents the percentage of the released antioxidants at infinity time,  $k_r$  denotes the release constant,  $t$  is the sampling time, and  $n$  is the diffusion exponent (related to the release mechanism).

Weibull model (Ye et al., 2019), Equation 9:

$$\ln[-\ln(1 - Q_t)] = \ln(\alpha) + \beta \ln t \quad [9]$$

Where  $\alpha$  represents the scale parameter that defines the timescale of the process,  $\beta$  denotes the curve shape factor, and  $t$  is the sampling time.

Based on the  $r^2$  values and Akaike information criterion (AIC), the best model to describe the kinetics and mechanisms of antioxidants released was identified (Jahromi et al., 2020).

## Statistical Analysis

All measurements were performed in triplicates and reported as mean value  $\pm$  SD. The data were analyzed by one-way or two-way analysis of variance (ANOVA) using Minitab Statistical Software Release 16 (Minitab, LLC., Pennsylvania, USA), followed by Tukey's post hoc test.

## RESULTS AND DISCUSSION

### Nanoemulsion Formulation

#### *Influence of Oil Types on the Solubility of Carotenes and Thermal Stability of Antioxidants*

Long-chain triacylglycerols, known as ripening inhibitors, were selected as the carrier oil for the current nanoemulsion formulation. Since TRF and AT used in this study were

in oil form, and carotenes are sparingly oil-soluble, the solubility of carotenes in various long-chain triacylglycerols was determined. Results showed that the solubility of carotenes was not significantly different ( $p > 0.05$ ) among the tested long-chain triacylglycerols (Table 2). Further investigation was done to determine the thermal stability of total antioxidants dissolved in these long-chain triacylglycerols, considering heat generated during nanoemulsion preparation using high-pressure homogenization can degrade the antioxidants easily (Kruszewski et al., 2021). It was found that the retention efficiency of total antioxidants in red palm oil (RPO) was significantly higher than ( $p < 0.05$ ) other oils, with no evidence of antioxidant degradation at 45°C (Table 2). Findings obtained following 1 hr heat treatment at 60°C showed that the retention efficiency in RPO was slightly lower than in rice bran oil. However, this difference did not reach statistical significance ( $p > 0.05$ ) (Table 2). Current results show that RPO provided greater thermal stability to antioxidants and was chosen as the carrier oil for subsequent experiments.

Table 2

*Solubility of carotenes and thermal stability of total antioxidants in different long-chain triacylglycerols*

Oil	Rice bran	Olive	Canola	Sunflower	Red palm
<b>Solubility of carotenes (mg/g of oil)</b>					
	43.13 ± 1.58 <sup>a</sup>	42.93 ± 1.59 <sup>a</sup>	44.68 ± 1.67 <sup>a</sup>	44.33 ± 1.74 <sup>a</sup>	44.81 ± 0.28 <sup>a</sup>
<b>Total antioxidant retention (%) after 1 hr thermal treatment</b>					
<b>Temperature</b>					
45°C	97.22 ± 0.41 <sup>a</sup>	98.94 ± 0.28 <sup>b</sup>	97.21 ± 0.51 <sup>a</sup>	99.47 ± 0.27 <sup>b</sup>	100.96 ± 0.29 <sup>c</sup>
60°C	95.64 ± 0.75 <sup>a</sup>	98.65 ± 0.61 <sup>b</sup>	95.57 ± 0.66 <sup>a</sup>	95.20 ± 0.35 <sup>a</sup>	97.49 ± 0.63 <sup>b</sup>
75°C	93.97 ± 1.01 <sup>a</sup>	94.23 ± 0.86 <sup>a</sup>	91.32 ± 0.29 <sup>b</sup>	93.07 ± 0.45 <sup>ab</sup>	94.59 ± 0.65 <sup>a</sup>

*Note.* Different superscript alphabets a, b and c in the same row denote statistical significance ( $p < 0.05$ )

### ***Process Conditions of High-speed Homogenization***

Although coarse emulsion formation using high-speed homogenization is a preparatory step before nanoemulsion formation, it may affect the resulting nanoemulsion's mean droplet size and PDI (Galvão et al., 2018). This experiment used a high-shear mixer with a fixed workhead (emulsor screens) to prepare coarse emulsions. The effects of homogenization speed, time and temperature on coarse emulsion formation were evaluated. A significant inverse relation existed between homogenization time and mean droplet size of coarse emulsion when homogenization speed was kept constant (Table 3). A significant negative correlation was also found between the homogenization speed and mean droplet size when homogenization time was fixed at 1 min and 5 min. With 10 min of homogenization, the mean droplet size of coarse emulsion was significantly reduced when the homogenization speed increased from 5000 to 7000 rpm ( $p < 0.05$ ); a further increment from 7000 to 9000 rpm did not reduce the mean droplet size. Synchronously, PDI and CI of coarse emulsion remained constant after 10 min of homogenization at speeds varying from 7000 to 9000 rpm (Table 3).

Hence, homogenization speed and time at 7000 rpm and 10 min were selected and applied in the screening experiment of homogenization temperature. When the homogenization temperature increased from 30°C to 60°C, the viscosity of emulsion phases decreased, and higher-intensity disruptive forces could be generated. Still, the coarse emulsion formed depicted no significant change ( $p > 0.05$ ) in mean droplet size (Table 4). Previous studies (Jafari et al., 2008; Kuhn & Cunha, 2012; Peng et al., 2015; Qian & McClements, 2011) have reported that the mean droplet size of nanoemulsion is an equilibrium result of droplet disintegration and recoalescence during homogenization. At this point, surfactants absorb and cover the new interface of the small droplets formed before they collide to recoalesce. However, when the timescale of collision is shorter than the timescale of surfactant absorption, a high recoalescence rate increases the mean droplet size of nanoemulsion, implying the effects of overprocessing conditions; thus, when the temperature increases, the intensity of the disruptive forces increases with increasing viscosity. The intensity of disruptive forces generated and the time exposure greatly affect

Table 3  
*Effects of high-shear mixer's homogenization speed and time on the mean droplet size, PDI and CI of coarse emulsions*

Homogenization speed (rpm)	Homogenization time (min)		
	1	5	10
Mean droplet size (nm)			
5000	7226.3 ± 280.4 <sup>A,a</sup>	831.1 ± 63.4 <sup>B,a</sup>	470.7 ± 19.9 <sup>C,a</sup>
6000	4824.5 ± 215.8 <sup>A,b</sup>	801.9 ± 45.8 <sup>B,a</sup>	358.4 ± 29.2 <sup>C,b</sup>
7000	1711.0 ± 111.1 <sup>A,c</sup>	452.5 ± 23.0 <sup>B,b</sup>	236.5 ± 10.1 <sup>C,c</sup>
8000	1089.0 ± 50.7 <sup>A,d</sup>	410.9 ± 35.2 <sup>B,bc</sup>	235.2 ± 11.4 <sup>C,c</sup>
9000	665.4 ± 25.7 <sup>A,c</sup>	374.1 ± 19.8 <sup>B,c</sup>	232.0 ± 7.5 <sup>C,c</sup>
<b>PDI</b>			
5000	0.229 ± 0.041 <sup>A,a</sup>	0.229 ± 0.041 <sup>A,a</sup>	0.229 ± 0.041 <sup>A,a</sup>
6000	0.472 ± 0.051 <sup>A,b</sup>	0.472 ± 0.051 <sup>A,b</sup>	0.472 ± 0.051 <sup>A,b</sup>
7000	1.000 ± 0.000 <sup>A,c</sup>	1.000 ± 0.000 <sup>A,c</sup>	1.000 ± 0.000 <sup>A,c</sup>
8000	1.000 ± 0.000 <sup>A,c</sup>	1.000 ± 0.000 <sup>A,c</sup>	1.000 ± 0.000 <sup>A,c</sup>
9000	1.000 ± 0.000 <sup>A,c</sup>	1.000 ± 0.000 <sup>A,c</sup>	1.000 ± 0.000 <sup>A,c</sup>
<b>CI (%)</b>			
5000	27.76 ± 2.19 <sup>A,a</sup>	27.76 ± 2.19 <sup>A,a</sup>	27.76 ± 2.19 <sup>A,a</sup>
6000	24.12 ± 0.74 <sup>A,b</sup>	24.12 ± 0.74 <sup>A,b</sup>	24.12 ± 0.74 <sup>A,b</sup>
7000	19.82 ± 0.25 <sup>A,c</sup>	19.82 ± 0.25 <sup>A,c</sup>	19.82 ± 0.25 <sup>A,c</sup>
8000	19.43 ± 0.48 <sup>A,c</sup>	19.43 ± 0.48 <sup>A,c</sup>	19.43 ± 0.48 <sup>A,c</sup>
9000	18.49 ± 0.53 <sup>A,c</sup>	18.49 ± 0.53 <sup>A,c</sup>	18.49 ± 0.53 <sup>A,c</sup>

*Note.* Different capital superscript alphabets A, B and C in the same row, while different small superscript alphabets a, b and c in the same column denote statistical significance ( $p < 0.05$ ). PDI = polydispersity index; CI = creaming index

the emulsification efficiency, which may affect the droplet size. However, a considerable improvement in PDI and CI was detected when the processing temperature increased to 45°C, with no additional improvement observed at 60°C (Table 4). Considering these results, the process conditions at 7000 rpm and 45°C for 10 min were chosen to prepare coarse emulsion.

Table 4

*Effects of high-speed homogenization processing temperature on the mean droplet size, PDI and creaming index of coarse emulsions*

Processing temperature	30°C	45°C	60°C
Mean droplet size (nm)	263.6 ± 16.9 <sup>a</sup>	262.8 ± 4.7 <sup>a</sup>	262.8 ± 8.3 <sup>a</sup>
Polydispersity Index (PDI)	0.746 ± 0.016 <sup>a</sup>	0.725 ± 0.005 <sup>b</sup>	0.715 ± 0.011 <sup>b</sup>
Creaming index (%)	14.21 ± 0.80 <sup>a</sup>	11.95 ± 0.88 <sup>b</sup>	10.98 ± 0.55 <sup>b</sup>

*Note.* Different superscript alphabets a and b in the same row denote statistical significance ( $p < 0.05$ )

### ***Influence of High-Pressure Homogenization's Process Conditions***

Theoretically, when a coarse emulsion is subjected to high-pressure homogenization, the intensity of disruptive forces generated and the time exposure greatly affect the emulsification efficiency of the surfactant. Therefore, the influence of homogenization pressures and cycles on the formation of nanoemulsion was examined. Overall, nanoemulsion's mean droplet size and PDI decreased modestly with increasing homogenization pressures and cycles (Table 5). The presence of a creaming layer evidenced that a single homogenization cycle at all homogenization pressures could not produce a stable nanoemulsion (Table 5). At low pressures varied from 250 to 500 bar, nanoemulsion with small mean droplet size and PDI < 0.200 could not be generated (Table 5). At higher pressure (750 to 1250 bar), it was observed that the mean droplet size and PDI of nanoemulsion remained consistent from the 5<sup>th</sup> to 8<sup>th</sup> homogenization cycles. During the 5<sup>th</sup> homogenization cycle, an increase in homogenization pressure from 750 to 1250 bar did not decrease mean droplet size and PDI. Since the mean droplet size and PDI did not reduce significantly after homogenization at 750 bars for five cycles, these settings were used throughout the following experiments to prepare nanoemulsion.

### ***Influence of Types of Surfactants and Surfactant-to-Oil Ratio***

Non-ionic surfactants that pose low skin irritation and safety issues are preferably used in dermatological products. In this study, the influence of four types of non-ionic surfactants (Tween 85, Kolliphor® EL, Tween 80 and Tween 20) at different surfactant-to-oil ratios on mean droplet size, PDI, CI and irritation potential was examined. All the tested surfactants at any surfactant-to-oil ratio formed a stable nanoemulsion with no creaming issue. When

Table 5

*Effects of high-pressure homogenization pressures and cycles on the mean droplet size, CI and PDI of nanoemulsion*

Cycle	Homogenization pressure (bar)				
	250	500	750	1000	1250
	<b>Mean droplet size (nm)</b>				
1	219.7 ± 1.5 <sup>A,a</sup>	184.4 ± 4.6 <sup>B,a</sup>	166.4 ± 1.6 <sup>C,a</sup>	157.2 ± 0.7 <sup>C,a</sup>	163.6 ± 9.1 <sup>C,a</sup>
2	197.6 ± 2.0 <sup>A,b</sup>	170.9 ± 0.3 <sup>B,b</sup>	152.2 ± 1.9 <sup>C,b</sup>	143.0 ± 0.9 <sup>B,b</sup>	147.0 ± 7.7 <sup>CD,b</sup>
3	193.3 ± 1.9 <sup>A,bc</sup>	165.3 ± 0.2 <sup>B,c</sup>	144.5 ± 2.6 <sup>C,c</sup>	137.7 ± 1.4 <sup>C,c</sup>	142.3 ± 7.9 <sup>C,b</sup>
4	190.4 ± 1.4 <sup>A,bcd</sup>	159.8 ± 0.6 <sup>B,d</sup>	138.1 ± 3.9 <sup>C,c</sup>	134.4 ± 0.8 <sup>C,d</sup>	138.9 ± 5.9 <sup>CD,b</sup>
5	188.9 ± 3.2 <sup>A,cd</sup>	157.1 ± 0.4 <sup>B,de</sup>	134.7 ± 3.0 <sup>C,d</sup>	131.5 ± 1.5 <sup>C,e</sup>	135.4 ± 2.4 <sup>C,b</sup>
6	186.8 ± 5.5 <sup>A,cd</sup>	153.2 ± 0.5 <sup>B,ef</sup>	132.5 ± 3.5 <sup>C,d</sup>	130.4 ± 1.0 <sup>C,e</sup>	136.2 ± 5.2 <sup>C,b</sup>
7	183.8 ± 3.9 <sup>A,d</sup>	151.2 ± 1.5 <sup>B,fg</sup>	131.3 ± 2.5 <sup>C,d</sup>	129.3 ± 0.5 <sup>C,e</sup>	134.1 ± 2.7 <sup>C,b</sup>
8	183.5 ± 4.4 <sup>A,d</sup>	148.6 ± 0.9 <sup>B,g</sup>	130.4 ± 3.2 <sup>C,d</sup>	129.1 ± 1.3 <sup>C,e</sup>	134.7 ± 4.1 <sup>C,b</sup>
	<b>PDI</b>				
1	0.302 ± 0.015 <sup>A,a</sup>	0.302 ± 0.015 <sup>A,a</sup>	0.302 ± 0.015 <sup>A,a</sup>	0.302 ± 0.015 <sup>A,a</sup>	0.302 ± 0.015 <sup>A,a</sup>
2	0.256 ± 0.009 <sup>A,b</sup>	0.256 ± 0.009 <sup>A,b</sup>	0.256 ± 0.009 <sup>A,b</sup>	0.256 ± 0.009 <sup>A,b</sup>	0.256 ± 0.009 <sup>A,b</sup>
3	0.250 ± 0.008 <sup>A,bc</sup>	0.250 ± 0.008 <sup>A,c</sup>	0.250 ± 0.008 <sup>A,bc</sup>	0.250 ± 0.008 <sup>A,bc</sup>	0.250 ± 0.008 <sup>A,bc</sup>
4	0.238 ± 0.012 <sup>A,bcd</sup>	0.238 ± 0.012 <sup>A,bcd</sup>	0.238 ± 0.012 <sup>A,bcd</sup>	0.238 ± 0.012 <sup>A,bcd</sup>	0.238 ± 0.012 <sup>A,bcd</sup>
5	0.236 ± 0.007 <sup>A,bcd</sup>	0.236 ± 0.007 <sup>A,bcd</sup>	0.236 ± 0.007 <sup>A,bcd</sup>	0.236 ± 0.007 <sup>A,bcd</sup>	0.236 ± 0.007 <sup>A,bcd</sup>
6	0.232 ± 0.013 <sup>A,cd</sup>	0.232 ± 0.013 <sup>A,d</sup>	0.232 ± 0.013 <sup>A,cd</sup>	0.232 ± 0.013 <sup>A,cd</sup>	0.232 ± 0.013 <sup>A,cd</sup>
7	0.230 ± 0.006 <sup>A,cd</sup>	0.230 ± 0.006 <sup>A,d</sup>	0.230 ± 0.006 <sup>A,cd</sup>	0.230 ± 0.006 <sup>A,cd</sup>	0.230 ± 0.006 <sup>A,cd</sup>
8	0.221 ± 0.006 <sup>A,d</sup>	0.221 ± 0.006 <sup>A,d</sup>	0.221 ± 0.006 <sup>A,d</sup>	0.221 ± 0.006 <sup>A,d</sup>	0.221 ± 0.006 <sup>A,d</sup>
	<b>CI (%)</b>				
1	5.34 ± 0.57	2.26 ± 0.01	2.28 ± 0.01	2.27 ± 0.02	1.70 ± 0.02
2	2.24 ± 0.04	1.13 ± 0.01	-	-	-
3	0.83 ± 0.02	-	-	-	-
4	0.58 ± 0.01	-	-	-	-
5	-	-	-	-	-
6	-	-	-	-	-
7	-	-	-	-	-
8	-	-	-	-	-

*Note.* Different capital superscript alphabets A, B and C in the same row, while different small superscript alphabets a - d in the same column denote statistical significance ( $p < 0.05$ ). PDI = polydispersity index; CI = creaming index

the surfactant-to-oil ratio increased, the mean droplet size of the nanoemulsion decreased, but the PDI increased (Table 6). At all surfactant-to-oil ratios, Tween 85 and Tween 20 produced nanoemulsion with appreciably higher mean droplet size than Kolliphor® EL and Tween 80, probably due to the ability of Kolliphor® EL and Tween 80 to adsorb at the interface and cover the newly formed droplets more rapidly during droplets disruption before they collide to recombine. As shown in Figure 1, it is noted that the irritation potential was remarkably lower in Kolliphor® EL than in Tween 80 at all surfactant-to-oil ratios.

AD patients are associated with a lower sensitization threshold and epidermal defects; hence, avoiding surfactants related to the high irritation potential and cytotoxicity in topical products is advisable. From this perspective, Kolliphor® EL seems more advantageous than Tween 80 for AD management. Considering that Ostwald ripening is prone to happen

Table 6  
Effects of types of surfactants and surfactant-to-oil ratio on the mean droplet size and PDI of nanoemulsion

Surfactant-to-oil ratio	Tween 85	Kolliphor® EL	Tween 80	Tween 20
<b>Mean droplet size (nm)</b>				
1.0:8.0	200.9 ± 2.0 <sup>A,a</sup>	187.6 ± 1.0 <sup>B,a</sup>	181.0 ± 0.5 <sup>C,a</sup>	188.8 ± 0.1 <sup>B,a</sup>
1.5:8.0	175.6 ± 1.1 <sup>A,b</sup>	164.8 ± 2.2 <sup>B,b</sup>	157.7 ± 1.0 <sup>C,b</sup>	166.3 ± 1.2 <sup>B,b</sup>
2.0:8.0	163.1 ± 2.0 <sup>A,c</sup>	146.1 ± 1.1 <sup>B,c</sup>	138.2 ± 2.0 <sup>C,c</sup>	157.2 ± 1.1 <sup>D,c</sup>
2.5:8.0	148.6 ± 1.8 <sup>A,d</sup>	121.6 ± 3.2 <sup>B,d</sup>	130.0 ± 1.6 <sup>C,d</sup>	144.1 ± 1.0 <sup>D,d</sup>
3.0:8.0	134.0 ± 1.8 <sup>A,e</sup>	114.5 ± 1.5 <sup>B,e</sup>	117.5 ± 1.3 <sup>C,e</sup>	139.8 ± 0.6 <sup>D,e</sup>
3.5:8.0	125.4 ± 1.6 <sup>A,f</sup>	110.5 ± 0.1 <sup>B,f</sup>	111.0 ± 0.6 <sup>B,f</sup>	133.7 ± 3.3 <sup>C,f</sup>
4.0:8.0	135.1 ± 2.3 <sup>A,e</sup>	100.3 ± 0.9 <sup>B,g</sup>	111.3 ± 3.6 <sup>C,f</sup>	125.7 ± 1.5 <sup>D,g</sup>
<b>PDI</b>				
1.0:8.0	0.136 ± 0.012 <sup>A,a</sup>	0.117 ± 0.008 <sup>B,a</sup>	0.140 ± 0.008 <sup>AC,a</sup>	0.152 ± 0.010 <sup>C,a</sup>
1.5:8.0	0.147 ± 0.012 <sup>A,a</sup>	0.130 ± 0.010 <sup>B,ab</sup>	0.154 ± 0.010 <sup>AC,a</sup>	0.164 ± 0.008 <sup>C,a</sup>
2.0:8.0	0.168 ± 0.012 <sup>A,b</sup>	0.145 ± 0.009 <sup>B,b</sup>	0.198 ± 0.007 <sup>C,b</sup>	0.184 ± 0.010 <sup>C,b</sup>
2.5:8.0	0.197 ± 0.007 <sup>A,c</sup>	0.178 ± 0.010 <sup>B,c</sup>	0.242 ± 0.007 <sup>C,c</sup>	0.194 ± 0.007 <sup>A,bc</sup>
3.0:8.0	0.242 ± 0.009 <sup>A,d</sup>	0.213 ± 0.011 <sup>B,d</sup>	0.262 ± 0.007 <sup>C,d</sup>	0.207 ± 0.004 <sup>B,cd</sup>
3.5:8.0	0.243 ± 0.003 <sup>A,d</sup>	0.225 ± 0.010 <sup>B,dc</sup>	0.275 ± 0.004 <sup>C,dc</sup>	0.216 ± 0.007 <sup>B,dc</sup>
4.0:8.0	0.245 ± 0.006 <sup>A,d</sup>	0.239 ± 0.009 <sup>AB,c</sup>	0.281 ± 0.008 <sup>C,e</sup>	0.228 ± 0.006 <sup>B,c</sup>

Note. Different capital superscript alphabets A-C in the same row, while different small superscript alphabets a-g in the same column denote statistical significance ( $p < 0.05$ ). PDI = polydispersity index

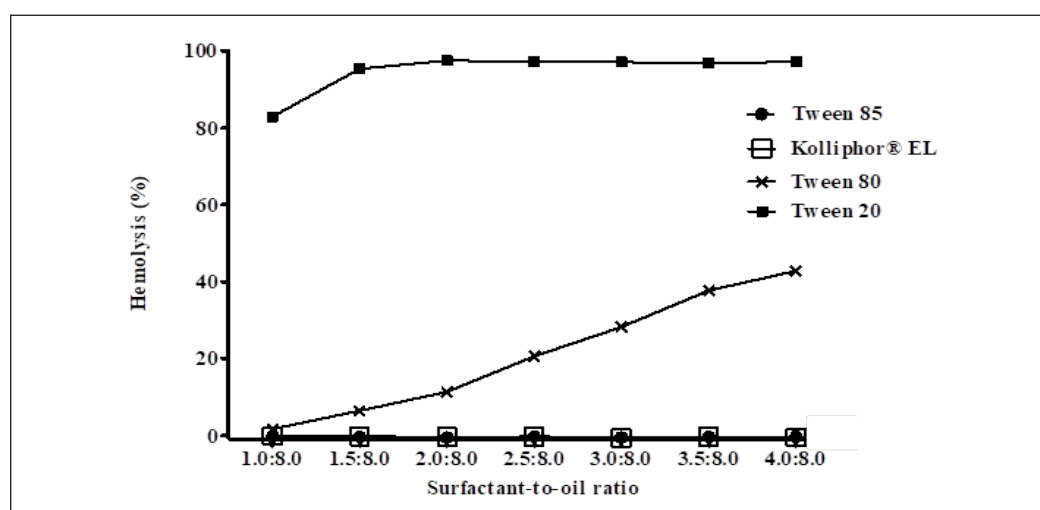


Figure 1. Effect of types of surfactants and surfactant-to-oil ratio on the irritation potential

in highly polydisperse nanoemulsion, it is often ideal for producing nanoemulsion with  $PDI < 0.200$ , as narrower size distribution will be more stable against Ostwald ripening. In this context, Kolliphor® EL, at a surfactant-to-oil ratio of 2.5:8.0, which could produce nanoemulsion with small mean droplet size ( $< 200\text{nm}$ ) and  $PDI < 0.200$ , was chosen as the optimal nanoemulsion formulation in this study.

## Moisturizer Cream Formulation

### *Physical Stability and Spreadability*

The current formulated cream base was composed of a mixture of oil and aqueous phases stabilized by an emulsifier, which is generally inherently unstable and will eventually separate phases. The time needed to show the first sign of instability depends on the oil phase and emulsifier concentrations. Centrifugation is a quick technique to evaluate the physical stability of the formulated products. It was evident that TC02, TC03, TC04, TC07, TC08 and TC12 creams showed signs of physical instability (Table 7), probably due to an insufficient amount of emulsifier to cover the high concentration of oil droplets formed in the creams. Another critical attribute evaluated was spreadability, which refers to the ability of the formulation to spread on the skin.

Overall, the spreadability was decreased with the increments in the oil phase and emulsifying wax concentrations (Table 7). The formulations TC15, TC16, TC18, TC19, and TC20 were semistiff creams, which could influence the patients' compliance as they were not easy to apply. The formulations TC01, TC02 and TC05 were fluid creams, which may result in the uneven spread of the creams and, thus, the dose of antioxidants administered at the application area. The rest of the formulations were classified as semifluid creams, indicating the formulated creams can be spread readily and evenly on the skin during application besides being not too runny to influence the delivery of the correct dose of antioxidants (Chen et al., 2016). Collectively, formulations TC06, TC09, TC10, TC11, TC13, TC14 and TC17 exhibited excellent physical stability and spreadability and were selected for the subsequent evaluations.

Table 7  
*Physical stability and spreadability of formulated creams*

Formulation	Physically unstable upon centrifugation		Spreadability	
	Samples stored at 25°C	Samples stored at 40°C	Spread diameter (cm)	Classification
TC01	*No	No	$8.0 \pm 0.2^a$	Fluid
TC02	No	*Yes	$7.3 \pm 0.1^b$	Fluid
TC03	No	Yes	$6.9 \pm 0.1^c$	Semifluid
TC04	Yes	Yes	$6.8 \pm 0.1^d$	Semifluid



Table 7 (continue)

Formulation	Physically unstable upon centrifugation		Spreadability	
	Samples stored at 25°C	Samples stored at 40°C	Spread diameter (cm)	Classification
TC05	No	No	7.2 ± 0.2 <sup>b</sup>	Fluid
TC06	No	No	6.4 ± 0.3 <sup>e</sup>	Semifluid
TC07	No	Yes	6.1 ± 0.1 <sup>f</sup>	Semifluid
TC08	No	Yes	5.8 ± 0.1 <sup>g</sup>	Semifluid
TC09	No	No	6.8 ± 0.2 <sup>d</sup>	Semifluid
TC10	No	No	6.1 ± 0.1 <sup>f</sup>	Semifluid
TC11	No	No	5.7 ± 0.1 <sup>g</sup>	Semifluid
TC12	No	Yes	5.4 ± 0.2 <sup>h</sup>	Semifluid
TC13	No	No	6.7 ± 0.2 <sup>d</sup>	Semifluid
TC14	No	No	5.8 ± 0.3 <sup>g</sup>	Semifluid
TC15	No	No	5.0 ± 0.1 <sup>i</sup>	Semistiff
TC16	No	No	4.9 ± 0.1 <sup>ij</sup>	Semistiff
TC17	No	No	6.6 ± 0.2 <sup>d</sup>	Semifluid
TC18	No	No	4.9 ± 0.1 <sup>ij</sup>	Semistiff
TC19	No	No	4.8 ± 0.1 <sup>jk</sup>	Semistiff
TC20	No	No	4.7 ± 0.1 <sup>k</sup>	Semistiff

Note. Different superscript alphabets a-k in the same column denote statistical significance ( $p < 0.05$ ). \*No indicates that the samples were not physically unstable upon centrifugation at that temperature. \*Yes indicates that the samples were physically unstable upon centrifugation at that temperature

### Rheological Behaviors

The rheological behaviors analysis was conducted for the selected cream formulations as it provides more detailed information about the cream's physical stability and behaviors during topical application. Figure 2 shows the viscosity flow curve of the TC06, TC09, TC10, TC11, TC13, TC14 and TC17 creams at 25°C, demonstrating that the evaluated creams exhibited shear thinning or pseudoplastic flow behavior (non-Newtonian), a desirable rheological behavior for a topical cream. This observation was corroborated by the calculated flow indices, with values  $< 1$  for all the evaluated creams (Table 8). Looking into more detail on the viscosity profile, under low shear conditions ( $0.1 \text{ s}^{-1}$ ), the high viscosity displayed by the formulations contributes to greater retention on the applied skin area for a long-lasting effect and the firmness feel of the creams (Table 8) (Demma et al., 2018). When shear was increased from  $0.1$  to  $100 \text{ s}^{-1}$ , a steady decrease in viscosity to  $< 5 \text{ Pa.s}$ , suggesting the easiness of the cream being extruded from a tube and applied over the skin to form a coherent film and covering a large skin area (Krishnaiah et al., 2014), from all the evaluated formulations, it was found that TC11 showed slightly higher viscosity at low ( $0.1 \text{ s}^{-1}$ ) and medium ( $1 \text{ s}^{-1}$ ) shear rates but relatively lower viscosity at the high

shear rate ( $100 \text{ s}^{-1}$ ) and was accompanied by a lower flow index. The consistency index was also calculated, representing the creams' consistency and defining the formulation's effectiveness in inhibiting the repeated collisions of globules in the cream that can promote coalescence and phase separation across time. When compared to other formulations, TC11 demonstrated a slightly higher index value (Table 8). These results suggested that formulation TC11 would possess higher physical stability and ensure good shear-thinning and application attributes on the skin.

Table 8

*Apparent viscosity (at low, medium and high shear rates), consistency and flow indices and in vitro occlusion factors of formulated creams*

Formulation	Apparent viscosity (Pa.s)			Power law		Occlusion factor (%)
	Shear rate at $0.01 \text{ s}^{-1}$	Shear rate at $1 \text{ s}^{-1}$	Shear rate at $100 \text{ s}^{-1}$	Consistency index (Pa.sn)	Flow index (n)	
TC06	$742.6 \pm 67.9^a$	$94.9 \pm 4.2^a$	$2.0 \pm 0.1^{ab}$	$98.89 \pm 4.77^{ab}$	$0.113 \pm 0.006^{ab}$	$72.15 \pm 2.41^a$
TC09	$670.0 \pm 42.9^a$	$89.7 \pm 5.3^a$	$1.9 \pm 0.1^a$	$90.19 \pm 4.97^a$	$0.136 \pm 0.006^c$	$69.09 \pm 2.60^a$
TC10	$788.3 \pm 53.7^{ab}$	$103.2 \pm 4.9^{ab}$	$2.1 \pm 0.2^{abc}$	$102.24 \pm 6.17^b$	$0.130 \pm 0.012^{cd}$	$72.41 \pm 1.78^a$
TC11	$902.9 \pm 81.4^{bc}$	$118.1 \pm 5.9^{bc}$	$2.2 \pm 0.1^{bc}$	$113.18 \pm 3.47^{cd}$	$0.111 \pm 0.004^a$	$79.29 \pm 2.30^b$
TC13	$795.4 \pm 34.9^{ab}$	$103.4 \pm 3.4^{ab}$	$2.2 \pm 0.1^{bc}$	$104.57 \pm 5.54^{bd}$	$0.132 \pm 0.009^c$	$69.98 \pm 1.84^a$
TC14	$998.8 \pm 42.0^c$	$127.9 \pm 5.5^c$	$2.6 \pm 0.1^d$	$116.75 \pm 3.80^e$	$0.116 \pm 0.001^{abd}$	$71.64 \pm 0.59^a$
TC17	$899.5 \pm 86.1^{bc}$	$113.5 \pm 12.7^{bc}$	$2.3 \pm 0.1^{cd}$	$108.83 \pm 5.24^{bcd}$	$0.127 \pm 0.003^{bcd}$	$70.80 \pm 2.19^a$

Note. Different superscript alphabets a-d in the same column denote statistical significance ( $p < 0.05$ )

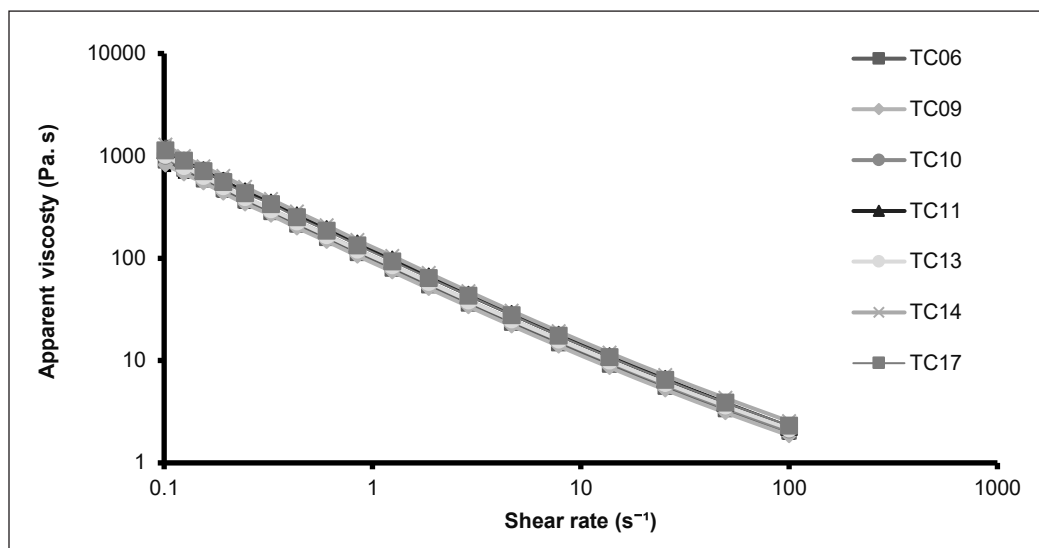


Figure 2. Viscosity flow curves of the formulated creams

### *In vitro Occlusive*

The occlusion effect is one of the critical features of moisturizers to ameliorate AD symptoms via TEWL prevention and skin rehydration (Hebert et al., 2020). Current results demonstrate that the occlusion factor of formulation TC11 was significantly higher than all other formulations (Table 8). It could prevent an additional about 7.14% to 10.2% water loss. The results indicated that applying TC11 could form a thin film to prevent water loss through evaporation, giving greater skin hydration efficiency. The highest concentration of petrolatum and mineral oil incorporated into TC11 and the desirable rheological behaviors exhibited by TC11 would have contributed to this attribute.

## **Characterization of the Selected Nanoemulsion and Moisturizer Cream Formulations**

### *Morphological Study*

A transmission electron microscope is an instrument that allows point-to-point measurement of a single droplet's size of nanoemulsion. The results in Figure 3A showed that the nanoemulsion droplets of the selected formulation were in the nanoscale range with spherical shape and uniform size. It confirms the results obtained from dynamic light scattering measurement ( $121.5 \pm 1.8$  nm). These results were similar to those reported by Chong et al. (2018). The microscopic images of the freshly prepared TC11 cream indicate that the moisturizer cream's microstructure was spherical (Figure 3B).

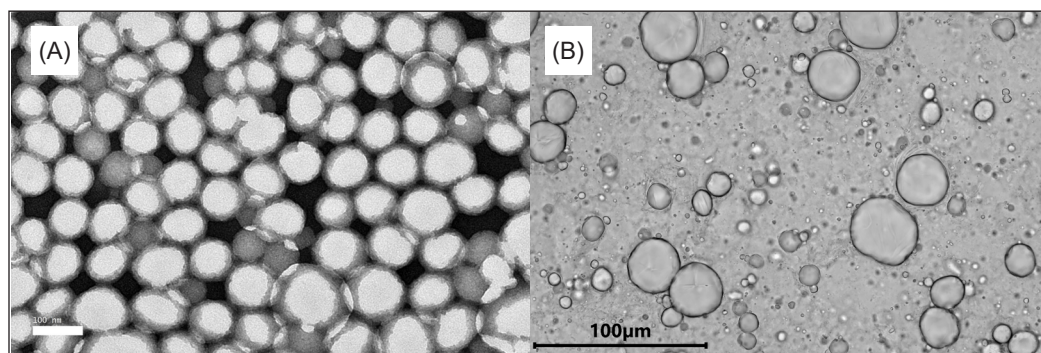


Figure 3. The morphology of the selected (A) nanoemulsion and (B) cream formulations was examined using the transmission electron microscope and light microscope, respectively

### *In vitro Release*

Figure 4 illustrates the antioxidant release profiles for the selected nanoemulsion and cream formulations, showing a concave down-like shape. Within the nanoemulsion matrix, it was observed that the cumulative amount of the released antioxidants per unit of the surface area increased as a function of time until a plateau was attained at 5 hr from the start of the

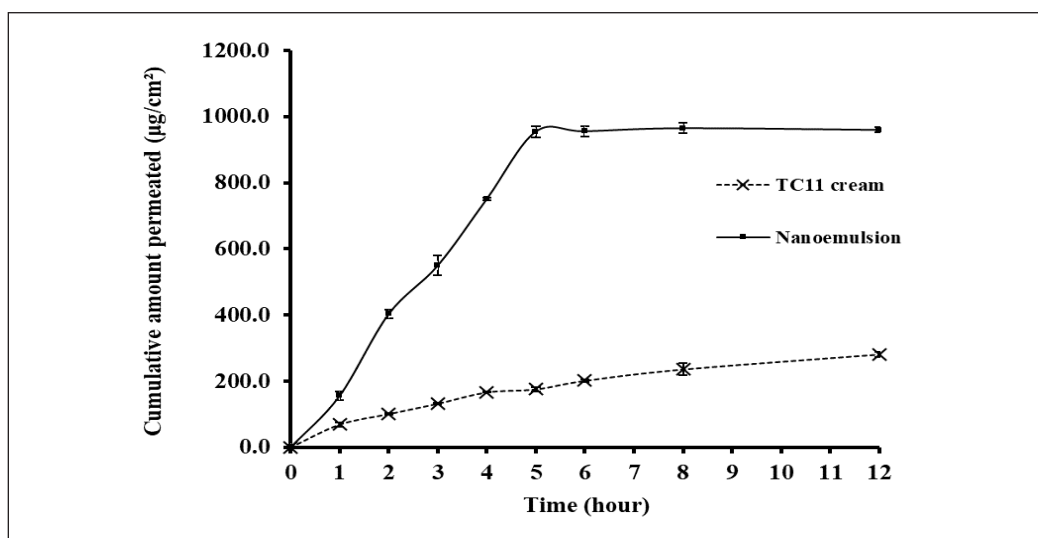


Figure 4. *In vitro* release profiles of encapsulated antioxidants from formulated nanoemulsion and moisturizer cream for 12 hr

analysis. With the TC11 topical cream base matrix, the cumulative amount of the released antioxidants per unit of surface area gradually increased until the end of the investigation. After 12 h, the total release mean percentages of antioxidants were 100% and 30.88% for nanoemulsion and TC11 cream, respectively, evidencing that the cumulative release of antioxidants was greater in nanoemulsion than in TC11 cream. Based on these results, the antioxidants release and diffusion through the membrane could be highly dependent on the delivery matrices or physicochemical properties of the formulation, with the slow release of antioxidants from TC11 cream probably due to the gelling attribute of the carbomer 940 and high viscosity of the cream base. The results were then fitted to the release kinetic models to give an idea of the release rate and mechanisms of antioxidants if used in topical application for the nanoemulsion and when the nanoemulsion was incorporated into the TC11 cream base. The results of the  $r^2$ , Akaike information criterion (AIC) and the corresponding constant values for each studied model were summarised in Table 9. Usually, the best-fit model can be identified based on the  $r^2$ , and if more than one model is accepted, the best-fit model can be further determined using AIC with the smallest value (Heredia et al., 2022).

Correspondingly, it was observed that the antioxidants released for nanoemulsion have a better adjustment to the zero-order model based on the calculated  $r^2$  value, indicating the release mechanism is independent of the initial concentration of antioxidants but as a function of time only. On the other hand, the TC11 cream base with a slower antioxidant release can fit with Higuchi, Korsmeyer-Peppas and Weibull models based on similar  $r^2$  values. Still, the Korsmeyer-Peppas and Weibull models were the best-fit models identified through AIC. With the  $\beta$  more than one in the Weibull model, the shape of the curve may

probably follow a sigmoidal form during release (Jahromi et al., 2020). Concurrently, the  $n$  value was located between 0.5 and 1.0 in the Korsmeyer-Peppas model, further suggesting that the release mechanism from the TC11 cream base might be following an anomalous non-Fickian transport (Paarakh et al., 2018).

## CONCLUSION

Using factorial design methodology, the present study successfully formulated nanoemulsion and moisturizer cream containing TRF, AT and carotenes. The ideal formulation and fabrication conditions of nanoemulsion were successfully screened. The preferred homogenization speed, time and temperature for coarse emulsion preparation using a high-shear mixer were 7000 rpm, 10 min and 45°C, respectively. The optimized homogenization pressure and cycles of high-pressure homogenizer for nanoemulsion formation were 750 bar and five cycles, respectively. The ideal formulation contains 73.75% w/w deionized water, 20% w/w red palm oil and 6.25% w/w Kolliphor® EL. When processed using the abovementioned conditions, nanoemulsion with mean droplet size between 100 to 200 nm and uniform size distribution (PDI < 0.200) was formed. Meanwhile, the moisturizer cream formulation showed that the ideal formulation consisted of 66.8% w/w deionized water, 10% w/w formulated nanoemulsion, 7.5% w/w petrolatum, 7.5% w/w mineral oil, 5% w/w glycerol, 3% w/w emulsifying wax and 0.2% w/w carbomer 940, with a final concentration of 0.1% w/w TRF, 0.1% w/w AT and 0.01% w/w carotenes. This optimally formulated cream could display the preferred shear-thinning behavior during topical application, increase skin hydration with its high occlusion factor, and exhibit Korsmeyer-Peppas and Weibull release kinetic mechanisms during in vitro release.

Table 9

In vitro, release kinetic study for the antioxidants released from formulated nanoemulsion and moisturizer cream

Model	Nanoemulsion	Cream
<b>Zero-order</b>		
$r^2$	0.9989	0.9466
AIC	121.09	1377.27
$k_0$	19.788	3.189
<b>First-order</b>		
$r^2$	0.9493	0.9401
AIC	4.04	4.00
$k_1$	4.734	4.552
<b>Higuchi</b>		
$r^2$	0.9587	0.9982
AIC	4454.08	51.04
$k_H$	37.121	8.843
<b>Korsmeyer-Peppas</b>		
$r^2$	0.9898	0.9943
AIC	4.02	4.01
$k_r$	0.094	-0.053
$n$	1.102	0.580
<b>Weibull</b>		
$r^2$	0.8647	0.9958
AIC	12.79	4.06
$\infty$	0.138	0.079
$\beta$	2.0859	0.6361

Note. AIC = Akaike information criterion;  $r^2$  = Coefficient of determination;  $k_0$  = the rate constant of zero-order release kinetics;  $k_1$  = the rate constant of first-order release kinetics;  $k_H$  = Higuchi dissolution constant;  $\infty$  - scale parameter that defines the timescale of the process;  $\beta$  = curve shape factor

## ACKNOWLEDGEMENTS

This study was supported by the Fundamental Research Grant Scheme (FRGS), Ministry of Higher Education Malaysia, under grant number FRGS/1/2017/STG05/UPM/01/6. The authors wish to express sincere appreciation to Shimadzu Malaysia Sdn. Bhd. for the HPLC instruments and technical assistance provided, which contributed to the success of this project.

## REFERENCES

- Amin, M. N., Liza, K. F., Sarwar, Md. S., Ahmed, J., Adnan, Md. T., Chowdhury, M. I., Hossain, M. Z., & Islam, M. S. (2015). Effect of lipid peroxidation, antioxidants, macro minerals and trace elements on eczema. *Archives of Dermatological Research*, 307(7), 617–623. <https://doi.org/10.1007/s00403-015-1570-2>
- Babaye-Nazhad, S., Amirmia, M., Khodaeyani, E., Afza, P. N., Alikhah, H., & Naghavi-Behzad, M. (2013). Effect of oral vitamin E on atopic dermatitis. *Journal of Clinical Research & Governance*, 2, 66–69. <https://doi.org/10.13183/jcrg.v2i2.55>
- Bruschi, M. (2015). Mathematical models of drug release. In M. Bruschi (Eds.), *Strategies to modify the drug release from pharmaceutical systems* (pp. 63–86). Wood head Publishing. <https://doi.org/10.1016/B978-0-08-100092-2.00005-9>
- Chellapa, P., Mohamed, A. T., Keleb, E. I., Elmahgoubi, A., Eid, A. M., Issa, Y. S., & Elmarzugli, N. A. (2015). Nanoemulsion and nanoemulgel as a topical formulation. *IOSR Journal of Pharmacy*, 5(10), 43–47.
- Chen, M. X., Alexander, K. S., & Baki, G. (2016). Formulation and evaluation of antibacterial creams and gels containing metal ions for topical application. *Journal of Pharmaceutics*, 2016(1), 5754349. <https://doi.org/10.1155/2016/5754349>
- Chong, W.-T., Tan, C.-P., Cheah, Y.-K., Lajis, A. F., Dian, N. L. H. M., Sivaruby, K., & Lai, O.-M. (2018). Optimization of process parameters in preparation of tocotrienol-rich red palm oil-based anoemulsion stabilized by Tween 80-Span 80 using response surface methodology. *PLoS ONE*, 13(8), e0202771. <https://doi.org/10.1371/journal.pone.0202771>
- Dantas, M. G. B., Reis, S. A. G. B., Damasceno, C. M. D., Rolim, L. A., Rolim-Neto, P. J., Carvalho, F. O., Quintans-Junior, L. J., & Da Silva Almeida, J. R. G. (2016). Development and evaluation of stability of a gel formulation containing the monoterpene borneol. *The Scientific World Journal*, 2016(1), 7394685. <https://doi.org/10.1155/2016/7394685>
- De Pascale, M. C., Bassi, A. M., Patrone, V., Villacorta, L., Azzi, A., & Zingg, J.-M. (2006). Increased expression of transglutaminase-1 and PPAR $\gamma$  after vitamin E treatment in human keratinocytes. *Archives of Biochemistry and Biophysics*, 447(2), 97–106. <https://doi.org/10.1016/j.abb.2006.02.002>
- Demma, A., Sartor, F., Tontini, G., Pastorelli, L., & Vecchi, M. (2018). Rheological characterization of two different suspension formulations of beclomethasone dipropionate enemas for rectal administration. *Journal of Pharmaceutical Technology and Drug Research*, 7, 1. <https://doi.org/10.7243/2050-120X-7-1>

- Galvão, K. C. S., Vicente, A. A., & Sobral, P. J. A. (2018). Development, characterization, and stability of o/w pepper nanoemulsions produced by high-pressure homogenization. *Food and Bioprocess Technology*, *11*(2), 355–367. <https://doi.org/10.1007/s11947-017-2016-y>
- Hayashi, D., Sugaya, H., Ohkoshi, T., Sekizawa, K., Takatsu, H., Shinkai, T., & Urano, S. (2012). Vitamin E improves biochemical indices associated with symptoms of atopic dermatitis-like inflammation in nc/nga mice. *Journal of Nutritional Science and Vitaminology*, *58*(3), 161–168. <https://doi.org/10.3177/jnsv.58.161>
- Hebert, A. A., Rippke, F., Weber, T. M., & Nicol, N. H. (2020). Efficacy of nonprescription moisturizers for atopic dermatitis: An updated review of clinical evidence. *American Journal of Clinical Dermatology*, *21*(5), 641–655. <https://doi.org/10.1007/s40257-020-00529-9>
- Hemrajani, C., Negi, P., Parashar, A., Gupta, G., Jha, N. K., Singh, S. K., Chellappan, D. K., & Dua, K. (2022). Overcoming drug delivery barriers and challenges in topical therapy of atopic dermatitis: A nanotechnological perspective. *Biomedicine & Pharmacotherapy*, *147*, 112633. <https://doi.org/10.1016/j.biopha.2022.112633>
- Heredia, N. S., Vizuete, K., Flores-Calero, M., V, K. P., Pilaquina, F., Kumar, B., & Debut, A. (2022). Comparative statistical analysis of the release kinetics models for nanoprecipitated drug delivery systems based on poly (lactic-co-glycolic acid). *PLOS ONE*, *17*(3), e0264825. <https://doi.org/10.1371/journal.pone.0264825>
- Hiragun, M., Hiragun, T., Oseto, I., Uchida, K., Yanase, Y., Tanaka, A., Okame, T., Ishikawa, S., Mihara, S., & Hide, M. (2016). Oral administration of  $\beta$ -carotene or lycopene prevents atopic dermatitis-like dermatitis in HR-1 mice. *The Journal of Dermatology*, *43*(10), 1188–1192. <https://doi.org/10.1111/1346-8138.13350>
- Jafari, S. M., Assadpoor, E., He, Y., & Bhandari, B. (2008). Re-coalescence of emulsion droplets during high-energy emulsification. *Food Hydrocolloid*, *22*(7), 1191–1202. <https://doi.org/10.1016/j.foodhyd.2007.09.006>
- Jaffary, F., Faghihi, G., Mokhtarian, A., & Hosseini, S. M. (2015). Effects of oral vitamin E on treatment of atopic dermatitis: A randomized controlled trial. *Journal of Research in Medical Sciences*, *20*(11), 1053. <https://doi.org/10.4103/1735-1995.172815>
- Jahromi, L. P., Ghazali, M., Ashrafi, H., & Azadi, A. (2020). A comparison of models for the analysis of the kinetics of drug release from PLGA-based nanoparticles. *Heliyon*, *6*(2), e03451. <https://doi.org/10.1016/j.heliyon.2020.e03451>
- Javanbakht, M. H., Keshavarz, S. A., Djalali, M., Siassi, F., Eshraghian, M. R., Firooz, A., Seirafi, H., Ehsani, A. H., Chamari, M., & Mirshafiey, A. (2011). Randomized controlled trial using vitamins E and D supplementation in atopic dermatitis. *Journal of Dermatological Treatment*, *22*(3), 144–150. <https://doi.org/10.3109/09546630903578566>
- Ji, H., & Li, X.-K. (2016). Oxidative stress in atopic dermatitis. *Oxidative Medicine and Cellular Longevity*, *2016*(1), 2721469. <https://doi.org/10.1155/2016/2721469>
- Jung, Y. J., Yoon, J.-H., Kang, N. G., Park, S. G., & Jeong, S. H. (2012). Diffusion properties of different compounds across various synthetic membranes using Franz-type diffusion cells. *Journal of Pharmaceutical Investigation*, *42*(5), 271–277. <https://doi.org/10.1007/s40005-012-0040-5>

- Kake, T., Imai, M., & Takahashi, N. (2019). Effects of  $\beta$ -carotene on oxazolone-induced atopic dermatitis in hairless mice. *Experimental Dermatology*, 28(9), 1044–1050. <https://doi.org/10.1111/exd.14003>
- Kapun, A. P., Salobir, J., Levart, A., Kalcher, G. T., Svete, A. N., & Kotnik, T. (2014). Vitamin E supplementation in canine atopic dermatitis: Improvement of clinical signs and effects on oxidative stress markers. *Veterinary Record*, 175(22), 560–560. <https://doi.org/10.1136/vr.102547>
- Kato, E., & Takahashi, N. (2012). Improvement by sodium dl- $\alpha$ -tocopheryl-6-O-phosphate treatment of moisture-retaining ability in stratum corneum through increased ceramide levels. *Bioorganic & Medicinal Chemistry*, 20(12), 3837–3842. <https://doi.org/10.1016/j.bmc.2012.04.029>
- Kim, K. P., Shin, K.-O., Park, K., Yun, H. J., Mann, S., Lee, Y. M., & Cho, Y. (2015). Vitamin c stimulates epidermal ceramide production by regulating its metabolic enzymes. *Biomolecules & Therapeutics*, 23(6), 525–530. <https://doi.org/10.4062/biomolther.2015.044>
- Krishnaiah, Y. S. R., Xu, X., Rahman, Z., Yang, Y., Katragadda, U., Lionberger, R., Peters, J. R., Uhl, K., & Khan, M. A. (2014). Development of performance matrix for generic product equivalence of acyclovir topical creams. *International Journal of Pharmaceutics*, 475(1), 110–122. <https://doi.org/10.1016/j.ijpharm.2014.07.034>
- Kruszewski, B., Zawada, K., & Karpiński, P. (2021). Impact of high-pressure homogenization parameters on physicochemical characteristics, bioactive compounds content, and antioxidant capacity of blackcurrant juice. *Molecules*, 26(6), 1802. <https://doi.org/10.3390/molecules26061802>
- Kuhn, K. R., & Cunha, R. L. (2012). Flaxseed oil – whey protein isolate emulsions: Effect of high-pressure homogenization. *Journal of Food Engineering*, 111(2), 449–457. <https://doi.org/10.1016/j.jfoodeng.2012.01.016>
- Laughter, M. R., Maymone, M. B. C., Mashayekhi, S., Arents, B. W. M., Karimkhani, C., Langan, S. M., Dellavalle, R. P., & Flohr, C. (2021). The global burden of atopic dermatitis: Lessons from the global burden of disease study 1990–2017\*. *British Journal of Dermatology*, 184(2), 304–309. <https://doi.org/10.1111/bjd.19580>
- Lee, J. H., Jeon, Y.-J., Choi, J. H., Kim, H. Y., & Kim, T.-Y. (2017). Effects of vitabride<sup>12</sup> on skin inflammation. *Annals of Dermatology*, 29(5), 548–558. <https://doi.org/10.5021/ad.2017.29.5.548>
- Leveque, N., Robin, S., Muret, P., Mac-Mary, S., Makki, S., & Humbert, P. (2003). High iron and low ascorbic acid concentrations in the dermis of atopic dermatitis patients. *Dermatology*, 207(3), 261–264. <https://doi.org/10.1159/000073087>
- Myriam, M., Sabatier, M., Steiling, H., & Williamson, G. (2006). Skin bioavailability of dietary vitamin E, carotenoids, polyphenols, vitamin C, zinc and selenium. *British Journal of Nutrition*, 96(2), 227–238. <https://doi.org/10.1079/BJN20061817>
- Oladimeji, F. A., Akinkunmi, E. O., Raheem, A. I., Abiodun, G. O., & Bankole, V. O. (2015). Evaluation of topical antimicrobial ointment formulations of essential oil of *Lippia multiflora* moldenke. *African Journal of Traditional, Complementary and Alternative Medicines*, 12(5), 135–144. <https://doi.org/10.4314/ajtcam.v12i5.18>
- Paarakh, M. P., Jose, P. A., Setty, C., & Christopher, G. V. P. (2018). Release kinetics – concepts and applications. *International Journal of Pharmacy Research & Technology (IJPRT)*, 8(1), 12–20. <https://doi.org/10.31838/ijprt/08.01.02>



- Packer, L., Weber, S. U., & Rimbach, G. (2001). Molecular aspects of  $\alpha$ -tocotrienol antioxidant action and cell signalling. *The Journal of Nutrition*, *131*(2), 369S-373S. <https://doi.org/10.1093/jn/131.2.369S>
- Parish, W. E., Read, J., & Paterson, S. E. (2005). Changes in basal cell mitosis and transepidermal water loss in skin cultures treated with vitamins C and E. *Experimental Dermatology*, *14*(9), 684–691. <https://doi.org/10.1111/j.0906-6705.2005.00340.x>
- Pasonen-Seppänen, S., Suhonen, M. T., Kirjavainen, M., Suihko, E., Urtti, A., Miettinen, M., Hyttinen, M., Tammi, M., & Tammi, R. (2001). Vitamin C enhances differentiation of a continuous keratinocyte cell line (REK) into epidermis with normal stratum corneum ultrastructure and functional permeability barrier. *Histochemistry and Cell Biology*, *116*(4), 287–297. <https://doi.org/10.1007/s004180100312>
- Peng, J., Dong, W. J., Li, L., Xu, J. M., Jin, D. J., Xia, X. J., & Liu, Y. L. (2015). Effect of high-pressure homogenization preparation on mean globule size and large-diameter tail of oil-in-water injectable emulsions. *Journal of Food and Drug Analysis*, *23*(4), 828-835. <https://doi.org/10.1016/j.jfda.2015.04.004>
- Qian, C., & McClements, D. J. (2011). Formation of nanoemulsions stabilized by model food-grade emulsifiers using high-pressure homogenization: Factors affecting particle size. *Food Hydrocolloid*, *25*(5), 1000-1008. <https://doi.org/10.1016/j.foodhyd.2010.09.017>
- Rocha-Filho, P. A., Ferrari, M., Maruno, M., Souza, O., & Gumiero, V. (2017). In vitro and in vivo evaluation of nanoemulsion containing vegetable extracts. *Cosmetics*, *4*(3), 32. <https://doi.org/10.3390/cosmetics4030032>
- Roohinejad, S., Oey, I., Wen, J., Lee, S. J., Everett, D. W., & Burritt, D. J. (2015). Formulation of oil-in-water  $\beta$ -carotene microemulsions: Effect of oil type and fatty acid chain length. *Food Chemistry*, *174*, 270–278. <https://doi.org/10.1016/j.foodchem.2014.11.056>
- Sakai, S., Sugawara, T., & Hirata, T. (2011). Inhibitory effect of dietary carotenoids on dinitrofluorobenzene-induced contact hypersensitivity in mice. *Bioscience, Biotechnology, and Biochemistry*, *75*(5), 1013–1015. <https://doi.org/10.1271/bbb.110104>
- Salamanca, C. H., Barrera-Ocampo, A., Lasso, J. C., Camacho, N., & Yarce, C. J. (2018). Franz diffusion cell approach for pre-formulation characterisation of ketoprofen semi-solid dosage forms. *Pharmaceutics*, *10*(3), 148. <https://doi.org/10.3390/pharmaceutics10030148>
- Sato, Y., Akiyama, H., Suganuma, H., Watanabe, T., Nagaoka, M. H., Inakuma, T., Goda, Y., & Maitani, T. (2004). The feeding of  $\beta$ -carotene down-regulates serum ige levels and inhibits the type i allergic response in mice. *Biological and Pharmaceutical Bulletin*, *27*(7), 978–984. <https://doi.org/10.1248/bpb.27.978>
- Savini, I., Rossi, A., Duranti, G., Avigliano, L., Catani, M. V., & Melino, G. (2002). Characterization of keratinocyte differentiation induced by ascorbic acid: Protein kinase c involvement and vitamin c homeostasis. *Journal of Investigative Dermatology*, *118*(2), 372–379. <https://doi.org/10.1046/j.0022-202x.2001.01624.x>
- Siska, B., Snejdrova, E., Machac, I., Dolecek, P., & Martiska, J. (2019). Contribution to the rheological testing of pharmaceutical semisolids. *Pharmaceutical Development and Technology*, *24*(1), 80–88. <https://doi.org/10.1080/10837450.2018.1425432>
- Sivaranjani, N., Rao, S. V., & Rajeev, G. (2013). Role of reactive oxygen species and antioxidants in atopic dermatitis. *Journal of Clinical and Diagnostic Research*, *7*(12), 2683–2685. <https://doi.org/10.7860/JCDR/2013/6635.3732>

- Swarnavalli, G. C. J., Dinakaran, S., & Divya, S. (2016). Preparation and characterization of nanosized Ag/SLN composite and its viability for improved occlusion. *Applied Nanoscience*, *6*(7), 1065–1072. <https://doi.org/10.1007/s13204-016-0522-2>
- Tsudoku, T., Kuriyama, K., Nakagawa, K., & Miyazawa, T. (2013). Tocotrienol (unsaturated vitamin e) suppresses degranulation of mast cells and reduces allergic dermatitis in mice. *Journal of Oleo Science*, *62*(10), 825–834. <https://doi.org/10.5650/jos.62.825>
- Uluata, S., Decker, E. A., & McClements, D. J. (2016). Optimization of nanoemulsion fabrication using microfluidization: Role of surfactant concentration on formation and stability. *Food Biophysics*, *11*(1), 52–59. <https://doi.org/10.1007/s11483-015-9416-1>
- Weber, T. M., Samarin, F., Babcock, M. J., Filbry, A., & Rippke, F. (2015). Steroid-free over-the-counter eczema skin care formulations reduce risk of flare, prolong time to flare, and reduce eczema symptoms in pediatric subjects with atopic dermatitis. *Journal of Drugs in Dermatology*, *14*(5), 478–485.
- Williamson, S., Merritt, J., & De Benedetto, A. (2020). Atopic dermatitis in the elderly: A review of clinical and pathophysiological hallmarks. *British Journal of Dermatology*, *182*(1), 47–54. <https://doi.org/10.1111/bjd.17896>
- Yarce, C. J., Pineda, D., Correa, C. E., & Salamanca, C. H. (2016). Relationship between surface properties and in vitro drug release from a compressed matrix containing an amphiphilic polymer material. *Pharmaceuticals*, *9*(3), 34. <https://doi.org/10.3390/ph9030034>
- Ye, M., Duan, H., Yao, L., Fang, Y., Zhang, X., Dong, L., Yang, F., Yang, X., & Pan, W. (2019). A method of elevated temperatures coupled with magnetic stirring to predict real time release from long acting progesterone PLGA microspheres. *Asian Journal of Pharmaceutical Sciences*, *14*(2), 222–232. <https://doi.org/10.1016/j.ajps.2018.05.010>
- Zuuren, E. J. van, Fedorowicz, Z., Christensen, R., Lavrijsen, A. P., & Arents, B. W. (2017). Emollients and moisturisers for eczema. *Cochrane Database of Systematic Reviews*, *2*(2). <https://doi.org/10.1002/14651858.CD012119.pub2>

## Sequential Cropping Productivity Evaluation of Corn, Mung Bean, and Sweet Potato Intercrop under Coconut Field in Zamboanga del Sur, Philippines

Nelmie Bendanillo Pongao-Ponio<sup>1\*</sup> and Ma. Stella M. Paulican<sup>2</sup>

<sup>1</sup>Faculty, School of Agriculture, Forestry and Environmental Studies, J.H. Cerilles State College Mati, San Miguel, 7029, Zamboanga del Sur, Philippines

<sup>2</sup>Faculty, College of Agriculture, Central Mindanao University, Musuan, Maramag, 8710 Bukidnon, Philippines

### ABSTRACT

Multiple cropping and sequential cropping system strategies with existing perennial crops would augment soil productivity per unit area, which optimizes crop production for food security. The study evaluated the effects of cropping patterns on the agronomic and yield performance, total productivity and profitability of corn, mung bean, and sweet potato planted under coconut ground in Zamboanga del Sur, Philippines. There were eight cropping patterns (CP) [(CP<sub>1</sub>—corn followed by mung bean), (CP<sub>2</sub>—corn followed by sweet potato), (CP<sub>3</sub>—corn intercropped with mung bean followed by sweet potato), (CP<sub>4</sub>—corn intercropped with sweet potato followed by mung bean), (CP<sub>5</sub>—mung bean followed by corn), (CP<sub>6</sub>—sweet potato followed by corn), (CP<sub>7</sub>—mung bean followed corn intercropped with sweet potato), (CP<sub>8</sub>—sweet potato followed by corn intercropped with mung bean)] arranged in Randomized Complete Block Design (RCBD). The results revealed that growing in a cropping pattern relative to the cropping period affected the days of tasseling and silking, plant and ear height, percent shelling, weight of 1000 seeds, and grains of corn. Sole corn and mung bean intercrop showed the same results, while Corn + Sweet potato intercropping decreased plant height and grain yield in corn regardless of the cropping pattern. Mung beans are affected by the cropping season in terms of the days of flowering, maturity, plant height, weight of 1000 seeds, and yield. Sweet potatoes showed the best performance in a number of lateral vines, maturity, and yield when placed first in the cropping pattern. However, sweet potato intercropping resulted in a reduction in yield. Further, CP<sub>6</sub>—sweet potato, followed by corn, had a notable total yield with a 98% return on investment and as a recommended intercropping pattern under coconut ground in the area.

### ARTICLE INFO

#### Article history:

Received: 22 April 2024

Accepted: 24 July 2024

Published: 28 January 2025

DOI: <https://doi.org/10.47836/pjtas.48.1.07>

#### E-mail addresses:

[nbpongao@gmail.com](mailto:nbpongao@gmail.com) (Nelmie Bendanillo Pongao-Ponio)

[bingmarquezpaulican@gmail.com](mailto:bingmarquezpaulican@gmail.com) (Ma. Stella M. Paulican)

\*Corresponding author

**Keywords:** Agroeconomic crops, cropping pattern, crop placement, intercropping, productivity

## INTRODUCTION

The global demand for food, as a result of the growing population, denotes more ample solutions and intensification in agricultural production to ensure food security (Lirio et al., 2023). Declining agricultural production as a result of land conversion, climate change, and biodiversity considerations are just a few of the obstacles that need to be overcome to satisfy demands (Rondhi et al., 2018). A single crop used for mass production necessitates the excessive application of synthetic fertilizers and pesticides, which increases pollution, reduces agricultural diversity, and ultimately results in food insecurity (Smith et al., 2020). As those are part of the growing concern in agriculture, adaptability in crop diversification programs using multiple cropping systems may alleviate crop productivity and aggravate negative impact, loss of biodiversity, and crop losses due to climate effects (Hufnagel et al., 2020; Food and Agriculture Organization, 2001). The multiple cropping approach combines certain perennial crops with agronomic crops to increase crop productivity, income, and food supply, benefiting both economically and ecologically (Waha et al., 2020).

In concept, multiple cropping comes into many examples, such as intercropping, double cropping and crop rotation. However, one must understand the variety of techniques in cropping patterns, growing crops in succession in one field at a particular time, considering climatic factors (Negash et al., 2017). Further, crop rotation practice is planting a series of different crops right after the other with a short harvest period (Tariq et al., 2019). Intercropping practice is cultivating short-period main or cash crops like root crops or vegetables under tall perennial crops like coconut and fruit-bearing trees (Fan et al., 2020). The time, space and arrangement of crops in a particular land area would enable increased crop productivity, production efficiency, land use efficiency, and economic return (Castellazzi et al., 2008). Likewise, the practice of intensive cropping systems under perennials with sequential patterns and crop rotations is extremely important. It enhances sustainable system productivity by efficiently using resources like microclimate and nutrient dynamics (Amosse et al., 2014).

Undeniably, coconut is one of the most well-known permanent crops for export (Moreno et al., 2020) in the Philippines while simultaneously importing corn and rice (Davidson, 2018). Under these conditions, intercropping agro-economic crops with sequential crop rotation and crop patterns will boost the land's economic value of coconuts and productivity instead of lone-produced crops and the income of coconut growers from coconut alone. In the Philippines, the primary coconut-producing regions include the Davao Region, CALABARZON, Northern Mindanao, and the Zamboanga Peninsula. Among these, the Zamboanga Peninsula ranks as the second-largest contributor to national coconut production, accounting for 13.6% of the total output. According to the Philippine Coconut Authority (2019), the region has a gross production spanning 1.747 million hectares. The intercropping system under coconut is an old practice of the local farmers with a continuous corn-corn-fallow sequential cropping pattern. Sowing usually starts in the first to the second

week of April, and the crop is harvested in the first to the second week of August. It is followed by cultivating another batch of corn to be planted in the third to fourth week of September and harvested at the end of January. After harvesting corn, the land is allowed to fallow for one and a half months.

Thus, there was a need to explore a study on cropping patterns using some agronomic crops to be grown under coconut. This study evaluated the cropping pattern and placement of some agronomic crops, such as corn, mung bean, and sweet potato, planted under coconuts. The specific objectives were (1) to evaluate and determine the key performance parameters of agronomic crops planted under coconut conditions; (2) to evaluate the total productivity of the crops grown under coconut; (3) assess the profitability of growing some agronomic crops under coconut in different cropping patterns in Zamboanga del Sur condition; and (4) determine the best cropping pattern under coconut to be recommended to farmers in Zamboanga del Sur. The study results would give farmers insight into the maximization of space between coconuts through intercropping.

## **MATERIALS AND METHODS**

### **Description of the Experimental Site**

The study was conducted at Bagong Oroquieta, Guipos, Zamboanga del Sur. The municipality of Guipos is a landlocked coastal province of Zamboanga del Sur. It has a land area of 9,104.60 hectares, accounting for 2.01% of the Zamboanga del Sur's total area. The town is approximately 7° 44' North, 123° 19' East, with an elevation estimated at 151.5 meters or 496.9 feet above mean sea level. The total land area covered by coconut production in the municipality is 1,126.98 hectares out of the total area of the province. There are 1,350 farmers owning an area of less than 5 hectares in size. A total of 40,091 coconut trees are within three years of planting, 66,055 coconut trees are more than 3 to 60 years old from planting, and only 99 coconut trees are more than 60 years old.

Coconut areas in the locality are usually intercropped with agronomic crops such as corn, rice, sweet potato, cassava, mung bean, peanut and some vegetables. The most adopted cropping patterns are corn-corn-fallow, corn-legumes-fallow, rice-corn and corn-root crops. This study was superimposed on the existing coconut plantation approximately seven years after its establishment. The variety of coconuts planted has not been identified. These are grown at a planting distance of 10 x 10 meters. It was previously intercropped with corn for five successive years except for the last cropping year, 2018, when it was planted with mung beans for a short-term study.

### **Experimental Design and Treatments**

The study was conducted in a 1,100 m<sup>2</sup> area under tall, statured perennial coconut trees and was prepared thoroughly. It was divided into three blocks, and each block was further

divided into eight plots, with a dimension of 8m × 3.5m. The alleys between blocks were four meters, and between plots, one meter to facilitate operations in the field. RCBD with eight treatments replicated three times was used. The different cropping pattern (CP) treatments were as follows: CP<sub>1</sub>—corn followed by mung bean sequential pattern (Corn-Mung bean). CP<sub>2</sub>—corn followed by sweet potato sequential pattern (Corn-Sweet potato). CP<sub>3</sub>—corn + mung bean intercrop followed by sweet potato (Corn + Mung bean-Sweet potato). CP<sub>4</sub>—Corn + Sweet potato intercrop followed by mung bean (Corn + Sweet potato-Mung bean). CP<sub>5</sub>—Mung bean followed by corn sequential pattern (Mung bean – Corn). CP<sub>6</sub>—Sweet potato followed by corn sequential pattern (Sweet potato-Corn). CP<sub>7</sub>—Mung bean followed by Corn + Sweet potato (Mung bean-Corn + Sweet potato). CP<sub>8</sub>—Sweet potato followed by corn + mung bean (Sweet potato-Corn + Mung bean).

### Cropping Period and Rainfall Data

The cropping period, comprising two seasons, started from September 2019 to March 2021. The first cropping was conducted from October 2019 to March 2020, and the second was conducted from May 2020 to March 2021. The rainfall data of the experimental area was taken to the nearest agro-meteorological weather station (Figure 1). The crops received total mean rainfall of 200.64 mm and 286.58 mm during the cropping period of 2019–2020 and 2020–2021, respectively. The month of June 2019 received the heaviest rainfall record and regularly decreased until the end of the cropping season. On the other hand, more than 70% of the rain was received on the second cropping from May 2020 to February 2021. Thus, in the same month of 2020 (June), the plant received the highest rainfall, and the decreases continued until the end of the cropping pattern. Hence, January 2021 had the lowest rainfall received by the plant.

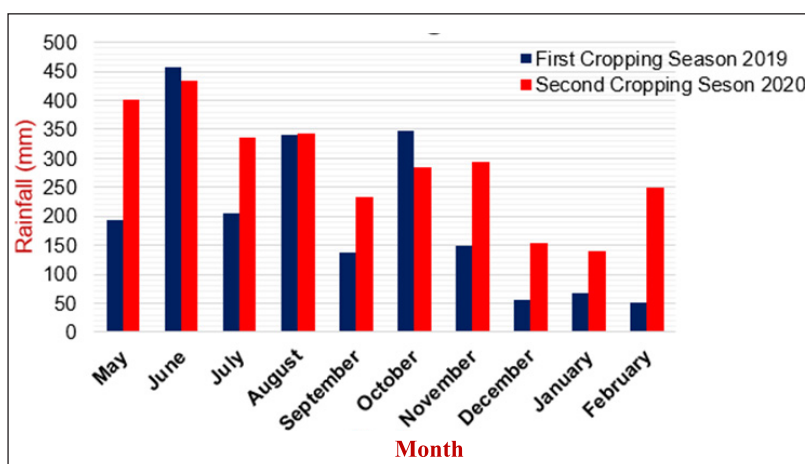


Figure 1. Mean monthly rainfall (mm), May 2019 - February 2021

## **Crop Management and Harvesting**

### ***Land Preparation***

The experimental area between coconut trees spaced  $10 \times 10$  meters was plowed twice using the animal-drawn moldboard plow and harrowed once before planting. This provided good soil condition and tilth for root development and minimized the weed problem. Furrows were prepared one meter away from the coconut trees with a spacing of 60 cm and about 8 cm depth for corn, mung bean and sweet potato intercrops.

### ***Planting of Sole Crops***

- A. Corn— The seeds were planted by sowing at a planting distance of 60 cm by 25 cm and covered with fine soil about 2 cm thick. Thinning was also done one week after planting, leaving only one plant per hill. At this time, the missing hills were replanted.
- B. Mung bean—Planting was performed by sowing the seeds at a planting spacing of 60 cm by 25 cm. Sown seeds were covered with fine soil around 2 cm thick. Thinning was executed one week after germination, leaving only two plants per hill. Replanting of missing hills was simultaneously done with thinning.
- C. Sweet potato—Vine cuttings around 25 cm in length were secured. These were planted in beds spaced at a planting distance of 60 cm by 25 cm with one cutting per hill. Prior to planting, defoliation was done on each stem cutting to prevent over-transpiration in the field. In planting, two-thirds of the cuttings were buried in the soil and then covered with soil. The replanting of missing plants was done two weeks after planting.

### ***Planting of Intercrop Mixes***

- A. Corn + Mung bean—The replacement method was used for intercrops with a planting ratio of 1:1. Each plot had seven rows of mung bean and six rows of corn in an alternate arrangement. Planting was done by sowing the seeds on the furrows at 60 cm by 25 cm spacing and covering them with 2 cm thick soil. Thinning was done one week after germination, leaving only one plant per hill for corn and two plants for mung bean. The missing hills for both crops were replanted at the same time.
- B. Corn + Sweet potato—A replacement method was used with a planting ratio of 1:1. The plot had seven rows of sweet potatoes and six rows of corn in an alternate arrangement. Corn was planted by sowing the seeds on the furrows, whereas sweet potato cuttings were buried on the bed at least two-thirds of its length. They were spaced at 60 cm by 25 cm and covered with a 2 cm thick soil. For corn, thinning was done after one week, leaving only one plant per hill. On the other hand, replanting missing hills for corn was performed during that time. However, sweet potato was replanted two weeks after planting.

### ***Fertilization***

Based on the soil analysis results, the entire experimental site was applied with vermicast. The sweet potato recommended rates of three tons per hectare were used in the study, with 8.4 kg per experimental plot. The vermicast was applied during the final harrowing of the area to incorporate the organic nutrient source into the soil. It was done one week before planting. No organic fertilizers were applied in the next cropping.

### ***Weed Management***

The experimental area was weed-free through regular hand weeding operations to minimize competition between the plants and weeds for moisture, nutrients and other field resources. Hand weeding started two weeks after planting, depending on the weed density in the area. Manual hilling-up for sole and intercrops was done at 30 DAP. Further, spot weeding was done as often as necessary.

### ***Pest Management***

Insect pests and disease infestations were observed by cropping pattern per cropping season. Fermented Kakawati leaves were applied during the vegetative stage of the first cropping to control cutworm insect pests. Proper monitoring was taken into action as often as necessary until the crops reached maturity.

### ***Water Management***

The soil moisture was monitored during the critical stages of growth and development (germination, vegetative, flowering and pod/seed filling stages) of the crops.

### ***Harvesting***

- A. Corn ears were harvested 103 days after sowing when the grains matured, as indicated by glazed kernels and 90% browning of the leaves. The harvested ears were shelled and sundried until 14% moisture content was attained.
- B. Mung bean pods were harvested 60–80 days after sowing when they were brown or black, and as soon as 75% of the pods dried up. Priming was done every three days for at least three priming. Harvested pods were placed in a net bag before sun drying to facilitate easy threshing. The beans were sundried to 12% moisture content for safe storage.
- C. Sweet potato fresh roots were harvested 153 DAP (5 months) on the first cropping and 294 DAP (10 months) on the second cropping. When fleshy roots reached the desired size and passed the maturity test, they were cut crosswise and exposed to the air. When the cut surface dried up, the roots were already mature, but when sap still flowed, this



meant these were immature. All harvested roots were graded as marketable and non-marketable based on a set of criteria.

Criteria	Marketable Fleshy Root	Non-marketable fleshy roots
Root Length	At least 10 cm, uniform length	Very variable, slender
Root diameter	At least 4 cm, uniform diameter	Very variable, rough
Shape	Long to oblong	Various shape
Smoothness	Smooth to rough	Generally rough
General	Generally free from blemishes	Damaged, very badly bruised and diseased

## Data Gathering Procedure

### *Growth and Yield Parameter for Corn*

Days to emergence were taken when 80% of the seeds sown in a plot had emerged or germinated. The plant height (cm) was measured at harvest maturity with a meter stick. The plant height was measured from the base of the plant to the tip of the flag leaf of 10 representative sample hills per plot. Days to tasseling were taken from sowing up to when 80% of the plants in the plot had tassels. Days to silking were determined from the date of sowing up to when at least 80% of the plants per treatment had a 3 cm length of silk. Ear height (cm) was measured by measuring the distance of the ear node from the ground using ten representative samples per treatment. The yield and yield components were obtained. The weight (g) of 1000 seeds was obtained by weighing 1000 randomly selected seeds from each treatment. The shelling percentage was determined by weighing the shelled grains from ten randomly selected ear samples divided by the weight of unshelled ears multiplied by 100. The grain yield (kg/ha) was obtained from the seven data rows in each plot and expressed in kilograms per hectare (kg/ha). Grain yield was adjusted to 14% Moisture Content (MC) using the formula:

$$\text{Grain yield (kg/ha)} = \frac{\text{Plot yield (g)}}{1,000 \text{ g/kg}} \times \frac{10,000 \text{ m}^2/\text{ha}}{\text{Effective harvest area (EHA) (m}^2\text{)}} \times \frac{100 - \text{MC}}{86}$$

where, EHA = Effective harvest area, 8.4 m<sup>2</sup>.

### *Growth and Yield Parameter for Mung Bean*

Days to emergence were taken when 80% of the seeds sown had emerged in each plot. The number of days to flower was recorded from planting to when at least 50% of the plants per treatment flowered. The plant height (cm) was measured at harvest maturity. Plant height was measured from the base of the plant to the tip of the leaf for 10 representative sample

hills per plot using a meter stick. The days to maturity were taken at harvest based on the days from sowing to the first priming when 80% of the pods in a plot were turned brown or black. The yield and yield components were obtained. The pod length (cm) was based on the average length of 10 randomly selected pods from ten sample plants per treatment. The number of seeds per pod was determined by counting the number of seeds of 10 randomly selected pods from ten sample plants per treatment. The weight (cm) of 1000 seeds was obtained by weighing 1000 randomly selected seeds from each treatment using a triple beam balance. The bean yield (kg/ha) was obtained from the seven data rows in each plot and expressed in kilograms per hectare (kg/ha). The grain yield was adjusted to 12% MC using the formula above.

### ***Growth and Yield Parameters for Sweet Potato***

The length (cm) of the main vines was measured from the base to the tip of the vines of ten sample plants per treatment taken at harvest using a meter stick. The number of lateral vines was taken from the same sample plants per treatment taken at harvest. Days to maturity were recorded from the time of planting to the harvesting of fleshy roots. The yield and yield components were obtained. The length (cm) and diameter (cm) of marketable fleshy roots were taken from ten randomly selected fleshy roots of ten sample plants per treatment. The number of marketable fleshy roots was determined by counting all marketable fleshy roots from ten sample plants per plot. Weight (kg/ha) of marketable fleshy roots was determined by weighing the same marketable fleshy roots from the seven data rows and computed on a per hectare basis as follows:

$$\text{Weight of marketable fleshy roots (kg/ha)} = \frac{\text{Plot yield (g)}}{1,000 \text{ g/kg}} \times \frac{10,000\text{m}^2/\text{ha}}{\text{EHA (m}^2\text{)}}$$

where, EHA = Effective harvest area, 8.4 m<sup>2</sup>.

Further, the percentage of marketable fleshy root. It was determined by converting the data obtained from the number of marketable fleshy roots and computed as follows:

$$\text{Marketable fleshy roots (\%)} = \frac{\text{No. of marketable fleshy roots}}{\text{Total number of fleshy roots}} \times 100\%$$

While the number of non-marketable fleshy roots. It was determined by counting all non-marketable fleshy roots from the same sample plants per plot. Then, the weight (kg/ha) of non-marketable fleshy roots. It was determined by weighing the same non-marketable fleshy roots from the seven data rows and computed on a per-hectare basis:

$$\text{Weight of non-marketable fleshy roots (kg/ha)} = \frac{\text{Plot yield (g)}}{1,000 \text{ g/kg}} \times \frac{10,000 \text{ m}^2/\text{ha}}{\text{EHA (m}^2\text{)}}$$

where, EHA = Effective harvest area, 8.4 m<sup>2</sup>.

The percentage of non-marketable fleshy roots was determined by converting the data obtained from a number of non-marketable fleshy roots and computed as follows:

$$\text{Non-marketable fleshy roots (\%)} = \frac{\text{No. of non-marketable fleshy roots}}{\text{Total number of fleshy roots}} \times 100\%$$

### ***Productivity Measurements***

The total yield equivalent (PHP) was determined by adding the main crop and the intercrop yield. Further, the economic profitability was computed with the cost. The return of the experiment per treatment was computed to measure the Return on Investment (ROI), and this was calculated using the formula:

$$\text{ROI} = \frac{\text{Net income}}{\text{Cost of production}} \times 100$$

### **Statistical Analysis**

Agronomic characteristics, yield performance, productivity and profitability of corn, mung bean, and sweet potato were gathered. After collecting and tabulating, data were analyzed using statistical Analysis of Variance (ANOVA) in RCBD using Statistical Tool for Agricultural Research (STAR) software version 2.0.1. The Honestly Significant Difference (HSD) test determined significant differences among treatments.

## **RESULTS AND DISCUSSION**

### **Agronomic and Yield Performance of Corn**

Growing corn in cropping patterns resulted in varying plant and ear heights at maturity. The plant and ear heights of corn were significantly influenced by the placement of the crop in the pattern (Table 1). Plant height was generally shorter at 185.30–216.78 cm for corn grown from October 2019 to January 2020 (first cropping) compared to corn grown from May to August 2020 (second cropping) with 214.63–242.43 cm plant heights. The shortest plant height of corn was observed in CP4, Corn + Sweet potato-mung bean, with 185.30 cm. It may be due to competition between the corn and sweet potato components for Nitrogen.

There was no significant difference in plant height for corn planted in sole cropping or intercropping with mung bean within the same season at alpha 0.05 because lone corn cropping offers sufficient nutrition to the corn as there is no nutrient competition. Although the mung bean's capacity to fix nitrogen, which contributes N to the neighboring corn plants, causes a relatively small increase in the mean plant height of corn interplanted with it. As per the findings of Gong et al. (2021), the intercropping system's heightened competition facilitates the mung bean's capacity to enhance the biological fixation of nitrogen, propelling the intercrops' growth. This benefit of using atmospheric and complementing soil N for mung bean intercropping reduces competition for N nutrients (Balde et al., 2011).

However, the results showed that corn with sweet potato intercropping during the first cropping produced a significantly shorter plant height than corn planted in sole cropping or monocropping at the second cropping. Further, sole corn in the first and second cropping yielded no significant difference, yet higher means were observed in the second cropping after mung bean and sweet potato. This observation might be due to the changes in soil moisture relative to the amount of rainfall received, not directly to the effect of non-leguminous or leguminous cropping patterns.

The ear height of corn differed significantly in the cropping pattern. The same trend was observed with the plant height of corn in different cropping patterns. Ear height in corn planted from the first cropping was significantly shorter at 65.88–83.60 cm than in corn grown in the second cropping, with heights ranging from 96.0–116.57 cm. No significant difference was observed in the ear height of corn planted in sole cropping or intercropped within the same cropping season. Intercropping of Corn + Sweet potato (CP4) had a significantly shorter ear height of 65.88 cm than corn planted in sole cropping or intercropping in the second cropping season. It confirmed the observation that sweet potato was a strong competitor for corn in terms of nutrients and available resources in the soil. Opposing to the result of the study by Goulart et al. (2011) indicated that sweet potato intercrop with sweet corn does not affect the height of sweetcorn.

Furthermore, the yield and yield components of corn, such as the weight of 1,000 seeds and the grain yield of corn in the cropping pattern grown under coconut, are presented in Table 2. There was a significant variation in the weight of 1000 seeds (268 to 270 g) as affected by cropping patterns. Both monocrop corn intercropped on the first cropping have a heavier grain than the corn produced in the second. In the cropping pattern, Corn + Mung bean (CP3) had heavier grains, 270 grams, in the first cropping. However, there was no significant difference in either sole corn or intercropping during the season. Corn planted on the second cropping showed no significant difference; thus, CP8, Sweet Potato-Corn + Mung bean, had heavier grains of 231.67 grams compared to corn sole and intercropped with sweet potato. Two cropping seasons determined that intercropping of Corn + Mung bean produced heavy grains in corn.

Table 1

*Plant and ear height (cm) at maturity of corn under coconut in various cropping patterns*

Treatment	Cropping patterns		Plant height (cm)	Ear height (cm)
	1 <sup>st</sup> cropping	2 <sup>nd</sup> cropping		
CP1	Corn	Mung bean	207.17 <sup>ab</sup>	72.80 <sup>bc</sup>
CP2	Corn	Sweet potato	216.38 <sup>ab</sup>	83.60 <sup>bc</sup>
CP3	Corn + Mung bean	Sweet potato	216.78 <sup>ab</sup>	82.83 <sup>bc</sup>
CP4	Corn + Sweet potato	Mung bean	185.30 <sup>b</sup>	65.88 <sup>c</sup>
CP5	Mung bean	Corn	229.37 <sup>a</sup>	108.50 <sup>a</sup>
CP6	Sweet potato	Corn	242.43 <sup>a</sup>	116.57 <sup>a</sup>
CP7	Mung bean	Corn + Sweet potato	214.63 <sup>ab</sup>	96.00 <sup>ab</sup>
CP8	Sweet potato	Corn + Mung bean	240.83 <sup>a</sup>	110.13 <sup>a</sup>
F- Test			**	**
% CV			5.75	9.07

*Note.* Means with the same letter(s) are not significantly different by least significant difference,  $p \geq 0.05$ , based on the Honestly Significant Difference test; \*\* = significant at  $p \leq 0.01$

Table 2

*Weight of 1,000 seeds and grain yield of corn under coconut in various cropping patterns*

Treatment	Cropping patterns		Weight of 1,000 seeds (g)	Grain yield (kg/ha)
	1 <sup>st</sup> cropping	2 <sup>nd</sup> cropping		
CP1	Corn	Mung bean	268.33 <sup>a</sup>	2176.60 <sup>ab</sup>
CP2	Corn	Sweet potato	251.67 <sup>ab</sup>	2855.17 <sup>a</sup>
CP3	Corn + Mung bean	Sweet potato	270.00 <sup>a</sup>	2345.27 <sup>ab</sup>
CP4	Corn + Sweet potato	Mung bean	241.67 <sup>abc</sup>	1115.10 <sup>b</sup>
CP5	Mung bean	Corn	225.00 <sup>bc</sup>	2948.42 <sup>a</sup>
CP6	Sweet potato	Corn	218.33 <sup>c</sup>	3067.47 <sup>a</sup>
CP7	Mung bean	Corn + Sweet potato	211.67 <sup>c</sup>	1281.75 <sup>b</sup>
CP8	Sweet potato	Corn + Mung bean	231.67 <sup>bc</sup>	2400.80 <sup>ab</sup>
F- Test			**	**
% CV			4.68	22.90

*Note.* Means with the same letter(s) are not significantly different by least significant difference,  $p \geq 0.05$ , based on the Honestly Significant Difference test; \*\* = significant at  $p \leq 0.01$

The cropping pattern significantly influenced the grain yield of corn per hectare. Thus, corn planted on the second cropping produced a higher grain yield at 2948.42–3067.47 kg/ha than corn grown on the first cropping. Corn planted in the first season showed significant differences among patterns. Two sole corn and corn intercropped with mung bean yielded 2176.60–2855.17 kg/ha, but when corn was intercropped with sweet potato, the yield of

corn was reduced. After mung bean, corn was observed to be higher because leguminous crops such as mung bean would help to nurture and replenish the soil (Arangote et al., 2022; Rani et al., 2019). The lowest grain yield was observed in CP4 (Corn + Sweet potato-mung bean) at 1115.10 kg/ha, comparable to Corn + Sweet potato planted after mung bean (CP7) at 1281.75 kg/ha. These values were significantly lower than corn in either sole or Corn + Mung bean intercropping. Altogether, 1000 grains of corn are greater in the first season compared to the second season, but the yield of corn is greater in the second season compared to the first season. This might be due to the number of grains. Some factors like cropping placement, mono or intercropping pattern, and their respective influence on soil condition, fertility, and rainfall received each cropping period. Besides, inter-specific competition between plants for above- and below-ground growth variables, such as soil moisture, nutrients, space, and solar radiation, may cause yield differences (Khan et al., 2012; Syafruddin, 2020). Similar data observed the oppositeness on the result of means in terms of 1000 grain weight but lower yield and higher yield but lower in 1000 grain weight because of the ecological factors and treatment (Musahraf et al., 2013; Nasar et al., 2023).

It confirms the study of Islam et al. (2014) that the intercropping of regular corn row + 1-row sweet potato yields 2.3 tons/ha compared to sole corn, which yields 5.2 tons/ha. It implies that corn intercropped with mung bean produced the exact outcome of sole corn, while corn intercropped with sweet potato has a low corn grain yield. Opposing the result of Johnson and Gurr (2016), rice, finger millet, maize, and pigeonpea yield was higher when intercropped with sweet potato compared to sole crops. Amaya et al. (2021) added that the presence of sweet potato in the planophile improves the intercrops yield.

### **Agronomic and Yield Performance of Mung bean**

The cropping patterns significantly influenced the plant height of mung beans (Table 3). The mung bean from the first cropping is shorter at 58.33–64.93 cm than the second at 78.43–85.07 cm. The plant height of mung bean planted after Corn + Sweet potato during the second cropping exhibited the tallest plant height at 85.05 cm. Although taller plants were observed during the second cropping (78.43–85.07 cm), the results show no significant difference from those planted in the first cropping. However, the shortest heights were observed at 58.33–59.80 cm in cropping patterns. CP3 and CP5 (first cropping) were significantly lower than CP4 (second cropping). No difference was observed when mung beans were planted in sole or intercropping. The bean yield of mung beans was significantly different among cropping patterns. Planting sole mung bean as the first crops (CP5 and CP7) produced the highest yield at 277.77–363.13 kg/ha over mung bean intercropped with corn (CP3). These mung bean yields were significantly higher than those planted in varying crop patterns during the second cropping. The second cropping of mung bean increases once compared with the cropping pattern of sole corn followed by mung bean (CP1) and

(CP4) Corn + Sweet potato; this might be due to the improved aeration of soil condition in cultivation with sweet potato. This result might be affected by the environmental condition. Bean yield increment on the first cropping was due to favorable climatic conditions; thus, the rainfall affected the second cropping. According to Ro et al. (2023), the mung bean, as drought-resistant in nature, cannot tolerate excess water. Mung bean requires relatively less water than other legumes for good growth and production. Nevertheless, no significant difference was observed when mung beans were planted in sole and intercropping within the season (Parida & Das, 2005). Mung bean intercropped with corn has a lower yield than sole mung bean, particularly on the first cropping, but almost the same on the second cropping, considering there was another yield from the companion crop. In conformity with this result, Alemayehu et al. (2018) found significant differences among seed yields of common bean varieties in maize + common bean intercropping. Likewise, Bekele et al. (2016) proved that grain yield per hectare of soybean was significantly affected by maize + soybean intercropping. In line with the result, Nasar et al. (2023) stated that intercropping reduced the mung bean yield by 28% compared to sole cropping of mung bean in maize + mung bean intercropping. Similarly, Arshad et al. (2020) obtained a significantly highest grain yield of sole mung bean in maize + mung bean intercropping.

Table 3

*Plant height and bean yield of mung bean under coconut in various cropping patterns*

Treatment	Cropping patterns		Plant height (cm)	Bean yield (kg/ha)
	1 <sup>st</sup> cropping	2 <sup>nd</sup> cropping		
CP3	Mung bean + Corn	Sweet potato	59.80 <sup>b</sup>	119.07 <sup>b</sup>
CP5	Mung bean	Corn	58.33 <sup>b</sup>	277.77 <sup>a</sup>
CP7	Mung bean	Corn + Sweet potato	64.93 <sup>ab</sup>	363.13 <sup>a</sup>
CP1	Corn	Mung bean	79.97 <sup>ab</sup>	89.29 <sup>b</sup>
CP4	Corn + Sweet potato	Mung bean	85.07 <sup>a</sup>	105.16 <sup>b</sup>
CP8	Sweet potato	Corn+ Mung bean	78.43 <sup>ab</sup>	71.43 <sup>b</sup>
F- Test			**	**
% CV			11.51	25.59

*Note.* Means with the same letter(s) are not significantly different by least significant difference,  $p \geq 0.05$ , based on Honestly Significant Difference test; \*\* = significant at  $p \leq 0.01$

### **Agronomic and Yield Performance of Sweet Potato**

The length of the main vine and the number of lateral vines of sweet potato are presented in Table 4. The length of the main vine of sweet potato shows no significant difference in the cropping pattern. The main vine was generally shorter at 378.47–416.28 cm for sweet potato grown on the first cropping than the second cropping with 429.7–485.7 cm length. The shortest main vines of sweet potato were recorded in CP6 (Sweet potato-Corn) with

378.47 cm, while the longest vine was also recorded in CP7, sweet potato intercropped with corn previously planted with mung bean with 485.7 cm. The vines that were the length of the sole sweet potato intercropped with corn did not vary in the two cropping seasons.

A significant influence in the number of lateral vines was observed in the cropping pattern. Sweet potato intercropped with corn (CP4) shows significantly more lateral vines of 6 compared to the other cropping patterns in two seasons except for the sole sweet potato of CP8 (Sweet potato-Corn + Mung bean), which had five lateral vines. The sweet potato planted on the first cropping has a more substantial number of lateral vines, with 4–6 than the sweet potato planted on the second cropping, with 3–4 vines. Moreover, sweet potato intercropped to corn as the first crop has significantly more vines compared to sole sweet potato (CP4). No significant difference was observed during the second cropping, either sole or intercropped.

Table 4

*Length of main vine and number of lateral vines of sweet potato under coconut in various cropping patterns*

Treatment	Cropping patterns		Length of the main vine (cm)	No. of lateral vines
	1 <sup>st</sup> cropping	2 <sup>nd</sup> cropping		
CP4	Sweet potato + Corn	Mung bean	388.07	6 <sup>a</sup>
CP6	Sweet potato	Corn	378.47	4 <sup>b</sup>
CP8	Sweet potato	Corn + Mung bean	416.28	5 <sup>ab</sup>
CP2	Corn	Sweet potato	459.70	4 <sup>b</sup>
CP3	Corn + Mung bean	Sweet potato	429.70	3 <sup>b</sup>
CP7	Mung bean	Sweet potato + Corn	485.70	3 <sup>b</sup>
F- Test			ns	**
% CV			15.69	16.32

*Note.* Means with same the letter(s) are not significantly different by least significant difference,  $p \geq 0.05$ , based on the Honestly Significant Difference test; \*\* = significant at  $p \leq 0.01$ ; ns = Not significant

### ***Yield and Yield Components of Sweet Potato***

The length, diameter and weight of marketable fleshy roots are presented in Table 5. The data revealed a significant influence on the size of marketable fleshy roots of sweet potatoes. The longest marketable roots of 13.39 cm were in CP6 (Sweet potato-Corn). It is significantly longer than the roots harvested in the second cropping in sole and intercrop sweet potatoes. However, CP6 did not differ from the other pattern planted on the first cropping. Sweet potato-Corn has a 13.39 cm length of roots, while CP2, Corn-Sweet potato has the shortest root length of 10.89 cm.

The sweet potato alone did not show significant variation among the sweet potato intercropped with corn. It implies that sweet potato with corn did not affect the length of the fleshy roots of sweet potato. The diameter of marketable fleshy roots did not vary



among the cropping patterns. The sweet potato planted on the first cropping has a diameter of 5.65–6.37 cm, while roots harvested on the second cropping have a diameter range from 5–5.79 cm. The sole sweet potato produced in the first cropping has a slightly wider diameter from 6.04–6.37 cm than sweet potato roots planted from intercropping in the same season—both sole and intercropped sweet potato had grown on the second cropping. The diameter of sweet potato intercropping was slightly shorter than the roots produced from sole sweet potato. There was a significant variation in the weight of marketable fleshy roots. The sole sweet potato planted on the first cropping (CP6 and CP8) produced the highest root yields at 8684.55–10263.93 kg/ha compared to sweet potato intercropped with corn (CP4).

These marketable root yields were significantly higher than those sweet potatoes planted in varying cropping patterns during the second cropping. Sweet potatoes planted in the second cropping yielded low weight ranges from 2,111–3,484.13 kg/ha regardless of the plant previously planted. Among the possible factors that affected the yield of sweet potatoes were the rainfall and soil temperature. Generally, higher temperatures on the soil surface could be attributed to greater numbers of living organisms and greater biological activities. During the second cropping, the experimental site received more rainfall (Figure 1), resulting in high soil moisture and, subsequently, soil having a low temperature. Sweet potato is much less tolerant of excess water than of drought. It confirms the study of Han et al. (2014) that sweet potato is considered a drought-tolerant crop; during the rainy season, soils are saturated with water over days. Thus, this causes a decrease in the size and number of tuberous roots but increases the fresh weight of the shoots.

Table 5  
*Length, diameter, and weight of roots of sweet potato under coconut in various cropping patterns*

Treatment	Cropping patterns		Length roots (cm)	Diameter roots (cm)	Weight of roots (kg/ha)
	1 <sup>st</sup> cropping	2 <sup>nd</sup> cropping			
CP4	Sweet potato + Corn	Mung bean	12.78 <sup>ab</sup>	5.65	4621.05 <sup>bc</sup>
CP6	Sweet potato	Corn	13.39 <sup>a</sup>	6.37	10263.92 <sup>a</sup>
CP8	Sweet potato	Corn + Mung bean	12.63 <sup>ab</sup>	6.04	8684.55 <sup>a</sup>
CP2	Corn	Sweet potato	10.89 <sup>b</sup>	5.79	3484.13 <sup>c</sup>
CP3	Corn + Mung bean	Sweet potato	11.06 <sup>b</sup>	5.00	2111.11 <sup>c</sup>
CP7	Mung bean	Sweet potato + Corn	10.96 <sup>b</sup>	5.01	2271.83 <sup>c</sup>
F- Test			*	ns	*
% CV			8.20	11.21	23.24

*Note.* Means with same letter(s) are not significantly different by least significant difference,  $p \geq 0.05$ , based on the Honestly Significant Difference test; \* = significant at  $p \leq 0.05$ ; ns= Not significant

## Total Yield Equivalent

Table 6 presents the total yield and equivalent of corn, mung bean, and sweet potato in a cropping pattern grown under coconut. The total yield in the cropping pattern was determined by adding the main crop and intercrop yield in two cropping seasons. Results show that total yield had significantly varied among the different cropping patterns. The cropping pattern of sweet potato-corn (CP6) yielded 13,331.4 kg/ha and had considerably higher compared to the cropping patterns mung bean - corn (CP5), which obtained 3,226.19 kg/ha, Corn + Mung bean-Sweet potato (CP3) with 4,575.45 kg/ha, mung bean-Corn + Sweet potato (CP7) 3,916.71 kg/ha and corn-mung bean (CP1) that incurred the lowest total yield of 2,265.89 kg/ha. However, CP2 (Corn-Sweet potato), CP4 (Corn + Sweet potato-Mung bean), and CP8 (Sweet potato-Corn + Mung bean) show no significant difference among cropping patterns. The cropping pattern planted with sweet potato, either in the first or second cropping, showed a much higher total yield than corn and mung bean.

Table 6

*Total yield and equivalent of corn, mung bean and sweet potato under coconut in various cropping patterns*

Treatment	Cropping patterns		Total yield (kg/ha)	Total yield equivalent (PHP)
	1 <sup>st</sup> cropping	2 <sup>nd</sup> cropping		
CP1	Corn	Mung bean	2,265.89 <sup>c</sup>	36,221 <sup>c</sup>
CP2	Corn	Sweet potato	6,339.30 <sup>abc</sup>	77,669 <sup>abc</sup>
CP3	Corn + Mung bean	Sweet potato	4,575.45 <sup>bc</sup>	61,053 <sup>bc</sup>
CP4	Corn + Sweet potato	Mung bean	5,841.31 <sup>abc</sup>	67,143 <sup>bc</sup>
CP5	Mung bean	Corn	3,226.19 <sup>c</sup>	55,337 <sup>bc</sup>
CP6	Sweet potato	Corn	13,331.40 <sup>a</sup>	148,651 <sup>a</sup>
CP7	Mung bean	Corn + Sweet potato	3,916.71 <sup>bc</sup>	56,470 <sup>bc</sup>
CP8	Sweet potato	Corn + Mung bean	11,156.78 <sup>ab</sup>	125,715 <sup>ab</sup>
F- Test			**	**
% CV			41.96	32.45

*Note.* Means with same the letter(s) are not significantly different by least significant difference,  $p \geq 0.05$ , based on the Honestly Significant Difference test; \*\* = significant at  $p \leq 0.01$

The total equivalent yield was data converted by multiplying the yield of each crop price and adding to the main crop of corn. The crop prices were corn at 15 pesos, mung bean at 40 pesos, and sweet potato at 10 per kilo, which is very low due to the high supply of the season. Results revealed highly significant differences among cropping patterns. The cropping pattern of sweet potato-corn (CP6) had a total equivalent yield of PHP 148,651, which was a significant difference from other cropping patterns except for the cropping pattern Sweet Potato-Corn + Mung bean (CP8) with the monetary amount of PHP 125,715 and CP2, Corn-Sweet potato with PHP 77,669 total yield equivalent. The result implies

that total yield and equivalent were higher in cropping patterns planted with sweet potato, either sole or intercropped, due to its heavyweight characteristic. Thus, all cropping patterns planted with sweet potato outclass in overall total crop production.

### Economic Profitability

The production cost and return analysis are presented in Table 7. Data shows that the cropping pattern Sweet potato-Corn + Mung bean (CP8) has recorded the highest crop production cost, amounting to 75,850 pesos, followed by all cropping patterns planted with sweet potato. Note that NSIC SP 30 sweet potato variety cuttings were brought from the Visayas State University (VSU), Baybay, Leyte, for 0.50 pesos per cutting. Nevertheless, CP6, Sweet potato-Corn got a gross monetary return of PHP 73,601 with an ROI of 98%, followed by the cropping pattern Sweet potato-Corn + Mung bean (CP8) with a net income of PHP 49,865 and ROI of 66%. Subsequently, cropping patterns of Corn + Mung bean-Sweet potato (CP3) had the lowest income and had no return. Return of investment values was high, according to the cropping pattern planted with sweet potato, either solely or intercropped on the first cropping. Thus, sweet potatoes and corn excel in all cropping patterns.

Table 7  
*Production cost and return analyses in various cropping patterns grown under coconut*

Treatment	Cropping patterns		Total yield equivalent (PHP)	Production cost (PHP)	Net income (PHP)	ROI (%)
	1 <sup>st</sup> cropping	2 <sup>nd</sup> cropping				
CP1	Corn	Mung bean	36,221	42,600	(6,379)	-15
CP2	Corn	Sweet potato	77,669	75,050	2,619	3
CP3	Corn + Mung bean	Sweet potato	61,053	75,050	(14,797)	-20
CP4	Corn + Sweet potato	Mung bean	67,143	59,625	7,518	13
CP5	Mung bean	Corn	55,337	42,600	12,737	30
CP6	Sweet potato	Corn	148,651	75,050	73,601	98
CP7	Mung bean	Corn + Sweet potato	56,470	59,625	(3,155)	-5
CP8	Sweet potato	Corn + Mung bean	125,715	75,850	49,865	66

*Note.* Price of corn @ PHP 15.00/kg; Price of wholesale mung bean @ PHP 40.00/kg; Price of wholesale sweet potato @ PHP 10.00/kg

## CONCLUSION

Based on the study's findings, the conclusions were that corn plants, ear height, and grain yield are best when corn is placed as the second crop in the pattern. However, Corn + Sweet potato intercropping results in a decrease in plant height and grain yield of corn. Mung bean plant height and bean yield are improved regardless of its placement in the cropping pattern, either in sole or intercropped with corn. Sweet potato has the best performance on root yields when placed as the first crop in the cropping pattern—however, sweet potato intercropping results in a reduction in yield. Therefore, provided by the ROI percentage, the cropping patterns of sweet potato followed by corn (CP6) and the same placement in the crop pattern of sweet potato followed by mutlicrop of Corn + Mung bean (CP8) showed the best performance and are recommended for the coconut farmers in Zamboanga del Sur.

## ACKNOWLEDGEMENTS

The authors thank the Commission on Higher Education Philippines for supporting the dissertation grants under the K12 Transition Scholarship Program and the J.H. Cerilles State College.

## REFERENCES

- Alemayehu, D., Shumi, D., & Afeta, T. (2018). Effect of variety and time of intercropping of common bean (*Phaseolus vulgaris* L.) with maize (*Zea mays* L.) on yield components and yields of associated crops and productivity of the system at mid-land of Guji, Southern Ethiopia. *Advances in Crop Science Technology*, 6(1), 324. <https://doi.org/10.4172/2329-8863.1000324>
- Amaya, Y. M. Q., Carvajal, J. E. V., Montaña, J. P. G., Ramos, O. M., & Quijano, E. B. (2021). High population density in arracacha (*Arracacia xanthorrhiza* Bancroft) increase radiation interception, yield, and profitability. *Agronomía Mesoamericana*, 32(2), 399-421. <https://doi.org/10.15517/am.v32i2.43281>
- Amosse, C., Jeuffroy, M. H., Mary, B., & David, C. (2014). Contribution of relay intercropping with legume cover crops on nitrogen dynamics in organic grain systems. *Nutrient Cycling in Agroecosystems*, 98(1), 1–14. <https://doi.org/10.1007/s10705-013-9591-8>
- Arangote, V. R., Saura, R. B. D. L., & Rollon, R. J. C. (2019). Growth and yield response of peanut, (*Arachis hypogaea* L.) and soil characteristics with application of inorganic and organic fertilizer and dolomite addition. *International Journal of Biosciences*, 15(6), 164-173.
- Arshad, M., Nawaz, R., Ahmad, S., Razaq, A., Ranamukhaarachchi, S. L., & Rahman, S. (2020). Relative production efficiency of maize-legume intercroppings at different altitudes. *Journal of the National Science Foundation of Sri Lanka*, 48(4), 409-420. <https://doi.org/10.4038/jnsfsr.v48i4.9331>
- Balde, A. B., Scope, L. E., Affholder, F., Corbeels, M., Da Silva, F. A. M., Xavier, J. H. V., & Wery, J. (2011). Agronomic performance of no-tillage relay intercropping with maize under smallholder conditions in Central Brazil. *Field Crop Research*, 124(2), 240–251. <https://doi.org/10.1016/j.fcr.2011.06.017>

- Bekele, W., Belete, K., & Tana, T. (2016). Effect of soybean varieties and nitrogen fertilizer rates on yield, yield components and productivity of associated crops under maize/soybean intercropping at Mechara, Eastern Ethiopia. *Agriculture, Forestry and Fisheries*, 5(1), 1-7. <http://doi.org/10.11648/j.aff.20160501.11>
- Castellazzi, M. S., Wood, G. A., Burgess, P. J., Morris, J., & Conrad, K. F. (2008). A systematic representation of crop rotations. *Journal of Agricultural Science*, 97(1-2), 26-33. <https://doi.org/10.1016/j.agsy.2007.10.006>
- Davidson, J. S. (2018). Rice imports and electoral proximity: The Philippines and Indonesia compared. *Pacific Affairs*, 91(3), 445-470. <https://doi.org/10.5509/2018923445>
- Fan, Y., Wang, Z., Liao, D., Raza, M. A., Wang, B., Zhang, J., Chen, J., Feng, L., Wu, X., Liu, C., Yang, W., & Yang, F. (2020). Uptake and utilization of nitrogen, phosphorus and potassium as related to yield advantage in maize-soybean intercropping under different row configurations. *Scientific Reports*, 10(1), 9504. <https://doi.org/10.1038/s41598-020-66459-y>
- Food and Agriculture Organization. (2001). *Crop diversification in the Asia-Pacific region*. [https://coin.fao.org/coin-static/cms/media/9/13171763115260/2001\\_03\\_high.pdf?utm\\_](https://coin.fao.org/coin-static/cms/media/9/13171763115260/2001_03_high.pdf?utm_)
- Gong, X., Dang, K., Lv, S., Zhao, G., Wang, H., & Feng, B. (2021). Interspecific competition and nitrogen application alter soil coenzymatic stoichiometry, microbial nutrient status, and improve grain yield in broomcorn millet/mung bean intercropping systems. *Field Crops Research*, 270, 108227. <https://doi.org/10.1016/j.fcr.2021.108227>
- Goulart, J. M., Rocha, A. A., Espindola, J. A. A., Araújo, E. S., & Guerra, J. G. M. (2021). Agronomic performance of sweet potato crop in succession to leguminous plants in monocropping and intercropped with corn. *Brazilian Horticulture*, 39(2), 186-191. <http://doi.org/10.1590/s0102-0536-20210209>
- Han, H., Pan, R., Buitrago, S., Abou-Elwafa, S. F., Peng, Y., Liu, Y., Zhang, W. Y., & Yang, X. S. (2021). The physiological basis of genotypic variations in low-oxygen stress tolerance in the vegetable sweet potato. *Russian Journal of Plant Physiology*, 68(6), 1236-1246. <https://doi.org/10.1134/S1021443721060054>
- Hufnagel, J., Reckling, M., & Ewert, F. (2020). Diverse approaches to crop diversification in agricultural research. A review. *Agronomy for Sustainable Development*, 40, 14. <https://doi.org/10.1007/s13593-020-00617-4>
- Islam, M. N., Akhteruzzaman, M., Alom, M. S., & Salim, M. (2014). Hybrid maize and sweet potato intercropping: a technology to increase productivity and profitability for poor hill farmers in Bangladesh. *Saarc Journal of Agriculture*, 12(2), 101-111. <https://doi.org/10.3329/sja.v12i2.21922>
- Johnson, A. C., & Gurr, G. M. (2016). Invertebrate pests and diseases of sweetpotato (*Ipomoea batatas*): A review and identification of research priorities for smallholder production. *Annals of Applied Biology*, 168(3), 291-320. <https://doi.org/10.1111/aab.12265>
- Khan, M. A., Khalid Naveed, K. N., Kawsar Ali, K. A., Bashir Ahmad, B. A., & Samin Jan, S. J. (2012). Impact of mungbean-maize intercropping on growth and yield of mungbean. *Pakistan Journal of Weed Science Research*, 18(2), 191-200.
- Lirio, G. A., Cerado, J. Jr., Esteban, J. T., Ferrer, J. A., & Salvedia, C. (2023). Growth performance of broiler chicken supplemented with *Bacillus velezensis* D01Ca and *Bacillus siamensis* G01Bb isolated from goat

- and duck microbiota. *Pertanika Journal of Tropical Agricultural Science*, 46(4), 1097-1110. <https://doi.org/10.47836/pjtas.46.4.02>
- Moreno, M. L., Kuwornu, J. K. M., & Szabo, S. (2020). Overview and constraints of the coconut supply chain in the Philippines. *International Journal of Fruit Science*, 20(2), 524-541. <https://doi.org/10.1080/15538362.2020.1746727>
- Nasar, J., Zhao, C. J., Khan, R., Gul, H., Gitari, H., Shao, Z., Abbas, G., Haider, I., Iqbal, Z., Ahmed, W., Rehman, R., Liang, Q. P., Zhou, X. B., & Yang, J. (2023). Maize-soybean intercropping at optimal N fertilization increases the N uptake, N yield and N use efficiency of maize crop by regulating the N assimilatory enzymes. *Frontiers in Plant Science*, 13, 1077948. <https://doi.org/10.3389/fpls.2022.1077948>
- Negash, F., Muluaem, T., & Fikirie, K. (2018). Effect of cropping sequence on agricultural crops: Implications for productivity and utilization of natural resources. *Advances in Crop Science and Technology*, 6(1), 326. <https://doi.org/10.4172/2329-8863.1000326>
- Parida, A. K., & Das. A. B. (2005). Salt tolerance and salinity effects on plants: A review. *Ecotoxicology and Environmental Safety*, 60(3), 24–349. <https://doi.org/10.1016/j.ecoenv.2004.06.010>
- Philippine Coconut Authority. (2019). *Department of Agriculture, Philippine Coconut Authority annual report 2019*. [https://www.pca.gov.ph/images/pdf/annualreport/PCA\\_2019\\_Annual\\_Report.pdf](https://www.pca.gov.ph/images/pdf/annualreport/PCA_2019_Annual_Report.pdf)
- Rani, K., Sharma, P., Kumar, S., Wati, L., Kumar, R., Gurjar, D.S., Kumar, D., & Kumar, R. (2019). Legumes for sustainable soil and crop management. In R. Meena, S. Kumar, J. Bohra & M. Jat (Eds.), *Sustainable management of soil and environment* (pp. 193-215). Springer Nature. [https://doi.org/10.1007/978-981-13-8832-3\\_6](https://doi.org/10.1007/978-981-13-8832-3_6)
- Ro, S., Roeurn, S, Sroy, C., & Prasad, P. V. V. (2023). Agronomic and yield performance of maize-mungbean intercropping with different mungbean seed rates under loamy sand soils of Cambodia. *Agronomy*, 13(5), 1293. <https://doi.org/10.3390/agronomy13051293>
- Rondhi, M., Pratiwi, P., Handini, V., Sunartomo, A., & Budiman, S. (2018). Agricultural land conversion, land economic value, and sustainable agriculture: A case study in East Java, Indonesia. *Land*, 7(4), 148. <https://doi.org/10.3390/land7040148>
- Smith, P., Calvin, K., Nkem, J., Campbell, D., Cherubini, F., Grassi, G., Korotkov, V., Le Hoang, A., Lwasa, S., McElwee, P., & Nkonya, E. (2020). Which practices co-deliver food security, climate change mitigation and adaptation, and combat land degradation and desertification? *Global Change Biology*, 26(3), 1532-1575. <https://doi.org/10.1111/gcb.14878>
- Syafruddin, S. (2020). Intercropping of maize-mungbean to increase the farmer's income. *IOP Conference Series: Earth and Environmental Science*, 484, 012054. <https://doi.org/10.1088/1755-1315/484/1/012054>
- Tariq, M. Ali, H., Hussain, N., Nasim, W., Mubeen, M., Ahmad, S., & Hasanuzzaman, M. (2019). Fundamentals of crop rotation in agronomic management. In M. Hasanuzzaman (Ed.), *Agronomic crops* (pp. 545-559). Springer. [https://doi.org/10.1007/978-981-32-9151-5\\_24](https://doi.org/10.1007/978-981-32-9151-5_24)
- Waha, K., Dietrich, J. P., Portmann, F. T., Siebert, S., Thornton, P. K., Bondeau, A., & Herrero, M. (2020). Multiple cropping systems of the world and the potential for increasing cropping intensity. *Global Environmental Change*, 64, 102-131. <https://doi.org/10.1016/j.gloenvcha.2020.102131>

*Review Article*

## Prevailing Knowledge on Aquaculture of Abalone in Southeast Asia: A Review

Nur-Syahirah Mamat<sup>1</sup>, Yuzine Esa<sup>1,2,3\*</sup>, Hidayah Manan<sup>4</sup>, Nur Leena W. S. Wong<sup>1,2</sup>, Julia D. Sigwart<sup>5,6</sup>, Siti-Azizah Mohd Nor<sup>7</sup>, Nazia Abdul Kadar<sup>8</sup>, Hon Jung Liew<sup>4</sup>, Jalilah Mohamad<sup>4</sup>, Suhairi Mazelan<sup>4</sup>, Khor Waiho<sup>4</sup> and Aziz Arshad<sup>2</sup>

<sup>1</sup>International Institute of Aquaculture and Aquatic Sciences, Universiti Putra Malaysia, 71050 Port Dickson, Negeri Sembilan, Malaysia

<sup>2</sup>Department of Aquaculture, Faculty of Agriculture, Universiti Putra Malaysia, 43400 Serdang, Selangor, Malaysia

<sup>3</sup>Department of Aquaculture, Faculty of Fisheries and Marine, Universitas Airlangga, Campus C Jalan Mulyorejo, Surabaya, 60115 East Java, Indonesia

<sup>4</sup>Higher Institution Centre of Excellence, Institute of Tropical Aquaculture and Fisheries, Universiti Malaysia Terengganu, 21030 Kuala Nerus, Terengganu, Malaysia

<sup>5</sup>Department of Marine Zoology, Senckenberg Research Institute and Museum, Frankfurt, Germany

<sup>6</sup>Queen's University Belfast, Marine Laboratory, Portaferry, Northern Ireland

<sup>7</sup>Institute of Marine Biotechnology, Universiti Malaysia Terengganu, 21030 Kuala Nerus, Terengganu, Malaysia

<sup>8</sup>Borneo Marine Research Institute, Universiti Malaysia Sabah, 88400 Kota Kinabalu, Sabah, Malaysia

### ABSTRACT

Abalone is a marine gastropod mollusc with significant economic importance in global fisheries and aquaculture. Currently, the abalone culture is actively engaged in Southeast Asia and has gained

significant popularity among aquaculturists and aquafarmers in Indonesia, the Philippines, Thailand, Vietnam, and Malaysia. Abalone also has emerged as a highly profitable source of income for fish farmers in Asian countries. The exquisite taste of abalone has made it a sought-after delicacy, particularly in Chinese cuisine. However, scanty documentation of this marine gastropod has been reported on the development of aquaculture production in Southeast Asia. Therefore, to help bridge the gap, this review emphasised the information and collated ideas on the industrial culture of abalone in Southeast Asia. In this review paper, all issues on abalone culture will be summarised and highlighted,

#### ARTICLE INFO

*Article history:*

Received: 24 June 2024

Accepted: 29 July 2024

Published: 28 January 2025

DOI: <https://doi.org/10.47836/pjtas.48.1.08>

*E-mail addresses:*

nsyahirahmamat@gmail.com (Nur-Syahirah Mamat)

yuzine@upm.edu.my (Yuzine Esa)

hidayahmanan@umt.edu.my (Hidayah Manan)

nurleena@upm.edu.my (Nur Leena W. S. Wong)

julia.sigwart@senckenberg.de (Julia D. Sigwart)

s.azizah@umt.edu.my (Siti-Azizah Mohd Nor)

nazia@ums.edu.my (Nazia Abdul Kadar)

honjung@umt.edu.my (Hon Jung Liew)

jalilah@umt.edu.my (Jalilah Mohamad)

suhairi@umt.edu.my (Suhairi Mazelan)

waiho@umt.edu.my (Khor Waiho)

azizarshad@upm.edu.my (Aziz Arshad)

\*Corresponding author

especially on the aquaculture industries of abalone, challenges and constraints in developing the aquaculture of *Haliotis* spp., and biological features of the abalone. This review paper could be a valuable reference for abalone aquaculture practices in Southeast Asia, with the aim of boosting production and conservation efforts of these marine gastropod molluscs, thereby benefiting abalone aqua farmers in Southeast Asian countries.

*Keywords:* Abalone, aquaculture, *Haliotis* spp., marine gastropod, Southeast Asia

---

## AN OVERVIEW OF AQUACULTURE ABALONE

Since the late 1990s, there has been a significant global demand for abalone products, mostly from Asian countries, relative to market supply (Cook & Gordon, 2010). In Southeast Asia, the Philippines was identified as the major producer of abalone from commercial capture fisheries, where in 1996, the Philippines recorded as much as 448 metric tons per year of harvested abalone. Commercial abalone aquaculture and fisheries in the Philippines have been developed rapidly with the well-established seed production, hatchery and grow-out culture of *Haliotis asinina* (Fermin, 2001). Abalone production in the Philippines showed increasing trends as demand in seafood markets increased in Asian countries (Salayo et al., 2020). Since 1991, the Philippines has also successfully exported abalone to several countries, such as Hong Kong, Japan, the United States, Singapore, and Australia. The success in the hatchery and nursery of abalone aquaculture has produced seed stocks for growing abalone in the Philippines (Lebata-Ramos et al., 2021; Mabuhay-Omar et al., 2021).

*Haliotis asinina*, a donkey's ear abalone, is a native species in Thailand, Indonesia, Malaysia, Vietnam, and the Philippines. It is a species with significant aquaculture potential in Southeast Asia due to its fast growth rate, high percentage of edible parts, and high survival rate when cultured either on land or in a sea-based culture system compared to other abalone species (Fermin, 2001; Kua et al., 2011). This species has the ability to spawn and mature within one year (Wood et al., 2015). This species is also commercially high-value seafood harvested by fishers (Salayo et al., 2020). Previous research papers published show that this species was successfully cultured in Thailand (Nuurai et al., 2010), Vietnam (Minh et al., 2010), Indonesia (Maulidya et al., 2021), the Philippines (Lebata-Ramos et al., 2021) also in Malaysia (Kua et al., 2011) through the hatchery and farming culture operation.

In Malaysia, Sabah was identified as an area with a high abundance of *H. asinina*, where this species is collected for domestic uses and exported (Kua et al., 2011; Wood et al., 2015). As far as literature is concerned, studies on aquaculture abalone in Malaysia used only samples from the coastal water of Sabah with only from *H. asinina* species (Nhan et al., 2010; Kua et al., 2011; Wood et al., 2015). Harvesting was unregulated; therefore,



no data on the population status was available. The distributions of abalone species in Peninsular Malaysia are still in question, and no documented reports exist. Sabah Parks initiated abalone breeding in the mid-1990s at Boheydulang island, Semporna (Sabah waters), to support local livelihood solely depending on fishing abalone (Wood et al., 2015). Then, in the 2000s, abalone breeding was conducted by the Fisheries Research Institute (FRI) due to high demand among Malaysia's Chinese populations. Species of *H. asinina* identified appear in the shallow reefs around the Sabah waters, including Mantanani Island and islands surrounding the Semporna waters (Kua et al., 2011). Omadal and Kulapuan islands located at Semporna have an active abalone fishery and supplied broodstock where the abalone price can reach up to RM 25 per kg (~USD5) (Wood et al., 2015).

Meanwhile, in 1991, the Coastal Development Centre in Rayong Province of Thailand successfully increased the fecundity of *H. asinina* (Apisawetakan et al., 1997), and in 1996, the first commercial abalone plantation was established on Phuket Island in southern Thailand (Wetchateng et al., 2010). Due to high meat yield, most abalone farms in Thailand culture the native species, *H. asinina*, as the selective type of abalone species to be cultured (Wetchateng et al., 2010). In the past decade, Thailand also have conducted research on the culturing of *H. asinina* (Jarayabhand & Paphavasit, 1996; Thongrod et al., 2003) with more updated studies on *H. asinina* on aspects of culture, including energy gained from feeding (Ganmanee et al., 2010), effects of stocking density on growth performance (Jarayabhand et al., 2010) and effects of hormone on reproduction (Nuurai et al., 2010).

Since 1997, Vietnam has also conducted a series of research on the aquaculture of abalone in a few species, including *H. asinina* (Minh et al., 2010; Minh & Hong, 2000), *Haliotis ovina* (Thao et al., 2020) and *Haliotis diversicolor* (Chieu et al., 2016). Among the studies are on reproductive biology (Minh & Hong, 2000), growth performance (Minh et al., 2010) and seed production (Chieu et al., 2016). In Indonesia, live abalone is much more expensive and can be sold at Rp. 150,000 (~ USD10) per kg; meanwhile, for dry abalone, the price is from Rp. 350,000 (~ USD23) and can reach up to Rp. 500,000 (~ USD32) per kg (Grandiosa, 2020). In the Philippines, live abalones command a high price of P300 (~USD5) per kg (15–20 pieces), and the blanched meat is sold at P550 (~USD10) per kg (Gallardo & Salayo, 2003). In addition to legal (overfishing) and illegal (poaching) harvesting as well as habitat disturbance, this situation has led to the depletion of abalone stock in nature of Southeast Asia, particularly Indonesia, Philippines, Thailand, and Malaysia (Sososutiksno & Gasperz, 2017). The deterioration of abalone stock is also identified as being affected by the disease, increased predation, and habitat degradation. The abalone aquaculture industry and its development through research in various parts of the world is increasing rapidly. It focuses on developing broodstock management, larval rearing, nursery and growth techniques (Grandiosa, 2020).

## BIOLOGY AND IMPORTANCE OF ABALONE IN AQUACULTURE

Abalone is a herbivorous marine gastropod from the only genus in the Haliotidae family, *Haliotis*, with a univalve (single spiral shell) and a row of holes along the left margin of the shell (Geiger & Poppe, 2000) (Figure 1). The shell is on the top and covers most of the abalone's body (Figure 2). Abalone is a nocturnal mollusc, and its feeding habits mainly occur at nighttime by consuming benthic diatoms during the larvae stage and actively grazing on micro and macro algae at the adult stage (Grandiosa, 2020). Abalone is considered one of the most vital marine molluscs in fisheries and aquaculture worldwide. The global production of abalone has increased significantly in recent years, and its production now relies mostly on aquaculture, although previously, the production depended primarily on fisheries (Hernández-Casas et al., 2023).

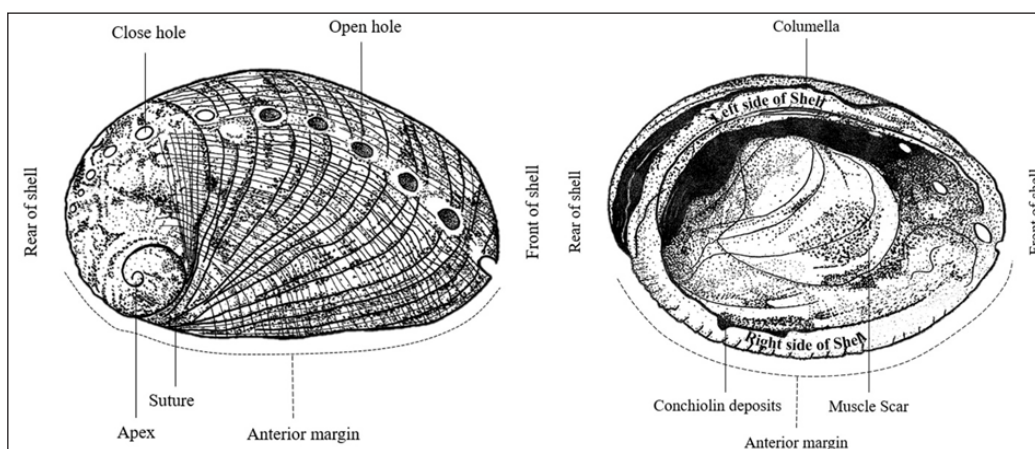


Figure 1. Diagram of external anatomy of abalone modified from Geiger and Poppe (2000)

Due to high demand and high price, abalone has become a profitable income source for fish farmers in Asian countries, especially in Indonesia (Sososutiksno & Gasperz, 2017), the Philippines (Capinpin et al., 2015), Vietnam (Chieu et al., 2016) and Malaysia (Wood et al., 2015). In Asian traditions, abalone is consumed as a premium and luxury seafood product that symbolises “wealth and power” and is referred to as “table gold” (Li et al., 2022). The significantly high market value of abalone aquaculture renders it commercially appealing due to the delicacy of its unique texture and flavour, which has an exquisite taste. Abalone also perceived the benefits of increasing vitality and nutrition (Grandiosa, 2020).

Concordant with the development of the economy, consumers have paid attention to the nutritional quality of abalone, which enhances health, decreases the occurrence of diseases, and extends lifespan by consuming essential nutrients (Li et al., 2022). The composition of abalone muscle contains protein, carbohydrate, fat, and ash (Shi et al., 2020). Proteins play

a crucial role in determining the nutritional content of food, and abalone muscle is rich in high-quality protein. The rich source of protein in abalone assists in preserving a wide range of health aspects. In addition, abalone can assist in the absorption of polyunsaturated fatty acids and essential amino acids, which contribute to developing cardioprotective dietary patterns (Tsai et al., 2018). Abalone also has a reduced caloric content compared to other types of shellfish (De Zoysa, 2013).

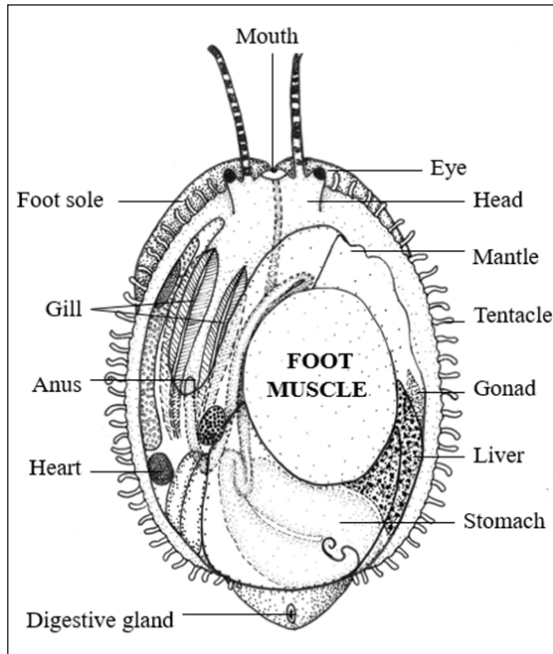


Figure 2. Diagram of the internal anatomy of abalone modified from Geiger and Poppe (2000)

Abalone is recognised to have bioactive components that can benefit health in addition to being consumed, including anticancer, antioxidant, anti-microbial, anti-coagulant, and benefits for cosmetics (Nguyen et al., 2013). Due to various benefits exhibited to human health, abalone is known as “the emperor of the seashells,” “ginseng in the ocean,” or “mother of shellfish” (De Zoysa, 2013). Abalone shells are renowned for their magnificent iridescent features. They have been used for numerous purposes in many cultures and industries, as shells are used for decoration, art crafts and souvenirs. Shells are also used to make jewellery such as buttons, necklaces, rings, bracelets and beads (Grandiosa, 2020; Maulidya et al., 2021). Meanwhile, in indigenous cultures, abalone shells have been used in traditional ceremonies and rituals (Gamble, 2017). Therefore, it is economically viable for aquaculture as there is a significant market demand for abalone in various markets around the world, contributing to the sustainability and profitability of seafood production.

## CULTURE TECHNIQUE AND RESEARCH FOR ABALONE AQUACULTURE

There are three main parts of abalone culture: (1) the larvae-rearing phase, (2) seed production, and (3) the grow-out phase of juveniles to marketable size. Wood et al. (2015) stated that the dividing phase is based on the abalone life cycle, which can comprise two different ways of living: a) free-swimming and non-feeding larval stages (trochophore and veliger) and b) settling down on substrate and eating microalgae plus algae (juvenile and adult stage). Larvae production in the hatchery is usually done inland, while grow-out production can be land- or sea-based. A full understanding of the abalone pelago-benthic life cycle is needed to properly plan and manage their culture, as it is highly susceptible to environmental changes. Hatchery production focused on rearing trochophore and veliger phase larvae until they successfully formed into the juvenile stage. The schematic diagram of the abalone life stage is shown in Figure 3.

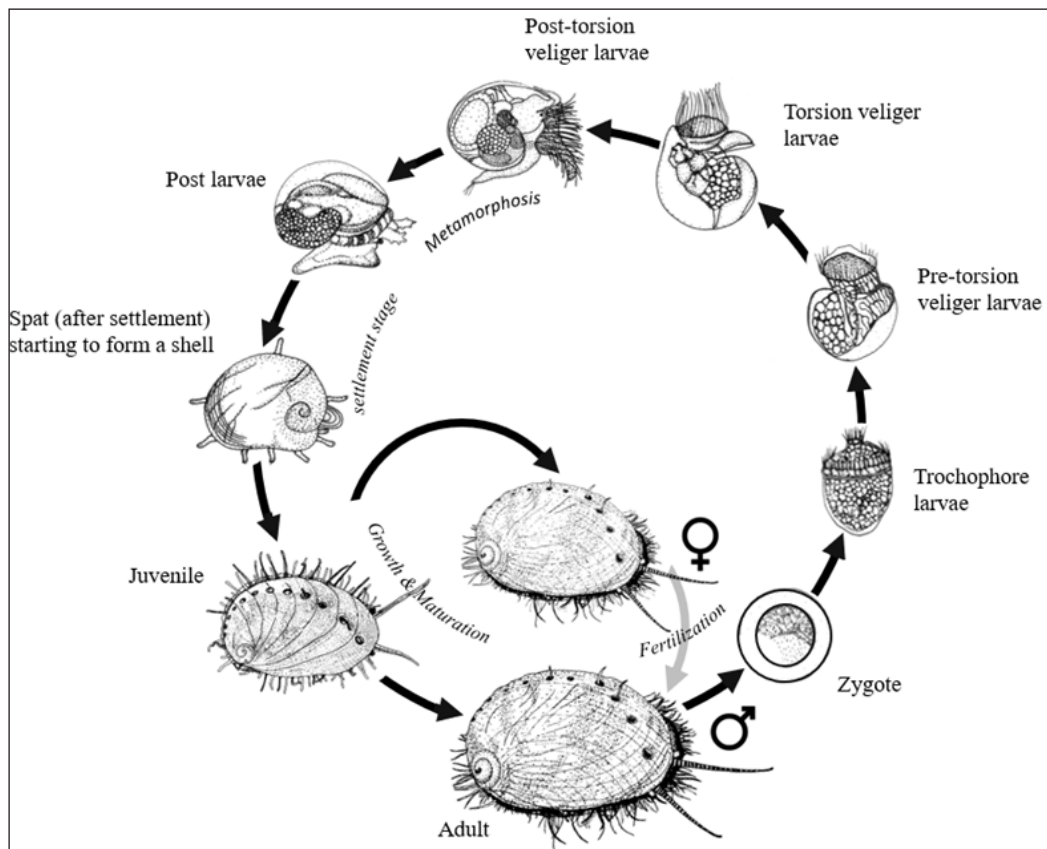


Figure 3. The pelago-benthic life cycle of abalone started from zygote to trochophore, changed to veliger larvae, then changed to post larvae, then changed to spat, then changed to juvenile and lastly, adult stages modified from Jardillier et al. (2008)

## Larvae Rearing Phase

The newly hatched trochophore larvae are free-swimming towards the light (positively phototactic), 200 µm in size per each, surrounded by ciliated named prototroch, only depends on nutrition from yolk sack or and in groups, they can be seen as the light green-white dots under the surface of the water (Wood et al., 2015). After 22 h, the prototroch of trochophore larvae progressively transformed into an organ called velum, and at this time, the larvae enter into the veliger phase larvae. At the veliger phase, the larvae are still in free-swimming form and start absorbing the soluble nutrients from their surroundings through the skin, but they still depend on the remaining egg yolk. The veliger phase larvae are actively searching for suitable settlement spots of the substrate and gradually attempt to settle until contentment. However, the distance and a total attempt to settle are limited and depend on the remaining energy of the yolk supply.

At most, the free-swimming larvae take seven days or less (depending on temperature) to settle to substrates in the rearing tank and become postlarvae (Najmudeen & Victor, 2004; Wu & Zhang, 2016). Post larvae fully shed their cilia, settle on the substrate, establish the shell, and develop into adult form. However, transitioning from the veliger stage to becoming benthic post larvae is extremely challenging. At this time, a high mortality rate is identified, around 10% or less of survival rates (Wood et al., 2015). Furthermore, the low quality of eggs, low water quality and microorganism contamination can contribute to mortality. Post-larval cultures are still in the hatchery phase and reared over 60 days or until they become juvenile size at 5-10 mm at the size that is able to eat macroalgae. The post larvae are tempted to settle on the substrate coated with layers of diatom (microalgae) with an optimum density of 3000 cells/mm<sup>2</sup> as food for the larvae (Wood et al., 2015).

The quality and quantity provided as feed on settlement plates determine the survival rates of the larvae. The common diatom selected as a starter food for abalone post-larval is *Navicula* sp., *Amphora* sp. and *Nitzschia* sp. (Avendaño-Herrera et al., 2007). A study by Gallardo and Buen (2003) also found that larval attachment was higher on mucus and *Navicula* than on other diatoms. The diatom film can be established in the culture tank by natural colonisation or seeding with cultivated stock. In the larval settlement process, substrate difference and feed type affect abalone growth's success rate (Williams et al., 2008). After 60 days of feeding with diatoms, the post larvae entered the juvenile stages. They were introduced to macroalgae, seaweed such as *Ulva lactuca*, green filamentous algae, and coralline red algae as food. According to Najmudeen and Victor (2004), the different types of seaweed can affect the colourizations of the juvenile shell, and the tropical abalone, *Haliotis varia*, which feeds with coralline red algae, displayed the best growth rate performance. The developing juvenile is left to grow in the hatchery at the rearing phase for three to four months until the size becomes 10mm long.

Conventionally, abalone spawning and nursery processes are done under controlled conditions in a hatchery before they reach juvenile size for the grow-out process in the open ocean until market size (Wood et al., 2015). With the advancement in abalone farming technology, farming abalone is now cultured fully indoors from larvae to adult market size by using a raceway system where super filtered and sterilized sea water continuously flows over the rearing tanks, delivering oxygen and carrying away waste (Heasman & Savva, 2007). Table 1 lists water quality for breeding abalone in Southeast Asia countries, including Malaysia, Indonesia, the Philippines, Thailand and Vietnam. Most studies were conducted on *H. asinina*, the most widespread species in Indo-Pacific oceans.

Table 1  
List of water quality for breeding of abalone in Southeast Asia

Country	Species	Temperature (°C)	pH	DO (mg/L)	Salinity (ppt)	Reference
Malaysia	<i>Haliotis asinina</i>	25–31	6.5–8.5	6.0–7.5	29–33	Nhan et al. (2010)
Indonesia	<i>Haliotis asinina</i>	26–28.5	7.5–7.8	5.7–7.6	32–34.5	Hamzah (2012)
	<i>Haliotis squamata</i>	28.1–29.9	7–8.5	8.2–10.1	29.6–34	Sahetapy and Latuihamallo (2014)
	<i>Haliotis squamata</i>	27–28	7–8	> 4	30–35	Ardi et al. (2020)
	<i>Haliotis squamata</i>	27–28	-	-	32–33	Hadijah et al. (2021)
	<i>Haliotis asinina</i>	27–31	8.3–8.4	5–5.6	28–35	Amin et al. (2020)
Philippines	<i>Haliotis asinina</i>	26–30	7.9–8.8	4.1–6.4	30–35	Fermin and Buen (2001)
	<i>Haliotis asinina</i>	28–31	8.3–8.4	5–5.6	28–32	Bautista-Teruel et al. (2003)
	<i>Haliotis asinina</i>	27–29	-	-	32–35	Gallardo and Salayo (2003)
	<i>Haliotis asinina</i>	26–27	7–8.2	-	35–38	Jumah et al. (2016)
Thailand	<i>Haliotis asinina</i>	27–30	8.3–8.4	6	29–32	Thongrod et al. (2003)
	<i>Haliotis asinina</i>	25–26	-	-	25–32	Stewart et al. (2008)
	<i>Haliotis asinina</i>	28	-	-	31	Ganmanee et al. (2010)
Vietnam	<i>Haliotis asinina</i>	27–28	-	-	30–34	Minh and Hong (2000)
	<i>Haliotis asinina</i>	23–31	7.8–8.4	4.5–6	30–32	Minh et al. (2010)

## Seed Production

The availability of a reliable seed supply is crucial for commercial production (Hamka & Shearer, 2009). Other countries have developed many abalone hatcheries to produce abalone seed for commercial farming and to improve natural stocks (Setyono, 2005). The

seed of production of *H. asinina* in Indonesia started in 1997 but only succeeded in 2003 after five years of research (Hamka & Shearer, 2009). Hamzah et al. (2012) compared the effect of different densities of abalone seeds (75, 50 and 25 individuals per tank) on survival and growth. General findings indicated that the highest survival rate was observed in the tank with 75 individuals, while the highest growth rate was recorded in the tank with 50 individuals. However, research showed that the abalone seed density does not influence the growth and survival of abalone seeds. This is due to the characteristics of abalone, which stick together in groups and only spread during feeding time (Hamzah et al., 2012).

The abalone seedlings are assumed to continue to be produced in aquaculture centres owned by the government in Indonesia due to the availability of established protocols (Grandiosa, 2020). In addition, feeding with immunostimulants, such as probiotics, may significantly boost the immunity and the survival of abalone seeds towards the disease, leading to fast abalone growth. The Aquaculture Department of the Southeast Asian Fisheries Development Centre (SEAFDEC/AQD) in the Philippines has classified abalone as a species for enhancement programs aiming to boost production. It has successfully produced *H. asinina* seeds in the hatchery (Lebata-Ramos et al., 2013). It is suggested that the minimum size of seeds of *H. asinina* for release is 3 cm shell length (SL) (Lebata-Ramos et al., 2013), which is supported by a study from Masuda and Tsukamoto (1998) that indicated that after one year of release (SL of 2, 3, and 4 cm), the survival rates were 10%, 30-60%, and 70-80%, respectively.

The larger size showed a higher survival rate compared to the smaller size, indicating that a release of larger abalone is ecologically more productive for survival in the wild. In Vietnam, a massive quantity of abalone seeds of *Haliotis diversicolor* has been produced from artificial reproduction conducted by the Research Institute for Marine Fisheries, aiming to restock and increase the income of local communities (Chieu et al., 2016). Abalone seeds can be managed based on a few techniques: (1) the seeds are stocked in protected areas, and (2) the seeds are commercially maintained using containers until certain periods (size suitable for sale) before being harvested and sold to consumers (Eny & Setyono, 2007). A study by Supriyono et al. (2020) suggests that a flow-through system can produce abalone seed production as this system can improve abalone's growth and survival rate. The authors also suggest that an additional 15 mg/L of calcium oxide (CaO) will increase the survival rate of abalone seed production.

Abalone with shell lengths between 2-3cm are selected for enlargement of abalone seeds. Poly Vinyl Chloride (PVC) pipe was commonly used for commercial abalone seed techniques in which the seeds will attach to that PVC pipe (Figure 4). This cut PVC pipe is beneficial as a substrate and a shelter and allows abalone seeds to adjust to the environment (Maulidya et al., 2021). It is also reported that the survival rate of abalone seeds was high using this technique (Lebata-Ramos et al., 2013). With the advance in technology upgrades,

it is expected that the seed production of *H. asinina* and *Haliotis squamata* in Indonesia will be capable of pursuing the production target of at least 1 billion seeds by 2023 to support the target of increasing exports in 2024 (Grandiosa, 2020).

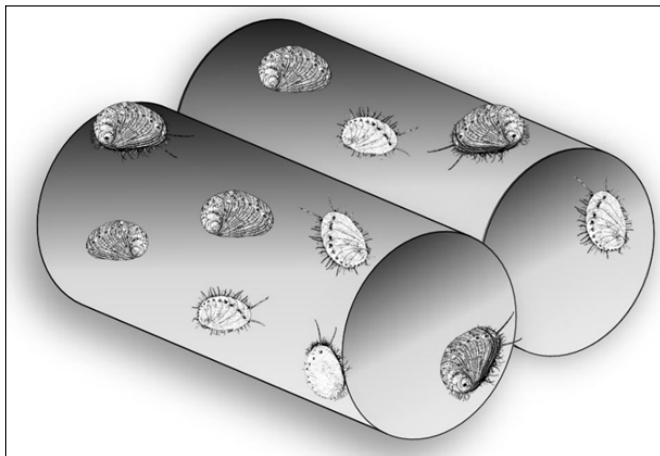


Figure 4. Abalone seeds were attached to the cut of PVC pipes that act as a substrate and shelters modified from Maulidya et al. (2021)

## Grow Out Culture

The juvenile that enters the grow-out phase will transfer to grow-out facilities if the culture is land-based or to the selected area in the open sea if the culture is sea-based. Land-based cultures can be found in onshore ponds, raceways, or tanks. Sea-based cultures are kept in intertidal ponds, cages, barrels, enclosed piles of rocks, or through sea ranching (Gallardo & Salayo, 2003). Minh and Hong (2010) emphasised that the most suitable size for transferring juveniles from hatchery to grow-out site sites cannot be more than 10 to 11 mm to ensure the optimal survival rate. The open sea-based is the best option over land-based for the grow-out phase of abalone due to several reasons: (1) can accommodate a large amount of growing abalone at one time without limit as long as the selected area is broad and suitable, (2) lower fund and management costs, (3) having natural water exchange that can control water quality and water temperature instabilities minimally occur, (4) easy access for the local community to enter the site, and (5) can possibly accommodate the polyculture system set up for culturing other species together with abalone and thus save cost plus making largest profits, for an example culturing seaweed above the abalone cages (Wood et al., 2015; Wu & Zhang, 2016).

Even though farmers rarely choose land-based grow-out facilities due to high operational costs and limited culture space for growing abalone, which depends on the size of built facilities, the management and maintenance of culture stock and disease control can be monitored easily compared to open sea-based grow-out. Sufficient food and



moderate temperature alongside suitable stocking densities in land-based grow-out facilities can ensure a higher survival rate and optimum growth rate of abalone (Huang & Hseu, 2010). In addition, cultured tropical abalone species normally achieve marketable size in only one year compared to temperate species, which take two to three years (Gallardo & Salayo, 2003; Gao et al., 2023). However, if high-tech systems were used in the cultured environment such as systems that allow easy control of temperature and water quality, the opportunity to speed up the harvestable period is possible, and farm profits may also be increased.

The most grow-out systems selected by farmers for open sea-bases are (1) mesh cages and/or (2) plastic containers with cut-out windows (or perforated baskets) for water flow movement (Wood et al., 2015). The facilities required for the hatching process, such as a net floating cage as the main rearing media, an aquarium as media to prepare gonad ripened broodstock, fibre tanks used for egg hatching and larva rearing media, and concrete tanks also used for larva rearing. A net floating cage is practical economically and financially for abalone culture with an Rp. income of 45000 (~USD 3) and a profit of Rp. 22800 (~USD1.5) (Sososutiksno & Gasperz, 2017). The structure of net cages can be rectangular or circular, and they also use unused tyres covered by a net (Setyono, 2005). Previous studies have proved the high successful survival rates of juveniles cultured of *H. asinina* in net cages offshore of Pemenang, West Lombok of Indonesia was around 93% to 95%. In a commercial application, net cages can be changed to cages made from rattan, wood, or bamboo, which provide more proper shelter for the juveniles while allowing adequate water to flow through the cages (Setyono, 2005).

Previous research by Setyono and Aswandy (2010) investigated the most suitable technique for culturing abalones using two structure types (TNC = tyre net cage and CNC = circular net cage). Results identified showed that the juveniles of *H. asinina* have better growth when cultured offshore using TNC compared to CNC. Another study by Capinpin et al. (2015) uses PVC pipes as shelter to compare the difference in the behaviour, rate of growth and recovery rates of hatchery-reared abalone juveniles with wild abalone. After one day of deployment, the wild abalone is able to immediately disperse into the surrounding environment. Meanwhile, wild seed abalone growth rates were similar to those of abalone culture in tanks. In terms of recovery rates, both hatchery-reared and wild abalone showed recovery rates of 3% - 4% after 105 days, which indicated that although the implementation of stock enhancement was very costly, it was able to help restore the depleted populations of marine animals (Capinpin et al., 2015).

A study by Ardi et al. (2020) uses different shelter shapes: (1) Round, (2) Square, and (3) Without shelter to examine the growth and survival of abalone (*H. squamata*). The shelter is made from PVC piping. Findings from this study showed that the use of shelter has a significant and better effect on the growth of abalone culture, which is also supported by previous studies that the growth of patterns of both shell length and wet weight

abalone were higher than abalone without shelter (Lloyd & Bates, 2008). The finding also discovered that abalone preferred to grow on and be sheltered in the culture rather than without sheltered and increased surface area (Ardi et al., 2020). Among the shelter shapes, a round shape showed the best result for growing abalone in the tidal area. The other study was conducted on the nursery and grow-out culture of *H. asinina* on a reef flat using four different culture containers: cage, recycled oil container, tray (control) and tube with the main purpose of comparing the growth and survival rates (Lebata-Ramos et al., 2021).

According to Lebata-Ramos (2018), the culture container is one of the most crucial inputs for large-scale grow-out culture. These containers ought to be affordable to both local low-wage earners and capitalists, reusable for several culture runs, and able to endure strong wind conditions. Findings showed that growth rates of *H. asinina* vary greatly depending on the culture conditions. However, with proper culture containers, optimum culture environment and sufficient food, non-significant differences in SL of abalone in the three culture containers in both nursery and grow-out cultures were found. Among the containers, tubes are most recommended for use when doing culture, particularly on reef flats, as these tubes are the most stable and durable enough to withstand harsh environmental conditions (Lebata-Ramos et al., 2021). All these examples indicate that the optimisation of production systems is critical as these systems directly affect the growth and survival of the species in culture.

## CONSTRAINTS AND CHALLENGE IN ABALONE CULTURE

As the demand for abalone keeps increasing, there is a need to make the production of abalone robust. One of the initiatives that can be applied is the systematic breeding programme for both wild population enhancement and aquaculture purposes. However, various challenges emerged that have limited abalone aquaculture production, such as disease infections, environmental changes, slow growth rate, and lack of quality seed and feeding behaviour (Wiradana et al., 2018; Wu & Zhang, 2016). Therefore, prior to future studies, it is crucial to know the factors that can affect the abalone culture as knowledge is needed to develop and expand abalone aquaculture in Asia (Wetchateng et al., 2010).

### Disease Infections

The development of aquaculture based on the intensification and commercialisation of marine products, including abalone, will raise the prevalence towards significant diseases as the movement of animals can lead to the spread of pathogens to the susceptible host during the harvesting and handling process (Mabuhay-Omar et al., 2021; Wiradana et al., 2018). Past research has shown numerous pathogens that cause serious abalone diseases have been reported from different abalone species around the world, such as *Haliotis tuberculata* (Nicolas et al., 2002), *Haliotis diversicolor* (Wang et al., 2004) and *Haliotis*

*gigantea* (Kamaishi et al., 2010). *Vibrio* species are the most commonly encountered bacterial agents associated with diseases in marine and brackishwater systems in tropical environments (Handlinger et al., 2005).

*Vibrio* is a ubiquitous opportunistic pathogen that is constantly present in water. *Vibrio* species are problems in molluscan shellfish hatcheries, including abalone (Handlinger et al., 2005; Kua et al., 2011). The disease outbreak only occurred in disease-supporting environments, indicating that environmental factors have a significant impact on vibriosis epidemics (Istiqomah & Isnansetyo, 2020). Among the major *Vibrio* species that infect abalone species are *Vibrio parahaemolyticus*, *Vibrio harveyi*, *Vibrio splendidus*, *Vibrio aglycolyticus*, *Vibrio anguillarum*, and *Vibrio vulnificus* (Cai et al., 2006; Handlinger et al., 2005; Pitchon et al., 2013). Outbreaks of vibriosis also have been reported in the population of abalone in Southeast Asia, such as in Indonesia (Giri et al., 2014), Thailand (Tangtrongpiros & Chansue, 1999; Wetchateng et al., 2010), the Philippines (Mabuhay et al., 2021; Santiago & Mabuhay-Omar, 2019) including Malaysia (Kua et al., 2011).

The outbreak can be detected in different parts of the abalone, such as the mantle, gill, gut, digestive tract, and foot (Giri et al., 2014; Kua et al., 2011; Mabuhay et al., 2021). A study by Giri et al. (2014) showed that an infection caused by *Vibrio* species bacteria is indicated by the presence of mantle epithelium and digestive tract epithelium erosion with abundant secretion and degradation, as well as the presence of mantle muscular abscess. A study by Yasa et al. (2020) reported that *H. squamata* will respond to the infection of *V. aglycolyticus* with a rapidly increasing level of heat shock protein (HSP70 and HSP90) expression. Meanwhile, in Thailand, the first observation of the Withering syndrome (WS) in abalone that was recorded in the small abalone, *Haliotis diversicolor supertexta*, was caused by an infection with the Rickettsia-like organism (RLO) ‘Candidatus Xenohaliotis californiensis’ (WS-RLO) agent (Wetchateng et al., 2010).

Other previous research conducted in Thailand reported that the occurrence of abdominal swelling disease in *H. asinina* was caused by *Vibrio cholerae*, *Escherichia coli* and *Pseudomonas fluorescens* detected in the blood and gastrointestinal tract (Tangtrongpiros & Chansue, 1999). In Malaysia, the high mortality rate of *H. asinina* was recorded with white lesions and necrosis on foot caused by *Pasteurella* sp. and *Vibrio* spp. (Kua et al., 2011). To date, a study in the Philippines reported that most of the pathogenic bacteria can be found in the gut of abalone (Mabuhay-Omar et al., 2021). The finding supported the previous finding, indicating that more microorganisms can be found in the abalone gut than in the gills and mantle (Santiago & Mabuhay-Omar, 2019).

## Survival Rate

Among the major problems in abalone farming is the extremely low survival rate during early juveniles (Hamka & Shearer, 2009; Minh et al., 2010). It occurs due to the small

size of the abalone, which becomes a potential prey to other marine animals. Growth and survival rates of abalone at low densities (40–60 pcs/cage) were higher than the abalone at higher densities (80–100 pcs/cage) (Minh et al., 2010). The movement of abalone was limited in high stock density to reach out for food as they had to compete with other individuals. Indirectly, this will impact their feeding and living conditions, including growth and survival rate (Huchette et al., 2003). The techniques applied to release the abalones significantly influence the survival rate. The survival rate can be boosted with better maintenance practices.

In this case, the government has to play a significant role in helping local fishermen boost abalone harvest in either sea ranching or stock enhancement programmes. In addition, to properly govern the harvesting of marine resources, the implementation of legislation for the management of marine protected areas (MPAs) or fish sanctuaries must be strengthened. For example, in Indonesia, there were three main centres operating abalone hatcheries that produce seeds and culture of local abalone species under the Directorate General of Aquaculture, Ministry of Marine Affairs and Fisheries namely Tigarong Abalone Hatchery (Bali), Marine Aquaculture Development Centre (MADC) (Lombok) and the Centre for Brackishwater Aquaculture Development (Makassar) (Hamka & Shearer, 2009).

### **Feeding Behaviour**

Food is one of the main criteria that determines the success of abalone aquaculture (Prihadi et al., 2018). Abalone needs macroalgae, such as seaweed, as a source of energy for growth and survival (Octaviani, 2007). It is suggested that three main factors affect the abalone preference for algae: morphology and texture, metabolite compounds, and the essential nutrients for the growth of abalone (Paul et al., 2006). However, the lack of information on good feed quality for abalone development and survival is another difficulty in abalone aquaculture (Hadijah et al., 2021). For example, insufficient amounts of *Gracilaria* sp. in some areas have affected abalone growth (Hamka & Shearer, 2009).

Commonly, the use of macroalgae as a natural abalone diet would result in malnutrition (Hwang et al., 2014), and due to its high moisture content, it probably can cause diseases and infection (Bautista-Teruel & Fermin, 2003). However, studies indicated that abalone fed with macroalgae significantly improves their health, product quality, and feeding behaviour compared to a formulated diet (Bansemmer et al., 2016). It was in concordance with a study by Hadijah (2017), which recommended that *Gracilaria* sp. of marine algae contributed to the most optimal growth and survivability of abalone compared to other varieties of feed. Larger juvenile abalones eat macroalgae, while benthic diatoms are important food for newly settled abalones (Daume, 2006).

A balanced abalone diet must include carbohydrates, protein, lipids, vitamins, and minerals. Algae for abalone is characterised by low lipid and high carbohydrate content

(Viera et al., 2005). Range of lipid requirements from 3%–5%, protein content ranged from 20%–35% while other minerals such as calcium and phosphorus in artificial feed are only needed in small amounts, 0.5% of calcium in diets and 0.7% of phosphorus in the diet can improve the growth rate of abalone. Although there is no information on vitamin supplements in the diet, it is suggested that natural foods suffice (Viera et al., 2005). Therefore, it is crucial to understand the cultivation techniques of these algae so that farmers can produce seaweed crops throughout the year for the abalone industry.

### **Other Factors**

One of the keys to the success of abalone farming is reliable and reproducible spawning, which results in high-quality larvae for grow-out (Nguyen et al., 2022). Therefore, the availability of high-quality seeds is critical to the sustainability of the long-term abalone aquaculture industry. However, the post-larvae stage becomes a main problem in many countries as in this phase, the larvae undergo a change in dietary patterns from zooplankton to periphyton (Grandiosa, 2020). In addition, in abalone hatcheries that are typically located distant from grow-out farms and restocking regions, abalone transport is needed because a higher rate of mortality occurs during the transport of live juveniles. Therefore, this issue needs to be addressed to promote effective aquaculture of abalones. Furthermore, the main remaining hurdle in abalone aquaculture is the slow growth rate of abalone (Nguyen et al., 2022).

### **CONCLUSION AND FUTURE RECOMMENDATIONS IN AQUACULTURE**

Abalone farming and culture have developed rapidly and have gained so much popularity in Southeast Asian countries, especially in Sabah (Malaysia), Southeast Sulawesi (Indonesia), Iloilo (Philippines), Khanh Hoa (Vietnam) and also popular cultured in Thailand waters. Many fundamental studies still have to be resolved in the abalone industry, where there is still a lack of data on population status, species availability and distribution, and research on the optimisation of abalone culture. At its current state of development, the aquaculture of abalone should focus on improving their survival and growth by optimising various culture parameters, such as stocking density, water depth in net cage, water stability, water temperature and photoperiod, pH, diet and different shelter types. In addition, the success of abalone seed production greatly influences its viability for commercial production and wild population restocking programmes.

Although abalone seed production is feasible in most countries, further optimisation of the culture parameters will enhance the survival and overall production output, as most physical parameters are region-specific. Furthermore, future research on the potential use of land-based grow-out production will further shorten the production time of abalones as culture conditions can be monitored and controlled compared to the common open sea

culture system. Various genomic selection programs for abalone can also be introduced to select desirable traits selectively. For example, the genome-wide association studies (GWAS) approach was used to identify single nucleotide polymorphisms (SNPs) and candidate genes related to heat tolerance, paving the way for selective breeding programs of abalone that can tolerate future climate scenarios. Similarly, other traits, such as fast growth, high disease resistance, and high fecundity, can be selected for trait improvement of abalone.

## ACKNOWLEDGEMENTS

This work was supported by the Science and Technology Research Partnership for Sustainable Development (SATREPS) Program entitled ‘Development of Advanced Hybrid Ocean Thermal Energy Conversion (OTEC) Technology for Low Carbon Society and Sustainable Energy System: First Experimental OTEC Plant of Malaysia’ funded by Japan Science and Technology Agency (JST) and Japan International Cooperation Agency (JICA) and Ministry of Higher Education Malaysia (MoHE) and led by the Institute of Ocean Energy Saga University (IOES) of Japan and UTM Ocean Thermal Energy Centre (UTM OTEC), Universiti Teknologi Malaysia (UTM). Registered Program Cost Centre: #R.K120000.78094L887, Project [Cost centre: #6300235].

## REFERENCES

- Amin, M., Bolch, C. J., Adams, M. B., & Burke, C. M. (2020). Growth enhancement of tropical abalone, *Haliotis asinina* L, through probiotic supplementation. *Aquaculture International*, 28, 463-75. <https://doi.org/10.1007/s10499-019-00473-4>
- Apisawetakan, S., Thongkukiatkul, A., Wanichanon, C., Linthong, V., Kruatrachue, M., Upatham, E., Poomthong, T., & Sobhon, P. (1997). The gametogenic processes in a tropical abalone, *Haliotis asinina* Linnaeus. *Journal of the Scientific Society*, 23, 225-240. <https://doi.org/10.2306/scienceasia1513-1874.1997.23.225>
- Ardi, I., Setiadi, E., & Pranowo, W. S. (2020). The grow-out of abalone (*Haliotis squamata*) at different shelter shape on growth and survival and its marine environmental influences at Lembongan Bay coastal waters. In *IOP Conference Series: Earth and Environmental Science* (Vol. 441, p. 012001). IOP Publishing. <https://doi.org/10.1088/1755-1315/441/1/012001>
- Avendaño-Herrera, R. E., & Riquelme, C. E. (2007). Production of a diatom-bacteria biofilm in a photobioreactor for aquaculture applications. *Aquacultural Engineering*, 36(2), 97-104. <https://doi.org/10.1016/j.aquaeng.2006.08.001>
- Bansemer, M. S., Qin, J. G., Harris, J. O., Howarth, G. S., & Stone, D. A. J. (2016). Nutritional requirements and use of macroalgae as ingredients in abalone feed. *Reviews in Aquaculture*, 8(2), 121-135. <https://doi.org/10.1111/raq.12085>
- Bautista-Teruel, M. N., Fermin, A. C., & Koshio, S. S. (2003). Diet development and evaluation for juvenile abalone, *Haliotis asinina*: Animal and plant protein sources. *Aquaculture*, 219(1-4), 645-653. [https://doi.org/10.1016/S0044-8486\(02\)00410-6](https://doi.org/10.1016/S0044-8486(02)00410-6)

- Cai, J., Han, Y., & Wang, Z. (2006). Isolation of *Vibrio parahaemolyticus* from abalone (*Haliotis diversicolor supertexta* L.) postlarvae associated with mass mortalities. *Aquaculture*, 257(1-4), 161-166. <https://doi.org/10.1016/j.aquaculture.2006.03.007>
- Capinpin, J. E. C., Parreno, S. C., & Abalos, R. S. (2015). Growth of abalone *Haliotis asinina* fed with *Hydropuntia edulis*, singly or in combination with other red algae in sea cages in Tondol, Anda, Pangasinan, Northern Philippines. *Philippine Journal of Science*, 144, 43-49.
- Chieu, H. D., Phuong, L. D., Duy, D. A., Tuan, B. M., & Thoa, N. K. (2016). Aquaculture-based enhancement and restoration of many-colored abalone resources (*Haliotis diversicolor* Reeve, 1846) in Bach Long VI national marine protected area, Vietnam. In H. Kawamura, T. Iwata, Y. Theparoonrat, N. Manajit & V. T. Sulit (Eds.), *Consolidating the strategies for fishery resources enhancement in Southeast Asia* (pp. 174-176). SEAFDEC Publications. <http://repository.seafdec.or.th/handle/20.500.12067/718>
- Cook, P. A., & Gordon, H. R. (2010). World abalone supply, markets, and pricing. *Journal of Shellfish Research*, 29(3), 569-571. <https://doi.org/10.2983/035.029.0303>
- Daume, S. (2006). The roles of bacteria and micro and macro algae in abalone aquaculture: A review. *Journal of Shellfish Research*, 25, 151-157. [https://doi.org/10.2983/0730-8000\(2006\)25\[151:TROBAM\]2.0.CO;2](https://doi.org/10.2983/0730-8000(2006)25[151:TROBAM]2.0.CO;2)
- De Zoysa, M. (2013). Nutritional value, bioactive compounds, and health-promoting properties of abalone. *Marine Nutraceuticals: Prospects and Perspectives*, 57, 57-68. <https://doi.org/10.1201/b13904-11>
- Eny, D., & Setyono, D. (2007). *Prospek usaha budidaya kekerangan di Indonesia* [Prospects for shellfish cultivation business in Indonesia]. *Oseana*, 32, 33-38.
- Fermin, A. C., & Buen, S. M. A. (2001). Grow-out culture of tropical abalone, *Haliotis asinina* (Linnaeus) in suspended mesh cages with different shelter surface areas. *Aquaculture International*, 9(6), 499-508. <https://doi.org/10.1023/A:1020535301193>
- Gallardo, W. G., & Buen S. M. A. (2003). Evaluation of mucus, *Navicula*, and mixed diatoms as larval settlement inducers for the tropical abalone *Haliotis asinina*. *Aquaculture*, 221(1-4), 357-364. [https://doi.org/10.1016/S0044-8486\(03\)00121-2](https://doi.org/10.1016/S0044-8486(03)00121-2)
- Gallardo, W. G., & Salayo, N. D. (2003). Abalone culture: A new business opportunity. *SEAFDEC ASIAN Aquaculture*, 25(3), 25-28.
- Gamble, L. H. (2017). Feasting, ritual practices, social memory, and persistent places: New interpretations of shell mounds in southern California. *American Antiquity*, 82(3), 427-451. <https://doi.org/10.1017/aaq.2017.5>
- Ganmanee, M., Sirirustananun, N., & Jarayabhand, P. (2010). Energy budget of the Thai abalone *Haliotis asinina* reared in a semiclosed recirculating land-based system. *Journal of Shellfish Research*, 29(3), 637-642. <https://doi.org/10.2983/035.029.0312>
- Gao, X., Zhang, M., Luo, X., You, W., & Ke, C. (2023). Transitions, challenges and trends in China's abalone culture industry. *Reviews in Aquaculture*, 15(4), 1274-1293. <https://doi.org/10.1111/raq.12769>
- Geiger, D. L., & Poppe, G. T. (2000). *A conchological iconography: Family Haliotidae*. Conchbooks. <https://www.vetigastropoda.com/abstracts/iconography/index.html>

- Giri, I. N. A., Sutarmat, T., Yudha, H. T., Rusdi, I. & Susanto, B. (2014). Grow-out of abalone *Haliotis squamata* in floating cages fed different proportions of seaweed and with reduction of stocking density. *Indonesian Aquaculture Journal*, 9(1), 15-21.
- Grandiosa, R. (2020). Increasing awareness of abalone culture to support sustainable aquaculture in Indonesia. *Global Scientific Journal*, 8(6), 315-321.
- Hadijah, H. (2017). Effect of natural feed on feed consumption level and feed conversion ratio of tropical abalone *Haliotis asinina* on sea cage. *Applied Mechanics and Materials*, 862, 121-126. <https://doi.org/10.4028/www.scientific.net/AMM.862.121>
- Hadijah, H., Mardiana, M., Indrawati, E., Budi, S., & Zainuddin, Z. (2021). The use of artificial feed in *Haliotis squamata* farming in submerged cage culture system at Lae-Lae island, Makassar. *Revista Ambiente & Água*, 16(4), 1-12. <https://doi.org/10.4136/ambi-agua.2719>
- Hamka, I. J. E., & Shearer, D. (2009). *Abalone industry enhancement in eastern Indonesia*. Australian Centre for International Agricultural Research. [https://www.aciar.gov.au/sites/default/files/2021-07/C2007102\\_abalone\\_industry\\_enhancement\\_eastern\\_indonesia\\_1.pdf](https://www.aciar.gov.au/sites/default/files/2021-07/C2007102_abalone_industry_enhancement_eastern_indonesia_1.pdf)
- Hamzah, M. S., Dwiono, S. A. P., & Hafid, S. (2012). Growth and survival of tropical abalone *Haliotis asinina* seed in concrete tanks at different stocking density. *Jurnal Ilmu dan Teknologi Kelautan Tropis*, 4(2), 191-197. <https://doi.org/10.29244/jitkt.v4i2.7781>
- Handlinger, J., Carson, J., Donachie, L. L. Gabor., & D. Taylor (2005). Bacterial infection in Tasmanian farmed abalone: Causes, pathology, farm factors and control options. In P. Walker, R. Lester & M. G. Bondad-Reantaso (Eds.), *Diseases in Asian aquaculture* (pp. 289-299). Asian Fisheries Society. [https://www.fhs-afs.net/daa\\_v\\_files/Chapter5\\_Diseases\\_of\\_Molluscs/Bacterial%20Infection%20in%20Tasmanian.pdf](https://www.fhs-afs.net/daa_v_files/Chapter5_Diseases_of_Molluscs/Bacterial%20Infection%20in%20Tasmanian.pdf)
- Heasman, M., & Savva, N. (2007). *Manual for intensive hatchery production of abalone*. NSW Department of Primary Industries. [https://www.dpi.nsw.gov.au/\\_data/assets/pdf\\_file/0013/222331/Manual-for-intensive-hatchery-production-of-abalone-section1.pdf](https://www.dpi.nsw.gov.au/_data/assets/pdf_file/0013/222331/Manual-for-intensive-hatchery-production-of-abalone-section1.pdf)
- Hernández-Casas, S., Seijo, J. C., Beltrán-Morales, L. F., Hernández-Flores, Á., Arreguín-Sánchez, F., & Ponce-Díaz, G. (2023). Analysis of supply and demand in the international market of major abalone fisheries and aquaculture production. *Marine Policy*, 148, 1-9. <https://doi.org/10.1016/j.marpol.2022.105405>
- Huang, W.-B., & Hseu, J.-R. (2010). Changes in growth characteristics of the small abalone *Haliotis diversicolor* (Reeve, 1846) after one decade in a closed culture system: A comparison with wild populations. *Fisheries Science Research*, 76, 131-137. <https://doi.org/10.1007/s12562-009-0190-1>
- Huchette, S. M., Koh, C. S., & Day, R. W. (2003). Growth of juvenile blacklip abalone (*Haliotis rubra*) in aquaculture tanks: Effects of density and ammonia. *Aquaculture*, 219(1-4), 457-470. [https://doi.org/10.1016/S0044-8486\(02\)00627-0](https://doi.org/10.1016/S0044-8486(02)00627-0)
- Hwang, E. K., Hwang, I. K., Park, E. J., Gong, Y. G., & Park, C. S. (2014). Development and cultivation of F2 hybrid between *Undariopsis peterseniana* and *Undaria pinnatifida* for abalone feed and commercial mariculture in Korea. *Journal of Applied Phycology*, 26, 742-752. <https://doi.org/10.1007/s10811-013-0164-7>



- Istiqomah, I., & Isnansetyo, A. (2020). Review vibriosis management in Indonesian marine fish farming. In *The 3<sup>rd</sup> International Symposium on Marine and Fisheries Research* (p. 01001). EDP Sciences. <https://doi.org/10.1051/e3sconf/202014701001>
- Jarayabhand, P., Kruiroongroj, W., & Chaisanit, C. (2010). Effects of stocking density on growth performance of Thai abalone, *Haliotis asinina*, Linnaeus 1758, reared under a semiclosed recirculating land-based system. *Journal of Shellfish Research*, 29(3), 593-597. <https://doi.org/10.2983/035.029.0307>
- Jarayabhand, P., & Paphavasit, N. (1996). A review of the culture of tropical abalone with special reference to Thailand. *Aquaculture*, 140, 159-168. [https://doi.org/10.1016/0044-8486\(95\)01194-3](https://doi.org/10.1016/0044-8486(95)01194-3)
- Jardillier, E., Rousseau, M., Gendron-Badou, A., Fröhlich, F., Smith, D. C., Martin, M., Helléouet, M. N., Huchette, S., Doumenc, D., & Auzoux-Bordenave, S. (2008). A morphological and structural study of the larval shell from the abalone *Haliotis tuberculata*. *Marine Biology*, 154(4), 735-744. <https://doi.org/10.1007/s00227-008-0966-3>
- Jumah, Y. U., Traifalgar, R. F., Jumah, D. S., Reyes, L.R., & Mero, F. F. (2016). Feeding rate and sexes affect gonad growth of donkey ear abalone *Haliotis asinina* Linnaeus, 1758. *Animal Biology & Animal Husbandry*, 8(1), 10-14.
- Kamaishi, T., Miwa, S., Goto, E., Matsuyama, T., & Oseko, N. (2010). Mass mortality of giant abalone *Haliotis gigantea* caused by a *Francisella* sp. bacterium. *Diseases of Aquatic Organisms*, 89, 145-154. <https://doi.org/10.3354/dao02188>
- Kua, B. C., Ramly, R., Devakie, M. N., Groman, D., & Berthe, C. J. F. (2011). Investigating a mortality in hatchery cultured tropical abalone, *Haliotis asinina* Linnaeus, 1758 in Malaysia. *Disease Asian Aquaculture*, 7, 103-110.
- Lebata-Ramos, M. J. H. (2018). *Grow-out culture of abalone in small islands and/or community. Terminal Report: National Abalone R&D Program*. Southeast Asian Fisheries Development Center.
- Lebata-Ramos, M. J. H., Doyola-Solis, E. F. C., Abroguena, J. B. R., Ogata, H., Sumbing, J. G., & Sibonga, R. C. (2013). Evaluation of post-release behavior, recapture, and growth rates of hatchery-reared abalone *Haliotis asinina* released in Sagay Marine Reserve, Philippines. *Reviews in Fisheries Science*, 21(3-4), 433-440. <https://doi.org/10.1080/10641262.2013.836445>
- Lebata-Ramos, M. J. H., Hazel, J., & Solis, E. F. D. (2021). Can *Ulva reticulata* replace *Gracilariopsis heteroclada* as natural food for the abalone *Haliotis asinina*? *Journal of Applied Phycology*, 33(3), 1869-1872. <https://doi.org/10.1007/s10811-021-02407-1>
- Li, Q., Lu, J., Chang, Y., Shen, G., & Feng, J. (2022). Effect of different cooking methods on nutritional intake and different storage treatments on nutritional losses of abalone. *Food Chemistry*, 377, 1-11. <https://doi.org/10.1016/j.foodchem.2022.132047>
- Lloyd, M. J., & Bates, A. E. (2008). Influence of density-dependent food consumption, foraging and stacking behaviour on the growth rate of the Northern abalone, *Haliotis kamtschatkana*. *Aquaculture*, 277(1-2), 24-29. <https://doi.org/10.1016/j.aquaculture.2008.01.039>
- Mabuhay-Omar, J. A., Cayabo, G. D. B., & Creencia, L. A. (2021). Bacteriological quality of cage-cultured abalone *Haliotis asinina*. *Aquaculture Research*, 4(2), 151-159. <https://doi.org/10.3153/AR21012>

- Masuda, R., & Tsukamoto, K. (1998). Stock enhancement in Japan: Review and perspective. *Bulletin of Marine Science*, 62(2), 337-358.
- Maulidya, K. D., Wiradana, P. A., Putranto, T. W. C., & Soegianto, A. (2021). Abalone (*Haliotis squamata*) enlargement technique using a floating net cage method as a preliminary study of mariculture. *Ecology, Environment and Conservation*, 27(2), 685-689.
- Minh, N. D., & Hong, L. T. (2000). Embryonic, larval and postlarval development of *Haliotis asinina* Linneù 1758 in laboratory condition. *Collection of Marine Research Works*, 10, 190-194.
- Minh, N. D., Petpiroon, S., Jarayabhand, P., Meksumpun, S., & Tunkijjanukij, S. (2010). Growth and survival of abalone, *Haliotis asinina* Linnaeus 1758, reared in suspended plastic cages. *Kasetsart Journal (Natural Science)*, 44(4), 621-630.
- Najmudeen, T. M., & Victor, A. C. C. (2004). Seed production and juvenile rearing of the tropical abalone *Haliotis varia* Linnaeus 1758. *Aquaculture*, 234, 277-292. <https://doi.org/10.1016/j.aquaculture.2003.12.013>
- Nguyen, T. V., Alfaro, A. C., Mundy, C., Petersen, J., & Ragg, N. L. (2022). Omics research on abalone (*Haliotis* spp.): Current state and perspectives. *Aquaculture*, 547, 1-15. <https://doi.org/10.1016/j.aquaculture.2021.737438>
- Nguyen, T. V., Qian, Z. J., Ryu, B., Kim, K. N., Kim, D., Kim, Y. M., Jeon, Y. J., Park, W. S., Choi, I. W., Kim, G. H., & Je, J. Y. (2013). Matrix metalloproteinases (MMPs) inhibitory effects of an octameric oligopeptide isolated from abalone *Haliotis discus hannai*. *Food Chemistry*, 141(1), 503-509. <https://doi.org/10.1016/j.foodchem.2013.03.038>
- Nhan, H. T., Jung, L. H., Ambak, M. A., Watson, G. J., & Siang, H. Y. (2010). Evidence for sexual attraction pheromones released by male tropical donkey's ear abalone (*Haliotis asinina*), (L.). *Invertebrate Reproduction & Development*, 54(4), 169-176. <https://doi.org/10.1080/07924259.2010.9652330>
- Nicolas, J. L., Basuyaux, O., Mazurie, J., & Thébault, A. (2002). *Vibrio carchariae*, a pathogen of the abalone *Haliotis tuberculata*. *Disease of Aquatic Organisms*, 50(1), 35-43. <https://doi.org/10.3354/dao050035>
- Nuurai, P., Engsusophon, A., Poomtong, T., Sretarugsa, P., Hanna, P., Sobhon, P., & Wanichanon, C. (2010). Stimulatory effects of egg-laying hormone and gonadotropin-releasing hormone on reproduction of the tropical abalone, *Haliotis asinina* Linnaeus. *Journal of Shellfish Research*, 29(3), 627-635. <https://doi.org/10.2983/035.029.0311>
- Octaviany, M. J. (2007). Beberapa catatan tentang aspek biologi dan perikanan abalon [Some notes on aspects of abalone biology and fisheries]. *Oseana*, 32(4), 39-47.
- Paul, N. A., De Nys, R., & Steinberg, P. D. (2006). Seaweed-herbivore interactions at a small scale: Direct tests of feeding deterrence by filamentous algae. *Marine Ecology Progress Series*, 323, 1-9. <https://doi.org/10.3354/meps323001>
- Pitchon, D., Cudennec, B., Huchette, S., Djediat, C., Renault, T., Paillard, C., & Auzoux-Bordenave, S. (2013). Characterization of abalone *Haliotis tuberculata* *Vibrio harveyi* interactions in gill primary cultures. *Cytotechnology*, 65, 759-772. <http://doi.org/10.1007/s10616-013-9583-1>
- Prihadi, T. H., Ardi, I., Widiyati, A., & Wiyanto, D. B. (2018). Potency of different seaweeds as diets for developing abalone (*H. squamata*) culture in Nusa Penida Island, Bali. In *2<sup>nd</sup> Scientific Communication in Fisheries and Marine Sciences* (p. 02004). EDP Sciences. <https://doi.org/10.1051/e3sconf/20184702004>

- Sahetapy, J. M., & Latuihamallo, M. (2014). The growth of abalone (*Haliotis squamata*) in net floating cage at Hulaliu Waters, Central District of Moluccas. *Aquacultura Indonesiana*, 15, 21-25. <https://doi.org/10.21534/ai.v15i1.28>
- Salayo, N. D., Azuma, T., Castel, R. J., Barrido, R. T., Tormon-West, D. H., & Shibuno, T. (2020). Stock enhancement of abalone, *Haliotis asinina*, in multi-use buffer zone of Sagay Marine Reserve in the Philippines. *Aquaculture*, 523, 1-10. <https://doi.org/10.1016/j.aquaculture.2020.735138>
- Santiago, C. H. S., & Mabuhay-Omar, J. A. (2019). Isolation and characterization of antimicrobial-producing bacteria from the donkey's ear abalone *Haliotis asinina*. *Journal of Shellfish Research*, 38(2), 413-416. <https://doi.org/10.2983/035.038.0224>
- Setyono, D. (2005). Abalone (*Haliotis asinina* L): Early juvenile rearing and ongrowing culture. *Oseana*, 30(2), 1-10. <https://doi.org/10.14203/mri.v30i0.420>
- Setyono, D. E. D., & Aswandy, I. (2010). Ongrowing techniques for juvenile donkey ear abalone (*Haliotis asinina*) at Pemenang Waters, North Lombok, Indonesia. *Marine Research in Indonesia*, 35(2), 15-22. <https://doi.org/10.14203/mri.v35i2.473>
- Shi, L., Hao, G., Chen, J., Ma, S., & Weng, W. (2020). Nutritional evaluation of Japanese abalone (*Haliotis discus hannai* Ino) muscle: Mineral content, amino acid profile and protein digestibility. *International Food Research*, 129, 1-8. <https://doi.org/10.1016/j.foodres.2019.108876>
- Sososutiksno, C., & Gasperz, J. (2017). Economic and financial feasibility of abalone culture development in Hulaliu village, District of Maluku Tengah, Maluku Province. *Aquaculture, Aquarium, Conservation & Legislation*, 10(6), 1492-1498.
- Stewart, P., Soonklang, N., Stewart, M. J., Wanichanon, C., Hanna, P. J., Poomtong, T., & Sobhon, P. (2008). Larval settlement of the tropical abalone, *Haliotis asinina* Linnaeus, using natural and artificial chemical inducers. *Aquaculture Research*, 39(11), 1181-1189. <https://doi.org/10.1111/j.1365-2109.2008.01982.x>
- Supriyono, E., Liubana, D. V., Budiardi, T., & Effendi, I. (2020). The addition of calcium oxide with different doses in the recirculation system to improve the abalone *Haliotis squamata* seed production. *Jurnal Akuakultur Indonesia*, 19(2), 199-206. <https://doi.org/10.19027/jai.19.2.199-206>
- Tangtrongpiros, J., & Chansue, N. (1999). *Use of antibiotics for therapeutic treatment of abdominal swelling disease in donkey's ear abalone (Haliotis asinina)*. Food and Agriculture Organization of the United Nations. <https://agris.fao.org/search/en/providers/122623/records/6472457153aa8c8963043de1>
- Thao, N. T., An, C. M., Hai, T. N., Dinh, T. D., & Khanh, L. V. (2020). Reproductive cycle of oval abalone (*Haliotis ovina* Gmelin, 1791) distributed on Nam Du island, Kien Giang province. *Can Tho University Journal of Science*, 5, 175-83. <https://doi.org/10.22144/ctu.jsi.2020.053>
- Thongrod, S., Tamtin, M., Chairat, C., & Boonyaratpalin, M. (2003). Lipid to carbohydrate ratio in donkey's ear abalone (*Haliotis asinina*, Linne) diets. *Aquaculture*, 225(1-4), 165-174. [https://doi.org/10.1016/S0044-8486\(03\)00287-4](https://doi.org/10.1016/S0044-8486(03)00287-4)
- Tsai, C. L., Shiau, C. Y., & Sung, W. C. (2018). Effects of blanching and refrigerated storage on quality attributes of hybrid abalone (*Haliotidae discus hannai* × *H. diversicolor diversicolor*). *Journal of Food Processing and Preservation*, 42(5), 1-10. <https://doi.org/10.1111/jfpp.13608>

- Viera, M. P., Pinchetti, J. G., De Viçose, G. C., Bilbao, A., Suárez, S., Haroun, R. J., & Izquierdo, M. S. (2005). Suitability of three red macroalgae as a feed for the abalone *Haliotis tuberculata* coccinea Reeve. *Aquaculture*, 248(1-4), 75-82. <https://doi.org/10.1016/j.aquaculture.2005.03.002>
- Wang, J., Guo, Z., Feng, J., Liu, G., Xu, L., Chen, B., & Pan, J. (2004). Virus infection in cultured abalone, *Haliotis diversicolor* Reeve in Guangdong Province, China. *Journal of Shellfish Research*, 23(4), 1163-1169.
- Wetchateng, T., Friedman, C. S., Wight, N. A., Lee, P. Y., Teng, P. H., Sriurairattana, S., Wongprasert, K., & Withyachumnarnkul, B. (2010). Withering syndrome in the abalone *Haliotis diversicolor* supertexta. *Disease of Aquatic Organisms*, 90(1), 69-76. <https://doi.org/10.3354/dao02221>
- Williams, E. A., Craigie, A., Yeates, A., & Degnan, S. M. (2008). Articulated coralline algae of the Genus *Amphiroa* are effective natural inducers of settlement in the tropical abalone *Haliotis asinina*. *The Biological Bulletin*, 215, 98-107. <https://doi.org/10.2307/25470687>
- Wiradana, P. A., Yusup, D. S., & Soegianto, A. (2018). Preliminary study of biomonitoring *Escherichia coli* and coliform contamination in abalone (*Haliotis squamata*) cultivation pond in Musi Village, Gerokgak Sub District, Buleleng-Bali. *Aquacultura Indonesiana*, 20(1), 32-40. <http://dx.doi.org/10.21534/ai.v20i1.143>
- Wood, E. M., Mapait, J. B., Bavoh, E. M., Ng, J. V., & Yusah, H. M. (2015). *Abalone culture and farming in Tun Sakaran Marine Park, Sabah*. Marine Conservation Society. <https://lighthouse-foundation.org/Binaries/Binary1063/Abalone-culture-and-farming-in-TSMP-2015.pdf>
- Wu, F., & Zhang, G. (2016). Pacific abalone farming in China: Recent innovations and challenges. *Journal of Shellfish Research*, 35, 703-710. <https://doi.org/10.2983/035.035.0317>
- Yasa, N. S., Murwantoko, M., Handayani, N. S., Triastutik, G., & Anshory, L. (2020). Physiological, biochemical and HSP70 and HSP90 gene expression profiles of tropical abalone *Haliotis squamata* in response to *Vibrio alginolyticus* infection. *Indonesian Journal of Biotechnology*, 25(1), 12-20. <https://doi.org/10.22146/ijbiotech.51322>

## Identifying Collagenase (MMP-1, -8, -13) Expression and Correlation with Periodontitis Progression Using the Rat Model

Fazle Khuda<sup>1</sup>, Badiyah Baharin<sup>2</sup>, Nur Najmi Mohamad Anuar<sup>3</sup>, Putri Ayu Jayusman<sup>1</sup>, Mariati Abdul Rahman<sup>1</sup> and Nurrul Shaqinah Nasruddin<sup>1\*</sup>

<sup>1</sup>Department of Craniofacial Diagnostics and Biosciences, Faculty of Dentistry, Universiti Kebangsaan Malaysia, Jalan Raja Muda Abdul Aziz, 50300 Kuala Lumpur, Malaysia

<sup>2</sup>Department of Restorative Dentistry, Faculty of Dentistry, Universiti Kebangsaan Malaysia, Jalan Raja Muda Abdul Aziz, 50300 Kuala Lumpur, Malaysia

<sup>3</sup>Programme of Biomedical Science, Centre for Toxicology and Health Risk Studies, Faculty of Health Sciences, Universiti Kebangsaan Malaysia, Jalan Raja Muda Abdul Aziz, 50300 Kuala Lumpur, Malaysia

### ABSTRACT

Collagenase (MMP-1, -8, and -13) is one of the groups of the matrix metalloproteinases (MMPs) that is responsible for the breakdown of collagen, particularly type-I collagen, which is found in profusion in the extracellular matrix (ECM). It is essential to understand the role of a group of biomarkers in the progression of periodontal disease. This study aims to evaluate the expression of MMP-1, -8, and -13 combined in the periodontitis progression induced by wire ligation and *Enterococcus faecalis* inoculation using the rat model. Twelve rats were allocated uniformly between the control group 0-day, experimental group 7- and 14-days. Orthodontic wire (0.2 mm) was placed between the proximal space of the right upper first and second molar tooth area and 0.5 µl of  $1.5 \times 10^8$  cfu/ml. Rats in the experimental groups received an injection of *E. faecalis* suspension into their gingival sulcus. After the respective induction time, the rats were euthanised. Gingival tissue and maxillary jaw samples were obtained from all rats for quantitative real-time PCR and histological examination. The results showed a significant increase in mRNA expression within the tissue samples from the gingiva of MMP-1 ( $p < 0.05$ ), -8 ( $p < 0.01$ ), and -13 ( $p < 0.01$ ) in 7 days as compared to the control. The MMP-8 expression levels were also significantly reduced ( $p < 0.05$ ). Histological analysis

showed a higher inflammatory cell infiltration and the presence of osteoclast in the 7 days, which was reduced in the 14 days. MMP-1, -8, and -13 levels were positively correlated with the presence of inflammatory cells. Therefore, identifying a group of collagenases might be a useful biomarker to detect the progression of periodontitis.

**Keywords:** Collagenase, matrix metalloproteinase, MMP-1, MMP-8, MMP-13, periodontitis

### ARTICLE INFO

#### Article history:

Received: 25 October 2023

Accepted: 26 February 2024

Published: 28 January 2025

DOI: <https://doi.org/10.47836/pjtas.48.1.09>

#### E-mail addresses:

hillo170@yahoo.com (Fazle Khuda)

shaqinah@ukm.edu.my (Nurrul Shaqinah Nasruddin)

badiyah@ukm.edu.my (Badiyah Baharin)

numajmi@ukm.edu.my (Nur Najmi Mohamad Anuar)

mariati\_ar@ukm.edu.my (Mariati Abdul Rahman)

putriayu@ukm.edu.my (Putri Ayu Jayusman)

\*Corresponding author

## INTRODUCTION

The gingiva, periodontal ligament, radicular cementum, and alveolar bone around the teeth are all affected by periodontal disease, a pathological condition (Beck et al., 2020). According to the World Health Organization (WHO), severe periodontitis appears to be the sixth most common disease worldwide, affecting around 10% of the global population (Jacob, 2012). The estimated disability-adjusted life year (DALY) for severe periodontitis was stated to be relatively high, ranking at number 77 (Dom et al., 2016). In Malaysia, moderate and severe periodontitis incidence was 30.3 and 18.2%, respectively, based on the National Oral Health Survey for adults. The disease is more prevalent in the adult population, while adolescents are less likely to be affected. Subgingival microbiota, a specific periodontopathogenic bacteria and host immune-inflammatory response are accountable towards the progression of the disease (Preethanath, 2020). In addition, more than 700 species of oral microorganisms are equally responsible for the disease progression (de Molon et al., 2016). *Enterococcus faecalis* is a facultative, Gram-positive microorganism and an important bacterium in endodontic infection, though it is less important as a periodontal pathogen. However, an association between *E. faecalis*-induced endodontic lesion and periodontal disease has been demonstrated in several studies (Alghamdi & Shakir, 2020; Souto et al., 2006). Bacteria in infected gingival tissue around the teeth cause inflammation by breaking down the barrier between the gingiva and the underlying connective tissue. After bacteria enter the sites, their byproducts cause periods of inflammation exacerbation and remission, which increases the generation of MMPs and proinflammatory cytokines (Ramadan et al., 2020).

Collagenase (MMP-1, -8, and -13) is one of the most significant MMP groups. It breaks down collagen, particularly type-I collagen, in the ECM (Khuda et al., 2021). Collagenase group member MMP-1 is sometimes referred to as fibroblast collagenase, interstitial collagenase, and collagenase 1. Most periodontal tissue matrix is made up of MMP-1, which is typically expressed by fibroblasts, osteoblasts, keratinocytes, macrophages, endothelial cells, platelets, chondrocytes, and tumour cells (Pirhan et al., 2008). Collagenase 2, or neutrophilic collagenase, another name for MMP-8, plays a key contributor in the aetiology of periodontal disease. The key host cell-derived collagenase generated from neutrophils causes gingival and periodontal collagen to break down and tissue destruction (Kraft-Neumärker et al., 2012). Osteoclastic activities, such as bone resorption and destruction, are carried out by MMP-13, which is also known as collagenase 3 (Checchi et al., 2020).

In the periodontal inflammatory process, microorganisms initiate an inflammatory and immune response that leads to tissue damage, particularly in susceptible hosts. Therefore, there is a lot of interest in identifying, validating, and clinically using biomarkers for periodontal disease. Early identification is essential for improving the management of the condition since periodontal disease is a global health problem linked to several systemic disorders (Hajishengallis & Chavakis, 2021). Numerous studies have pointed

to MMP-8 as a prognostic marker for periodontal health and disease (Rathnayake et al., 2017). Furthermore, an MMP-8 point-of-care chairside test kit has also been developed to diagnose periodontal disease. Combining biomarkers can be useful for better diagnostic performance than just a single biomarker. It is crucial to comprehend the part played by this set of biomarkers in developing periodontal disease to improve diagnostic procedures. This study aims to assess the expression of the MMPs-1, -8, and -13 combined in the periodontitis progression by wire ligation and *E. faecalis* inoculation using the rat model.

## MATERIALS AND METHODS

### Animals

The Universiti Kebangsaan Malaysia Animal Ethical Committee (UKMAEC) and the National Institutes of Health (NIH) both gave their approval for the animal studies to be carried out in accordance with the “Guide for the Care and Use of Laboratory Animals” (FD/2018/NURRUL SHAQINAH/28-NOV./967-NOV.-2018-JAN. -2020). The Sprague Dawley rats used in this study were grown under specific pathogen-free settings in the Laboratory Animal Resource Unit, Universiti Kebangsaan Malaysia, maintained in the standard environment ( $25 \pm 1^\circ\text{C}$ , 55% humidity, 12–12 days–night pattern) with water and food provided ad libitum. Before the experiment, four rats were housed in a cage and given a week to get used to the environment. Twelve male rats, weighing about ~180 g and aged six weeks old, were divided into 0-day (control), 7- and 14-days (experimental) groups. This study followed the ARRIVE 2.0 reporting guidelines (du Sert et al., 2020). The rats were weighed on 0 day and every 3 days throughout the experimental schedule. The degree of freedom used in the analysis of variance (ANOVA) computation to determine sample sizes has an “E” value that must be between 10 and 20 ( $E = \text{Total number of animals} - \text{Total number of groups}$ ) (Ilyas et al., 2017). Rats were assigned 4 per group, with no losses of the rats from the groups at the end of the experiment. Two investigators blinded to treatments evaluated the rats for at least one hour each day for behavioural and physical symptoms of animal welfare, and the rats remained within acceptable, humane endpoint criteria, with no indication of pain or discomfort outside of the experimental stimulus.

### Experimental Procedure

An intraperitoneal injection of a 10% ketamine (100 mg/kg, Ketamil, Australia) and a 2% xylazine® (Pharmika India Pvt. Ltd., India), (10 mg/kg) body weight combination was used to administer general anaesthesia (Davis, 2001). Anaesthesia was installed in 4–5 min after administration. The sterile endodontic file #8, #10 (Dentsply Sirona, USA) was carefully placed between the interdental spaces of the upper right first and second molar teeth. The gentle push and pull movements were repeated a few times to make a space without damaging the gingival tissue (Li et al., 2020). Then, using a needle holder, a 0.2 mm

sterile orthodontic wire with a length of 5 mm was bent into the shape of a “(“ and gently placed into the space. The procedure was performed carefully to prevent any damage to the tissue. An oral examination was performed twice a week to check the wire placement.

*Enterococcus faecalis* strain was obtained from the American Type Culture Collection® (ATCC 29212, USA). The strain was cultured in an anaerobic chamber at 37°C for 24 hr using a brain heart infusion (BHI, Oxoid, United Kingdom) agar medium. The bacterial solution was prepared using sterile PBS in  $1.5 \times 10^8$  cfu/ml bacteria and standardised using McFarland standards. A Hamilton syringe (Hamilton, USA) was used to carefully inject 0.5 µl of the bacterial inoculation once a week into the gingival sulcus of the upper right first and second molar region over the respective induction period after the insertion of a ligature wire.

### Sample Collection

Rats were euthanised at 0-, 7-, and 14-days post-induction by using a mixture of 10% ketamine (200 mg/kg) and 2% xylazine (20 mg/kg) followed by cervical displacement. The control group (0 day) was sacrificed after the 14-day induction period. A gross examination of the oral cavity and the general appearance of the rats was performed. Tissue samples from the gingiva around the molar teeth area were obtained for RNA and DNA extraction. The RNA and DNA extraction samples were rinsed with a cold, sterile saline solution and immediately kept at -80°C until further use. Instantly after being extracted from the maxillary jaw for histopathological analysis, the samples were preserved in 10% neutral buffered formalin (Leica, USA) for at least 48 hr.

### RNA and DNA Extraction

The 20 mg of samples from gingival tissue were used to extract and purify total RNA using the Innu PREP® RNA Mini Kit 2.0 (Analytik Jena, Germany). Reverse mRNA transcription to cDNA was performed using a High-quality ReverTra Ace® qPCR RT Master Mix with gDNA Remover (TOYOBO, Japan) according to protocol. Using the Nucleospin® DNA extraction kit (Macherey-Nagel, Germany), total DNA was extracted and purified from 25 mg of gingival tissues in accordance with the manufacturer’s guidelines. The quantity and integrity of the extracted total RNA and DNA was measured by a NanoDrop (ND-2000, Thermo Fisher Scientific, USA). The study did not include RNA or DNA samples with 260/280 ratios greater than 1.8.

### RT-qPCR Assay

Quantitative real-time PCR (RT-qPCR) was carried out using a ready-to-use 2× concentration of ChamQ Universal SYBR® qPCR master mix (Vazyme, China). The master mix contains dNTPs, Mg<sup>2+</sup>, Champagne Taq DNA polymerase, and Specific ROX reference



dye. The 10 µl real-time PCR reactions consisted of 5 µl master mix, 0.5 µl of reverse and forward primers, cDNA template of 1 µl, and RNase-free water of 3 µl. The tubes were sealed and briefly centrifuged to remove all air bubbles. The specific gene sequence was amplified using a CFX96 Connect™ RT-PCR Thermal cycler (Bio-Rad, USA). A two-step amplification protocol for collagenase and inflammatory cytokines was set, as shown in Table 1. The primer sequences and their specific qPCR settings are listed in Table 1. All reactions were prepared in triplicate, and any contamination presence was determined by running a no-template control, which contained the reaction mixture without template DNA with every qPCR run. Melting peaks were used to determine PCR specificity. Results were normalised using the housekeeping gene glyceraldehyde-3-phosphate dehydrogenase (GAPDH), and data were evaluated using the  $2^{-\Delta\Delta CT}$  technique (Livak & Schmittgen, 2001).

Table 1

*Primer sequence for quantitative real-time polymerase chain reaction assays*

Gene name	5'-3' primer sequence	Annealing temperature (°C)	Amplification cycle	Reference
MMP-1	Forward ACAACCTGCCAAATGGGCTTGA	60, 30s	40	Hirate et al. (2012)
	Reverse CTGTCCCTGAACAGCCCAGACTTA			
MMP-8	Forward TCCTTGCCCATGCCTTTCAA	60, 30s	40	Matsui et al. (2011)
	Reverse CCAAACTATGCTTACAGAGAACCC			
MMP-13	Forward AGAAGTGTGACCCAGCCCTATC	65, 30s	32	Matsui et al. (2011)
	Reverse GCATACGAGCATCCATCCCGA			
<i>Enterococcus faecalis</i>	Forward GGAATTGTTCTTGCATCCGT	60, 30s	40	Liu (2011)
	Reverse ACAATTAAGTATTCTACGCC			
GAPDH	Forward TGCTGGTGCTGAGTATGTCG	60, 30s	40	Kuo et al. (2019)
	Reverse ATTGAGAGCAATGCCAGCC			

*Note.* MMP = Matrix metalloproteinases; GAPDH = Glyceraldehyde-3-phosphate dehydrogenase

## **Histological Examination**

Tissue samples from the maxillae were collected and processed for histological analysis. Soft tissues that would be examined histopathologically were fixed instantly and immersed in 10% buffered formalin for at least two days. Following a 21-day decalcification period in 10% buffered ethylenediaminetetraacetic acid (EDTA, Sigma-Aldrich, Germany) solution, the maxillary specimens were sectioned into 5  $\mu\text{m}$  and subjected to Hematoxylin and Eosin staining (H&E staining, Leica, USA) in accordance with established processes.

## **Analysis of Inflammatory Cells**

All the tissue sections were examined under a microscope at magnifications of 4 $\times$ , 10 $\times$ , and 40 $\times$ , and the Image-Pro Plus system (Media Cybernetics, USA) digitally captured the images — the distinctive morphology of inflammatory cells (neutrophils, macrophages, lymphocytes) allowed for their identification. Only whole, clearly blue-stained inflammatory cells were counted. The inflammatory cells were counted using the ImageJ software bundled with Java 1.8.0\_172 and presented in a bar graph. The histopathology results were qualitatively reported, and the group descriptions were contrasted.

## **Statistical Analysis**

On day 0 and at the conclusion of the experimental period, body weight was analysed through a one-way ANOVA. The data were presented as mean values with either standard deviation (SD) or standard errors (SE), and these analyses were carried out using IBM SPSS data editor version 23.0 (IBM, USA). If a statistically significant difference was observed, a pairwise multiple comparison test (Tukey post-hoc) was executed to assess distinctions among the groups. The RT-qPCR fold change results were logarithmically transformed, and statistical analysis was performed. The ANOVA was employed to assess distinctions in group means, and a Tukey post-hoc test was utilised to identify which means differed significantly from the other groups. In the current study, *P* values less than 0.05 were accepted as statistically significant. The Pearson correlation was performed to evaluate the correlation between collagenase (MMP-1, -8, -13) expression and inflammatory cell count.

# **RESULTS**

## **Body Weight Measurement**

The mean body weight of all the rats at the beginning of the experiment was around 180 g, and there was no significant variation among the groups ( $p > 0.05$ ). The average body weight of the animals in all three experimental groups had increased significantly by the end of the experimental period, with a significant difference between them ( $p < 0.05$ ). The control group (0 day) gained significantly more ( $p < 0.05$ ) weight during the study than the

7- and 14-day groups. The final mean body weight of 0- and 7-day groups after the 7-day experimental period was  $231.25 \pm 14.34$  and  $194.50 \pm 6.95$ , respectively, as shown in Figure 1 (a). The final mean body weight of 0- and 14-day groups after the 14-day experimental period was  $260.50 \pm 15.93$  and  $221.25 \pm 7.68$ , respectively, as shown in Figure 1 (b).

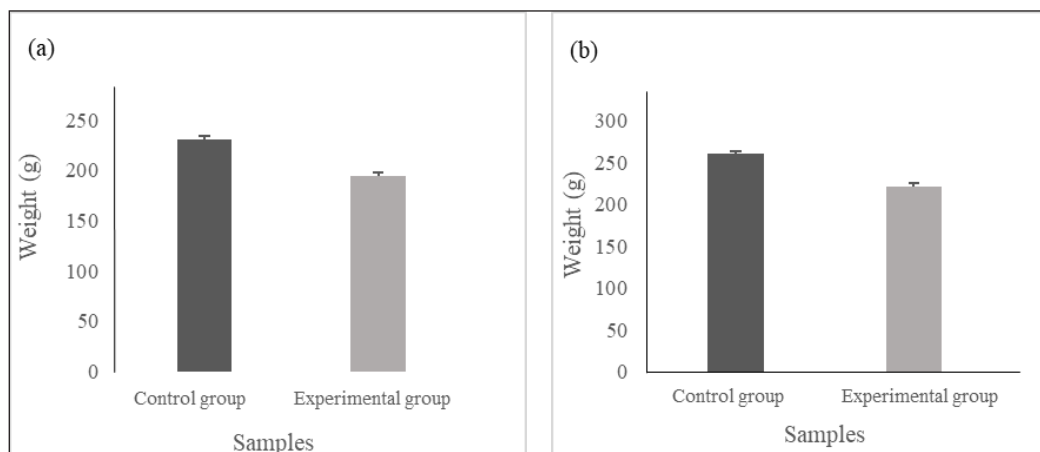


Figure 1. The final mean body weight of (a) 0- and 7-days groups after the 7 days experimental period; (b) 0- and 14-days groups after the 14 days experimental period

### Expression of Collagenase (MMP-1, -8, -13) in Gingival Tissue Samples

This study found an upregulation of collagenase significantly, MMP-1 ( $p < 0.01$ ), MMP-8 ( $p < 0.01$ ), and MMP-13 ( $p < 0.01$ ), as shown in Figure 2 in gingival tissue samples at 7 days post-induction. There was a notable variation in the MMP-8 expression between 7 and 14 days ( $p < 0.05$ ), as shown in Figure 2 (b). However, in comparison to the 0-day group, MMP-1 and MMP-8 were substantially elevated at 7 and 14 days ( $p < 0.01$ ); the upregulation of MMP-13 expression at 14 days in the gingival tissue samples was not significant statistically ( $p > 0.05$ ) as shown in Figure 2.

### *Enterococcus faecalis* Bacterial Load Analysis in the Gingival Tissue Samples

The cycle threshold (Ct) value is a semi-quantitative measure of bacterial load, where the greater the amount of bacterial DNA, the lower the Ct value. There was a significant difference in the *E. faecalis* gene Ct values of the gingival tissue samples at the 7 days ( $p < 0.01$ ) and 14 days ( $p < 0.05$ ) post-induction group as compared to the control group (Ct 34.41). Moreover, a considerable difference was seen between the 7- and 14-days groups ( $p < 0.01$ ). At 7 days, the Ct value was lowered (Ct 28.72) but then increased at 14 days (Ct 32.81). All results are shown in Figure 3.

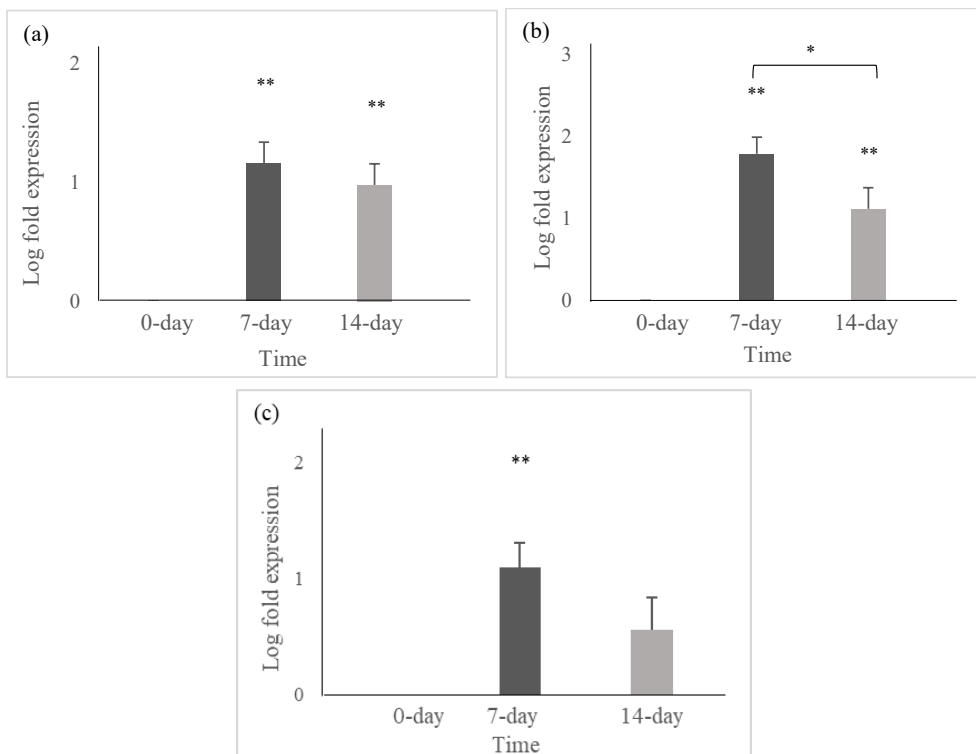


Figure 2. Expression of MMP-1, -8, -13 in gingival tissue samples shows (a) significant upregulation of MMP-1 at 7 and 14 days ( $p < 0.01$ ) as compared to 0-day group; (b) significant upregulation of MMP-8 at 7 and 14 days ( $p < 0.01$ ) as compared to 0-day group, a significant difference between 7 and 14 days group ( $p < 0.05$ ); (c) significant upregulation of MMP-13 at 7 days ( $p < 0.01$ ) as compared to 0-day group  
 Note. \* =  $p < 0.05$ ; \*\* =  $p < 0.001$

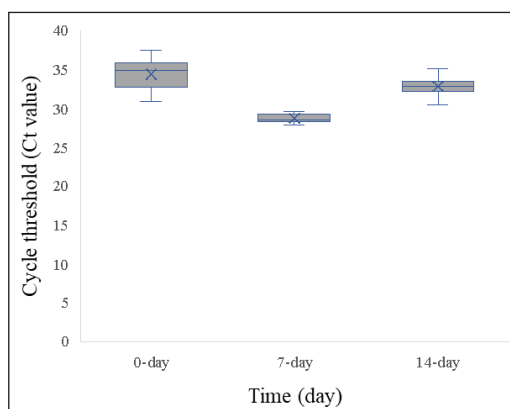
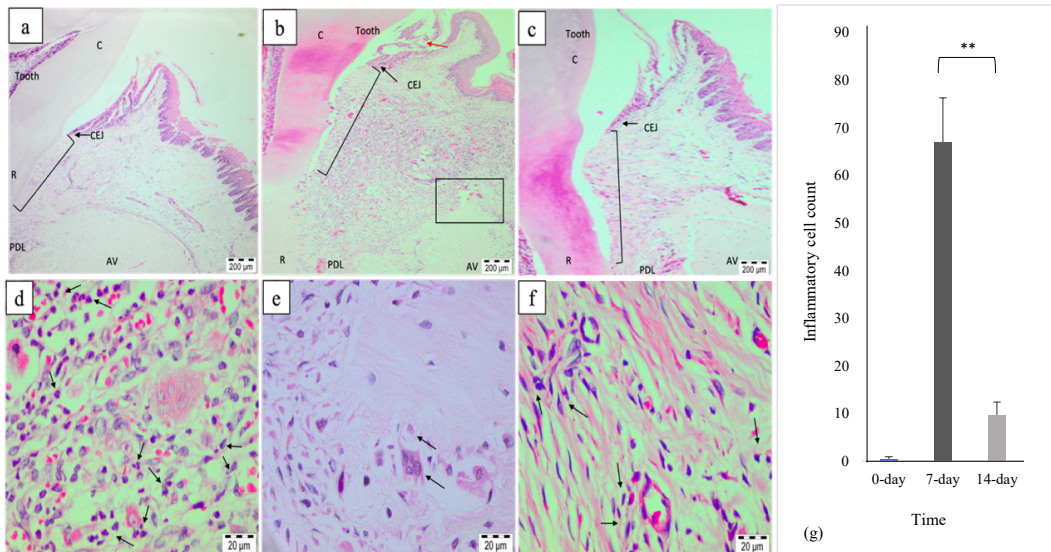


Figure 3. The cycle threshold (Ct) values of the *Enterococcus faecalis* gene in gingival tissue samples. At 7 days, the Ct value was (Ct 28.72), then increased at the 14 days (Ct 32.81). There was a significant difference between the 7- and 14-days groups ( $p < 0.01$ )  
 Note. \*\* =  $p < 0.001$

## Histopathological Changes in the Periodontium

The histopathological analysis of the periodontium of the 7 days post-induction group showed thin and ulcerated junctional epithelium (JE), migration of the JE apically, loss of attachment at the cemento enamel junction (CEJ) as shown in Figure 4 (b), inflammatory cells infiltration mostly neutrophils, macrophages as shown in Figure 4 (d) as well as the presence of osteoclasts and alveolar bone (AV) resorption as shown in Figure 4 (e). In the 14-day post-induction group, inflammatory cell infiltration was less as compared to the 7-day post-induction group as shown in Figure 4(f), even though the migration of the JE apically and attachment loss from the CEJ were observed as shown in Figure 4 (f). In the control group, the JE was normal; there was no attachment loss from CEJ, inflammatory cell infiltration and resorption of the alveolar bone surface within the periodontium as shown in Figure 4 (a). When compared to the 14-day group, the 7-day group exhibited a notably greater quantity of inflammatory cells ( $p < 0.01$ ), as shown in Figure 4 (g).



**Figure 4.** Histopathological images were shown in figures (a, b, c, d, e, f) and the number of inflammatory cells was shown in figure (g). (a) Images of normal histological structure within the periodontium at 0-day; (b) Image of a thin and ulcerated junctional epithelium (JE), apical migration of the JE, attachment loss from the cemento enamel junction (CEJ) at 7 days; (c) Images of attachment loss from CEJ at 14 days; (d) Images of inflammatory cells infiltration mostly neutrophils and macrophages; (e) Images of presence of osteoclasts and alveolar (AV) bone resorption; (f) Images of less inflammatory cells infiltration at 14 days as compared to the 7 days PI group, even though the migration of the JE apically and attachment loss from the CEJ were observed using 4x, 10x, and 40x magnifications; (g) Image of bar graph shows significantly higher inflammatory cell count ( $p < 0.01$ ) in the 7-day group as compared to the 14-day group. Note. C = Crown; R = Root; PDL = Periodontal ligament; \*\* in figure (g) =  $p < 0.001$

### Correlation Between Collagenase (MMP-1, -8, -13) Expression and Inflammatory Cells Count

The Pearson correlation method was applied to determine if a correlation exists between the gene expression (based on qPCR data) and inflammatory cell count. The analysis showed a highly positive correlation of MMP-1 ( $r = 0.926$ ), MMP-8 ( $r = 0.890$ ), and MMP-13 ( $r = 0.823$ ) in 7-day with the inflammatory cells, as shown in Figure 5 (a, b, c). Furthermore, the correlation between MMP-1 ( $r = 0.873$ ), MMP-8 ( $r = 0.906$ ), and MMP-13 ( $r = 0.914$ ) in 14 days was highly positive with the inflammatory cells, as shown in Figure 5 (d, e, f).

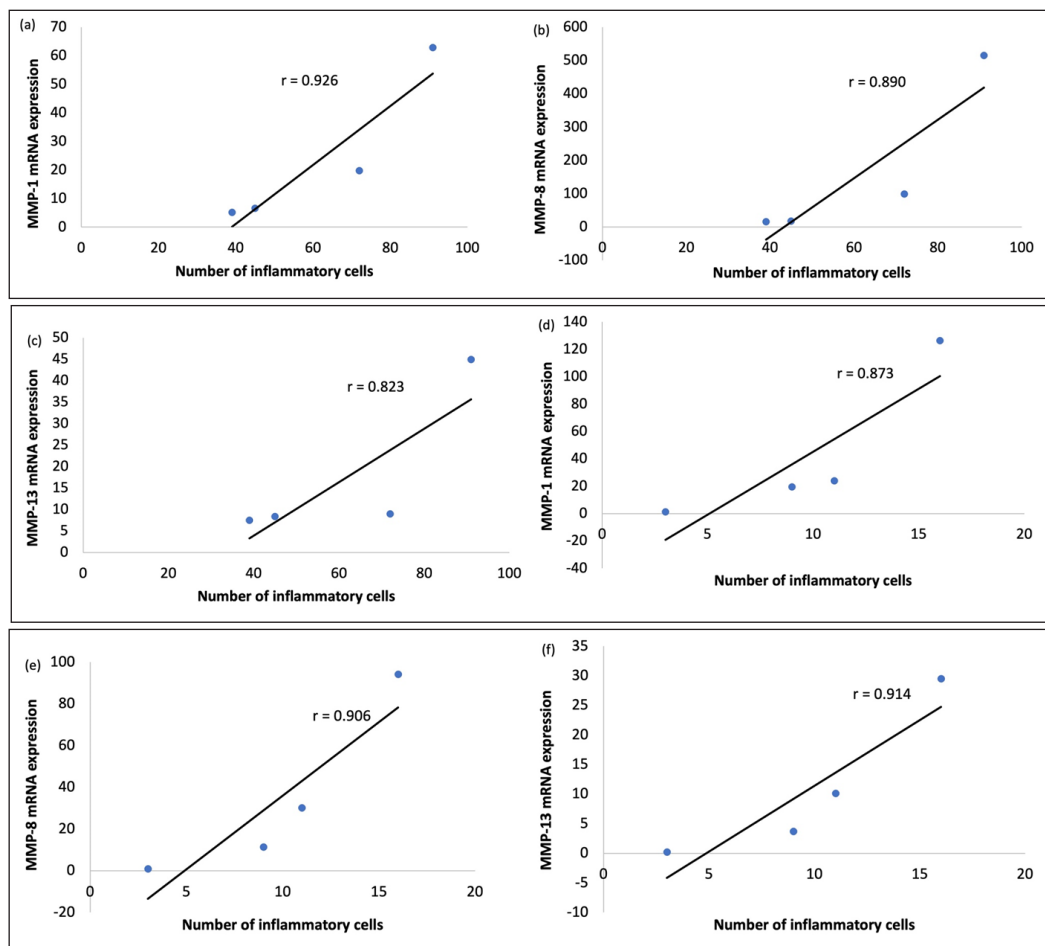


Figure 5. A correlation between collagenase (MMP-1, -8, -13) expression and inflammatory cell count was performed. There was a highly positive correlation of MMP-1, -8, -13 mRNA expression with the number of inflammatory cells at 7 days (a, b, c) and a highly positive correlation of MMP-1, -8, -13 mRNA expression at 14 days with the number of inflammatory cells (d, e, f)

## DISCUSSION

MMP-1, -8, -13 expression is generally low; nonetheless, the enzymes are activated in a variety of physiological conditions when ECM remodelling is necessary. The findings of this study highlight the utility of combining disease mediators, such as MMP-1, -8, and -13, to assess a patient's condition more precisely. Based on varied regulatory mechanisms among distinct MMPs, the current study hypothesised that individual MMPs may play a variety of potentially conflicting functions in oral inflammatory conditions. Their varying temporal expression levels are possible. Hence, utilising an experimentally generated periodontitis animal model, the mRNA expression levels of collagenase were examined at various time points following simultaneous injection with *E. faecalis* and ligature wire infection.

Once the gingival surface has been successfully colonised, bacteria multiply within the host and induce immunological responses in local resident cells and circulating immune cells, producing proinflammatory cytokines, prostaglandins, proteinases, and MMPs. The immune system's cells are generally distributed throughout the body, and when an infection develops, the inflammatory response enables the marshalling of immune system components to certain areas. Early stages of the inflammatory response to an infection are typically not clinically detectable. In the current study, a considerable rise in the body weight of the control group shows the healthy states of the animals. However, the experimental group's weight was increased over their respective induction periods, though it was still lower than the control groups, indicating an inflammatory process within the experimental groups (Choubaya et al., 2019).

The current investigation examined gingiva tissue samples taken from 0-, 7-, and 14-days following wire ligation and concurrent infection with *E. faecalis* inoculation to evaluate the bacterial load of the *E. faecalis* gene using qPCR assay. This study has detected a higher bacterial load of the *E. faecalis* gene in the gingival tissue at 7 days post-induction. However, the bacterial load was lower at 14 days compared to the 7 days groups. The lower Ct value of *E. faecalis* in the 7-day post-induction period suggested that periodontal inflammation may favour the establishment of this organism. According to a study conducted by Chidambar et al. (2019), a significantly higher frequency of *E. faecalis* was detected in the subgingival biofilms of the periodontitis group (41.7%), compared to gingivitis (5.9%) and healthy group (0%) (Chidambar et al., 2019). In the current study, wire ligation acts as a biofilm retentive factor, which helps to accumulate complex microbiota within the periodontal pocket. The complex microbiota, along with the inflammatory process, may produce a variety of nutrients and binding sites for developing this microorganism.

Collagenase is a member of the MMP group, capable of degrading nearly every kind of collagen found within the ECM and contributing to tissue destruction. However, the pattern of MMP-8 and MMP-13 expressions in the periodontium is still under research.

The current study has demonstrated upregulated MMP-1, -8, -13 mRNA expression levels in the gingival tissue at 7- and 14-days post-induction. There were significant differences in MMP-1, -8, and -13 mRNA expression levels in gingival tissue at 7 days post-induction compared to the control group. This study also discovered a substantial positive association between the number of inflammatory cells and the levels of the MMP-1, -8, and -13 genes, which suggests that the presence of inflammatory cells that have migrated to the infection site because of experimentally induced periodontitis regulates the gene expression. MMP-8, also known as neutrophilic collagenase, is mostly secreted by neutrophils. Moreover, a significant elevation of the collagenase levels, particularly for MMP-8, within the gingival tissue indicates that the destruction of the periodontal tissue occurred during the event.

Furthermore, a significant decrease in MMP-8 expression at 14 days suggested a reduction in the inflammatory activity within the periodontium (Yang et al., 2013). This finding is supported by the histological analysis of the periodontium, which showed that the infiltration of inflammatory cells, mostly neutrophils and macrophages, was higher within the tissue at 7 days and was notably reduced at 14 days. Yang et al. (2013) observed a significant decrease in MMP-8 staining on days 5 and 7, which continued from days 11 to 21. A significant decrease in MMP-8 expression was observed on days 5 and 7, and this decrease continued from 11 to 21, which is consistent with our findings. Furthermore, we found that the upregulation of MMP-1, also known as fibroblastic collagenase, steadily decreased at 14 days. Compared to the 7 days, histopathological analysis of the 14-day sample showed that the neutrophils and macrophages were significantly reduced, with fibroblast cells present.

The physiologic remodelling of bones and bone resorption are both regulated by MMP-13. So, it is probable that the presence of osteoclasts during the 7 days caused MMP-13 to be upregulated. Interestingly, we did not see any osteoclasts after 14 days, suggesting that the MMP-13 expression was likely lower than at 7 days. According to previous studies, MMP-13 expression peaked on day 7 and subsequently began to decline from days 11 to 21. This study's results are consistent with previous studies (Yang et al., 2013).

The innate immune system is activated while neutrophil and macrophages are deployed to clear the microbial challenge within the periodontal tissue, significantly elevating these collagenases. More importantly, the current study has observed that all the inflammatory processes started to decrease at 14 days, although it was not significant, except for the MMP-8 expression, which was significantly reduced compared to 7 days. When the *E. faecalis* gene expression was compared to the histological analysis, it was noticed that the bacterial loads were lowered at 14 days post-induction, and histologically, fewer inflammatory cells were observed. It is postulated that the inflammatory process started to decrease due to the development of the host's immune response to resist the microbial challenge. The decreased inflammation severity over time could be attributed to a protective



feature of the periodontal tissue in response to microbial challenges. Previous studies by de Molon et al. (2014) and de Souza et al. (2011) have also reported a reduction in the inflammatory response with time, which agrees with the present study (de Molon et al., 2014; de Souza et al., 2011).

## CONCLUSION

Our results showed that MMP-1, MMP-8, and MMP-13 were expressed at different levels in each sample of periodontitis, along with the accompanying inflammatory cells. The findings imply that the degree of inflammation was correlated with a reduction in MMP-1, -8, and -13 expressions. The study found that identifying the MMP-1, -8, and -13 groups could be beneficial for detecting numerous aspects of periodontitis progression. Knowing the activities of the groupings of biomarkers in periodontitis might play an essential role in the early identification of periodontitis and more effective disease treatment. This study provides significant insight into the severity of periodontal disease based on its biomarker activities. Future research is still required to develop precise diagnostic tools to improve the predictability of diseases in treatment.

## ACKNOWLEDGEMENTS

This work is supported by GP-2021-K021271 from Universiti Kebangsaan Malaysia.

## REFERENCES

- Alghamdi, F., & Shakir, M. (2020). The influence of *Enterococcus Faecalis* as a dental root canal pathogen on endodontic treatment: A systematic review. *Cureus*, *12*(3), e7257. <https://doi.org/10.7759/cureus.7257>
- Beck, J., Philips, K., Moss, K., Sen, S., Morelli, T., Preisser, J., & Pankow, J. (2020). Periodontal disease classifications and incident coronary heart disease in the Atherosclerosis Risk in Communities study. *Journal of Periodontology*, *91*(11), 1409–1418. <https://doi.org/10.1002/JPER.19-0723>
- Checchi, V., Maravic, T., Bellini, P., Generali, L., Consolo, U., Breschi, L., & Mazzoni, A. (2020). The role of matrix metalloproteinases in periodontal disease. *International Journal of Environmental Research and Public Health*, *17*(14), 4923. <https://doi.org/10.3390/ijerph17144923>
- Chidambar, C. K., Shankar, S. M., Raghu, P., Gururaj, S. B., Bushan, K. S. (2019). Detection of *Enterococcus faecalis* in subgingival biofilm of healthy, gingivitis and chronic periodontitis subjects. *Journal of Indian Society of Periodontology*, *23*(5), 416-418. [https://doi.org/10.4103/jisp.jisp\\_44\\_19](https://doi.org/10.4103/jisp.jisp_44_19)
- Choubaya, C., Chahine, R., Zalloua, P., & Salameh, Z. (2019). Periodontitis and diabetes interrelationships in rats: Biochemical and histopathological variables. *Journal of Diabetes and Metabolic Disorders*, *18*, 163-172. <https://doi.org/10.1007/s40200-019-00403-4>
- Davis, J. A. (2001). Mouse and rat anesthesia and analgesia. *Current Protocols in Neuroscience*, *5*(1), A.4B.1-A.4B.7. <https://doi.org/10.1002/0471142301.nsa04bs15>

- de Molon, R. S., de Avila, E. D., Nogueira A. V. B., de Souza, J. A. C., Avila-Campos, M. J., de Andrade, C. R., & Cirelli, J. A. (2014). Evaluation of the host response in various models of induced periodontal disease in mice. *Journal of Periodontology*, *85*(3), 465–477. <https://doi.org/10.1902/jop.2013.130225>
- de Molon, R. S., Mascarenhas, V. I., de Avila, E. D., Finoti, L. S., Toffoli, G. B., Spolidorio, D. M. P., Scarel-Caminaga, R. M., Tetradis, S., & Cirelli, J. A. (2016). Long-term evaluation of oral gavage with periodontopathogens or ligature induction of experimental periodontal disease in mice. *Clinical Oral Investigations*, *20*, 1203–1216. <https://doi.org/10.1007/s00784-015-1607-0>
- de Souza, J. A. C., Nogueira, A. V. B., de Souza, P. P. C., Cirelli, J. A., Garlet, G. P., & Rossa Jr., C. (2011). Expression of suppressor of cytokine signaling 1 and 3 in ligature-induced periodontitis in rats. *Archives of Oral Biology*, *56*(10), 1120–1128. <https://doi.org/10.1016/j.archoralbio.2011.03.022>
- Dom, T. N. M., Ayob, R., Muttalib, K. A., & Aljunid, S. M. (2016). National economic burden associated with management of periodontitis in Malaysia. *International Journal of Dentistry*, *2016*, 1891074. <https://doi.org/10.1155/2016/1891074>
- du Sert, N. P., Hurst, V., Ahluwalia, A., Alam, S., Avey, M. T., Baker, M., Browne, W. J., Clark, A., Cuthill, I. C., Dirnagl, U., Emerson, M., Garner, P., Holgate, S. T., Howells, D. W., Karp, N. A., Lazic, S. E., Lidster, K., MacCallum, C. J., Macleod, M., ... Würbel, H. (2020). The ARRIVE guidelines 2.0: Updated guidelines for reporting animal research. *BMC Veterinary Research*, *16*, 242. <https://doi.org/10.1186/s12917-020-02451-y>
- Hajishengallis, G., & Chavakis, T. (2021). Local and systemic mechanisms linking periodontal disease and inflammatory comorbidities. *Nature Reviews Immunology*, *21*, 426–440. <https://doi.org/10.1038/s41577-020-00488-6>
- Hirate, Y., Yamaguchi, M., & Kasai, K. (2012). Effects of relaxin on relapse and periodontal tissue remodeling after experimental tooth movement in rats. *Connective Tissue Research*, *53*(3), 207–219. <https://doi.org/10.3109/03008207.2011.628060>
- Ilyas, M. N., Adzim, M. K. R., Simbak, N. B., & Atif, A. B. (2017). Sample size calculation for animal studies using degree of freedom (E); An easy and statistically defined approach for metabolomics and genetic research. *Current Trends in Biomedical Engineering and Biosciences*, *10*(2), 555785. <https://doi.org/10.19080/ctbeb.2017.10.555785>
- Jacob, S. (2012). Global prevalence of periodontitis: A literature review. *International Arab Journal of Dentistry*, *3*(1), 6.
- Khuda, F., Anuar, N. N. M., Baharin, B., & Nasruddin, N. S. (2021). A mini review on the associations of matrix metalloproteinases (MMPs) -1, -8, -13 with periodontal disease. *AIMS Molecular Science*, *8*(1), 13–31. <https://doi.org/10.3934/molsci.2021002>
- Kraft-Neumärker, M., Lorenz, K., Koch, R., Hoffmann, T., Mäntylä, P., Sorsa, T., & Netuschil L. (2012). Full-mouth profile of active MMP-8 in periodontitis patients. *Journal of Periodontal Research*, *47*(1), 121–128. <https://doi.org/10.1111/j.1600-0765.2011.01416.x>
- Kuo, P.-J., Fu, E., Lin, C.-Y., Ku, C.-T., Chiang, C.-Y., Fu, M. M., Fu, M.-W., Tu, H.-P., & Chiu, H.-C. (2019). Ameliorative effect of hesperidin on ligation-induced periodontitis in rats. *Journal of Periodontology*, *90*(3), 271–280. <https://doi.org/10.1002/JPER.16-0708>

- Li, D., Feng, Y., Tang, H., Huang, L., Tong, Z., Hu, C., Chen, X., & Tan, J. (2020). A simplified and effective method for generation of experimental murine periodontitis model. *Frontiers in Bioengineering and Biotechnology*, 8, 444. <https://doi.org/10.3389/fbioe.2020.00444>
- Liu, D. (Ed.) (2011). *Molecular detection of human bacterial pathogens* (1<sup>st</sup> ed.). CRC Press. <https://doi.org/10.1201/b10848>
- Livak, K. J., & Schmittgen, T. D. (2001). Analysis of relative gene expression data using real-time quantitative PCR and the  $2^{-\Delta\Delta CT}$  method. *Methods*, 25(4), 402–408. <https://doi.org/10.1006/meth.2001.1262>
- Matsui, H., Yamasaki, M., Nakata, K., Amano, K., & Nakamura, H. (2011). Expression of MMP-8 and MMP-13 in the development of periradicular lesions. *International Endodontic Journal*, 44(8), 739–745. <https://doi.org/10.1111/j.1365-2591.2011.01880.x>
- Pirhan, D., Atilla, G., Emingil, G., Sorsa, T., Tervahartiala, T., & Berdeli, A. (2008). Effect of MMP-1 promoter polymorphisms on GCF MMP-1 levels and outcome of periodontal therapy in patients with severe chronic periodontitis. *Journal of Clinical Periodontology*, 35(10), 862–870. <https://doi.org/10.1111/j.1600-051x.2008.01302.x>
- Preethanath, R. S., Ibraheem, W. I., & Anil, A. (2020). Pathogenesis of gingivitis. In G. Sridharan, A. Sukumaran, & A. E. O. Al Ostwani (Eds.), *Oral diseases*. IntechOpen. <https://doi.org/10.5772/intechopen.91614>
- Ramadan, D. E., Hariyani, N., Indrawati, R., Ridwan, R. D., & Diyatri, I. (2020). Cytokines and chemokines in periodontitis. *European Journal of Dentistry*, 14(3), 483–495. <https://doi.org/10.1055/s-0040-1712718>
- Rathnayake, N., Gieselmann, D.-R., Heikkinen, A. M., Tervahartiala, T., & Sorsa, T. (2017). Salivary diagnostics — Point-of-care diagnostics of MMP-8 in dentistry and medicine. *Diagnostics*, 7(1), 7. <https://doi.org/10.3390/diagnostics7010007>
- Souto, R., de Andrade, A. F. B., Uzeda, M., & Colombo, A. P. V. (2006). Prevalence of “non-oral” pathogenic bacteria in subgingival biofilm of subjects with chronic periodontitis. *Brazilian Journal of Microbiology*, 37, 208–215. <https://doi.org/10.1590/S1517-83822006000300002>
- Yang, D., Wang, J., Ni, J., Shang, S., Liu, L., Xiang, J., & Li, C. (2013). Temporal expression of metalloproteinase-8 and -13 and their relationships with extracellular matrix metalloproteinase inducer in the development of ligature-induced periodontitis in rats. *Journal of Periodontal Research*, 48(4), 411–419. <https://doi.org/10.1111/jre.12019>



# Floristic Composition and Diversity of Plants Across Three Vegetation Zones of Gashaka Gumti National Park, Northeastern Nigeria

Salihu Abba Hammanjoda<sup>1,2</sup>, Rosimah Nulit<sup>1</sup>, Chee Kong Yap<sup>1</sup>, Umaru Buba Nformi<sup>3</sup>, George Nodza<sup>4</sup>, Abdulwakil Olawale Saba<sup>1</sup>, Edward Entalai Besi<sup>1</sup> and Rusea Go<sup>1\*</sup>

<sup>1</sup>Department of Biology, Faculty of Science, Universiti Putra Malaysia, 43400 UPM Serdang, Selangor, Malaysia

<sup>2</sup>Department of Biological Sciences, Faculty of Science, Taraba State University, PMB 1167, Jalingo, Taraba State, Nigeria

<sup>3</sup>Department of Forestry, Faculty of Agriculture, Taraba State University, PMB 1167, Jalingo, Taraba State, Nigeria

<sup>4</sup>Molecular Systematics Laboratory, Department of Botany, University of Lagos, Akoka, Lagos State, Nigeria

## ABSTRACT

Gashaka Gumti National Park (GGNP) is Nigeria's biggest national park, with an elevation range of 300 m to its highest peak at 2400 m. Although GGNP has a wide range of plant species, particularly woody ones, there is limited information regarding its floristic composition along the vegetation zones. This study examined the floristic composition and species diversity of GGNP by systematically sampling plant species using quadrats of 25 m × 25 m and a point-centered quadrat (PCQ). A total of 228 plant species belonging to 114 genera and 49 families were recorded across the three major vegetation zones. Fabaceae was the most species-rich family (34 species), representing 14.9% of the species, followed by Malvaceae (18 species), representing 7.9%.

Other important species include Moraceae and Rubiaceae, 15 species each, representing 6.6% of the species, respectively, while Combretaceae (10 species) represents 4.4% of the species recorded. The Lowland Tropical Rain Forest (LTRF) recorded 137 species in 42 families, and Montane Highland (MH) recorded 146 species in 43 families. In comparison, the Savannah Woodland (SW) recorded 68 species in 28 families. Twenty-five species, which account for 11% of the total, are threatened. Among them, 10 species are Vulnerable, six are Endangered,

## ARTICLE INFO

### Article history:

Received: 20 March 2024

Accepted: 5 July 2024

Published: 28 January 2025

DOI: <https://doi.org/10.47836/pitas.48.1.10>

### E-mail addresses:

salihujoda01@gmail.com (Salihu Abba Hammanjoda)

rosimahn@upm.edu.my (Rosimah Nulit)

yapchee@upm.edu.my (Chee Kong Yap)

bumami2004@yahoo.com (Umaru Buba Nformi)

gnodza@unilag.edu.ng (George Nodza)

saba@upm.edu.my (Abdulwakil Olawale Saba)

edwardentalai@upm.edu.my (Edward Entalai Besi)

rusea@upm.edu.my (Rusea Go)

\*Corresponding author

five are Critically Endangered, and four are Near Threatened, according to the International Union for Conservation of Nature (IUCN) Red List status. Across all plots, average Shannon-Weiner's species diversity indices of 2.40, 2.40, and 2.25 were recorded for MH, LTRF, and SW, respectively. According to Sorensen's similarity coefficient, LTRF and SW (33.42%) habitats recorded the highest species similarity, while MH, as against SW habitats, recorded the lowest (18.92%). The importance value indicated that the SW had the most important species based on the importance value (0.581) compared to other vegetation zones. The overall evenness values for LTRF, SW, and MH are 0.77, 0.78, and 0.77, respectively. This study offers significant insights into the flora variety and conservation situation of Gashaka Gumti National Park. It emphasizes the need for more research and conservation initiatives to save its distinct habitats and endangered species.

*Keywords:* Anthropogenic threats, biological conservation, Fabaceae family, flora diversity, Lowland Tropical Rainforest, montane vegetation, Savanna Woodland

---

## INTRODUCTION

Nigeria boasts a wide variety of vegetation, encompassing nearly all African types (Nodza et al., 2021). This vegetational variety spans geopolitical zones, making it one of the most biodiverse countries in Africa (Ayodele & Yang, 2012). Despite this impressive biodiversity, Nigeria faces several environmental challenges that contribute to the decline of the country's vegetation resources. The most prominent environmental issues include deforestation, desertification, erosion, expansion of agricultural land, overgrazing, unsustainable utilization of biological resources, invasion of exotic species, and overexploitation for various purposes such as firewood, charcoal, construction material, farm implements, and timber (Bello et al., 2019; Borokini et al., 2023; Imarhiagbe et al., 2020; Okon et al., 2021). Ecosystem degradation occurs alarmingly, affecting designated conservation areas (Gumnior & Sommer, 2012). By 2006, almost 90% of Nigeria's rainforests had been cleared, with habitat destruction extending beyond forests, threatening various habitats through urbanization and unsustainable human practices. The widespread disregard for environmental protection and the high poverty rate exacerbates this ecological loss (Ayodele & Yang, 2012).

Nigerian authorities have established several parks, including Gashaka Gumti National Park (GGNP), the largest of Nigeria's eight gazetted national parks, covering 6731 km<sup>2</sup> of landmass to combat biodiversity loss (Sommer & Ross, 2011). Situated in the eastern highlands of Nigeria (Umar et al., 2019), the GGNP has great ecological and cultural importance (Febnteh et al., 2023), featuring diverse vegetation zones, ranging from lowland forests and savanna vegetation to mountains that harbor unique montane vegetation typical of Nigeria (Nodza et al., 2022a). However, the flora of GGNP remains poorly documented, with only a few botanical exploration records reported. For instance, Ezukanma et al. (2017) specifically cataloged the bryophyte species within the eastern highlands, encompassing

areas such as the Gashaka Gumti National Park (GGNP), documenting 27 species. Similarly, Chapman and Chapman (2001) identified no fewer than 24 plant species facing threats within the montane forests of Taraba State. In another study, Nodza et al. (2022a) concentrated solely on orchids, revealing a richness of 80 orchid species across 38 genera within the confines of the GGNP.

Recently, the GGNP has faced severe anthropogenic activities, such as illegal logging, intensive cattle grazing, and artisanal mining (Nodza et al., 2022b). Illegal logging of Rosewood (*Pterocarpus erinaceus*) has been a significant threat due to high demand in China and other Asian countries (Chen et al., 2022; Dumenu, 2019; Kombat & Chen, 2022; Siritwat & Nijman, 2023), a trend observed across tropical Africa (Adjonou et al., 2020; Kossi et al., 2021), including Taraba State (Ahmed et al., 2016), where GGNP is located. Massive logging of various timber species, such as *Afzelia africana*, *Erythrophleum suaveolens*, and *Pseudospondias macrocarpa* has significantly impacted the park. These activities have led to insecurity within the park, making it nearly inaccessible due to kidnapping, armed robbery, and cattle rustling. Herdsmen have encroached on park habitats, looping branches of *A. africana* and other species to feed their cattle in savanna vegetation (Nodza et al., 2022b).

Hence, the need for this study, as floristic studies play a crucial role in providing essential data on species numbers, forest variety, and vegetation types, aiding in forest management and enhancing our understanding of forest ecology and ecosystem functions (Anamo et al., 2023; Hammanjoda et al., 2022; Haq et al., 2023; Negesse & Woldearegay, 2022; Sewale & Mammo, 2022; van Rooyen et al., 2019). The objectives of this study are to identify and classify floristic species in the various vegetation zones of the GGNP and to assess the richness, similarity, and diversity of species in the different vegetation zones of the park.

## MATERIALS AND METHODS

### Study Area

The Gashaka Gumti National Park (GGNP) is the biggest in Nigeria, spanning roughly 6,700 square kilometers. It is situated in the country's northeastern region and is of great importance to national and international conservation efforts. The park extends from the Taraba state (Plateau), running northwards along the boundary with Cameroon and Africa's Gulf of Guinea forests. It continues to Adamawa State, reaching as far as Toungo, known for its high biodiversity (Sommer & Ross, 2011). The region is situated between 06°55' latitude and 08°13' longitude North and between 11°13' latitude and 12°11' longitude East (Figure 1). Pictures showing parts of the vegetation zones sampled in the GGNP are presented in Figure 2.

GGNP, located in Nigeria's Northern state, shares many ecological similarities with southern regions (Sommer & Ross, 2011). The park features extensive mountainous areas, part of the Eastern highlands, with altitudes ranging from 300 m to over 2,400 m above sea level. Chabbal Wadde (the highest mountain in Nigeria) is situated southeast of the park, near the Nigeria-Cameroon boundary (Sommer & Ross, 2011).

Gashaka Gumti is typically found in the Guinea savanna zone, although it stands out from other central habitats because of its lengthy and distinct dry season. It is common to lack rainfall over three months, from December to February. The onset of the rainy season often occurs in March or early April and concludes in mid-November. The park has a variation in annual rainfall, with the northern region receiving around 1200 mm and the southern region receiving over 3000 mm. The mountains facilitate high rainfall by causing the humidity from the Atlantic to rise to higher altitudes, cool down, and condense into clouds that produce rain. It enables the development of lush forests (Dishan et al., 2010; Nodza et al., 2022b).

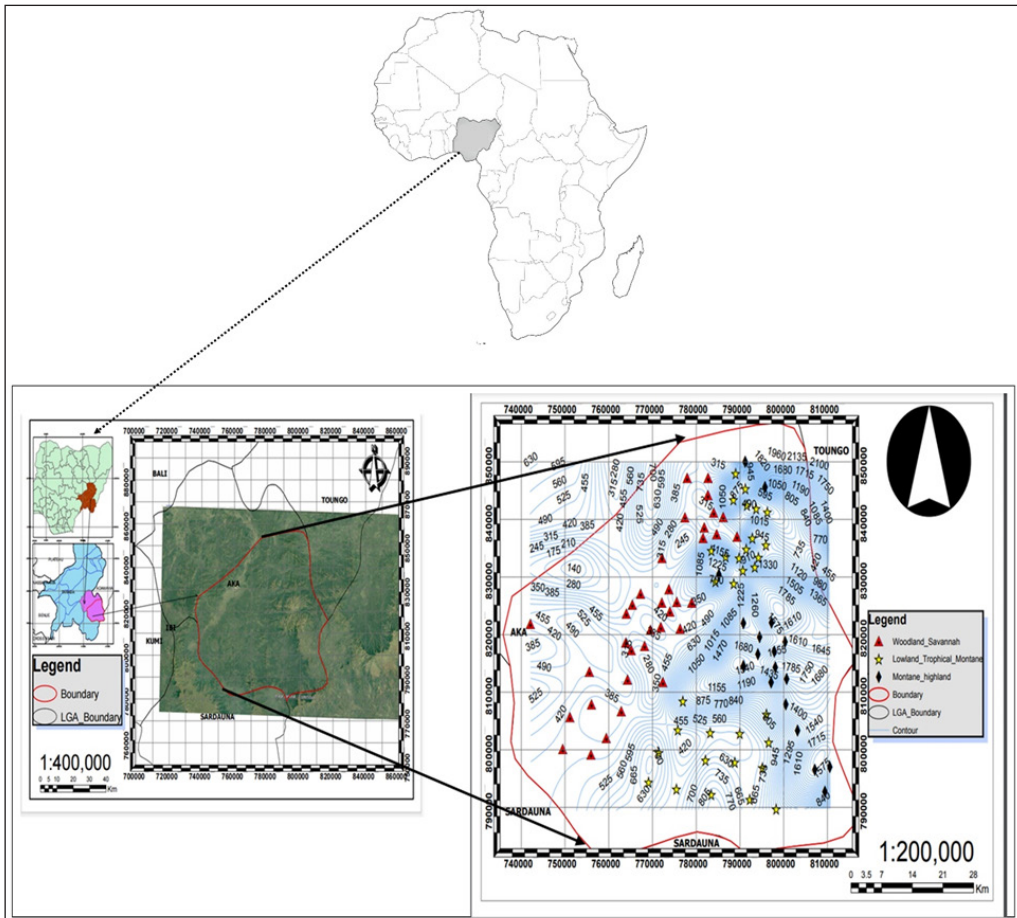
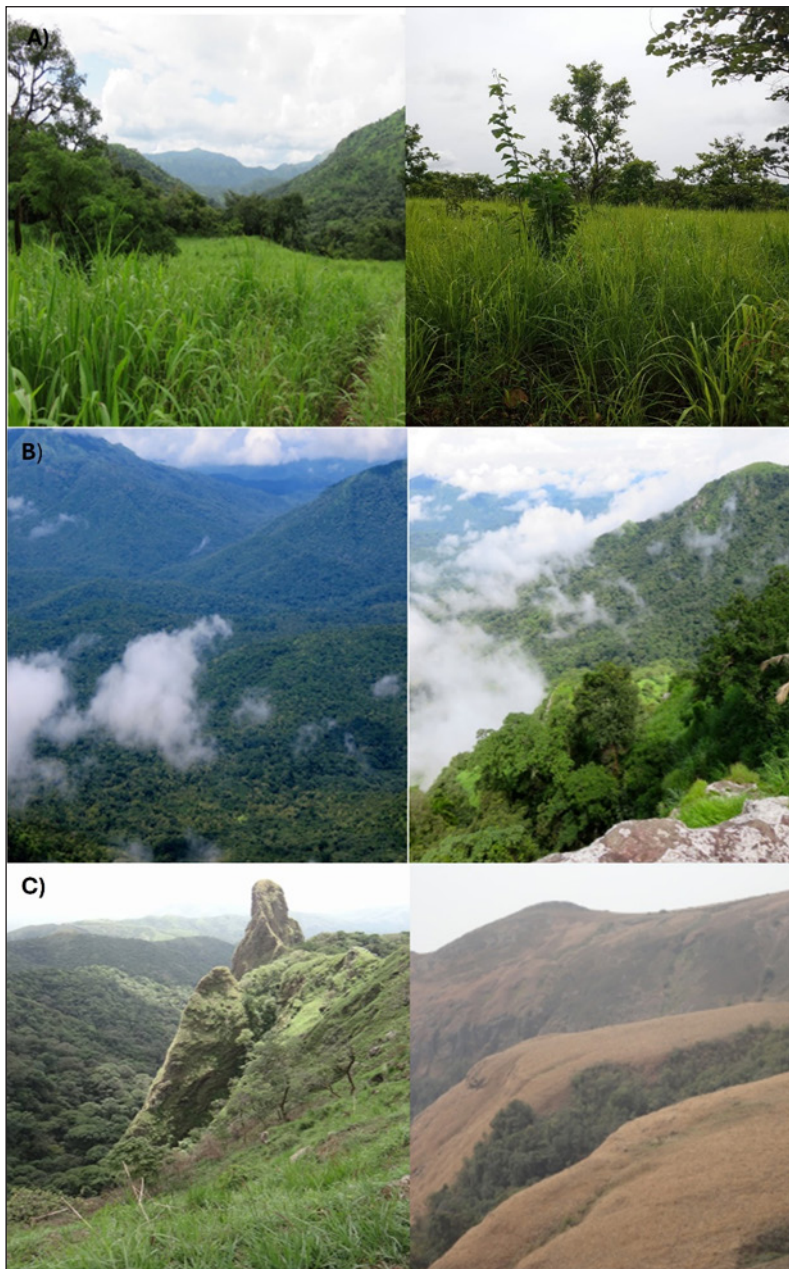


Figure 1. Sampling sites in the three vegetation zones of the Gashaka Gumti National Park





*Figure 2.* Picture showing parts of the sampled vegetation such as A) Savanna woodland, B) Lowland tropical rainforest, and C) Montane highland

The flora has been extensively modified by the cumulative and lasting impacts of fire, farming, and grazing activities (Dishan et al., 2010). Currently, the Park has a total of seven distinct habitat categories. These habitats include lowland gallery forests (specialized

forests along rivers and streams in tropical regions, characterized by unique vegetation and ecological characteristics), montane grassland, riverine or riparian forest, Southern guinea savanna, Northern guinea savanna, montane forest, and derived savanna. The Northern (Gumti) region mostly consists of forests, distinguished by trees with relatively short trunks, wide leaves, and tall grasses (Nodza et al., 2022b). The savanna is home to many often-seen tree species, such as *A. africana*, *Acacia* sp., *Danielia oliverii*, *Khaya senegalensis*, *Vitellera paradoxa*, and *Isoberlinia doka*. The forest in the southern (Gashaka) region is mainly covered by moist Southern Guinea savanna. The dominant tree species in this area include *A. africana*, *Albizia gummifera*, *Symphonia globulifera*, *Aubrevillea kerstingii*, and *Triplochiton schleroxylon*. The montane vegetation in Gangirwal is characterized by elevated montane grassland, while a typical montane forest dominates the valleys. The dominant plant species in this forest are *Loudetia simplex*, *Rhytachne* sp., and *Elionurus argenteus* (Nodza et al., 2022b).

### Sampling Procedure

We conducted a reconnaissance survey of all the different vegetation zones in GGNP starting from March 2023 (dry season). It was finalized in April 2023 (wet season) based on topographic and vegetation maps of the reserve (Sommer & Ross, 2012). The sample collection occurred at the onset of the rainy season, namely from mid-April to September 2023, by an average of nine individuals throughout the sampling period. The recorded data included geographical locations obtained via a Global Positioning System (GPS) device, namely the GARMIN GPS 12®. The latitudes and elevations were measured following the methodology described by Kumar and Moore (2002). We collected data on habitat type, topography, altitude, human activities, physical features of woody species, and land use patterns. The PCQ sampling approach, as described by Blydenstein (1967), was used to sample forest ecosystems characterized by challenging terrains, such as steep escarpments. We systematically sampled plant species using 25 m × 25 m quadrats and a PCQ. During the research period, 150 sample plots were surveyed, 50 in each vegetation zone. The quadrat dimension utilized in this study is a regularly used size for tropical forest sampling (van Rooyen et al., 2019). The number of plant species on each plot was tallied during the fieldwork, and their common names were documented.

### Species Identification and Classification

Specimen identification was conducted in the field by a plant taxonomist. For those specimens that could not be identified in the field, voucher specimens were collected and brought to the Lagos University Herbarium (LUH) for identification by the same expert using taxonomic keys, descriptions, and illustrations, as described by Hutchinson and Dalziel (1927). The final scientific names and authorities were determined using the ‘Plants

of the World Online' (POWO: <https://powo.science.kew.org/>). Plant classification followed species lists in the Angiosperm Phylogeny Group (APG) (APG, 2016). The IUCN red list was used to assess the conservation status of the species (IUCN: <https://www.iucn.org/>).

### Diversity Indices

Shannon-Weiner diversity index, Sorensen's similarity coefficient, important value index, and evenness index were computed. The Shannon-Weiner diversity index was applied based on the following Equation 1:

$$H' = - \sum P_i \ln P_i \quad [1]$$

where  $H'$  = Shannon-Wiener Diversity Index

$P_i = n_i/N$  = number of individuals within species ( $n_i$ ) /total number of individuals ( $N$ ).

$\ln$  = natural logarithm

The evenness index ( $J'$ ) was also calculated as Equation 2:

$$J' = \frac{H'}{\ln(S)} \quad [2]$$

where  $H'$  = Shannon-Wiener Diversity Index

$H' \text{ max} = \ln S$  where  $S$  refers to the number of species.

Sorensen's Similarity Coefficient was determined using the Equation 3:

$$S = \frac{2a}{2a + b + c} \quad [3]$$

where,

$a$  is the number of species shared between the two habitats (or sampling sites).

$b$  is the number of species unique to the first habitat (or sampling site).

$c$  is the number of species unique to the second habitat (or sampling site).

The Importance Value Index of species (IVI) was determined using the Equation 4:

$$IVI = \frac{RF + RD + RDo}{3} \quad [4]$$

where,

$RF$  = Relative Frequency

$RD$  = Relative Density

$RDo$  = Relative Dominance

## RESULTS

### Floristic Composition and Conservation Status

A total of 228 plant species belonging to 114 genera and 49 families were identified from the 150 plots in the study area (Table 1). Fabaceae was the most species-rich family, with 34 species, followed by Malvaceae, with 18 species. Moraceae and Rubiaceae each had 15 species, while Combretaceae had 10 species. (Figure 3). The LTRF recorded 137 species in 42 families, with Fabaceae having the highest frequency (22 species). Malvaceae followed with 12 species, Moraceae (nine species), Apocynaceae (eight species), and Anacardiaceae (seven species) (Figure 4).

The MH recorded 146 species in 43 families, with Fabaceae having the highest frequency of 15 species. Moraceae followed with 11 species, Rubiaceae and Malvaceae recorded nine species each, while Phyllanthaceae, Lamiaceae, and Apocynaceae recorded six species, respectively (Figure 5). The SW recorded 68 species in 28 families, with Fabaceae having the highest number of species (15). Combretaceae followed with six species, Moraceae and Malvaceae, five species each, while Rubiaceae and Phyllanthaceae recorded four species each (Figure 6). Conservation assessment revealed that 25 species (11% of the total) are threatened, with 10 Vulnerable, Six Endangered, Six Critically Endangered, and Four Near Threatened, according to the IUCN Red List status. Trees (T) dominate the landscape, making up 78.5% of the vegetation (Figure 9). It is important to note that many of these trees serve as hosts for epiphytes, including delicate orchids. In addition to trees, other life forms are also present. Shrubs (S) comprise 9.2% of the overall composition, while herbs (H) account for 7.0% of the plant community. Climbers (CL), lianas (L), and small herbs (SH) contribute the remaining percentages such as 2.2%, 2.2%, and 0.4%, respectively (Figure 7).

Table 1

List of floristic species distribution across the three vegetation zones of the Gashaka Gumti National Park

S/N	Family	Species Name	LTRF	MH	SW	CS
1	Acanthaceae	<i>Justicia striata</i> (Klotzsch) Bullock	-	×	-	1
2	Anacardiaceae	<i>Anacardium occidentale</i> L.	×	-	-	2
3		<i>Lannea acida</i> A.Rich.	×	×	×	1
4		<i>Lannea barteri</i> (Oliv.) Engl.	×	×	×	2
5		<i>Lannea nigritana</i> (Scott Elliot) Keay	×	×	-	1
6		<i>Lannea schimperi</i> (Hochst. ex A. Rich.) Engl.	-	×	-	1
7		<i>Mangifera indica</i> L.	×	×	×	3
8		<i>Pseudospondias microcarpa</i> (A.Rich.) Engl.	×	-	-	1
9		<i>Pseudospondias cf microcarpa</i> Engl.	×	-	-	2
10	Annonaceae	<i>Annona senegalensis</i> Pers.	×	×	×	2

Table 1 (continue)

S/N	Family	Species Name	LTRF	MH	SW	CS
11		<i>Isolona deightonii</i> Keay	×	×	-	4
12		<i>Xylopia aethiopica</i> (Dunal) A.Rich.	×	-	-	2
13	Apocynaceae	<i>Alstonia boonei</i> De Wild.	×	-	×	2
14		<i>Calotropis procera</i> (Aiton) W.T.Aiton	×	×	×	2
15		<i>Landolphia owariensis</i> P.Beauv.	×	×	-	1
16		<i>Landolphia togolana</i> (Hallier f.) Pichon	×	-	-	1
17		<i>Rauvolfia vomitoria</i> Wennberg	×	×	-	2
18		<i>Tabernaemontana</i> sp.	×	×	-	2
19		<i>Voacanga africana</i> Stapf	×	×	-	2
20		<i>Voacanga thouarsii</i> Roem. & Schult.	×	×	-	2
21	Aquifoliaceae	<i>Ilex mitis</i> (L.) Radlk.	×	-	×	4
22	Araceae	<i>Anchomanes difformis</i> (Blume) Engl.	-	-	×	2
23	Araliaceae	<i>Polyscias fulva</i> (Hiern) Harms	×	-	×	2
24		<i>Cussonia arborea</i> Hochst. ex A.Rich.	×	×	-	2
25		<i>Cussonia barberi</i> Seem.	×	-	-	NA
26		<i>Schefflera abyssinica</i> (Hochst. ex A.Richa.) Harms	-	×	-	4
27		<i>Schefflera mannii</i> (Hook.f.) Harms	-	×	-	4
28		<i>Strombosia scheffleri</i> Engl.	-	×	-	2
29	Arecaceae	<i>Borassus aethiopum</i> Mart.	×	-	×	2
30		<i>Elaeis guineensis</i> Jacq.	×	-	-	2
31		<i>Phoenix reclinata</i> Jacq.	×	×	-	2
32		<i>Raphia hookeri</i> G.Mann & H.Wendl.	×	×	-	1
33		<i>Raphia mambillensis</i> Otedoh	×	×	-	2
34	Asparagaceae	<i>Drimia coromandeliana</i> (Roxb.) Lekhak & P.B.Yadav	×	×	-	1
35		<i>Drimia indica</i> (Roxb.) Jessop	-	×	-	1
36	Asteraceae	<i>Aspilia africana</i> (Pers.) C. D. Adams	-	×	×	1
37		<i>Bidens pilosa</i> L	-	×	-	1
38		<i>Chromolaena alternifolia</i> Gardner	×	-	-	1
39		<i>Chromolaena</i> DC	×	-	-	1
40		<i>Chromolaena odorata</i> (L.) R.M.King & H.Rob.	×	×	-	1
41		<i>Guizotia abyssinica</i> (L.f.) Cass.	-	×	-	1
42		<i>Vernonia glabra</i> (Steetz) Vatke.	×	×	-	1
43	Bignonaceae	<i>Newbouldia laevis</i> (P. Beauv.) Seem. ex Bureau	×	×	-	2
44		<i>Daniella oliveri</i> Hutch. & Dalziel	×	-	×	NA
45		<i>Kigelia africana</i> (Lam.) Benth.	-	×	-	2
46		<i>Spathodea campanulata</i> P.Beauv.	-	×	-	2
47		<i>Stereospermum acuminatissimum</i> K.Schum.	×	-	-	2
48	Burseraceae	<i>Boswellia dalzielii</i> Hutch.	×	-	×	1

Table 1 (continue)

S/N	Family	Species Name	LTRF	MH	SW	CS
49		<i>Canarium schweinfurthii</i> Engl.	×	×	-	2
50		<i>Canarium vulgare</i> Leenh.	-	×	-	2
51		<i>Santiria trimera</i> (Oliv.) Aubrév.	×	×	-	2
52	Cannabaceae	<i>Celtis gomphophylla</i> Baker	×	-	-	1
53		<i>Trema guineense</i> (Schumach. & Thonn.)	-	×	-	2
54		<i>Trema orientale</i> (L.) Blume	×	×	-	2
55	Caricaceae	<i>Carica papaya</i> L	×	×	×	1
56	Celastraceae	<i>Maytenus elliptica</i> (Lam.) Krug & Urb.	-	×	-	2
57	Chrysobalanaceae	<i>Parinari excelsa</i> Sabine	×	-	-	1
58	Clusiaceae	<i>Garcinia ovalifolia</i> Oliv.	-	×	-	1
59		<i>Garcinia smeathmanii</i> (Planch. & Triana) Oliv.	-	×	-	1
60		<i>Symphonia acuminata</i> Baker	×	-	-	2
61		<i>Symphonia globulifera</i> L.f.	-	×	-	2
62		<i>Symphonia grandifolia</i> Spreng	×	×	-	2
63	Combretaceae	<i>Anogeissus leiocarpa</i> (DC.) Guill. & Perr.	×	-	×	2
64		<i>Combretum micranthum</i> G.Don	×	×	-	1
65		<i>Combretum molle</i> R.Br. ex G.Don	×	×	×	2
66		<i>Combretum nigricans</i> Lepr. ex Guill. & Perr.	-	-	×	2
67		<i>Terminalia catappa</i> L.	-	×	-	2
68		<i>Terminalia glaucescens</i> Planch. ex Benth.	-	-	×	2
69		<i>Terminalia laxiflora</i> Engl.	-	×	-	2
70		<i>Terminalia superba</i> Engl. & Diels	×	-	-	1
71		<i>Strephonema mannii</i> Benth. & Hook.f.	-	×	×	2
72		<i>Terminalia schimperiana</i> Hochst	-	-	×	2
73	Cyatheaceae	<i>Cyathea manniana</i> (Diels) Tardieu	-	×	-	1
74	Dilleniaceae	<i>Tetracera alnifolia</i> Willd.	×	-	-	1
75	Euphorbiaceae	<i>Macaranga barteri</i> Müll.Arg.	×	×	×	2
76		<i>Macaranga occidentalis</i> Mull.Arg.	-	×	-	1
77		<i>Croton macrostachyus</i> Hochst. ex Delile	×	×	-	2
78		<i>Manihot esculenta</i> Crantz	×	×	-	3
79		<i>Jatropha curcas</i> var. <i>rufa</i> McVaugh	-	×	-	2
80	Fabaceae	<i>Acacia albida</i> Delile	×	-	-	1
81		<i>Acacia guianensis</i> (Aubl.) Willd.	×	-	×	NA
82		<i>Acacia nilotica</i> (L.) Willd. ex Delile	×	×	-	2
83		<i>Vachellia sieberiana</i> (DC.) Kyal. & Boatwr.	×	-	×	2
84		<i>Afrormosia laxiflora</i> (Benth. ex Baker) Harms	×	-	×	NA
85		<i>Azelia africana</i> Sm. ex Pers.	-	-	×	2
86		<i>Albizia gummifera</i> (J.F.Gmel.) C.A.Sm.	-	×	-	2
87		<i>Albizia zygia</i> (DC.) J.F.Macbr.	×	×	-	2
88		<i>Anthonotha macrophylla</i> P.Beauv.	×	-	-	2

Table 1 (continue)

S/N	Family	Species Name	LTRF	MH	SW	CS
89		<i>Anthonotha noldeae</i> (Rossbach) Exell & Hille.	×	×	-	1
90		<i>Brachystegia eurycoma</i> Harms	×	-	-	2
91		<i>Acacia seyal</i> f. <i>fistula</i> (Schweinf.) Cufod.	-	-	×	2
92		<i>Burkea africana</i> Hook.	×	-	×	2
93		<i>Chamaecrista mimosoides</i> (L.) Greene	-	×	-	2
94		<i>Dalbergia lactea</i> Vatke	×	×	-	2
95		<i>Detarium macrocarpum</i> Harms	×	×	-	1
96		<i>Entada abyssinica</i> Steud. ex A.Rich.	×	×	-	2
97		<i>Entada africana</i> Guill. & Perr.	-	-	×	2
98		<i>Erythrina abyssinica</i> Lam.	-	×	-	2
99		<i>Erythrina senegalensis</i> DC.	×	-	-	2
100		<i>Isoberlinia doka</i> Craib & Stapf	-	-	×	2
101		<i>Isoberlinia tomentosa</i> (Harms) Craib & Stapf	-	-	×	1
102		<i>Millettia conraui</i> Harms	-	×	-	6
103		<i>Newtonia buchananii</i> (Baker) G.C.C.Gilbert & Boutique	×	×	-	2
104		<i>Entandofragma</i> sp.	-	-	×	NA
105		<i>Papilionoideae</i> DC.	-	×	-	2
106		<i>Parkia bicolor</i> A.Chev.	×	×	-	2
107		<i>Parkia biglobosa</i> (Jacq.) R.Br. ex G.Don	×	-	×	2
108		<i>Piliostigma thonningii</i> (Schumach.) Milne-Redh.	×	-	×	2
109		<i>Prosopis africana</i> (Guill. & Perr.) Taub.	×	-	×	1
110		<i>Pterocarpus erinaceus</i> Poir.	-	×	-	6
111		<i>Tamarindus indica</i> L.	×	-	×	2
112		<i>Vachellia seyal</i> (Delile) P.J.H.Hurter	×	-	×	NA
113		<i>Erythrophleum suaveolens</i> (Guill. & Perr.) Brenan	×	×	-	2
114	Gentianaceae	<i>Anthocleista vogelii</i> Planch.	×	×	×	2
115	Hypericaceae	<i>Harungana madagascariensis</i> Lam. ex Poir.	×	×	-	1
116		<i>Psorospermum aurantiacum</i> Engl.	×	×	-	2
117		<i>Psorospermum febrifugum</i> Spach	-	×	-	1
118		<i>Psorospermum senegalense</i> Spach	-	×	-	1
119	Lamiaceae	<i>Gmelina arborea</i> Roxb. ex Sm.	×	-	×	NA
120		<i>Platostoma africanum</i> P.Beauv.	-	×	-	1
121		<i>Vitex doniana</i> Sweet	×	×	×	2
122		<i>Vitex macrophylla</i> H.J.Lam	-	×	-	3
123		<i>Vitex rotundifolia</i> L.f.	×	×	-	1
124		<i>Tectona grandis</i> L.f.	-	×	×	1
125		<i>Platostoma rotundifolium</i> (Briq.)	-	×	-	NA

Table 1 (continue)

S/N	Family	Species Name	LTRF	MH	SW	CS
126	Lauraceae	<i>Beilschmiedia mannii</i> (Meisn.) Benth. & Hook.f. ex B.D.Jacks.	-	×	-	2
127		<i>Persea americana</i> Mill.	-	×	×	1
128	Malvaceae	<i>Adansonia digitata</i> L.	-	-	×	NA
129		<i>Bombax costatum</i> Pellegr. & Vuillet	×	-	×	2
130		<i>Ceiba pentandra</i> (L.) Gaertn.	×	-	×	2
131		<i>Cola nitida</i> (Vent.) Schott & Endl.	×	×	-	2
132		<i>Cola acuminata</i> (P.Beauv.) Schott & Endl.	×	-	-	2
133		<i>Cola gigantea</i> A.Chev.	×	-	-	2
134		<i>Cola hispida</i> Brenan & Keay	×	-	-	NA
135		<i>Cola millenii</i> K.Schum.	×	×	-	2
136		<i>Cola verticillata</i> (Thonn.) Stapf ex A.Chev.	×	×	-	1
137		<i>Dombeya buettneri</i> K.Schum.	-	×	-	1
138		<i>Dombeya ledermannii</i> Engl.	×	×	-	7
139		<i>Grewia mollis</i> Juss.	×		×	2
140		<i>Pavonia urens</i> Cav.	-	×	-	1
141		<i>Pterospermum acerifolium</i> (L.) Willd.	×	-	-	2
142		<i>Sida acuminata</i> DC.	-	×	-	1
143		<i>Sterculia oblonga</i> Mast.	-	×	-	4
144		<i>Sterculia setigera</i> Delile	-	-	×	2
145		<i>Sterculia tragacantha</i> Lindl.	×	×	-	2
146	Melastomataceae	<i>Melastomastrum afzelii</i> (Hook.f.) A.Fern. & R.Fern.	-	×	-	NA
147	Meliaceae	<i>Azadirachta indica</i> A.Juss.	-	-	×	2
148		<i>Carapa grandiflora</i> Sprague	-	×	-	2
149		<i>Carapa procera</i> DC.	×	×	-	2
150		<i>Entandrophragma angolense</i> (Welw.) C.DC.	×	×	-	5
151		<i>Guarea cedrata</i> (A.Chev.) Pellegr.	-	×	-	5
152		<i>Khaya grandifoliola</i> C.DC.	×	-	-	4
153		<i>Khaya senegalensis</i> (Desr.) A.Juss	×	-	×	4
154		<i>Lovoa trichilioides</i> Harms	×	-	-	2
155		<i>Pseudocedrela kotschyi</i> (Schweinf.) Harms	-	-	×	2
156	Moraceae	<i>Ficus asperifolia</i> Miq.	-	×	-	2
157		<i>Ficus capensis</i> Thunb	×	×	×	2
158		<i>Ficus congesta</i> Roxb	-	-	×	2
159		<i>Ficus exasperata</i> Vahl	×	×	-	2
160		<i>Ficus lutea</i> Vahl	×	×	×	2
161		<i>Ficus sur</i> Forssk.	-	×	-	2
162		<i>Ficus sycomorus</i> L.	×	×	×	2
163		<i>Ficus thonningii</i> Blume	-	×	-	2



Table 1 (continue)

S/N	Family	Species Name	LTRF	MH	SW	CS
164		<i>Ficus todayensis</i> Elmer	×	-	-	2
165		<i>Milicia excelsa</i> (Welw.) C.C.Berg	×	×	-	1
166		<i>Ficus auticulata</i> Lour.	×	-	×	NA
167		<i>Ficus</i> sp.	-	×	-	NA
168		<i>Trilepisium gymnandrum</i> (Baker) J.Gerlach	×	-	-	7
169		<i>Trilepisium madagascariense</i> DC.	-	×	-	2
170		<i>Uapaca albida</i> De Wild.	×	×	-	2
171	Moringaceae	<i>Moringa oleifera</i> Lam.	×	×	×	2
172	Urticaceae	<i>Musanga cecropioides</i> R.Br. ex Tedlie	×	×	-	2
173	Myrtaceae	<i>Psidium guajava</i> L.	×	×	×	2
174		<i>Syzygium guineense</i> (Willd.) DC.	×	×	-	2
175		<i>Syzygium macrocarpum</i> (Blume) Bahadur & R.C.Gaur	×	×	-	6
176		<i>Eugenia gilgii</i> Engl. & Brehmer.	×	×	-	6
177	Ochnaceae	<i>Lophira alata</i> Banks ex C.F.Gaertn.	×	-	×	4
178		<i>Lophira lanceolata</i> Tiegh. ex Keay	×	-	-	2
179	Oleaceae	<i>Strombosia grandifolia</i> Hook.f. ex Benth.	×	×	-	2
180	Pandanaceae	<i>Pandanus candelabrum</i> P.Beauv	×	×	×	2
181		<i>Pandanus panayensis</i> Merr.	×	-	-	6
182	Phyllanthaceae	<i>Antidesma laciniatum</i> Müll.Arg.	-	×	-	2
183		<i>Antidesma venosum</i> E.Mey. ex Tul.	-	×	-	2
184		<i>Bridelia ferruginea</i> Benth.	×	-	×	2
185		<i>Bridelia micrantha</i> (Hocks) Bail	-	×	-	2
186		<i>Bridelia speciosa</i> Müll.Arg.	×	×	×	1
187		<i>Hymenocardia acida</i> Tul.	×	×	×	2
188		<i>Phyllanthus niruri</i> L.	-	×	-	2
189		<i>Uapaca togoensis</i> Pax	×	-	×	2
190	Primulaceae	<i>Maesa lanceolata</i> Forssk.	-	×	-	2
191	Proteaceae	<i>Protea madiensis</i> Oliv.	-	×	-	2
192	Ranunculaceae	<i>Clematis grandiflora</i> DC	-	×	-	2
193		<i>Clematis hirsutissima</i> Pursh	-	×	-	1
194	Rosaceae	<i>Prunus africana</i> (Hook.f.) Kalkman	×	-	-	4
195		<i>Rubus fellatae</i> A.Chev.	-	×	-	2
196	Rubiaceae	<i>Rytigynia senegalensis</i> Blume	-	×	-	2
197		<i>Canthium</i> sp.	-	×	-	NA
198		<i>Coffea ambongensis</i> J.-F.Leroy ex A.P.Davis & Rakotonas.	×	-	-	6
199		<i>Crossopteryx febrifuga</i> (Afzel. ex G.Don) Benth.	-	-	×	2
200		<i>Gardenia aqualla</i> Stapf & Hutch.	-	-	×	7

Table 1 (continue)

S/N	Family	Species Name	LTRF	MH	SW	CS
201		<i>Nauclea latifolia</i> Sm.	-	-	×	2
202		<i>Oxyanthus racemosus</i> (Schumach. & Thonn.) Keay	×	-	-	2
203		<i>Oxyanthus speciosus</i> DC.	×	×	×	2
204		<i>Psychotria lanata</i> Müll.Arg.	-	×	-	NA
205		<i>Psychotria pedunculata</i> Sw.	-	×	-	5
206		<i>Psychotria succulenta</i> (Hiern) E.M.A.Petit	-	×	-	2
207		<i>Rothmannia annae</i> (E.P.Wright) Keay	-	×	-	7
208		<i>Rothmannia buchananii</i> (Oliv.) Fagerl.	-	×	-	2
209		<i>Rothmannia octomera</i> (Hook.) Fagerl.	×	-	-	2
210		<i>Rothmannia urcelliformis</i> (Hiern) Bullock ex Robyns	-	×	-	2
211	Rutaceae	<i>Clausena anisata</i> (Willd.) Hook.f. ex Benth.	×	×	-	2
212		<i>Zanthoxylum lepieurii</i> Guill. & Perr.	×	-	-	2
213	Sapindaceae	<i>Allophylus africanus</i> P.Beauv.	×	×	×	2
214		<i>Deinbollia pinnata</i> (Poir.) Schumach. & Thonn.	-	×	-	2
215		<i>Paullinia paullinioides</i> Radlk	-	×	-	2
216		<i>Paullinia pinnata</i> L.	-	×	-	1
217	Sapotaceae	<i>Aningeria altissima</i> (A.Chev.) Aubrév. & Pellegr.apo	×	×	-	2
218		<i>Faurea rochetiana</i> (A.Rich.) Chiov. ex Pic. Serm.	-	×	-	2
219		<i>Pouteria altissima</i> (A.Chev.) Baehni	×	-	-	1
220		<i>Pouteria macrophylla</i> (Lam.) Eyma.	-	×	-	2
221		<i>Strephenomina mannii</i> Benth. & Hook.f.	×	-	-	NA
222		<i>Vitellaria paradoxa</i> C.F.Gaertn.	×	-	×	4
223	Smilacaceae	<i>Smilax anceps</i> L.	×	-	-	2
224	Stilbaceae	<i>Nuxia congesta</i> R.Br. ex Fresen.	×	×	-	2
225	Thymelaeaceae	<i>Aquilaria crassna</i> Pierre ex Lecomte	×	-	-	7
226	Vitaceae	<i>Leea guineensis</i> G.Don	×	×	-	1
227		<i>Cissus purpurea</i> Roxb. ex Steud.	-	×	-	1
228	Zingiberaceae	<i>Aframomum angustifolium</i> (Sonn.)	-	×	-	2

Note. × = Presence of species, Dash (-) = Absence, CS = IUCN Conservation Status, LTRF = Lowland Tropical Rainforest, MH = Montane Highland, SW = Savanna Woodland, NE (Not Evaluated) = 1, LC (Least Concern) = 2, DD (Data Deficient) = 3, VU (Vulnerable) = 4, NT (Near Threatened) = 5, EN (Endangered) = 6, CR (Critically Endangered) = 7

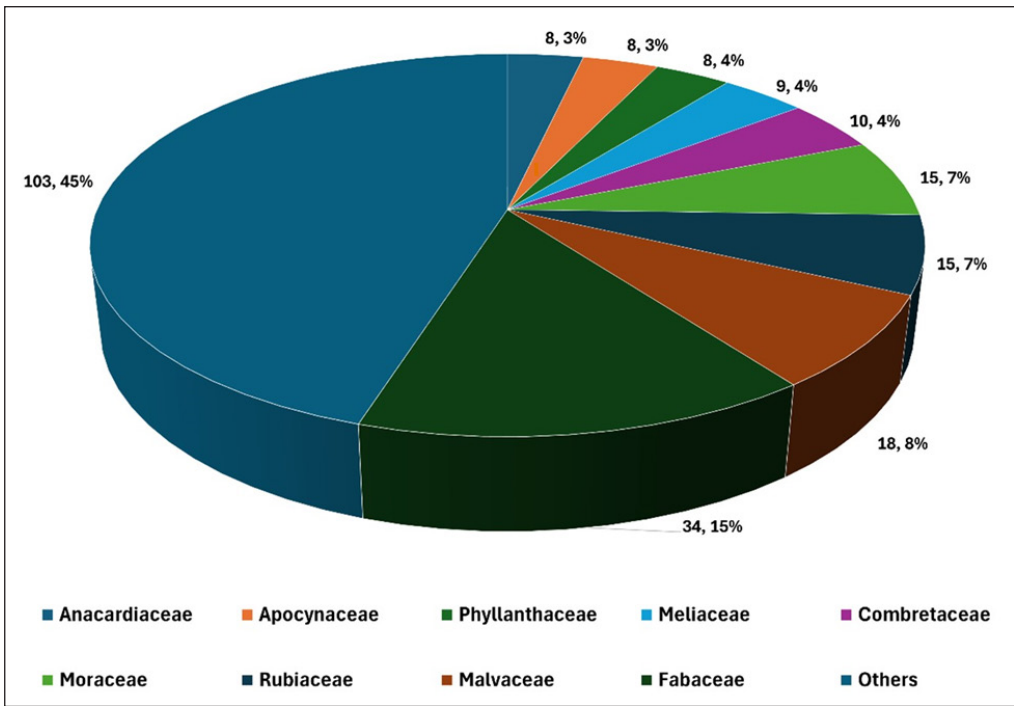


Figure 3. Frequency and percentage frequency of sampled plants by family from the three vegetation zones

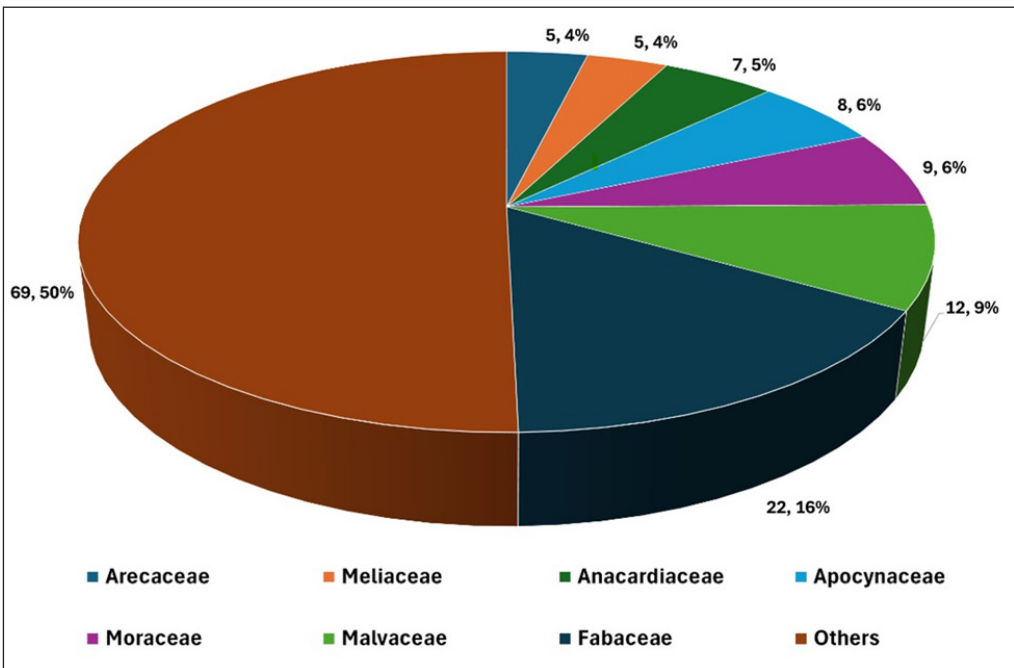


Figure 4. Frequency and percentage frequency of sampled plants by family from the Lowland Tropical Rainforest

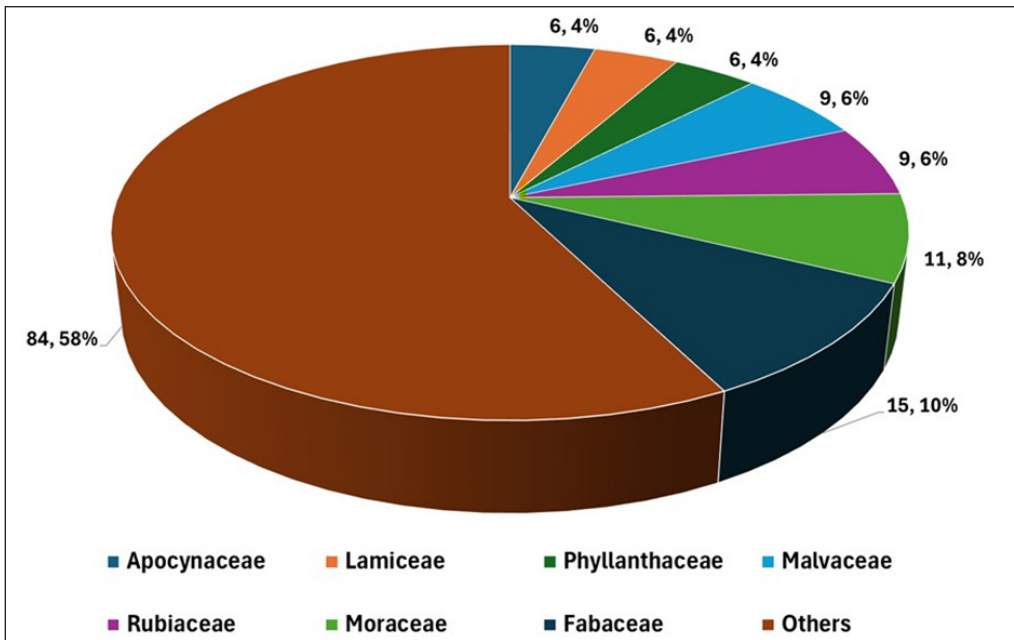


Figure 5. Frequency and percentage frequency of sampled plants by family from the Montane Highlands

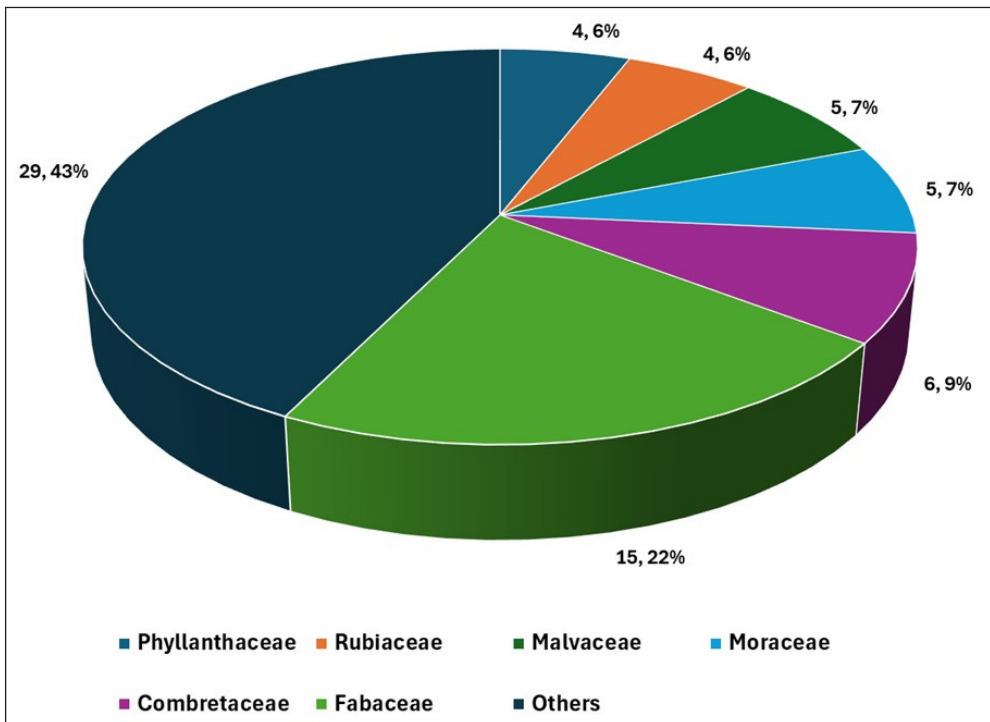


Figure 6. Frequency and percentage frequency of sampled plants by family from the Savannah Woodland

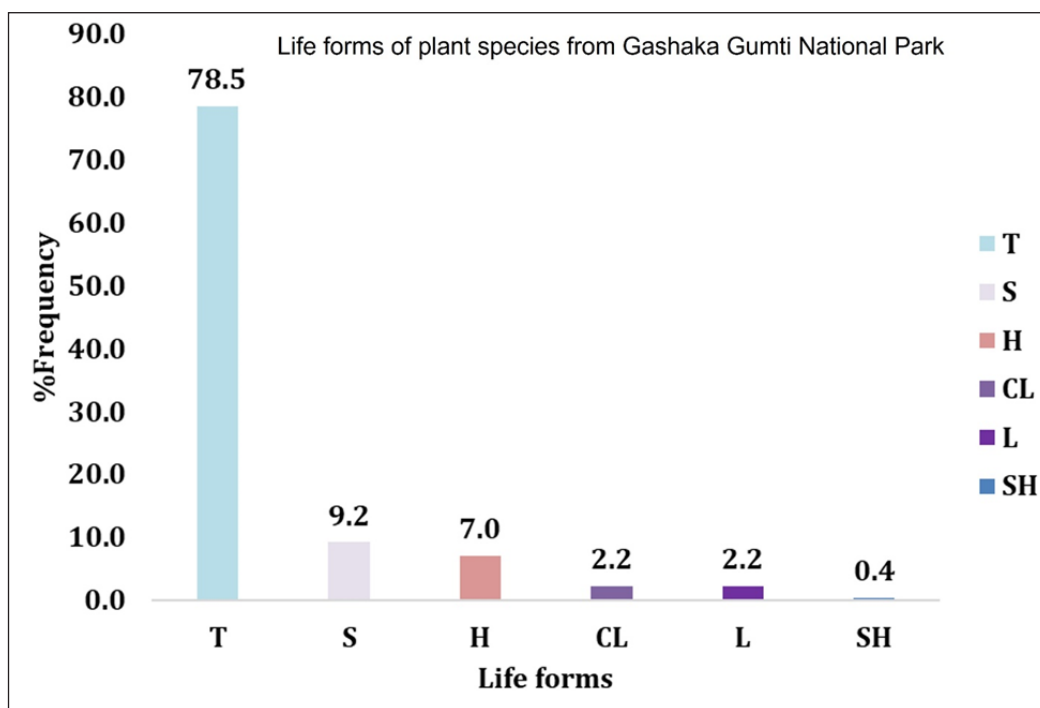


Figure 7. Summary of the life forms of the species in the study area

Note. T = Trees, S = Shrubs, H = Herbs, CL = Climbers, L = Lianas, SH = Small herbs

### Diversity Indices

Across all plots, average Shannon-Weiner's species diversity indices of 2.40, 2.40, and 2.25 were recorded for MH, LTRF, and SW, respectively. It shows that LTRF has the highest species diversity, while MH has the lowest (Supplementary File 1).

Supplementary File 2 shows the plot-by-plot richness of species across the three habitats. According to Sorensen's similarity coefficient, LTRF and SW (33.42%) habitat recorded the highest species similarity, while MH, as against SW habitat, recorded the lowest (18.92%) (Figure 8). Based on the Importance Value (IVI), the most significant species within the habitat documented from the SW. with a value of 0.581, followed by lowland with a value of 0.548, while montane has the least important species across the three habitats with a value of 0.272. The Species evenness per plot across the three vegetation zones is shown in Supplementary File 3. The overall evenness values for LTRF, SW, and MH are 0.77, 0.78, and 0.77. Figure 9 shows the number of species shared across the three vegetation zones.

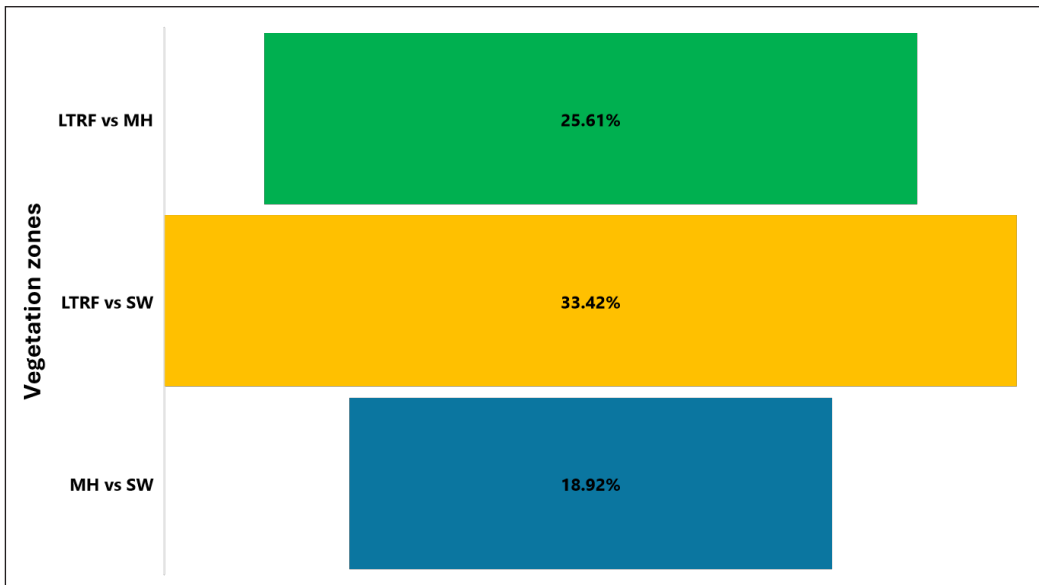


Figure 8. Sorensen's similarity coefficient of floristic species for the three different vegetation zones in the Gashaka Gumti National Park

Note. MH = Montane Highlands, SW = Savannah Woodland, LTRF = Lowland Tropical Rain Forest

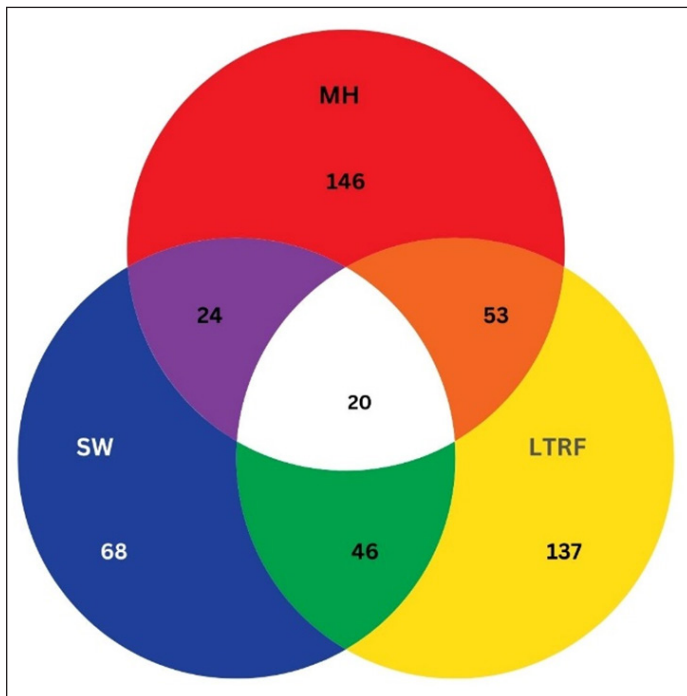


Figure 9. Venn diagram showing the species distribution from the three vegetation zones

Note. MH = Montane Highlands, SW = Savannah Woodlands, LTRF = Lowland Tropical Rain Forest

## DISCUSSION

This study presents an updated checklist and explores the flora diversity across three distinct vegetation zones within Gashaka Gumti National Park (GGNP). The recorded total of 228 species surpasses the previous report of 77 species by Chapman & Chapman (2002), indicating a significant augmentation in species richness. The frequency of families and species reported in this study is also higher than that reported by Abiem et al. (2018), who reported 134 species from 44 families for a forest reserve in Jos, Nigeria, and the study of Mato et al. (2024) who reported 38 species in 19 families for the biological garden of the Nigerian Defence Academy. One possible explanation for this is the vastness of the GGNP, the largest national park in Nigeria, and Abiem et al. (2018) focused only on the woody species. Throughout the vegetation zones, the family Fabaceae was the most notable. This aligns with the findings of Abba et al. (2022) and Mato et al. (2024), who also reported that the Fabaceae family was the dominant plant family in their study areas.

Compared to previous reports, the high number of threatened species underscores the urgency for enhanced conservation efforts within the park. Our findings highlight only a slight disparity in plant species diversity and evenness across different regions, with the MH and LTRF vegetation strata exhibiting the highest species diversity. Therefore, the three zones can be said to possess similarly high species diversity and evenness. Despite the closeness of these two habitats in richness, evenness, and diversity, they recorded a lower similarity compared to the LTRF as against SW. Moreover, SW recorded the highest importance, indicating that it harbors the most important species. The Shannon-Weiner diversity index provided in this research is comparatively lower than the findings of Abiem et al. (2018). The possible reason for this variance might be attributed to the fact that our study area includes three distinct vegetation zones, in contrast to their previous research, which concentrated only on woodlands. Additionally, variations in the methods used to collect samples and the number of samples taken in each study could contribute to the differences in diversity index values.

Factors such as altitude, seedling regeneration, and seed quality may have contributed to the differences in species diversity. Naidu and Kumar (2016) emphasized the significance of biotic factors in maintaining tree diversity. Another possibility is that the montane habitat's varied terrain, natural forests, and limited human disturbances create favorable conditions for a diverse range of plant species. The savanna woodland displayed lower species diversity, which could be attributed to heightened anthropogenic activities such as land clearing for agriculture, logging, and bush burning, leading to habitat loss, biodiversity decline, and ecosystem degradation (Skarpe & Hester, 2008). Habitats with high-importance values support specialized species but do not significantly increase species diversity. These species sometimes serve as keystone species in ecosystems, maintaining habitat health and function (Narango et al., 2020).

Human settlements and associated activities further exacerbate habitat fragmentation and introduce invasive species, negatively impacting plant diversity. Bush-burning Fires can strip away vegetation and expose soil to erosion, leading to sedimentation of water bodies and reduced soil fertility (Birhanu et al., 2019). Conservation strategies must prioritize mitigating these anthropogenic impacts to safeguard the health of this ecosystem. Human settlements can fragment natural habitats and introduce invasive species that can compete with indigenous species in harnessing available resources (Tadele et al., 2014). More so, uncontrolled or excessive grazing can lead to the removal of too much vegetation through consumption and trampling saplings, seeds, and seedlings, causing soil erosion, reduction in soil fertility, and degrading pastures and ecosystems (Gebeyehu et al., 2019; Sartorello et al., 2020).

This study highlights the crucial significance of comprehending the intricate interaction between human activities and environmental elements in determining the patterns of plant diversity. This knowledge may guide conservation and management initiatives to protect these areas with high biodiversity. Similarly, the practice of selective cutting leads to a shortage of seed sources and the opening of the canopy, which exposes the surface to high temperatures, light, and evaporative transpiration. These factors limit plant regeneration and promote certain species' development. In addition, variables such as elevated temperatures, fluctuations in weather patterns, decreased vegetation coverage, and restricted water availability may have a role in the reported decrease in plant variety in these ecosystems (Kelly & Goulden, 2008). In their study, Hejda et al. (2009) found a significant reduction of almost 90% in the number of species in the buffer zones of some protected areas due to anthropogenic disturbances. Conservation efforts should prioritize the mitigation of these consequences to preserve the environment's biodiversity.

## CONCLUSION

This research provides valuable insights into the flora diversity and conservation condition of Gashaka Gumti National Park (GGNP), emphasizing its importance as the biggest park in Nigeria. The cataloging of 228 plant species across three vegetation zones highlights the substantial botanical diversity found within GGNP. The results of our study indicate differences in the variation of species and diversity measures seen in various environments, highlighting the crucial role of habitat heterogeneity in influencing the organization of plant communities. Moreover, recognizing endangered species highlights the immediate need for aggressive conservation efforts to protect the park's biodiversity. The significant resemblance in species composition between the LTRF and SW habitats and the prevalence of certain plant families, such as Fabaceae, offers an essential understanding of the ecological processes in GGNP. Nevertheless, the dearth of research on the park's botanical diversity emphasizes the need for ongoing scientific investigation and conservation initiatives to address risks and save its unique ecosystems and endangered organisms.



## ACKNOWLEDGEMENTS

We appreciate the Nigerian National Parks Service approving this study with the NPH/GEN/121/XXXII/681 approval number. The authors also appreciate the entire management and staff of the Gashaka Gumti National Park, the African Nature Investors (ANI), Mr. Sabastine Nubuyag, Mr. Elisha Emmanuel, Mr. Markson, Mr. Abdulwasiyu, and Mr. Sule Zarto, for their support during data collection for this study. The corresponding author provided the funds to publish this paper through KRIBB-UPM grant no. 6384300.

## REFERENCES

- Abba, H. M., Yuguda, U. A., Yila, C. N., & Zhigila, A. D. (2022). Woody species composition and diversity of Wawa-Zange Forest, Gombe State, Nigeria. *Asian Journal of Plant Biology*, 4(1), 30-35. <https://doi.org/10.54987/ajpb.v4i1.701>
- Abiem, I., Saha, S., Manu, S. A., & Elisha, E. B. (2018). Woody vegetation composition and diversity in woodlands inside and outside a forest reserve in Jos, Nigeria. *African Journal of Ecology*, 56(2), 202-207. <https://doi.org/10.1111/aje.12433>
- Adjonou, K., Abotsi, K. E., Segla, K. N., Rabiou, H., Houetcheignon, T., Sourou, K. N. B., Johnson, B. N., Ouinsavi, C. A. I. N., Kokutse, A. D., Mahamane, A., & Kokou, K. (2020). Vulnerability of African rosewood (*Pterocarpus erinaceus*, Fabaceae) natural stands to climate change and implications for silviculture in West Africa. *Heliyon*, 6(6), e04031. <https://doi.org/10.1016/j.heliyon.2020.e04031>
- Ahmed, Y., Oruonye, E., & Ayuba, H. (2016). Socio-economic impact of commercial production of rosewood (*P. erinaceus*) in Taraba State, Nigeria. *Journal of Agriculture and Ecology Research International*, 7(3), 1–9. <https://doi.org/10.9734/jaeri/2016/25151>
- Anamo, A., Mammo, S., & Temesgen, M. (2023). Floristic composition and community analysis of woody species in Hereje Natural Forest, southwest Ethiopia. *SN Applied Sciences*, 5(1), 48. <https://doi.org/10.1007/s42452-022-05265-9>
- The Angiosperm Phylogeny Group, Chase, M. W., Christenhusz, M. J. M., Fay, M. F. Byng, J. W., Judd, W. S., Soltis, D. E. Mabberley, D. J. Sennikov, A. N., Soltis, P. S., & Stevens, P. F. (2016). An update of the Angiosperm Phylogeny Group classification for the orders and families of flowering plants: APG IV. *Botanical Journal of the Linnean Society*, 181(1), 1–20. <https://doi.org/10.1111/boj.12385>
- Ayodele, A. E., & Yang, Y. (2012). *Diversity and distribution of vascular plants in Nigeria*. Qingdao Publishing House.
- Bello, A., Jamaladdeen, S., Elder, M. T., Yaradua, S. S., Kankara, S. S., Wagini, N. H., Stirton, C. H., & Muasya, M. (2019). Threatened medicinal and economic plants of the Sudan Savanna in Katsina State, northwestern Nigeria. *Bothalia*, 49(1), 1-17. <https://doi.org/10.4102/abc.v49i1.2325>
- Birhanu, B. Z., Traoré, K., Gumma, M. K., Badolo, F., Tabo, R., & Whitbread, A. M. (2019). A watershed approach to managing rainfed agriculture in the semiarid region of southern Mali: Integrated research on water and land use. *Environment, Development and Sustainability*, 21, 2459-2485. <http://doi.org/10.1007/s10668-018-0144-9>

- Blydenstein, J. (1967). *Tropical savanna vegetation of the Llanos of Colombia*. The University of Arizona Press. <https://doi.org/10.2307/1933412>
- Borokini, I. T., Kortz, A., Anibaba, Q. A., Witt, A., Aigbokhan, E. I., Hejda, M., & Pyšek, P. (2023). Alien flora of Nigeria: Taxonomy, biogeography, habitats, and ecological impacts. *Biological Invasions*, 25(12), 3677-3696. <https://doi.org/10.1007/s10530-023-03140-1>
- Chapman, H. M., Olson, S. M., & Trumm, D. (2004). An assessment of changes in the montane forests of Taraba State, Nigeria, over the past 30 years. *Oryx*, 38(03). <https://doi.org/10.1017/s0030605304000511><https://doi.org/10.2307/4110842>
- Chapman, J. D., & Chapman, H. M. (2001). The forests of Taraba and Adamawa States, Nigeria. An ecological account and plant species checklist. *Kew Bulletin*, 57(1), 239-240. <https://doi.org/10.2307/4110842>
- Chen, B., Yeboah, F. K., Abdullahi, B. N., & Paa-Kwesi, C. C. (2022). Macroeconomic determinants of forest trade between China and ECOWAS member states: Income disparity approach. *Open Access Library Journal*, 9(5), 1-19. <https://doi.org/10.4236/oalib.1108794>
- Dishan, E. E., Agishi, R., & Akosim, C. (2010). Women's involvement in non-timber forest products utilization in support zones of Gashaka Gumti National Park. *Journal of Research in Forestry, Wildlife and Environment*, 2(1), 73-84.
- Dumenu, W. K. (2019). Assessing the impact of felling/export ban and cites designation on exploitation of African rosewood (*Pterocarpus erinaceus*). *Biological Conservation*, 236, 124–133. <https://doi.org/10.1016/j.biocon.2019.05.044>
- Ezukanma, I. O., Ogundipe, O. T., Nodza, G. I., & Pócs, T. (2017). Bryophyte records from the eastern Nigerian highlands. *Polish Botanical Journal*, 62(2), 203-212. <https://doi.org/10.1515/pbj-2017-0030>
- Fazan, L., Song, Y. G., & Kozłowski, G. (2020). The woody planet: From past triumph to manmade decline. *Plants*, 9(11), 1593. <https://doi.org/10.3390/plants9111593>
- Febnteh, E. B., Jatau, D. F., & Schombi, S. O. (2023). Assessment of the economic benefits of conservation activities at Kwano chimpanzee forest habitat in Gashaka Gumti National Park (GGNP), Nigeria. *Asian Journal of Research in Agriculture and Forestry*, 9(3), 189-199. <https://doi.org/10.9734/ajraf/2023/v9i3223>
- Gebeyehu, G., Soromessa, T., Bekele, T., & Teketay, D. (2019). Species composition, stand structure, and regeneration status of tree species in dry afro-montane forests of Awi Zone, northwestern Ethiopia. *Ecosystem Health and Sustainability*, 5(1), 199-215. <https://doi.org/10.1080/20964129.2019.1664938>
- Gumnior, M., & Sommer, V. (2012). Multi-scale, multi-temporal vegetation mapping and assessment of ecosystem degradation at Gashaka Gumti National Park (Nigeria). *Research Journal of Environmental and Earth Sciences*, 4(4), 397-412.
- Hammanjoda, S. A., Barau, B. W., Buba, U., Usman, D. D., Fauziya, K. M., & Maikeri, T. C. (2022). Diversity and population status of tree species in Bakin-Dutse of Ardo-Kola LGA, Taraba State, Nigeria. *Nigerian Journal of Environmental Sciences and Technology*, 6(2), 379–390. <https://doi.org/10.36263/nijest.2022.02.0383>
- Haq, S. M., Amjad, M. S., Waheed, M., Bussmann, R. W., & Proćkó, J. (2022). The floristic quality assessment index as ecological health indicator for forest vegetation: A case study from Zabarwan Mountain Range, Himalayas. *Ecological Indicators*, 145, 109670. <https://doi.org/10.1016/j.ecolind.2022.109670>

- Haq, S. M., Khoja, A. A., Lone, F. A., Waheed, M., Bussmann, R. W., Mahmoud, E. A., & Elansary, H. O. (2023). Floristic composition, life history traits and phylogeographic distribution of forest vegetation in the Western Himalaya. *Frontiers in Forests and Global Change*, 6, 1169085. <https://doi.org/10.3389/ffgc.2023.1169085>
- Hejda, M., Pyšek, P., & Jarošík, V. (2009). Impact of invasive plants on the species richness, diversity and composition of invaded communities. *Journal of Ecology*, 97(3), 393–403. <https://doi.org/10.1111/j.1365-2745.2009.01480.x>
- Hutchinson, J., & Dalziel J. M. (1927). *Flora of West Tropical Africa*. Crown Agents. [https://www.abebooks.com/servlet/BookDetailsPL?bi=30627038313&ref\\_o\\_3\\_ac](https://www.abebooks.com/servlet/BookDetailsPL?bi=30627038313&ref_o_3_ac)
- Imarhiagbe, O., Egbotuku, W. O., & Nwankwo, B. J. (2020). A review of the biodiversity conservation status of Nigeria. *Journal of Wildlife and Biodiversity*, 4(1), 73–83. <https://doi.org/10.22120/jwb.2019.115501.1096>
- Kelly, A. E., & Goulden, M. L. (2008). Rapid shifts in plant distribution with recent climate change. *Proceedings of the national academy of sciences*, 105(33), 11823–11826. <https://doi.org/10.1073/pnas.0802891105>
- Kombat, G. P., & Chen, X. (2022). The study of impact factors on timber trade between Ghana and China. *Forestry Economics Review*, 4(2), 78–98. <https://doi.org/10.1108/fer-01-2022-0002>
- Kossi, A., Towanou, H., Habou, R., Novinyo, S. K., Elikplim, A. K., Nathalie, J. B., Pyoabalo, A., Nougbodé, O. C. A., Marie-Luce, Q. A., Dzifa, K. A., Ali, M., & Kouami, K. (2021). Challenges of conservation and sustainable management of African rosewood (*Pterocarpus erinaceus*) in West Africa. In E. R. Rhodes & H. Nasser (Eds.), *Natural resources management and biological sciences* (pp. 386). IntechOpen. <https://doi.org/10.5772/intechopen.88796>
- Kumar, S., & Moore, K. B. (2002). The evolution of global positioning system (GPS) technology. *Journal of Science Education and Technology*, 11(1), 59–80. <https://doi.org/10.1023/a:1013999415003>
- Mato, I. B., Ajibade, G. A., Madu, A. H., Suleiman, M. Z., & Imam, I. U. (2024) Diversity and conservation status of tree species in the Nigerian defense academy biological garden. *World Scientific Journal*, 190(2), 200-215.
- Mubi, A., & Tukur, A. (2012). Species density and diversity along geomorphic gradient in Gashaka-Gumti National Park (GGNP), Nigeria. *Ethiopian Journal of Environmental Studies and Management*, 5(4), 513-520. <https://doi.org/10.4314/ejesm.v5i4.s11>
- Naidu, M. T., & Kumar, O. A. (2016). Tree diversity, stand structure, and community composition of tropical forests in eastern ghats of Andhra Pradesh, India. *Journal of Asia-Pacific Biodiversity*, 9(3), 328–334. <https://doi.org/10.1016/j.japb.2016.03.019>
- Narango, D. L., Tallamy, D. W., & Shropshire, K. J. (2020). Few keystone plant genera support the majority of Lepidoptera species. *Nature communications*, 11, 5751. <https://doi.org/10.1038/s41467-020-19565-4>
- Negesse, G., & Woldearegay, M. (2022). Floristic diversity, structure and regeneration status of Menfeskidus monastery forest in Berehet District, North Shoa, central Ethiopia. *Trees, Forests and People*, 7, 100191. <https://doi.org/10.1016/j.tfp.2022.100191>
- Nodza, G., Anthony, R., Onuminya, T., & Ogundipe, O. (2021). Floristic studies on herbaceous and grass species growing in the University of Lagos, Nigeria. *Tanzania Journal of Science*, 47(1), 80-90.

- Nodza, G. I., Onuminya, T. O., & Ogundipe, O. T. (2022a). Preliminary conservation checklist of orchid of Gashaka Gumti National Park, Nigeria. *Journal of Tropical Biology and Conservation*, *19*, 29–46. <https://doi.org/10.51200/jtbc.v19i.3936>
- Nodza, I. N., Onuminya, T., Igbari, A. D., Ogundipe, T. O., & Abdulhameed, A. (2022b). Ethno veterinary practice for the treatment of cattle diseases in the eastern highlands of Nigeria. *Ethnobotany Research and Applications*, *24*(7), 1-16. <https://doi.org/10.32859/era.24.7.1-16>
- Ochayi, C. (2018, November 27). FG partners ANI to revitalize Gashaka Gumti Nat'l Parks. *Vanguard Newspapers*. <https://www.vanguardngr.com/2018/11/environment-fg-partners-ani-to-revitalize-gashaka-gumti-natl-parks/>
- Okon, E. M., Falana, B. M., Solaja, S. O., Yakubu, S. O., Alabi, O. O., Okikiola, B. T., Awe, T. E., Adesina, B. T., Tokula, B. E., Kipchumba, A. K., & Edeme, A. B. (2021). Systematic review of climate change impact research in Nigeria: Implication for sustainable development. *Heliyon*, *7*(9), e07941. <https://doi.org/10.1016/j.heliyon.2021.e07941>
- Riki, J. T. B., Maiguru, A. A., Zaku, S. S., & Auta, B. J. B. (2021). Investigation of under-utilised wood species for potential utilisations in Taraba State, Nigeria. *European Journal of Agriculture and Food Sciences*, *3*(5), 106–112. <https://doi.org/10.24018/ejfood.2021.3.5.366>
- Sartorello, Y., Pastorino, A., Bogliani, G., Ghidotti, S., Viterbi, R., & Cerrato, C. (2020). The impact of pastoral activities on animal biodiversity in Europe: A systematic review and meta-analysis. *Journal for Nature Conservation*, *56*, 125863. <https://doi.org/10.1016/j.jnc.2020.125863>
- Sewale, B., & Mammo, S. (2022). Analysis of floristic composition and plant community types in Kenech Natural Forest, Kaffa Zone, Ethiopia. *Trees, Forests & People*, *7*, 100170. <https://doi.org/10.1016/j.tfp.2021.100170>
- Siriwat, P., & Nijman, V. (2023). Quantifying the illegal high-value rosewood trade and criminal trade networks in the Greater Mekong Region. *Biological Conservation*, *277*, 109826. <https://doi.org/10.1016/j.biocon.2022.109826>
- Skarpe, C., & Hester, A. J. (2008). Plant traits, browsing and grazing herbivores, and vegetation dynamics. In I. J. Gordon & H. H. T. Prins (Eds.). *The ecology of browsing and grazing*. (pp. 217-261). Springer. [https://doi.org/10.1007/978-3-540-72422-3\\_9](https://doi.org/10.1007/978-3-540-72422-3_9)
- Sommer, V., & Ross, C. (Eds.). (2011). *Primates of Gashaka*. Springer. <https://doi.org/10.1007/978-1-4419-7403-7>
- Tabuti, J. R. S. (2012). Important woody plant species, their management and conservation status in Balawoli Sub-county, Uganda. *Ethnobotany Research and Applications*, *10*, 269-286. <https://doi.org/10.17348/era.10.0.269-286>
- Tadele, D., Lulekal, E., Damtie, D., & Assefa, A. (2014). Floristic diversity and regeneration status of woody plants in Zengena Forest, a remnant montane forest patch in northwestern Ethiopia. *Journal of Forestry Research*, *25*, 329-336. <https://doi.org/10.1007/s11676-013-0420-3>
- Umar, I. A., Yaduma, Z. B., Dishan, E. E., & Adaeze, J. E. (2019). Landcover change of Gashaka Gumti National Park within 21 years window (1991 to 2011) using satellite imageries. *Open Access Library Journal*, *6*(9), 1–4. <https://doi.org/10.4236/oalib.1105750>

- van Rooyen, M. W., van Rooyen, N., Miabangana, E. S., Nsongola, G., Gaugris, C. V., & Gaugris, J. Y. (2019). Floristic composition, diversity and structure of the Rainforest in the Mayoko District, Republic of Congo. *Open Journal of Forestry*, 9(1), 16–69. <https://doi.org/10.4236/ojf.2019.91002>
- Wajim, J. (2020). Impacts of deforestation on socio-economic development and environment in Nigeria. *The International Journal of Social Sciences and Humanities Invention*, 7(3), 5852-5863. <https://doi.org/10.18535/ijsshi/v7i03.04>



## Effects of Temperature on Growth and Biochemical Composition of Arctic *Pseudanabaena* sp. and Tropical *Synechococcus* sp.

Nurul Farhanah Azlee<sup>1</sup>, Azmir Hamidi<sup>1</sup>, Zoya Khan<sup>2</sup>, Faradina Merican<sup>1</sup>, Jerzy Smykla<sup>3</sup>, Siti Aisyah Alias<sup>4,5</sup> and Wan Maznah Wan Omar<sup>1\*</sup>

<sup>1</sup>School of Biological Sciences, Universiti Sains Malaysia, 11800 Penang, Malaysia

<sup>2</sup>Centre for Marine and Coastal Studies (CEMACS), Universiti Sains Malaysia, 11800 Penang, Malaysia

<sup>3</sup>Department of Ecology, W. Szafer Institute of Botany, Polish Academy of Sciences, Lubicz 46, 31-512 Krakow, Poland

<sup>4</sup>National Antarctic Research Centre, Universiti Malaya, 50603 Kuala Lumpur, Malaysia

<sup>5</sup>Institute of Ocean and Earth Sciences, Universiti Malaya, 50603 Kuala Lumpur, Malaysia

### ABSTRACT

This study examines the effect of temperature on the growth and biochemical composition of two cyanobacteria: *Pseudanabaena* sp. from the Arctic region and *Synechococcus* sp. from a tropical region. Cyanobacterial isolates were cultivated under three different temperatures: 4±2°C, 15±2°C and 25±2°C. The growth rate of *Pseudanabaena* sp. at 4±2°C, 15±2°C and 25±2°C was 1.61 day<sup>-1</sup>, 1.62 day<sup>-1</sup> and 1.53 day<sup>-1</sup>, while the doubling time was 0.11, 0.18 and 0.08 days, respectively. The growth rate of *Synechococcus* sp. was slightly lower. At 4±2°C, 15±2°C and 25±2°C, the growth rate was recorded at 0.65 day<sup>-1</sup>, 0.94 day<sup>-1</sup> and 1.06 day<sup>-1</sup>, while the doubling time was 0.003, 0.07 and 0.25 days, respectively. Total carbohydrate for *Pseudanabaena* sp. at 4±2°C, 15±2°C and 25±2°C was 207.16±10.03 mg/L, 329.57±189.65 mg/L and 63.32±41.02 mg/L, respectively. At the same temperature, the total carbohydrate for *Synechococcus* sp. was 269.44±81.29 mg/L, 321.15±73.31 mg/L and 1556.84±243.38 mg/L, respectively. It illustrates higher total carbohydrate in *Synechococcus* sp. compared to *Pseudanabaena* sp. At 4±2°C, 15±2°C and 25±2°C, total protein for *Pseudanabaena* sp. was recorded as 5.59±0.09 mg/L, 5.23±0.21 mg/L, and 4.34±0.47 mg/L. Meanwhile, for *Synechococcus* sp., total protein recorded at temperatures 4±2°C, 15±2°C and 25±2°C was 0.47±0.01 mg/L, 0.45±0.01 mg/L and 0.39±0.05 mg/L, respectively. This study shows that the growth rate and biochemical composition of Arctic *Pseudanabaena* sp. and tropical *Synechococcus* sp. were influenced by different temperature levels.

### ARTICLE INFO

#### Article history:

Received: 20 March 2024

Accepted: 30 July 2024

Published: 28 January 2025

DOI: <https://doi.org/10.47836/pjtas.48.1.11>

#### E-mail addresses:

farhanahazlee@student.usm.my (Nurul Farhanah Azlee)

azmir\_kkb@yahoo.com (Azmir Hamidi)

zoyakhan2908@gmail.com (Zoya Khan)

faradina@usm.my (Faradina Merican)

jerzysmykla@yahoo.com (Jerzy Smykla)

saa@um.edu.my (Siti Aisyah Alias)

wmaznah@usm.my (Wan Maznah Wan Omar)

\* Corresponding author

**Keywords:** Arctic, cyanobacteria, growth, tropical, temperature

## INTRODUCTION

Temperature is an environmental condition that controls the growth and biological chemistry of cyanobacteria, green algae, diatom and others (Gani et al., 2019; Juneja et al., 2013; Morgan-Kiss et al., 2006). Cyanobacteria are prokaryotic, photosynthetic, gram-negative microorganisms that can adapt to environments ranging from low temperatures in the Polar region to high temperatures of more than 80°C in hot springs. They are highly adaptable to a wide range of environmental conditions, including variations in temperature, ultraviolet (UV) irradiance, photo-oxidation, drought and desiccation, nitrogen starvation, heat-cold shocks, anaerobiosis, osmotic and salinity stresses, all of which influence their physiological traits and metabolic activities (Nandagopal et al., 2021; Yadav et al., 2022). Cyanobacteria have evolved exclusive survival strategies to cope with these challenges by producing bioactive compounds that act as protective regulators against external factors. These bioactive metabolites play crucial roles in ensuring the survival of cyanobacteria under diverse environmental conditions (Nandagopal et al., 2021).

Cyanobacteria have various strategies to cope with low temperatures, including the modulation of key enzyme kinetics, the evolution of cold shock and ice-structuring proteins, and the development of liquid biomembranes through the accumulation of polyunsaturated fatty acyl chains (Morgan-Kiss et al., 2006). At low temperatures, cyanobacteria have a dark fixation that decreases the photosynthetic process controlled by enzymes (Tang et al., 1997). Moreover, fatty acid desaturases facilitate the incorporation of polyunsaturated fatty acyl chains into the membrane lipids of cyanobacteria. These enzymes increase the degree of unsaturation in fatty acid chains by adding double bonds at specific positions, forming polyunsaturated fatty acyl chains. Consequently, the buildup of these polyunsaturated fatty acyl chains improves membrane fluidity and helps cyanobacteria sustain cellular activity (Los & Mironov, 2015; Murata & Wada, 1995). This adaptation is important for cyanobacteria to survive in a very harsh environment. Therefore, cyanobacteria is a group of phototrophic microorganisms that can dominate in cold ecosystems, such as the Polar Region, including the Arctic and Antarctic (Vincent, 2007).

*Pseudanabaena* sp. is a non-heterocystous cyanobacteria belonging to the order Oscillatoriales from the family Pseudanabaenaceae (Acinas et al., 2008; Gao et al., 2018). Simple trichomes characterise this species with a width of less than 4µm. Somehow, the morphology of *Pseudanabaena* sp. is often confused with *Limnothrix* (Meffert, 1987). This species can be found in brackish and freshwater ecosystems and has a strong adaptability and tolerance to various environmental factors such as temperature, low light disturbance and phosphorus deficiency. *Pseudanabaena* sp. is a harmful species, as it often dominates freshwater reservoirs, likely due to its adaptability to these disturbances (Gao et al., 2018). *Synechococcus* sp. is a unicellular cyanobacterium belonging to the order Chroococcales. The natural habitat of *Synechococcus* sp. includes marine and freshwater environments.



This species is one of the major sources of primary production in its habitats and crucial in nutrient cycling, supporting the growth of other marine organisms commonly in the temperate to tropical oceans (Christie-Oleza et al., 2017; Kim et al., 2018; Wang et al., 2011). It has a rod-shaped to coccoid shape less than 3  $\mu\text{m}$  in diameter. *Synechococcus* sp. undergoes binary fission, dividing into equal halves, producing two identical daughter cells in a single plane. This study aims to elucidate the impact of elevated temperature on the growth and biochemical compounds of these two cyanobacteria and compare the response of Arctic and tropical cyanobacteria under different temperature regimes.

## MATERIALS AND METHODS

### Isolation and Growth Conditions

This study investigated two different regions: the Arctic and the tropical regions. *Pseudanabaena* sp. was isolated from Svalbard Island, Norway (Latitude: 78°N; Longitude: 19.2°E), which represents the polar while *Synechococcus* sp. was isolated from Niah Cave, Malaysia (Latitude: 3.8°N; Longitude: 113.7°E), which represents the tropics. Both isolated species (*Pseudanabaena* sp. and *Synechococcus* sp.) were collected in sterile small containers and transported to the laboratory for further analysis.

Single isolates of *Pseudanabaena* sp. and *Synechococcus* sp. were obtained using streaking and serial dilution methods. Both species were streaked onto BG-11 agar media and maintained in an incubator (Protech, Malaysia) at  $15\pm 2^\circ\text{C}$ . The cultures were observed daily to monitor their growth. Serial dilutions were performed several times until pure unialgal strains were obtained. Cultures were grown in BG-11 liquid media. *Pseudanabaena* sp. was incubated at a temperature of  $15\pm 2^\circ\text{C}$ ; photoperiod of 12L: 12D, with a light intensity of 2000 lux. Meanwhile, *Synechococcus* sp. was grown at  $25\pm 2^\circ\text{C}$ , a photoperiod of 12L: 12D, with a light intensity of around 2,000 lux.

### Experimental Design

For the experiment, 18 lab flasks (Schott Duran, 250 ml) were filled with 100 ml of BG-11 liquid media. Flasks were divided into two sets: *Pseudanabaena* sp. and *Synechococcus* sp. Each group has three subsets with triplicates that represent  $4\pm 2^\circ\text{C}$ ,  $15\pm 2^\circ\text{C}$  and  $25\pm 2^\circ\text{C}$ , respectively. The three temperature ranges ( $4\pm 2^\circ\text{C}$ ,  $15\pm 2^\circ\text{C}$ , and  $25\pm 2^\circ\text{C}$ ) were chosen to represent the native habitats of *Pseudanabaena* sp. (Arctic region) and *Synechococcus* sp. (tropical region). A temperature of  $4^\circ\text{C}$  represents the cold conditions of the Arctic, where the *Pseudanabaena* sp. was natively found,  $15^\circ\text{C}$  represents a moderate temperature, and  $25^\circ\text{C}$  represents the warm conditions of the tropics, where the *Synechococcus* sp. was found. For both species, 10% of its initial inoculum was inoculated into the flask. Each flask was incubated under  $4\pm 2^\circ\text{C}$ ,  $15\pm 2^\circ\text{C}$  and  $25\pm 2^\circ\text{C}$ , respectively.

## Cyanobacterial Growth Analysis

Cell count was done daily by measuring growth using a Neubauer haemocytometer (MC, China). Before harvesting for carbohydrate and protein analysis, counting was done under a light microscope until the 25<sup>th</sup> day. The net growth rate of each population was determined using Equation 1:

$$\mu = \ln [Nt/N0]/t \quad [1]$$

where,  $\mu$  is the population growth rate ( $d^{-1}$ ),  $N0$  and  $Nt$  are initial and final cell densities, and  $t$  is the incubation duration in days. The unit for growth rate is  $day^{-1}$ .

Equation 1 is used to calculate doubling time,  $T_g$ :

$$T_g = \ln 2 / \mu = 0.6931 / \mu \quad [2]$$

Each culture was harvested by centrifugation at  $1500 \times g$  for 15 minutes. The supernatant was discarded, and the pellet was freeze-dried to make powder. Protein and carbohydrates were extracted to measure both species' total protein and carbohydrates. Total protein was measured by Bradford's methods (1976), while total carbohydrates were determined by Dubois' methods (Dubois et al., 1956).

## Statistical Analysis

Statistical analysis was done using Statistical Package for the Social Sciences (SPSS) software (IBM SPSS Statistic 20). All values represent the mean of triplicate samples for each treatment. Error bars in the figures illustrate the standard deviations of these triplicates. Significant differences ( $p < 0.05$ ) between values were determined using two-way Analysis of Variance (ANOVA) and Duncan's Post Hoc Test to identify which specific group means are significantly different.

## RESULTS

### Biomass Productivity

For 25 days, *Pseudanabaena* sp. and *Synechococcus* sp. biomass productivity was evaluated at various temperatures. Two-way ANOVA, between-groups analysis of variance, was conducted to explore the impact of different temperatures on growth and biochemical compounds. The highest growth rate achieved for *Pseudanabaena* sp. was at  $15 \pm 2^\circ C$  ( $1.62 \text{ day}^{-1}$ ) (Table 1, Figure 1) with the highest doubling time of 0.18 day (Table 1, Figure 2). At  $4 \pm 2^\circ C$ , *Pseudanabaena* sp. showed a growth rate of  $1.61 \text{ day}^{-1}$  (Figure 1) and a doubling time of 0.11 day (Figure 2), which is almost adjacent to the readings at  $15 \pm 2^\circ C$ . Post-hoc comparisons using the Duncan Test indicated that the growth rate and doubling time for *Pseudanabaena* sp. at three diverse temperatures were nearly identical ( $p > 0.05$ ) (Table

1). For *Synechococcus* sp., the maximum growth rate was observed at  $25\pm 2^\circ\text{C}$  ( $1.06\text{ day}^{-1}$ ) (Table 1, Figure 1), and the highest doubling time was recorded at  $0.25\text{ day}^{-1}$  (Table 1, Figure 2). The lowest growth rate for *Synechococcus* sp. was at  $4\pm 2^\circ\text{C}$ , while the lowest doubling time was determined at  $0.003\text{ day}^{-1}$ . Duncan Test showed that the same growth rate for three temperatures was significant ( $p > 0.05$ ), while the doubling time for  $25\pm 2^\circ\text{C}$  was significantly different from other temperatures ( $p < 0.05$ ).

Table 1

Functional growth performance parameters for *Pseudanabaena* sp. and *Synechococcus* sp. cells grown under three different temperatures

Isolates and growth		Temperature ( $^\circ\text{C}$ )		
		4	15	25
<i>Pseudanabaena</i> sp.	Growth rate ( $\text{day}^{-1}$ )	$1.61\pm 0.60^b$	$1.62\pm 0.08^b$	$1.50\pm 0.70^{a,b}$
	Doubling time (day)	$0.11\pm 0.02^{a,b}$	$0.18\pm 0.04^{b,c}$	$0.08\pm 0.06^{a,b}$
<i>Synechococcus</i> sp.	Growth rate ( $\text{day}^{-1}$ )	$0.63\pm 0.12^a$	$0.95\pm 0.80^{a,b}$	$1.06\pm 0.05^{a,b}$
	Doubling time (day)	$0.003\pm 0.001^a$	$0.070\pm 0.015^{a,b}$	$0.250\pm 0.090^c$

Note. Values given are the means with a standard deviation of measurements on triplicate cultures. Different superscript letters indicate significant differences in values ( $p < 0.05$ )

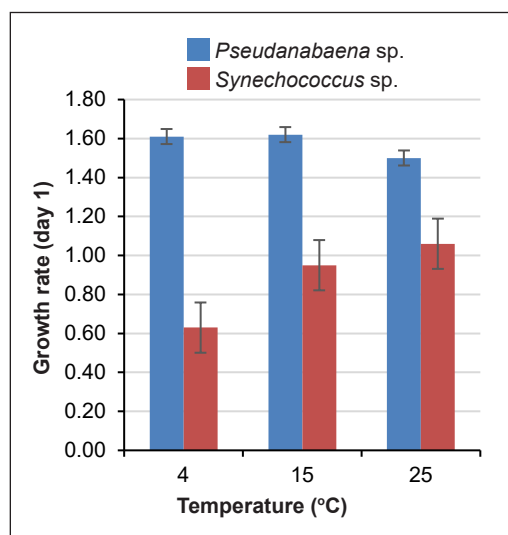


Figure 1. The growth rate of *Pseudanabaena* sp. and *Synechococcus* sp. at different temperature regimes (mean growth rate  $\pm$  standard deviation)

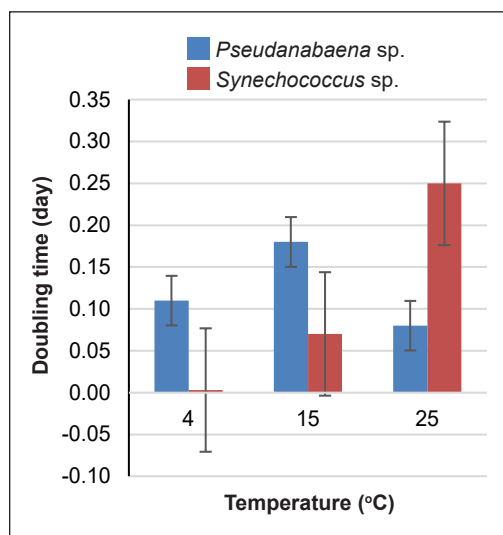


Figure 2. Doubling time of *Pseudanabaena* sp. and *Synechococcus* sp. at different temperature regimes (mean doubling time  $\pm$  standard deviation)

## Total Carbohydrate and Total Protein

Table 2 illustrates the total carbohydrates for *Pseudanabaena* sp. and *Synechococcus* sp. at different temperatures. For *Pseudanabaena* sp., the highest total carbohydrate was recorded at  $15\pm 2^\circ\text{C}$  ( $329.57\pm 189.65\text{ mg/L}$ ), while the lowest total carbohydrate was recorded

at 25±2°C (63.32±41.02 mg/L). For *Synechococcus* sp., the highest total carbohydrate was recorded at 25±2°C (1556.84±243.38 mg/L), while the lowest total carbohydrate was recorded at 4±2°C (269.44±81.29 mg/L). Post-hoc Duncan Test (Table 2) showed that total carbohydrates for *Pseudanabaena* sp. were not significant ( $p > 0.05$ ), whereas total carbohydrates for *Synechococcus* sp. at 25±2°C were dramatically higher than other temperatures ( $p = 0.001$ ). Figure 4 examined the total protein for *Pseudanabaena* sp. and *Synechococcus* sp. *Pseudanabaena* sp. recorded higher total protein than *Synechococcus* sp. The total protein for *Pseudanabaena* sp. and *Synechococcus* sp. was highest at 4±2°C when compared to 15±2°C and 25±2°C ( $p < 0.05$ ). The total protein of both cyanobacteria showed the same prototype- total protein declined as the temperature increased.

Table 2  
Functional biochemical growth parameters for *Pseudanabaena* sp. and *Synechococcus* sp. cells grown under three different temperatures

Isolates and biochemical components	Temperature (°C)		
	4	15	25
<i>Pseudanabaena</i> sp. Carbohydrates (mg/L)	252.35±52.35 <sup>ab</sup>	329.57±189.65 <sup>b</sup>	63.32±41.02 <sup>a</sup>
<i>Pseudanabaena</i> sp. Protein (mg/L)	5.6±0.008 <sup>f</sup>	5.2±0.060 <sup>e</sup>	4.5±0.040 <sup>d</sup>
<i>Synechococcus</i> sp. Carbohydrates (mg/L)	269.44±81.29 <sup>ab</sup>	322.45±75.26 <sup>ab</sup>	1556.84±243.38 <sup>c</sup>
<i>Synechococcus</i> sp. Protein (mg/L)	0.4±0.010 <sup>c</sup>	0.3±0.011 <sup>b</sup>	0.2±0.006 <sup>a</sup>

Note. Values given are the means with standard deviations of measurements on triplicate cultures. Different superscript letters indicate significant differences in values ( $p < 0.05$ )

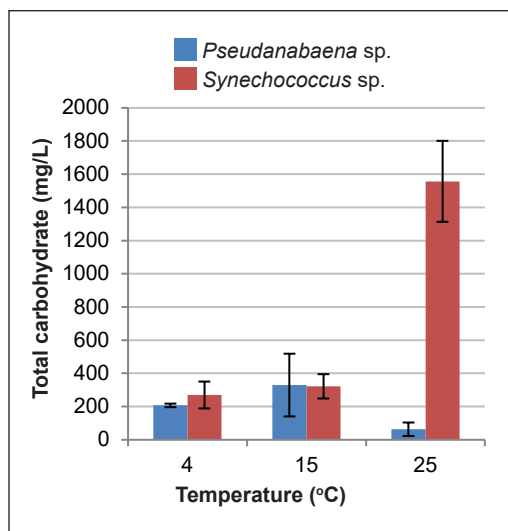


Figure 3. Total carbohydrate of *Pseudanabaena* sp. and *Synechococcus* sp. at different temperature regimes (mean total carbohydrates ± standard deviation)

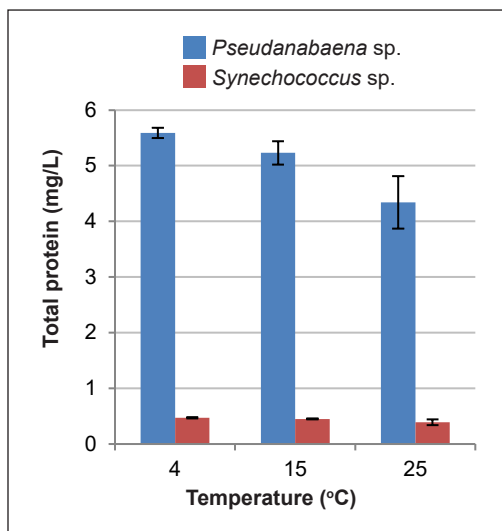


Figure 4. Total protein of *Pseudanabaena* sp. and *Synechococcus* sp. at different temperature regimes (mean total protein ± standard deviation)

## DISCUSSION

One of the aims of this investigation is to determine if temperature acts as a controlling factor for cyanobacteria growth. In some cases, *Pseudanabaena* sp. responded better to experimental conditions with different temperatures than *Synechococcus* sp. (Gao et al., 2018). However, temperature did have a marked effect on *Synechococcus* sp. growth rate. Cell division rates for *Pseudanabaena* sp. remained unaffected by the experimental temperature changes. Based on Figure 1, we can conclude that the *Pseudanabaena* sp. is a psychrotolerant or psychrotrophic species. According to Moyer and Morita (2007), psychrotolerant or psychrotrophic is a species of organism from a cold environment that can adapt to temperatures higher than the ambient temperature of 15°C. However, Figures 1 and 2 also illustrated that *Pseudanabaena* sp. had the lowest growth rate and doubling time as temperature increased. This result is the same as recorded by Tang et al. (1997), where the growth of psychrotrophic species will decrease as temperature increases.

Additionally, previous studies have demonstrated that the Antarctic and Arctic strains of the genus *Pseudanabaena* are psychrotolerant, exhibiting optimal growth temperatures ranging from 8°C to 15°C; they are also able to grow and develop at temperatures exceeding 20°C (Averina et al., 2020; Khan et al., 2017). It may be due to thermal instability and denaturation of molecular compounds in the cyanobacteria. At higher temperatures, proteins and nucleic acids lose the basic conformational structure in their native state, leading to cell activity disruption and probably cell death. The sudden growth from day 0 to day 3 was because of the exponential accumulation of cyanobacteria biomass in stock culture (Tang et al., 1997) due to the change in temperature from 15°C to 4°C. Experiment results indicated that temperature above 15°C limits the growth of *Pseudanabaena* sp.

Figure 1 shows that as the temperature increases, the growth rate of *Synechococcus* sp. increases. Figure 2 demonstrated a similar pattern, with doubling time directly proportional to temperature. A previous study by Prihantini et al. (2016) also observed that *Synechococcus* strains achieved their highest cell densities and optimal growth temperatures between 30°C and 35°C, indicating that an increase in temperature within this range can enhance their growth due to the increase of metabolic rate in algae that can enhance the activity of the species. The enzyme that catalyses the biochemical reaction rate depends on temperature changes (Sakamoto et al., 1998). According to Beardall and Raven (2004), temperature will increase the reaction rate of Ribulose-1, 5-bisphosphate carboxylase oxygenase (RUBISCO) and enhance the growth rate of cyanobacteria, given that inorganic carbon or other factors do not limit the growth. Tropical *Synechococcus* sp. showed the lowest growth at 4°C as protein is less stable and is difficult to synthesise at low temperatures (Sanfelice & Temussi, 2016). It is another mechanism that can limit growth at low temperatures. Some research suggested that low temperature decreases the rate of nutrient uptake from the environment, which could be the rate-limiting step for the growth of microorganisms (Nedwell & Rutter, 1994).

As shown in Figure 3, the total carbohydrate for *Synechococcus* sp. at  $25\pm 2^{\circ}\text{C}$  was higher than *Pseudanabaena* sp. because carbohydrate accumulates in cyanobacterial cells due to osmotic reactions (Warr et al., 1985). The accumulation of carbohydrates keeps water in the cell, which protects it from dehydration. Because *Synechococcus* sp. was isolated from Niah Cave, the existence of light might affect the accumulation of carbohydrates. It might stress this species as its natural environment is dark. Thus, the production of carbohydrates is part of the defence in response to stress conditions (De Philippis & Vincenzini, 1998; Otero & Vincenzini, 2003; Trabelsi et al., 2009; Wingender et al., 1999). Khajepour et al. (2015) reported that *Nostoc calcicola* shows high carbohydrate and carotenoid content when light intensity increases. Besides temperature, salinity also occurs in the accumulation of carbohydrates in cyanobacteria because of the osmotic reaction that prevents dehydration (Hershkovitz et al., 1991; Reed & Stewart, 1985). The form of mucopolysaccharides or exopolymeric substances (EPS) can make the liquid water flow slowly when freezing up and thawing. In addition, the EPS may force ice crystal formation to create well away from cyanobacterial cells (Vincent, 2007). It is also shown in *Nostoc commune*, where EPS protects cyanobacterium from desiccation and freezing up (Tamaru et al., 2005; Vincent, 2007). Increased production of EPS and sucrose in the algal cells protects them from osmotic damage by maintaining the cellular osmotic equilibrium between the intracellular and extracellular environment (Chen et al., 2006).

To tolerate stress conditions, protein profiling and newly forming proteins can help cyanobacteria survive (Weber & Jung, 2002). In Figure 4, the total protein for *Pseudanabaena* sp. was higher than *Synechococcus* sp. in all degrees of temperature. *Pseudanabaena* sp. was isolated from the Arctic region since there was a change in temperature from  $15^{\circ}\text{C}$  (stock culture) to  $4^{\circ}\text{C}$ . This species can have high total protein because the accumulation of proteins such as dehydrins might be how Arctic cyanobacteria adapt to survive in cold environments (Dasauni et al., 2021). This adaptation is known as cyano-dehydrins. During osmotic adaptation, the protein acts as a regulator that prevents osmotic stress due to the adaptation in a cold environment that operates within desiccation-tolerant in cyanobacterial cells (Close & Lammers, 1993). Thus, Arctic cyanobacteria can have higher total protein than tropic cyanobacteria. At low temperatures, membrane lipid unsaturation increases (Zheng et al., 2011), and this can be considered an acclimatised response to balance the decreased functionality of biological membranes at low temperatures by increasing the membrane fluidity for cellular viability under temperature stress. Its increase in membrane lipid unsaturation is a conserved adaptation response that allows cells to maintain the appropriate fluidity of membrane lipid bilayers, ensuring cell viability under temperature stress (Uemura et al., 2005). The susceptibility of a protein to high-temperature degradative reactions

seems to be dependent on the conformational integrity of the protein at that particular temperature (Daniel et al., 1996). Figure 4 also shows that protein content decreased as the temperature increased. Temperature affects phytoplankton growth, especially when enzyme kinetics are controlled.

In response to low temperatures, an increase in protein content prompts the production of enzymes to prevent the loss of membrane fluidity, highlighting the essential role of generating cold-active enzymes in microalgae to maintain cellular functions and ensure survival under low-temperature stress conditions (Gao et al., 2023; Georlette et al., 2004). This pattern of the graph (Figure 4) was similar to some marine microalgae such as *Pavlova lutheri*, *Skeletonema costatum* and also *Euglena gracilis* (Carvalho et al., 2009; Cook, 1963; Falkowski, 1977).

## CONCLUSION

This research concludes that *Pseudanabaena* sp. and *Synechococcus* sp. showed higher responses at their ambient temperature. This finding suggested that cyanobacteria are highly adaptive to their native environment but can survive in extreme conditions. This adaptive nature is based on the mechanism that allows its adaptation, the rate of adaptation, the cost of fitness, the growth rate, and the photosynthetic efficiency of this adaptation. *Pseudanabaena* sp. from the Arctic region is a psychrotrophic species. The growth pattern of this species indicates that, after reaching the optimum temperature, the growth of cold-tolerant cyanobacteria decreases with rising temperatures. For future research, this study will consider the employment and comparison of cyanobacteria from polar and tropic regions for biofuel production. Biofuel is the most promising solution for global energy calamity and climate change.

## ACKNOWLEDGEMENTS

This study was funded and supported by a Flagship grant (304/PBIOLOGI/650723/P131) under the Ministry of Science, Technology and Innovation, Malaysia.

## REFERENCES

- Acinas, S. G., Haverkamp, T., Huisman, J., & Stal, L. J. (2008). Phenotypic and genetic diversification of *Pseudanabaena* spp. (cyanobacteria). *The ISME Journal*, 3(1), 31–46. <https://doi.org/10.1038/ismej.2008.78>
- Averina, S., Tsvetkova, S. A., Poliakova, E. Y., Величко, Н. В., & Pinevich, A. V. (2020). Antarctic cyanobacteria of the genus *Pseudanabaena* – an example of psychrotolerant microorganisms. *Issues of Modern Algology*, 2(23), 57–62. [https://doi.org/10.33624/2311-0147-2020-2\(23\)-57-62](https://doi.org/10.33624/2311-0147-2020-2(23)-57-62)
- Beardall, J., & Raven, J. A. (2004). The potential effects of global climate change on microalgal photosynthesis, growth and ecology. *Phycologia*, 43(1), 26–40. <https://doi.org/10.2216/i0031-8884-43-1-26.1>

- Bradford, M. M. (1976). A rapid and sensitive method for the quantitation of microgram quantities of protein utilizing the principle of protein-dye binding. *Analytical Biochemistry*, 72(1–2), 248–254. [https://doi.org/10.1016/0003-2697\(76\)90527-3](https://doi.org/10.1016/0003-2697(76)90527-3)
- Carvalho, A. P., Monteiro, C. M., & Malcata, F. X. (2009). Simultaneous effect of irradiance and temperature on biochemical composition of the microalga *Pavlova lutheri*. *Journal of Applied Phycology*, 21(5), 543–552. <https://doi.org/10.1007/s10811-009-9415-z>
- Chen, L., Li, D., Song, L., Hu, C., Wang, G., & Liu, Y. (2006). Effects of salt stress on carbohydrate metabolism in desert soil alga *Microcoleus vaginatus* Gom. *Journal of Integrative Plant Biology*, 48(8), 914–919. <https://doi.org/10.1111/j.1744-7909.2006.00291.x>
- Christie-Oleza, J. A., Sousoni, D., Lloyd, M., Armengaud, J., & Scanlan, D. J. (2017). Nutrient recycling facilitates long-term stability of marine microbial phototroph–heterotroph interactions. *Nature Microbiology*, 2, 17100. <https://doi.org/10.1038/nmicrobiol.2017.100>
- Close, T. J., & Lammers, P. J. (1993). An osmotic stress protein of cyanobacteria is immunologically related to plant dehydrins. *Plant Physiology*, 101(3), 773–779. <https://doi.org/10.1104/pp.101.3.773>
- Cook, J. R. (1963). Adaptations in growth and division in *Euglena* effected by energy supply\*. *The Journal of Protozoology*, 10(4), 436–444. <https://doi.org/10.1111/j.1550-7408.1963.tb01703.x>
- Daniel, R. M., Dines, M., & Petach, H. H. (1996). The denaturation and degradation of stable enzymes at high temperatures. *Biochemical Journal*, 317(1), 1–11. <https://doi.org/10.1042/bj3170001>
- Dasauini, K., Divya, N., & Nailwal, T. K. (2021). Cyanobacteria in cold ecosystem: Tolerance and adaptation. In R. Goel, R. Soni, D. C. Suyal & M. Khan (Eds.), *Survival strategies in cold-adapted microorganisms* (pp. 1–29). Springer. [https://doi.org/10.1007/978-981-16-2625-8\\_1](https://doi.org/10.1007/978-981-16-2625-8_1)
- De Philippis, R., & Vincenzini, M. (1998). Exocellular polysaccharides from cyanobacteria and their possible applications. *Fems Microbiology Reviews*, 22(3), 151–175. <https://doi.org/10.1111/j.1574-6976.1998.tb00365.x>
- DuBois, M., Gilles, K. A., Hamilton, J. K., Rebers, P. T., & Smith, F. (1956). Colorimetric method for determination of sugars and related substances. *Analytical chemistry*, 28(3), 350–356. <https://doi.org/10.1021/ac60111a017>
- Falkowski, P. G. (1977). The adenylate energy charge in marine phytoplankton: The effect of temperature on the physiological state of *Skeletonema costatum* (Grev.) Cleve. *Journal of Experimental Marine Biology and Ecology*, 27(1), 37–45. [https://doi.org/10.1016/0022-0981\(77\)90052-1](https://doi.org/10.1016/0022-0981(77)90052-1)
- Gani, P., Sunar, N. M., Matias-Peralta, H. M., & Apandi, N. (2019). An overview of environmental factor's effect on the growth of microalgae. *Journal of Applied Chemistry and Natural Resources*, 1(2), 1–5.
- Gao, B., Hong, J., Chen, J., Zhang, H., Ren, H., & Zhang, C. (2023). The growth, lipid accumulation and adaptation mechanism in response to variation of temperature and nitrogen supply in psychrotrophic filamentous microalga *Xanthonema hormidioides* (Xanthophyceae). *Biotechnology for Biofuels and Bioproducts*, 16, 12. <https://doi.org/10.1186/s13068-022-02249-0>
- Gao, J., Zhu, J., Wang, M., & Dong, W. (2018). Dominance and growth factors of *Pseudanabaena* sp. in drinking water source reservoirs, Southern China. *Sustainability*, 10(11), 3936. <https://doi.org/10.3390/su10113936>



- Georlette, D., Blaise, V., Collins, T., D'Amico, S., Gratia, E., Hoyoux, A., Marx, J., Sonan, G., Feller, G., & Gerday, C. (2004). Some like it cold: Biocatalysis at low temperatures. *Fems Microbiology Reviews*, 28(1), 25–42. <https://doi.org/10.1016/j.femsre.2003.07.003>
- Hershkovitz, N., Oren, A., & Cohen, Y. (1991). Accumulation of trehalose and sucrose in cyanobacteria exposed to matric water stress. *Applied and Environmental Microbiology*, 57(3), 645–648. <https://doi.org/10.1128/aem.57.3.645-648.1991>
- Juneja, A., Ceballos, R. M., & Murthy, G. S. (2013). Effects of environmental factors and nutrient availability on the biochemical composition of algae for biofuels production: A review. *Energies*, 6(9), 4607–4638. <https://doi.org/10.3390/en6094607>
- Khajepour, F., Hosseini, S. A., Nasrabadi, R. G., & Μάρκου, Γ. (2015). Effect of light intensity and photoperiod on growth and biochemical composition of a local isolate of *Nostoc calcicola*. *Applied Biochemistry and Biotechnology*, 176(8), 2279–2289. <https://doi.org/10.1007/s12010-015-1717-9>
- Khan, Z., Omar, W. M. W., Merican, F., Azizan, A. A., Foong, C. P., Convey, P., Najimudin, N., Smykla, J., & Alias, S. A. (2017). Identification and phenotypic plasticity of *Pseudanabaena catenata* from the Svalbard archipelago. *Polish Polar Research*, 38(4), 445–458. <https://doi.org/10.1515/popore-2017-0022>
- Kim, Y., Jeon, J., Kwak, M. S., Kim, G. H., Koh, I., & Rho, M. (2018). Photosynthetic functions of *Synechococcus* in the ocean microbiomes of diverse salinity and seasons. *PloS One*, 13(1), e0190266. <https://doi.org/10.1371/journal.pone.0190266>
- Los, D. A., & Mironov, K. S. (2015). Modes of fatty acid desaturation in cyanobacteria: An update. *Life*, 5(1), 554–567. <https://doi.org/10.3390/life5010554>
- Meffert, M. E. (1987). Planktic unsheathed filaments (Cyanophyceae) with polar and central gas-vacuoles. I: Their morphology and taxonomy. *Archiv für Hydrobiologie. Supplementband. Monographische Beiträge*, 76(4), 315–346.
- Morgan-Kiss, R. M., Priscu, J. C., Pockock, T., Gudynaite-Savitch, L., & Hüner, N. P. A. (2006). Adaptation and acclimation of photosynthetic microorganisms to permanently cold environments. *Microbiology and Molecular Biology Reviews*, 70(1), 222–252. <https://doi.org/10.1128/mmbr.70.1.222-252.2006>
- Morita, R. Y. (1975). Psychrophilic bacteria. *Bacteriological reviews*, 39(2), 144–167. <https://doi.org/10.1128/br.39.2.144-167.1975>
- Moyer, C. L., & Morita, R. Y. (2007). *Psychrophiles and psychrotrophs*. John Wiley & Sons. <https://doi.org/10.1002/9780470015902.a0000402.pub2>
- Murata, N., & Wada, H. (1995). Acyl-lipid desaturases and their importance in the tolerance and acclimatization to cold of cyanobacteria. *Biochemical Journal*, 308(1), 1–8. <https://doi.org/10.1042/bj3080001>
- Nandagopal, P., Steven, A. N., Chan, L., Rahmat, Z., Jamaluddin, H., & Noh, N. I. M. (2021). Bioactive metabolites produced by cyanobacteria for growth adaptation and their pharmacological properties. *Biology*, 10(10), 1061. <https://doi.org/10.3390/biology10101061>
- Nedwell, D. B., & Rutter, M. A. (1994). Influence of temperature on growth rate and competition between two psychrotolerant Antarctic bacteria: Low temperature diminishes affinity for substrate uptake. *Applied and Environmental Microbiology*, 60(6), 1984–1992. <https://doi.org/10.1128/aem.60.6.1984-1992.1994>

- Otero, A., & Vincenzini, M. (2003). Extracellular polysaccharide synthesis by *Nostoc* strains as affected by N source and light intensity. *Journal of Biotechnology*, 102(2), 143-152. [https://doi.org/10.1016/S0168-1656\(03\)00022-1](https://doi.org/10.1016/S0168-1656(03)00022-1)
- Prihantini, N. B., Addana, F., Sjamsuridzal, W., & Yokota, A. (2016). The effect of temperature on the growth of genus *Synechococcus* isolated from four Indonesian hot springs and Agathis small lake of Universitas Indonesia. *Proceedings of the 1<sup>st</sup> International Symposium on Current Progress in Mathematics and Sciences*, 1729(1), 020063. <https://doi.org/10.1063/1.4946966>
- Reed, R. H., & Stewart, W. D. P. (1985). Osmotic adjustment and organic solute accumulation in unicellular cyanobacteria from freshwater and marine habitats. *Marine Biology*, 88, 1-9. <https://doi.org/10.1007/BF00393037>
- Sakamoto, T., Shen, G., Higashi, S., Murata, N., & Bryant, D. A. (1997). Alteration of low-temperature susceptibility of the cyanobacterium *Synechococcus* sp. PCC 7002 by genetic manipulation of membrane lipid unsaturation. *Archives of microbiology*, 169, 20-28. <https://doi.org/10.1007/s002030050536>
- Sanfelice, D., & Temussi, P. A. (2016). Cold denaturation as a tool to measure protein stability. *Biophysical Chemistry*, 208, 4–8. <https://doi.org/10.1016/j.bpc.2015.05.007>
- Tamaru, Y., Takani, Y., Yoshida, T., & Sakamoto, T. (2005). Crucial role of extracellular polysaccharides in desiccation and freezing tolerance in the terrestrial cyanobacterium *Nostoc commune*. *Applied and Environmental Microbiology*, 71(11), 7327–7333. <https://doi.org/10.1128/aem.71.11.7327-7333.2005>
- Tang, E. P. Y., Tremblay, R., & Vincent, W. F. (1997). Cyanobacterial dominance of polar freshwater ecosystems: are high-latitude mat-formers adapted to low temperature?<sup>1</sup>. *Journal of Phycology*, 33(2), 171–181. <https://doi.org/10.1111/j.0022-3646.1997.00171.x>
- Trabelsi, L., Ouada, H. B., Bacha, H., & Ghouil, M. (2008). Combined effect of temperature and light intensity on growth and extracellular polymeric substance production by the cyanobacterium *Arthrospira platensis*. *Journal of Applied Phycology*, 21(4), 405–412. <https://doi.org/10.1007/s10811-008-9383-8>
- Uemura, M., Tominaga, Y., Nakagawara, C., Shigematsu, S., Minami, A., & Kawamura, Y. (2005). Responses of the plasma membrane to low temperatures. *Physiologia Plantarum*, 126(1), 81–89. <https://doi.org/10.1111/j.1399-3054.2005.00594.x>
- Vincent, W. F. (2007). Cold tolerance in cyanobacteria and life in the cryosphere. In J. Seckbach (Eds.), *Cellular origin, life in extreme habitats and astrobiology* (pp. 287–301). Springer. [https://doi.org/10.1007/978-1-4020-6112-7\\_15](https://doi.org/10.1007/978-1-4020-6112-7_15)
- Wang, K., Wommack, K. E., & Chen, F. (2011). Abundance and distribution of *Synechococcus* spp. and Cyanophages in the Chesapeake Bay. *Applied and Environmental Microbiology*, 77(21), 7459–7468. <https://doi.org/10.1128/aem.00267-11>
- Warr, S. R. C., Reed, R. H., & Stewart, W. D. P. (1985). Carbohydrate accumulation in osmotically stressed cyanobacteria (blue-green algae): Interactions of temperature and salinity. *New Phytologist*, 100(3), 285–292. <https://doi.org/10.1111/j.1469-8137.1985.tb02779.x>
- Weber, A., & Jung, K. (2002). Profiling early osmostress-dependent gene expression in *Escherichia coli* using DNA macroarrays. *Journal of Bacteriology*, 184(19), 5502–5507. <https://doi.org/10.1128/jb.184.19.5502-5507.2002>

- Wingender, J., Neu, T. R., & Flemming, H. C. (1999). What are bacterial extracellular polymeric substances? In J. Wingender, T. R. Neu & H. C. Flemming (Eds.), *Microbial extracellular polymeric substances* (pp. 1-19). Springer. [https://doi.org/10.1007/978-3-642-60147-7\\_1](https://doi.org/10.1007/978-3-642-60147-7_1)
- Yadav, P., Singh, R. P., Rana, S., Joshi, D., Kumar, D., Bhardwaj, N., Gupta, R. K., & Kumar, A. (2022). Mechanisms of stress tolerance in Cyanobacteria under extreme conditions. *Stresses*, 2(4), 531–549. <https://doi.org/10.3390/stresses2040036>
- Zheng, G., Tian, B., Zhang, F., Tao, F., & Li, W. (2011). Plant adaptation to frequent alterations between high and low temperatures: Remodelling of membrane lipids and maintenance of unsaturation levels. *Plant, Cell & Environment*, 34(9), 1431–1442. <https://doi.org/10.1111/j.1365-3040.2011.02341.x>



## Heavy Metals Assessment in Selected Leafy Vegetables from Selangor, Malaysia

Sian Nee See<sup>1</sup>, Mohd Sabri Pak Dek<sup>1</sup>, Maimunah Sanny<sup>1,2</sup>, Radhiah Shukri<sup>3</sup> and Nurul Shazini Ramli<sup>1\*</sup>

<sup>1</sup>Department of Food Science, Faculty of Food Science and Technology, Universiti Putra Malaysia, 43400 Serdang, Selangor, Malaysia

<sup>2</sup>Laboratory of Food Safety and Food Integrity, Institute of Tropical Agriculture and Food Security, Universiti Putra Malaysia, 43400 Serdang, Selangor, Malaysia

<sup>3</sup>Department of Food Technology, Faculty of Food Science and Technology, Universiti Putra Malaysia, 43400 Serdang, Selangor, Malaysia

### ABSTRACT

Leafy vegetables may contain heavy metals that possess negative impacts on human health. However, no structured monitoring has been available so far in terms of the heavy metal content of vegetables sold in markets across the country. Thus, the present study aimed to investigate heavy metals concentration [aluminium (Al), cadmium (Cd), chromium (Cr), copper (Cu), iron (Fe) and lead (Pb)] in selected leafy vegetables (*Brassica oleracea* subsp. *capitata* L., *Brassica juncea* Czern., *Spinacia oleracea* L., and *Brassica rapa* var. *chinensis*) from Selangor wholesale wet markets using inductively coupled plasma–optical emission spectrometry. Potential health risks linked to their consumption were assessed by estimating daily intake of toxic metals (EDI) and calculating both cancer and non-cancer risks, including hazard index and target hazard quotient (THQ). Results showed that the average concentrations of Al and Fe in vegetable samples were within the permissible limits, with the greatest amount of Al found in spinach (41.37 mg/kg). The mean levels of Fe in cabbage, mustard, spinach, and pak choi were  $6.30 \pm 5.78$ ,  $4.12 \pm 1.84$ ,  $13.59 \pm 4.73$ , and  $4.14 \pm 0.31$  mg/kg, respectively. However, Cd, Cr, Cu, and Pb were undetected in all samples. THQ values derived from the EDI of heavy metals were discovered to be less than one,

suggesting a low likelihood of adverse health effects. In conclusion, although leafy vegetables present negligible health risks, consumers should vary their vegetable intake to prevent long-term health effects.

### ARTICLE INFO

#### Article history:

Received: 29 April 2024

Accepted: 29 May 2024

Published: 28 January 2025

DOI: <https://doi.org/10.47836/pjtas.48.1.12>

#### E-mail addresses:

sianneese@gmail.com (Sian Nee See)

mhdsabri@upm.edu.my (Mohd Sabri Pak Dek)

s\_maimunah@upm.edu.my (Maimunah Sanny)

radhiah@upm.edu.my (Radhiah Shukri)

shazini@upm.edu.my (Nurul Shazini Ramli)

\* Corresponding author

**Keywords:** Dietary exposure, health hazard assessment, heavy metal, inductively coupled plasma-optical emission spectrometry

## INTRODUCTION

Vegetables contain varied micronutrients and dietary fibre essential for preventing diseases and maintaining human physiological functions (Mallor, 2023). Nevertheless, vegetables are considered one of the principal routes of heavy metal exposure to human beings, especially green leafy vegetables (Martín-León et al., 2023). Toxic metals such as Cd and Pb have been shown to accumulate at higher concentrations on leaves compared to the stems and fruity varieties (Guo et al., 2020). Consuming vegetables polluted by heavy metals resulted in different disorders, including anemia, pulmonary illness, hyperactivity, male infertility, cancer, and death (Najmi et al., 2023).

Various elements contribute to the accumulation of heavy metals in plants. For instance, there is widespread application of fertilizers, the utilization of human-made sources in agricultural areas, and environmental pollutants. A report from Iran indicated higher levels of Pb in vegetables collected from the sites close to traffic highways due to the atmospheric lead deposits originating from the leaded petrol combustion in cars (Tajdar-Oranj et al., 2022). Furthermore, a study conducted by Shi et al. (2022) found high concentrations of heavy metals in leafy vegetables from the mining areas in China. The studies proved that plants absorbed heavy metals from soils and deposited them in the leave tissues.

In Malaysia, a previous dietary exposure study on leafy vegetables (pak choi, amaranth, and caisim) cultivated in Pahang, Malaysia, showed a possible health risk to consumers due to the high lifetime cancer risk (LCR) values for arsenic (As) and Pb (Sulaiman et al., 2020). Similarly, Pb and Cd concentrations in spinach (*S. oleracea*) from the conventional farms in Kuala Selangor exceeded the World Health Organization (WHO) standard for leafy vegetables (Mohamad & Kamaludin, 2019). Besides, Aweng et al. (2020) found four types of heavy metals, including Fe, Cu, zinc (Zn), and manganese (Mn) in spinach (*S. oleracea*) collected from Pasar Siti Khadijah, Kota Bharu, Kelantan. However, the concentration of heavy metals was below the maximum level allowed by the Malaysian Food Act (1983) and Food Regulation (1985) (Malaysia & International Law Book Services, 2019). Nevertheless, sustained exposure to low concentrations of heavy metals, especially for vulnerable groups such as children, still needs attention. Therefore, ensuring the safety of leafy vegetables remains a significant public health priority.

Selangor is an urban state with the highest population density in Malaysia. For this reason, vegetables and other perishable products are not only produced in the state but also supplied from the rural and semi-urban regions of the country, especially from Cameron Highlands, Pahang. As mentioned, the heavy metals from agricultural soils are subsequently transferred to the plants, which have been discovered in Pahang and Kuala Selangor (Aweng et al., 2020; Sulaiman et al., 2020). It could be due to the greater usage of chicken manure and chemical fertilizers in the plantation areas that increased the

heavy metal content in the soil, such as Pb, Zn, and Cu (Aljohani, 2023). Additionally, rapid urbanization, economic development, and increased motorization in the Klang Valley area (including the Kuala Lumpur Federal Territory and Selangor State) have contributed to higher pollution levels, resulting in decreased water and air quality (Loi et al., 2022). As a result, the atmospheric heavy metals might be deposited in the plants cultivated in the adjacent areas.

Pasar Borong Selangor in Seri Kembangan is one of the largest wet markets in Selangor. The leafy vegetables sold in this market are a significant food source for locals, especially those in the Klang Valley. Due to the rapid industrial development in the state, plants, including vegetables grown in this area, might become contaminated with heavy metals. However, no structured monitoring system currently tracks heavy metals in vegetables sold across the nation's markets. Only a few papers have been published investigating human exposure to metal contaminants from vegetables in the urban state. It is hypothesized that the leafy vegetables sold in Selangor wet markets are contaminated with heavy metals, and long-term consumption of these leafy vegetables poses adverse health effects. Hence, the present study aimed to investigate the concentrations of heavy metals (Al, Cd, Cr, Cu, Fe, and Pb) in commonly consumed vegetables sourced from Pasar Borong Selangor, Seri Kembangan. Four types of leafy vegetables, including cabbage (*B. oleracea* subsp. *capitata* L.), mustard (*B. juncea* Czern.), spinach (*S. oleracea* L.), and pak choi (*B. rapa* var. *chinensis*), were selected based on the highest economic importance globally (Ribera et al., 2021) and the most consumed vegetables in the country (Nurul Izzah et al., 2012). Besides, the conceivable health risks related to dietary exposure to hypothetically harmful metals are determined via the calculations of the hazard index (HI), THQ, EDI, and target cancer risk (TCR).

## MATERIALS AND METHODS

### Materials

Four types of vegetables (about 350 g each) being randomly collected once per week (for three consecutive weeks: 19 October 2022, 26 October 2022, and 2 November 2022) from Pasar Borong Selangor, Seri Kembangan, namely cabbage (*B. oleracea* subsp. *capitata* L.), mustard (*B. juncea* Czern.), spinach (*S. oleracea* L.), and pak choi (*B. rapa* var. *chinensis*). Pasar Borong Selangor is a rapidly growing area in the south region of Selangor and is surrounded by high-density areas (Department of Statistics Malaysia, 2023), as shown in Figure 1. Meanwhile, the selections of sellers were kept constant along these three consecutive weeks of sample collections, which were Lot 167 (spinach and pak choi,  $n = 3$ ), Lot 183 (cabbage,  $n = 3$ ), and Lot 207 (mustard,  $n = 3$ ). After each purchase, all samples were put into a clean plastic bag, sealed, and immediately brought to the laboratory for further processing.

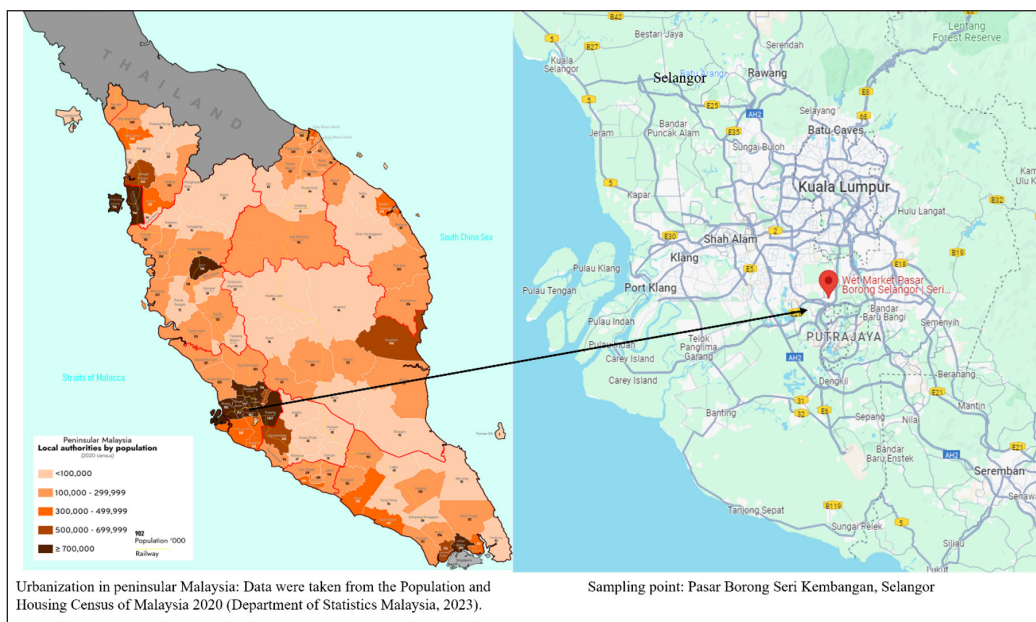


Figure 1. Selangor and sampling point (Pasar Borong, Seri Kembangan)

## Sample Preparation

Bruised or rotten portions of the vegetables were eliminated, and the edible parts were utilized (Aweng et al., 2020; Gebeyehu & Bayissa, 2020). The freshly collected edible parts of samples were washed in running water to remove the adsorbed dust and particulate matter, followed by three washings with distilled water in the laboratory to prevent contamination. Consequently, the samples were dried using the tissue papers. The samples were cut into smaller pieces using a clean knife; then, at about 400 g of cut, samples were stored in the small airtight polyethene bags and kept in a low-temperature freezer (Fisher Scientific, USA) until digestion and analysis. All samples were analysed for the targeted heavy metals (Al, Cd, Cr, Cu, Fe, and Pb).

## Digestion Procedures

The optimization procedures were adopted from Gebeyehu and Bayissa (2020), wherein a mixture of 9 ml of nitric acid ( $\text{HNO}_3$ ) and 3 ml of hydrochloric acid (HCl) (Fisher Scientific, USA) was utilized during digestion for 45 min under pressure and at a temperature of 80 W and  $180^\circ\text{C}$ , respectively. In a microwave digestion vessel, 0.5 g of homogenized vegetable sample was placed with 9 ml of 10 M  $\text{HNO}_3$  and 3 ml of 10 M HCl. The vessels were firmly sealed and positioned in the batch microwave digestion system (MARS<sup>TM</sup> 6, United Kingdom), and digestion was performed at  $180^\circ\text{C}$  for 45 min until a colourless solution was obtained. The transparent and colourless solution obtained was filtered



through the Whatman No. 42 filter paper. Subsequently, the analysis of heavy metals using inductively coupled plasma—optical emission spectrometry (ICP–OES, Avio 550 Max, United Kingdom) was immediately conducted using the prepared solutions after adjustment using 2% of HNO<sub>3</sub>. The digestion and analysis were repeated three times. The results are presented as mean ± standard deviation. Similar steps were taken to prepare the 1,000 ppm stock standard solutions in accordance with the defined ideal circumstances, and they were then examined.

### Heavy Metal Analysis

The concentrations of Al, Cd, Cr, Cu, Fe, and Pb in the samples were determined using the ICP–OES, which integrated with high throughput system (HTS) (PerkinElmer, United Kingdom) — a distinctive flow injection sample introduction segment. A workflow-based software —Syngistix™ for ICP Software was adopted to support customized reporting capabilities for diverse peripherals. For the instrument adjustment conditions, a peristaltic pump, operating at a flow rate of 2.5 ml/min through Tygon-type PVC peristaltic pump tubes, was employed to introduce the digested sample into the ICP–OES system. The ICP-OES system was powered at 1,400 W, with the radiofrequency generator operating at 40 MHz. The argon gas flow rates were set at 0.73 L/min for the nebulizer, 0.8 L/min for the auxiliary, and 13 L/min for the plasma. All analyses were conducted weekly (for three consecutive weeks) after the appropriate calibration of the instrument by calibration blank. All calibration techniques were assessed according to their associated correlation coefficients ( $r^2 \geq 0.998$ ) (Gebeyehu & Bayissa, 2020).

### Health Hazard Assessment

#### *Estimated Daily Intake (EDI)*

The EDI of heavy metals was anticipated using the equation below, as stated by Chen et al. (2011):

$$EDI = \frac{E_f \times E_D \times F_{IR} \times C_M \times C_f}{B_W \times T_A} \times 0.001 \quad [1]$$

where,  $E_f$  = exposure rate (365 days of whole year);  $E_D$  = exposure period (65 years — equivalent to average lifetime) (Woldetsadik et al., 2017);  $F_{IR}$  = average vegetable consumption (240g/person/day for low fruit and vegetables intake) (WHO, 2002);  $C_M$  = metal concentration (mg/kg for dry weight);  $C_f$  = 0.085 (concentration conversion factor for fresh to dry vegetable weight) (Harmanescu et al., 2011);  $B_W$  = 70 kg (reference body weight for an adult) (Woldetsadik et al., 2017);  $T_A$  = average exposure time (65 years × 365 days); 0.001 = unit conversion factor.

### ***Target Hazard Quotient (THQ)***

Various biomagnifying pollutants have both cancer-causing and non-cancerous impacts on human bodies (Hussain et al., 2022). The THQ is adopted to evaluate non-carcinogenic impacts (Agoro et al., 2020). The evaluation of potential non-carcinogenic health risks to the population resulting from the vegetable intake that was contaminated with heavy metals was conducted by determining the THQ using the equation described by Chen et al. (2011):

$$THQ = \frac{EDI}{RfD} \quad [2a]$$

where, *EDI* = estimated daily meal intake of the population (mg/day/kg body weight); *RfD* = oral reference dose (mg/kg/day) values for all metals determined.

The likelihood of non-carcinogenic consequences is generally low if the THQ value is less than one. In other words, the exposed population is unlikely to encounter apparent adverse effects. If the THQ value is more than one, it is generally assumed that non-carcinogenic effects are possible. As the value increases, the possibility also heightens (Antoine et al., 2017).

The following equation is used to calculate the *RfD* as stated by the United States Environmental Protection Agency (US EPA) (1993):

$$RfD = \frac{NOAEL}{(UF \times MF)} \quad [2b]$$

where, *NOAEL* = no-observed-adverse-effect-level (mg/kg/day); *UF* = standard uncertainty factor (*UF* = 10-fold factor); *MF* = modifying factor (*MF* = 1).

Values of *RfD* for each metal of relevance adopted for the calculation of THQs was Al: 1, Cd: 0.001 (Antoine et al., 2017), Cr: 0.003 (Chang et al., 2014), Cu: 0.04, Fe: 0.7 (Javed & Usmani, 2016), and Pb: 0.0035 (Chang et al., 2014) in mg/kg/day.

### ***Hazard Index (HI)***

The hazard index (HI) is the accumulation effect of consuming contaminated vegetables, resulting in the health risks associated with heavy metals (Esmaeilzadeh et al., 2019). The HI of individual heavy metals was calculated using the equation as follows by Antoine et al. (2017) (Equation 3):

$$HI = \sum_{n=1}^i THQ_n; i = 1,2,3, \dots, n \quad [3]$$

where, *HI* = cumulative of all potential pollution risks.

When the HI value is less than one, it indicates that the exposure to the heavy metal appears to have no negative impacts on health. If the HI value is more than one, it shows

the possible health effect consequence. If HI is greater than 10, it suggests a significant chronic health implication (Esmailzadeh et al., 2019; Gebeyehu & Bayissa, 2020).

### **Target Cancer Risk (TCR).**

The TCR refers to the population's cancer risk due to the consumption of specific metals. The was determined using the equation delineated by Gebeyehu and Bayissa (2020):

$$CR = EDI \times CPS_0 \quad [4]$$

where,  $EDI$  = estimated daily metal ingestion of the populace in mg/day/kg;  $CPS_0$  = oral cancer slope factor in (mg/kg/day)

The cancer slope factor is established when evaluating the quantitative risk of substances or agents considered carcinogens. It serves as a gauge of the likelihood of developing cancer after being exposed to a chemical throughout a lifespan. It is often expressed in terms of the percentage of the population impacted per milligrams of substance per kilogramme of body weight per day (expressed in units of reciprocal dose (mg/ kg/ day)<sup>-1</sup> (Farris & Ray, 2014). As the carcinogenic potential of Al and Fe has not been established, only the CR values for Pb, Cd, Cu, and Cr were calculated to assess their carcinogenic effects (US EPA, 2010). The  $CPS_0$  values adopted for CR calculation were Cd: 0.38 (Yang et al., 2018), Cr: 0.5 (Zeng et al., 2015), Cu: 1.7 (Soumaoro et al., 2021), Pb: 0.0085 (Kamunda et al., 2016) in (mg/kg/day).

The target cancer risk (TCR) from the consumption of heavy metals such as Cd, Cr, Cu, and Pb was assessed using the equation provided by Kamunda et al. (2016) as follows:

$$TCR = \sum_{n=1}^i CR; i = 1, 2, 3, \dots, n \quad [4b]$$

where,  $n$  = number of heavy metals taken into account for cancer risk calculation.

### **Statistical Analysis**

The experimental results were analysed using Minitab software (Minitab Version 21.1), and the confidence level was fixed at 95%. The mean and standard deviation (SD) of each heavy metal in vegetable samples were calculated and expressed as milligrams per kilogram fresh weight (FW) of the composite samples. The acquired data were subjected to a one-way analysis of variance (ANOVA) analysis and Pearson's correlation test, respectively, to compare the mean concentration of heavy metals between the selected leafy vegetables and determine their correlation level. Pearson's correlation test was performed to identify potential causative factors of heavy metal pollution and how specific the heavy metals affect their contents.

## RESULTS AND DISCUSSION

### Heavy Metal Analysis

The present study investigated heavy metal concentrations in leafy vegetables and their health risks. Based on the results in Table 1, the mean levels of Al in cabbage, mustard, spinach, and pak choi were  $11.12 \pm 3.76$ ,  $28.97 \pm 5.33$ ,  $41.37 \pm 8.53$ , and  $25.69 \pm 6.32$  mg/kg, respectively. The values of Al metals obtained revealed a statistically significant difference ( $p < 0.05$ ) between mustard, cabbage, and pak choi (Table 1). As no information is available for Al standards on vegetable values in Malaysia, this study adopted the provisional tolerable weekly intake (PTWI) for Al metal of 2 mg/kg introduced by the Joint Food and Agriculture Organization (FAO) and World Health Organization (WHO) Expert Committee on Food Additives (JECFA) in June 2011 (Food and Agriculture Organization of the United Nations & World Health Organization [FAO/WHO], 2011).

Among the leafy vegetables tested, spinach contains the greatest amount of Al (41.37 mg/kg). The results indicated that spinach is more capable of taking in hazardous substances and heavy metals from the rhizosphere and transforming them into palatable sections than other fruits and root vegetables (Bashir et al., 2020). This finding was in line with Ghasemidehkordi et al. (2018), who reported the highest Al value of 37.19 mg/kg in

Table 1

*Heavy metals concentration (mg/kg fresh weight) in leafy vegetables collected from a wet market in Seri Kembangan, Selangor*

Metals	Mean levels of heavy metals (mg/kg fresh weight)				Allowable levels (mg/kg)	
	Cabbage	Mustard	Spinach	Pak choi	Malaysia	FAO/WHO
Al	$11.12 \pm 3.76^a$	$28.97 \pm 5.33^a$	$41.37 \pm 8.53^{ab}$	$25.69 \pm 6.32^b$	N/A	2.0 <sup>B</sup>
Cd	ND	ND	ND	ND	1.0 <sup>A</sup>	0.2 <sup>B</sup>
Cr	ND	ND	ND	ND	N/A	2.3 <sup>C</sup>
Cu	ND	ND	ND	ND	N/A	73.3 <sup>B</sup>
Fe	$6.30 \pm 5.78^a$	$4.12 \pm 1.84^a$	$13.59 \pm 4.73^b$	$4.14 \pm 0.31^a$	N/A	425.5 <sup>B</sup>
Pb	ND	ND	ND	ND	N/A	0.3 <sup>B</sup>

*Note.* Results are presented in mean  $\pm$  standard deviation

Al = Aluminium; Cd = Cadmium; Cr = Chromium; Cu = Copper; Fe = Iron; Pb = Lead

ND = Not detected; N/A = Not available in Malaysia Food Regulation 1985, Fourteenth Schedule (Regulation 38) Table 1 (Malaysia & International Law Book Services, 2019)

The detection limits for Cd and Pb were  $<0.004$  mg/kg, while for Cr and Cu were  $<0.01$  mg/kg

Means in the same row with different superscript letters are significantly different ( $p < 0.05$ ) after comparing the mean levels of heavy metals among different leafy vegetables using parametric one-way analysis of variance and Tukey's honestly significant difference tests at 95% confidence level

<sup>A</sup> – Malaysia Food Regulations 1985, Fourteenth Schedule (Regulation 38) Table 1 (Malaysia & International Law Book Services, 2019)

<sup>B</sup> – Joint Food and Agriculture Organization of the United Nations & World Health Organization Expert Committee on Food Additives (JECFA), June 2011 (FAO/WHO, 2011)

<sup>C</sup> – Food and Agriculture Organization of the United Nations & World Health Organization (FAO/WHO, 2014)

spinach when compared to other vegetables, including fenugreek, parsley, cress, allium, radish, tarragon, and coriander, collected from the agricultural sites in Iran. Similarly, these results are like those previously reported by Martín-León et al. (2023), in which spinach, lettuce, and chard were classified as having a high Al content (41.94 mg/kg).

Al is the third most prevalent metal in the crust, accounting for 7-8% of its mass, after oxygen and silicon (Muhammad et al., 2019). The presence of Al is easily flagged in all life forms as it is an integral part of mineral soils (Rahman et al., 2018). However, active Al ions are hazardous to plants, specifically to root tip meristem, by constraining root elongation. In humans, dietary exposure to Al accumulates in the organ tissues, increasing the risk for hypertension and vascular dysfunctions (Martinez et al., 2017). In acidic soils with low pH (4.3), Al is solubilized into hydrated metal ion salt  $[Al(H_2O)_6]^{3+}$ , which is commonly denoted to aluminium cation ( $Al^{3+}$ ).  $Al^{3+}$  is the most toxic form, enormously influencing plant growth and development (Singh et al., 2017). The soil pH was not assessed in the present study; therefore, the impact of soil pH could not be confirmed.

The mean levels of Fe in cabbage, mustard, spinach, and pak choi were  $6.30 \pm 5.78$ ,  $4.12 \pm 1.84$ ,  $13.59 \pm 4.73$ , and  $4.14 \pm 0.31$  mg/kg, respectively (Table 1). Among these, spinach had the highest concentration of Fe metal ( $p < 0.05$ ). As Fe levels in vegetables have yet to be regulated in Malaysia Food Regulations 1985 [Fourteenth Schedule (Regulation 38) Table 1], thus this study solely compared the stipulated limits by FAO/WHO for Fe metal of 425.50 mg/kg (FAO/WHO, 2011). The information presented in Table 1 shows that the concentration of Fe in all examined vegetables falls below the permissible limits. Dark green leafy vegetables are a good source of iron, particularly the non-haem form, with spinach containing the highest amount ranging from 400 to 500 mg/kg (National Coordinating Committee on Food and Nutrition [NCCFN], 2017). The lower amount of iron detected in the present study could be attributed to the crops' limited iron absorption from the soil. It has been previously reported that excessive carbonate and calcium levels can increase soils' pH levels (Kasowska et al., 2018), decreasing iron solubility. This limitation in iron uptake by the plant roots and various plant parts, including leaves, may occur despite ample iron in the soil.

These findings are consistent with those of Akhtar et al. (2022), who reported higher levels of iron than the maximum permissible level in soil in District Sargodha, irrigated with urban wastewater. However, the iron concentrations in crop samples were lower than the limit, ranging from 4.09 to 32.58 mg/kg. Consistent with the literature, the mean Fe levels of the studied vegetables were within a similar range. In addition to excessive use of chemical fertilizers and pesticides, consistent use of sewage water for irrigation can also lead to the build-up of heavy metals in plants (Sandeep et al., 2019). Fe can produce hydroxyl radicals that are detrimental to DNA, proteins, and lipids, which eventually lead to cell death, known as ferroptosis (McMillen et al., 2022). In humans, shortcomings

associated with Fe overload increase the risk of bacterial infection and cardiomyopathy (Dasa & Abera, 2018). Fe builds up in the liver, causing fibrosis, cirrhosis, and damage to liver function, resulting in complications and death if left untreated (NCCFN, 2017).

As shown in Table 1, cadmium (Cd) was not detected in all tested leafy vegetables (cabbage, mustard, spinach, and pak choi), suggesting safe consumption. The WHO (2019) classified Cd as a human carcinogen. According to FAO/WHO (2014), leafy vegetables containing Cd at levels higher than 0.20 mg/kg represent a major risk to human health. Different plant types and genotypes have varying capacities for Cd absorption, transport, and accumulation (Zhao et al., 2023). In general, more heavy metals were retained in the root portion of the plant as opposed to the leaves, as Sulaiman et al. (2020) reported. The metal binding site in roots was more effective at absorbing heavy metals as compared to leaves (Sagagi et al., 2022). Dietary Cd intake due to ingestion of ecologically polluted rice and other foods was related to an augmented risk of postmenopausal breast cancer (Itoh et al., 2013). As soon as in the human body, it can persist in metabolism for 16 to 33 years, as has been correlated with many health issues, including kidney damage and atypical urinary protein excretion disorders in the liver, kidney, testicles, pancreas, and bones (Fu & Xi, 2020).

In the present study, Cr metals in all leafy vegetables (cabbage, mustard, spinach, and pak choi) were lesser than the detection limit of 0.01 mg/kg — not detected (ND) (Table 1). Simultaneously, the metal content was lower than the allowable limit by FAO/WHO (2011) of 2.3 mg/kg (for leafy vegetables). According to Oliveira (2012), plants should have a Cr content of less than 0.001 mg/kg under normal circumstances. Therefore, the results indicated that these vegetables are fit for human consumption. These results reflect those of Khairiah et al. (2002), who also found that Cr content in black mustard (*Brassica nigra*) and water spinach (*Ipomoea aquatica*) was very low at their sampling locations in Sepang and Bangi, Selangor. Cr metal was also not detected in spinach and coriander leaves irrigated using wastewater in Allahabad, India (Chandel & Bharose, 2020).

Most investigations have revealed that even when growth is restricted to dangerous levels, Cr in plants is less than 1 to 2 mg/kg (dry weight). The increase in the contents of Cr in roots may be due to the defensive measure of Cr sequestration in the vacuoles of root cells (Mangabeira et al., 2011). The concentration of Cr translocated from the roots towards the aerial shoots is rather low, which relies on the chemical form of Cr in the tissue (Shahid et al., 2017). Consequently, this mechanism gives plants some built-in resistance to Cr toxicity. Besides, Cr is essential for insulin action and DNA transcription in organisms, specifically humans (Ametepey et al., 2018).

The present study found that (Cu) content in various leafy vegetables such as cabbage, mustard, spinach, and pak choi was consistently below the detection limit (< 0.01 mg/kg). It suggests that these vegetables do not present an immediate threat to human health in terms of copper toxicity. Notably, the levels detected were significantly lower than the

established safety limit of 73.3 mg/kg suggested by Mensah et al. (2009). However, it is important to acknowledge that current regulations in Malaysia, specifically under the Food Regulations 1985, do not address copper content in food, highlighting a potential regulatory gap that may warrant attention.

Copper, a vital trace element, plays essential roles in plant physiology and human health. It serves diverse functions in plants, including electron transport during photosynthesis, hormone signalling, and cell wall metabolism. Cu overload leads to oxidative stress in plants via the augmentation in the generation of reactive oxygen species (ROS). Cu necessitates an intricate absorption, sequestration, and transportation system due to its dual nature (essential and possibly detrimental) (Mir et al., 2021). However, excessive accumulation of copper can induce oxidative stress, impacting plant health. Similarly, copper is crucial for various physiological processes in humans, but deficiency and excess can lead to adverse health effects such as gastrointestinal discomfort and liver damage. Copper is an indispensable component, although evidence has shown that larger concentrations can have harmful impacts, and overexposure (200 mg/kg) can lead to fatality (FAO/WHO, 2011).

The Pb contents of the leafy vegetables were also under the detection limits ( $< 0.004$  mg/kg) (Table 1). The fact that all Pb concentrations for all vegetable samples were less than the permissible limits of 0.3 and 2.0 mg/kg (FAO/WHO, 2014) indicated that these vegetables are relatively fit for human consumption. This study supports evidence from previous observations on leafy vegetables, whereby Pb metal was not detected in smooth amaranth (Ogunkunle et al., 2014), kale, lettuce, and watercress (Thang et al., 2021), as well as tarragon, parsley, and celery (Bora et al., 2022). In contrast, Martín-León et al. (2023) found that spinach contains the highest concentration of Pb compared to other studied green leafy vegetables, such as lettuce and chard.

Due to phosphate and carbonate precipitation controlling the solubility of Pb metal, Pb was the slightest concentrated in the plants (Li et al., 2021). Plant roots may accumulate phosphate or carbonate from fertilizer solutions or the ditch where the plants were dug up (Xia & Ma, 2006). Owing to physical obstacles in roots that prevent metal from travelling to the aerial regions, Lu et al. (2004) also noted that stems and leaves accumulate heavy metals at lower rates than roots of the water hyacinth. Furthermore, high metal concentrations in the roots suggest it could filter out heavy metals via rhizofiltration (Sulaiman et al., 2020).

Pb is one of the most accumulative metals that can penetrate the body system via food, water, and air, and it cannot be easily eliminated by washing produce (Collin et al., 2022). Some plants have elevated amounts of Pb, which could have been caused by pollution in irrigation water, agricultural soil or public road traffic (Shetty et al., 2023). Pb poisoning can impact the kidneys and nervous system, as most doctors reported that acute lead exposure can result in anaemia, which in turn causes heme suppression and red blood cell destruction (Fu & Xi, 2020).

In brief, Cd, Cr, Cu, and Pb were not detected in cabbage, mustard, spinach, and pak choi. Therefore, the overall levels of aluminium accumulated in leafy vegetable samples followed the order of spinach > mustard > pak choi > cabbage, while the concentrations of iron in leafy vegetable samples followed the order of pak choi > cabbage > spinach > mustard. It is worth mentioning here that leafy vegetables have a greater tendency for heavy metal accumulation than fruiting and tuber vegetable varieties. This statement is in line with the research findings revealed by Sultana et al. (2022) and Xu et al. (2022), which showed that Leafy vegetables typically contain higher concentrations of heavy metals compared to non-leafy vegetables.

## Health Hazard Assessment

### *Estimated Daily Intake (EDI) of Heavy Metals*

In this study, the adult population's estimated daily intake (EDI) of heavy metals was determined by calculating the average metal concentrations in each leafy vegetable. The results were compiled in Table 2. For cabbage, the EDI values for Al and Fe were  $3.241 \times 10^{-3}$  and  $1.816 \times 10^{-3}$  mg/day, respectively, based on a consumption rate of 240 g/day. However, the Pb Cr, Cd, and Cu concentrations were below the detection limits (ND). Thus, their corresponding EDI values resulting from the consumption of the selected leafy vegetables were not available (NA).

Table 2

*Estimated daily intake (EDI) (mg/day/kg) of toxic metals for the adult population due to the consumption of leafy vegetables*

Metals	EDI values (mg/day/kg)				Total EDI via consumption of selected leafy vegetables (mg/day/kg)	Maximum tolerable daily intake (mg/day)
	Cabbage	Mustard	Spinach	Pak choi		
Al	$3.241 \times 10^{-3}$	$8.443 \times 10^{-3}$	$12.056 \times 10^{-3}$	$7.487 \times 10^{-3}$	$3.123 \times 10^{-3}$	1 <sup>D</sup>
Cd	ND	ND	ND	ND	N/A	0.02 – 0.07 <sup>A, B, C, D</sup>
Cr	ND	ND	ND	ND	N/A	0.035 – 0.2 <sup>A, C</sup>
Cu	ND	ND	ND	ND	N/A	2.5 – 3 <sup>B, C</sup>
Fe	$1.816 \times 10^{-3}$	$1.201 \times 10^{-3}$	$3.961 \times 10^{-3}$	$1.206 \times 10^{-3}$	$8.184 \times 10^{-3}$	2 – 5 <sup>A, C</sup>
Pb	ND	ND	ND	ND	N/A	0.21 <sup>A</sup>
Total	0.005057	0.009644	0.01602	0.008693	0.03941	

*Note.* Al = Aluminium; Cd = Cadmium; Cr = Chromium; Cu = Copper; Fe = Iron; Pb = Lead  
 ND = Not detected; N/A = Not available in Malaysia Food Regulation 1985, Fourteenth Schedule (Regulation 38) Table 1 (Malaysia & International Law Book Services, 2019).

The detection limits for Cd and Pb were <0.004 while for Cr and Cu were <0.01

<sup>A</sup> – The maximum tolerable daily intake is based on the values reported by Shaheen et al. (2016)

<sup>B</sup> – The maximum tolerable daily intake is based on the values reported by Zheng et al. (2007)

<sup>C</sup> – The maximum tolerable daily intake is based on the values reported by Naser et al. (2012)

<sup>D</sup> – European Food Safety Authority (EFSA) (2013)



The EDI of heavy metals linked to the consumption of cabbage follows a descending pattern as  $Al > Fe > Cd > Cr > Cu > Pb$ . Meanwhile, the EDI values for Al and Fe metals owing to the identical amount of consumption of mustard were  $8.443 \times 10^{-3}$  and  $1.201 \times 10^{-3}$  mg/day, respectively. The EDI of corresponding heavy metals obtained by eating mustard followed a descending sequence as  $Al > Fe > Cd > Cr > Cu > Pb$ . For a 240 g/day consumption of spinach, the EDI values for Al and Fe metals were found to be  $12.056 \times 10^{-3}$  and  $3.961 \times 10^{-3}$  mg/day. Similarly, the intake of these metals is based on spinach consumption in the declining sequence as  $Fe > Al > Cd > Cr > Cu > Pb$ . Furthermore, the EDI values for Al and Fe metals resulting from the consumption of pak choi at a rate of 240 g/day were  $7.487 \times 10^{-3}$  and  $1.206 \times 10^{-3}$  mg/day, respectively. The EDI of heavy metals from pak choi consumption exhibited a descending order as follows:  $Al > Fe > Cd > Cr > Cu > Pb$ .

The EDI of both Al and Fe metals observed in this work due to the 240 g/day consumption of cabbage, mustard, spinach, and pak choi are less than the maximum tolerable daily intake (MTDI) of each metal reported by the previous research (Basha et al., 2014; Shaheen et al., 2016; Zheng et al., 2007). In a recent study, the EDI of aluminium from spinach was the highest, contributing 12 and 4% to the toxic reference value for adults and children, respectively (Martín-León et al., 2023). It suggests that chronic exposure, even at very small concentrations, might negatively affect health, especially at the early stages of the lifecycle. According to Hussain et al. (2022), though heavy metals have lower EDI compared to MTDI, they can pose a variety of *in vivo* effects, both carcinogenic and non-carcinogenic, due to how they accumulate in organisms. Research has indicated that certain heavy metal elements could impair children's spatial learning abilities and indirectly influence their memory (Porru et al., 2024). Moreover, this investigation solely concentrated on cabbage, mustard, spinach, and pak choi to evaluate the potential health hazards to the population within the Seri Kembangan area. It implies that only a portion, rather than the entirety, of the hazards to the population was considered.

### ***Target Hazard Quotient (THQ)***

The correlation between health threats and pollutants depends on the level of exposure and absorption within the human body (Shetty et al., 2023). In this context, the quantity of vegetables ingested, and an individual's weight play pivotal roles in determining the health threats associated with vegetable consumption. Therefore, it is crucial to forecast the exposure levels and assess the health impact of contaminants by considering the exposure routes to the organisms. The THQ was calculated to assess the associated human health risks based on the mean concentration of Pb, Fe, Al, Cu, Cr, and Cd. THQ is an effective tool for assessing the risk level associated with a specific pollutant. When the THQ exceeds one, it indicates a potentially carcinogenic effect on the human body; conversely, a THQ less than one suggests no non-carcinogenic effect (Hussain et al., 2022). The THQ values for the studied leafy

vegetables are shown in Table 3. Notably, the THQs of Al in cabbage, mustard, spinach, and pak choi were  $3.241 \times 10^{-3}$ ,  $8.443 \times 10^{-3}$ ,  $12.056 \times 10^{-3}$ , and  $7.487 \times 10^{-3}$ , respectively. Similarly, the THQs of Fe in cabbage, mustard, spinach, and pak choi were  $2.623 \times 10^{-3}$ ,  $1.716 \times 10^{-3}$ ,  $5.659 \times 10^{-3}$ , and  $1.723 \times 10^{-3}$  respectively. Estimating hazard quotients for metals in the tested leafy vegetables revealed insignificant health threats associated with their ingestion.

The cumulative THQs resulting from the consumption of cabbage, mustard, spinach, and pak choi (GTHQ) for Al and Fe were less than one, with values of 0.03123 and 0.01172, respectively. It clearly indicates that the adult population faces no substantial health risks through the consumption of these metals in general or from the increasing levels of metals specifically found in the leafy vegetables (cabbage, mustard, spinach, and pak choi) consumed and cultivated in the region.

In contrast to our results, Pavlíková et al. (2023) reported that Cd, Zn, and Cr in leafy vegetables, especially lettuce, showed the highest THQ values compared to root and legume vegetables, except for Pb in carrots. It suggests potential adverse health effects of non-carcinogenic diseases due to the consumption of these vegetables. Also, Gupta et al. (2021) previously confirmed that the THQ values greater than one for Pb and Cd carcinogenic elements in spinach and carrots. Consistent with previous findings, a recent study conducted in the southern region of Northeast Thailand indicated that the THQ values for Cd, Mn, and Pb in the analyzed spinach exceeded one (Tongprung et al., 2024). Although the present study found no risks associated with the consumption of cabbage, mustard, spinach, and pak choi, regular structured monitoring of irrigation water, soil, and crops is still needed to prevent food chain contamination, especially in the younger segment of the population in the urban area.

Table 3

*Target hazard quotient (THQ) and hazard index to heavy metals due to consumption of leafy vegetables (cabbage, mustard, spinach, and pak choi) for the adult population*

Metals	Target hazard quotient				GTHQ <sup>A</sup>
	Cabbage	Mustard	Spinach	Pak choi	
Al	$3.241 \times 10^{-3}$	$8.443 \times 10^{-3}$	$12.056 \times 10^{-3}$	$7.487 \times 10^{-3}$	0.03123
Cd	ND	ND	ND	N/A	N/A
Cr	ND	ND	ND	N/A	N/A
Cu	ND	ND	ND	N/A	N/A
Fe	$2.623 \times 10^{-3}$	$1.716 \times 10^{-3}$	$5.659 \times 10^{-3}$	$1.723 \times 10^{-3}$	0.01172
Pb	ND	ND	ND	N/A	N/A
Hazard index	0.005864	0.0102	0.01772	0.00921	0.04299

*Note.* Al = Aluminium; Cd = Cadmium; Cr = Chromium; Cu = Copper; Fe = Iron; Pb = Lead

ND = Not detected; N/A = Not available in Malaysia Food Regulation 1985, Fourteenth Schedule (Regulation 38) Table 1 (Malaysia & International Law Book Services, 2019).

The detection limits for Cd and Pb were  $<0.004$ ; while for Cr and Cu were  $<0.01$

<sup>A</sup>Global Target Hazard Quotient (GTHQ) is the total of distinct metals THQ for the selected leafy vegetables

### ***Hazard Index (HI)***

The HI, which accounts for the cumulative effect of consuming different potentially harmful metals from a range of vegetables (Hussain et al., 2022), is depicted in Table 3. The HI values, which represent the cumulative THQ of respective metals for each leafy vegetable analysed (cabbage, mustard, spinach, and pak choi), were found to be less than one, with HI values of 0.005864, 0.0102, 0.01772, and 0.00921, respectively. These values individually indicate acceptable adverse health effects from consuming these non-carcinogenic leafy vegetables. Therefore, the recorded HI suggests that the contribution of heavy metals did not result in an aggregate threat through the intake of these vegetables.

Findings from the present work contradict other authors who found heavy metals, including Pb and Cd, significantly contributed to higher HI values (Pavlíková et al., 2023). However, the bioavailability of toxic elements is less than 40%, indicating that a HI value of less than two may not result in a concerning health hazard. Laboni et al. (2023) suggested that humans are exposed to chronic hazards when the HI value is more than 10. Vegetables exhibiting elevated HI values typically indicate significant health risks for consumers. Variations in heavy metal intake, individual body weight, and duration of exposure largely account for the differences in THQ values (Ametepey et al., 2018).

A great deal of previous research has been conducted on the health risk assessments of vegetables, which takes into consideration both the total and bioaccessibility of heavy metals. The effects of consuming vegetables from roadside open-air markets faced by the population in Johannesburg, South Africa, were recently studied by Adhikari and Struwig (2024). The authors concluded that the residents were at high risk of cancer when consuming both washed and unwashed leafy vegetables from the local markets, likely due to the deposition of dust containing hazardous elements (Cd, Ni, Cr, Hg, and Pb). These results are consistent with those reported by Tajdar-Oranj et al. (2024), in which the daily consumption of parsley, coriander, dill, and cress from the local market in Tehran, Iran, contaminated with Cd posed a high health risk. Likewise, the population in the Příbram district of the Czech Republic had a high risk of cancer from consuming vegetables when lead-silver mining activities in the area caused the deposition of toxic elements in the atmosphere (Pavlíková et al., 2023). Collectively, these studies outline the critical role of researchers and local authorities in continuous studies and monitoring to prevent adverse health effects due to heavy metals from the daily consumption of leafy vegetables.

It is crucial to note that the HI, THQ, and EDI values in this study were calculated based on the assumed daily intake of selected leafy vegetables: 240 g for cabbage, mustard, spinach, and pak choi. Consequently, it is possible that the EDI and THQ values reported were underestimated, which may also have affected the HI values. It should be noted that this study solely considered cabbage, mustard, spinach, and pak choi while estimating potential health threats, such as carcinogenic and non-carcinogenic effects, for the adult

population. Since only a portion of the population was included in the study's findings, there is a possibility that the health threats associated with heavy metal exposure from consuming selected leafy vegetables may have been underestimated.

## CONCLUSION

The current study indicates that the levels of heavy metals, namely, lead, iron, copper, aluminium, chromium and cadmium, in the selected leafy vegetables (cabbage, mustard, spinach, and pak choi) are within permissible limits established by both local and international regulatory. Furthermore, as evaluated by the HI, the combined non-carcinogenic impacts of various heavy metals were below one, indicating either the absence or reduced significant health risks associated with consuming these leafy vegetables. Based on these findings, it can be inferred that consuming cabbage, mustard, spinach, and pak choi poses low potential health risks. However, regular monitoring conducted by relevant authorities can help mitigate the health risks associated with consuming vegetables contaminated with heavy metals. Chronic exposure to multiple heavy metals from daily vegetable consumption may lead to adverse health effects, especially for consumers at early stages of their lifecycle, such as children. It is recommended that people vary their vegetable intake to fulfill daily vegetable consumption requirements in their diet while simultaneously decreasing their exposure to and accumulation of both carcinogenic and non-carcinogenic contaminants. Further investigations are warranted to thoroughly examine the health threats related to the daily consumption of leafy vegetables among the local population, especially focusing on vulnerable groups. Future research could focus on increasing the variety of vegetables and assessing comprehensive health risks among the population nationwide.

## ACKNOWLEDGEMENTS

The authors acknowledge the financial support from the Ministry of Higher Education (MOHE) [LRGS/1/2019/UKM-UPM/5/4] and the facilities provided by the Faculty of Food Science and Technology, Universiti Putra Malaysia, for conducting the research.

## REFERENCES

- Adhikari, S., & Struwig, M. (2024). Concentrations and health risks of selected elements in leafy vegetables: A comparison between roadside open-air markets and large stores in Johannesburg, South Africa. *Environmental Monitoring and Assessment*, 196, 170. <https://doi.org/10.1007/s10661-023-12283-6>
- Agoro, M. A., Adeniji, A. O., Adefisoye, M. A., & Okoh, O. O. (2020). Heavy metals in wastewater and sewage sludge from selected municipal treatment plants in Eastern Cape Province, South Africa. *Water*, 12(10), 2746. <https://doi.org/10.3390/w12102746>
- Akhtar, S., Luqman, M., Awa, M. U. F., Saba, I., Khan, Z. I., Ahmad, K., Muneeb, A., Nadeem, M., Batool, A. I., Shahzadi, M., Memona, H., Shad, H. A., Mustafa, G., & Zubair, R. M. (2022). Health risk implications

- of iron in wastewater soil-food crops grown in the vicinity of peri urban areas of the District Sargodha. *PLOS One*, 17(11), e0275497. <https://doi.org/10.1371/journal.pone.0275497>
- Aljohani, A. S. M. (2023). Heavy metal toxicity in poultry: A comprehensive review. *Frontiers in Veterinary Science*, 10, 1161354. <https://doi.org/10.3389/fvets.2023.1161354>
- Ametepey, S. T., Cobbina, S. J., Akpabey, F. J., Duwiejuah, A. B., & Abuntori, Z. N. (2018). Health risk assessment and heavy metal contamination levels in vegetables from Tamale Metropolis, Ghana. *International Journal of Food Contamination*, 5, 5. <https://doi.org/10.1186/s40550-018-0067-0>
- Antoine, J. M. R., Fung, L. A. H., & Grant, C. N. (2017). Assessment of the potential health risks associated with the aluminium, arsenic, cadmium and lead content in selected fruits and vegetables grown in Jamaica. *Toxicology Reports*, 4, 181-187. <https://doi.org/10.1016/j.toxrep.2017.03.006>
- Aweng, E. R., Lim, J. H., Arham Muchtar, A. B., Sharifah Aisyah, S. O., Salam, M. A., & Liyana, A. A. (2020). Concentration of heavy metal in selected vegetables sold in Pasar Siti Khadijah, Kota Bharu, Kelantan, Malaysia. *Solid State Technology*, 63(2s), 3128-3133.
- Basha, A. M., Yasovardhan, N., Satyanarayana, S. V., Reddy, G. V. S., & Kumar, A. V. (2014). Trace metals in vegetables and fruits cultivated around the surroundings of Tummalapalle uranium mining site, Andhra Pradesh, India. *Toxicology Reports*, 1, 505-512. <https://doi.org/10.1016/j.toxrep.2014.07.011>
- Bashir, S., Ali, U., Shaaban, M., Gulshan, A. B., Iqbal, J., Khan, S., Husain, A., Ahmed, N., Mehmood, S., Kamran, M. & Hu, H. (2020). Role of sepiolite for cadmium (Cd) polluted soil restoration and spinach growth in wastewater irrigated agricultural soil. *Journal of Environmental Management*, 258, 110020. <https://doi.org/10.1016/j.jenvman.2019.110020>
- Bora, F. D., Bunea, A., Pop, S. R., Baniță, S. I., Dușa, D. Ș., Chira, A., & Bunea, C.-I. (2022). Quantification and reduction in heavy metal residues in some fruits and vegetables: A case study Galați County, Romania. *Horticulturae*, 8(11), 1034. <https://doi.org/10.3390/horticulturae8111034>
- Chandel, S. S., & Bharose, R. (2020). Evaluation of heavy metal contamination in green leafy vegetables grown in Allahabad. *International Journal of Environment, Agriculture and Biotechnology*, 5(5), 1220-1225. <https://doi.org/10.22161/ijecab.55.5>
- Chang, C. Y., Yu, H. Y., Chen, J. J., Li, F. B., Zhang, H. H., & Liu, C. P. (2014). Accumulation of heavy metals in leaf vegetables from agricultural soils and associated potential health risks in the Pearl River Delta, South China. *Environmental Monitoring and Assessment*, 186, 1547-1560. <https://doi.org/10.1007/s10661-013-3472-0>
- Chen, C., Qian, Y., Chen, Q., & Li, C. (2011). Assessment of daily intake of toxic elements due to consumption of vegetables, fruits, meat, and seafood by inhabitants of Xiamen, China. *Journal of Food Science*, 76(8), T181-T188. <https://doi.org/10.1111/j.1750-3841.2011.02341.x>
- Collin, M. S., Venkatraman, S. K., Vijayakumar, N., Kanimozhi, V., Arbaaz, S. M., Stacey, R. G. S., Anusha, J., Choudhary, R., Lvov, V., Tovar, G. I., Senatov, F., Koppala, S., & Swamiappan, S. (2022). Bioaccumulation of lead (Pb) and its effects on human: A review. *Journal of Hazardous Materials Advances*, 7, 100094. <https://doi.org/10.1016/j.hazadv.2022.100094>
- Dasa, F., & Abera, T. (2018). Factors affecting iron absorption and mitigation mechanisms: A review. *International Journal of Agricultural Science and Food Technology*, 4(2), 24-30. <https://doi.org/10.17352/2455-815X.000033>

- Department of Statistics Malaysia. (2023). *Selangor*. <https://open.dosm.gov.my/dashboard/kawasanku/Selangor>
- Esmacilzadeh, M., Jaafari, J., Mohammadi, A. A., Panahandeh, M., Javid, A., & Javan, S. (2019). Investigation of the extent of contamination of heavy metals in agricultural soil using statistical analyses and contamination indices. *Human and Ecological Risk Assessment: An International Journal*, 25(5), 1125-1136. <https://doi.org/10.1080/10807039.2018.1460798>
- European Food Safety Authority. (2013). Dietary exposure to aluminium-containing food additives. *European Food Safety Authority*, 10(4), 411E. <https://doi.org/10.2903/sp.efsa.2013.EN-411>
- Farris, F. F., & Ray, S. D. (2014). Cancer potency factor. In C. P. Wild (Ed.), *Encyclopedia of toxicology* (pp. 642-644). Academic Press. <https://doi.org/10.1016/B978-0-12-386454-3.00448-6>
- Food and Agriculture Organization of the United Nations & World Health Organization. (2011). *Joint FAO/WHO Food Standards Programme Codex Committee on Contaminants in Foods. CF/5 INF/1, 1-89*. FAO/WHO. <https://iris.who.int/handle/10665/89285>
- Food and Agriculture Organization of the United Nations & World Health Organization. (2014). *General Standard for Contaminants and Toxins in Food and Feed (CXS 193-1995). Joint FAO/WHO Food Standards Programme Codex Committee on Contaminants in Foods*. FAO/WHO. <https://www.fao.org/fao-who-codexalimentarius/thematic-areas/contaminants/en/>
- Fu, Z., & Xi, S. (2020). The effects of heavy metals on human metabolism. *Toxicology Mechanisms and Methods*, 30(3), 167-176. <https://doi.org/10.1080/15376516.2019.1701594>
- Gebeyehu, H. R., & Bayissa, L. D. (2020). Levels of heavy metals in soil and vegetables and associated health risks in Mojo area, Ethiopia. *PLOS One*, 15(1), e0227883. <https://doi.org/10.1371/journal.pone.0227883>
- Ghasemidehkordi, B., Nazem, H., Malekirad, A. A., Fazilati, M., Salavati, H., & Rezaei, M. (2018). Human health risk assessment of aluminium via consumption of contaminated vegetables. *Quality Assurance and Safety of Crops and Foods*, 10(2), 115-123. <https://doi.org/10.3920/QAS2017.1101>
- Gupta, N., Yadav, K. K., Kumar, V., Prasad, S., Cabral-Pinto, M. M., Jeon, B. H., & Alsukaibia, A. K. D. (2022). Investigation of heavy metal accumulation in vegetables and health risk to humans from their consumption. *Frontiers in Environmental Science*, 10(2022), 791052. <https://doi.org/10.3389/fenvs.2022.791052>
- Guo, J., Guo, Y., Yang, J., Yang, J., Zheng, G., Chen, T., Li, Z., Wang, X., Bian, J., & Meng, X. (2020). Effects and interactions of cadmium and zinc on root morphology and metal translocation in two populations of *Hylotelephium spectabile* (Boreau) H. Ohba, a potential Cd-accumulating species. *Environmental Science and Pollution Research*, 27, 21364-21375. <https://doi.org/10.1007/s11356-020-08660-0>
- Harmanescu, M., Alda, L. M., Bordean, D. M., Gogoasa, I., & Gergen, I. (2011). Heavy metals health risk assessment for population via consumption of vegetables grown in old mining area; A case study: Banat County, Romania. *Chemistry Central Journal*, 5, 64. <https://doi.org/10.1186/1752-153X-5-64>
- Hussain, N., Ahmed, K. S., Asmatullah, Ahmed, M. S., Hussain, S. M., & Javid, A. (2022). Potential health risks assessment cognate with selected heavy metals contents in some vegetables grown with four different irrigation sources near Lahore, Pakistan. *Saudi Journal of Biological Sciences*, 29(3), 1813-1824. <https://doi.org/10.1016/j.sjbs.2021.10.043>

- Itoh, H., Iwasaki, M., Sawada, N., Takachi, R., Kasuga, Y., Yokoyama, S., Onuma, H., Nishimura, H., Kusama, R., Yokoyama, K., & Tsugane, S. (2014). Dietary cadmium intake and breast cancer risk in Japanese women: A case-control study. *International Journal of Hygiene and Environmental Health*, 217(1), 70-77. <https://doi.org/10.1016/j.ijheh.2013.03.010>
- Javed, M., & Usmani, N. (2016). Accumulation of heavy metals and human health risk assessment via the consumption of freshwater fish *Mastacembelus armatus* inhabiting, thermal power plant effluent loaded canal. *SpringerPlus*, 5, 776. <https://doi.org/10.1186/s40064-016-2471-3>
- Kamunda, C., Mathuthu, M., & Madhuku, M. (2016). Health risk assessment of heavy metals in soils from Witwatersrand Gold Mining Basin, South Africa. *International Journal of Environmental Research and Public Health*, 13(7), 663. <https://doi.org/10.3390/ijerph13070663>
- Kasowska, D., Gediga, K., & Spiak, Z. (2018). Heavy metal and nutrient uptake in plants colonizing post-flotation copper tailings. *Environmental Science and Pollution Research*, 25, 824-835. <https://doi.org/10.1007/s11356-017-0451-y>
- Khairiah, J., Yin, Y. H., Ibrahim, K. N., Wee, A. W., Aminah, A., Maimon, A., Zalifah, M. K., Giber, G. A. K. (2002). Bioavailability of chromium in vegetables of selected agricultural areas of Malaysia. *Pakistan Journal of Biological Sciences*, 5(4), 471-473. <https://doi.org/10.3923/pjbs.2002.471.473>
- Laboni, F. A., Ahmed, M. W., Kaium, A., Alam, M. K., Parven, A., Jubayer, M. F., Rahman, M. A., Meftaul, I. M., & Khan, M. S. I. (2023). Heavy metals in widely consumed vegetables grown in industrial areas of Bangladesh: A potential human health hazard. *Biological Trace Element Research*, 201, 995-1005. <https://doi.org/10.1007/s12011-022-03179-6>
- Li, X., Huang, S., & McBride, M. B. (2021). Rhizosphere effect on Pb solubility and phytoavailability in Pb-contaminated soils. *Environmental Pollution*, 268(Part B), 115840. <https://doi.org/10.1016/j.envpol.2020.115840>
- Loi, J. X., Chua, A. S. M., Rabuni, M. F., Tan, C. K., Lai, S. H., Takemura, Y., & Syutsubo, K. (2022). Water quality assessment and pollution threat to safe water supply for three river basins in Malaysia. *Science of The Total Environment*, 832, 155067. <https://doi.org/10.1016/j.scitotenv.2022.155067>
- Lu, X., Kruatrachue, M., Pokethitiyook, P., & Homyok, K. (2004). Removal of cadmium and zinc by water hyacinth, *Eichhornia crassipes*. *Science Asia*, 30, 93-103. <https://doi.org/10.2306/scienceasia1513-1874.2004.30.093>
- Malaysia & International Law Book Services. (2019). *Malaysian Food Act 1983 (Act 281) and Regulations 1985*. International Law Book Services. <https://hq.moh.gov.my/fsq/akta-makanan-1983>
- Mallor, C., Bertolín, J. R., Paracuellos, P., & Juan, T. (2023). Nutraceutical potential of leafy vegetables landraces at microgreen, baby, and adult stages of development. *Foods*, 12(17), 3173. <https://doi.org/10.3390/foods12173173>
- Mangabeira, P. A., Ferreira, A. S., de Almeida, A.-A. F., Fernandes, V. F., Lucena, E., Souza, V. L., dos Santos Júnior, Oliveira, A. H., Grenier-Loustalot, M. F., Barbier, F., & Silva, D. C. (2011). Compartmentalization and ultrastructural alterations induced by chromium in aquatic macrophytes. *Biometals*, 24, 1017-1026. <https://doi.org/10.1007/s10534-011-9459-9>

- Martinez, C. S., Piagette, J. T., Escobar, A. G., Martín, Á., Palacios, R., Peçanha, F. M., Vassallo, D. V., Exley, C., Alonso, M. J., Miguel, M., Salaices, M., & Wiggers, G. A. (2017). Aluminium exposure at human dietary levels promotes vascular dysfunction and increases blood pressure in rats: A concerted action of NAD(P)H oxidase and COX-2. *Toxicology*, *390*, 10-21. <https://doi.org/10.1016/j.tox.2017.08.004>
- Martín-León, V., Rubio, C., Rodríguez-Hernández, Á., Zumbado, M., Acosta-Dacal, A., Henríquez-Hernández, L. A., Boada, L. D., del Mar Travieso-Aja, M., & Luzardo, O. P. (2023). Evaluation of essential, toxic and potentially toxic elements in leafy vegetables grown in the Canary Islands. *Toxics*, *11*(5), 442. <https://doi.org/10.3390/toxics11050442>
- McMillen, S. A., Dean, R., Dihadja, E., Ji, P., & Lönnerdal, B. (2022). Benefits and risks of early life iron supplementation. *Nutrients*, *14*(20), 4380. <https://doi.org/10.3390/nu14204380>
- Mensah, E., Kyei-Baffour, N., Ofori, E., & Obeng, G. (2009). Influence of human activities and land use on heavy metal concentrations in irrigated vegetables in Ghana and their health implications. In E. K. Yanful (Ed.), *Appropriate technologies for environmental protection in the developing world* (pp. 9-14). Springer. [https://doi.org/10.1007/978-1-4020-9139-1\\_2](https://doi.org/10.1007/978-1-4020-9139-1_2)
- Mir, A. R., Pichtel, J., & Hayat, S. (2021). Copper: Uptake, toxicity and tolerance in plants and management of Cu-contaminated soil. *Biometals*, *34*, 737-759. <https://doi.org/10.1007/s10534-021-00306-z>
- Mohamad, A., & Kamaludin, F. (2019). *Determination of heavy metal in leafy and fruit vegetables from conventional farms in Kuala Selangor district* [Unpublished Bachelor's dissertation]. Universiti Teknologi Mara.
- Muhammad, N., Zvobgo, G., & Zhang, G.-P. (2019). A review: The beneficial effects and possible mechanisms of aluminium on plant growth in acidic soil. *Journal of Integrative Agriculture*, *18*(7), 1518-1528. [https://doi.org/10.1016/S2095-3119\(18\)61991-4](https://doi.org/10.1016/S2095-3119(18)61991-4)
- Najmi, A., Albratty, M., Al-Rajab, A. J., Alhazmi, H. A., Javed, S. A., Ahsan, W., ur Rehman, Z., Hassani, R., & Alqahtani, S. S. (2023). Heavy metal contamination in leafy vegetables grown in Jazan region of Saudi Arabia: Assessment of possible human health hazards. *International Journal of Environmental Research and Public Health*, *20*(4), 2984. <https://doi.org/10.3390/ijerph20042984>
- Naser, H. M., Sultana, S., Gomes, R., & Shamsun, N. (2012). Heavy metal pollution of soil and vegetable grown near roadside at Gazipur. *Bangladesh Journal of Agricultural Research*, *37*(1), 9-17. <https://doi.org/10.3329/bjar.v37i1.11170>
- National Coordinating Committee on Food & Nutrition. (2017). *Recommended nutrient intakes for Malaysia: A report of the technical working group on nutritional guidelines*. Ministry of Health Malaysia. <https://hq.moh.gov.my/nutrition/wp-content/uploads/2023/12/FA-Buku-RNI.pdf>
- Nurul Izzah, A., Aminah, A., Md Pauzi, A., Lee, Y. H., Wan Rozita, W. M., & Siti Fatimah, D. (2012). Patterns of fruits and vegetable consumption among adults of different ethnics in Selangor, Malaysia. *International Food Research Journal*, *19*(3), 1095-1107.
- Oliveira, H. (2012). Chromium as an environmental pollutant: Insights on induced plant toxicity. *Journal of Botany*, *2012*, 375843. <https://doi.org/10.1155/2012/375843>
- Pavlíková, D., Zemanová, V., & Pavlík, M. (2023). Health risk and quality assessment of vegetables cultivated on soils from a heavily polluted old mining area. *Toxics*, *11*(7), 583. <https://doi.org/10.3390/toxics11070583>



- Porru, S., Esplugues, A., Llop, S., & Delgado-Saborit, J. M. (2024). The effects of heavy metal exposure on brain and gut microbiota: A systematic review of animal studies. *Environmental Pollution*, 348, 123732. <https://doi.org/10.1016/j.envpol.2024.123732>
- Rahman, M. A., Lee, S.-H., Ji, H. C., Kabir, A. H., Jones, C. S., & Lee, K.-W. (2018). Importance of mineral nutrition for mitigating aluminium toxicity in plants on acidic soils: Current status and opportunities. *International Journal of Molecular Sciences*, 19(10), 3073. <https://doi.org/10.3390/ijms19103073>
- Ribera, J. M., Morgades, M., Ciudad, J., Montesinos, P., Esteve, J., Genescà, E., & Orfao, A. (2021). Chemotherapy or allogeneic transplantation in high-risk Philadelphia chromosome-negative adult lymphoblastic leukemia. *Blood, The Journal of the American Society of Hematology*, 137(14), 1879-1894. <https://doi.org/10.1182/blood.2020007311>
- Sagagi, B. S., Bello, A. M., & Danyaya, H. A. (2022). Assessment of accumulation of heavy metals in soil, irrigation water, and vegetative parts of lettuce and cabbage grown along Wawan Rafi, Jigawa State, Nigeria. *Environmental Monitoring and Assessment*, 194, 699. <https://doi.org/10.1007/s10661-022-10360-w>
- Sandeep, G., Vijayalatha, K. R., & Anitha, T. (2019). Heavy metals and its impact in vegetable crops. *International Journal of Chemical Studies*, 7(1), 1612-1621.
- Shaheen, N., Irfan, N. M., Khan, I. N., Islam, S., Islam, M. S., & Ahmed, M. K. (2016). Presence of heavy metals in fruits and vegetables: Health risk implications in Bangladesh. *Chemosphere*, 152, 431-438. <https://doi.org/10.1016/j.chemosphere.2016.02.060>
- Shahid, M., Shamshad, S., Rafiq, M., Khalid, S., Bibi, I., Niazi, N. K., Dumat., C., & Rashid, M. I. (2017). Chromium speciation, bioavailability, uptake, toxicity, and detoxification in soil-plant system: A review. *Chemosphere*, 178, 513-533. <https://doi.org/10.1016/j.chemosphere.2017.03.074>
- Shetty, S. S., Deepthi, D., Harshitha, S., Sonkusare, S., Naik, P. B., Suchetha Kumari, N., & Madhyastha, H. (2023). Environmental pollutants and their effects on human health. *Heliyon*, 9(9), e19496. <https://doi.org/10.1016/j.heliyon.2023.e19496>
- Shi, Z., Yong, L., Liu, Z., Wang, Y., Sui, H., Mao, W., Zhang, L., Li, Y., Liu, J., Wei, S., & Song, Y. (2022). Risk assessment of rare earth elements in fruits and vegetables from mining areas in China. *Environmental Science and Pollution Research*, 29, 48694-48703. <https://doi.org/10.1007/s11356-022-19080-7>
- Singh, S., Tripathi, D. K., Singh, S., Sharma, S., Dubey, N. K., Chauhan, D. K., & Vaculík, M. (2017). Toxicity of aluminium on various levels of plant cells and organism: A review. *Environmental and Experimental Botany*, 137, 177-193. <https://doi.org/10.1016/j.envexpbot.2017.01.005>
- Soumaoro, I., Pitala, W., Gnandi, K., & Kokou, T. (2021). Health risk assessment of heavy metal accumulation in broiler chickens and heavy metal removal in drinking water using *Moringa oleifera* seeds in Lomé, Togo. *Journal of Health Pollution*, 11(31), 210911. <https://doi.org/10.5696/2156-9614-11.31.210911>
- Sulaiman, F. R., Ibrahim, N. H., & Ismail, S. N. S. (2020). Heavy metal (As, Cd, and Pb) concentration in selected leafy vegetables from Jengka, Malaysia, and potential health risks. *Discover Applied Sciences*, 2, 1430. <https://doi.org/10.1007/s42452-020-03231-x>
- Sultana, R., Tanvir, R. U., Hussain, K. A., Chamon, A. S., & Mondol, M. N. (2022). Heavy metals in commonly consumed root and leafy vegetables in Dhaka City, Bangladesh, and assessment of associated public health risks. *Environmental Systems Research*, 11, 15. <https://doi.org/10.1186/s40068-022-00261-9>

- Tajdar-Oranj, B., Javanmardi, F., Parastouei, K., Taghdir, M., Fathi, M., & Abbaszadeh, S. (2024). Health risk assessment of lead, cadmium, and arsenic in leafy vegetables in Tehran, Iran: The concentration data study. *Biological Trace Element Research*, *202*, 800-810. <https://doi.org/10.1007/s12011-023-03707-y>
- Thang, N. Q., Tho, N. T. M., & Phuong, N. T. K. (2021). Nitrate, nitrite, and lead contamination in leafy vegetables collected from local market sites of Go Vap district, Ho Chi Minh City. *Vietnam Journal of Chemistry*, *59*(1), 79-86. <https://doi.org/10.1002/vjch.202000124>
- Tongprung, S., Wibuloutai, J., Dechakhamphu, A., & Samaneein, K. (2024). Health risk assessment associated with consumption of heavy metal-contaminated vegetables: A case study in the southern area of Northeast Thailand. *Environmental Challenges*, *14*, 100845. <https://doi.org/10.1016/j.envc.2024.100845>
- United States Environmental Protection Agency. (1993). *Reference Dose (RfD): Description and use in health risk assessments*. US EPA. <https://www.epa.gov/iris/reference-dose-rfd-description-and-use-health-risk-assessments#1.7>
- United States Environmental Protection Agency. (2010). *Toxics Release Inventory (TRI) national analysis*. US EPA. <https://www.epa.gov/trinationalanalysis>
- Woldetsadik, D., Drechsel, P., Keraita, B., Itanna, F., Erko, B., & Gebrekidan, H. (2017). Microbiological quality of lettuce (*Lactuca sativa*) irrigated with wastewater in Addis Ababa, Ethiopia and effect of green salads washing methods. *International Journal of Food Contamination*, *4*, 3. <https://doi.org/10.1186/s40550-017-0048-8>
- World Health Organization. (2019). *Preventing disease through healthy environments: Exposure to cadmium: A major public health concern*. WHO. <https://iris.who.int/handle/10665/329480>
- Xia, H., & Ma, X. (2006). Phytoremediation of ethion by water hyacinth (*Eichhornia crassipes*) from water. *Bioresource Technology*, *97*(8), 1050-1054. <https://doi.org/10.1016/j.biortech.2005.04.039>
- Xu, Z., Peng, J., Zhu, Z., Yu, P., Wang, M., Huang, Z., Huang, Y., & Li, Z. (2022). Screening of leafy vegetable varieties with low lead and cadmium accumulation based on foliar uptake. *Life*, *12*(3), 339. <https://doi.org/10.3390/life12030339>
- Yang, J., Ma, S., Zhou, J., Song, Y., & Li, F. (2018). Heavy metal contamination in soils and vegetables and health risk assessment of inhabitants in Daye, China. *Journal of International Medical Research*, *46*(8), 3374-3387. <https://doi.org/10.1177/0300060518758585>
- Zeng, F., Wei, W., Li, M., Huang, R., Yang, F., & Duan, Y. (2015). Heavy metal contamination in rice-producing soils of Hunan province, China and potential health risks. *International Journal of Environmental Research and Public Health*, *12*(12), 15584-15593. <https://doi.org/10.3390/ijerph121215005>
- Zhao, J., Yu, B., Wang, X., Chen, L., Akhtar, K., Tang, S., Lu, H., He, J., Wen, R., & He, B. (2023). Differences in the response mechanism of cadmium uptake, transfer, and accumulation of different rice varieties after foliar silicon spraying under cadmium-stressed soil. *Frontiers in Plant Science*, *13*, 1064359. <https://doi.org/10.3389/fpls.2022.1064359>

*Review Article*

## Effects of Different Extraction Methods on Yield, Polyunsaturated Fatty Acids, Antioxidants, and Stability Improvement of Chia Seed Oil: A Review

Izzreen Ishak<sup>1</sup>, Ranil Coorey<sup>3</sup>, Maaruf Abd Ghani<sup>4</sup>, Chin Ping Tan<sup>2</sup>, Nazamid Saari<sup>2</sup> and Norhayati Hussain<sup>1,2\*</sup>

<sup>1</sup>Halal Products Research Institute, Universiti Putra Malaysia, Putra Infoport, 43400 Serdang, Selangor, Malaysia

<sup>2</sup>Faculty of Food Science and Technology, Universiti Putra Malaysia, 43400 Serdang, Selangor, Malaysia

<sup>3</sup>School of Molecular and Life Sciences, Faculty of Science and Engineering, Curtin University, Perth, Western Australia, Australia

<sup>4</sup>Faculty of Fisheries and Food Science, Universiti Malaysia Terengganu, 21030 Kuala Nerus, Terengganu, Malaysia

### ABSTRACT

There has been an increasing trend in the use of chia seed oil (CSO) rich in polyunsaturated fatty acids (PUFA), mainly  $\alpha$ -linolenic and linoleic acids, accompanied by antioxidants like tocopherols, phytosterols, carotenoids and polyphenols, which may benefit to human health. Various conventional (solvent and mechanical pressing) and alternative extractions (supercritical fluid extraction using carbon dioxide and ultrasound-assisted method) have been utilised to extract oil from chia seed based on selected conditions and types of solvent, which affect the oil yield and nutritional composition. Alternative extractions like ultrasound-assisted with solvent (time: 40 min, temperature: 50°C and solvent-to-seed ratio: 12 ml of ethyl acetate/g of chia seed) and supercritical fluid extraction (SFE) using carbon dioxide enriched with 10% acetone (time: 300 min, temperature: 70°C and pressure: 280 bar) can be applied to improve the amount of oil (up to 27.1% and 33.9% for ultrasound-

assisted with solvent and SFE, respectively) and PUFA extracted from the chia seed. SFE is recommended as a highly desirable alternative to traditional methods (Soxhlet and pressing) for extracting tocopherol and phytosterol from CSO. Incorporating acetone with SFE could enhance the number of polyphenols and carotenoids in CSO compared to pure supercritical carbon dioxide. However, CSO is highly susceptible to oxidation due to its high concentration of PUFA (more than 80%). Recent research on the

### ARTICLE INFO

*Article history:*

Received: 07 May 2024

Accepted: 02 July 2024

Published: 28 January 2025

DOI: <https://doi.org/10.47836/pjtas.48.1.13>

*E-mail addresses:*

[izzreen99@gmail.com](mailto:izzreen99@gmail.com) (Izzreen Ishak)

[R.Coorey@curtin.edu.au](mailto:R.Coorey@curtin.edu.au) (Ranil Coorey)

[maaruf@umt.edu.my](mailto:maaruf@umt.edu.my) (Maaruf Abd Ghani)

[tanep@upm.edu.my](mailto:tanep@upm.edu.my) (Chin Ping Tan)

[nazamid@upm.edu.my](mailto:nazamid@upm.edu.my) (Nazamid Saari)

[aryatihussain@upm.edu.my](mailto:aryatihussain@upm.edu.my) (Norhayati Hussain)

\* Corresponding author

nutritional qualities of CSO has explored the impact of improvement techniques to prevent loss of nutritional quality. Therefore, natural antioxidants and blends of vegetable oils have been applied to improve CSO's oxidative stability and shelf life.

*Keywords:* Chia seed oil, conventional extraction, oxidative stability, polyunsaturated fatty acids, supercritical fluid extraction, tocopherols, ultrasonic-assisted extraction

---

## INTRODUCTION

Chia seed (*Salvia hispanica* L.) is originally from Mexico and Guatemala, where it has been consumed for thousands of years (Ixtaina, Mattea, et al., 2011). Countries such as Australia, Argentina, Columbia, America, and Europe have successfully cultivated chia plants and become the largest chia seed producers over the past few years (Grancieri et al., 2019). The high demand for chia seeds is the reason for its continually high share in the global market. Future Market Insights (2023) has estimated that the overall market value for whole chia seed will reach US\$390.3 billion over the prediction period (2023–2033). The demand for chia seeds is predicted to report a 7% Compound Annual Growth Rate (CAGR) (2023–2033), higher than the previous performance (2018–2022) with a CAGR of 2.4% (Future Market Insights, 2023).

Food products enriched with polyunsaturated fatty acids (PUFA) from plant sources have gained customer attention for their significant role in positively affecting human health (Kus-Yamashita et al., 2016). The primary dietary source of PUFA is fish oil, but the current need has led to the overexploitation of certain fish species, impacting global fish stocks (Lenihan-Geels & Bishop, 2016). Furthermore, plant oils are cheaper, have higher oxidation resistance and yield higher than fish oil (Tacon & Metian, 2008). Therefore, vegetable oil is investigated as a sustainable alternative source to fulfil the demand for PUFA worldwide. A higher concentration of PUFA in chia seed oil (CSO) is identified and compared with other known plant food sources. Generally, CSO contains about 63.64%  $\alpha$ -linolenic acid (ALA), 19.84% linoleic acid (LA), 7.07% palmitic acid (PA), 5.5% oleic acid (OA) and 2.81% stearic acid (SA) (Shen et al., 2018). CSO is characterised by their high PUFA content and as a good source of antioxidants (Dąbrowski et al., 2018a; Dąbrowski et al., 2016). The extraction of high-quality CSO is a recent development globally, and the demand for CSO is growing.

Different extraction methods (conventional and alternative) influenced the composition of PUFA, antioxidants and oil yield (Dąbrowski et al., 2016). Vegetable oil extractions use traditional methods, including solvent extraction or Soxhlet, distillation, and mechanical pressing (hot and cold). However, these methods involve long extraction times that could remove antioxidant compounds in the extracted oil (Scapin et al., 2017). As a result, many researchers nowadays seek the latest extraction techniques to solve these matters. Novel vegetable oil extraction methods from different seeds, like supercritical fluid extraction

(SFE) and ultrasound-assisted extractions, have been studied lately (Ferrentino et al., 2020; Senrayan & Venkatachalam, 2020).

Lipid oxidation is one of the chemical reactions contributing to the deterioration of vegetable oil quality (Fruehwirth et al., 2020). Different approaches and processes were carried out to improve CSO's oxidative stability from lipid oxidation. To our knowledge, there is a limited review of the bioactive compounds (PUFA and antioxidants) of CSO extracted by conventional and alternative extraction methods. It is also the first review paper to report the different improvement techniques for the oxidative stability of CSO from lipid oxidation. Therefore, this review has summarised an overview of current research in CSO extraction and its effect on yield, PUFA and antioxidants. Moreover, different techniques for improving CSO stability, such as natural antioxidants and vegetable oil blending against lipid oxidation, are discussed.

Lipid oxidation is one of the chemical reactions contributing to the deterioration of vegetable oil quality (Fruehwirth et al., 2020). Different approaches and processes were carried out to improve CSO's oxidative stability from lipid oxidation. To our knowledge, there is a limited review of the PUFA and antioxidants in CSO extracted by conventional and alternative extraction methods. It is also the first review paper to report the different improvement techniques for the oxidative stability of CSO from lipid oxidation. Therefore, this review summarises the research on CSO extraction and its effect on yield, PUFA, and antioxidants. Moreover, different techniques for improving CSO stability, such as natural antioxidants and vegetable oil blending against lipid oxidation, are discussed.

## **EXTRACTION METHODS OF CHIA SEED OIL**

The extraction process is one of the vital stages in oil production from seeds. The conventional oil extraction processes are mechanical and solvent extraction. Research groups have evaluated the potential of using alternative extraction technologies to improve CSO yield and nutritional value. Table 1 summarises the advantages and drawbacks of various CSO extraction methods.

### **Pressing**

Pressing is a commonly used technique for the industrial production of CSO. Screw pressing is less expensive than solvent extraction because it does not require costly chemicals to squeeze the oil from chia seed (Martínez et al., 2012). In addition, mechanical pressing can be carried out at a low temperature, preserving the PUFA, tocopherols and carotenoids of CSO. However, pressing is slow and laborious and provides incomplete oil extraction production, thus producing a low yield of CSO (Dąbrowski et al., 2016; Fernandes et al., 2019; Ixtaina, Martínez, et al., 2011). Another disadvantage of pressing is that it accelerates the process of CSO oxidation (Ali et al.,

Table 1  
*Advantages and drawbacks of methods to extract chia seed oil*

Extraction method	Advantage	Drawback	References
Pressing	<ul style="list-style-type: none"> <li>• Less expensive than solvent extraction (does not require solvent)</li> <li>• Simple technology</li> <li>• Cold pressing conducted at low temperatures to preserve the quality of the CSO</li> </ul>	<ul style="list-style-type: none"> <li>• Slow and time-consuming</li> <li>• Lower oil yield (20.11%-26.3%) than solvent extraction (19.28%-35.8%)</li> <li>• Produces high peroxide value of oil, especially at a higher temperature</li> </ul>	<p>Fernandes et al. (2019); Dąbrowski et al. (2016); Ali et al. (2012); Martínez et al. (2012); Ixtaina, Martínez, et al. (2011)</p>
Solvent extraction (Soxhlet and Folch)	<ul style="list-style-type: none"> <li>• Extract more lipids than other extraction methods</li> <li>• A straightforward methodology and little training needed</li> <li>• Elevated temperature extracted a higher amount of oil from chia seed</li> </ul>	<ul style="list-style-type: none"> <li>• High flammability and toxicity</li> <li>• Long time for extraction (up to 18 hr)</li> <li>• Large volume of solvent wasted, which causes environmental problems</li> </ul>	<p>Dąbrowski et al. (2016)</p>
Ultrasound-assisted extraction	<ul style="list-style-type: none"> <li>• Better penetration of solvent into cellular materials</li> <li>• Improves extraction yield and PUFA content with shorter extraction time compared to solvent extraction and SFE (without ultrasound-assisted)</li> </ul>	<ul style="list-style-type: none"> <li>• Prolonged sonication may lead to degradation of bioactive compounds and changes in extracted oil from chia seed</li> </ul>	<p>Rosas-Mendoza et al. (2017)</p>
Supercritical fluid extraction (Fluid: carbon dioxide)	<ul style="list-style-type: none"> <li>• Environmentally friendly solvent</li> <li>• Supercritical carbon dioxide (SC-CO<sub>2</sub>) is readily available</li> <li>• SC-CO<sub>2</sub> has a high solvation power and diffusivity for better penetration to extract lipid components (oils and bioactive compounds)</li> <li>• Polar co-solvent (acetone) can be applied together with SC-CO<sub>2</sub> to extract higher oil yield, polyphenols and carotenoids</li> </ul>	<ul style="list-style-type: none"> <li>• Unsuitable for the extraction of polar antioxidants (polyphenols)</li> <li>• Require more expensive equipment than other conventional methods</li> <li>• Lower oil yield (9.5%-33.9%) than Soxhlet extraction</li> </ul>	<p>Bubalo et al. (2018); Dąbrowski et al. (2018b); Bubalo et al. (2015)</p>

2012) due to the high friction force applied during extraction, leading to hydroperoxide formation and triggering oxidative reactions.

A high peroxide value (PV) of 10.98 mEq O<sub>2</sub>/kg oil was observed in CSO obtained by pressing, exhibiting a high vulnerability to lipid oxidation (Fernandes et al., 2019). The result obtained for PV of pressed CSO agreed with those reported by previous authors (Martínez et al., 2012), who found that higher pressing temperatures (50°C–70°C) presented a higher susceptibility towards oxidation compared to lower temperatures (20°C and 30°C). As a result, the PV is higher than those allowed by the Commission Implementing Regulation (EU) 2014, which declares that PV for CSO obtained by cold pressing must not be more than 10 mEq O<sub>2</sub>/kg oil.

The yield of pressed CSO (20.01%–26.3%) was lower than other extraction methods like Soxhlet, SFE and ultrasound-assisted extraction (Dąbrowski et al., 2016; Fernandes et al., 2019; Ixtaina, Martínez, et al., 2011). Based on the oil yield extracted by different mechanical pressing, hot screw pressing conducted at a high temperature (110°C) for 1 hr could maximise the yield of CSO (26.27%) compared to cold pressing without using high temperature (24.1%) (Dąbrowski et al., 2016). However, the different values of CSO yield obtained are not significant ( $p \geq 0.05$ ). It is similar to Martínez et al. (2012), who stated that different pressing temperatures (30°C–70°C) had no significant effect on CSO yield. Pressing temperature negatively affected the peroxide value of the CSO, but the different temperatures did not significantly influence the oil yield.

### Solvent Extraction

The Soxhlet and Folch procedures are the standard methods for total lipid extraction from food materials. Solvent extraction methods are the most effective, with 98% of total oil recovery (Dąbrowski et al., 2016). The different solvents used in extracting CSO include hexane, petroleum ether, acetone and a mixture of chloroform and methanol. Hexane is the most common solvent used for CSO extraction. It is highly effective for vegetable oil extraction due to its high oil recovery, low boiling point temperature (63°C–69°C), and excellent non-polar nature (Liu & Mamidipally, 2005). However, hexane has led to several severe impacts, such as hazardous pollution to the environment, toxicological effects on human health, and residual solvents in the final product (Kumar et al., 2017).

According to their polarity, four solvents were also used to extract CSO in isolating bioactive compounds and oil recovery. These solvents include petroleum ether, chloroform, methanol, and acetone. The oils extracted are strongly affected by the solubility and extractability of lipids in the solvents (Ramluckan et al., 2014). However, less oil yield was obtained from polar solvents due to the difficulty in molecular interaction between substances in the sample matrix and solvent. The yield of CSO from solvent extraction methods was proven to be higher than other alternative extractions (19.28%–36.1%)

(Dąbrowski et al., 2016; Dąbrowski et al., 2018a; Dąbrowski et al., 2018b; Fernandes et al., 2019; Ishak, Ghani, Yuen, 2020; Oteri et al., 2023; Rosas-Mendoza et al., 2017; Shen et al., 2018; Timilsena et al., 2017).

Few studies reported the low yield of CSO obtained using cold extraction without applying the Soxhlet apparatus at room temperature. Low oil recovery of CSO was observed using hexane and petroleum ether (19.28% and 26.6%, respectively) under cold extraction conditions (Fernandes et al., 2019; Timilsena et al., 2017). High oil yield from chia seed (more than 30%) was achieved with hexane under hot extraction conditions using the Soxhlet apparatus. In general, lipids' solubility can be improved with increased temperature by breaking the strong molecular oil interactions and enhancing the extraction rate of oils from the molecule (Ritcher et al., 1996). These findings suggested that the oil from chia seed under hot extraction conditions is more efficient than cold extraction.

### **Ultrasound-assisted Solvent Extraction**

Using ultrasound technology in various food industries has numerous potentials for efficiency, yield and selectivity (Chemat et al., 2017). Ultrasound-assisted extraction (UAE) is the latest technique with many advantages to improve CSO yield. UAE is a rapid method to provide higher extraction oil yield than conventional extraction procedures without using ultrasound-assisted. Generally, ultrasonic power above 20 kHz leads to cavitation, which involves microbubble shock formed by excess vibration and generating pressure until the bubble explodes on the contact surface between the sample matrix and a liquid solvent (Rosas-Mendoza et al., 2017). Thus, such reactions break the sample's cell wall, and the extraction of lipid components into the solvent is enhanced (Chemat et al., 2017).

Applying ultrasound on chia seed samples in ethyl acetate and petroleum ether resulted in significantly higher oil yield than extraction without ultrasound (de Mello et al., 2017; Rosas-Mendoza et al., 2017). The ultrasonic extraction using optimal conditions at 40 min, temperature of 50°C and solvent-to-seed ratio (12 ml of ethyl acetate/g of seed) produced a CSO yield of 27.19% higher than without ultrasound (22.12%) (de Melo et al., 2017). Meanwhile, the extraction oil yield of chia seed is increased by 3.2% after being treated with ultrasonic power at 40 kHz for 90 min compared to the stirring method (Rosas-Mendoza et al., 2017). Therefore, the organic solvents used for CSO extraction assisted by ultrasound treatment are appropriate for replacing hexane. The warming effect during ultrasound treatment also affects the oil recovery from chia seed.

In comparison with the study (de Melo et al., 2017; Rosas-Mendoza et al., 2017), the yield of CSO was slightly higher at hot extraction 50°C (27.19%) compared to cold extraction without heat treatment (25.0%). It shows that using an ultrasound bath, the CSO extraction has improved with increased temperature. An increase in extraction temperature



enhanced the speed rate of microbubble breaking, and this process would promote the penetration of solvent into the cell wall of the sample and increase the extraction rate of lipid compounds into the solvent (Li et al., 2016). Applying ultrasound as a sample pretreatment before SFE is the best option to improve CSO yield for a shorter extraction time. Fernandes et al. (2019) reported that the use of ultrasound treatment on chia seed for 15 min before SFE increased the total oil yield (24.5%) compared with SFE without using ultrasound (22.2%). The authors also examined the different durations of the ultrasound process on chia seed oil extraction at 30 and 60 min, which showed similar oil content of chia seed (24.5%). Extending the extraction time using ultrasound may lead to a decrease or no changes in the CSO yield due to the maximum release of lipid components at the beginning of the extraction. After a certain period, the CSO extraction process was completed. Therefore, using ultrasonic treatment with appropriate extraction time and temperature would improve the CSO recovery using extraction methods.

### **Supercritical Fluid Extraction**

Most SFE has been performed with supercritical carbon dioxide (SC-CO<sub>2</sub>) as a supercritical solvent due to its critical conditions (temperature: 31.1°C and pressure: 73.8 bar), non-explosive, inexpensive, user-friendly and easy to remove from the product. Thus, it can be applied to food (Bubalo et al., 2015). SC-CO<sub>2</sub> has low viscosity and high diffusivity due to the high pressure, which promotes better transport properties by rapidly penetrating the sample molecules, resulting in faster extraction rates than liquids. SC-CO<sub>2</sub> is suitable for extracting less polar compounds like fatty acids (Herrero et al., 2006). The oil content of chia seed extracted by SFE highly varied (9.5%–33.9%) according to the different extraction conditions (Dąbrowski et al., 2018b; Fernandes et al., 2019; Ishak et al., 2021; Ixtaina et al., 2010; Ixtaina, Mattea, et al., 2011).

The extraction pressure is the main parameter that influences the extraction efficiency of CSO, as reported by Ishak et al. (2021), Fernandes et al. (2019), Dąbrowski et al. (2018b), Ixtaina, Vega, et al. (2011) and Ixtaina et al. (2010). Increased extraction pressure typically enhances the desired compound's solubility (Bubalo et al., 2018). An increase in pressure resulted in higher extraction oil yields from chia seed, which is elevated from approximately 3.9% at 150 bar to almost 17.45% at 250 bar (Fernandes et al., 2019). High pressure generally improved the oil yield due to increased SC-CO<sub>2</sub> density (Soh et al., 2018). Higher pressure would then facilitate the oil movement into the surface of the sample matrix (Ghoreishi et al., 2016). Extraction temperature and time also affected the oil recovery from chia seed. At the constant pressure (250 bar), a higher amount of CSO (17.45%) is obtained at a lower temperature (40°C) compared to oil extracted at 60°C (11.96%) (Fernandes et al., 2019). The authors stated that an increase in temperature reduced the SC-CO<sub>2</sub> density, which led to a decrease in the oil yield.

Meanwhile, the yield of CSO improved by 5% after extending the extraction time from 60 to 75 min at constant pressure (250 bar) and temperature (40°C) (Fernandes et al., 2019). The range of extraction time to recover the oil from chia seed based on previous studies is 75–300 min (Dąbrowski et al., 2018b; Fernandes et al., 2019; Ixtaina et al., 2010; Ixtaina, Mattea, et al., 2011; Scapin et al., 2017). The extraction consists of two periods, which include a fast extraction period (initial linear and transition phase) and a slow extraction period (second linear phase) (Ixtaina, Mattea, et al., 2011; Ixtaina et al., 2010). Most CSO extraction mainly occurred in the fast extraction period based on the accumulated extraction curves for oil removal by SC-CO<sub>2</sub> (Ixtaina, Mattea, et al., 2011). The result showed that the total extraction time for CSO extracted by higher pressure (450 bar) at 40°C and 60°C were 135 and 138 min, respectively. In contrast, oil extracted at a lower pressure (250 bar) indicated longer total extraction time at 40°C and 60°C (285 and 423 min, respectively). CSO extracted by the SFE process varied from 9.5% (60 min with SC-CO<sub>2</sub>) to 33.9% (300 min with SC-CO<sub>2</sub> enriched by 10% acetone) with the pressure of 280 bar at 70°C (Dąbrowski et al., 2018b).

An increased extraction time from 60–300 min for pure SC-CO<sub>2</sub> significantly improved CSO yield (9.5%–32.7%). Moreover, acetone yielded more CSO and minimised the extraction time. The extraction enriched with 10% acetone obtained a higher yield of CSO (22.2%) than pure SC-CO<sub>2</sub> (9.5%) at 60 min of extraction time. These findings agree with Fernandes et al. (2019), who reported that the addition of 30% ethanol as a polar co-solvent in the SFE process produced more oil yield (25.10%) than the pure SC-CO<sub>2</sub> (22.24%) for 75 min of extraction. SC-CO<sub>2</sub> polarity has difficulty extracting polar substances (phenolic compounds). Ethanol and acetone are mainly used as co-solvents to improve the polarity of SC-CO<sub>2</sub>, enhancing its solvating power to extract phenolic compounds (Bubalo et al., 2015). Besides that, different particle sizes of ground chia seed influenced the oil extraction using SC-CO<sub>2</sub> (Ishak et al., 2021). The authors reported that intermediate particle sizes of ground chia seed (100–400 µm) based on the grinding time of 10 s has higher surface area (0.0350 m<sup>2</sup>/g) to contact with SC-CO<sub>2</sub> compared to larger particle sizes of ground sample (0.066 m<sup>2</sup>/g), resulting in oil extracted quickly from the surface of the sample matrix. Therefore, the overall fat content of chia seed (9.5%–35.8%) is significantly affected by conditions and parameters employed during oil extraction, such as temperature, solvent type, extraction time, pressure, co-solvent and particle size of the ground sample.

## **EFFECTS OF EXTRACTION METHODS ON POLYUNSATURATED FATTY ACIDS AND ANTIOXIDANTS OF CHIA SEED OIL**

Lipids contain PUFA and antioxidants (phytosterols and tocopherols), which are soluble in non-polar organic solvents but poorly soluble in polar solvents. Polyphenols are the minor antioxidant compounds in CSO. The composition of CSO (fatty acids and antioxidants) is based on the different extraction methods presented in Table 2.

Table 2

*Composition of chia seed oil (fatty acids and antioxidants) based on the different extraction methods*

Composition	Unit	Range (minimum- maximum)	Extraction methods	References
<b>Fatty acids</b>				
Polyunsaturated fatty acids	%	73.69–89.84	Soxhlet (hexane and acetone), petroleum ether extraction using an orbital shaker,	Oteri et al. (2023); Ishak et al. (2021); Ishak, Ghani and Nasri (2020); Dąbrowski et al. (2018a); Shen et al. (2018); Hrnčič et al. (2018); Scapin et al. (2017); Ixtaina, Mattea, et al. (2011)
Saturated fatty acids	%	7.76–16.09	Folch procedure (chloroform and methanol), mechanical pressing (hot and cold), SFE (CO <sub>2</sub> and acetone), ultrasound-assisted extraction	
Monounsaturated fatty acids	%	2.43-10.53		
<b>Antioxidants</b>				
Tocopherols	mg/kg	100–1244	Soxhlet, mechanical pressing (hot and cold) and SFE (SC-CO <sub>2</sub> , acetone and <i>n</i> -propane)	Ishak et al. (2021); Dąbrowski et al. (2018a); Dąbrowski et al. (2018b); Shen et al. (2018); Dąbrowski et al. (2016); Zanqui et al. (2015); Ciftci et al. (2012); Ixtaina, Mattea, et al. (2011); Álvarez-Chávez et al. (2008)
Phytosterols	mg/kg	2272–12600		
Polyphenols	mg/kg	0–172		

*Note.* SFE=Supercritical fluid extraction, SC-CO<sub>2</sub>=supercritical carbon dioxide, UAE=Ultrasound-assisted extraction

### Polyunsaturated Fatty Acids

CSO is recommended as one of the healthiest oils in the market due to its high PUFA content (73.69%–89.84%) which consists of ALA (53.67%–69.3%) and LA (16.6%–23.21%) (Dąbrowski et al., 2018a; Hrnčič et al., 2018; Ishak, Ghani, Nasri, 2020; Ixtaina, Mattea, et al., 2011; Oteri et al., 2023; Scapin et al., 2017; Shen et al., 2018). Furthermore, saturated fatty acids (SFA), including PA (5.5%–11.5%) and SA (0.29%–7.89%), were calculated for 7.76%–16.09% of total fatty acids. The minor concentration of OA (2.43%–10.53%) is classified as monounsaturated fatty acids (MUFA), also present in CSO (Ciftci et al., 2012; Ixtaina et al., 2010; Segura-Campos et al., 2014). The CSO is rich in PUFA with more than 80% regardless of conventional extraction methods (Dąbrowski et al., 2016; Fernandes et al., 2019; Ixtaina, Martínez, et al., 2011).

Cold (conducted at room temperature) and hot mechanical pressing (110°C) showed no significant differences in the fatty acid composition of CSO. The PUFA content in cold-pressed CSO (82.2%) was higher ( $p \geq 0.05$ ) than in hot-pressed CSO (81.7%) (Dąbrowski et al., 2016). Most CSO extracted by different solvent extraction methods (Soxhlet, Folch and mixing) had a level of PUFA (more than 80%). This can be explained by the high operational temperature and solvent recycling related to the higher solute solubility and the interaction of

the sample and the solvent during extraction (Abdolshahi et al., 2015). It was also observed that non-polar solvents such as hexane and petroleum ether are excellent choices for non-polar lipids such as fatty acids. Therefore, the concentration of PUFA was not affected by different methods and solvents with polarity differences used to extract oil from the chia seed.

Applying ultrasound-assisted solvent extraction using ethyl acetate provided higher PUFA content in CSO than other extraction methods. The results showed that UAE extracted 82% PUFA content with less solvent used (1 g of chia seed in 12 ml of ethyl acetate), reduced extraction time (40 min) and higher selectivity (de Mello et al., 2017). Previous studies have reported that UAE provided better extraction of bioactive compounds in seeds by destroying plant cells due to the strong impact of ultrasonic waves (Tian et al., 2013). The application of UAE in the CSO industry is considered the best option to improve extraction efficiency by performing low operation temperatures, which may prevent heat damage to the oil and preserve the nutritional qualities of the oil.

Several authors have reported the research on the fatty acid composition of CSO extracted by SC-CO<sub>2</sub> compared with the conventional method (Ixtaina, Mattea, et al., 2011; Ixtaina, Martínez, et al., 2011). Ixtaina et al. (2010) are the first authors to report on the fatty acids of CSO extracted by SFE at different conditions of pressure (250, 350 and 450 bar), temperature (40°C, 60°C and 80°C) and time (60, 150 and 240 min). The results showed that wide variations were observed in the amount of each fatty acid in CSO, including ALA (44.4%–63.4%), LA (19.6%–35%), PA (6.8%–14%), SA (2.5%–13%) and OA (3.9%–11.1%) based on the different SFE operating conditions and extraction time significantly affected ( $p \leq 0.05$ ) the concentration of ALA and LA. The highest oil yield of chia seed based on the optimal conditions (80°C, 450 bar and 300 min) was compared with hexane extraction for the fatty acid composition. It is indicated that the fatty acid profile for both oils obtained was not significantly different ( $p \geq 0.05$ ). Ixtaina et al. (2011a) also revealed that no significant differences ( $p \geq 0.05$ ) were detected in the fatty acid composition of CSO obtained by both extraction methods, except that the amount of LA was significantly higher in oil extracted by SFE (pressure: 250 and 450 bar and temperature: 40°C and 60°C) compared to solvent extraction. Dąbrowski et al. (2018b) conducted a study to show the impact of acetone as a modifier at different concentrations and times with SC-CO<sub>2</sub> on the fatty acid composition of CSO. Results showed that the CSO were relatively similar in PUFA level (78.5%–82.2%) regardless of acetone addition and extraction time. Therefore, adding acetone as a high-polarity solvent in the SFE systems did not change the concentration of the fatty acid profile in the CSO.

### **Tocopherols and Phytosterols**

Generally, oil extracted from plant seeds contains tocopherols and phytosterols, considered natural antioxidants (Hussain et al., 2021; Gharby et al., 2017). Tocopherols and phytosterols

in CSO varied from 100–1244 mg/kg and 2998.8–12600 mg/kg, respectively. Tocopherols in CSO consist mainly of  $\gamma$ - with more than 90% of the total, followed by a minor amount of  $\alpha$ - (about 5%) and  $\delta$ - (around 3%). Meanwhile, the main representative of phytosterols was  $\beta$ -sitosterol (1829–7960 mg/kg), followed by stigmastanol (2180–2770 mg/kg), stigmasterol (173–1830 mg/kg), campesterol (271–924.6 mg/kg), 25-hydroxy-24-methylcholesterol (430.1–683.2 mg/kg),  $\Delta^5$ -avenasterol (355 mg/kg), 24-methylenecycloartanol (127.4–146.8 mg/kg) and other sterol compounds (2180–2770 mg/kg) was present in CSO (Álvarez-Chávez et al., 2008; Ciftci et al., 2012; Dąbrowski et al., 2016; Dąbrowski et al., 2018a; Ishak et al., 2021; Ixtaina, Mattea, et al., 2011; Ixtaina, Martínez, et al., 2011; Shen et al., 2018; Zanqui et al., 2015). The variability is highly dependent on the oil extraction method and the origin of the seeds.

Tocopherols and phytosterols were observed in CSO for alternative and conventional extraction methods. Dąbrowski et al. (2016) reported the composition of tocopherols and phytosterols of CSO obtained by Soxhlet extraction using different solvents (hexane and acetone) and screw pressing (cold and hot conditions). CSO obtained by hexane extraction has significantly higher total phytosterol contents than other extraction methods, indicating that hexane is the best non-polar solvent to extract the highest amount of phytosterols. Meanwhile, both oils extracted at different pressing conditions contained the lowest total phytosterols.  $\beta$ -sitosterol is the primary compound with 61% of the total content. Other studies also reported that  $\beta$ -sitosterol is the major sterol compound in CSO (Álvarez-Chávez et al., 2008; Ciftci et al., 2012; Shen et al., 2018). Tocopherol of CSO extracted by conventional methods showed  $\gamma$ -tocopherol is the main compound obtained regardless of the extraction method used. CSO extracted by cold pressing showed significantly higher total tocopherols than Soxhlet using different solvents and hot pressing at 110°C (Dąbrowski et al., 2016) due to no heat involved from cold pressing and did not degrade tocopherols (Wang et al., 2010).

A higher yield of tocopherols and phytosterols extraction was found in CSO obtained by SFE compared to conventional methods (Dąbrowski et al., 2016). The results showed that the extraction of phytosterols in CSO was higher in SFE at 70°C. In contrast, the higher temperature at 90°C increased the greatest yield of tocopherols at 300 min of extraction time. They reported that high temperatures in the Soxhlet extraction and hot pressing degraded the number of tocopherols and phytosterols in CSO. Furthermore, acetone's addition as co-solvent at different percentages with SC-CO<sub>2</sub> decreased the extraction of tocopherols and phytosterols in the CSO compared to pure SC-CO<sub>2</sub>, indicating these compounds are diluted with the presence of acetone (Dąbrowski et al., 2018b).

The extraction pressure and temperature of SFE can be varied to select the highest amount of targeted bioactive compounds (Follegatti-Romero et al., 2009). Ixtaina, Mattea, et al. (2011) reported that CSO extracted at a higher pressure (450 bar) contained significantly higher tocopherol contents compared to lower pressure (250 bar). Peng et al. (2020) stated

that applying high pressure (300 bar) would improve the interaction between SC-CO<sub>2</sub> and the sample matrix, contributing to the higher diffusivity of  $\gamma$ -tocopherol in CSO during extraction. It is also related to the internal mass transfer rate and diffusivity enhanced during the extraction process, thus improving the tocopherol levels (Wang et al., 2017). The CSO extraction by compressed liquefied petroleum gas (LPG) and SC-CO<sub>2</sub> to evaluate the quality of oils obtained regarding  $\alpha$ -tocopherol,  $\beta$ -sitosterol and antioxidant activity. CSO obtained by SC-CO<sub>2</sub> at lower pressure and temperature (100 bar and 20°C) achieved higher antioxidant activity (87%),  $\alpha$ -tocopherol (22.95 mg 100 g<sup>-1</sup>) and  $\beta$ -sitosterol (77.10 mg 100 g<sup>-1</sup>) than CSO extracted by LPG. Different parameters for both solvents influenced the qualities of CSO (Scapin et al., 2017). However, LPG is classified as toxic and highly flammable compared to SC-CO<sub>2</sub>, which is generally considered safe (Abaide et al., 2017). Therefore, the extraction of CSO using SC-CO<sub>2</sub> is the best choice to obtain more lipophilic antioxidant compounds than LPG.

### Polyphenols

Polyphenols exhibit various positive human health effects, such as anti-inflammatory, anti-cancer, and antioxidant activities (Yeo et al., 2015). Polyphenol in CSO ranged from 0 mg/kg (cold pressing) to 172 mg/kg (Soxhlet using acetone). The polyphenolic compounds present in CSO extracted by different extraction methods were caffeic acid, chlorogenic acid, myricetin, quercetin and kaempferol (Ixtaina, Mattea, et al., 2011; Ixtaina, Martínez, et al., 2011). Even though lower levels of phenolic compounds are found in oils than in whole seeds, the same compounds are detected in chia whole seeds (Reyes-Caudillo et al., 2008). Hence, this may be due to polyphenols being polar and hydrophilic, which are not soluble in lipids (Ixtaina, Mattea, et al., 2011a).

SC-CO<sub>2</sub> alone may not be able to extract polar compounds such as polyphenols. Co-solvents are employed during extraction at a small percentage (1%–10%) for better extraction of polyphenols. The modifiers with higher polarity than CO<sub>2</sub> by expanding the range of targeted compounds (Bimakr et al., 2011). Generally, the modifiers used with CO<sub>2</sub> extraction are ethanol, methanol, acetone and mixtures of several solvents (de Melo et al., 2014). Dąbrowski et al. (2018b) reported that incorporating acetone as a modifier in the SFE system progressively increased the polyphenol concentration of CSO. The higher modifier (up to 10%) added into the SC-CO<sub>2</sub> for a short period at 1 hr improved the polyphenol concentrations to the maximum level until 33 mg/kg of CSO. Acetone is commonly used as a polar solvent to extract plant polyphenols (Haminiuk et al., 2014). According to the extraction method, CSO extracted by the Soxhlet method using acetone obtained 24 times higher total phenolic contents than oil extracted by SFE at 90°C (Dąbrowski et al., 2016). It can be concluded that extraction methods using acetone as modifiers to produce CSO contain relatively high polarity of polyphenols known for their antioxidant activity.

## STABILITY IMPROVEMENT OF CHIA SEED OIL

Previous research has reported that the induction period (IP) of the bulk CSO is short due to the high concentration of PUFA (>80%), as these are highly unsaturated and can quickly oxidise when subjected to high temperature and overflow air-based conditions (Dąbrowski et al., 2016; Dąbrowski et al., 2018a; Ishak, Ghani, Nasri, 2020; Ixtaina, Mattea, et al., 2011; Ixtaina, Martínez, et al., 2011; Shen et al., 2018; Timilsena et al., 2017). The shorter the IP of oils, the more decomposition products containing fatty acids are released from lipid oxidation (Santos et al., 2013). Generally, lipid oxidation causes many challenges during food processing and storage, including off-flavours in food by the formation of secondary oxidation products (aldehydes and ketones) (Let et al., 2005), reducing nutritional qualities of the oils (essential fatty acids and lipid-soluble vitamins) (Arab-Tehrany et al., 2012) and possessing adverse effect on human health (Jacobsen et al., 1999). Regarding the high content of PUFA in CSO, the formation rate of primary oxidation products increased by higher unsaturated double bonds present in oil (Maszewska et al., 2018). Thus, immediate oxidation occurs in the CSO, which is related to the highest amount of PUFA, with the most prominent fatty acid composed of ALA (53.67%–69.3%). Therefore, the oxidative stability of CSO can be improved by adding antioxidants and in combination with other vegetable oils.

### Addition of Antioxidants

Natural or synthetic antioxidants can improve the shelf life of food products by delaying lipid oxidation. Natural antioxidants from plant sources are considered the best option to replace synthetic antioxidants due to their potential health benefits and safety (Lourenço et al., 2019). Lipid oxidation commonly occurs in food products when exposed to oxygen, heat, and light (Carocho et al., 2014). Natural plant extracts proved to be thermally stable during processing and exhibited antioxidant activity (Taghvaei & Jafari, 2015). A few research have evaluated the effectiveness of various natural antioxidants on the oxidative stability of CSO by pressing and analysing using the Rancimat method and storage study (Aliabadi et al., 2023; Bodoira et al., 2017; Ixtaina et al., 2012; Jung et al., 2021).

Aliabadi et al. (2023) reported that the highest concentration of oregano (*Origanum vulgare* L.) extract (1800 ppm) had the highest oxidative stability index of CSO (8.31 hr) compared to oil containing yarrow (*Achillea millefolium*) extracts (600–1800 ppm) according to the Rancimat conditions (110°C and an airflow rate of 20 L/hr). Furthermore, CSO enriched with oregano extract at 1800 ppm had the lowest acid, peroxide, anisidine and total oxidation values under accelerated oxidation conditions for five days in the oven at 90°C. Ixtaina et al. (2012) reported that applying different antioxidants improved CSO's shelf life. The best antioxidant effects recorded in CSO with the addition of ascorbyl palmitate (AP) (2,500 and 5,000 ppm), rosemary extract at the highest concentration studied (5,000 ppm) and the mixture of green extract and rosemary extract (1:1) (Ixtaina et

al., 2012). However, adding tocopherols (more than 1500 ppm) decreased the IP of CSO, showing that tocopherols are less effective against lipid oxidation than other antioxidants tested. It can be explained mainly by the polar paradox, which is based on the different antioxidant polarities in which tocopherols might be passive in bulk CSO and sensitive to high temperatures (Ixtaina et al., 2012).

Other studies also supported these findings, where only tocopherol added (200 mg/kg) in the CSO showed the least performance as an antioxidant compared to other antioxidants and their combinations (Bodoira et al., 2017). However, the oxidative stability of CSO improved significantly by the synergistic effect between the mixture of tocopherols (200 mg/kg) and rosemary extract (8000 mg/kg). In contrast, the addition of natural antioxidants in low concentrations (200 mg/kg) demonstrated no significant effect ( $p \geq 0.05$ ) on the oxidative stability of CSO obtained by hexane extraction (Souza et al., 2017). However, tert-butylhydroquinone (TBHQ), a synthetic antioxidant applied in the CSO, was the most efficient against lipid oxidation. The synergistic antioxidant effect between TBHQ and rosemary extract at the concentration of 200 mg/kg increased the oxidative stability of CSO (IP: 11.43 hr) significantly compared to the addition of rosemary extract alone (IP: 1.53 hr). Thus, the increased IP of CSO with enhanced concentrations and combinations of selected antioxidants was observed (Bodoira et al., 2017; Ixtaina et al., 2012; Souza et al., 2017).

### **Blending of Vegetable Oils**

Blending edible oils from plants is one of the most straightforward procedures to enhance stability and nutritional properties at affordable prices (Bordón et al., 2019). The blending of cold-pressed CSO with other vegetable oils (walnut, almond, virgin and roasted sesame oils) based on the different proportions (20:80, 30:70 and 40:60) were compared in terms of their oxidative stability by conducting the Rancimat method (flow rate: 20 L/hr and temperature: 100°C) and accelerated stability test (40°C for 12 days) (Bordón et al., 2019). Pure CSO contained the lowest oxidative stability index ( $p \leq 0.05$ ) compared to other CSO blended with other vegetable oils according to the Rancimat method. Sesame oil blends (both virgin and roasted) with CSO were observed as the most stable against oxidation, while walnut oil mixed with CSO had the lowest oxidative stability among all oil blends (Bordón et al., 2019).

Meanwhile, similar trends were observed for the oxidative stability of CSO blends using accelerated storage conditions. The low stability of oil blends (chia seed and walnut) was observed due to the high content of PUFA (more than 70%). The oil blends with almond and sesame oil (both virgin and roasted) presented higher oxidative stability by yielding a small number of oxidation products based on the peroxide values lower than 3 mEq O<sub>2</sub>/kg throughout the entire accelerated study for 12 days (Bordón et al., 2019). The oxidative stability of the mixture of sunflower and cold-pressed chia seed oil (90:10 and 80:20) with the addition of natural antioxidants was evaluated at different storage temperatures (4°C



and 20°C) for 360 days. CSO blends with rosemary extract, and AP presented the best oxidative stability throughout the storage study (360 days) compared to other CSO samples without antioxidants (Guiotto et al., 2014). The authors suggested that the addition of antioxidants in the oil blends increased the activation energy and decreased the rate constant, showing an improvement in the oxidative stability of the CSO. Therefore, increased storage temperature and unsaturated fatty acids significantly reduced the oxidative stability of oil blends (sunflower and CSO) during oxidation (Guiotto et al., 2014).

## CONCLUSION

CSO has been extracted using various methods such as pressing (hot and cold), solvent extraction (Soxhlet and Folch), SC-CO<sub>2</sub> and ultrasound-assisted extraction. The conventional techniques heated at boiling temperature according to the different types of solvent obtained a higher yield of CSO than other extraction methods. However, mechanical pressing produced the lowest CSO recovery. The improvement in CSO yield can be achieved by conducting an ultrasound extraction system using conventional or alternative methods. Meanwhile, most CSOs contain more than 80% PUFA, obtained by different extraction methods. CSO mainly composes ALA and LA, which may help reduce cardiovascular disease risk. The content of PUFA in CSO was not affected by solvent extraction with different polarity and the addition of acetone in the SFE method. It was found that the application of ultrasound-assisted solvent extraction improved the PUFA level of CSO. Meanwhile, CSO extraction using SC-CO<sub>2</sub> has a high tocopherol and phytosterol content comparable to oils extracted by hexane and LPG. The addition of acetone with SC-CO<sub>2</sub> significantly improved the level of polyphenols in CSO. CSO has emerged as a new source of edible oil with functional properties that can be applied to food products and used as healthy supplements rich in PUFA. The stability of CSO is the primary concern that needs to be focused on since it is high in PUFA, which is very susceptible to oxidation, thus shortening its shelf life when subjected to improper storage temperature. This problem can be solved by adding natural antioxidants in combination with other vegetable oils to maintain the nutritional quality and improve the oxidative stability of CSO. In future, extensive research should be conducted to reveal more applications of recent extraction methods such as aqueous enzymatic, microwave or pulsed electric field-assisted to produce higher oil yield and several lipophilic compounds, including PUFA, tocopherols, phytosterols and polyphenols in chia seed.

## ACKNOWLEDGEMENTS

The authors wish to thank the support of Research University Grants: Universiti Putra Malaysia Grant (GP/2018/9643600) and (GP/IPS/2017/9537200) as well as (GUP-2018-018) and Prime Impact Grant (DIP-2018-036) from Universiti Kebangsaan Malaysia.

## REFERENCES

- Abaide, E. R., Zabot, G. L., & Tres, M. V. (2017). Yield, composition, and antioxidant activity of avocado pulp oil extracted by pressurized fluids. *Food and Bioproducts Processing*, *102*, 289-298. <https://doi.org/10.1016/j.fbp.2017.01.008>
- Abdolshahi, A., Majd, M. H., Rad, J. S., Taheri, M., Shabani, A., & da Silva, J. A. T. (2015). Choice of solvent extraction technique affects fatty acid composition of pistachio (*Pistacia vera* L.) oil. *Journal of Food Science and Technology*, *52*(4), 2422–2427. <https://doi.org/10.1007/s13197-013-1183-8>
- Ali, N. M., Yeap, S. K., Ho, W. Y., Beh, K. B., Tan, S. W., & Tan, S. G. (2012). The promising future of chia, *Salvia hispanica* L. *Journal of Biomedicine and Biotechnology*, *2012*(1), 171956. <https://doi.org/10.1155/2012/171956>
- Aliabadi, F. K., Dastgerdi, A. A., & Nimavard, J. T. (2023). The oxidative stability of chia seed oil enriched with oregano (*Origanum vulgare* L.) and yarrow (*Achille millefolium*) extracts. *Journal of Food Quality*, *2023*(1), 6263692. <https://doi.org/10.1155/2023/6263692>
- Álvarez-Chávez, L. M., Valdivia-López, M. D. L. A., Aburto-Juárez, M. D. L., & Tecante, A. (2008). Chemical characterization of the lipid fraction of Mexican chia seed (*Salvia hispanica* L.). *International Journal of Food Properties*, *11*(3), 687-697. <https://doi.org/10.1080/10942910701622656>
- Arab-Tehrany, E., Jacquot, M., Gaiani, C., Imran, M., Desobry, S., & Linder, M. (2012). Beneficial effects and oxidative stability of omega-3 long-chain polyunsaturated fatty acids. *Trends in Food Science and Technology*, *25*(1), 24-33. <https://doi.org/10.1016/j.tifs.2011.12.002>
- Bimakr, M., Rahman, R. A., Taip, F. S., Ganjloo, A., Salleh, L. M., Selamat, J., Hamid, A., & Zaidul, I. S. M. (2011). Comparison of different extraction techniques for isolation of major bioactive flavonoid compounds from spearmint (*Mentha spicata* L.) leaves. *Food and Bioproducts Processing*, *89*(1), 67-72. <https://doi.org/10.1016/j.fbp.2010.03.002>
- Bodoira, R. M., Penci, M. C., Ribotta, P. D., & Martínez, M. C. (2017). Chia (*Salvia hispanica* L.) oil stability: Study of the effect of natural antioxidants. *LWT-Food Science and Technology*, *75*, 107-113. <https://doi.org/10.1016/j.lwt.2016.08.031>
- Bordón, M. G., Meriles, S. P., Ribotta, P. D., & Martinez, M. L. (2019). Enhancement of composition and oxidative stability of chia (*Salvia hispanica* L.) seed oil by blending with specialty oils. *Journal of Food Science*, *84*(5), 1035-1044. <https://doi.org/10.1111/1750-3841.14580>
- Bubalo, M. C., Vidović, S., Redovniković, I. R., & Jokić, S. (2018). New perspective in extraction of plant biologically active compounds by green solvents. *Food and Bioproducts Processing*, *109*(2), 52–73. <https://doi.org/10.1016/j.fbp.2018.03.001>
- Bubalo, M. C., Vidović, S., Redovniković, I. R., & Jokić, S. (2015). Green solvents for green technologies. *Journal of Chemical Technology and Biotechnology*, *90*(9), 1631–1639. <https://doi.org/10.1002/jctb.4668>
- Carocho, M., Barreiro, M. F., Morales, P., Ferreira, I. C., & Gomez, P. M. (2014). Adding molecules to food, pros and cons: A review on synthetic and natural food additives. *Comprehensive Reviews on Food Science and Food Safety*, *13*(4), 377–399. <https://doi.org/10.1111/1541-4337.12065>

- Chemat, F., Rombaut, N., Sicaire, A.-G., Meullemiestre, A., Fabiano-Tixier, A.-S., & Abert-Vian, M. (2017). Ultrasound assisted extraction of food and natural products. Mechanisms, techniques, combinations, protocols and applications: A review. *Ultrasonic Sonochemistry*, *34*, 540-560. <https://doi.org/10.1016/j.ultsonch.2016.06.035>
- Ciftci, O. N., Przybylski, R., & Rudzińska, M. (2012). Lipid components of flax, perilla, and chia seeds. *European Journal of Lipid Science and Technology*, *114*(7), 794-800. <https://doi.org/10.1002/ejlt.201100207>
- Dąbrowski, G., Konopka, I., Czaplicki, S., & Tańska, M. (2016). Composition and oxidative stability of oil from *Salvia hispanica* L. seeds in relation to extraction method. *European Journal of Lipid Science and Technology*, *119*(5), 16002-16009. <https://doi.org/10.1002/ejlt.201600209>
- Dąbrowski, G., Konopka, I., & Czaplicki, S. (2018a). Variation in oil quality and content of low molecular lipophilic compounds in chia seed oils. *International Journal of Food Properties*, *21*(1), 2016–2029. <https://doi.org/10.1080/10942912.2018.1501699>
- Dąbrowski, G., Konopka, I., & Czaplicki, S. (2018b). Supercritical CO<sub>2</sub> extraction in chia oils production: Impact of process duration and co-solvent addition. *Food Science and Biotechnology*, *27*(3), 677-686. <https://doi.org/10.1007/s10068-018-0316-2>
- de Mello, B. T. F., Garcia, V. A. S., & da Silva, C. (2017) Ultrasound-assisted extraction of oil from chia (*Salvia hispânica* L.) seeds: Optimization extraction and fatty acid profile. *Journal of Food Process Engineering*, *40*(1), 1–8. <https://doi.org/10.1111/jfpe.12298>
- de Melo, M. M. R., Silvestre, A. J. D., & Silva, C. M. (2014). Supercritical fluid extraction of vegetable matrices: Applications, trends and future perspectives of a convincing green technology. *Journal of Supercritical Fluids*, *92*, 115-176. <https://doi.org/10.1016/j.supflu.2014.04.007>
- Fernandes, S. S., Tonato, D., Mazutti, M. A., de Abreu, B. R., Cabrera, D. D. C., D'Oca, C. D. R. M., Prentice-Hernández, C., & Salas-Mellado, M. D. L. M. (2019). Yield and quality of chia oil extracted via different methods. *Journal of Food Engineering*, *262*, 200–208. <https://doi.org/10.1016/j.jfoodeng.2019.06.019>
- Ferrentino, G., Giampiccolo, S., Morozova, K., Haman, N., Spilimbergo, S., & Scampicchio, M. (2020). Supercritical fluid extraction of oils from apple seeds: Process optimization, chemical, characterization and comparison with a conventional solvent extraction. *Innovative Food Science & Emerging Technologies*, *64*, 102428. <https://doi.org/10.1016/j.ifset.2020.102428>
- Follegatti-Romero, L. A., Piantino, C. R., Grimaldi, R., & Cabral, F. A. (2009). Supercritical CO<sub>2</sub> extraction of omega-3 rich oil from sacha inchi (*Plukenetia volubilis* L.) seeds. *Journal of Supercritical Fluids*, *49*(3), 323–329. <https://doi.org/10.1016/j.supflu.2009.03.010>
- Fruehwirth, S., Zehentner, S., Salim, M., Sterneder, S., Tiroch, J., Lieder, B., Zehl, M., Somoza, V., & Pignitter, M. (2020). *In vitro* digestion of grape seed oil inhibits phospholipid-regulating effects of oxidized lipids. *Biomolecules*, *10*(5), 708. <https://doi.org/10.3390/biom10050708>
- Future Market Insights. (2023). *Chia seed market*. <https://www.futuremarketinsights.com/reports/chia-seed-market>

- Gharby, S., Harhar, H., Bouzoubaa, Z., Asdadi, A., El Yadini, A., & Charrouf, Z. (2017). Chemical characterization and oxidative stability of seeds and oil of sesame grown in Morocco. *Journal of the Saudi Society of Agricultural Sciences*, 16(2), 105-111. <https://doi.org/10.1016/j.jssas.2015.03.004>
- Ghoreishi, S. M., Hedayati, A., & Mohammadi, S. (2016). Optimization of periodic static dynamic supercritical CO<sub>2</sub> extraction of taxifolin from *Pinus nigra* bark with ethanol as entrainer. *Journal of Supercritical Fluids*, 113, 53–60. <https://doi.org/10.1016/j.supflu.2016.03.015>
- Grancieri, M., Martino, H. S. D., & de Mejia, E. G. (2019). Chia seed (*Salvia hispanica* L.) as a source of proteins and bioactive peptides with health benefits: A review. *Comprehensive Reviews on Food Science and Food Safety*, 18(2), 480–499. <https://doi.org/10.1111/1541-4337.12423>
- Guiotto, E. N., Ixtaina, V. Y., Nolasco, S. M., & Tomás, M. C. (2014). Effect of storage conditions and antioxidants on the oxidative stability of sunflower-chia oil blends. *Journal of the American Oil Chemists' Society*, 91(5), 767-776. <https://doi.org/10.1007/s11746-014-2410-9>
- Haminiuk, C. W. I., Plata-Oviedo, M. S. V., de Mattos, G., Carpes, S. T., & Branco, I. G. (2014). Extraction and quantification of phenolic acids and flavonols from *Eugenia pyriformis* using different solvents. *Journal of Food Science and Technology*, 51(10), 2862–2866. <https://doi.org/10.1007/s13197-012-0759-z>
- Herrero, M., Cifuentes, A., & Ibáñez, E. (2006). Sub- and supercritical fluid extraction of functional ingredients from different natural sources: Plants, food-by-products, algae and microalgae: A review. *Food Chemistry*, 98(1), 136-148. <https://doi.org/10.1016/j.foodchem.2005.05.058>
- Hrnčič, M. K., Cör, D., & Knez, Z. (2018). Subcritical extraction of oil from black and white chia seeds with n-propane and comparison with conventional techniques. *The Journal of Supercritical Fluids*, 140, 182-187. <https://doi.org/10.1016/j.supflu.2018.06.017>
- Hussain, I., Ishak, I., Coorey, R., Ghani, M. A., & Ping, T. C. (2021). Tocopherols. In M. Mushtaq & F. Anwar (Eds.), *A centum of valuable plant bioactives* (pp. 707-731). Academic Press. <https://doi.org/10.1016/B978-0-12-822923-1.00011-X>
- Ishak, I., Ghani, M. A., & Nasri, N. N. S. (2020). Effect of extraction solvents on the oxidative stability of chia seed (*Salvia hispanica* L.) oil stored at different storage temperatures. *Food Research*, 4(6), 2103-2113. [https://doi.org/10.26656/fr.2017.4\(6\).259](https://doi.org/10.26656/fr.2017.4(6).259)
- Ishak, I., Ghani, M. A., & Yuen, J. Z. (2020). Effects of extraction solvent and time on the oil yield, total phenolic content, carotenoid and antioxidant activity of Australian chia seed (*Salvia hispanica* L.) oil. *Food Research*, 4(Suppl. 4), 27-37. [https://doi.org/10.26656/fr.2017.4\(S4\).006](https://doi.org/10.26656/fr.2017.4(S4).006)
- Ishak, I., Hussain, N., Coorey, R., & Ghani, M. A. (2021). Optimization and characterization of chia seed (*Salvia hispanica* L.) oil extraction using supercritical carbon dioxide. *Journal of CO<sub>2</sub> Utilization*, 45, 101430. <https://doi.org/10.1016/j.jcou.2020.101430>
- Ixtaina, V. Y., Martínez, M. L., Spotorno, V., Mateo, C. M., Maestri, D. M., Diehl, B. W. K., Nolasco, S. M., & Tomás, M. C. (2011). Characterization of chia seed oils obtained by pressing and solvent extraction. *Journal of Food Composition and Analysis*, 24(2), 166–174. <https://doi.org/10.1016/j.jfca.2010.08.006>
- Ixtaina, V. Y., Mattea, F., Cardarelli, D. A., Mattea, M. A., Nolasco, S. M., Tomás, M. C. (2011). Supercritical carbon dioxide extraction and characterization of Argentinean chia seed oil. *Journal of the American Oil Chemists' Society*, 88(2), 289–298. <https://doi.org/10.1007/s11746-010-1670-2>

- Ixtaina, V. Y., Nolasco, S. M., & Tomás, M. C. (2012). Oxidative stability of chia (*Salvia hispanica* L.) seed oil: Effect of antioxidants and storage conditions. *Journal of the American Oil Chemists' Society*, 89(6), 1077-1090. <https://doi.org/10.1007/s11746-011-1990-x>
- Ixtaina, V. Y., Vega, A., Nolasco, S. M., Tomás, M. C., Gimeno, M., Bárzana, E., & Tecante, A. (2010). Supercritical carbon dioxide extraction of oil from Mexican chia seed (*Salvia hispanica* L.): Characterization and process optimization. *The Journal of Supercritical Fluids*, 55(1), 192–199. <https://doi.org/10.1016/j.supflu.2010.06.003>
- Jacobsen, C., Hartvigsen, K., Lund, P., Meyer, A. S., Adler-Nissen, J., Holstborg, J., & Hølmer, G. (1999). Oxidation in fish-oil-enriched mayonnaise 1. Assessment of propyl gallate as an antioxidant by discriminant partial least squares regression analysis. *European Food Research and Technology*, 210, 13-30. <https://doi.org/10.1007/s002170050526>
- Jung, H., Kim, I., Jung, S., & Lee, J. (2021). Oxidative stability of chia seed oil and flax seed oil and impact of rosemary (*Rosmarinus officinalis* L.) and garlic (*Allium cepa* L.) extracts on the prevention of lipid oxidation. *Applied Biological Chemistry*, 64, 6. <https://doi.org/10.1186/s13765-020-00571-5>
- Kumar, S. P. J., Prasad, S. R., Banerjee, R., Agarwal, D. K., Kulkarni, K. S., & Ramesh, K. V. (2017). Green solvents and technologies for oil extraction from oilseeds. *Chemistry Central Journal*, 11, 9. <https://doi.org/10.1186/s13065-017-0238-8>
- Kus-Yamashita, M. M. M., Filho, J. M. McDonald, B., Ravacci, G., Rogero, M. M., Santos, R. D., Waitzberg, D., Reyes, M. S., Yehuda, S., Gierke, J., Cori, H., Pires, T., & Lajolo, F. M. (2016). Polyunsaturated fatty acids: Health impacts. *European Journal of Nutrition and Food Safety*, 6(3), 111-131. <https://doi.org/10.9734/EJNFS/2016/23018>
- Lenihan-Geels, G., & Bishop, K. S. (2016). Alternative origins for omega-3 fatty acids in the diet. In M. V. Hegde, A. A. Zanwar & S. P. Adekar (Eds.), *Omega-3 fatty acids: Keys to nutritional health* (pp. 475-486). Springer International Publishing. [https://doi.org/10.1007/978-3-319-40458-5\\_34](https://doi.org/10.1007/978-3-319-40458-5_34)
- Liu, S. X., & Mamidipally, P. K. (2005). Quality comparison of rice bran oil extracted with d-limonene and hexane. *Cereal Chemistry*, 82(2), 209–215. <https://doi.org/10.1094/CC-82-0209>
- Lourenço, S. C., Moldão-Martins, M., & Alves, V. D. (2019). Antioxidants of natural plant origins: From sources to food industry applications. *Molecules*, 24(22), 4132. <https://doi.org/10.3390/molecules24224132>
- Martínez, M. L., Marín, M. A., Faller, C. M. S., Revol, J., Penci, M. C., & Ribotta, P. D. (2012). Chia (*Salvia hispanica* L.) oil extraction: Study of processing parameters. *LWT - Food Science and Technology*, 47(1), 78-82. <https://doi.org/10.1016/j.lwt.2011.12.032>
- Maszewska, M., Florowska, A., & Dłużewska, E. (2018). Oxidative stability of selected edible oils. *Molecules*, 23(7), 1746. <https://doi.org/10.3390/molecules23071746>
- Oteri, M., Bartolomeo, G., Rigano, F., Aspromonte, J., Trovato, E., Purcaro, G., Dugo, P., Mondello, L., & Beccaria, M. (2023). Comprehensive chemical characterization of chia (*Salvia hispanica* L.) seed oil with a focus on minor lipid components. *Foods*, 12(1), 23. <https://doi.org/10.3390/foods12010023>
- Peng, W. L., Mohd-Nasir, H., Setapar, S. H. M., Ahmad, A., & Lokhat, D. (2020). Optimization of process variables using response surface methodology for tocopherol extraction from roselle seed oil by

- supercritical carbon dioxide. *Industrial Crops and Products*, 143, 111886. <https://doi.org/10.1016/j.indcrop.2019.111886>
- Ramluckan, K., Moodley, K. G., & Bux, F. (2014). An evaluation of the efficacy of using selected solvents for the extraction of lipids from algal biomass by the Soxhlet extraction method. *Fuel*, 116, 103-108. <https://doi.org/10.1016/j.fuel.2013.07.118>
- Reyes-Caudillo, E., Tecante, A., & Valdivia-López, M. A. (2008). Dietary fibre content and antioxidant activity of phenolic compounds present in Mexican chia (*Salvia hispanica* L.) seeds. *Food Chemistry*, 107(2), 656–663. <https://doi.org/10.1016/j.foodchem.2007.08.062>
- Richter, B. E., Jones, B. A., Ezzell, J. L., & Porter, N. L. (1996). Accelerated solvent extraction: A technique for sample preparation. *Analytical Chemistry*, 68(6), 1033-1039. <https://doi.org/10.1021/ac9508199>
- Rosas-Mendoza, M. E., Coria-Hernández, J., Meléndez-Pérez, R., & Arjona-Román, J. L. (2017). Characteristics of chia (*Salvia hispanica* L.) seed oil extracted by ultrasound assistance. *Journal of the Mexican Chemical Society*, 61(4), 326-335. <https://doi.org/10.29356/jmcs.v61i4.463>
- Santos, O. V., Corrêa, N. C. F., Carvalho Jr., R. N., Costa, C. E. F., & Lannes, S. C. S. (2013). Yield, nutritional quality, and thermal-oxidative stability of Brazil nut oil (*Bertolletia excelsa* H. B. K) obtained by supercritical extraction. *Journal of Food Engineering*, 117(4), 499–504. <https://doi.org/10.1016/j.jfoodeng.2013.01.013>
- Scapin, G., Abaide, E. R., Nunes, L. F., Mazutti, M. A., Vendruscolo, R. G., Wagner, R., & da Rosa, C. S. (2017). Effect of pressure and temperature on the quality of chia oil extracted using pressurized fluids. *Journal of Supercritical Fluids*, 127, 90-96. <https://doi.org/10.1016/j.supflu.2017.03.030>
- Senrayan, J., & Venkatachalam, S. (2020). Ultrasonic acoustic-cavitation as a novel and emerging energy efficient technique for oil extraction from kapok seeds. *Innovative Food Science and Emerging Technologies*, 62, 102347. <https://doi.org/10.1016/j.ifset.2020.102347>
- Shen, Y., Zheng, L., Jin, J., Li, X., Fu, J., Wang, M., Guan, Y., & Song, X. (2018). Phytochemical and biological characteristics of Mexican chia seed oil. *Molecules*, 23(12), 3219. <https://doi.org/10.3390/molecules23123219>
- Soh, S. H., Agarwal, S., Jain, A., Lee, L. Y., Chin, S. K., & Jayaraman, S. (2019). Mathematical modeling of mass transfer in supercritical fluid extraction of patchouli oil. *Engineering Reports*, 1(4), 12051. <https://doi.org/10.1002/eng2.12051>
- Souza, A. L., Martínez, F. P., Ferreira, S. B., & Kaiser, C. R. (2017). A complete evaluation of thermal and oxidative stability of chia oil. *Journal of Thermal Analysis and Calorimetry*, 130, 1307-1315. <https://doi.org/10.1007/s10973-017-6106-x>
- Tacon, A. G., & Metian, M. (2008). Aquaculture feed and food safety: The role of the food and agriculture organization and the Codex Alimentarius. *Annals of the New York Academy of Sciences*, 1140, 50–59. <https://doi.org/10.1196/annals.1454.003>
- Taghvaei, M., & Jafari, S. M. (2015). Application and stability of natural antioxidants in edible oils in order to substitute synthetic additives. *Journal of Food Science and Technology*, 52(3), 1272-1282. <https://doi.org/10.1007/s13197-013-1080-1>

- Tian, Y., Xu, Z., Zheng, B., & Lo, Y. M. (2013). Optimization of ultrasonic-assisted extraction of pomegranate (*Punica granatum* L.) seed oil. *Ultrasonic Sonochemistry*, 20(1), 202–208. <https://doi.org/10.1016/j.ultsonch.2012.07.010>
- Timilsena, Y. P., Vongsvivut, J., Adhikari, R., & Adhikari, B. (2017). Physicochemical and thermal characteristics of Australian chia seed oil. *Food Chemistry*, 228, 394–402. <https://doi.org/10.1016/j.foodchem.2017.02.021>
- Wang, S., Hwang, H., Yoon, S., & Choe, E. (2010). Temperature dependence of autoxidation of perilla oil and tocopherol degradation. *Journal of Food Science*, 75(6), 498-505. <https://doi.org/10.1111/j.1750-3841.2010.01681.x>
- Wang, X., Wang, C., Zha, X., Mei, Y., Xia, J., & Jiao, Z. (2017). Supercritical carbon dioxide extraction of  $\beta$ -carotene and  $\alpha$ -tocopherol from pumpkin: A box–behken design for extraction variables. *Analytical Methods*, 9(2), 294-303. <https://doi.org/10.1039/C6AY02862D>
- Yeo, J.-S., Seong, D.-W., & Hwang, S.-H. (2015). Chemical surface modification of lignin particle and its application as filler in the polypropylene composites. *Journal of Industrial and Engineering Chemistry*, 31, 80-85. <https://doi.org/10.1016/j.jiec.2015.06.010>
- Zanqui, A. B., de Morais, D. R., da Silva, C. M., Santos, J. M., Chiavelli, L. U. R., Bittencourt, P. R. S., Eberlin, M. N., Visentainer, J. V., Cardozo-Filho, L., & Matsushita, M. (2015). Subcritical extraction of *Salvia hispanica* L. oil with *n*-propane: Composition, purity and oxidation stability as compared to the oils obtained by conventional solvent extraction methods. *Journal of the Brazilian Chemical Society*, 26(2), 282-289. <http://doi.org/10.5935/0103-5053.20140278>





## Dietary Administration of Karonda (*Carissa carandas*) on the Growth, Digestive Enzymes, Skin Mucosal Immunity, and Pigmentation in Siamese Fighting Fish (*Betta splendens*)

Kotchaporn Ponsin, Janeeya Khunchalee and Phukphon Munglue\*

Faculty of Science, Ubon Ratchathani Rajabhat University, Ubon Ratchathani 34000, Thailand

### ABSTRACT

Karonda (*Carissa carandas*) fruit contains natural colorants; however, no research has investigated its effects on fish growth and coloration. Thus, this study examined the impacts of *C. carandas* fruit powder (CCFP) on growth, skin mucosal immunity, digestive enzymes, and pigmentation in Siamese fighting fish (*Betta splendens*). Flavonoids ( $15.97 \pm 0.48$  mg quercetin equivalent/g CCFP), phenolics ( $43.52 \pm 1.73$  mg gallic acid equivalent/g CCFP), terpenoids ( $350.00 \pm 15.66$  mg linalool equivalent/g CCFP), tannins ( $40.97 \pm 0.15$  mg tannic acid equivalent/g CCFP), carotenoids ( $5.53 \pm 0.73$   $\mu\text{g/g}$  CCFP), and  $\beta$ -carotene ( $0.67 \pm 0.05$   $\mu\text{g/g}$  CCFP) were estimated in CCFP. In the 2,2-diphenyl-1-picrylhydrazyl assay, CCFP showed antioxidant activity with an  $\text{IC}_{50}$  of  $256.12 \pm 7.68$   $\mu\text{g/ml}$ . Fish ( $0.42 \pm 0.02$  g weight and  $3.20 \pm 0.07$  cm length) were fed diets containing CCFP at 0 (control), 3, 6, and 9 g/kg for 8 weeks. The results showed that CCFP administration significantly enhanced final weight, length, weight gain, specific growth rate, and average daily gain ( $p < 0.05$ ). No changes in feed conversion ratio, survival, and condition factor were observed ( $p > 0.05$ ). Dietary CCFP significantly increased skin mucus lysozyme, alkaline phosphatase, IgM, myeloperoxidase, total protein, antioxidant capacity, catalase, and superoxide dismutase. Fish treated with CCFP showed significant increases in intestinal protease, lipase, and amylase activity, as well as skin, muscle, and fin carotenoid levels. In conclusion, the administration of CCFP at 9 g/kg is optimal for improving growth, digestive enzymes, skin mucosal immunity, and pigmentation in *B. splendens*.

*Keywords:* Aquaculture, feed additive, feed utilization, natural colorants, ornamental fish, phytochemicals

### ARTICLE INFO

#### Article history:

Received: 26 July 2024

Accepted: 05 August 2024

Published: 28 January 2025

DOI: <https://doi.org/10.47836/pjtas.48.1.14>

#### E-mail addresses:

kotchaporn.pg61@ubru.ac.th (Kotchaporn Ponsin)

janeeya\_g@hotmail.com (Janeeya Khunchalee)

phukphon.m@ubru.ac.th (Phukphon Munglue)

\* Corresponding author

### INTRODUCTION

The Siamese fighting fish (*Betta splendens*) is one of the most significant ornamental fish species in Thailand. The export value of this species in 2016 reached 529 million baht, the most valuable among ornamental

fish (Krueahong et al., 2022). The primary sources of *B. splendens* in the ornamental fish market are generally obtained from cultivation processes and natural water sources. Recently, the natural habitat of *B. splendens* has been threatened by the expansion of modern agriculture, pesticide use, and increasing water pollution. Some contaminants can alter reproductive system function and decrease hatch rates, leading to a decline in the *B. splendens* population in nature (Paulos et al., 2010). Ornamental fish production systems have been developed for large-scale export. However, raising fish under intensive conditions can result in infectious diseases and significant mortality rates (Gruneck et al., 2022). Moreover, fish stress responses to long-term capture, starvation, water pollution, and low-quality feed may substantially decrease skin pigmentation (Nascimento et al., 2019; Pailan et al., 2012).

Fish skin color is a specific feature that needs to be controlled according to market demands (Pailan et al., 2012). The factors affecting skin color in fish include the carotenoid content in their diet. Like other aquatic animals, fish cannot synthesize carotenoids and must obtain them through digestion (Thongprajukaew et al., 2011). In the ornamental fish industry, various additives, such as sex hormones, synthetic carotenoids, and astaxanthin, have been incorporated into diets to improve coloration (Karşlı, 2021; Keleştemur & Çoban, 2016; Wang et al., 2006). On the other hand, fish that receive continuous hormone administration may experience stress, liver enlargement, and abdominal edema. Furthermore, according to Paulos et al. (2010), using artificial colorants increases production costs and harms fish. This report suggests that natural colors from plants or animals can be a more affordable option for fish culture than chemicals. Interestingly, natural supplements may improve fish growth and health (Clotfelter et al., 2007; Wang et al., 2006).

Karonda (*Carissa carandas*) is a member of the flowering plants of the Apocynaceae family. It is a huge shrub with 3 to 5-cm long branches and stems covered in thick, sharp spines. It features clusters of white blooms and single leaves. The fruit has smooth, waxy skin and is rounded or slightly oval. When young, the fruit is white and gradually turns pink and dark red as it ripens. The analysis of the phytochemicals in different parts of *C. carandas* indicated the existence of flavonoids, alcohol, cardiac glycosides, terpenoids, saponins, tannins, and phenolics (Itankar et al., 2011; Singh et al., 2020). Gas chromatography-mass spectrometry (GC-MS) identified various phytochemical substances in the extract of dried *C. carandas* fruit. These chemicals include myo-inositol, 4-c-methyl, 2*R*-acetoxymethyl-1,3,3-trimethyl-4*t*-(3-methyl-2-buten-1-yl)-1*t*-cyclohexanol, dichloroacetic acid, 2-ethylhexyl ester, 12-Oleanen-3-yl acetate, (3- $\alpha$ ), 2*R*-acetoxymethyl-1,3,3-trimethyl-4*t*-(3-methyl-2-buten-1-yl)-1*t*-cyclohexanol, and 1-pentatriacontanol (Anupama et al., 2014). Previous research has shown that *C. carandas* has antioxidant, anti-inflammatory, analgesic, anticancer, antidiabetic, and hepatoprotective activities (Itankar et al., 2011; Neimkhum et al., 2021). Additionally, *C. carandas* has demonstrated efficacy in treating diabetes, diarrhea, fever, ulcers, pain, asthma, and malaria in the application of traditional

medicine (Singh et al., 2020; Verma et al., 2015). Importantly, data indicates that the fruit of *C. carandas* has the potential to be used as a natural pigment in the dietary supplement, fabric, and pharmaceutical industries (Manicketh et al., 2020). As a result, these findings support the use of *C. carandas* fruit as a supplement in ornamental fish production.

The specific growth rate and weight gain are commonly used as indicators of the growth-promoting properties of herbs or their derivatives in aquaculture studies (Hoseinifar et al., 2019; Jahazi et al., 2020). Digestive enzymes are crucial for the breakdown of nutrients in fish diets. Diets enriched with herbal plants increase the activities of digestive enzymes, leading to potential improvements in fish development, feed intake, and feed efficiency (Mohammady et al., 2022). Fish are protected from infectious disorders caused by different pathogens through the secretion of skin mucus by goblet cells. Fish skin mucus is a non-specific immunological defense mechanism and contains vital biological molecules such as lysozymes, myeloperoxidase, and antimicrobial peptides (Hoseinifar et al., 2015). Medicinal plants in fish diets enhance skin mucus components, indicating an improvement of innate immune function by certain phytochemicals (Promprom et al., 2024). As stated above, lighter coloration in fish is directly related to the consumption of dietary carotenoids. Previous studies have suggested that incorporating carotenoids or  $\beta$ -carotene into the diet could increase the pigmentation levels in numerous fish species (Keleştemur & Çoban, 2016; Wang et al., 2006; Yanar et al., 2007). Therefore, it is postulated that incorporating natural products containing carotenoids and  $\beta$ -carotene into the diet of ornamental fish could be beneficial in enhancing their coloration (Dananjaya et al., 2015; Sathyaruban et al., 2021).

As mentioned above, different parts of *C. carandas* have been used to treat various ailments in folk medicine. However, no scientific research has documented the utilization of *C. carandas* in aquafeed or any other animal species. A recent study performed an acute toxicity test on male Wistar rats and observed that administering acetone extracts of *C. carandas* fruits at doses ranging from 500 to 5000 mg/kg body weight did not cause any deleterious effects or mortality (Saher et al., 2020). Moreover, *C. carandas* fruit contains natural pigments such as carotenoids and  $\beta$ -carotene. These findings suggest that *C. carandas* fruit could be utilized as a feed additive without toxicity. Thus, this work investigates the impacts of dietary administration of *C. carandas* fruit powder (CCFP) on the growth, digestive enzymes, skin mucosal immunology, and pigmentation in *B. splendens*.

## MATERIALS AND METHODS

### Chemicals and Reagents

Unless otherwise specified, the chemicals and reagents used throughout the present research were of analytical grade and obtained from Sigma-Aldrich (St. Louis, USA).

## Plant Samples

Ripe fruits of *C. carandas* were collected from a local market in the Khueang Nai District, Ubon Ratchathani, Thailand. A plant specimen was collected and taxonomically classified to the species level by the plant taxonomist. The plant specimen (Munglue 0018) was kept for future reference in the Biology program of the Faculty of Science, Ubon Ratchathani Rajabhat University.

## Preparation of *C. carandas* Fruit Powder

The sample of CCFP was made according to the method of Santos et al. (2019) with minor modifications. The fruits were rinsed with flowing tap water, and the seeds were separated. The seedless fruits were dried in a hot air oven at 60°C for three days and blended using an electronic blender. The dried sample was mixed with distilled water at the ratio of 100 mg/ml and boiled at 100°C for 15 min. The solution was then passed through a filter paper of Whatman No. 1. The filtrate was mixed with maltodextrin (1:1 w/w) and processed in a Büchi mini spray dryer (Büchi Labortechnik AG, B-290, Switzerland). The conditions of operation for spray drying were as follows: the inlet air temperature was 150°C, and the outlet air temperature was 107°C. The atomization pressure was 4 bars. The average feed rate was 0.5 L/h, and the average drying air flow rate was 75.63 m<sup>3</sup>/h. The sample was kept at -20°C for use in experiments.

## Phytochemical Determination

The colorimetric method of Jankham et al. (2024) was used to measure total flavonoid concentration in mg quercetin equivalent per gram of CCFP (mg QE/g CCFP). The Folin-Ciocalteu reagent method evaluated total phenolic content (Verma et al., 2015), reported as mg gallic acid equivalent per gram of CCFP (mg GAE/g CCFP). The terpenoid level was assessed using the methodology developed by Łukowski et al. (2022), and the outcomes are quantified as milligrams of linalool equivalent per gram of CCFP (mg LNOLE/g CCFP). The tannin concentration was determined using the Folin-Ciocalteu method (Anh & Tan, 2023), and the findings are shown as milligrams of tannic acid equivalent per gram of CCFP (mg TAE/g CCFP). The carotenoid content was assessed using the Foss et al. (1984) method, and the findings are shown as micrograms of carotenoids per gram of CCFP (µg/g CCFP). The β-carotene content was evaluated using the Biswas et al. (2011) method, and the findings are reported as µg of β-carotene per gram of CCFP (µg/g CCFP). All phytochemical tests were triplicated using a microplate reader (SPECTRO Star Nano, BMG LabTech, Germany).

## Antioxidant Activity

The 2,2-diphenyl-1-picrylhydrazyl (DPPH) test was used to assess the antioxidant activity of CCFP (Verma et al., 2015). The CCFP was diluted to final 0–1000 µg/ml concentrations

in methanol. After mixing 2 ml of each concentration with 1 ml of 0.2 mM DPPH reagent, the mixture was incubated at room temperature for 30 min. The absorbance was measured at 517 nm using a UV-visible spectrophotometer (Lambda 12, PerkinElmer, Connecticut, USA). The standard reference used in this research was ascorbic acid. IC<sub>50</sub> values and percentages of DPPH inhibition were computed.

## Diet Preparation

The fish diet (Product name: Higade 9006T) used in this study was obtained from Charoen Pokphand Foods PCL, Bangkok, Thailand. The levels of CCFP used were 0 (control), 3, 6, and 9 g/kg diet, based on the reports of Doan et al. (2020) and Pailan et al. (2012) with some modifications. The diet samples were combined with distilled water (1:4 w/v), homogenized using an electric meat mincer to produce extruded string shapes, and dried at 40°C for 24 h. The diets were then crushed into small pellets (1 mm) and kept at 4°C for future use. The basal diet's moisture, crude protein, crude fat, and ash were measured using Association of Official Analytical Chemists methods (AOAC, 2019). The fiber content was quantified following the methodology outlined by AOAC (2010). The proximate analysis of the basal diet is provided in Table 1.

Table 1  
*Proximate analysis of the basal diet used in this research*

Proximate analysis	Results (%)
Moisture	8.10
Crude protein	43.37
Crude lipid	6.26
Nitrogen-free extract	30.62
Ash	10.48
Fiber	1.16

*Note.* The crude protein, crude lipid, moisture, ash, and fiber were measured values. The nitrogen-free extract was calculated value

## Animal Ethics and Regulation

The study was carried out at the Ubon Ratchathani Rajabhat University Farm with permission from the Institutional Animal Care and Use Committee (AN64003).

## Fish Preparation

Male *B. splendens* with a solid red phenotypic was purchased from Ubon Ratchathani Fish Cooperatives and acclimatized in the laboratory for two weeks. Daily monitoring was conducted during the acclimatization period to observe the experimental fish's exterior appearance, general behavior, and health. Fish with an initial weight of  $0.42 \pm 0.02$  g and an initial length of  $3.20 \pm 0.07$  cm were raised individually in plastic beakers of 11.5 cm in height and 8 cm in diameter, filled with 250 ml of dechlorinated water and exposed to a 12-hour light/12-hour dark cycle. The basal diet was given to the fish twice a day, at 8:00 and 17:00. Water quality parameters, including temperature ( $29.51 \pm 0.34^\circ\text{C}$ ), pH ( $7.65 \pm 0.17$ ), alkalinity ( $110.02 \pm 1.68$  mg/L), nitrite ( $0.0029 \pm 0.0003$  mg/L), nitrate ( $0.042$

$\pm 0.005$  mg/L), and dissolved oxygen ( $6.78 \pm 0.20$  mg/L), were checked and maintained under standard conditions for *B. splendens* cultivation (Thongprajukaew et al., 2011). The water in the containers was changed daily.

## Experimental Design

The study used a completely randomized design (CRD). There were four treatments, each with three replications with 20 fish. The treatments included a control group (0 g CCFP/kg) and three experimental groups (3, 6, and 9 g CCFP/kg). The experiment was carried out over eight weeks.

## Growth and Survival Rate

At the end of the experimental period, the fish were starved for 24 h. All the fish from each replicate were harvested for the evaluation of growth and survival using the following equations:

$$\text{Weight gain (WG, g)} = \text{Final weight (g)} - \text{Initial weight (g)} \quad [1]$$

$$\text{Specific growth rate (SGR, \%/day)} = \frac{\text{Ln final weight (g)} - \text{Ln initial weight (g)}}{\text{the experimental period}} \times 100 \quad [2]$$

$$\text{Average daily gain (ADG, g/day)} = \frac{\text{(final weight (g)} - \text{initial weight (g)})}{\text{the experimental period}} \quad [3]$$

$$\text{Feed conversion ratio} = \frac{\text{feed consumed by fish (g)}}{\text{final fish weight (g)}} \quad [4]$$

$$\text{Condition factor (g/cm}^3\text{)} = 100 \times [\text{fish weight (g)}]/[\text{fish length}^3 \text{ (cm)}] \quad [5]$$

$$\text{Survival rate (\%)} = \frac{\text{number of fish at the end of the experiment}}{\text{number of fish at the beginning of the experiment}} \quad [6]$$

## Skin Mucus Collection

Four fish per replication were subjected to a 24-hour starvation period, after which skin mucus was collected using the method mentioned by Hoseinifar et al. (2015). The fish were anesthetized using clove oil (5 ml/L) in an appropriate container with an electric air pump. Each fish was placed in a plastic bag with 10 ml of 50 mM NaCl. To collect the skin mucus, the fish were moved gently by hand for 1 min. The skin sample was then transferred to a test tube and centrifuged at  $3000 \times g$  for 5 min at  $4^\circ\text{C}$ . After being collected, the supernatant was kept at  $-20^\circ\text{C}$  for use in other tests.

## Skin Mucus Assays

The gram-positive bacterium *Micrococcus lysodeikticus* was lysed using the turbidimetric method to evaluate lysozyme activity. Alkaline phosphatase (ALP) activity was quantified

using *p*-nitrophenyl phosphate as a substrate (Wangkahart et al., 2022). Hoseinifar et al. (2015) used the method to measure total immunoglobulin M (IgM). The activity of mucosal myeloperoxidase (MPO) was determined based on the protocol of Doan et al. (2020). Skin mucus protein levels were estimated using a Lowry assay (Lowry et al., 1951), with bovine serum albumin as the standard reference. The ferric ion-reducing antioxidant power assay, as reported by Fernández-Alacid et al. (2019), was used to determine the total antioxidant capacity (T-AOC). The activities of catalase (CAT) and superoxide dismutase (SOD) were assessed using the protocols described by Wangkahart et al. (2022).

### Digestive Enzyme Collection

After a 24-hour starvation period, four fish from each replicate were harvested and anesthetized individually using a specific dose of clove oil. The abdominal wall was then opened, and the internal organs were collected, cleared of connective tissues, cleaned with 0.90% normal saline solution, and weighed. The digestive tract was extracted using 0.2 M Na<sub>2</sub>HPO<sub>4</sub>-NaH<sub>2</sub>PO<sub>4</sub> buffer (pH 8) at a ratio of 1:10 (w/v). After that, the samples were centrifuged for 30 minutes at -4°C at 15,000 × *g*. The supernatants were kept at -20°C until analysis.

### Digestive Enzyme Activities and Protein Content

Soluble starch served as the substrate to test the amylase activity. A standard curve of reducing sugar was used to compare the absorbance, which was determined at 540 nm (Willora et al., 2022). The lipase activity was evaluated using *p*-nitrophenyl palmitate (*p*-NPP) as a substrate, as Winkler and Stuckmann (1979) reported. The solutions were quantified at a wavelength of 410 nm and compared to a standard curve of *p*-nitrophenol. The assessment of protease activity was conducted using the method presented by Wangkahart et al. (2022), using azocasein as a substrate. The solutions were measured at 440 nm and compared with a standard curve of tyrosine. The specific digestive enzyme activities are given in units per milligram of total protein (U/mg total protein). Lowry et al. (1951) outlined the method to determine the total protein concentration in the digestive tract supernatant. The activities of digestive enzymes were calculated using the following equation (Willora et al., 2022):

$$\text{Specific enzyme activities (U/mg total protein)} = \frac{(\Delta Abs \times V_{total})}{\epsilon \times V_{sample} \times t} \times \frac{\text{ml}}{\text{mg total protein}} \quad [7]$$

Where,  $\Delta Abs$  represents the test samples' absorbance,  $V_{total}$  is the total volume of the reaction solution,  $\epsilon$  is the molar extinction coefficient,  $V_{sample}$  is the volume of the supernatant used in the reaction, and  $t$  is the reaction time.

## **Carotenoid Contents**

The carotenoid content in the fish was assayed according to the method of Thongprajukaew et al. (2012). Briefly, four fish from each replicate were starved for 24 hours. Each fish was then anesthetized with a specific concentration of clove oil in an appropriate container equipped with an electric air pump. Skin, muscle, pectoral fin, caudal fin, pelvic fin, dorsal fin, and anal fin samples were collected and stored separately in centrifuge tubes. Three milligrams of each sample were introduced into microcentrifuge tubes containing 1 ml of 90% acetone and stored in the dark at 4°C for three days. The samples were shaken twice daily. To determine the carotenoid content, the samples were centrifuged at  $5000 \times g$  for 10 mins at a temperature of 4°C. Collected supernatants were measured at 474 nm. The carotenoid content was calculated according to Thongprajukaew et al. (2012). The results are presented as  $\mu\text{g}$  per gram of sample ( $\mu\text{g/g}$  wet weight).

## **Data Analysis**

Kolmogorov–Smirnov and Levene’s tests were used to test data normality and variance homogeneity, respectively. If the data distribution was abnormal, square-root and arcsine transformations were used. The data are shown as mean  $\pm$  SEM (standard error of the mean). Duncan’s multiple range test and one-way analysis of variance (ANOVA) were used to assess significant variations among treatments. There was a statistically significant difference between the treatments when the  $p$ -value was less than 0.05.

## **RESULTS**

### **Phytochemical Determination and Antioxidant Activity**

The results of the phytochemical determination in CCFP are presented in Table 2. The phytochemical compounds found in CCFP were flavonoids, phenolics, terpenoids, tannins, carotenoids, and  $\beta$ -carotene. Moreover, the  $\text{IC}_{50}$  value of the antioxidant activity estimated by the DPPH assay in CCFP was  $256.12 \pm 7.68 \mu\text{g/ml}$ , lower than the  $\text{IC}_{50}$  value of ascorbic acid.

### **Growth Parameters**

The final weight, length, WG, ADG, and SGR of the fish fed the CCFP diets were significantly greater than those of the control fish ( $p < 0.05$ ; Table 3). However, the FCR, condition factor, and survival rate were not significantly different among the treatments after eight weeks of experimentation ( $p > 0.05$ ).

### **Mucosal Skin Immune Activity**

Figure 1 illustrates the effects of CCFP diets on skin mucus immune parameters. After an eight-week experimental period, dietary supplementation with CCFP led to a significant



Table 2

*Qualitative determination and antioxidant activity of C. carandas fruit powder*

Phytochemicals	Results
Total flavonoid content (mg QE/g CCFP)	15.97 ± 0.48
Total phenolic content (mg GAE/g CCFP)	43.52 ± 1.73
Terpenoids (mg LNOLE/g CCFP)	350.00 ± 15.66
Tannins (mg TAE/g CCFP)	40.97 ± 0.15
Carotenoids (µg/g CCFP)	5.53 ± 0.73
β-carotene (µg/g CCFP)	0.67 ± 0.05
DPPH assay (IC <sub>50</sub> )	
CCFP (µg/ml)	256.12 ± 7.68
Ascorbic acid (µg/ml)	60.97 ± 0.48

Note. Data are represented as mean ± SEM,  $n = 3$  for each test, QE = quercetin equivalent, GAE = gallic acid equivalent, LNOLE = linalool equivalent, TAE = tannic acid equivalent, DPPH = 2,2-diphenyl-1-picrylhydrazyl

Table 3

*Growth parameters of B. splendens fed C. carandas fruit powder diets and control diet for eight weeks*

Parameters	CCFP (g/kg diet)			
	0 (Control)	3	6	9
IW (g)	0.42 ± 0.03	0.38 ± 0.02	0.44 ± 0.03	0.41 ± 0.02
FW (g)	0.92 ± 0.05 <sup>b</sup>	1.14 ± 0.06 <sup>a</sup>	1.25 ± 0.13 <sup>a</sup>	1.27 ± 0.07 <sup>a</sup>
IL (cm)	3.12 ± 0.09	3.13 ± 0.09	3.26 ± 0.06	3.30 ± 0.06
FL (cm)	4.37 ± 0.15 <sup>b</sup>	5.02 ± 0.14 <sup>a</sup>	5.00 ± 0.25 <sup>a</sup>	5.27 ± 0.16 <sup>a</sup>
WG (g)	0.49 ± 0.03 <sup>b</sup>	0.76 ± 0.06 <sup>a</sup>	0.81 ± 0.11 <sup>a</sup>	0.85 ± 0.07 <sup>a</sup>
ADG (mg/day)	8.92 ± 0.02 <sup>b</sup>	13.57 ± 0.12 <sup>a</sup>	14.46 ± 0.25 <sup>a</sup>	15.35 ± 0.14 <sup>a</sup>
SGR (%/day)	1.04 ± 0.07 <sup>b</sup>	1.33 ± 0.02 <sup>a</sup>	1.19 ± 0.08 <sup>a</sup>	1.36 ± 0.05 <sup>a</sup>
FCR	1.46 ± 0.08	1.41 ± 0.09	1.28 ± 0.17	1.41 ± 0.09
CF (g/cm <sup>3</sup> )	1.07 ± 0.12	0.92 ± 0.08	1.03 ± 0.11	0.87 ± 0.04
SR (%)	100.00 ± 0.00	100.00 ± 0.00	100.00 ± 0.00	100.00 ± 0.00

Note. The different superscripts indicated in each row show a significant difference at  $p < 0.05$ . Data are represented as mean ± SEM. IW = initial weight (g), FW = final weight (g), IL = initial length (cm), FL = final length (cm), WG = weight gain (g), ADG = average daily gain (mg/day), SGR = specific growth rate (%/day), FCR = feed conversion ratio, CF = condition factor (g/cm<sup>3</sup>), SR = survival rate (%)

increase in lysozyme, IgM, and myeloperoxidase levels compared to the basal diet. According to the results, fish fed a 3 g CCFP-containing diet showed a significant increase in ALP levels compared to other groups. The results also demonstrated that fish-fed diets containing 6 and 9 g of CCFP had substantially higher total protein concentrations than the control and 3 g CCFP-treated groups.

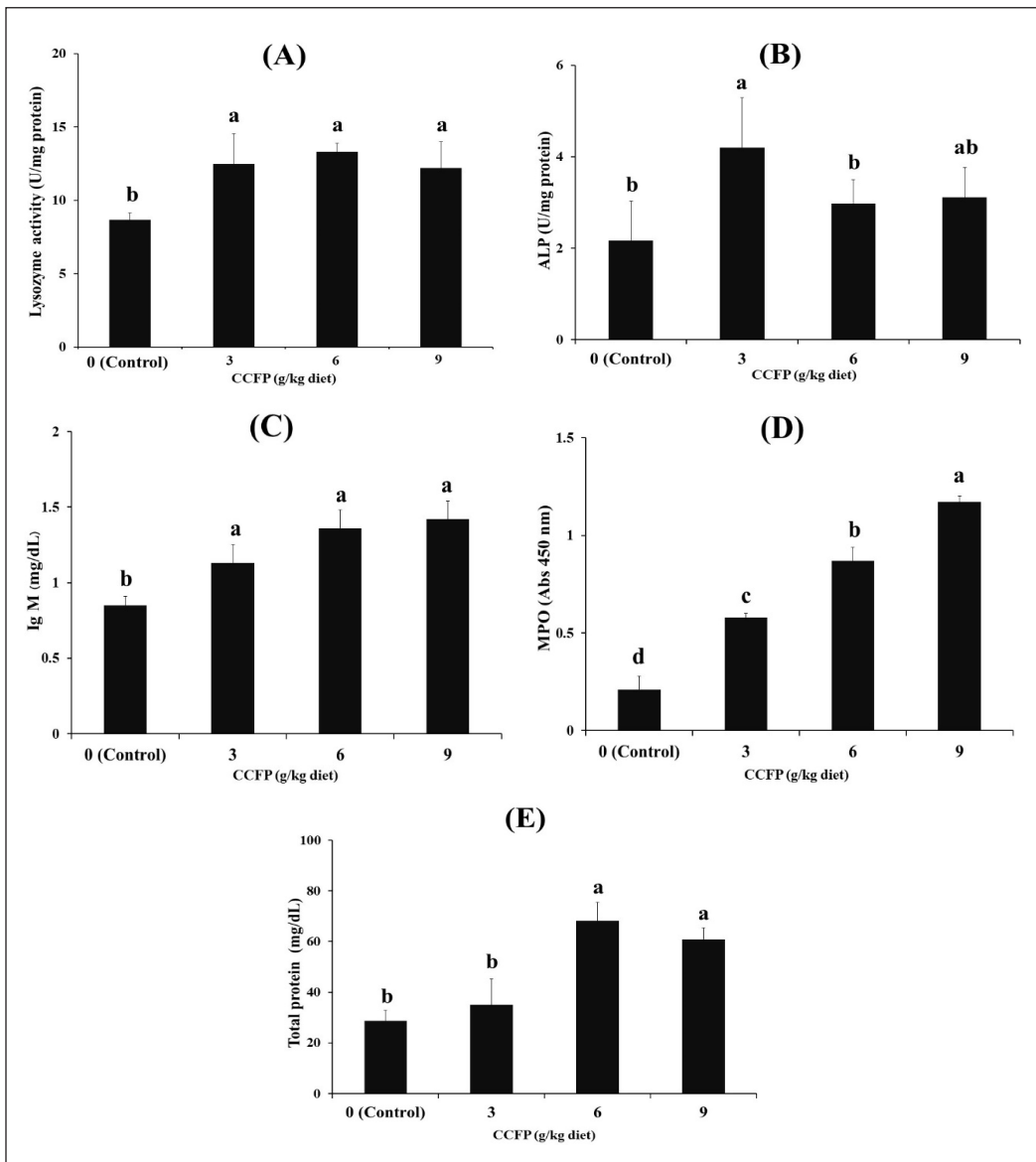


Figure 1. Non-specific skin mucus immune parameters of *B. splendens* fed *C. carandas* fruit powder diets and control diet for eight weeks. (A) Lysozyme activity, (B) Alkaline phosphatase (ALP), (C) Immunoglobulin M (IgM), (D) Myeloperoxidase (MPO), (E) Total protein. The different superscripts indicated a significant difference at  $p < 0.05$ .  $n = 12$  for each group. Data are represented as mean  $\pm$  SEM

### Antioxidant Capacity

The results illustrate the effects of dietary CCFP on the antioxidant capacity of *B. splendens*, as depicted in Figure 2. The levels of T-AOC in the fish-fed diets containing 6 and 9 g CCFP/kg were notably greater than those in the control fish. Moreover, fish fed a diet

containing 6 g CCFP/kg showed the highest CAT activity compared to the other groups. Also, the SOD activities in the experimental groups were significantly greater compared to those in the control group.

### Digestive Enzyme Activities and Protein Content

Figure 3 displays the levels of digestive enzyme activity, and protein content of fish fed different levels of CCFP. The results revealed that fish fed a 9 g CCFP/kg diet showed the highest protease activity compared to the other groups. Furthermore, the CCFP diets significantly increased fish lipase activity compared to the control diet. In addition, fish fed 6 and 9 g CCFP/kg diets had higher amylase activities than other groups. However, the total protein contents did not differ significantly among the groups.

### Carotenoid Contents

Table 4 presents the effects of dietary supplementation with CCFP on the carotenoid content of *B. splendens* over 8 weeks. The results indicated that fish fed 3 and 9 g CCFP/kg diets had a significant increase in carotenoid content in the skin compared with the other groups. In addition, fish fed a 3 g CCFP/kg diet showed the highest muscle carotenoid content. Furthermore, fish fed with CCFP-containing diets had higher carotenoid levels in their caudal fins than control fish. Fish fed a 9 g CCFP/kg diet showed the highest levels of carotenoid in the pectoral, pelvic, dorsal, and anal fins.

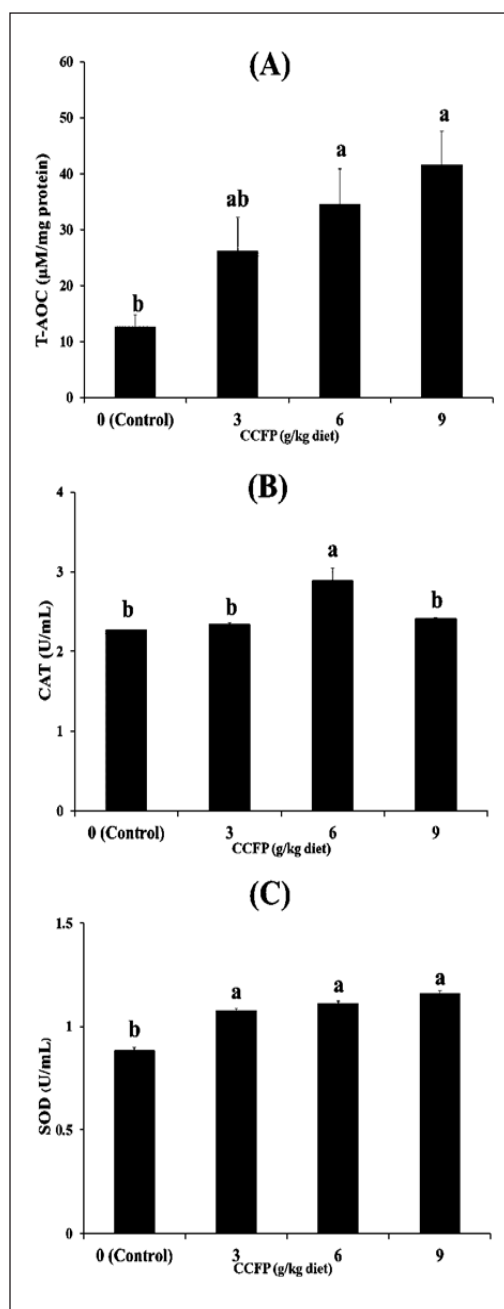


Figure 2. Antioxidative enzyme activity in *B. splendens* fed *C. carandas* fruit powder diets and control diet for eight weeks. (A) Total antioxidant capacity (T-AOC), (B) Catalase (CAT), (C) Superoxide dismutase (SOD). The different superscripts indicated a significant difference at  $p < 0.05$ .  $n = 12$  for each group. Data are represented as mean  $\pm$  SEM

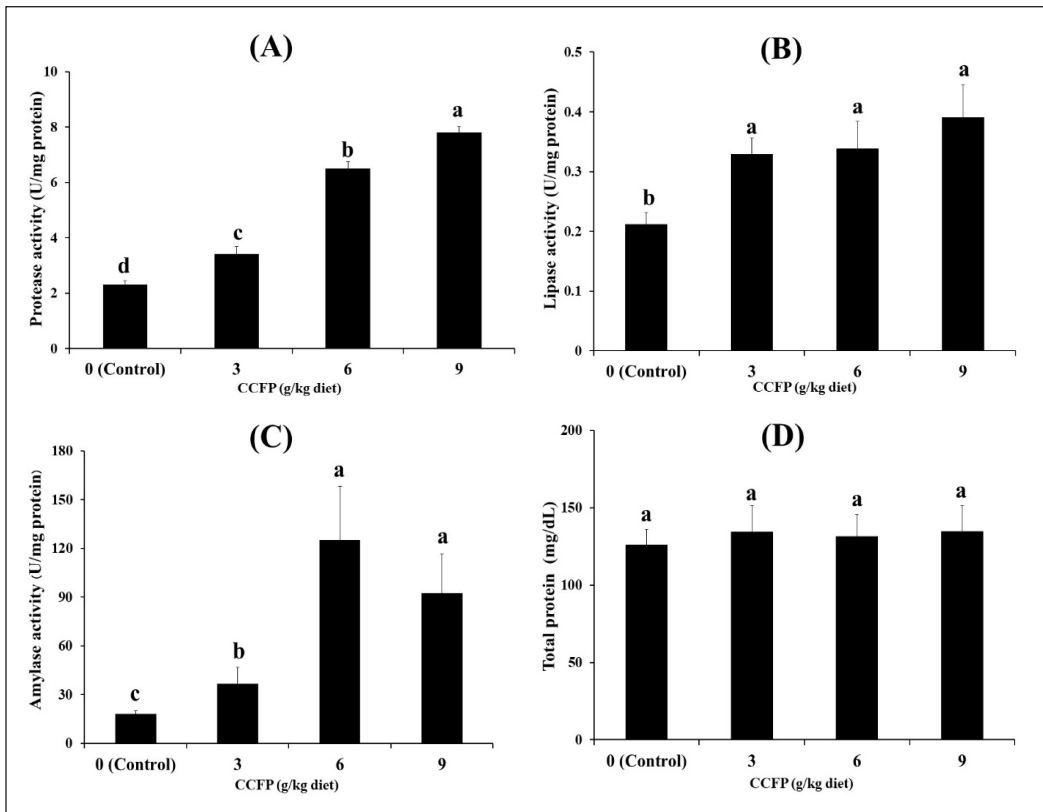


Figure 3. Digestive enzyme activities and protein contents in *B. splendens* fed *C. carandas* fruit powder diets and control diet for eight weeks. (A) Protease activity; (B) Lipase activity; (C) Amylase activity; (D) Total protein. The different superscripts indicated a significant difference at  $p < 0.05$ .  $n = 12$  for each group. Data are represented as mean  $\pm$  SEM

Table 4

Total carotenoid contents ( $\mu\text{g/g}$  wet weight) in skin, muscle, and fins of *B. splendens* fed *C. carandas* fruit powder diets and control diet for eight weeks

Parameters	CCFP (g/kg diet)			
	0 (Control)	3	6	9
Skin	21.34 $\pm$ 4.64 <sup>c</sup>	99.86 $\pm$ 2.39 <sup>a</sup>	80.25 $\pm$ 8.42 <sup>b</sup>	112.13 $\pm$ 5.84 <sup>a</sup>
Muscle	34.61 $\pm$ 9.85 <sup>c</sup>	86.24 $\pm$ 2.00 <sup>a</sup>	56.25 $\pm$ 1.38 <sup>b</sup>	60.33 $\pm$ 9.65 <sup>b</sup>
Pectoral fin	419.68 $\pm$ 25.18 <sup>c</sup>	473.80 $\pm$ 19.20 <sup>c</sup>	655.89 $\pm$ 37.74 <sup>b</sup>	1902.83 $\pm$ 78.52 <sup>a</sup>
Caudal fin	241.82 $\pm$ 19.63 <sup>b</sup>	717.79 $\pm$ 32.17 <sup>a</sup>	721.34 $\pm$ 12.67 <sup>a</sup>	724.53 $\pm$ 13.33 <sup>a</sup>
Pelvic fin	323.15 $\pm$ 19.00 <sup>c</sup>	775.07 $\pm$ 50.74 <sup>b</sup>	702.83 $\pm$ 34.07 <sup>b</sup>	1387.93 $\pm$ 57.88 <sup>a</sup>
Dorsal fin	319.64 $\pm$ 12.79 <sup>d</sup>	609.69 $\pm$ 16.88 <sup>c</sup>	787.15 $\pm$ 48.21 <sup>b</sup>	1847.33 $\pm$ 74.39 <sup>a</sup>
Anal fin	475.55 $\pm$ 17.90 <sup>d</sup>	696.55 $\pm$ 31.39 <sup>c</sup>	886.71 $\pm$ 88.32 <sup>b</sup>	1176.44 $\pm$ 81.74 <sup>a</sup>

Note. The different superscripts indicated in each row show a significant difference at  $p < 0.05$ .  $n = 12$  for each group. Data are represented as mean  $\pm$  SEM

## DISCUSSION

### Phytochemical Determination and Antioxidant Activity

The accumulation of reactive free radicals can damage cellular components. Natural products have been used to prevent oxidative processes in cells (Almarri et al., 2023). Plants contain a wide range of antioxidants, such as phenolics, flavonoids, and carotenoid pigments (Promprom et al., 2024). These compounds have been isolated and tested for their potential use in various applications (Dananjaya et al., 2015; Manicketh et al., 2020). The aquaculture industry has used medicinal herbs and their secondary metabolites as feed additives to enhance the growth and physiological features of several aquatic species (Hoseinifar et al., 2015; Jahazi et al., 2020; Jankham et al., 2024; Mohammady et al., 2022). This research indicated that CCFP consists of flavonoids, phenolics, terpenoids, tannins, carotenoids, and  $\beta$ -carotene. In addition, the CCFP exhibited antioxidant properties with an  $IC_{50}$  value of  $256.12 \pm 7.68$   $\mu\text{g/ml}$  as determined by the DPPH assay. As a result, this study supports using CCFP as a natural supplement to improve fish growth, health, and coloration.

### Growth Performance

In this study, dietary supplementation with CCFP at concentrations of 3, 6, and 9 g/kg for eight weeks resulted in significant increases in growth parameters compared to those in the control group. Moreover, the application of CCFP to the diet had no noticeable effects on FCR, CF, or SR in *B. splendens*. Similar to the previous study, juvenile *B. splendens* fed a microwave-irradiated diet showed a significant increase in body weight, CF, SGR, net weight, and ADG when compared with the control, gamma-irradiated diet, probiotic-containing diet, and carbohydrase-supplemented diet (Thongprajukaew et al., 2011). Furthermore, Patria et al. (2024) indicated that dietary supplementation with *Spirulina* powder from *Arthrospira maxima* at 15% significantly increased the growth of *B. splendens*. The improvement in growth and survival rates is crucial for ensuring the productivity and profitability of the aquaculture industry. The addition of plants or their bioactive compounds to feeds can improve growth and nutrient utilization in various aquatic species. The growth-promoting properties of CCFP detected in this research may be due to phytochemicals like flavonoids and phenolic compounds, which have been shown to stimulate appetite, enhance the secretion of digestive enzymes in the gastrointestinal tract, boost immune functions, resist bacterial infections, and mitigate environmental stress, ultimately promoting overall fish health (Jankham et al., 2024; Patel & Rao, 2013). This present study suggests that CCFP could be a useful novel dietary supplement to improve fish growth (Almarri et al., 2023). However, further investigations should focus on elucidating the effects of CCFP on nutrient digestion and absorption in different aquatic animals.

### **Mucus Immunological Parameters**

The findings of this study showed that fish fed CCFP diets had considerably higher levels of total protein, IgM, lysozyme, and ALP than fish fed a control diet. It is generally accepted that fish skin mucus acts as the first line of defense against pathogen invasion (Doan et al., 2020; Promprom et al., 2024). It contains various molecules, such as lysozyme, ALP, and IgM (Hoseinifar et al., 2015). Lysozyme plays a crucial role in disease prevention by lysing pathogenic bacteria. ALP is involved in the defense of fish against several pathogenic agents. IgM neutralizes invading antigens, and MPO protects by destroying foreign substances and pathogens through phagocytosis. The results of this study were in agreement with Motlagh et al. (2020), who noted that female guppy fish (*Poecilia reticulata*) fed diets supplemented with garlic extract showed a significant increase in lysozyme activity, IgM, and ALP when compared with the control. The improvement of immunological parameters in the skin mucus of *B. splendens* by CCFP is likely due to the effects of flavonoids, phenolics, and carotenoids, which regulate the production of active components in the immune system (Hoseinifar et al., 2015; Motlagh et al., 2020). Nevertheless, additional experiments are required to investigate the molecular mechanisms by which CCFP influences non-specific immunological responses in aquatic animals.

### **Antioxidant Capacity**

The present study demonstrated that dietary CCFP increased the activity of T-AOC, CAT, and SOD in *B. splendens* skin mucus. T-AOC is commonly used to assess the antioxidant potential of phytochemicals in fish (Hendam et al., 2024). The primary function of CAT is to degrade H<sub>2</sub>O<sub>2</sub> into water and oxygen, thereby preventing oxidative damage to cells and their components (Shekarabi et al., 2022). SOD plays a crucial role in reducing free superoxide anion radicals in the body (Hendam et al., 2024). It is possible that phenolics, flavonoids, tannins, terpenoids, and carotenoids found in CCFP may be responsible for a significant increase in the antioxidant capacity in skin mucus (Neimkhum et al., 2021). Therefore, the increase in antioxidant enzyme activity caused by dietary CCFP would reduce oxidative stress in fish (Singh et al., 2020; Verma et al., 2015). A possible reason for this is that CCFP may enhance the expression of fish antioxidant genes (Mohammady et al., 2022). Nevertheless, more research is necessary to verify this hypothesis.

### **Digestive Enzyme Activities and Protein Content**

The present investigation showed that CCFP supplementation in fish diets significantly increased intestinal protease, lipase, and amylase activities in *B. splendens*. Similar research by Thongprajukaew et al. (2011) noted that *B. splendens* fed a microwave-irradiated diet revealed a significant increase in amylase activity when compared with the other modified

diets. Moreover, the application of curcumin to the diet at 5 g/kg produced a significant enhancement of trypsin and lipase activities in the intestine of crucian carp (*Carassius auratus*) (Jiang et al., 2016). It is well-established that the activity of digestive enzymes is a major indicator of digestive processes in animals (Jiang et al., 2016; Mohammady et al., 2022). The addition of medicinal plants to diets can increase digestive enzyme activity in the tract, resulting in growth improvements in cultured fish (Mohammady et al., 2022; Promprom et al., 2024). It has been reported that phytochemicals such as phenolics, flavonoids, tannins, and pigments have been reported to promote the secretion of digestive enzymes (Almarri et al., 2023; Jiang et al., 2016). Based on the findings of this study, the flavonoids, phenolics, and tannins present in CCFP may be responsible for the elevated digestive enzyme activities in *B. splendens* (Almarri et al., 2023). Therefore, the increased digestive enzyme activities could support the growth of fish.

### Carotenoid Contents

This study revealed that dietary supplementation with CCFP significantly increased the total carotenoid contents in various parts of *B. splendens*. It was found by Patria et al. (2024) that a 15% spirulina power-supplemented diet significantly enhanced the color brightness in *B. splendens* when compared with the control diet. The coloration of fish is influenced by the accumulation of pigments, such as carotenoids, in chromatophores. Carotenoids are absorbed in the intestinal mucosa and distributed in various organs of fish, including the skin, muscle, reproductive organs, and liver, through the action of lipoproteins (Sathyaruban et al., 2021). Genetics, the life cycle, stress, diet compositions, and environmental conditions are among the factors influencing the distribution and accumulation patterns of carotenoids in fish (Nascimento et al., 2019; Thongprajukaew et al., 2011; Sathyaruban et al., 2021). Ornamental fish are unable to synthesize carotenoid pigments and must obtain coloring pigments from their diet. The application of synthetic carotenoids to fish feed can enhance the integument coloration (Keleştemur & Çoban, 2016; Wang et al., 2006). However, using synthetics increases the cost of fish production (Dananjaya et al., 2015). Therefore, there is a need to develop novel feed additives with skin color-promoting properties for cultivating ornamental fish (Sathyaruban et al., 2021). The present study showed that dietary supplementation of CCFP enhanced the carotenoid contents in the skin, muscles, and fins of *B. splendens*. The current study also revealed that CCFP contains significant amounts of carotenoids and  $\beta$ -carotene. Previous research has indicated that the skin pigmentation of fish can be enhanced by the application of plants that contain carotenoids, flavonoids, and betalains (Thongprajukaew et al., 2012; Sathyaruban et al., 2021; Yanar et al., 2007). According to the results of this investigation, CCFP may be used as a natural carotenoid source to improve skin color in ornamental fish.

## CONCLUSION

This research indicates that *C. carandas* fruit powder (CCFP) is a promising novel feed additive for enhancing various aspects of *B. splendens* health and performance. Specifically, CCFP supplementation improved fish growth, the mucosal immune response, digestive enzyme activity, and skin pigmentation. The estimated optimal CCFP supplementation concentration was 9 g/kg of diet.

## ACKNOWLEDGMENTS

This research was partially funded by a grant from Ubon Ratchathani Rajabhat University (Grant No. UBRU\_2565). The authors express their gratitude to Miss Pattra Srihabandit and Miss Tucsaporn Suwannakoot for their support and assistance in conducting this study.

## REFERENCES

- Almarri, S. H., Khalil, A. A., Mansour, A. T., & El-Houseiny, W. (2023). Antioxidant, immunostimulant, and growth-promoting effects of dietary *Annona squamosa* leaf extract on Nile tilapia, *Oreochromis niloticus*, and its tolerance to thermal stress and *Aeromonas sobria* infection. *Animals*, *13*(4), 746. <https://doi.org/10.3390/ani13040746>
- Anh, C. H., & Tan, M. L. (2023). Screening of medicinal plant extracts in Vietnam and investigation of their combination for preventing and treating gout. *Fine Chemical Technologies*, *18*(1), 38-47. <https://doi.org/10.32362/2410-6593-2023-18-1-38-47>
- Anupama, N., Madhumitha, G., & Rajesh, K. S. (2014). Role of dried fruits of *Carissa carandas* as anti-inflammatory agents and the analysis of phytochemical constituents by GC-MS. *BioMed Research International*, *2014*(1), 512369. <https://doi.org/10.1155/2014/512369>
- Biswas, A. K., Sahoo, J., & Chatli, M. K. (2011). A simple UV-Vis spectrophotometric method for determination of  $\beta$ -carotene content in raw carrot, sweet potato and supplemented chicken meat nuggets. *LWT - Food Science and Technology*, *44*(8), 1809–1813. <https://doi.org/10.1016/j.lwt.2011.03.017>
- Clotfelter, E. D., Ardia, D. R., & McGraw, K. J. (2007). Red fish, blue fish: Trade-offs between pigmentation and immunity in *Betta splendens*. *Behavioral Ecology*, *18*(6), 1139–1145. <https://doi.org/10.1093/beheco/arm090>
- Dananjaya, S. H. S., Munasinghe, D. M. S., Ariyaratne, H. B. S., Lee, J., & De Zoysa, M. (2015). Natural bixin as a potential carotenoid for enhancing pigmentation and colour in goldfish (*Carassius auratus*). *Aquaculture Nutrition*, *23*(2), 255–263. <https://doi.org/10.1111/anu.12387>
- Doan, H. V., Hoseinifar, S. H., Jaturasitha, S., Dawood, M. A. O., & Harikrishnan, R. (2020). The effects of berberine powder supplementation on growth performance, skin mucus immune response, serum immunity, and disease resistance of Nile tilapia (*Oreochromis niloticus*) fingerlings. *Aquaculture*, *520*, 734927. <https://doi.org/10.1016/j.aquaculture.2020.734927>
- Fernández-Alacid, L., Sanahuja, I., Ordóñez-Grande, B., Sánchez-Nuño, S., Herrera, M., & Ibarz, A. (2019). Comparison between properties of dorsal and ventral skin mucus in Senegalese sole: Response to an acute stress. *Aquaculture*, *513*, 734410. <https://doi.org/10.1016/j.aquaculture.2019.734410>



- Foss, P., Storebakken, T., Schiedt, K., Liaaen-Jensen, S., Austreng, E., & Streiff, K. (1984). Carotenoid in diets for salmonids: I. Pigmentation of rainbow trout with the individual optical isomers of astaxanthin in comparison with canthaxanthin. *Aquaculture*, *41*(3), 213-226. [https://doi.org/10.1016/0044-8486\(84\)90284-9](https://doi.org/10.1016/0044-8486(84)90284-9)
- Gruneck, L., Jinatham, V., Therdtatha, P., & Popluechai, S. (2022). Siamese fighting fish (*Betta splendens* Regan) gut microbiota associated with age and gender. *Fishes*, *7*, 347. <https://doi.org/10.3390/fishes7060347>
- Hendam, B. M., Baromh, M. Z., Khafaga, A. F., Shukry, M., El-Son, M. A. M., & Abdel-Latif, H. M. R. (2024). Effects of dietary baobab, *Adansonia digitata* on growth, haemato-immunological status, antioxidant biomarkers, intestinal histomorphometry, gene expression responses, and disease resistance in Nile tilapia, *Oreochromis niloticus*. *Aquaculture*, *581*, 740473. <https://doi.org/10.1016/j.aquaculture.2023.740473>
- Hoseinifar, S. H., Khalili, M., Rufchaei, R., Raehsi, M., Attar, M., Cordero, H., & Esteban, M. Á. (2015). Effects of date palm fruit extracts on skin mucosal immunity, immune related genes expression and growth performance of common carp (*Cyprinus carpio*) fry. *Fish & Shellfish Immunology*, *47*(2), 706–711. <https://doi.org/10.1016/j.fsi.2015.09.046>
- Hoseinifar, S. H., Zou, H. K., Doan, H. V., Harikrishnan, R., Yousefi, M., Paknejad, H., & Ahmadifar, E. (2019). Can dietary jujube (*Ziziphus jujuba* Mill.) fruit extract alter cutaneous mucosal immunity, immune related genes expression in skin and growth performance of common carp (*Cyprinus carpio*)? *Fish and Shellfish Immunology*, *94*, 705–710. <https://doi.org/10.1016/j.fsi.2019.09.016>
- Itankar, P. R., Lokhande, S. J., Verma, P. R., Arora, S. K., Sahu, R. A., & Patil, A. T. (2011). Antidiabetic potential of unripe *Carissa carandas* Linn. fruit extract. *Journal of Ethnopharmacology*, *135*(2), 430–433. <https://doi.org/10.1016/j.jep.2011.03.036>
- Jahazi, M. A., Hoseinifar, S. H., Jafari, V., Hajimoradloo, A., Doan, H. V., & Paolucci, M. (2020). Dietary supplementation of polyphenols positively affects the innate immune response, oxidative status, and growth performance of common carp, *Cyprinus carpio* L. *Aquaculture*, *517*, 734709. <https://doi.org/10.1016/j.aquaculture.2019.734709>
- Jankham, A., Promprom, W., Chatan, W., Somnate, K., Khambaione, S., & Munglue, P. (2024). Effects of dietary star apple (*Chrysophyllum cainito* L.) peel extract on growth performance, intestinal histology, hematology, and non-specific immune parameters in common lowland frog (*Rana rugulosa* Wiegmann). *Natural and Life Sciences Communications*, *23*(1). e2024009. <https://doi.org/10.12982/nlsc.2024.009>
- Jiang, J., Wu, X.-Y., Zhou, X.-Q., Feng, L., Liu, Y., Jiang, W.-D., Wu, P., & Zhao, Y. (2016). Effects of dietary curcumin supplementation on growth performance, intestinal digestive enzyme activities and antioxidant capacity of crucian carp *Carassius auratus*. *Aquaculture*, *463*, 174–180. <https://doi.org/10.1016/j.aquaculture.2016.05.040>
- Karshi, Z. (2021). Effects of synthetic androgen (17 $\alpha$ -methyltestosterone) and estrogen (17 $\beta$ -estradiol) on growth and skin coloration in emperor red cichlid, *Aulonocara nyassae* (Actinopterygii: Cichliformes: Cichlidae). *Acta Ichthyologica Et Piscatoria*, *51*(4), 357–363. <https://doi.org/10.3897/aiep.51.70223>
- Keleştemur, G. T., & Çoban, O. E. (2016). Effects of the  $\beta$ -carotene on the growth performance and skin pigmentation of rainbow trout (*Oncorhynchus mykiss*, W. 1792). *Journal of Fisheries and Livestock Production*, *4*(1), 1000162. <https://doi.org/10.4172/2332-2608.1000164>

- Krueahong, J., Srinoparatawatana, C., Prasoompon, S., & Panboonma, P. (2022). Promotion and development of fighting fish culture: A case study Siamese fighting fish farmers group, Bang muang sub-district, Mueang district, Nakhon Sawan province. *Journal of Agricultural Research and Extension*, 39(1), 114–126.
- Lowry, O. H., Rosebrough, N. J., Farr, A. L., & Randall, R. J. (1951). Protein measurement with the Folin phenol reagent. *Journal of Biological Chemistry*, 193(1), 265–275. [https://doi.org/10.1016/s0021-9258\(19\)52451-6](https://doi.org/10.1016/s0021-9258(19)52451-6)
- Łukowski, A., Jagiełło, R., Robakowski, P., Adamczyk, D., & Karolewski, P. (2022). Adaptation of a simple method to determine the total terpenoid content in needles of coniferous trees. *Plant Science*, 314, 111090. <https://doi.org/10.1016/j.plantsci.2021.111090>
- Manicketh, T. J., Francis, M. S., & Joseph, G. (2020). Extraction of natural colourants from mussaenda hybrid (*M. philippica* × *M. luteola*), *Carissa carandas* L. and *Syzygium cumini* L. for textile colouration. *Natural Product Research*, 35(21), 4159–4163. <https://doi.org/10.1080/14786419.2020.1741578>
- Mohammady, E. Y., Soaudy, M. R., Mohamed, A. E., El-Erian, M. M. A., Farag, A., Badr, A. M. M., Bassuony, N. I., Ragaza, J. A., El-Haroun, E. R., & Hassaan, M. S. (2022). Can dietary phytogetic mixture improve performance for growth, digestive enzyme activity, blood parameters, and antioxidant and related gene expressions of Nile tilapia, *Oreochromis niloticus*? *Animal Feed Science and Technology*, 290, 115369. <https://doi.org/10.1016/j.anifeedsci.2022.115369>
- Motlagh, H. A., Paolucci, M., Bami, L. M., & Safari, O. (2020). Sexual parameters, digestive enzyme activities, and growth performance of guppy (*Poecilia reticulata*) fed garlic (*Allium sativum*) extract supplemented diets. *Journal of the World Aquaculture Society*, 51(5), 1087–1097. <https://doi.org/10.1111/jwas.12729>
- Nascimento, L. da S., Reis, S. M., Ferreira, P. de M. F., Kanashiro, M. Y., Salara, A. L., & Zuanon, J. A. S. (2019). Effects of *Curcuma longa* rhizome on growth, skin pigmentation, and stress tolerance after transport of *Trichogaster labiosa*. *Revista Brasileira de Zootecnia*, 48, e20160282. <https://doi.org/10.1590/rbz4820160282>
- Neimkhum, W., Anuchapreeda, S., Lin, W.-C., Lue, S.-C., Lee, K.-H., & Chaiyana, W. (2021). Effects of *Carissa carandas* Linn. fruit, pulp, leaf, and seed on oxidation, inflammation, tyrosinase, matrix metalloproteinase, elastase, and hyaluronidase inhibition. *Antioxidants*, 10(9), 1345. <https://doi.org/10.3390/antiox10091345>
- Pailan, G. H., Archana, S., & Mrinal, K. (2012). Rose petals meal as natural carotenoid source in pigmentation and growth of rosy barb (*Puntius Conchonus*). *Indian Journal of Animal Nutrition*, 29(3), 291–296.
- Patel, P. R., & Rao, T. V. R. (2013). Physiological changes in karanda (*Carissa carandus* L.) fruit during growth and ripening. *Nutrition and Food Science*, 43(2), 128–136. <https://doi.org/10.1108/00346651311313346>
- Patria, M. P., Amanda, S. P., Susanti, H., Susilaningsih, D., & Taufikurahman, T. (2024). Growth response and color brightness of betta fish (*Betta splendens* (Regan, 1910)) supplemented by spirulina powder from algae *Arthrospira maxima* (Setchell and N. L. Gardner 1917)). *Journal of Agricultural Science and Technology*, 26(1), 73–83.
- Paulos, P., Runnalls, T. J., Nallani, G., Point, T. L., Scott, A. P., Sumpter, J. P., & Huggett, D. B. (2010). Reproductive responses in fathead minnow and Japanese medaka following exposure to a synthetic progestin, Norethindrone. *Aquatic Toxicology*, 99(2), 256–262. <https://doi.org/10.1016/j.aquatox.2010.05.001>

- Promprom, W., Chatan, W., Khambaione, S., Somnate, K., & Munglue, P. (2024). Effects of dietary supplementation of spray dried hog plum (*Spondias pinnata* (L.f.) Kurz) fruit powder on growth, digestive enzyme activity, and skin mucus immune parameters of climbing perch (*Anabas testudineus* (Bloch, 1972). *Veterinary Integrative Sciences*, 22(1), 315–334. <https://doi.org/10.12982/vis.2024.023>
- Saher, S., Narnawre, S., & Patil, J. (2020). Evaluation of phytochemical and pharmacological activity of *Carissa carandas* L. fruits at three different stages of maturation. *Drug Research*, 70(02/03), 80–85. <https://doi.org/10.1055/a-0815-4832>
- Santos, S. S., Rodrigues, L. M., Costa, S. C., & Madrona, G. S. (2019). Antioxidant compounds from blackberry (*Rubus fruticosus*) pomace: Microencapsulation by spray-dryer and pH stability evaluation. *Food Packaging and Shelf Life*, 20, 100177. <https://doi.org/10.1016/j.fpsl.2017.12.001>
- Sathyaruban, S., Uluwaduge, D. I., Yohi, S., & Kuganathan, S. (2021). Potential natural carotenoid sources for the colouration of ornamental fish: A review. *Aquaculture International*, 29(4), 1507–1528. <https://doi.org/10.1007/s10499-021-00689-3>
- Shekarabi, S. P. H., Mehrgan, M. S., Ramezani, F., Dawood, M. A. O., Doan, H. V., Moonmanee, T., Hamid, N. K. A., & Kari, Z. A. (2022). Effect of dietary barberry fruit (*Berberis vulgaris*) extract on immune function, antioxidant capacity, antibacterial activity, and stress-related gene expression of Siberian sturgeon (*Acipenser baerii*). *Aquaculture Reports*, 23, 101041. <https://doi.org/10.1016/j.aqrep.2022.101041>
- Singh, S., Bajpai, M., & Mishra, P. (2020). *Carissa carandas* L. – Phyto-pharmacological review. *Journal of Pharmacy and Pharmacology*, 72(12), 1694–1714. <https://doi.org/10.1111/jphp.13328>
- Thongprajukaew, K., Kovitvadhi, S., Kovitvadhi, U., & Rungruangsak-Torrissen, K. (2012). Pigment deposition and *in vitro* screening of natural pigment sources for enhancing pigmentation in male Siamese fighting fish (*Betta splendens* Regan, 1910). *Aquaculture Research*, 45(4), 709–719. <https://doi.org/10.1111/are.12009>
- Thongprajukaew, K., Kovitvadhi, U., Kovitvadhi, S., Somsueb, P., & Rungruangsak-Torrissen, K. (2011). Effects of different modified diets on growth, digestive enzyme activities and muscle compositions in juvenile Siamese fighting fish (*Betta splendens* Regan, 1910). *Aquaculture*, 322–323, 1–9. <https://doi.org/10.1016/j.aquaculture.2011.10.006>
- Verma, K., Shrivastava, D., & Kumar, G. (2015). Antioxidant activity and DNA damage inhibition *in vitro* by a methanolic extract of *Carissa carandas* (Apocynaceae) leaves. *Journal of Taibah University for Science*, 9(1), 34–40. <https://doi.org/10.1016/j.jtusc.2014.07.001>
- Wang, Y.-J., Chien, Y.-H., & Pan, C.-H. (2006). Effects of dietary supplementation of carotenoids on survival, growth, pigmentation, and antioxidant capacity of characins, *Hyphessobrycon callistus*. *Aquaculture*, 261(2), 641–648. <https://doi.org/10.1016/j.aquaculture.2006.08.040>
- Wangkahart, E., Wachiraamonloed, S., Lee, P.-T., Subramani, P. A., Qi, Z., & Wang, B. (2022). Impacts of *Aegle marmelos* fruit extract as a medicinal herb on growth performance, antioxidant and immune responses, digestive enzymes, and disease resistance against *Streptococcus agalactiae* in Nile tilapia (*Oreochromis niloticus*). *Fish and Shellfish Immunology*, 120, 402–410. <https://doi.org/10.1016/j.fsi.2021.11.015>
- Willora, F. P., Vatsos, I. N., Mallioris, P., Bordignon, F., Keizer, S., Martinez-Llorens, S., Sørensen, M., & Hagen, Ø. (2022). Replacement of fishmeal with plant protein in the diets of juvenile lumpfish

(*Cyclopterus lumpus*, L. 1758): Effects on digestive enzymes and microscopic structure of the digestive tract. *Aquaculture*, 561, 738601. <https://doi.org/10.1016/j.aquaculture.2022.738601>

Winkler, U. K., & Stuckmann, M. (1979). Glycogen, hyaluronate, and some other polysaccharides greatly enhance the formation of exolipase by *Serratia marcescens*. *Journal of Bacteriology*, 138(3), 663–670. <https://doi.org/10.1128/jb.138.3.663-670.1979>

Yanar, Y., Büyükçapar, H., Yanar, M., & Göcer, M. (2007). Effect of carotenoids from red pepper and marigold flower on pigmentation, sensory properties and fatty acid composition of rainbow trout. *Food Chemistry*, 100(1), 326–330. <https://doi.org/10.1016/j.foodchem.2005.09.056>

## ***In Silico* Study of Neoagaro-Oligosaccharides (NAOS) Anti-Inflammatory Activity: Molecular Docking with iNOS and COX-2 Proteins**

**Pinki Anggrahini Puspitasari<sup>1</sup>, Visi Endah Pratitis<sup>1</sup>, Syahputra Wibowo<sup>1,2</sup>, Nastiti Wijayanti<sup>1</sup> and Fajar Sofyantoro<sup>1\*</sup>**

<sup>1</sup>*Department of Tropical Biology, Faculty of Biology, Universitas Gadjah Mada, 55281 Yogyakarta, Indonesia*

<sup>2</sup>*Eijkman Research Center for Molecular Biology, National Research and Innovation Agency, 16911 Bogor, Indonesia*

### **ABSTRACT**

Neoagaro-Oligosaccharides (NAOS) arise from the enzymatic hydrolysis of agarose employing  $\beta$ -agarases enzymes. Comprising diverse monomers such as neoagarobiose (NA2), neoagarotetraose (NA4), neoagarohexaose (NA6), and neoagarooctaose (NA8), NAOS are characterised by their Degree of Polymerization (DP). Extensive investigations have delineated the potential of various NAOS monomers, particularly anti-inflammatory agents, owing to their capability to impede iNOS and COX-2, pivotal mediators of inflammation. Nevertheless, the molecular interplay between NAOS and inflammatory mediators remains unexplored. Thus, this study aimed to elucidate the interaction dynamics between NAOS with iNOS and COX-2. Employing ligands neoagarobiose (ID: 275080182), neoagarotetraose (ID: 130476782), neoagarohexaose (ID: 131485243), and neoagarooctaose (ID: 54758640) in conjunction with target proteins iNOS (3E7G) and COX-2 (5F19), analyses were conducted utilising ProTox-II and SwissADME. Protein preparation was carried out using Discovery Studio, while ligand preparation entailed PyRx, with docking facilitated by CBDock2.0. Absorption, distribution, metabolism, and excretion (ADME) evaluations revealed that neoagarobiose, neoagarotetraose, neoagarohexaose, and neoagarooctaose did not adhere to Lipinski's Rule of Five. Docking simulations exhibited the capacity of all ligands to

engage with the binding site of iNOS, forming diverse bond types. Notably, neoagarobiose, neoagarotetraose, and neoagarohexaose demonstrated enhanced affinity towards COX-2, whereas neoagarooctaose exhibited heightened binding affinity towards iNOS.

### ARTICLE INFO

#### *Article history:*

Received: 12 March 2024

Accepted: 16 May 2024

Published: 28 January 2025

DOI: <https://doi.org/10.47836/pitas.48.1.15>

#### *E-mail addresses:*

[pinkianggrahinipuspitasari@mail.ugm.ac.id](mailto:pinkianggrahinipuspitasari@mail.ugm.ac.id) (Pinki Anggrahini Puspitasari)

[visiendahpratitis@mail.ugm.ac.id](mailto:visiendahpratitis@mail.ugm.ac.id) (Visi Endah Pratitis)

[syahputra.wibowo@brin.go.id](mailto:syahputra.wibowo@brin.go.id) (Syahputra Wibowo)

[nastiti\\_wijayanti@ugm.ac.id](mailto:nastiti_wijayanti@ugm.ac.id) (Nastiti Wijayanti)

[fajar.sofyantoro@ugm.ac.id](mailto:fajar.sofyantoro@ugm.ac.id) (Fajar Sofyantoro)

\*Corresponding author

**Keywords:** COX-2, iNOS, inflammation, molecular docking, NAOS

## INTRODUCTION

Inflammatory responses represent orchestrated actions by the immune system to combat pathogenic infection and restore homeostasis (Bennett et al., 2018; Chen et al., 2018). The manifestations of inflammation arise from the activities of diverse mediators, including but not limited to Nitric Oxide (NO), pro-inflammatory cytokines, prostaglandins (PGs), histamines, reactive oxygen species (ROS), and reactive nitrogen species (RNS), engendered during the inflammatory cascade (Patel & Patel, 2015).

Nitric Oxide (NO) assumes a pivotal role as a free radical species in modulating inflammatory responses, with its synthesis catalysed by members of the nitric oxide synthase (NOS) family, namely endothelial nitric oxide synthase (eNOS), neuronal nitric oxide synthase (nNOS), and inducible nitric oxide synthase (iNOS) (Vishwakarma et al., 2019). The biosynthesis of NO commences with the enzymatic hydrolysis of L-Arginine by NOS, yielding N-hydroxy-L-arginine, subsequently oxidised to L-Citrulline and NO. Upon interaction with superoxide ( $O_2^{\bullet-}$ ), NO undergoes conversion to peroxynitrite (ONOO<sup>-</sup>), eliciting deleterious effects on lipids, proteins, and deoxyribonucleic acid (DNA) integrity (Batra et al., 2007; Forstermann & Sessa, 2012).

Prostaglandins (PGs), derivatives of arachidonic acid (AA) metabolism catalysed by the cyclooxygenase (COX) enzyme, notably manifest the interplay between COX-1 and COX-2 isoenzymes. While both isoforms orchestrate PG production, COX-1 primarily regulates physiological homeostasis, whereas COX-2 assumes prominence in pathophysiological states such as inflammation (Rawat et al., 2019).

The shift from acute inflammation to a chronic condition signifies serious health consequences (Bennett et al., 2018; Chen et al., 2018). While traditional anti-inflammatory medications like aspirin and glucocorticoids relieve chronic inflammation, their extended usage is associated with various negative effects (Coutinho & Chapman, 2011; Harirforoosh et al., 2014; Sherwood et al., 2010). Thus, exploring natural alternatives to mitigate inflammation is imperative, among which Neogaro-oligosaccharides (NAOS) have emerged as promising candidates.

Agarose, derived from red algae (Rhodophyta), is highly valued for its diverse applications due to its unique chemical composition, which includes (1–4)-linked 3,6-anhydro- $\alpha$ -L-galactose and (1–3)-linked  $\beta$ -D-galactopyranose components (Fu & Kim, 2010). Widely employed as a gelling agent across food, cosmetic, and research domains, agarose undergoes enzymatic or chemical hydrolysis to yield NAOS and Agaroligosaccharides (AOS) (Pandey et al., 2019; Xu et al., 2018).

Neogaro-oligosaccharides (NAOS), enzymatic breakdown products of agarose facilitated by  $\beta$ -agarases, harbour  $\beta$ -D-galactose residues at their reducing ends (Cheong et al., 2018; Fu & Kim, 2010; Higashimura et al., 2013; Xu et al., 2018; Yun et al., 2017). Distinguished by their Degree of Polymerization (DP), NAOS encompass a spectrum of

oligomeric forms such as neoagarobiose (NA2), neoagarotetraose (NA4), neoagarohexaose (NA6), neoagarooctaose (NA8), neoagarodecaose (NA10), neoagarododecaose (NA12), and others (Qu et al., 2020; Wang et al., 2017).

The industrial, cosmetic, and pharmaceutical sectors recognise the utility of Agarooligosaccharides (AOS) and NAOS, leveraging their diverse bioactivities (Qu et al., 2020). Noteworthy among these are the antioxidant and prebiotic properties attributed to NAOS, along with their purported anti-diabetic and skin-whitening efficacies mediated through modulation of  $\alpha$ -glucosidase expression and melanin/tyrosine production, respectively (Hong et al., 2017; Zhang et al., 2019).

While existing literature has explored the anti-inflammatory potential of various NAOS monomeric forms based on their DP, investigations into their interactions with key inflammatory mediators, particularly iNOS and COX-2 proteins, remain nascent. Hence, this study aimed to elucidate the drug likeness profiles of diverse NAOS monomers based on their DP and their putative interactions with iNOS and COX-2 proteins via molecular docking analyses.

## MATERIAL AND METHODS

### Protein Data Acquisition and Preparation

Data pertaining to iNOS (PDB code: 3E7G) and COX-2 (PDB code: 5F19) were acquired from the Protein Data Bank (PDB) website (<http://www.rcsb.org/pdb>). Subsequently, the Ramachandran plots of both proteins were scrutinised utilising PDBSum (<http://www.ebi.ac.uk/thornton-srv/databases/pdbsum/>). These proteins' binding active sites were analysed using the PrankWeb platform (<https://prankweb.cz/>). The removal of water molecules and ligands from the protein structures was executed using the Discovery Studio 2016 Client application, followed by preserving the modified structures in (.pdb) format.

### Ligand Data Retrieval and Preparation

This investigation employed four ligands—neoagarobiose (ID: 275080182), neoagarotetraose (ID: 130476782), neoagarohexaose (ID: 131485243), neoagarooctaose (ID: 54758640), and aspirin (ID: 2244)—serving as positive controls. The three-dimensional (3D) conformers and two-dimensional (2D) structures of these ligands were obtained from PubChem (<https://pubchem.ncbi.nlm.nih.gov/>). A subsequent ligand toxicity assessment was performed using the ProTox-II website ([https://tox-new.charite.de/protox\\_II/](https://tox-new.charite.de/protox_II/)). The ligands' drug-likeness parameters and pharmacokinetic characteristics were evaluated via the SwissADME website (<http://www.swissadme.ch/>). Following, energy minimisation of the ligands was carried out utilising the PyRx application, and the resultant structures were saved in (.pdb) format.

## Molecular Docking

Blind docking simulations were executed utilising the CB-Dock2.0 website (<https://cadd.labshare.cn/cb-dock2/>), which facilitates blind docking of protein-ligand complexes based on AutoDock Vina. The docking procedure entails uploading the pre-processed protein and ligand structures, followed by cavity detection and blind docking exploration.

## RESULTS AND DISCUSSION

### Protein Characteristic

The study herein focused on the characterisation of proteins iNOS (3E7G) and COX-2 (5F19) as designated targets, being predicated upon Ramachandran Plot analyses (Jordan et al., 2023; Md Idris et al., 2022). Protein iNOS exhibited 90.6% of its residues within the Ramachandran plot's favoured regions (Ali et al., 2023), accompanied by a G-Factor normality value of 0.31 and a resolution of 2.20 Å. Conversely, protein COX-2 portrayed 90.7% of its residues nestled within the favoured regions of the Ramachandran plot, with a G-Factor normality value of 0.28 and a resolution of 2.04 Å. Notably, the normality values for both proteins marginally exceed the prescribed range. Per PROCHECK standards, the G-factor is ideally between 0 and 0.5, with optimal quality models reflecting values proximal to zero (Elengoe et al., 2014). P2Rank analysis elucidated 23 binding site pockets for iNOS (Figure 1A) and 16 for COX-2 (Figure 1B).

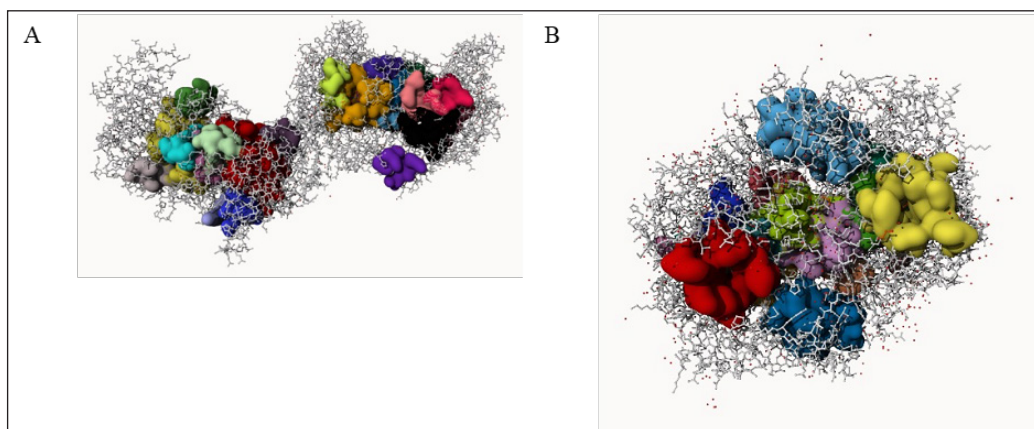


Figure 1. Protein binding sites pocket of (A) iNOS (3E7G) and (B) COX-2 (5F19)

### ADME Analysis

All ligands' toxicity and absorption, distribution, metabolism, and excretion (ADME) properties were assessed using ProTox-II and SwissADME (Table 1). Neoagarobiose, neoagarotetraose, neoagarohexaose, and neoagarooctaose exhibited identical toxicity



profiles, classified as level three toxicity with an LD50 value of 648 mg/kg. Furthermore, hepatotoxicity and carcinogenicity assays across all ligands demonstrated negligible activity, with a high probability of 0.91. Similarly, immunotoxicity assessment for these ligands indicated minimal activity, with a probability of 0.87. Moreover, all four ligands exhibited no mutagenic potential, with a probability of 0.75. Cytotoxicity analysis also revealed minimal activity for these ligands, with a probability of 0.63. Based on the toxicity evaluation, neoagarobiose, neoagarotetraose, neoagarohexaose, and neoagarooctaose share similarities with aspirin in their toxicity profiles.

Based on the toxicity assessment outcomes, neoagarobiose, neoagarotetraose, neoagarohexaose, and neoagarooctaose are included within the "danger if swallowed" category as per the classification on the ProTox-II website (Banerjee et al., 2018). Furthermore, the toxicity evaluation indicates that these four compounds are ostensibly safe according to their predicted lack of hepatotoxicity, carcinogenicity, mutagenicity, cytotoxicity, and immunotoxicity (Banerjee et al., 2018).

The outcomes of ADME physiochemical analysis using SwissADME for each ligand are shown in Table 2. The purpose of ADME analysis is to evaluate the pharmacokinetic properties of potential drug molecules and to determine the efficacy and safety of a drug candidate. Using tools like SwissADME makes it possible to assess various parameters such as molecular weight, lipophilicity, solubility, bioavailability, and likelihood of gastrointestinal absorption. These parameters provide insights into how efficiently a drug candidate can be absorbed into the bloodstream, distributed to the target tissues, metabolised by the body, and ultimately excreted. These are all critical considerations in drug development (Morak-Młodawska et al., 2023).

As shown in Table 2, neoagarobiose exhibited an molecular weight (MW) < 500 g/mol, whereas neoagarotetraose, neoagarohexaose, and neoagarooctaose surpassed this threshold. Consequently, neoagarobiose is postulated to undergo oral absorption more readily, while the latter compounds may be absorbed through alternative routes. Molar refractivity (MR) and Rotatable Bond Number (RBN) serve as parameters *in silico* for probing the pharmacokinetic properties of targeted compounds (Ibrahim et al., 2021). According to Lipinski's five rules, MR values falling between 40–130 are acceptable, whereas compounds with an RBN < 10 suggest favourable oral bioavailability. The convergence of acceptable MR and RBN values signifies robust intestinal absorption and oral bioavailability of the substance (Ibrahim et al., 2021). Notably, neoagarobiose and neoagarotetraose demonstrated MR values ranging from 64.77 to 126.18 and RBN values of 3–8, indicative of favourable intestinal absorption and oral bioavailability.

Hydrogen Bond Acceptor (HBA) and Hydrogen Bond Donor (HBD) indices are pivotal for analysing intermolecular interactions between macromolecules and chemicals, thereby influencing oral absorption (Ibrahim et al., 2021). As stipulated by Lipinski's 5 rules, the acceptable count of HBA should not exceed 10, with HBD not surpassing 5. However, all targeted compounds in Table 2 exhibited HBA counts exceeding 10, and HBD counts

Table 1  
Toxicity prediction using ProTox-II

Ligand	Toxicity class	Toxicity Tests				
		Hepato-toxicity	Carcinogenicity	Immuno-toxicity	Mutagenicity	Cyto-toxicity
Neoagarobiose	3 (LD <sub>50</sub> : 648mg/kg)	Inactive (prob: 0,91)	Inactive (prob: 0,91)	Inactive (prob: 0,87)	Inactive (prob: 0,75)	Inactive (prob: 0,63)
Neoagarotetrose	3 (LD <sub>50</sub> : 648mg/kg)	Inactive (prob: 0,91)	Inactive (prob: 0,91)	Inactive (prob: 0,87)	Inactive (prob: 0,75)	Inactive (prob: 0,63)
Neoagarohexaose	3 (LD <sub>50</sub> : 648mg/kg)	Inactive (prob: 0,91)	Inactive (prob: 0,91)	Inactive (prob: 0,87)	Inactive (prob: 0,75)	Inactive (prob: 0,63)
Neoagarooctaose	3 (LD <sub>50</sub> : 648mg/kg)	Inactive (prob: 0,91)	Inactive (prob: 0,91)	Inactive (prob: 0,87)	Inactive (prob: 0,75)	Inactive (prob: 0,63)
Aspirin	3 (LD <sub>50</sub> : 250mg/kg)	Inactive (prob: 0,51)	Inactive (prob: 0,86)	Inactive (prob: 0,99)	Inactive (prob: 0,97)	Inactive (prob: 0,94)

Table 2  
Ligand physicochemical analysis using SwissADME

	Physicochemical analysis			
	Neoagarobiose	Neoagarotetraose	Neoagarohexaose	Neoagarooctaose
Molecular weight (g/mol)	324,28	630,55	936,81	1243,08
Number of heavy atoms	22	43	64	85
Number of rotatable bonds	3	8	13	18
Number of hydrogen bond acceptors	10	19	28	37
Number of hydrogen bond donors	6	10	14	18
Molar refractivity	64,77	126,18	187,60	249,01
TPSA (Å <sup>2</sup> )	158,30	285,37	412,44	539,51
Lipophilicity (Log P)	-2,93	-5,28	-7,99	-10,17
Water solubility (Log S / ESOL)	0,70 (highly soluble)	0,86 (highly soluble)	1,02 (highly soluble)	1,18 (highly soluble)
				Aspirin 180,16

surpassing 5, suggesting potential challenges in oral absorption due to increased interactions with biological targets. Further investigation and optimisation to determine HBA and HBD compounds such as O, N, and H atoms using nuclear magnetic resonance (NMR) may be required to address these issues and improve the compounds' pharmacokinetic profiles (Wang et al., 2021).

As gauged by the Log P value, lipophilicity delineates a compound's solubility and permeability characteristics. Lipinski posits that compounds with a Log P < 5 hold promise as potential drugs. As per the results in Table 2, all four compounds exhibited a Log P value < 5, indicating their capacity to dissolve in both water and lipids. The negative Log P values denoted their hydrophilic nature, rendering them soluble in water, tolerable in the gastric milieu, and conducive to proper renal excretion (Al Mogren et al., 2020; Kadela-Tomanek et al., 2021). These findings align with the log S (water solubility) values, portraying the compounds as highly soluble in water.

According to Lipinski's criteria, a compound warrants consideration as a drug if it adheres to specific thresholds concerning molecular weight, lipophilicity, HBA, HBD, and molar refractivity (Riyadi et al., 2021). Furthermore, Lipinski stipulates that an orally active drug should not exceed one violation of these criteria (Ibrahim et al., 2017; Riyadi et al., 2021; Sen et al., 2021). Drug likeness analysis based on Lipinski's 5 rules suggested that neoagarobiose, neoagarotetraose, neoagarohexaose, and neoagarooctaose lacked the requisite chemical and physical properties to qualify as orally active drugs for human use.

Table 3 presents the drug-likeness analysis based on Lipinski's 5 rules. Lipinski's test aims to ascertain whether a target compound with known biological activity possesses chemical and physical characteristics conducive to oral consumption as medicine in humans. As shown in Table 3, it is evident that neoagarobiose, neoagarotetraose, neoagarohexaose, and neoagarooctaose failed to satisfy several Lipinski indicators. Specifically, neoagarobiose fulfilled 3 out of 5 Lipinski indicators, while neoagarotetraose satisfied only 2 out of 5. Neoagarohexaose and neoagarooctaose, however, fulfilled only 1 of the 5 indicators established by Lipinski.

### **Molecular Docking**

Using CBDock2.0, molecular docking simulations employed AutoDock Vina for ligand-protein interactions. The resultant binding affinities, quantified as Vina scores, reflect the strength of interaction between the ligands and the protein receptors (Hasan et al., 2023). Docking analyses of neoagarobiose, neoagarotetraose, neoagarohexaose, and neoagarooctaose with iNOS protein are depicted in Figure 2. These analyses revealed that neoagarooctaose exhibited the highest binding affinity, with a value of -10.6 kcal/mol, followed by neoagarohexaose (-9.2 kcal/mol) and neoagarotetraose (-8.8 kcal/mol). In contrast, neoagarobiose demonstrated the lowest binding affinity at -6.6 kcal/mol (Table 3).

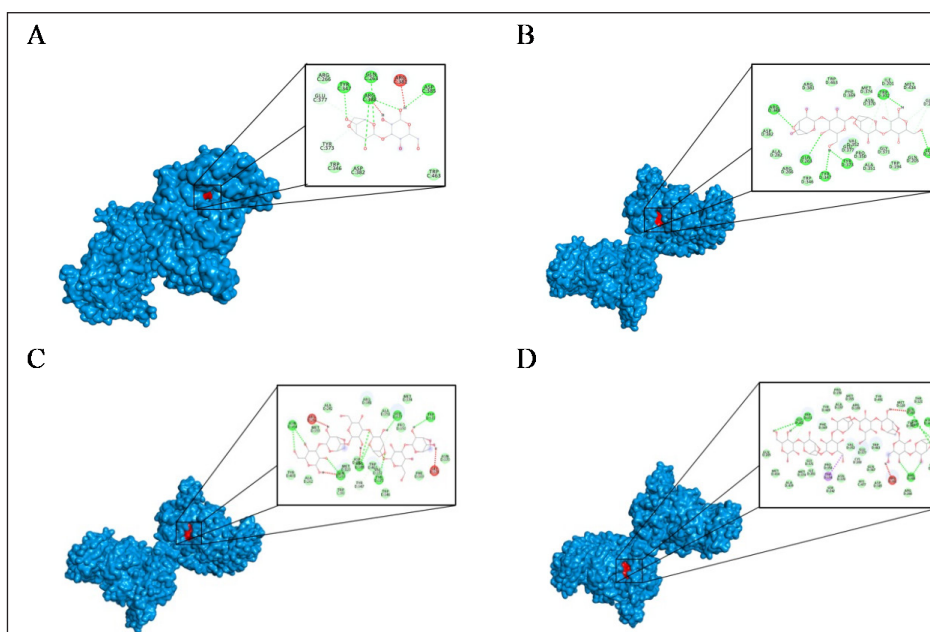


Figure 2. Molecular docking of interaction between (A) neoagarobiose and iNOS, (B) neoagarotetrose and iNOS, (C) neoagarohexaose and iNOS, (D) neoagarooctaose and iNOS

The outcomes of molecular docking analyses revealed the binding of neoagarobiose, neoagarotetraose, neoagarohexaose, and neoagarooctaose within the binding site pocket of the inducible nitric oxide synthase (iNOS) protein. Various bonds were formed between each ligand and iNOS, encompassing van der Waals interactions, conventional hydrogen bonds, carbon-hydrogen bonds, Pi-Sigma bonds, and bonds deemed unfavourable (Figure 3). Specifically, the interaction between neoagarobiose and iNOS was characterised by one unfavourable bond at residue ARG381. Likewise, in the case of neoagarooctaose, an unfavourable bond at residue ARG381 was observed, along with a Pi-Sigma bond at residue TRP194. Neoagarohexaose's interaction with iNOS was marked by two unfavourable bonds at residues ARG266 and GLY371. Conversely, the interaction involving neoagarotetraose did not exhibit any unfavourable bonds.

Figure 4 provides a visual representation elucidating the interaction dynamics between neoagarobiose, neoagarotetraose, neoagarohexaose, and neoagarooctaose with the COX-2 protein. Concurrently, Table 3 outlines the binding affinity values associated with the interactions of the ligands mentioned above with the COX-2 protein. Notably, neoagarohexaose exhibited the most favourable binding affinity value upon binding to the COX-2 protein, registering at -10.7 kcal/mol. Following this, neoagarotetraose demonstrates a binding affinity value of -10.3 kcal/mol, neoagarooctaose at -9.8 kcal/mol, and neoagarobiose exhibited the least favourable binding affinity value at -6.6 kcal/mol (Table 3).

Table 3  
Binding affinity and hydrogen form

Protein	Ligand	Binding affinity (Kcal/mol)	Hydrogen bond
iNOS (3E7G)	Neoagarobiose	-6,6	GLN263, TYR347, TYR373, GLU377, ASP385, ARG388
	Neoagarotetraose	-8,8	GLY202, SER242, GLN263, TYR347, TRP372, TYR373, ARG388
	Neoagarohexaose	-9,2	GLN263, TYR347, ASN354, TRP372, TYR373, GLU377, ARG388
	Neoagaroctaose	-10,6	CYS200, GLY202, GLN263, TRP372, TYR373, ASP382, ARG388
	Aspirin	-7,3	TRP194
COX-2 (5F19)	Neoagarobiose	-7,1	GLY225, ASN375, GLY533
	Neoagarotetraose	-10,3	GLY225, GLY227, ASN375, GLY533, VAL228, GLN374, ASN375, GLY536
	Neoagarohexaose	-10,7	GLY225, GLY235, GLN241, TYR373, ASN375, ARG376, VAL538
	Neoagaroctaose	-9,8	SER143, GLY225, GLU236, ASN375, GLU140, ASP229, ARG376
	Aspirin	-6,6	ALA202, THR206, TRP387

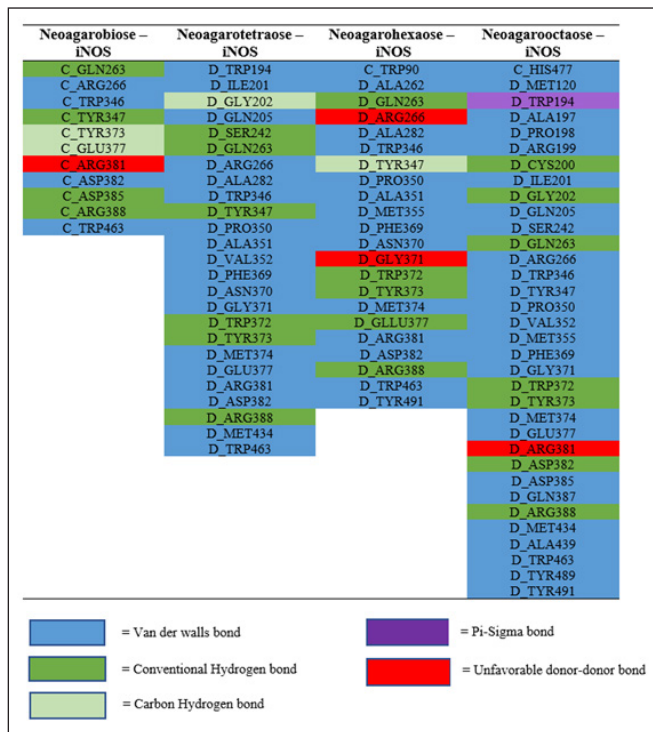


Figure 3. Residue bonds formed through interaction between neoagarobiose, neoagarotetraose, neoagarohexaose, neoagaroctaose interaction and iNOS protein (3E7G)

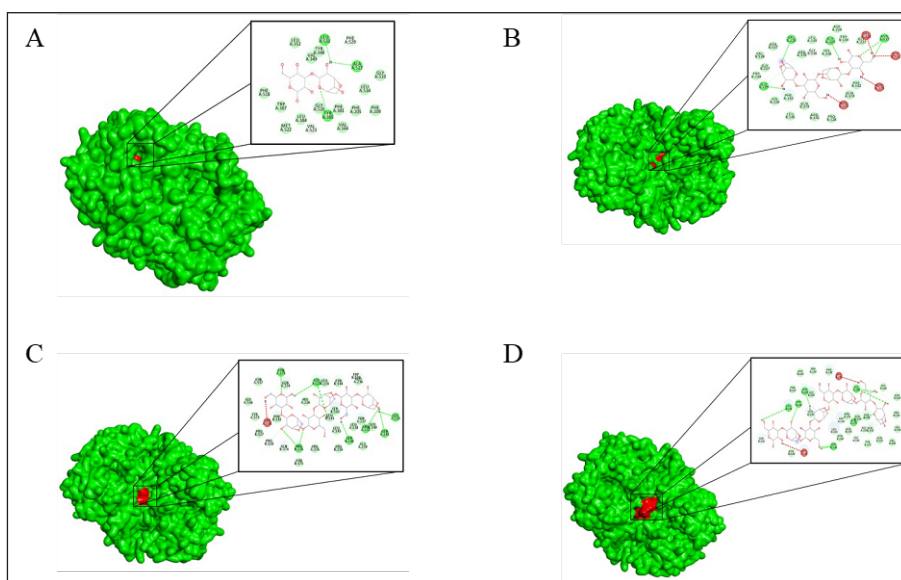


Figure 4. Molecular docking between (A) neogaroibiose and COX-2, (B) neogarotetraose and COX-2, (C) neogarohehexaose and COX-2, (D) neogarooctaose and COX-2

The binding interactions of neogaroibiose, neogarotetraose, neogarohehexaose, and neogarooctaose with the COX-2 binding site pocket resemble those observed with all ligands and iNOS. These interactions manifest through the formation of diverse bonds, including van der Waals bonds, conventional hydrogen bonds, carbon hydrogen bonds, and unfavourable donor-donor bonds, as depicted in Figure 5. Specifically, as illustrated in Figure 5, the interactions of neogaroibiose and neogarooctaose with COX-2 lacked residues exhibiting unfavourable donor-donor bonds. Conversely, the interaction between neogarotetraose and COX-2 entails one unfavourable donor-donor bond located at residue GLY225. Notably, the interaction of neogarohehexaose with COX-2 involved two unfavourable donor-donor bonds situated at residues LEU238 and SER143.

The outcomes of molecular docking analyses reveal the presence of hydrogen bond interactions between neogaroibiose, neogarotetraose, neogarohehexaose, and neogarooctaose with iNOS and COX-2, characterised by specific residues within the protein structures. Neogaroibiose exhibited hydrogen bonding with iNOS residues GLN263, TYR347, TYR373, GLU377, ASP385, and ARG388. Similarly, neogarotetraose engaged in hydrogen bonding interactions with iNOS residues GLY202, SER242, GLN263, TYR347, TRP372, TYR373, and ARG388, while with COX-2, it formed hydrogen bonds at GLY225, GLY227, ASN375, GLY533, VAL228, GLN374, ASN375, and GLY536 residues. Likewise, neogarohehexaose established hydrogen bonds with iNOS at GLN263, TYR347, ASN354, TRP372, TYR373, GLU377, and ARG388 residues, and with COX-2 at GLY225, GLY235, GLN241, TYR373, ASN375, ARG376, and VAL538 residues.

Additionally, neoagarooctose interacted via hydrogen bonding with iNOS residues CYS200, GLY202, GLN263, TRP372, TYR373, ASP382, and ARG388, and with COX-2 residues SER143, GLY225, GLU236, ASN375, GLU140, ASP229, and ARG376. These hydrogen bond formations signify robust binding of the ligands to the respective proteins, enhancing their stability (Wibowo et al., 2019; Wibowo et al., 2020; Wibowo et al., 2021; Wibowo et al., 2022).

Neoagarobiose –COX-2	Neoagarotetraose –COX-2	Neoagarohexaose –COX-2	Neoagarooctose –COX-2
A_LEU224	A_TRP139	A_LEU145	A_TRP139
A_GLY225	A_LEU145	A_LEU224	A_PHE142
A_GLY227	A_GLY225	A_GLY225	A_SER143
A_VAL228	A_GLY227	A_GLY235	A_LEU145
A_ASP229	A_VAL228	A_GLU236	A_LEU224
A_TYR373	A_ASP229	A_THR237	A_GLY225
A_ASN375	A_ASN375	A_LEU238	A_GLU236
A_GLY533	A_ARG376	A_GLN241	A_THR237
A_GLY536	A_GLY533	A_ARG333	A_LEU238
A_ASN537	A_GLY536	A_GLN374	A_GLN241
A_VAL538	A_ASN537	A_ASN375	A_ARG333
B_TRP139	B_TRP139	A_ARG376	A_TYR373
B_SER143	B_PHE142	A_GLY536	A_GLN374
B_LEU145	B_LEU145	A_ASN537	A_ASN375
B_GLN374	B_GLY225	A_VAL538	A_GLY536
B_ARG376	B_HIS226	B_TRP139	A_ASN537
	B_GLY227	B_GLU140	A_VAL538
	B_VAL228	B_PHE142	B_TRP139
	B_ASP229	B_SER143	B_GLU140
	B_GLN374	B_LEU145	B_PHE142
	B_ASN375	B_GLN374	B_SER143
	B_ARG376	B_ASN375	B_LEU145
	B_GLY533	B_ARG376	B_LEU224
	B_GLY536		B_GLY225
	B_ASN537		B_HIS226
	B_VAL538		B_ASP229
			B_GLN374
			B_ASN375
			B_ARG376

= Van der Waals bond

= Carbon Hydrogen bond

= Conventional Hydrogen bond

= Unfavorable donor-donor bond

Figure 5. Residues bond formed through interaction between neoagarobiose, neoagarotetraose, neoagarohexaose, neoagarooctose and COX-2 (5F19)

Docking simulations revealed that all four target compounds fit within the binding pockets of iNOS and COX-2 proteins. Molecular docking analyses further unveiled the presence of unfavourable bonds at specific residues, potentially compromising protein stability (Wibowo et al., 2019). Additionally, hydrogen bonds formed between the compounds and iNOS/COX-2 proteins played pivotal roles in fortifying their interactions. Neoagarobiose exhibited a propensity to inhibit COX-2 production to a greater extent than iNOS, as evidenced by its stronger binding affinity with COX-2 (-7.1 Kcal/mol) compared to iNOS (-6.6 Kcal/mol). Analogously, neoagarotetraose, neoagarohexaose, and neoagarooctose demonstrated stronger binding affinities with COX-2 relative to iNOS. These findings suggest a potential therapeutic advantage in targeting COX-2 over iNOS inhibition.

In summary, the comprehensive evaluation of neoagarobiose, neoagarotetraose, neoagarohexaose, and neoagarooctaose underscores their promising pharmacological attributes, particularly in gastrointestinal drug delivery and anti-inflammatory therapy.

## CONCLUSION

Based on the findings presented, the proteins iNOS and COX-2 have been thoroughly characterised, revealing their structural attributes and potential binding sites. The ligands neoagarobiose, neoagarotetraose, neoagarohexaose, and neoagarooctaose exhibited favourable toxicity profiles with negligible hepatotoxic, carcinogenic, mutagenic, cytotoxic, and immunotoxic properties. However, they failed to fulfil Lipinski's criteria for drug-likeness due to certain physicochemical characteristics. Molecular docking simulations highlighted the strong binding affinities of these ligands with both iNOS and COX-2 proteins, indicating their potential as inhibitors. Notably, neoagarobiose preferred to inhibit COX-2, suggesting a therapeutic advantage in targeting this pathway for anti-inflammatory purposes.

Future perspectives may involve further *in vitro* and *in vivo* studies to validate the therapeutic potential of these ligands, exploring their efficacy and safety profiles in relevant disease models. Additionally, structural optimisation efforts could be undertaken to enhance their drug-likeness properties and improve their pharmacological utility. Further investigations into the specific mechanisms underlying their interactions with iNOS and COX-2 would also contribute to a deeper understanding of their mode of action and potential clinical applications.

## ACKNOWLEDGEMENTS

This study received funding from Universitas Gadjah Mada, Indonesia, through the Rekognisi Tugas Akhir (RTA) 2023 grant under the reference number 5075/UN1.P.II/Dit-Lit/PT.01.01/2023.

## REFERENCES

- Al Mogren, M. M., Zerroug, E., Belaidi, S., BenAmor, A., & Al Harbi, S. D. A. (2020). Molecular structure, drug likeness and QSAR modeling of 1,2-diazole derivatives as inhibitors of enoyl-acyl carrier protein reductase. *Journal of King Saud University - Science*, 32(4), 2301–2310. <https://doi.org/10.1016/j.jksus.2020.03.007>
- Ali, A., Mir, G. J., Ayaz, A., Maqbool, I., Ahmad, S. B., Mushtaq, S., Khan, A., Mir, T. M., & Rehman, M. U. (2023). *In silico* analysis and molecular docking studies of natural compounds of *Withania somnifera* against bovine NLRP9. *Journal of Molecular Modeling*, 29(6), 171. <https://doi.org/10.1007/s00894-023-05570-z>
- Banerjee, P., Eckert, A. O., Schrey, A. K., & Preissner, R. (2018). ProTox-II: A webserver for the prediction of toxicity of chemicals. *Nucleic Acids Research*, 46(W1), W257–W263. <https://doi.org/10.1093/nar/gky318>



- Batra, J., Chatterjee, R., & Ghosh, B. (2007). Inducible nitric oxide synthase (iNOS): Role in asthma pathogenesis. *Indian Journal of Biochemistry & Biophysics*, *44*(5), 303–309.
- Bennett, J. M., Reeves, G., Billman, G. E., & Sturmberg, J. P. (2018). Inflammation–Nature’s way to efficiently respond to all types of challenges: Implications for understanding and managing “the epidemic” of chronic diseases. *Frontiers in Medicine*, *5*, 316. <https://doi.org/10.3389/fmed.2018.00316>
- Chen, L., Deng, H., Cui, H., Fang, J., Zuo, Z., Deng, J., Li, Y., Wang, X., & Zhao, L. (2018). Inflammatory responses and inflammation-associated diseases in organs. *Oncotarget*, *9*(6), 7204–7218. <https://doi.org/10.18632/oncotarget.23208>
- Cheong, K.-L., Qiu, H.-M., Du, H., Liu, Y., & Khan, B. (2018). Oligosaccharides derived from red seaweed: Production, properties, and potential health and cosmetic applications. *Molecules*, *23*(10), 2451. <https://doi.org/10.3390/molecules23102451>
- Coutinho, A. E., & Chapman, K. E. (2011). The anti-inflammatory and immunosuppressive effects of glucocorticoids, recent developments, and mechanistic insights. *Molecular and Cellular Endocrinology*, *335*(1), 2–13. <https://doi.org/10.1016/j.mce.2010.04.005>
- Elengoe, A., Naser, M., & Hamdan, S. (2014). Modeling and docking studies on novel mutants (K71L and T204V) of the ATPase domain of human Heat Shock 70 kDa Protein 1. *International Journal of Molecular Sciences*, *15*(4), 6797–6814. <https://doi.org/10.3390/ijms15046797>
- Forstermann, U., & Sessa, W. C. (2012). Nitric oxide synthases: Regulation and function. *European Heart Journal*, *33*(7), 829–837. <https://doi.org/10.1093/eurheartj/ehr304>
- Fu, X. T., & Kim, S. M. (2010). Agarase: Review of major sources, categories, purification method, enzyme characteristics and applications. *Marine Drugs*, *8*(1), 200–218. <https://doi.org/10.3390/md8010200>
- Harirforoosh, S., Asghar, W., & Jamali, F. (2014). Adverse effects of nonsteroidal antiinflammatory drugs: An update of gastrointestinal, cardiovascular and renal complications. *Journal of Pharmacy & Pharmaceutical Sciences*, *16*(5), 821. <https://doi.org/10.18433/J3VW2F>
- Hasan, T. N., Naqvi, S. S., Rehman, M. U., Ullah, R., Ammad, M., Arshad, N., Ain, Q. U., Perween, S., & Hussain, A. (2023). Ginger ring compounds as an inhibitor of spike binding protein of alpha, beta, gamma and delta variants of SARS-CoV-2: An in-silico study. *Narra J*, *3*(1). <https://doi.org/10.52225/narra.v3i1.98>
- Higashimura, Y., Naito, Y., Takagi, T., Mizushima, K., Hirai, Y., Harusato, A., Ohnogi, H., Yamaji, R., Inui, H., Nakano, Y., & Yoshikawa, T. (2013). Oligosaccharides from agar inhibit murine intestinal inflammation through the induction of heme oxygenase-1 expression. *Journal of Gastroenterology*, *48*(8), 897–909. <https://doi.org/10.1007/s00535-012-0719-4>
- Hong, S. J., Lee, J.-H., Kim, E. J., Yang, H. J., Chang, Y.-K., Park, J.-S., & Hong, S.-K. (2017). In vitro and in vivo investigation for biological activities of neoagarooligosaccharides prepared by hydrolyzing agar with  $\beta$ -agarase. *Biotechnology and Bioprocess Engineering*, *22*(4), 489–496. <https://doi.org/10.1007/s12257-017-0049-8>
- Ibrahim, E. I., Omer, R. A., Elsadig, A. H., Elkhatim, M., & Mohamed, S. B. (2017). In silico analysis of the structural and biochemical features of the Granulocyte-Macrophage Colony Stimulating Factor (GM-CSF), Interleukin-3 (IL-3) and Interleukin-5 (IL-5) receptors subunit  $\alpha$ . *American Journal of Bioinformatics Research*, *7*(1), 25–47. <https://doi.org/10.5923/j.bioinformatics.20170701.03>

- Ibrahim, Z. Y., Uzairu, A., Shallangwa, G. A., & Abechi, S. E. (2021). Pharmacokinetic predictions and docking studies of substituted aryl amine-based triazolopyrimidine designed inhibitors of *Plasmodium falciparum* dihydroorotate dehydrogenase (PfDHODH). *Future Journal of Pharmaceutical Sciences*, 7(1), 133. <https://doi.org/10.1186/s43094-021-00288-2>
- Jordan, P., Costa, A., Specker, E., Popp, O., Volkamer, A., Piske, R., Obrusnik, T., Kleissle, S., Stuke, K., Rex, A., Neuenschwander, M., Von Kries, J. P., Nazare, M., Mertins, P., Kettenmann, H., & Wolf, S. A. (2023). Small molecule inhibiting microglial nitric oxide release could become a potential treatment for neuroinflammation. *PLOS ONE*, 18(2), e0278325. <https://doi.org/10.1371/journal.pone.0278325>
- Kadela-Tomanek, M., Jastrzębska, M., Marciniak, K., Chrobak, E., Bębenek, E., & Boryczka, S. (2021). Lipophilicity, pharmacokinetic properties, and molecular docking study on SARS-CoV-2 target for betulin triazole derivatives with attached 1,4-Quinone. *Pharmaceutics*, 13(6), 781. <https://doi.org/10.3390/pharmaceutics13060781>
- Md Idris, M. H., Mohd Amin, S. N., Mohd Amin, S. N., Nyokat, N., Khong, H. Y., Selvaraj, M., Zakaria, Z. A., Shaameri, Z., Hamzah, A. S., Teh, L. K., & Salleh, M. Z. (2022). Flavonoids as dual inhibitors of cyclooxygenase-2 (COX-2) and 5-lipoxygenase (5-LOX): Molecular docking and in vitro studies. *Beni-Suef University Journal of Basic and Applied Sciences*, 11(1), 117. <https://doi.org/10.1186/s43088-022-00296-y>
- Morak-Młodawska, B., Jeleń, M., Martula, E., & Korlacki, R. (2023). Study of lipophilicity and ADME properties of 1,9-Diazaphenothiazines with anticancer action. *International Journal of Molecular Sciences*, 24(8), 6970. <https://doi.org/10.3390/ijms24086970>
- Pandey, S. P., Shukla, T., Dhote, V. K., K. Mishra, D., Maheshwari, R., & Tekade, R. K. (2019). Use of polymers in controlled release of active agents. In Tekade, R. K. (Eds.), *Basic fundamentals of drug delivery* (pp. 113–172). Elsevier. <https://doi.org/10.1016/B978-0-12-817909-3.00004-2>
- Patel, H., & Patel, V. H. (2015). Inflammation and metabolic syndrome: An overview. *Current Research in Nutrition and Food Science Journal*, 3(3), 263–268. <https://doi.org/10.12944/CRNFSJ.3.3.10>
- Qu, W., Wang, D., Wu, J., Chan, Z., Di, W., Wang, J., & Zeng, R. (2020). Production of neoagaro-oligosaccharides with various degrees of polymerization by using a truncated marine agarase. *Frontiers in Microbiology*, 11, 574771. <https://doi.org/10.3389/fmicb.2020.574771>
- Rawat, C., Kukal, S., Dahiya, U. R., & Kukreti, R. (2019). Cyclooxygenase-2 (COX-2) inhibitors: Future therapeutic strategies for epilepsy management. *Journal of Neuroinflammation*, 16(1), 197. <https://doi.org/10.1186/s12974-019-1592-3>
- Riyadi, P. H., Romadhon, Sari, I. D., Kurniasih, R. A., Agustini, T. W., Swastawati, F., Herawati, V. E., & Tanod, W. A. (2021). SwissADME predictions of pharmacokinetics and drug-likeness properties of small molecules present in *Spirulina platensis*. *IOP Conference Series: Earth and Environmental Science*, 890(1), 012021. <https://doi.org/10.1088/1755-1315/890/1/012021>
- Sen, D. J., Nandi, K., & Saha, D. (2021). Rule of five: The five men army to cross the blood brain barrier for therapeutically potent. *World Journal of Advance Healthcare Research*, 5(3), 206–211.
- Sherwood, A. R., Kurihara, A., Conklin, K. Y., Sauvage, T., & Presting, G. G. (2010). The Hawaiian Rhodophyta biodiversity survey (2006-2010): A summary of principal findings. *BMC Plant Biology*, 10(1), 258. <https://doi.org/10.1186/1471-2229-10-258>

- Vishwakarma, A., Wany, A., Pandey, S., Bulle, M., Kumari, A., Kishorekumar, R., Igamberdiev, A. U., Mur, L. A. J., & Gupta, K. J. (2019). Current approaches to measure nitric oxide in plants. *Journal of Experimental Botany*, 70(17), 4333–4343. <https://doi.org/10.1093/jxb/erz242>
- Wang, H., Zhao, Y., Zhang, F., Ke, Z., Han, B., Xiang, J., Wang, Z., & Liu, Z. (2021). Hydrogen-bond donor and acceptor cooperative catalysis strategy for cyclic dehydration of diols to access O-heterocycles. *Science Advances*, 7(22), eabg0396. <https://doi.org/10.1126/sciadv.abg0396>
- Wang, W., Liu, P., Hao, C., Wu, L., Wan, W., & Mao, X. (2017). Neoagaro-oligosaccharide monomers inhibit inflammation in LPS-stimulated macrophages through suppression of MAPK and NF- $\kappa$ B pathways. *Scientific Reports*, 7(1), 44252. <https://doi.org/10.1038/srep44252>
- Wibowo, S., Costa, J., Baratto, M. C., Pogni, R., Widyarti, S., Sabarudin, A., Matsuo, K., & Sumitro, S. B. (2022). Quantification and improvement of the dynamics of human serum albumin and glycated human serum albumin with astaxanthin/astaxanthin-metal ion complexes: Physico-Chemical and computational approaches. *International Journal of Molecular Sciences*, 23(9), 4771. <https://doi.org/10.3390/ijms23094771>
- Wibowo, S., Sumitro, S. B., & Widyarti, S. (2020). Computational study of Cu<sup>2+</sup>, Fe<sup>2+</sup>, Fe<sup>3+</sup>, Mn<sup>2+</sup>, and Mn<sup>3+</sup> binding sites identification on HSA 4K2C. *IOP Conference Series: Materials Science and Engineering*, 833(1), 012052. <https://doi.org/10.1088/1757-899X/833/1/012052>
- Wibowo, S., Widyarti, S., Sabarudin, A., Soeatmadji, D. W., & Sumitro, S. B. (2019). The role of astaxanthin compared with metformin in preventing glycated human serum albumin from possible unfolding: A molecular dynamic study. *Asian Journal of Pharmaceutical and Clinical Research*, 12(9), 276–282. <https://doi.org/10.22159/ajpcr.2019.v12i9.34617>
- Wibowo, S., Widyarti, S., Sabarudin, A., Soeatmadji, D. W., & Sumitro, S. B. (2021). DFT and molecular dynamics studies of astaxanthin-metal ions (Cu<sup>2+</sup> and Zn<sup>2+</sup>) complex to prevent glycated human serum albumin from possible unfolding. *Heliyon*, 7(3), e06548. <https://doi.org/10.1016/j.heliyon.2021.e06548>
- Xu, S.-Y., Kan, J., Hu, Z., Liu, Y., Du, H., Pang, G.-C., & Cheong, K.-L. (2018). Quantification of neoagaro-oligosaccharide production through enzymatic hydrolysis and its anti-oxidant activities. *Molecules*, 23(6), 1354. <https://doi.org/10.3390/molecules23061354>
- Yun, E. J., Yu, S., & Kim, K. H. (2017). Current knowledge on agarolytic enzymes and the industrial potential of agar-derived sugars. *Applied Microbiology and Biotechnology*, 101(14), 5581–5589. <https://doi.org/10.1007/s00253-017-8383-5>
- Zhang, Y.-H., Song, X.-N., Lin, Y., Xiao, Q., Du, X.-P., Chen, Y.-H., & Xiao, A.-F. (2019). Antioxidant capacity and prebiotic effects of *Gracilaria* neoagaro oligosaccharides prepared by agarase hydrolysis. *International Journal of Biological Macromolecules*, 137, 177–186. <https://doi.org/10.1016/j.ijbiomac.2019.06.207>



## Determination of the Pathogenicity of the Variant UPM 1432/2019 IBDV in SPF Chicken Eggs and Chicken Fibroblast Cell Line

Ali Youssif Mansour<sup>1,3</sup>, Abdul Rahman Omar<sup>2,3</sup>, Mohd Hair Bejo<sup>2,3</sup>, Noorjahan Banu Alitheen<sup>1,3</sup> and Nurulfiza Mat Isa<sup>1,3\*</sup>

<sup>1</sup>Faculty of Biotechnology and Biomolecular Sciences, Universiti Putra Malaysia, 43400 Serdang, Selangor, Malaysia

<sup>2</sup>Faculty of Veterinary Medicine, Universiti Putra Malaysia, 43400 Serdang, Selangor, Malaysia

<sup>3</sup>Institute of Bioscience, Universiti Putra Malaysia, 43400 Serdang, Selangor, Malaysia

### ABSTRACT

The infectious bursal disease virus (IBDV) is a nuisance to chicken productivity in the global poultry industry due to its high pathogenicity. In this study, the pathogenicity of the UPM 1432/2019 variant was evaluated using specific pathogen-free (SPF) chicken eggs and fibroblast cell lines. This viral strain was isolated from chickens displaying symptoms of watery diarrhoea and ruffled feathers. Following inoculation, the SPF chicken eggs, and cell lines were meticulously monitored for indicators of viral replication and the onset of cytopathic effects (CPE). The results showed that the virus could replicate in the SPF eggs and cell lines due to the presence of CPE in some cells. In addition, virus-induced weight loss in infected embryonated chicken eggs was evaluated. The UPM 1432/2019 and UPM 1219/2019 strains demonstrated similar mortality rates and CPE features. These findings indicate that the UPM 1432/2019 variant is pathogenic in SPF chicken eggs and fibroblast cell lines. Furthermore, the new UPM 1432/2019 variant caused IBD with pathogenic characteristics similar to the traditional UPM 1219/2019 variant. The emergence of the UPM 1432/2019 variant poses a risk to the economy and poultry production and is potentially resistant to the existing bursal disease vaccines. Consequently, the UPM 1432/2019 variant may significantly contribute to economic losses for chicken farm operators. Moreover, this study provides essential information on the potential virulence of the UPM 1432/2019 variant of IBDV and its potential impact on the poultry industry.

### ARTICLE INFO

#### Article history:

Received: 1 March 2024

Accepted: 15 May 2024

Published: 28 January 2025

DOI: <https://doi.org/10.47836/pjtas.48.1.16>

#### E-mail addresses:

gs58122@student.upm.edu.my (Ali Youssif Mansour)

aro@upm.edu.my (Abdul Rahman Omar)

mdhair@upm.edu.my (Mohd Hair Bejo)

noorjahan@upm.edu.my (Noorjahan Banu Alitheen)

nurulfiza@upm.edu.my (Nurulfiza Mat Isa)

\*Corresponding author

**Keywords:** CEF cells, cytopathic, embryonated, IBDV, inoculated, pathogenicity

### INTRODUCTION

Infectious bursal disease (IBD) is highly contagious and potentially fatal for

chickens. This viral disease is caused by the infectious bursal disease virus (IBDV) from the Avibirnavirus genus and Birnaviridae family, which targets the bursa of Fabricius imperative for immune cell development (Huang et al., 2021). The IBDV is a double-stranded RNA virus that codes for five viral proteins: VP1, VP2, VP3, VP4, and VP5 (Thai et al., 2021). The VP2 protein is the primary factor determining the virus's pathogenicity and ability to elicit a protective immune response. Therefore, sequencing the hVP2 gene and pathogenicity testing are the most reliable methods for identifying IBDV strains (Deorao et al., 2021). The first IBD outbreak in Malaysia was reported in 1991, where the very virulent IBDV (vvIBDV) strain resulted in catastrophic mortality in poultry farms (Aliyu et al., 2021). Local chicken farm operators experienced devastating economic losses, estimated at more than RM72 million annually. The symptoms of IBD include depression, watery diarrhoea, ruffled feathers, dehydration, and immunosuppression in chickens aged between three and six weeks (Eterradossi et al., 1999).

A critical pathological consequence of IBD is the bursa of Fabricius atrophy, characterised by diminished organ size and function. Consequently, the host's immune competence is compromised, making the chicken susceptible to secondary infections. Therefore, management and prevention strategies, particularly vaccination regimens, have been established to combat the threats posed by the disease on the poultry industry (Taghavian et al., 2013). Attenuated live, inactivated immune complex and recombinant vaccines have been developed to specifically target virulent infectious bursal disease Virus (vIBDV), classical virulent IBDV (cIBDV), and antigenic variant IBDV (avIBDV) strains, respectively (Jin et al., 2005).

The variant UPM1432/2019 IBDV was isolated from vaccinated poultry with watery diarrhoea and ruffled feathers. This Malaysian variant is more persistent in the bursa of chickens than the vvIBDV and UPM1056/2018 strains (Aliyu et al., 2022). The bursa atrophy caused by IBDV is a significant complication with possible long-term effects on chicken health and immunity (Yang et al., 2021). Thus, this research aims to determine the effects of the propagated UPM1432/2019 variant on specific pathogen-free (SPF) chicken eggs and fibroblast cell lines. The study findings could shed light on the pathogenic severity of the UPM1432/2019 variant compared to other IBDV strains. In addition, this study ascertained the 50% tissue culture infectious dose (TCID<sub>50</sub>) of the UPM1432/2019 variant in fibroblast cells of SPF chicken embryonated eggs. It determined the virus's mortality, persistence, and cytopathic effect on SPF chicken eggs and chicken embryonated fibroblast cells.

## MATERIALS AND METHODS

### Samples

A total of 70 SPF eggs and three viral isolates were used in this study. Two strains, UPM1219/2019 (accession no. MT431215) and UPM1432/2019 (accession no. MT505343), were obtained with other isolates from different commercial broiler farms across five states

in Malaysia between 2017 and 2019. The bursa samples exhibited haemorrhages, oedema, and lesions (Aliyu et al., 2021). Meanwhile, UPM081 (accession no. AY520910), a very virulent strain isolated from an outbreak in Malaysia back in 2000 (Lawal et al., 2018), was obtained as CAM homogenates and used as a comparison with the other isolates.

### **Titration (TCID<sub>50</sub>) of UPM1432/2019 Variant Isolates**

The TCID<sub>50</sub> was used to determine the number of virus particles required to infect 50% of the host cell. This assay measures a virus's virulence and compares the infectivity of different strains. First, the UPM1432/2019 variant was serially diluted, and each dilution was added to a separate well containing the host cell, the chicken embryo fibroblast (CEF) cells. The plate was incubated for a specified period, followed by a cell count of infected cells to determine the dilution at which 50% of the wells were infected (Jin et al., 2005).

### **Pathogenicity in Embryonated SPF Chicken Eggs**

Three cycles of freeze-thaw and homogenisation of the bursa tissues were performed in a sterile mortar and pestle containing 20% (w/v) suspension of sterile, pH 7.4 phosphate-buffered saline (PBS). Subsequently, the homogenised tissue suspension was centrifuged at 4,000 x g for 20 min at 4°C (Ebrahimi et al., 2013). The supernatant was filtered using 0.22 µm sterile syringe filters (Micro, Lab Scientific, China) and stored for 60 to 90 min at 40°C. Finally, the virus was inoculated in the 9–11-day-old SPF embryonated chicken eggs using the chorioallantois membrane (CAM) method and incubated at 37°C for eight days while continuously checking for mortality.

### **Primary Chicken Embryonated Fibroblast (CEF) Cell Culture**

Fibroblast cells obtained from 9–11-day-old SPF embryonated chicken eggs were used for cell culture preparation (Rekha et al., 2014). First, the CEF tissue was extracted and washed using 1 ml of PBS. The fibroblast tissue was cut into smaller pieces, transferred into a 15 ml tube containing 0.25% trypsin, mixed, and shaken for 20 min. Subsequently, the DMEM growth medium (high glucose, L-glutamine, and sodium pyruvate, Biosera, France) was supplemented with 10% fetal bovine serum (FBS) (Hyclone, USA) to stop the trypsinisation process. The cells were centrifuged at 350 x g for 5 min at 4°C, and the supernatant was discarded. The growth medium was then added to the cell pellets. The cell suspension (5 ml) was adjusted to a concentration of 5.0 x 10<sup>6</sup> cells/ml (SPL Lifesciences, South Korea) and seeded into a 25 ml flask. Complete monolayers in the flask were infected with 0.1 ml of the UPM1432/2019 variant and incubated at 37°C in 5% carbon dioxide (CO<sub>2</sub>). The cytopathic effect (CPE) was monitored daily, and the flasks were freeze-thawed thrice and centrifuged at 350 x g for 5 min upon CPE detection. The supernatants were collected and stored at -20°C.

### **Virus Inoculation in Chicken Embryonated Fibroblast (CEF) Cell Culture**

A full monolayer was formed in the flasks after 24 h. The flasks were washed thrice with 1 ml of pH 7.4 PBS and inoculated with 0.1 ml of the UPM1432/2019 variant. The flasks were incubated at 37 °C for 1 h to allow virus attachment. Subsequently, maintenance media containing DMEM, 2% FBS, and antibiotics were added to the flask. The cells were observed at 24, 48, and 72-h intervals and checked daily for cytopathic effects. Once CPE was visible, the cells were centrifuged, and the supernatant was stored at -20 °C for viral RNA extraction.

### **Immunofluorescence Assay (IFA)**

As mentioned, the CEF cells injected with wild-type UPM1432/2019 were prepared to identify their morphological characteristics. Immunofluorescent staining was performed on the cells at 24 and 48 hr. First, the plates were fixed for 10 min with 4% paraformaldehyde (Biotium, USA), followed by washing with 1 ml of PBS thrice every 5 min and carefully aspirated. Subsequently, 0.5 ml of 0.3% triton X-100 was added to each well for 10 min to catalyse permeabilisation and washed gently with PBS thrice at 5 min intervals. After adding 500 µl of 1% bovine serum albumin (Sigma-Aldrich, Germany) to each well for 30 mins, the plate was washed thrice at 5 min intervals using PBST (Thermo Scientific, USA). Each well received 40 µl of mouse primary IBDV antibody (Fitzgerald, USA) and incubated at 4°C overnight in the dark. All plates were covered with aluminium foil to maintain the dark condition.

The plates were thoroughly rinsed thrice with 1 ml of PBS after 18 hr, followed by the addition of 40 µl secondary rabbit antibody against mouse IgG1 conjugated with fluorescein isothiocyanate (FITC) (Abcam, UK) to each well. The plates were incubated for 2 hr at 4°C in the dark. After three PBS washes, the plates were left to dry. Once dried, the coverslip was carefully removed from the plates, mounted with 20 µl of Fluoroshield mounting media with Dapi (Abcam, UK), and rested for 30 min. Finally, the slides were examined under a fluorescence microscope. Fluorescent signals of varying magnitude are indicative of a successful IFA. The viral overlap in the nucleus was identified and captured using a camera (AxioCam MRm, Germany) to assess the localisation features of the UPM1432/2019 variant within the CEF cells.

## **RESULTS**

Figure 1 compares the pathogenicity of SPF chicken eggs inoculated with three strains (UPM1219, UPM081, and UPM1432/2019). The mortality rate was observed from day 1 to 8 post-infection, where UPM1432/2019 IBDV showed an increased mortality rate of about 30% from day seven post-infection.



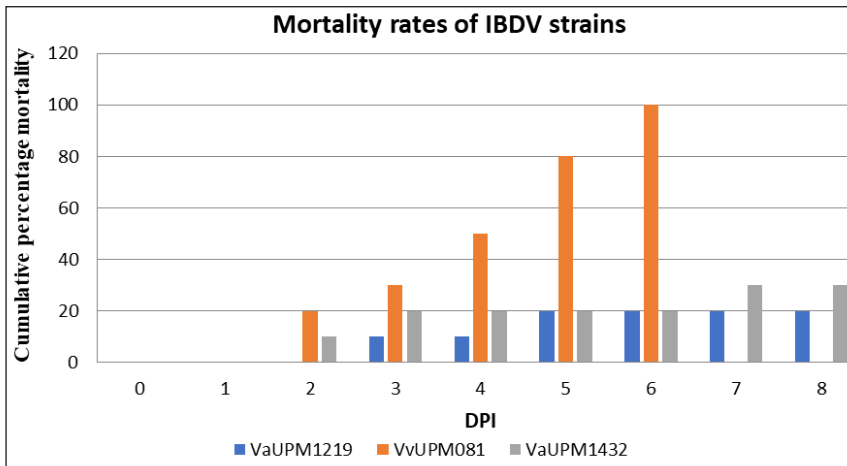


Figure 1. Cumulative mortality rates of IBDV variants inoculated in specific pathogen free (SPF) chicken eggs

Figure 2 shows gross lesions of the UPM 1432/2019, UPM 1219/2019, and UPM 081 in nine-day-old embryonated chicken eggs.

### Gross lesions

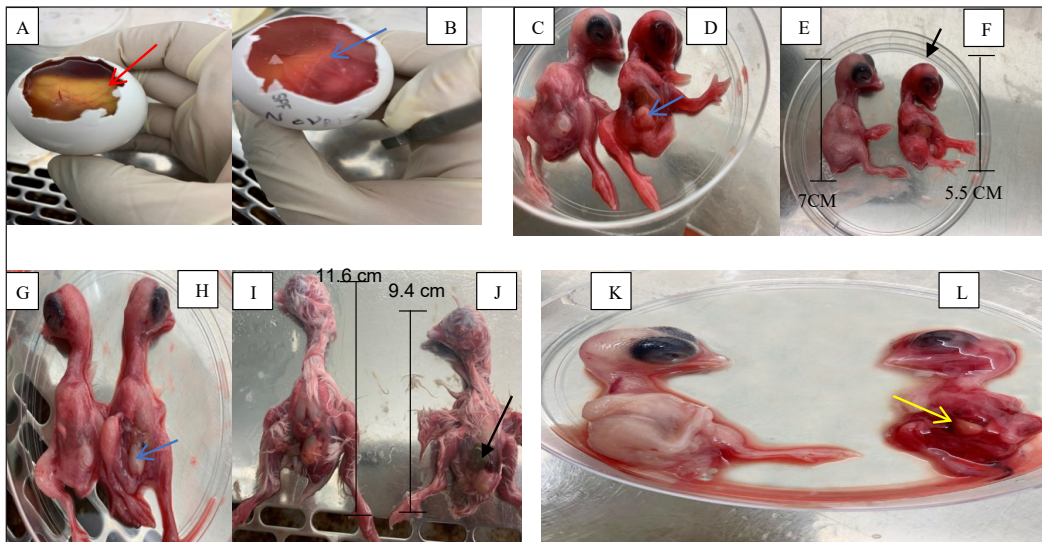


Figure 2. Gross lesions of UPM 1432/2019, UPM 1219/2019, and UPM 081 in nine-day-old embryonated chicken eggs. (A, C, E, G, I, and K): the control uninoculated embryo presents normal conditions. (A) shows normal transparent CAM (red arrow), (B, D, and F) infected group with UPM 1432/2019 displayed typical lesions on the bursa. Also, it showed cloudy CAM in the embryo (B) (blue arrow), head haemorrhagic (F) (black arrow), and swollen bursa (D) (blue arrow). (H and J) show chicken embryonated eggs inoculated with UPM 1219/2019, which represent swollen bursa (blue arrow) (H), dwarfing growth, and liver abnormality (black arrow) (J). (L) represent gross lesions in the infected nine-day-old embryonated chicken eggs and display congestion in the liver (yellow arrow) due to infection with the UPM 081 strain

The 50% tissue culture infectious dose (TCID<sub>50</sub>) value of the UPM 1432/2019 variant strain was also used to compare its infectivity to other IBDV strains and to monitor changes in virulence over time. The TCID<sub>50</sub> value was calculated using experimental data shown in Table 1.

Table 1  
*Estimation of fifty per cent tissue culture infective dose (TCID<sub>50</sub>) recorded UPM 1432/2019 variant virus data*

10-fold dilution	No. of positive CPE well	No. of negative CPE well	Accumulative	Number	Total number	Percentage
			Positive (A)	Negative (B)	A+B	A/(A+B)X 100%
10 <sup>-1</sup>	10	0	61	0	61	100.0
10 <sup>-2</sup>	10	0	52	1	53	98.0
10 <sup>-3</sup>	10	0	45	3	48	93.7
10 <sup>-4</sup>	10	0	37	5	42	88.0
10 <sup>-5</sup>	10	0	29	6	35	82.0
10 <sup>-6</sup>	9.0	0	21	9	30	70.0
10 <sup>-7</sup>	7.0	4	18	12	30	60.0
10 <sup>-8</sup>	5.0	6	12	19	31	38.0
10 <sup>-9</sup>	4.0	8	7.0	22	29	24.0
10 <sup>-10</sup>	2.0	8	2.0	29	31	6.0

Note. It is important to note that the TCID<sub>50</sub> assay is a simplified measure of virulence and does not consider other factors that may affect the ability of a virus to infect a host cell culture (Wang et al., 2021)

At dilution 10<sup>7</sup>, the dilution percentage immediately above 50% = 60%. At dilution 10<sup>8</sup>, the percentage of dilution immediately below 50% = 38%.

$$\text{Index calculation} = \frac{\text{Percentage on infectivity at dilution above 50\%} - 50}{\text{Percentage on infectivity at dilution above 50\%} - \text{Percentage on infectivity below 50\%}}$$

$$= \frac{60 - 50}{60 - 38} = 0.45$$

$$10^{7.45} / 0.1 \text{ ml} = 10^{8.45} \text{ TCID}_{50} / \text{ML}$$

It is important to note that the TCID<sub>50</sub> assay is a simplified measure of virulence and does not consider other factors that may affect the ability of a virus to infect a host cell culture (Wang et al., 2021).

Figure 3 shows specific features of each strain's CPE, such as cytoplasmic vacuolation, apoptosis, and necrosis. These features were used to differentiate between IBDV strains.

Figure 4 shows that a microscopic examination of a CEF monolayer demonstrates alterations in the nucleolus morphology of chicken embryo fibroblast cells post-infection with the UPM 1432/2019 variant virus at 24- and 48-hours post-infection (hpi).

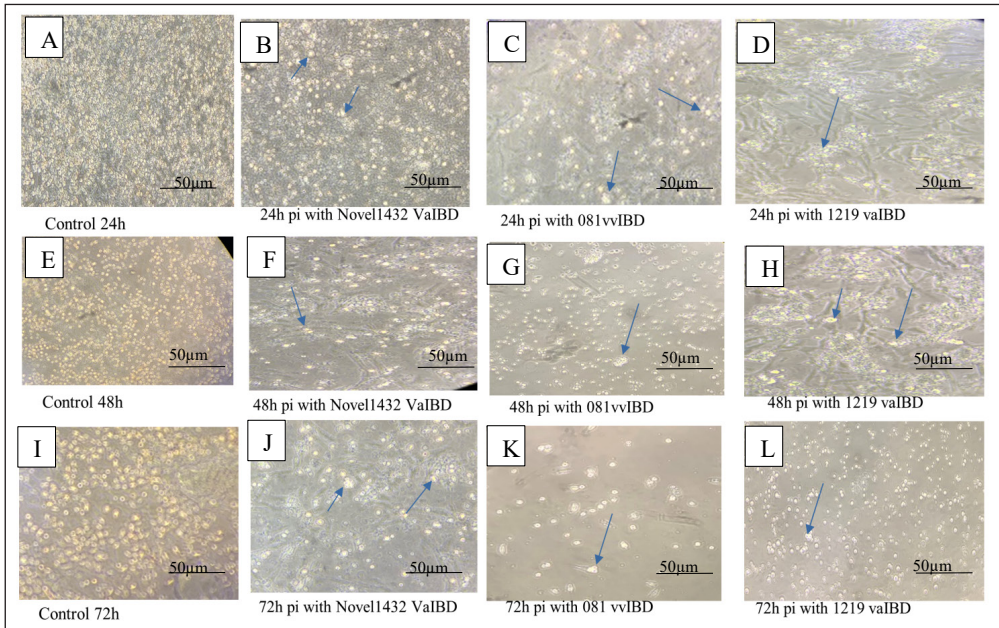


Figure 3. Microscopic view of chicken embryo fibroblast (CEF) cells monolayer after 24, 48, and 72-hours post-infection (hpi) by three different infectious bursal disease virus (IBDV) strains (variant UPM 1432/2019, very virulent UPM 081, and variant UPM 1219/2019). (A) indicates the control group

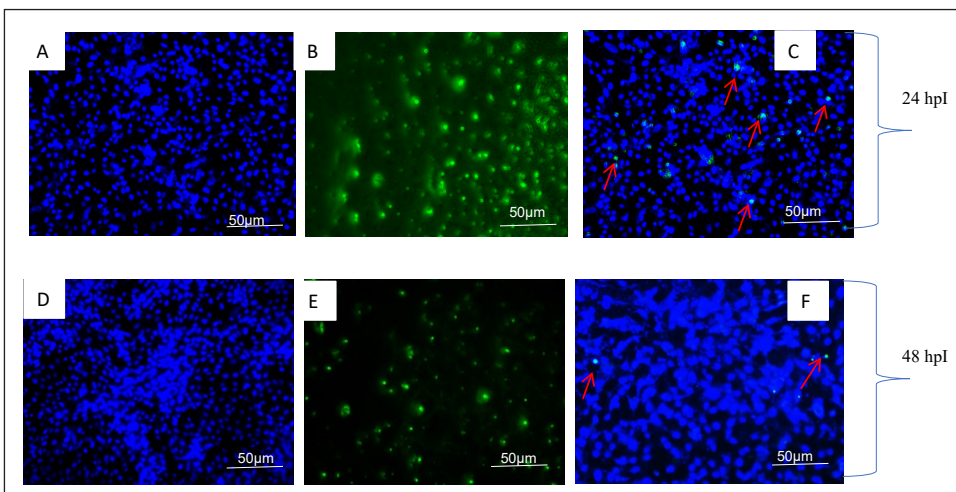


Figure 4. A microscopic examination of a chicken embryo fibroblast (CEF) monolayer demonstrates alterations in the nucleolus morphology of chicken embryo fibroblast cells post-infection with the UPM 1432 variant infectious bursal disease virus (IBDV) at 24 and 48-hours post-infection (hpi). The control group (A and D) displays a nucleus labelled with Dapi (blue) at 24 and 48 hpi, respectively, while infected CEFs (B and E) reveal the virus labelled with FITC in green at 24 and 48 hpi. Additionally, mixed staining of infected CEFs (C and F) exhibits a nucleus stained blue and the variant UPM1432 IBD virus stained with fluorescein isothiocyanate (FITC) green at 24 hpi and 48 hpi

## DISCUSSION

This study successfully propagated the UPM 1432/2019 and UPM 1219/2019 strains and UPM 081 virulent strains in SPF chicken embryonated eggs. The mortality rates of the IBDV strains varied depending on factors such as the chickens' age and immune states (Dey et al., 2019). The disease caused by vvIBDV is often more severe than those caused by avIBDV or clIBDV, where the former is characterised by severe depression, diarrhoea, and high mortality (Fan et al., 2020). The mortality rate for the clIBDV-infected chicken is typically low in SPF eggs. Conversely, a significant death rate may be evident among chickens infected with vvIBDV strain (Dey et al., 2019). Approximately 20% and 30% of the SPF eggs infected with UPM 1432/2019 and UPM 1219/2019 died on day 8 post-infection (Figure 1). Meanwhile, 100% mortality was observed in the SPF eggs at day 6 post-infection with the UPM 081 strain.

At nine days old, the SPF chicken embryonated eggs inoculated with the UPM1432/2019 variant demonstrated cloudy CAM in the embryo (Figure 2B), swelling, and a haemorrhagic in the bursa (Figure 2D). In contrast, those infected with UPM 081 had significant lesions in their bursa and liver (Figure 2L). Figure 1 also indicated that the UPM 1432/2019 infection did not result in high mortality, and the embryonated chicken could continue to propagate eight days post-infection. However, lesions were observed at their bursa (Figure 2D). This finding confirmed that the impacts of UPM 1432/2019 are more persistent and limited to the bursa, while the UPM 081 strain spreads its pathogenicity to other organs, such as the liver. Likewise, the SPF eggs infected with UPM 1432/2019 and UPM 1219/2019 also exhibited similar outcomes (Figure 2 D & H). Earlier studies reported that IBDV mainly targets the bursa of Fabricius in chickens, a reservoir for B lymphocytes (Reddy et al., 2022).

The CPE refers to changes in host cell post-viral infection, particularly in the cellular morphology and function. These alterations vary depending on the viral strain and host cell. The present study described the CPE of three viral strains on CEF cell culture (Figure 3). At 24 h post-infection (hpi) with the UPM 1432/2019 variant, the microscopic view of the CEF cell monolayer appeared relatively normal (Figure 3B). The cells are well-spread and adhered to the culture dish, with a normal cytoplasmic appearance. Meanwhile, cells inoculated with the UPM 081 strain had a slightly rounded appearance (Figure 3C). At 48 hpi (Figure 3G), the UPM 081-infected CEF cell monolayer was significantly altered and indicative of severe CPE, characterised by a rounded appearance and detachment from the culture dish. No morphological changes were observed in CEF infected with UPM 1432/2019 and UPM 1219/2019 strains after 48 h (Figure 3F & H). At 72 hpi, the monolayer of the UPM 081-infected CEF cells exhibited prominent CPE, evident from the rounded cells detached from the culture plate (Figure 3K). The cytoplasm of the infected cells was vacuolated and swollen, with a substantial decrease in cell proliferation compared to UPM 1432/2019 and UPM 1219/2019 CEFs, which demonstrated mild CPE and a slight reduction in cells (Figure 3J & L) (Deorao et al., 2021).

Similar CPE patterns were observed in the IFA (Figure 4). At 24 hpi, the CEF infected with the UPM1432/2019 variant overlapped with the nucleus (Figure 4C), acquired CPE, fully integrated into the CEF nucleus, and began to transform morphologically by 48 hpi (Figure 4F). Overall, the microscopic view of the CEF cell monolayer post-infection with the three IBDV strains exhibited clear CPE progression over time. The UPM1432/2019 and UPM1219/2019 IBDV strains caused mild CPE, whereas the UPM081 very virulent strain caused severe CPE (Aliyu et al., 2021). These changes in the CEF cell monolayer are a valuable tool for differentiating the IBDV strains. The IBDV disease severity is associated with strain virulence, and novel IBDV variants can possess stronger virulence than their predecessors (Aliyu et al., 2021). Moreover, vvIBDV can cause severe immunosuppression and high mortality rates, particularly in young birds. These strains also cause more severe bursal damage, loss, and systemic disease (Agnihotri et al., 2022). Besides the bursal lesions, other organs, such as the thymus, spleen, and liver, could be affected by vvIBDV, which is indicated by organ enlargement and congestion. The kidneys may also be impacted, indicated by tubular necrosis.

## CONCLUSION

The emergence of new IBDV variants continues to concern various stakeholders in the poultry industry. Controlling the spread of these variants is crucial to prevent severe disease spread and economic losses. In the current study, the UPM 1432/2019 variant was successfully propagated in SPF chicken embryonated eggs. The results indicate that this strain induces IBD with pathological features mimicking the conventional UPM 1219/2019 strain and UPM081 virulent strain. This finding highlighted the potential threat of the UPM 1432/2019 to the economy and poultry farming, as the existing IBD vaccines may not be effective against this variant. Therefore, it is recommended for future studies to develop a new and safe IBD vaccine that targets UPM 1432/2019, UPM 1219/2019, and UPM 081 IBDV to protect chickens against the disease.

## ACKNOWLEDGMENTS

This study was funded by the Institute of Bioscience, Higher Institute Centre of Excellence (IBS HICoE) grant (grant no. 5220002) under the Ministry of Higher Education, Malaysia.

## REFERENCES

- Agnihotri, A. A., Awandkar, S. P., Kulkarni, M. B., Chavhan, S. G., Kulkarni, R., & Chavan, V. G. (2022). Molecular phylodynamics of infectious bursal disease viruses. *Virus Genes*, *58*(4), 350–360. <https://doi.org/10.1007/s11262-022-01905-9>
- Aliyu, H. B., Hair-Bejo, M., Omar, A. R., & Ideris, A. (2021). Genetic diversity of recent infectious bursal disease viruses isolated from vaccinated poultry flocks in Malaysia. *Frontiers in Veterinary Science*, *8*, 643976. <https://doi.org/10.3389/fvets.2021.643976>

- Aliyu, H. B., Hamisu, T. M., Hair Bejo, M., Omar, A. R., & Ideris, A. (2022). Comparative pathogenicity of Malaysian variant and virulent infectious bursal disease viruses in chickens. *Avian Pathology*, 51(1), 76–86. <https://doi.org/10.1080/03079457.2021.2006604>
- Deorao, C. V., Rajasekhar, R., Ravishankar, C., Nandhakumar, D., Sumod, K., Palekkodan, H., John, K., & Chaithra, G. (2021). Genetic variability in VP1 gene of infectious bursal disease virus from the Kerala, India field outbreaks. *Tropical Animal Health and Production*, 53(3), 407. <https://doi.org/10.1007/s11250-021-02852-7>
- Dey, S., Pathak, D., Ramamurthy, N., Maity, H. K., & Chellappa, M. M. (2019). Infectious bursal disease virus in chickens: Prevalence, impact, and management strategies. *Veterinary Medicine: Research and Reports*, 2019(10), 85–97. <https://doi.org/10.2147/vmrr.s185159>
- Ebrahimi, M. M., Shahsavandi, S., Masoudi, S., & Ghodsian, N. (2013). Isolation, characterization and standardization of new infectious bursal disease virus for development of a live vaccine. *Iranian Journal of Virology*, 7(4), 29–36. <https://doi.org/10.21859/isy.7.4.2>
- Etteradossi, N., Arnauld, C., Tekai, F., Toquin, D., Le Coq, H., Rivallan, G., Guittet, M., Domenech, J., van den Berg, T. P. & Skinner, M. A. (1999). Antigenic and genetic relationships European virulent infectious bursal disease virus between strains and an early West African isolate. *Avian Pathology*, 28(1), 36–46. <https://doi.org/10.1080/0307945995028>
- Fan, L., Wu, T., Wang, Y., Hussain, A., Jiang, N., Gao, L., Li, K., Gao, Y., Liu, C., Cui, H., Pan, Q., Zhang, Y., & Qi, X. (2020). Novel variants of infectious bursal disease virus can severely damage the bursa of fabricius of immunized chickens. *Veterinary Microbiology*, 240, 108507. <https://doi.org/10.1016/j.vetmic.2019.108507>
- Huang, X., Liu, W., Zhang, J., Liu, Z., Wang, M., Wang, L., Zhou, H., Jiang, Y., Cui, W., Qiao, X., Xu, Y., Li, Y., & Tang, L. (2021). Very virulent infectious bursal disease virus-induced immune injury is involved in inflammation, apoptosis, and inflammatory cytokines imbalance in the bursa of fabricius. *Developmental and Comparative Immunology*, 114, 103839. <https://doi.org/10.1016/j.dci.2020.103839>
- Jin, R., Cheng, T., Liu, X., Jiang, T., Gu, H., & Zou, G. (2005). Development of recombinant VP2 vaccine for the prevention of infectious bursal disease of chickens. *Vaccine*, 23(40), 4844–4851. <https://doi.org/10.1016/j.vaccine.2005.05.015>
- Lawal, N., Hair-Bejo, M., Arshad, S. S., Omar, A. R., & Ideris, A. (2018). Propagation and molecular characterization of bioreactor adapted very virulent infectious bursal disease virus isolates of Malaysia. *Journal of Pathogens*, 2018(1), 1068758. <https://doi.org/10.1155/2018/1068758>
- Reddy, V. R. a. P., Nazki, S., Brodrick, A. J., Asfor, A. S., Urbaniec, J., Morris, Y., & Broadbent, A. J. (2022). Evaluating the breadth of neutralizing antibody responses elicited by infectious bursal disease virus genogroup A1 strains using a novel chicken B-Cell rescue system and neutralization assay. *Journal of Virology*, 96(18), e01255-22. <https://doi.org/10.1128/jvi.01255-22>
- Rekha, K., Sivasubramanian, C., Chung, I., & Thiruvengadam, M. (2014). Growth and replication of infectious bursal disease virus in the DF-1 cell line and chicken embryo fibroblasts. *BioMed Research International*, 2014(1), 494835. <https://doi.org/10.1155/2014/494835>

- Taghavian, O., Spiegel, H., Hauck, R., Hafez, H. M., Fischer, R., & Schillberg, S. (2013). Protective oral vaccination against infectious bursal disease virus using the major viral antigenic protein VP2 produced in *Pichia pastoris*. *PLOS ONE*, *8*(12), e83210. <https://doi.org/10.1371/journal.pone.0083210>
- Thai, T. N., Jang, I., Kim, H., Kim, H., Kwon, Y., & Kim, H. (2021). Characterization of antigenic variant infectious bursal disease virus strains identified in South Korea. *Avian Pathology*, *50*(2), 174–181. <https://doi.org/10.1080/03079457.2020.1869698>
- Wang, S., Yu, M., Liu, A., Bao, Y., Qi, X., Gao, L., Chen, Y., Liu, P., Wang, Y., Xing, L., Meng, L., Zhang, Y., Fan, L., Li, X., Pan, Q., Zhang, Y., Cui, H., Li, K., Liu, C., ... Wang, X. (2021). TRIM25 inhibits infectious bursal disease virus replication by targeting VP3 for ubiquitination and degradation. *PLoS Pathogens*, *17*(9), e1009900. <https://doi.org/10.1371/journal.ppat.1009900>
- Yang, D., Zhang, L., Duan, J., Huang, Q., Yu, Y., Zhou, J., & Lü, H. (2021). A single vaccination of IBDV subviral particles generated by *Kluyveromyces marxianus* efficiently protects chickens against novel variant and classical IBDV Strains. *Vaccines*, *9*(12), 1443. <https://doi.org/10.3390/vaccines9121443>





## Antioxidant Properties and Storage Stability of Spray-dried *Melastoma malabathricum* L. Fruit Extract for Natural Colorant

Nurul Syazwani Zahari<sup>1</sup>, Siti Fatimah Sabran<sup>1\*</sup>, Norhaidah Mohd Asrah<sup>2</sup>, Mohd Fadzelly Abu Bakar<sup>1</sup>, Furzani Pa'ee<sup>1</sup>, Norhayati Muhammad<sup>1</sup>, Fazleen Izzany Abu Bakar<sup>1</sup> and Mohd Khairil Said<sup>3</sup>

<sup>1</sup>Department of Technology and Natural Resources, Faculty of Applied Sciences and Technology, Universiti Tun Hussein Onn Malaysia (UTHM), Pagoh Education Hub, KM 1, Jalan Panchor, 84600 Muar, Johor, Malaysia

<sup>2</sup>Department of Mathematics and Statistics, Universiti Tun Hussein Onn Malaysia (UTHM), Pagoh Education Hub, KM 1, Jalan Panchor, 84600 Muar, Johor, Malaysia

<sup>3</sup>Tropical Bioessence Sdn. Bhd., No.43 Jalan Tiara Sentral 2, Nilai Utama Enterprise Park, 71800 Nilai, Negeri Sembilan, Malaysia

### ABSTRACT

*Melastoma malabathricum* L. is a plant that is rich in anthocyanin, though its anthocyanin is low in stability. Therefore, this study aims to characterize the physicochemical properties of the encapsulated fruit extracts of *M. malabathricum*, to determine the antioxidant activities before and after encapsulation using 2,2-Diphenyl-1-picrylhydrazyl (DPPH), 2,2-Azino-bis-3-ethylbenzothiazoline-6-sulphonic acid (ABTS), and Ferric Reducing Antioxidant Power (FRAP) assays, expressed as IC<sub>50</sub> values, and to assess the storage stability of the encapsulated fruit extract in different conditions based on the Total Anthocyanin Content (TAC) and Degradation Index (DI). The encapsulation was performed using a spray dryer and maltodextrin as the wall material. Crude extract with maltodextrin ratios of 1:1, 1:2 and 1:3 were tested, and TAC of the samples were determined using pH differential methods. The encapsulated extract was characterized according to their physical

and chemical properties. Stability was evaluated under different conditions, including 20°C, 4°C and 25°C in the dark, and 25°C with light exposure for 90 days. Ratio 1:3 exhibited the lowest moisture content (5.77%) and solubility time (3s), while ratio 1:1 demonstrated the lowest bulk and tapped densities (0.366 g/ml and 0.5 g/ml). All ratios were acidic and displayed spherical particles with irregular surfaces. Ratio 1:1 showed the highest antioxidant activity with IC<sub>50</sub> values of 28.50 µg/ml (DPPH), 49.03 µg/ml (ABTS), and 39.97 µg/ml (FRAP). The most

### ARTICLE INFO

#### Article history:

Received: 25 April 2024

Accepted: 4 July 2024

Published: 28 January 2025

DOI: <https://doi.org/10.47836/pjtas.48.1.17>

#### E-mail addresses:

syazwanizahari0206@gmail.com (Nurul Syazwani Zahari)

fatimahsb@uthm.edu.my (Siti Fatimah Sabran)

norhaida@uthm.edu.my (Norhaidah Mohd Asrah)

fadzelly@uthm.edu.my (Mohd Fadzelly Abu Bakar)

furzani@uthm.edu.my (Furzani Pa'ee)

norhayatim@uthm.edu.my (Norhayati Muhammad)

fazleen@uthm.edu.my (Fazleen Izzany Abu Bakar)

md.tbesb@gmail.com (Mohd Khairil Said)

\*Corresponding author

stable condition was at 4°C in the dark, while the ratio 1:2 was found to be the best ratio. Both factors can be considered to achieve stability for future applications.

*Keywords:* Antioxidant, anthocyanin, natural color, spray-dried, storage stability

---

## INTRODUCTION

The rising demand for all-natural products has sparked the exploration of novel natural colorants (Novais et al., 2022). Natural colorants pose no health risks to humans and biodegrade quickly, making them ideal for use (Usman et al., 2017). Besides, synthetic colorants have produced potentially harmful consequences compared to natural ones. It can be seen in the case of various studies on the harmful consequences of using synthetic colorants (Oplatowska et al., 2017). Thus, this issue has created an alarm for people to be concerned about the effects of shifting to a natural colorant.

Natural colorants are widely used in many industries but are most commonly used in food and beverage products. According to the market research report, the market for natural food colors was estimated to be worth USD 1.54 billion in 2021. By 2030, it is anticipated to expand at a compound annual growth rate (CAGR) of 7.4%. Due to the increasing demand for natural colorants, exploring new and alternative sources is crucial to focusing on the underutilized plant species (Adnan et al., 2011).

Numerous underutilized natural plant species have not been researched for a few reasons. As Malaysia has a tropical climate with the highest levels of biodiversity in the world, an underutilized plant known as senduduk, *Melastoma malabathricum* L., shown in Figure 1, is a promising candidate for becoming a source of natural colorant. Many



Figure 1. A mature plant of *Melastoma malabathricum* L. in its wild habitat

studies have demonstrated this plant's medicinal properties, which can benefit from all parts, including fruits, leaves, flowers, and roots.

The fruit of *M. malabathricum*, as shown in Figure 2, has been emerging as a promising source of natural colorants due to the presence of anthocyanin pigments, which are able to offer a color ranging from red to purple, marked as a significant advancement for different sectors. Anthocyanin from *M. malabathricum* has attracted attention lately because it possesses potential health benefits, especially as an antioxidant. Significantly, this plant's development of natural colorants aligns with the growing interest in food natural colorants with higher antioxidant activities. However, the food natural colorant from plant pigment faces challenges because they are vulnerable to degradation and low stability (Echegaray et al., 2020). They usually often lose their color, and their biological activity is particularly affected by the light, temperature of the storage, and pH (Roobha et al., 2011). Following storage stability testing by World Health Organization (WHO), the storage conditions were simulated to include room temperature, refrigerator, and freezer conditions. This finding broadly influences the selection of storage stability testing for anthocyanins due to their potential stability in stable conditions, as they are easily degraded at higher temperatures. Besides that, the pH will remain constant throughout the study to accurately depict how anthocyanins act in their native state.

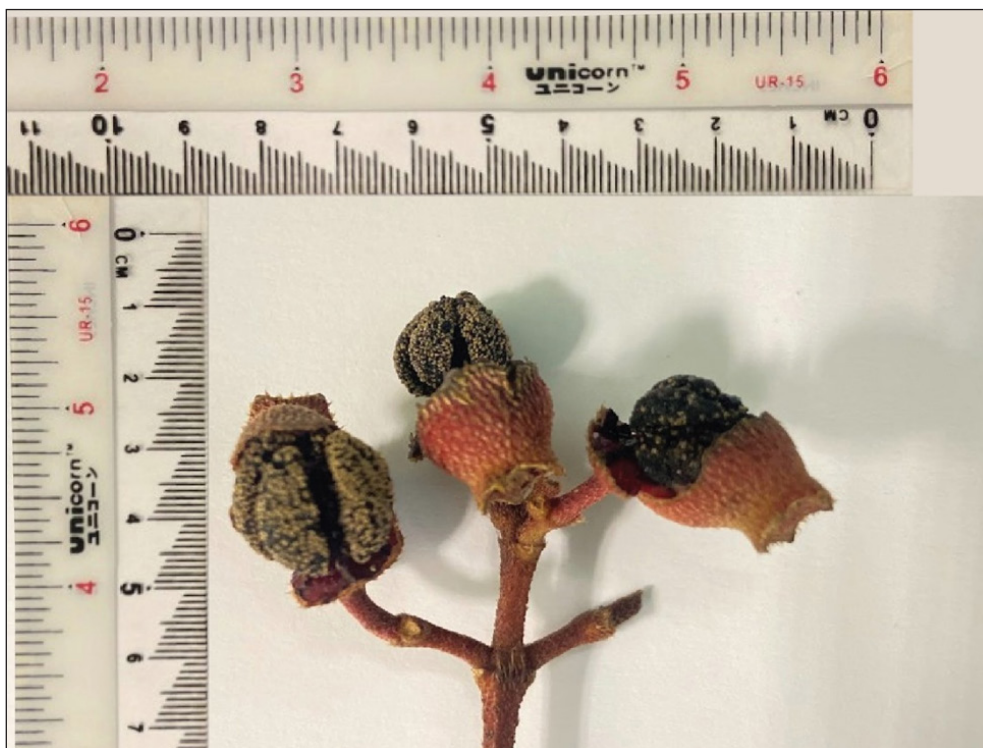


Figure 2. *Melastoma malabathricum* L. fruits

Existing studies on encapsulation of *M. malabathricum* fruit extracts have primarily focused on evaluating wall materials instead of stability. Therefore, this study has successfully established the connection by assessing the storage stability of the encapsulated fruit extract of *M. malabathricum* in different conditions based on the Total Anthocyanin Content (TAC) and Degradation Index (DI). These studies concern the physicochemical properties of the encapsulated fruit extract in producing high-quality powder and highlight its potential to provide health benefits, such as antioxidant activity.

## MATERIALS AND METHODS

### Sample Collection

Fresh samples of *M. malabathricum* fruits were collected from UTHM Campus Pagoh, Johor, Malaysia, from January to March during the northeast monsoon season. According to Kasunmala et al. (2020), the fruits were collected at two different maturation stages: maturity stage 2, which represents mature fruits, and maturity stage 3, which represents ripened fruits. *Melastoma malabathricum* L. species were identified and deposited at the National Herbarium in Forest Research Institute Malaysia (FRIM) Kepong. Subsequently, five kilograms of *M. malabathricum* fruits were washed, cleaned, and air-dried at room temperature. The dried samples were then ground using a blender and stored at 4°C until further use (Kasunmala et al., 2020).

### Sample Extraction

Ultrasound-Assisted Extraction (UAE) was conducted with some modifications. Fruits of *M. malabathricum* were extracted using a wt/vol ratio of 1:10 (mass of sample in g: volume of solvent in ml) with absolute ethanol (Thermo Fisher, America) in a beaker. The ultrasonic frequency and power set were fixed at 280 W 37 kHz, 70°C temperature, and 19 min extraction time. After that, the extract was filtered using Whatman No. 1 filter paper, and the solvent was removed using a rotary evaporator (Buchi Switzerland R-100, Switzerland) under 200 mbar at a temperature of 70°C to obtain the crude extract.

### Encapsulation Using Spray Dryer of *Melastoma malabathricum* L.

The spray-drying process was conducted using maltodextrin, following the methods outlined by Narayanan et al. (2018), Mokhtar et al. (2013), and Krishnainah et al. (2012) with certain modifications. Three different ratios of the encapsulated fruit extracts to maltodextrin were (1:1), (1:2), and (1:3). The maltodextrin (Sigma Aldrich, Malaysia) was mixed with the crude extract together with 1000 ml distilled water, as shown in Table 1. The mixture was then stirred using a magnetic stirrer for 1 hr (Nayak & Rastogi, 2010a). The mixture was spray dried using a spray dryer with an inlet of 160°C and an outlet temperature

maintained at 80°C. Then, the powders were stored over silica gel in desiccators at room temperature (25°C ± 2°C) for further experiments.

Table 1

*Total sample and maltodextrin in different ratio*

Ratio	Sample (g)	Maltodextrin (g)
1:1	50	50
1:2	33	66
1:3	25	75

### Encapsulation Efficiency (EE)

The encapsulation efficiency was the amount of anthocyanin encapsulated relative to the extract's content. It was calculated using the formula [1] (Kar et al., 2019).

$$EE (\%) = \frac{\text{Total Anthocyanin Content in the feed}}{\text{Total Anthocyanin Content in the powder}} \times 100 \quad [1]$$

### Physicochemical Properties of Encapsulated Extracts

#### *Moisture Content*

According to Kathiman et al. (2020), the encapsulated fruit extracts' moisture content was determined using a moisture analyzer (MX-50, A&D Weighing, Malaysia). One gram of the sample powder was placed into the moisture analyzer. The data was recorded, and the evaluation was done in triplicate.

#### *Bulk and Tapped Density*

The bulk density and tapped density of the encapsulated fruit extract were determined based on the weight-to-volume ratio. Two grams of powder were transferred to a 10 ml graduated cylinder, and the reading was recorded. For tapped density, the encapsulated fruit extracts were transferred and battered 20 times on a hard surface until the volume was fixed. All samples were run in triplicate (George et al., 2021). The density was calculated by using formula 2:

$$\text{Bulk and Tapped density } \left(\frac{g}{ml}\right) = \frac{\text{Weight of sample}}{\text{Volume of sample}} \quad [2]$$

#### *pH Value*

Ten grams of encapsulated fruit extracts were added to 90 ml of distilled water, and the pH value was determined using a pH meter (pH 700, Eutech Instruments, Singapore) (Caglar et al., 2020).

### ***Dissolution Test***

Fifty milligrams of encapsulated fruit extracts were added to 1 ml of distilled water at 25°C. The time required to reconstitute the powder was recorded using an electronic timer (s) (Quelal et al., 2023).

### ***Color Determination***

The color changes in the anthocyanin content of the encapsulated fruit extract and crude extracts were determined using a colorimeter (MSE-4500L, HunterLab, USA) based on CIELab color space. The data  $L^*a^*b^*$  from the colorimeter was then simulated into a color palette using the software easyrgb.com (EasyRGB 1.0, USA), according to Lam et al. (2023).

### ***Surface Morphology by Scanning Electron Microscopy (SEM)***

Five milligrams microcapsules were dried at 110°C for 24 hours before starting. SEM evaluated encapsulated fruit extracts and crude extracts at a voltage of 20 kV, and SEM images were recorded at different magnifications (George et al., 2021).

### ***Antioxidant Activities***

#### ***2,2-Diphenyl-1-picrylhydrazyl (DPPH) Assay***

The free radical scavenging activity was analyzed using the DPPH method with minor modifications (Chandra et al., 2014). Each prepared sample solution of the encapsulated fruit extracts and crude extract was mixed with 1 mM DPPH solution. The absorbance was measured at 517 nm using a UV-Vis spectrophotometer (U-3900H, Hitachi, Japan). The assay was done in triplicate. The free radical scavenging activity was calculated based on the following formula 3:

$$\text{Radical Scavenging activity (\%)} = \frac{\Delta C - \Delta S}{\Delta C} \times 100 \quad [3]$$

Where  $\Delta C$  is the absorbance reading of the negative control, and  $\Delta S$  is the absorbance reading of the sample.

#### ***2,2-Azino-bis-3-ethylbenzothiazoline-6-sulphonic Acid (ABTS) Assay***

The ABTS assay was performed by preparing 7 mM ABTS and mixing it with 2.45 mM Potassium persulfate (Sigma Aldrich, Malaysia). To each 1 ml of prepared solution, 10  $\mu$ l of each encapsulated fruit extract and crude extract was added. The mixtures were kept for 15 min at room temperature, and the absorbance was read at 734 nm. The assay was

done in triplicate. The free radical scavenging activity was calculated using the radical scavenging activity as formula [3] above.

### ***Ferric Reducing Antioxidant Power (FRAP) Assay***

The ferric-reducing activity (FRAP) of the encapsulated fruit extracts and crude extract was performed. Firstly, the FRAP reagent was prepared by mixing 25 ml of acetate (Merck, Germany) buffer, 2.5 ml of 2,4,6-tri(2-pyridyl)-1,3,5-triazine (TPTZ) solution, and 2.5 ml of Iron (III) chloride (Thermo Fisher, America). Fifty (50)  $\mu$ l aliquots of each extract or standard were mixed with 1.5 ml of the freshly prepared FRAP reagent. The absorbance was measured 30 minutes after the addition of the FRAP reagent. The percentage of ferric-reducing antioxidant activity was calculated using formula 4 (Bejeli et al., 2012). All determinations were carried out in triplicate.

$$FERIC\ reducing\ antioxidant\ activity\ (\%) = \frac{\Delta C - \Delta S}{\Delta C} \times 100 \quad [4]$$

Where  $\Delta C$  is the absorbance reading of the negative control, and  $\Delta S$  is the absorbance reading of the sample.

### **Total Anthocyanin Content (TAC)**

The total anthocyanin was measured using the pH-differential method by Giusti and Wrolstad (2001), using two buffer systems: (1) 0.025M potassium chloride (Merck, Germany) buffer at pH 1.0 and (2) 0.4 M sodium acetate (Merck, Germany), buffer at pH 4.5 as referenced in Association of Official Analytical Chemists (AOAC) (2005). One (1) ml of the encapsulated fruit extracts and the crude extract were added into a buffer solution of pH 1 and pH 4.5. Then, the absorbance of each sample was determined using a UV-Vis Spectrophotometer and was read at 520 nm and 700 nm. Absorbance (A) of dilutions was calculated using the following formula 5:

$$TAC \left( \frac{mg}{ml} \right) = \frac{A \times MW \times DF \times 1000}{\epsilon \times l} \quad [5]$$

Where,  $A = (A_{520nm} - A_{700nm})_{pH\ 1.0} - (A_{520nm} - A_{700nm})_{pH\ 4.5}$ .

$MW$  (molecular weight) = 449.2 g/mol for cyanidin-3-glucoside (cyd-3-glu).

$DF$  = dilution factor established in D.

$l$  = pathlength in cm.

$\epsilon$  = 26 900 molar extinction coefficients, in  $L \times mol^{-1} \times cm^{-1}$ , for cyd-3-glu

1000 = factor for conversion from g to mg

## Stability Test

The stability test of the encapsulated fruit extracts and crude extract was referred to the studies by Yusoff et al. (2014), and Janna et al. (2006), focusing on the anthocyanin stability of *M. malabathricum* under different light conditions and different storage temperatures. Encapsulated fruit extract from each ratio (1:1, 1:2, 1:3) and crude extract were located and evaluated at 4°C, -20°C, and 25°C with the absence of light wrapped with aluminum foil. In comparison, another sample for 25°C was located in the presence of light. The total anthocyanin content of each sample was recorded on days 0, 14, 30, 60, and 90 using a UV-Vis spectrophotometer in triplicate.

## Degradation Index (DI)

The degradation constant (K) for the anthocyanin content in the encapsulated fruit extracts and the crude extract was determined considering first-order degradation kinetics, as described by formula [6], where  $C_0$  represents the initial anthocyanin content, and  $C_t$  represents the anthocyanin content at a specified time.

$$\ln \frac{C_0}{C_t} = -Kt \quad [6]$$

## Statistical Analysis

All data in triplicate readings were recorded and reported as mean  $\pm$  standard deviation for every analysis. Experimental data were analyzed using one-way analysis of variance (ANOVA) in IBM SPSS Statistic 27. Tukey's test determined Significant differences between means (Kim, 2017). Minitab software 19 was also utilized to determine the best ratio and storage condition using a main effect plot graph (Qaziyani et al., 2019).

## RESULTS AND DISCUSSION

### Encapsulation Efficiency (EE%)

Encapsulation efficiency (EE) was calculated by considering the Total Anthocyanin Content (TAC) present in the solution before drying and in the powder after drying. Table 2 shows the TAC of the encapsulated fruit extracts and encapsulation efficiency with different ratios.

From Table 2, different ratios of maltodextrin showed a significant effect on TAC after encapsulation and EE, ranging from 69.76% to 96.82%. It indicates that the encapsulation process successfully preserved the anthocyanins in the fruit extract. EE increased significantly ( $p < 0.05$ ) with higher sample ratios or maltodextrin concentrations. Ratio 1:1 exhibited the highest EE at 89.10%, followed by ratio 1:2 (78.54%), and ratio 1:3 showed the lowest EE at 69.76%. What stands out in these results is the correlation between the



amount of TAC and EE, with a ratio of 1:1 showing the highest TAC after encapsulation and the most effective encapsulation percentage among the other ratios.

Table 2

Total anthocyanin content of the encapsulated fruit extracts and encapsulation efficiency with different ratios

Sample	Total Anthocyanin Content (TAC) after encapsulated (mg/ml)	Encapsulation efficiency % (EE)
1:1	246.66 ± 0.34 <sup>a</sup>	96.82 ± 0.13 <sup>a</sup>
1:2	184.54 ± 1.77 <sup>b</sup>	78.54 ± 0.81 <sup>b</sup>
1:3	155.99 ± 1.91 <sup>c</sup>	69.76 ± 0.79 <sup>c</sup>

Note. Data are expressed as means ± SD ( $n = 3$ ), means were compared by the Tukey test ( $p < 0.05$ ). The mean is significantly different  $p < 0.05$

Generally, TAC may decrease as maltodextrin concentration increases because a thicker wall surrounding the anthocyanin droplets due to higher maltodextrin concentrations may reduce the diffusion of water and other solutes into the droplets (Deng et al., 2023; Nafunisa et al., 2017; Padzil et al., 2018). As the amount of maltodextrin in the encapsulated fruit extracts increased, the TAC decreased, as depicted in Figure 3. It is likely because the bulky nature of maltodextrin as wall materials may dilute the anthocyanin sample. Interestingly, the samples before encapsulation had a substantially higher TAC than the encapsulated samples, even with the highest maltodextrin content. It suggests that anthocyanins can be effectively encapsulated and preserved even with a small amount of maltodextrin.

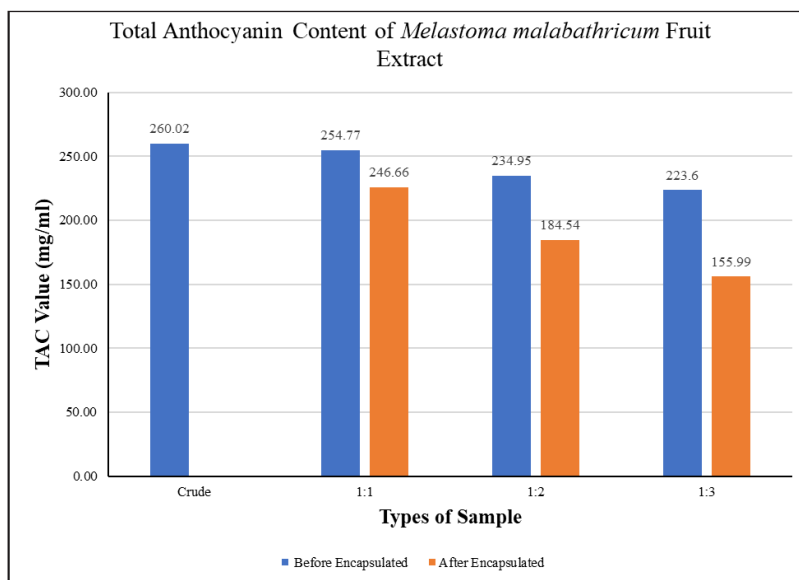


Figure 3. Total Anthocyanin Content (TAC) of *Melastoma malabathricum* L. fruit extract and encapsulated fruit extract 1:1, 1:2, and 1:3

Contradicting the findings, Akdeniz et al. (2017) subsequently stated that the EE decreased as the ratio of core to coating increased. The study revealed that a ratio of 1:10 has higher encapsulation efficiency than a ratio of 1:20. In addition, Akdeniz also acknowledged the use of maltodextrin as wall materials, giving higher encapsulation efficiency than gum Arabic.

### **Physicochemical Properties of Encapsulated Fruit Extract**

Physical and chemical properties were included in characterizing encapsulated fruit extracts from *M. malabathricum*. Table 3 summarizes the results of the physicochemical properties of the encapsulated samples, while Table 4 presents the surface morphology of the encapsulated fruit extracts and crude extract.




### **Moisture Content**

The moisture content of the encapsulated fruit extracts at different ratios is shown in Table 3, ranging from 5.77%–6.66 %. Ratio 1:3 exhibited the lowest moisture content (5.77%) compared to ratios 1:2 and 1:1, which were 6.22% and 6.66%, respectively. The differences in moisture content were attributed to the concentration of the encapsulating agent, where moisture content decreased as maltodextrin concentration increased. The lower moisture content observed in ratio 1:3 can be attributed to the higher amount of maltodextrin present in the sample compared to ratios 1:1 and 1:2. Generally, higher amounts of maltodextrin slow down the dispersion of water molecules, thus aiding in maintaining the moisture content of the encapsulated fruit extract.

Previous studies from Quelal et al. (2023) have also observed a reduction in moisture content with increasing maltodextrin concentration. Quelal et al. (2023) used different maltodextrin concentrations ranging from 3% to 7%, resulting in moisture content ranging from 5.44% to 1.96%. Similarly, findings from Narayanan et al. (2018) indicate that the moisture content decreases with increasing maltodextrin concentration. The water content of the feed significantly affects the final moisture content of the powder produced in a spray drying system.

Lower moisture content benefits the long-term storage and stability of the samples. According to Bell (2020), reduced moisture content improves chemical stability by lowering oxidation rates and hydrolytic degradation, which can degrade the active compounds and eventually reduce the sample's efficacy. At the same time, the safety of the sample and the extension of its shelf life depend on this microbial stability. Lower moisture content also prevents microbial growth (Rezaei & VanderGheynst, 2010), which means that contamination and deterioration are prevented by maintaining conditions in which bacteria, molds, and yeasts are unable to thrive. Physically, less moisture keeps the extract powder from caking and clumping, which happens when there is too much moisture, and the

Table 3  
Physicochemical properties of encapsulated fruit extracts

Ratio	Moisture content (%)	Bulk density (g/ml)	Tapped density (g/ml)	pH value	Solubility (s)	Color determination		Color simulation	
						L*	b*		
1:1	6.66 ± 0.27 <sup>a</sup>	0.36 ± 0.02 <sup>c</sup>	0.50 ± 0.00 <sup>c</sup>	5.35 ± 0.02 <sup>a</sup>	4.64 ± 0.36 <sup>a</sup>	56.86 ± 3.13 <sup>c</sup>	39.72 ± 4.43 <sup>c</sup>	2.43 ± 0.61 <sup>a</sup>	
1:2	6.22 ± 0.08 <sup>a</sup>	0.43 ± 0.02 <sup>b</sup>	0.60 ± 0.00 <sup>b</sup>	3.60 ± 0.02 <sup>b</sup>	3.94 ± 0.92 <sup>ab</sup>	70.51 ± 0.62 <sup>b</sup>	42.48 ± 0.26 <sup>ab</sup>	1.27 ± 0.17 <sup>a</sup>	
1:3	5.77 ± 0.18 <sup>b</sup>	0.50 ± 0.03 <sup>a</sup>	0.77 ± 0.00 <sup>a</sup>	2.87 ± 0.02 <sup>c</sup>	3.03 ± 0.06 <sup>b</sup>	76.75 ± 1.83 <sup>a</sup>	45.90 ± 0.77 <sup>a</sup>	1.75 ± 0.39 <sup>a</sup>	

Note. Data are expressed as mean ± SD ( $n = 3$ ), means were compared by the Tukey test ( $p < 0.05$ ). The mean is significantly different  $p < 0.05$

Table 4  
Surface morphology of the particles using Scanning-Electron Microscopy (SEM)

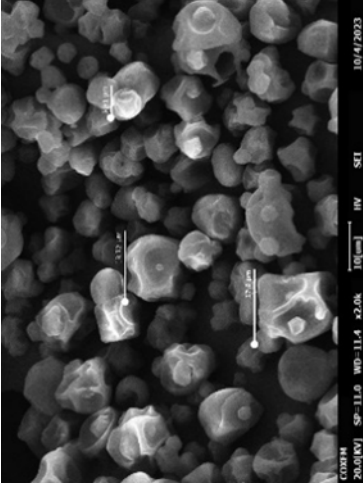
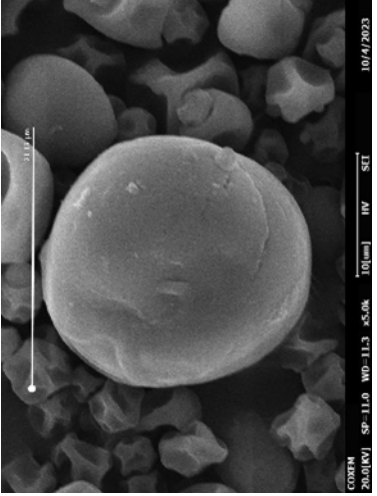
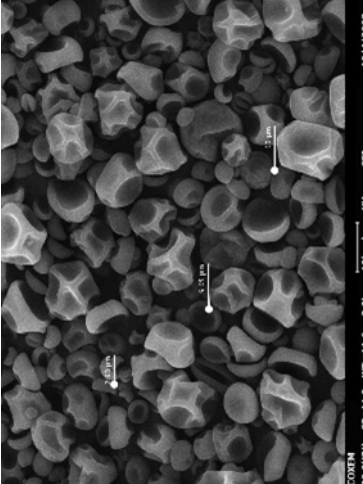
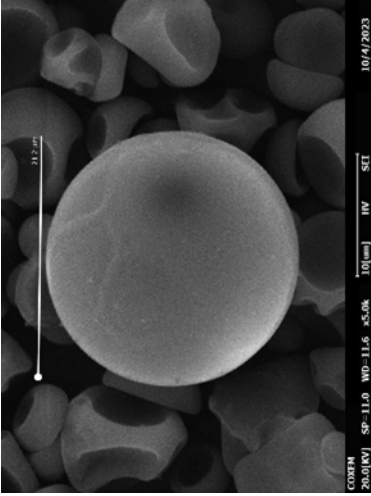
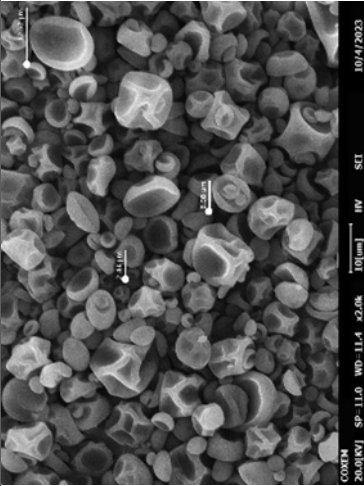
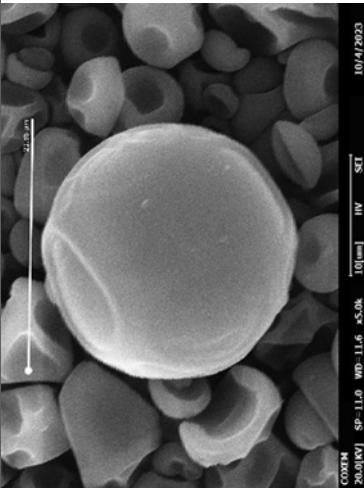
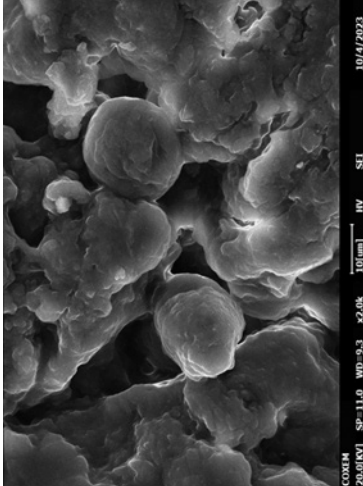
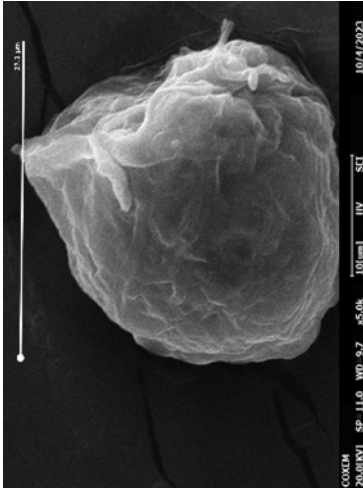
Ratio	Encapsulated fruit extract length ( $\mu\text{m}$ )	2000x	5000x
1:1	$21.13 \pm 0.78^b$		
1:2	$21.20 \pm 0.05^b$		

Table 4 (continue)

Ratio	Encapsulated fruit extract length ( $\mu\text{m}$ )	2000x	5000x
1:3	$21.35 \pm 0.19^b$		
Crude	$27.096 \pm 1.44^a$		

Note. Data are expressed as means  $\pm$  SD ( $n = 4$ ), means were compared by the Tukey test ( $p < 0.05$ ). The mean is significantly different  $p < 0.05$

particles attach (Carter, 2020). It ensures the powder will flow freely, making handling, processing, and dosing uniformly during manufacture easier. According to Gaikwad et al. (2019), lower moisture content extracts are less likely to absorb more moisture from the surroundings, which may reduce cost by reducing the need for expensive, specialized, moisture-proof packing materials. It also might improve storage efficiency while simultaneously reducing the cost of packaging. Maintaining batch-to-batch consistency and product reliability also depends on the sample's uniform physical and chemical qualities, which a stable moisture content ensures.

### **Bulk and Tapped Density**

The encapsulated fruit extracts at difference ratios (1:1,1:2,1:3) exhibited a bulk density range of 0.362–0.501 g/ml, and tapped density ranged from 0.5–0.769 g/ml, as shown in Table 3. Significant differences ( $p < 0.05$ ) in bulk density were observed among all ratios, indicating that the concentration of the wall material affected both bulk and tapped density. Ratio 1:1 showed the lowest values for both bulk dan tapped density (0.362 g/ml and 0.5 g/ml, respectively), followed by ratio 1:2 (0.429 g/ml and 0.601 g/ml), and ratio 1:3 had the highest values (0.501 g/ml and 0.769 g/ml). Many studies, including those by Al-Maqtari et al. (2021), Rashid et al. (2022), and Shadordizadeh et al. (2023), have found that tapped density is correlated with bulk density. To better understand this relationship, Amidon et al. (2017) explained that the tapped density is always higher than bulk density because tapping and vibration during the procedure compact the powder, reducing the spaces between particles.

The highest bulk density observed for ratio 1:3 can be attributed to the increase in maltodextrin concentration, which increases solid content in the feed solutions, making the particles heavier and enhancing bulk density (Rodríguez-Díaz et al., 2014). Similarly, moisture content affects the density of the powder, with higher maltodextrin concentrations typically resulting in lower moisture content. Bulk density and moisture content generally have an inverse relationship. As moisture content increases, bulk density decreases because water molecules take up space between sample particles, reducing the total volume filled by solid material. Previous studies from Šavikin et al. (2021) have also observed that the concentration of the wall material can affect the bulk density of encapsulated fruit extract. For instance, powders with 120% whey protein (WP) concentrations had higher bulk density than others.

The stability and long-term storage of extracts are significantly influenced by bulk and tapped densities, which affect a few important variables. First, space is used efficiently, and fewer materials are needed for packaging when bulk density-based optimization is used for packaging (Ding et al., 2020). Tapped density reduces empty areas inside the container by indicating how much a powder can be compacted. Reducing access to air and

moisture is crucial since these factors can trigger degradation processes such as oxidation and hydrolysis. The extract's shelf life can be increased by preserving its chemical stability by limiting exposure to these substances (Sornsomboonsuk et al., 2019). Moreover, higher densities enhance the extract powder's flow properties, which is helpful for consistent handling and dosing throughout the production and packaging stages (Akseli et al., 2019). This avoids problems like clumping or caking, which can reduce the effectiveness and efficacy of the extract. Optimized densities have the potential to decrease transportation and warehousing costs by enabling the transportation and storage of a greater quantity of products inside a given container. Furthermore, uniform bulk and tapped densities provide batch-to-batch consistency, essential for preserving the extract's purity and functionality in various applications (Stranzinger et al., 2019).

### pH Value

The results from Table 3 show a significant difference ( $p < 0.05$ ) in the pH value of the encapsulated fruit extracts of *M. malabathricum* across different ratios (1:1, 1:2, 1:3). The pH of the powder ranges from pH 5.35 to 2.87, with the highest pH value ( $5.35 \pm 0.02$ ) recorded for ratio 1:1, followed by ratio 1:2 with a pH value of  $3.60 \pm 0.02$ , and the lowest pH for ratio 1:3 ( $2.87 \pm 0.02$ ). Kobo et al. (2022) noted that these pH values indicate acidic conditions. The low and acidic pH values observed in this study suggest that all the powder samples may be stable on the shelf, indirectly contributing to the stability of the product.

It is important to consider that the pH of each ratio may have been affected by the amount of crude extract present in the ratio. For instance, in the sample ratio 1:1, which had the highest crude extract content compared to other ratios, the pH value was  $5.35 \pm 0.02$ . A study by Aishah et al. (2013) reported that the crude extract of *M. malabathricum* fruit collected from Muar, Johor, had a pH value of  $5.56 \pm 0.30$ , which is similar to the pH of ratio 1:1. In contrast, the pH values of ratios 1:2 and 1:3 was lower. It could be attributed to the decrease in crude extract content and increased maltodextrin concentration in these ratios, leading to a decrease in pH value. Additionally, Chatpun et al. (2016) found that as the concentration of maltodextrin increased from 1% to 10%, the pH of tapioca maltodextrin solutions containing DE1 slightly dropped from 5.4 to 5.1. It suggests that higher concentrations of maltodextrin can contribute to decreased pH.

### Solubility

The encapsulated fruit extracts of *M. malabathricum* at different ratios (1:1, 1:2, 1:3) exhibited solubility times ranging from 4.637 to 3.027 s. The results in Table 3 indicate significant differences ( $p < 0.05$ ) in solubility time among all ratios, suggesting that the different concentrations of maltodextrin affect the powder's solubility. Specifically, ratio 1:3 had the lowest solubility time ( $3.027 \pm 0.06$  s) compared to ratio 1:1 ( $4.637 \pm 0.36$  s) and ratio 1:2 ( $3.943 \pm 0.92$  s).

As Nawi et al. (2015) described, maltodextrin is highly soluble compared to other wall materials such as gum Arabic. Maltodextrin is produced exclusively through hydrolysis catalyzed by acids, resulting in linear chains that are easily retrograded. Thus, the high-water solubility of maltodextrins is achieved by combining acid catalysis with amylase-catalyzed hydrolysis (Tiefenbacher et al., 2017). The different ratios, representing varying maltodextrin concentrations, appear to be linked to the solubility of the powder. Ratio 1:3, which contained more maltodextrin compared to the other ratios, exhibited the highest solubility. The findings are consistent with those of George et al. (2021), who attributed the high solubility index of maltodextrin samples to its inherent solubility properties.

### Color Determination

Three variables typically represent color properties:  $L^*$ ,  $a^*$ , and  $b^*$ . The color properties of encapsulated fruit extracts with different ratios were analyzed (Table 3), and the powder color was presented using the Red, Green, Blue System (RGB) color palette. Ratio 1:1 showed the lowest  $L^*$  value ( $56.86 \pm 3.13$ ), followed by ratio 1:2 ( $70.505 \pm 0.62$ ), and the highest was ratio 1:3 ( $76.75 \pm 1.83$ ). Similarly, ratio 1:1 showed the lowest  $a^*$  value ( $39.72 \pm 4.43$ ), followed by 1:2 and 1:3 with  $42.48 \pm 0.26$  and  $45.90 \pm 0.77$ , respectively. However, the  $b^*$  value was highest for ratio 1:1 ( $2.43 \pm 0.61$ ), followed by ratio 1:2 ( $1.27 \pm 0.17$ ), and the lowest value was ratio 1:3 ( $1.75 \pm 0.39$ ).

It is noteworthy that increasing maltodextrin concentrations in the powder tends to increase lightness ( $L^*$ ) due to maltodextrin's white color. Similarly, an increase in the crude extract content in the sample reflects the dark purple nature of the original *M. malabathricum* fruit color. A study by Laqui-Vilca et al. (2018) supports the correlation between maltodextrin concentration and the  $L^*$  value of microencapsulated quinoa betalain. They found that  $L^*$  values increased as maltodextrin concentration increased. The betalain microencapsulated from beetroot juice has the highest  $L^*$  value with a 12.5% maltodextrin content. Similarly, Santiago et al. (2016) observed that anthocyanin pomegranate juice powder exhibited  $a^*$  value within the red range, indicating the presence of anthocyanins. Therefore, the analysis of the powder color shows the presence of anthocyanins and how wall materials influence the color values with a 12.5% maltodextrin content.

### Surface Morphology by the Scanning Electron Microscopy (SEM)

SEM micrographs of the encapsulated fruit extracts of *M. malabathricum*, with different ratios and the crude extract, obtained through spray drying at magnifications of 2000 and 5000 (Table 4). The encapsulated fruit extracts (1:1, 1:2, 1:3) displayed spherical particles and particles with irregular, concave, and wrinkled surfaces, all equal size with no significant differences observed ranging from  $21.13 \pm 0.78 \mu\text{m}$ ,  $21.20 \pm 0.05 \mu\text{m}$ , and  $21.35 \pm 0.19 \mu\text{m}$ , respectively. Meanwhile, the crude extract exhibited an agglomerated and disordered structure.



Quelal et al. (2023) attribute this phenomenon to spray drying, explaining that wrinkled particles are more susceptible to oxidation. However, their concavity and wrinkles facilitate quick moisture evaporation during spray drying. However, these features may also lead to agglomerate formation, impeding the dust's ability to disperse when reconstituted in a solvent (Kurniawan et al., 2019). In addition, mechanisms causing shrinkage and deformation are generally more obvious during drying, especially at low temperatures where slower water diffusion allows particles more time to shrink, collapse, and undergo other deformations. Previous studies by George et al. (2021) noted slight differences in the morphological shape of *Moringa oleifera* leaf powder due to the different encapsulation agents used.

### Antioxidant Activity

In this study, the encapsulated fruit extracts (1:1, 1:2, 1:3) and crude extract of *M. malabathricum* underwent screening for their potential antioxidant activities using DPPH, ABTS, and FRAP assay methods. The IC<sub>50</sub> values for DPPH and ABTS radicals were determined as the concentration required to achieve 50% inhibition, indicating the amount of antioxidants needed to reduce the initial concentration of the assay solution by half.

### DPPH and ABTS Radical Scavenging Activity

IC<sub>50</sub> values of the encapsulated fruit extracts and crude extract with positive controls (ascorbic acid) ranged from 25.17 ± 0.06 µg/ml to 178.5 ± 7.53 µg/ml (Table 5). From the table, ratio 1:1, crude extract and ascorbic acid exhibited no significant difference ( $p > 0.05$ ) and demonstrated excellent antiradical activity by inhibiting DPPH and ABTS assay with lower IC<sub>50</sub> values of (1:1, 28.5 ± 2.78 µg/ml), (crude, 27.37 ± 7.91 µg/ml), and (ascorbic acid, 25.17 ± 0.06 µg/ml) for DPPH assay. Similarly, for the ABTS assay, the IC<sub>50</sub> values were (1:1, 49.03 ± 5.94 µg/ml) (crude, 35.33 ± 3.4 µg/ml), and (ascorbic

Table 5  
The IC<sub>50</sub> value for both DPPH and ABTS assay of samples

IC <sub>50</sub> (µg/ml)	IC <sub>50</sub> (µg/ml)	
	2,2-Diphenyl-1-picrylhydrazyl (DPPH)	2,2'-Azino-bis(3-ethylbenzothiazoline-6-sulfonic acid (ABTS))
Ascorbic Acid	25.17 ± 0.06 <sup>c</sup>	26.67 ± 0.12 <sup>dc</sup>
Crude	27.37 ± 7.91 <sup>c</sup>	35.33 ± 3.40 <sup>cd</sup>
1:1	28.50 ± 2.78 <sup>c</sup>	49.03 ± 5.94 <sup>c</sup>
1:2	73.93 ± 4.06 <sup>b</sup>	67.43 ± 7.98 <sup>b</sup>
1:3	86.27 ± 2.61 <sup>a</sup>	92.83 ± 0.76 <sup>a</sup>

Note. Data are expressed as mean ± SD ( $n = 3$ ), means were compared by the Tukey test ( $p < 0.05$ ). The mean is significantly different  $p < 0.05$

acid  $26.67 \pm 0.12 \mu\text{g/ml}$ ). However, ratios 1:2 and 1:3 significantly differed from other DPPH and ABTS assay samples.

There is a significant difference ( $p < 0.05$ ) among the samples, ratio 1:1 showed the highest antioxidant activity followed by ratio 1:2 and ratio 1:3 for DPPH ( $28.5 \pm 2.78 \mu\text{g/ml}$ ,  $73.93 \pm 4.06 \mu\text{g/ml}$ ,  $86.27 \pm 2.61 \mu\text{g/ml}$ ) and ABTS assays ( $49.03 \pm 5.94$ ,  $67.43 \pm 7.98$ ,  $92.83 \pm 0.76$ ), respectively. With that, all the encapsulated fruit extracts were considered to have greater antioxidant activity. In addition, a ratio of 1:1 successfully preserved the antioxidant activity of the extract, as the results show no significant difference ( $p > 0.05$ ) compared to the crude extract. It can be proven by the previous result, where the encapsulation efficiency of ratio 1:1 was the highest among other ratios.

To date, little evidence has been found associating the different ratios of plant extract and/or wall material concentrations with the antioxidant activity of encapsulated fruit extract of *M. malabathricum*. However, the study by Sayuti et al. (2015) showed that the increasing amount of *M. malabathricum* fruit extract in jackfruit jam correlated with a lower IC<sub>50</sub> value, indicating higher antioxidant activity. It was related to the fruit's flavonoid content in the form of anthocyanin and phenolic compounds. Meanwhile, Wariyah and Riyanto (2016) showed that increasing the concentration of maltodextrin will decrease antioxidant activity. Adding maltodextrin caused the total phenol of the encapsulated fruit extract to become lower.

By contrast, the DPPH assay conducted by Purwaningsih et al. (2023) showed a higher IC<sub>50</sub> value for the methanolic extract of *M. malabathricum* fruit ( $99.79 \mu\text{g/ml}$ ) than the ethanolic extract reported by Isnaini et al., (2019) ( $16.82 \pm 0.24 \mu\text{g/ml}$ ). This difference can be explained by the presence of –OH groups bound to the carbon of the aromatic ring, which enables flavonoids and phenols to act as antioxidants. The ability of phenolic compounds to scavenge free radicals depends on the quantity and position of hydroxyl groups within the molecule. Greater antioxidant activity is generated in proportion to the quantity of hydroxyl groups present. Antioxidant activity may be influenced by how the compound interacts with DPPH free radicals (Shahidi & Ambigaipalan, 2015).

These results suggest that the antioxidant activity in both DPPH and ABTS assays may vary due to different concentrations and variations in localities and solvent extraction methods used to obtain the crude sample. This finding suggests that the fruit of *M. malabathricum* plants may serve as a promising source of natural colorants with higher antioxidant activity, holding potential for commercialization in the future.

### **FRAP Ferric Ion Reducing Activity**

Meanwhile, the FRAP assay determines antioxidant activity by measuring electron transport. The result of IC<sub>50</sub> values of the FRAP assay of the encapsulated fruit extracts ratios 1:1, 1:2, 1:3, and the crude extract sample is presented in Figure 4. The IC<sub>50</sub> values

ranged from 24.67 to 186.80  $\mu\text{g/ml}$ . A lower IC<sub>50</sub> value indicates a higher antioxidant activity in the sample. The graph depicted that the highest IC<sub>50</sub> value was observed for ratio 1:3, indicating a reducing activity of 50% at 84.93  $\mu\text{g/ml}$ , followed by ratio 1:2 (66.43  $\mu\text{g/ml}$ ). Additionally, there was no significant difference between ratios 1:1 and the crude extract ( $p > 0.05$ ), with IC<sub>50</sub> values of 39.97  $\mu\text{g/ml}$  and 28.03  $\mu\text{g/ml}$ , respectively. Moreover, the crude extract showed no significant difference compared to the standard.

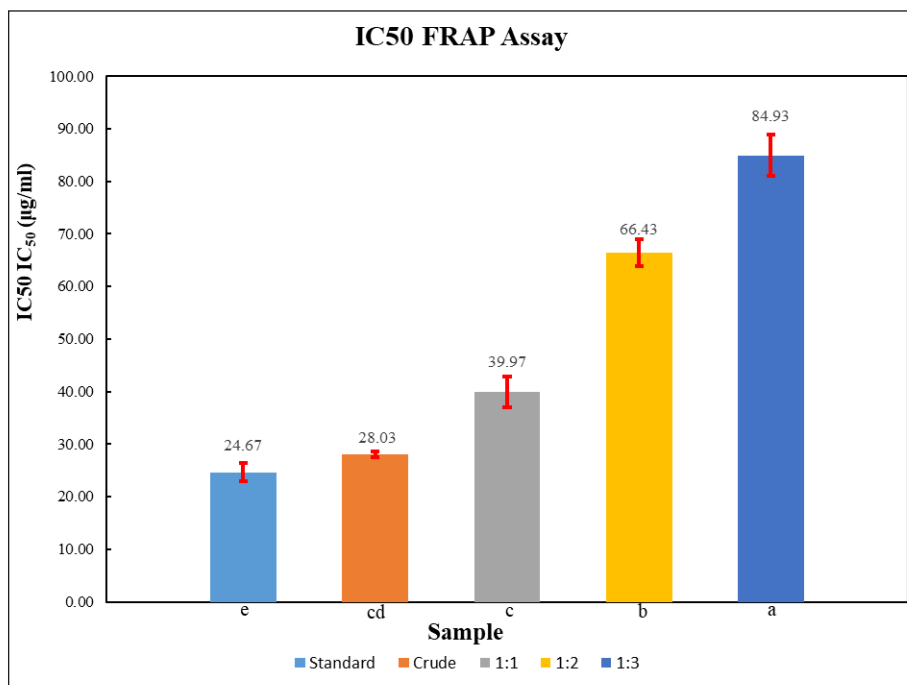


Figure 4. Comparison of IC<sub>50</sub> value for Ferric reducing antioxidant power (FRAP) assay of samples

Among the encapsulated fruit extracts, ratio 1:1 exhibited the lowest IC<sub>50</sub> value, indicating the highest antioxidant activity among the other ratios. The results showed a significant difference between the encapsulated fruit extracts, with a ratio of 1:1 at 39.97  $\mu\text{g/ml}$ , ratio 1:2 at 66.43  $\mu\text{g/ml}$ , and ratio 1:3 at 84.93  $\mu\text{g/ml}$ . Previous results indicate this outcome is due to the highest anthocyanin compound content. Anthocyanin compounds in the sample contribute to the antioxidant capacity by functioning as free radical scavengers against harmful oxidants, such as reactive oxygen and nitrogen species (Mattioli et al., 2020).

According to Karageçili et al. (2023), compounds capable of breaking the chain of free radicals by donating a hydrogen atom are associated with the reducing properties of any sample. Phenolic compounds, such as anthocyanins, act as hydrogen donors, singlet oxygen quenchers, and reducing agents due to their redox characteristics, exhibiting high

reducing power on Fe<sup>3+</sup>-TPTZ. The higher antioxidant activity in the FRAP assay for *M. malabathricum* is supported by previous studies by Nayak & Basak (2015) and Kasunmala et al. (2020), which found that *M. malabathricum* exhibits the highest FRAP.

### Stability Test

This study evaluated different storage conditions within 90 days for the encapsulated fruit extract ratios (1:1, 1:2, and 1:3) and crude extract based on Total Anthocyanin Content (TAC). Table 6 summarizes the TAC for each ratio and the crude extract from day 0 to day 90. Meanwhile, Figure 5 demonstrates the degradation of total anthocyanin content from day 0 under dark conditions at temperatures of -20°C, 4°C, and 25°C, as well as under conditions exposed to light at 25°C.

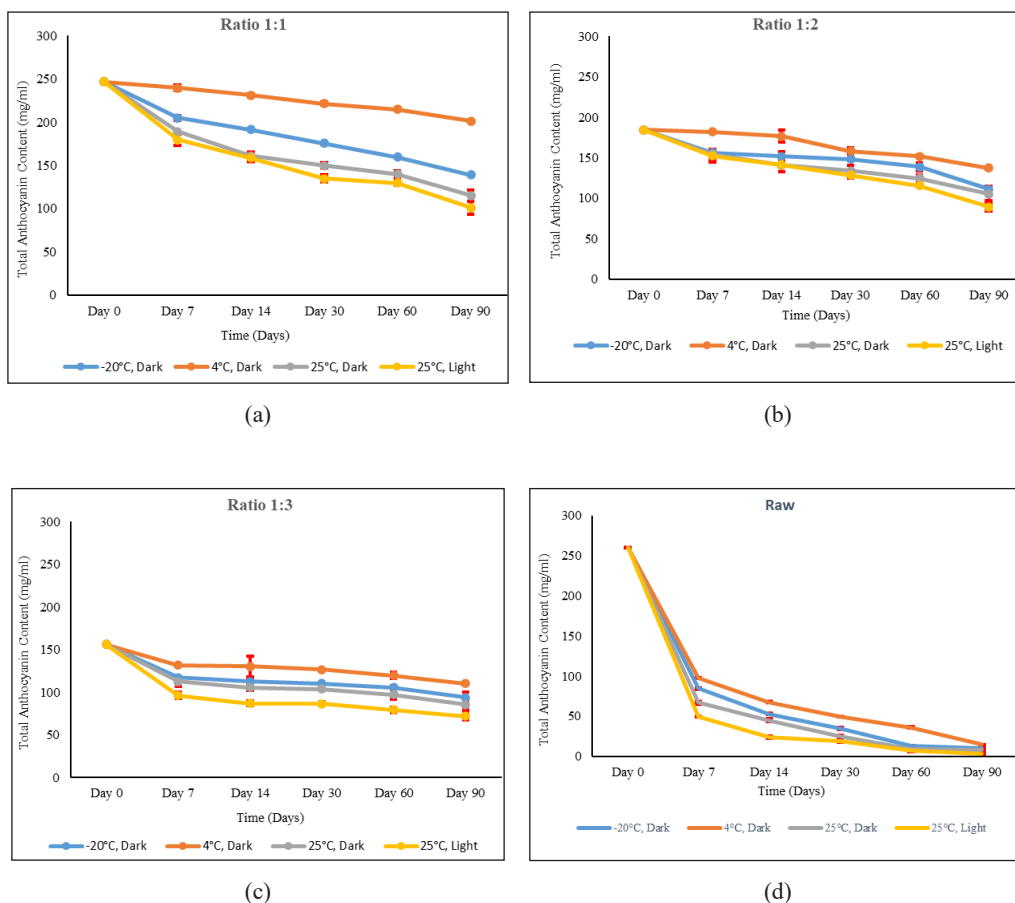


Figure 5. Degradation of Total Anthocyanin Content (TAC) at different storage conditions in 90 days for (a) Ratio 1:1, (b) Ratio 1:2, (c) Ratio 1:3, and (d) Crude

Table 6  
Total Anthocyanin Content (TAC) at different storage conditions in 90 days

Ratio	Condition	Total Anthocyanin Content (mg/ml)								
		Day 0	Day 7	Day 14	Day 30	Day 60	Day 90			
1:1	-20°C, Dark	246.66 ± 0.34 <sup>a</sup>	205.11 ± 6.33 <sup>b</sup>	191.40 ± 0.94 <sup>b</sup>	175.53 ± 3.85 <sup>b</sup>	159.58 ± 2.72 <sup>b</sup>	139.20 ± 0.77 <sup>b</sup>			
	4°C, Dark	246.66 ± 0.34 <sup>a</sup>	239.80 ± 5.93 <sup>a</sup>	231.35 ± 2.93 <sup>a</sup>	221.56 ± 3.38 <sup>a</sup>	214.94 ± 2.40 <sup>a</sup>	201.22 ± 1.71 <sup>a</sup>			
	25°C, Dark	246.66 ± 0.34 <sup>a</sup>	189.34 ± 1.10 <sup>bc</sup>	161.25 ± 8.25 <sup>cd</sup>	150.11 ± 5.80 <sup>cd</sup>	140.21 ± 6.73 <sup>cd</sup>	115.23 ± 11.37 <sup>cd</sup>			
	25°C, Light	246.66 ± 0.34 <sup>a</sup>	179.81 ± 11.73 <sup>c</sup>	158.85 ± 8.52 <sup>cd</sup>	134.96 ± 7.00 <sup>def</sup>	129.93 ± 5.16 <sup>def</sup>	101.02 ± 12.35 <sup>de</sup>			
1:2	-20°C, Dark	184.54 ± 1.91 <sup>b</sup>	156.36 ± 6.90 <sup>d</sup>	151.59 ± 9.67 <sup>de</sup>	110.39 ± 2.14 <sup>g</sup>	138.67 ± 8.15 <sup>de</sup>	111.14 ± 7.19 <sup>de</sup>			
	4°C, Dark	184.54 ± 1.91 <sup>b</sup>	182.30 ± 2.06 <sup>c</sup>	176.85 ± 13.15 <sup>bc</sup>	126.50 ± 7.36 <sup>f</sup>	151.84 ± 2.58 <sup>bc</sup>	137.28 ± 3.06 <sup>bc</sup>			
	25°C, Dark	184.54 ± 1.91 <sup>b</sup>	154.42 ± 11.13 <sup>d</sup>	140.90 ± 2.28 <sup>de</sup>	134.04 ± 12.18 <sup>ef</sup>	124.50 ± 7.04 <sup>ef</sup>	104.95 ± 14.55 <sup>def</sup>			
	25°C, Light	184.54 ± 1.91 <sup>b</sup>	152.46 ± 14.42 <sup>de</sup>	141.38 ± 14.24 <sup>de</sup>	86.62 ± 7.00 <sup>h</sup>	115.33 ± 2.69 <sup>fg</sup>	89.09 ± 8.51 <sup>efg</sup>			
1:3	-20°C, Dark	155.99 ± 1.77 <sup>b</sup>	117.14 ± 3.39 <sup>fg</sup>	112.77 ± 2.92 <sup>f</sup>	148.10 ± 1.88 <sup>de</sup>	105.87 ± 3.70 <sup>gh</sup>	93.96 ± 10.64 <sup>defg</sup>			
	4°C, Dark	155.99 ± 1.77 <sup>b</sup>	131.90 ± 0.91 <sup>ef</sup>	130.38 ± 20.59 <sup>ef</sup>	158.43 ± 2.12 <sup>e</sup>	119.85 ± 6.62 <sup>fg</sup>	110.11 ± 2.31 <sup>def</sup>			
	25°C, Dark	155.99 ± 1.77 <sup>b</sup>	112.56 ± 9.82 <sup>fg</sup>	105.54 ± 5.80 <sup>fg</sup>	103.84 ± 3.24 <sup>g</sup>	97.42 ± 9.20 <sup>h</sup>	85.78 ± 10.72 <sup>fg</sup>			
	25°C, Light	155.99 ± 1.77 <sup>b</sup>	96.43 ± 6.53 <sup>gh</sup>	87.17 ± 5.44 <sup>gh</sup>	128.30 ± 3.5 <sup>f</sup>	79.52 ± 5.99 <sup>i</sup>	71.79 ± 6.83 <sup>g</sup>			
Crude	-20°C, Dark	260.02 ± 1.33 <sup>c</sup>	84.52 ± 1.69 <sup>hi</sup>	52.91 ± 1.49 <sup>i</sup>	34.85 ± 2.22 <sup>ij</sup>	13.50 ± 1.15 <sup>k</sup>	9.88 ± 0.49 <sup>h</sup>			
	4°C, Dark	260.02 ± 1.33 <sup>c</sup>	98.24 ± 0.41 <sup>gh</sup>	67.45 ± 1.73 <sup>hi</sup>	49.89 ± 0.59 <sup>j</sup>	36.06 ± 1.73 <sup>j</sup>	14.82 ± 0.16 <sup>h</sup>			
	25°C, Dark	260.02 ± 1.33 <sup>c</sup>	67.12 ± 3.16 <sup>ij</sup>	45.06 ± 2.81 <sup>ij</sup>	25.08 ± 2.3 <sup>jk</sup>	9.55 ± 1.19 <sup>k</sup>	8.12 ± 0.91 <sup>h</sup>			
	25°C, Light	260.02 ± 1.33 <sup>c</sup>	49.61 ± 1.66 <sup>j</sup>	24.26 ± 2.31 <sup>j</sup>	18.83 ± 2.12 <sup>k</sup>	7.08 ± 0.29 <sup>k</sup>	3.35 ± 1.33 <sup>f</sup>			

Note. Data are expressed as mean ± SD ( $n = 3$ ), means were compared by the Tukey test ( $p < 0.05$ ). The mean is significantly different  $p < 0.05$

The overall trend shown in Figure 5 indicates that the anthocyanin contents were at their lowest at the highest temperature (25°C) and when exposed to light conditions. This result aligns with a previous study by Enaru et al. (2021), which stated that temperature affects the degradation of anthocyanin content. The hypothesis proposed by Hocine et al. (2018), suggesting that increasing temperature decreases the stability of encapsulated fruit extract, may closely correlate with their chemical structure. Indeed, the chemical structure of the encapsulated fruit extract plays a crucial role in determining its stability. This structure can accelerate chemical reactions, alter its configuration, facilitate the release of encapsulated material more easily, potentially induce degradation reactions, or render the powder more susceptible to environmental factors such as oxidation and moisture.

Research has indicated that anthocyanins undergo degradation during storage conditions (Enaru et al., 2021). Elevations in polymeric color values correspond with a reduction in total anthocyanin content. It is anticipated that during storage, anthocyanins undergo significant polymerization (Ochoa et al., 1999). There could be several reasons for the significant rise in polymeric color values and the consequent decrease in anthocyanins, such as residual enzyme activity or condensation interactions with other phenolics (Cheyner et al., 2012). Unfortunately, establishing the stability of anthocyanins is challenging due to their complex mechanisms, but their chemical structure strongly influences their stability.

These findings were also reported by Muche et al. (2018), indicating that temperature affects the rate of anthocyanin degradation at 25°C during storage, with higher temperatures resulting in a noticeably larger loss of anthocyanins. By the end of storage at 25°C, anthocyanin loss was significantly higher (95%–99.9%) than at 5°C, where the loss was 50%–60%. Additionally, light exposure contributes to reducing the anthocyanin content in the sample due to the absorption of light photons by organic molecules in the sample, causing chemical disruption to the conjugated double bonds, such as in aromatic rings, double rings, and compounds, including disulfide bonds, thereby reducing the anthocyanin stability.

The findings reveal that although encapsulation has some protective effect, it is not enough to stabilize anthocyanin considerably since Total Anthocyanin Content (TAC) decreases slowly over 90 days under various storage conditions. Compared to crude extracts, the encapsulation technique probably slows down the degradation process, which protects anthocyanins from direct exposure to conditions that can cause them to degrade, such as light, oxygen, and temperature changes. This result also can be seen clearly from the previous study in which Baeza et al. (2021) reported that the degradation of anthocyanins during storage indicates a half-life of 63 days at room temperature. Meanwhile, Tonon et al. (2010) evaluated the storage stability of spray-dried acai juice within six months and reported the degradation of anthocyanins during storage, indicating a decrease in anthocyanin content. The encapsulation methods or materials could not achieve

optimal protection, which could allow the slow deterioration to continue. It implies that while encapsulation slows down the rate at which anthocyanins break down, it does not completely resolve the anthocyanins' underlying instability under the studied conditions. Therefore, more encapsulating materials and technique optimization are required for better stabilization and storage conditions.

### Degradation Index (DI)

According to Nayak and Rastogi (2010b), the stability and quality of the anthocyanin DI were calculated for further analysis of deterioration. This study measured the first-order kinetics for anthocyanin degradation for different ratios from day 0 until the end of the 90-day storage period under different storage conditions.

Figure 6 shows the anthocyanin's DI of encapsulated fruit extract of *M. malabathricum* produced with different ratios and crude extract, following first-order kinetics throughout a 90-day storage period. From the figure, the results are consistent for all three ratios, and the crude extract showed an increase in DI from lower to higher temperatures, except for -20°C, with the encapsulated fruit extract at the highest temperature exposed to light

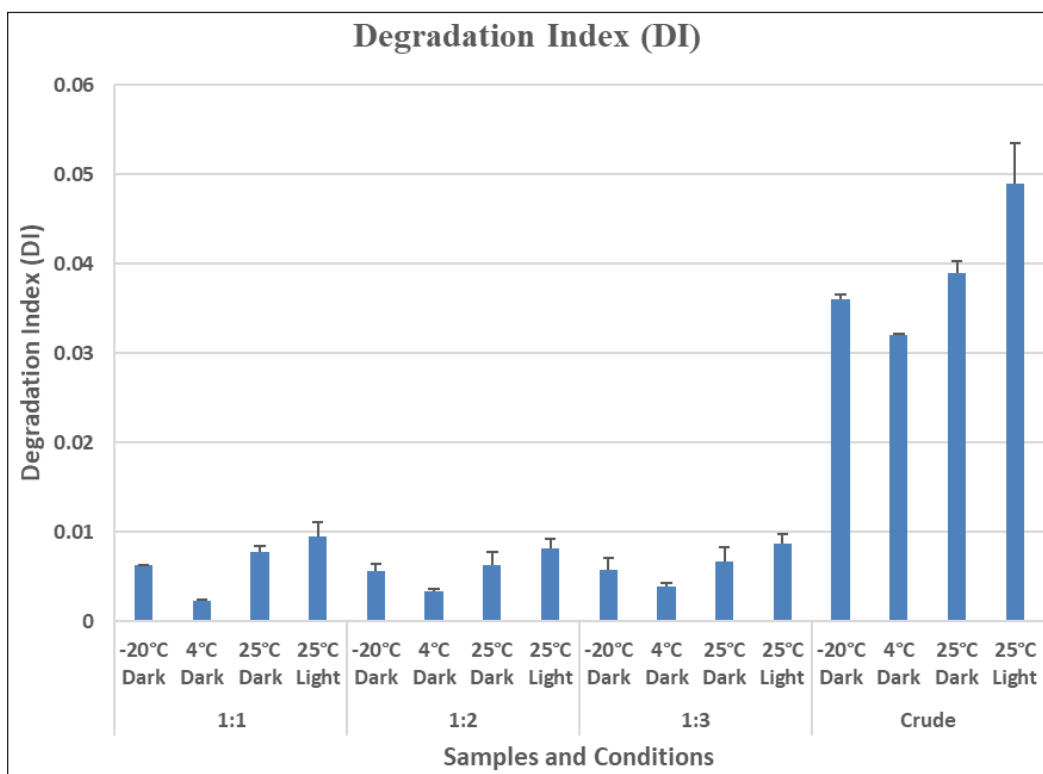


Figure 6. Degradation Index (DI) of encapsulated fruit extract of *Melastoma malabathricum* L. fruit extract

showing the highest DI value. The most distinctive pattern found for all different ratios and crude extract was that the DI of anthocyanin contents increased progressively when stored at 25°C in light conditions over 90 days. However, the DI of all three ratios and the crude extract was relatively low when the temperature was maintained at 4°C. The most likely causes of anthocyanin degradation are the compound's susceptibility to higher temperatures and light exposure. In addition, the results also showed that the sample is likely unsuitable at extremely low temperatures, -20°C.

Azarpazhooch et al. (2018) stated that, generally, the anthocyanin content of the encapsulated fruit extract decreased as the storage period increased. The degradation index measures the extent of degradation or damage to a material over time. A lower degradation index is considered more stable than a higher degradation index because it indicates that the anthocyanin content has experienced less degradation or deterioration, as demonstrated in the figure. The experimental results align with previous studies on the stability of *Melastoma malabathricum* L., as reported by Yusoff et al. (2014) and Janna et al. (2006). These studies found that anthocyanin pigments degraded more at higher temperatures, such as 25°C, compared to lower temperatures, like 4°C. Furthermore, Jiang et al. (2019) stated that the degradation and polymerization of anthocyanins at high temperatures ultimately cause a greater DI. Kirca et al. (2006) also demonstrated this scientific phenomenon and observed that black carrot anthocyanins degraded more quickly when stored at 37°C compared to refrigerated conditions at 4°C. Furthermore, Kumar et al. (2022) explained that the increase in DI is due to the reaction between two different compounds, tannins and anthocyanin. Reduced values of DI suggest increased anthocyanin stability and a decreased degradation rate. The formation of polymeric colors occurs when monomeric anthocyanins react with condensed tannins, such as epicatechin or catechin. The interaction between anthocyanins and other hydroxy residues from phenols in condensed tannins leads to the formation of a chemical complex, contributing to degradation.

### Storage Stability Determination

The analysis proceeded using ANOVA to determine the significant effects between two factors, the ratio and the condition, on the main effect (DI value). Table 7 indicates a significant effect ( $p < 0.05$ ) for the condition, while for the ratio, there is no significant effect ( $p > 0.05$ ). Similarly, the interaction for both factors showed no significance ( $p > 0.05$ ). Thus, these results suggest that the main factor affecting DI is the condition, contributing to lower DI values.

Figure 7 presents the main effect plot for each factor, condition, and ratio to assist in interpreting the results for stability determination. Since there is no significant interaction between the ratio and condition, both factors act as independent main effects. The condition, rather than the ratio, is the significant factor determining what most affects the lowest degradation value.



Table 7

Analysis of variance (ANOVA) of the main effect between two factors

Source	Degrees of Freedom (DF)	Adjusted Sum of Squares (Adj SS)	Adjusted Mean of Squares (Adj MS)	F-Value	p-Value
RATIO	2	0.000002	0.000001	1.13	0.340
CONDITON	3	0.000149	0.000050	46.98	0.000
RATIO*CONDITON	6	0.000009	0.000001	1.38	0.264
Error	24	0.000025	0.000001		
Total	35	0.000186			

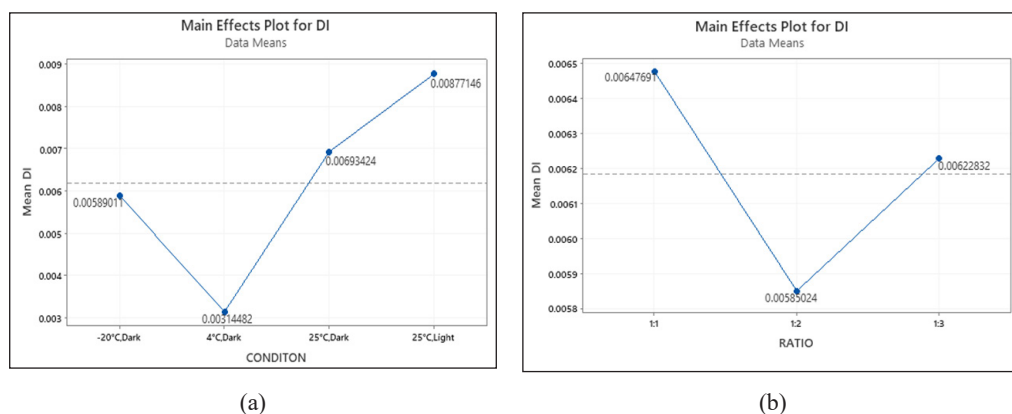


Figure 7. Main Effect Plot (a) Condition main effects plot for Degradation Index (DI), and (b) Ratio main effects plot for DI

As previously mentioned, a lower degradation index signifies greater stability, indicating less anthocyanin content degradation or deterioration. From the graph in Figure 7, the condition factor showed the lowest mean DI at 4°C (0.00314) in the dark, followed by -20°C (0.00589) in the dark, 25°C (0.00693) in the dark, and the highest DI was at 25°C (0.00877) in the light. As for the ratio, the lowest mean DI was ratio 1:2 (0.00585), followed by ratio 1:3 (0.006228), and the highest mean DI was 1:1 (0.00648). Limited research supports the stability of ratio 1:2 compared to other ratios. However, the composition of wall materials may contribute to why the ratio 1:2 was more stable. This finding is in line with a previous study by Dobroslavić et al. (2023), which suggested that a ratio of 1:2 may be more stable due to the optimal balance between the sample and maltodextrin, creating a suitable protective layer that protects against external factors and prevents anthocyanin degradation. In comparison, a ratio of 1:3 contains a higher amount of maltodextrin, which may delay structural formation and potentially lead to instability.

The study revealed notable differences in anthocyanin stability when stored under -20°C, 4°C, and 25°C. The DI at 4°C was  $1.282 \times 10^{-3}$ , slightly higher at -20°C with 1.286

$\times 10^{-3}$ , while at 25°C, the anthocyanin pigments degraded faster with a DI of  $6.261 \times 10^{-3}$ . A study by Yusof et al. (2014) observed a similar pattern for *Hibiscus rosa-sinensis* but not for *Codiaeum variegatum*, suggesting that anthocyanin pigments are more stable at -20°C. Thus, this suggests that the anthocyanin at -20°C provides good stability for three months, but the optimal temperature for storage stability was still 4°C. The analysis of the variance table and the main effect plot graph leads to the conclusion that the most stable condition was at 4°C in the dark, while the best ratio was 1:2. These factors can be considered essential in achieving a lower DI and indirectly ensuring stability for future applications.

## CONCLUSION

This research highlights the potential of encapsulated fruit extracts from *Melastoma malabathricum* L. as a valuable source of natural color. This study has demonstrated an overall characterization, including moisture content, bulk and tapped density, pH value, solubility, color, and surface morphology for potential future applications. Among the ratios tested, ratio 1:3 exhibited the lowest moisture content and solubility time, while ratio 1:1 showed the lowest values for bulk and tapped density. The pH of the encapsulated fruit extracts demonstrated an acidic condition. Regarding color properties, ratio 1:1 exhibited the lowest  $L^*$  and  $a^*$  values but the highest  $b^*$  value. All encapsulated fruit extracts showed the same shape, and no significant differences were observed in particle size among the ratios. This study also focused on assessing antioxidant activity before and after encapsulation. Ratio 1:1 exhibited no significant difference ( $p > 0.05$ ) compared to the crude extract from *M. malabathricum*, indicating successful preservation of antioxidant activity. For storage stability, the most stable condition was at 4°C in dark conditions, while a ratio of 1:2 was the best condition. These factors contribute to achieving lower DI values and indirectly enhance stability for future applications. To further enhance anthocyanin stability, optimizing methods like nanoencapsulation and using superior encapsulation materials could be applied and considered, especially during storage stability, by taking into account other parameters, including humidity levels and the type of containers used for storing the samples.

## ACKNOWLEDGEMENTS

This research was supported by Universiti Tun Hussein Onn Malaysia (UTHM) through RE-GG (vot Q209) and Tier 1 (vot Q148), and communication of this research is made possible through monetary assistance by the UTHM Publisher's Office via Publication Fund E15216.

## REFERENCES

- Adnan, M. A. F., Mat Nor, N. A., Aziz, N., & Taha, R. M. (2011). Colour analysis of potential natural colourant from *Ixora siamensis* and *Melastoma malabathricum*. *Materials Research Innovations*, 15, s176-s183. <https://doi.org/10.1179/143307511X13031890748939>
- Aishah, B., Nursabrina, M., Noriham, A., Norizzah, A. R., & Shahrimi, H. M. (2013). Anthocyanins from *Hibiscus sabdariffa*, *Melastoma malabathricum* and *Ipomoea batatas* and its color properties. *International Food Research Journal*, 20(2), 827-834.
- Akdeniz, B., Sumnu, G., & Sahin, S. (2017). The effects of maltodextrin and gum arabic on encapsulation of onion skin phenolic compounds. *Chemical Engineering Transactions*, 57, 1891-1896. <https://doi.org/10.3303/CET1757316>
- Akseli, I., Hilden, J., Katz, J. M., Kelly, R. C., Kramer, T. T., Mao, C., Osei-Yeboah, F., & Strong, J. C. (2019). Reproducibility of the measurement of bulk/tapped density of pharmaceutical powders between pharmaceutical laboratories. *Journal of Pharmaceutical Sciences*, 108(3), 1081-1084. <https://doi.org/10.1016/j.xphs.2018.10.009>
- Al-Maqtari, Q. A., Mohammed, J. K., Mahdi, A. A., Al-Ansi, W., Zhang, M., Al-Adeeb, A., Wei, M., Phyto, M. H., & Yao, W. (2021). Physicochemical properties, microstructure, and storage stability of *Pulicaria jaubertii* extract microencapsulated with different protein biopolymers and gum arabic as wall materials. *International Journal of Biological Macromolecules*, 187, 939-954. <https://doi.org/10.1016/j.ijbiomac.2021.07.180>
- Amidon, G. E., Secreast, P. J., & Mudie, D. (2017). Particle, powder, and compact characterization. In Y. Qiu, Y. Chen, G. Zhang, L. Liu & W. Porter (Eds.), *Developing solid oral dosage forms* (pp. 271-293). Academic Press. <https://doi.org/10.1016/B978-0-12-802447-8.00010-8>
- Azarpazhooh, E., Sharayei, P., Zomorodi, S., & Ramaswamy, H. S. (2019). Physicochemical and phytochemical characterization and storage stability of freeze-dried encapsulated pomegranate peel anthocyanin and *in vitro* evaluation of its antioxidant activity. *Food and Bioprocess Technology*, 12(2), 199-210. <https://doi.org/10.1007/s11947-018-2195-1>
- Baeza, R., & Chirife, J. (2021). Anthocyanin content and storage stability of spray/freeze drying microencapsulated anthocyanins from berries: A review. *International Journal of Food Engineering*, 17(12), 927-944. <https://doi.org/10.1515/ijfe-2021-0184>
- Bejeli, M., Rowshan, V., & Zakerin, A. (2012). Comparison of total phenolic content and antioxidant activity of five *Salvia* species by FRAP and DPPH assay. *International Journal of Pharmacy and Pharmaceutical Science*, 4(3), 572-5.
- Bell, L. N. (2020). Moisture effects on food's chemical stability. In G. V. Barbosa-Cánovas, A. J. Fontana Jr, S. J. Schmidt & T. P. Labuza (Eds.), *Water activity in foods: Fundamentals and applications* (pp. 227-253). <https://doi.org/10.1002/9781118765982.ch9>
- Caglar, N., Ermis, E., & Durak, M. Z. (2020). Spray-dried and freeze-dried sourdough powders: Properties and evaluation of their use in breadmaking. *Journal of Food Engineering*, 292, 110355. <https://doi.org/10.1016/j.jfoodeng.2020.110355>

- Carter, B. P. (2020). Applications for dynamic moisture sorption profiles in foods. In G. V. Barbosa-Cánovas, A. J. Fontana Jr, S. J. Schmidt & T. P. Labuza (Eds.), *Water activity in foods: Fundamentals and applications* (pp. 311-322). Wiley. <https://doi.org/10.1002/9781118765982.ch13>
- Chandra, S., Khan, S., Avula, B., Lata, H., Yang, M. H., ElSohly, M. A., & Khan, I. A. (2014). Assessment of total phenolic and flavonoid content, antioxidant properties, and yield of aeroponically and conventionally grown leafy vegetables and fruit crops: A comparative study. *Evidence-based Complementary and Alternative Medicine, 2014*(1), 253875. <https://doi.org/10.1155/2014/253875>
- Chatpun, S., Sawanyawisuth, K., Wansuksri, R., & Piyachomkwan, K. (2016). Characterization and physiological effect of tapioca maltodextrin colloid plasma expander in hemorrhagic shock and resuscitation model. *Journal of Materials Science, 27*, 1-12. <https://doi.org/10.1007/s10856-016-5708-3>
- Cheynier, V. (2012). Phenolic compounds: From plants to foods. *Phytochemistry Reviews, 11*, 153-177. <https://doi.org/10.1007/s11101-012-9242-8>
- Deng, W., Li, X., Ren, G., Bu, Q., Ruan, Y., Feng, Y., & Li, B. (2023). Stability of purple corn anthocyanin encapsulated by maltodextrin, and its combinations with gum arabic and whey protein isolate. *Foods, 12*(12), 2393. <https://doi.org/10.3390/foods12122393>
- Ding, H., Li, B., Boiarkina, I., Wilson, D. I., Yu, W., & Young, B. R. (2020). Effects of morphology on the bulk density of instant whole milk powder. *Foods, 9*(8), 1024. <https://doi.org/10.3390/foods9081024>
- Dobrosłavić, E., Elez Garofulić, I., Zorić, Z., Pedisić, S., Roje, M., & Dragović-Uzelac, V. (2023). Physicochemical properties, antioxidant capacity, and bioavailability of *Laurus nobilis* L. leaf polyphenolic extracts microencapsulated by spray drying. *Foods, 12*(9), 1923. <https://doi.org/10.3390/foods12091923>
- Echegaray, N., Munekata, P. E., Gull'on, P., Dzuvor, C. K., Gull'on, B., Kubi, F., & Lorenzo, J. M. (2020). Recent advances in food products fortification with anthocyanins. *Critical Reviews in Food Science and Nutrition, 62*, 1553-1567. <https://doi.org/10.1080/10408398.2020.1844141>
- Enaru, B., Dreţcanu, G., Pop, T. D., Stănilă, A., & Diaconeasa, Z. (2021). Anthocyanins: Factors affecting their stability and degradation. *Antioxidants, 10*(12), 1967. <https://doi.org/10.3390/antiox10121967>
- Gaikwad, K. K., Singh, S., & Ajji, A. (2019). Moisture absorbers for food packaging applications. *Environmental Chemistry Letters, 17*(2), 609-628. <https://doi.org/10.1007/s10311-018-0810-z>
- George, T. T., Oyenih, A. B., Rautenbach, F., & Obilana, A. O. (2021). Characterization of *Moringa oleifera* leaf powder extract encapsulated in maltodextrin and/or gum arabic coatings. *Foods, 10*(12), 3044. <https://doi.org/10.3390/foods10123044>
- Giusti, M. M., & Wrolstad, R. E. (2001). Characterization and measurement of anthocyanins by UV-visible spectroscopy. *Current Protocols in Food Analytical Chemistry, 00*(1), F1.2.1-F1.2.13. <https://doi.org/10.1002/0471142913.faf0102s00>
- Hocine, R., Farid, D., Yasmine, S., Khodir, M., Kapranov, V. N., & Kiselev, E. F. (2018). Recent advances on stability of anthocyanins. *Journal of Agronomy and Animal Industries, 13*(4), 257-286. <http://doi.org/10.22363/2312-797X-2018-13-4-257-286>
- Isnaini, I., Yasmina, A., & Nur'amin, H. W. (2019). Antioxidant and cytotoxicity activities of karamunting (*Melastoma malabathricum* L.) fruit ethanolic extract and quercetin. *Asian Pacific Journal of Cancer Prevention, 20*(2), 639. <https://doi.org/10.31557/APJCP.2019.20.2.639>

- Janna, O. A., Khairul, A., Maziah, M., & Mohd, Y. (2006). Flower pigment analysis of *Melastoma malabathricum*. *African Journal of Biotechnology*, 5(2), 170-174.
- Jiang, T., Mao, Y., Sui, L., Yang, N., Li, S., Zhu, Z., Wang, C., Yin, S., He, J., & He, Y. (2019). Degradation of anthocyanins and polymeric color formation during heat treatment of purple sweet potato extract at different pH. *Food Chemistry*, 274, 460-470. <https://doi.org/10.1016/j.foodchem.2018.07.141>
- Kar, A., Mahato, D. K., Patel, A. S., & Bal, L. M. (2019). The encapsulation efficiency and physicochemical characteristics of anthocyanin from black carrot (*Daucus carota* Ssp. *sativus*) as affected by encapsulating materials. *Current Agriculture Research Journal*, 7(1). <https://doi.org/10.12944/CARJ.7.1.04>
- Karageçili, H., Yilmaz, M. A., Alwasel, S. H., Arik, M., & Gülçin, İ. (2023). Comprehensively revealing the profile of *Pistacia vera* L. cv. Siirt turpentine-antioxidant, antidiabetic, anti-Alzheimer, and antiglaucoma effects. *Records of Natural Products*, 17(5), 918-937. <https://doi.org/10.25135/rnp.410.2305.2787>
- Kasunmala, I. G. G., Navaratne, S. B., & Wickramasinghe, I. (2020). Antioxidant activity and physicochemical properties changes of *Melastoma malabathricum* (L.) and *Syzygium caryophyllatum* (L.) fruit during ripening. *International Journal of Fruit Science*, 20, S1819-S1828. <https://doi.org/10.1080/15538362.2020.1834896>
- Kathiman, M. N., Mudalip, S. A., & Gimbin, J. (2020). Effect of encapsulation agents on antioxidant activity and moisture content of spray dried powder from Mahkota Dewa fruit extract. *Materials Science and Engineering*, 991(1), 012040. <https://doi.org/10.1088/1757-899X/991/1/012040>
- Kim, T. K. (2017). Understanding one-way ANOVA using conceptual figures. *Korean Journal of Anesthesiology*, 70(1), 22-26. <https://doi.org/10.4097/kjae.2017.70.1.22>
- Kirca, A., Özkan, M., & Cemeroglu, B. (2006). Stability of black carrot anthocyanins in various fruit juices and nectars. *Food Chemistry*, 97(4), 598e605. <https://doi.org/10.1016/j.foodchem.2005.05.036>
- Kobo, G. K., Kaseke, T., & Fawole, O. A. (2022). Micro-encapsulation of phytochemicals in passion fruit peel waste generated on an organic farm: Effect of carriers on the quality of encapsulated powders and potential for value-addition. *Antioxidants*, 11(8), 1579. <https://doi.org/10.3390/antiox11081579>
- Krishnainah, D., Hiaw, K. B., Sarbatly, R., Anisuzzaman, S. M., & Nithyanandam, R. (2012). Spray drying of *Morinda citrifolia* L. and *Beta vulgaris* L. fruit extract and its synergistic effect. *International Journal of Chemical Engineering and Applications*, 3(6), 380. <https://doi.org/10.7763/ijcea.2012.v3.223>
- Kumar, M., Dahuja, A., Sachdev, A., Tomar, M., Lorenzo, J. M., Dhumal, S., & Mekhemar, M. (2022). Optimization of the use of cellulolytic enzyme preparation for the extraction of health promoting anthocyanins from black carrot using response surface methodology. *Lebensmittel-Wissenschaft & Technologie*, 163, 113528. <https://doi.org/10.1016/j.foodchem.2005.05.036>
- Kurniawan, J. M., Yusuf, M. M., Azmi, S. S., Salim, K. P., Utami Prihastyanti, M. N., Indrawati, R., Heriyanto, Shioi, Y., Limantara, L., & Brotosudarmo, T. H. P. (2019). Effect of drying treatments on the contents of lutein and zeaxanthin in orange-and yellow-cultivars of marigold flower and its application for lutein ester encapsulation. *Materials Science and Engineering*, 509, 012060. <https://doi.org/10.1088/1757-899X/509/1/012060>
- Lam, T. (2023). *Color analysis and microfade testing of the 1918 Curtiss Jenny US airmail stamp*. [https://www.analyticalphilately.org/documents/Lam\\_Smith\\_Devine\\_Vicenzi.pdf](https://www.analyticalphilately.org/documents/Lam_Smith_Devine_Vicenzi.pdf)

- Laqui-Vilca, C., Aguilar-Tuesta, S., Mamani-Navarro, W., Montaña-Bustamante, J., & Condezo-Hoyos, L. (2018). Ultrasound-assisted optimal extraction and thermal stability of betalains from colored quinoa (*Chenopodium quinoa* Willd) hulls. *Industrial Crops and Products*, *111*, 606-614. <https://doi.org/10.1016/j.indcrop.2017.11.034>
- Mattioli, R., Francioso, A., Mosca, L., & Silva, P. (2020). Anthocyanins: A comprehensive review of their chemical properties and health effects on cardiovascular and neurodegenerative diseases. *Molecules*, *25*(17), 3809. <https://doi.org/10.3390/molecules25173809>
- Mokhtar, T. N., M, Kharidah., Mohd Adzahan, N., Suri, R. (2013). Evaluation of wall materials for encapsulation of natural colorant from Senduduk (*Melastoma malabathricum*) fruits. *Acta Horticulturae*, *1012*, 1435–1441. <https://doi.org/10.17660/ActaHortic.2013.1012.194>
- Muche, B. M., Speers, R. A., & Rupasinghe, H. P. V. (2018). Storage temperature impacts on anthocyanins degradation, color changes and haze development in juice of “Merlot” and “Ruby” grapes (*Vitis vinifera*). *Frontiers in Nutrition*, *5*, 100. <https://doi.org/10.3389/fnut.2018.00100>
- Nafiunisa, A., Aryanti, N., Wardhani, D. H., & Kumoro, A. C. (2017). Microencapsulation of natural anthocyanin from purple rosella calyces by freeze drying. *Journal of Physics: Conference Series*, *909*, 012084. <https://doi.org/10.1088/1742-6596/909/1/012084>
- Narayanan, M., Shanmugam, S., & Suresh, P. M. (2018). Physical properties of microencapsulated anthocyanin obtained by spray drying of red *Amaranthus* extract with maltodextrin. *Malaysian Journal of Nutrition*, *24*(1), 139–147.
- Nawi, M. N., Muhamad, I. I., & Mohd, M. A. (2015). The physicochemical properties of microwave-assisted encapsulated anthocyanins from *Ipomoea batatas* as affected by different wall materials. *Food Science and Nutrition*, *3*(2), 91-99. <https://doi.org/10.1002/fsn3.132>
- Nayak, C. A., & Rastogi, N. K. (2010a). Effect of selected additives on microencapsulation of anthocyanin by spray drying. *Drying Technology*, *28*(12), 1396-1404. <http://dx.doi.org/10.1080/07373937.2010.482705>
- Nayak, C. A., & Rastogi, N. K. (2010b). Forward osmosis for the concentration of anthocyanin from *Garcinia indica* Choisy. *Separation and Purification Technology*, *71*(2), 144-151. <https://doi.org/10.1016/j.seppur.2009.11.013>
- Nayak, J., & Basak, U. (2015). Analysis of some nutritional properties in eight wild edible fruits of Odisha, India. *International Journal of Current Science*, *5*(4), 55-62.
- Novais, C., Molina, A. K., Abreu, R. M., Santo-Buelga, C., Ferreira, I. C., Pereira, C., & Barros, L. (2022). Natural food colorants and preservatives: A review, a demand, and a challenge. *Journal of Agricultural and Food Chemistry*, *70*(9), 2789-2805. <https://doi.org/10.1021/acs.jafc.1c07533>
- Ochoa, M. R., Kessler, A. G., Vullioud, M. B., & Lozano, J. E. (1999). Physical and chemical characteristics of raspberry pulp: storage effect on composition and color. *LWT - Food Science and Technology*, *32*(3), 149-153. <https://doi.org/10.1006/fstl.1998.0518>
- Oplawska-Stachowiak, M., & Elliott, C. T. (2017). Food colors: Existing and emerging food safety concerns. *Critical reviews in Food Science and Nutrition*, *57*(3), 524-548. <https://doi.org/10.1080/10408398.2014.889652>

- Padzil, A. M., Aziz, A. A., & Muhamad, I. I. (2018). Physicochemical properties of encapsulated purple sweet potato extract: Effect of maltodextrin concentration, and microwave drying power. *Malaysian Journal of Analytical Sciences*, 22(4), 612-18. <https://doi.org/10.17576/mjas-2018-2204-06>
- Purwaningsih, I., Fathiah, F., Amaliyah, N., & Kuswiyanto, K. (2023). The phenolic, flavonoid, and anthocyanin content from methanol extract of senggani fruit and its antioxidant activity. *Indonesian Journal of Chemical Research*, 10(3), 195-202. <https://doi.org/10.30598/ijcr.2023.10-pur>
- Qaziyani, S. D., Pourfarzad, A., Gheibi, S., & Nasiraie, L. R. (2019). Effect of encapsulation and wall material on the probiotic survival and physicochemical properties of synbiotic chewing gum: Study with univariate and multivariate analyses, *Heliyon*, 5(7). <https://doi.org/10.1016/j.heliyon.2019.e02144>
- Quelal, M., Villacrés, E., Vizuete, K., & Debut, A. (2023). Physicochemical characterization of sangorache natural colorant extracts (*Amaranthus quitensis* L.) prepared via spray-and freeze-drying. *AIMS Agriculture and Food*, 8(2), 343-358. <https://doi.org/10.3934/agrfood.2023019>
- Rashid, R., Wani, S. M., Manzoor, S., Masoodi, F. A., & Altaf, A. (2022). Nanoencapsulation of pomegranate peel extract using maltodextrin and whey protein isolate. characterisation, release behaviour and antioxidant potential during simulated *in vitro* digestion. *Food Bioscience*, 50, 102135. <https://doi.org/10.1016/j.fbio.2022.102135>
- Rezaei, F., & VanderGheynst, J. S. (2010). Critical moisture content for microbial growth in dried food-processing residues. *Journal of the Science of Food and Agriculture*, 90(12), 2000-2005. <https://doi.org/10.1002/jsfa.4044>
- Rodríguez-Díaz, J. C., Tonon, R. V., & Hubinger, M. D. (2014). Spray Drying of blue shark skin protein hydrolysate: physical, morphological, and antioxidant properties. *Drying Technology*, 32(16), 1986-1996. <https://doi.org/10.1080/07373937.2014.928726>
- Roobha, J. J., Saravanakumar, M., Aravindhana, K. M., & Devi, P. S. (2011). The effect of light, temperature, pH on stability of anthocyanin pigments in *Musa acuminata* bract. *Research in Plant Biology*, 1(5), 5-12.
- Santiago, M. C. P. D. A., Nogueira, R. I., Paim, D. R. S. F., Gouvêa, A. C. M. S., Godoy, R. L. D. O., Peixoto, F. M., Pacheco, S., & Freitas, S. P. (2016). Effects of encapsulating agents on anthocyanin retention in pomegranate powder obtained by the spray drying process. *LWT-Food Science and Technology*, 73, 551-556. <https://doi.org/10.1016/j.lwt.2016.06.059>
- Šavikin, K., Nastić, N., Janković, T., Bigović, D., Miličević, B., Vidović, S., Menković, N., & Vladić, J. (2021). Effect of type and concentration of carrier material on the encapsulation of pomegranate peel using spray drying method. *Foods*, 10(9), 1968. <https://doi.org/10.3390/foods10091968>
- Sayuti, K., Azima, F., & Marisa, M. (2015). The antioxidant activity of straw jackfruit jam (*Artocarpus heterophyllus*, L.) was added "senduduk" fruit juice (*Melastoma malabathricum*, L.). *International Journal on Advanced Science, Engineering and Information Technology*, 5(6), 396-401. <https://doi.org/10.18517/ijaseit.5.6.599>
- Shadordizadeh, T., Mahdian, E., & Hesarinejad, M. A. (2023). Application of encapsulated *Indigofera tinctoria* extract as a natural antioxidant and colorant in ice cream. *Food Science and Nutrition*, 11(4), 1940-1951. <https://doi.org/10.1002/fsn3.3228>

- Shahidi, F., & Ambigaipalan, P. (2015). Phenolics and polyphenolics in foods, beverages and spices: Antioxidant activity and health effects – A review. *Journal of Functional Foods*, *18*, 820-897. <https://doi.org/10.1016/j.jff.2015.06.018>
- Sornsomboonsuk, S., Junyusen, T., Chatchavanthatri, N., Moolkaew, P., & Pamkhuntod, N. (2019). Evaluation of physicochemical properties of spray dried bael fruit powder during storage. *International Journal of Food Engineering*, *5*(3), 209-213. <http://dx.doi.org/10.18178/ijfe.5.3.209-213>
- Stranzinger, S., Faulhammer, E., Li, J., Dong, R., Khinast, J. G., Zeitler, J. A., & Markl, D. (2019). Measuring bulk density variations in a moving powder bed via terahertz in-line sensing. *Powder Technology*, *344*, 152-160. <https://doi.org/10.1016/j.powtec.2018.11.106>
- Tiefenbacher, K. F. (2017). *Wafer and waffle*. Academic Press. <https://doi.org/10.1016/B978-0-12-809438-9.00002-8>
- Tonon, R. V., Brabet, C., & Hubinger, M. D. (2010). Anthocyanin stability and antioxidant activity of spray-dried açai (*Euterpe oleracea* Mart.) juice produced with different carrier agents. *Food Research International*, *43*(3), 907-914. <https://doi.org/10.1016/j.foodres.2009.12.013>
- Usman, H. M., Abdulkadir, N., Gani, M., & Maiturare, H. M. (2017). Bacterial pigments and its significance. *MOJ Bioequivalence and Bioavailability*, *4*(3), 285-288. <https://doi.org/10.15406/mojbb.2017.04.00073>
- Wariyah, C., & Riyanto, R. (2016). Antioxidative activity of microencapsulated *Aloe vera* (*Aloe vera* var. *Chinensis*) powder with various concentrations of added maltodextrin. *International Food Research Journal*, *23*(2), 537-542.
- Yusoff, A., Kumara, N. T. R. N., Lim, A., Ekanayake, P., & Tennakoon, K. U. (2014). Impacts of temperature on the stability of tropical plant pigments as sensitizers for dye sensitized solar cells. *Journal of Biophysics*, *2014*(1), 739514. <https://doi.org/10.1155/2014/739514>



# REFEREES FOR THE PERTANIKA JOURNAL OF TROPICAL AGRICULTURAL SCIENCE

Vol. 48 (1) JAN. 2025

The Editorial Board of the *Pertanika* Journal of Tropical Agricultural Science wishes to thank the following:

Alev Er  
*University of Istanbul, Turkey*

Karun Thongprajukaew  
*PSU, Thailand*

Phebe Ding  
*UPM, Malaysia*

Amin Ismail  
*UPM, Malaysia*

Kingwascharapong  
Passakorn  
*KU, Thailand*

Seri Narti Edayu Sarchio  
*UPM, Malaysia*

Azman Abd Samad  
*UTM, Malaysia*

Lotanna Micah Nneji  
*Princeton University, USA*

Sirima Sinthusamran  
*KMITL, Thailand*

Earl Cranbrook  
*Great Glemham Farms, United Kingdom*

Lucio Cardozo-Filho  
*UEM, Brazil*

Siti Suriawati Badai  
*MPOB, Malaysia*

Farah Ain Zainee  
*UKM, Malaysia*

Monika Valdenegro  
*PUCV, Chile*

Sujatha Ramasamy  
*UM, Malaysia*

Gabriel Pavan Sabino  
*Unicamp, Brazil*

Muhammad Arshad  
*KIU, Pakistan*

Vivek Rangarajan  
*BITS Pilani, India*

Hairul Azman @ Amir  
Hamzah Roslan  
*UNIMAS, Malaysia*

Nor Fazliyana Mohtar  
*UMT, Malaysia*

Yu Choo Yee  
*UPM, Malaysia*

Izzati Adilah Azmir  
*UiTM, Malaysia*

Norhasnida Zawawi  
*UPM, Malaysia*

Zafar Iqbal Khan  
*UOS, Pakistan*

Janice Alano Ragaza  
*Pamantasan Ateneo de Manila, Philippines*

Nurul Izza Ab. Ghani  
*UPM, Malaysia*

---

*BITS Pilani* – Birla Institute of Technology and Science, Pilani – Goa Campus  
*KIU* – Karakoram International University  
*KMITL* – King Mongkut's Institute of Technology Ladkrabang  
*KU* – Kasetsart University  
*MPOB* – Malaysian Palm Oil Board  
*PSU* – Prince of Songkla University  
*PUCV* – Pontifical Catholic University of Valparaiso  
*UEM* – Universidade Estadual de Maringá  
*UiTM* – Universiti Teknologi MARA

*UKM* – Universiti Kebangsaan Malaysia  
*UM* – Universiti Malaya  
*UMT* – Universiti Malaysia Terengganu  
*Unicamp* – The State University of Campinas  
*UNIMAS* – Universiti Malaysia Sarawak  
*UOS* – University of Sargodha  
*UPM* – Universiti Putra Malaysia  
*UTM* – Universiti Teknologi Malaysia

---

While every effort has been made to include a complete list of referees for the period stated above, however if any name(s) have been omitted unintentionally or spelt incorrectly, please notify the Chief Executive Editor, *Pertanika* Journals at [executive\\_editor.pertanika@upm.edu.my](mailto:executive_editor.pertanika@upm.edu.my)

Any inclusion or exclusion of name(s) on this page does not commit the *Pertanika* Editorial Office, nor the UPM Press or the university to provide any liability for whatsoever reason.





Dietary Administration of Karonda ( <i>Carissa carandas</i> ) on the Growth, Digestive Enzymes, Skin Mucosal Immunity, and Pigmentation in Siamese Fighting Fish ( <i>Betta splendens</i> ) <i>Kotchaporn Ponsin, Janeeya Khunchalee and Phukphon Munglue</i>	259
<i>In silico</i> Study of Neoagaro-Oligosaccharides (NAOs) Anti-Inflammatory Activity: Molecular Docking with iNOS and COX-2 Proteins <i>Pinki Anggrahini Puspitasari, Visi Endah Pratitis, Syahputra Wibowo, Nastiti Wijayanti and Fajar Sofyantoro</i>	279
Determination of the Pathogenicity of the Variant UPM 1432/2019 IBDV in SPF Chicken Eggs and Chicken Fibroblast Cell Line <i>Ali Youssif Mansour, Abdul Rahman Omar, Mohd Hair Bejo, Noorjahan Banu Alitheen and Nurulfiza Mat Isa</i>	295
Antioxidant Properties and Storage Stability of Spray-dried <i>Melastoma malabathricum</i> L. Fruit Extract for Natural Colorant <i>Nurul Syazwani Zahari, Siti Fatimah Sabran, Norhaidah Mohd Asrah, Mohd Fadzelly Abu Bakar, Furzani Pa'ee, Norhayati Muhammad, Fazleen Izzany Abu Bakar and Mohd Khairil Said</i>	307

Sequential Cropping Productivity Evaluation of Corn, Mung Bean, and Sweet Potato Intercrop under Coconut Field in Zamboanga del Sur, Philippines <i>Nelmie Bendanillo Pongao-Ponio and Ma. Stella M. Paulican</i>	117
<i>Review Article</i>	
Prevailing Knowledge on Aquaculture of Abalone in Southeast Asia: A Review <i>Nur-Syahirah Mamat, Yuzine Esa, Hidayah Manan, Nur Leena W. S. Wong, Julia D. Sigwart, Siti-Azizah Mohd Nor, Nazia Abdul Kadar, Hon Jung Liew, Jalilah Mohamad, Suhairi Mazelan, Khor Waiho and Aziz Arshad</i>	137
Identifying Collagenase (MMP-1, -8, -13) Expression and Correlation with Periodontitis Progression Using the Rat Model <i>Fazle Khuda, Badiyah Baharin, Nur Najmi Mohamad Anuar, Putri Ayu Jayusman, Mariati Abdul Rahman and Nurul Shaqinah Nasruddin</i>	159
Floristic Composition and Diversity of Plants Across Three Vegetation Zones of Gashaka Gumti National Park, Northeastern Nigeria <i>Salihu Abba Hammanjoda, Rosimah Nulit, Chee Kong Yap, Umaru Buba Nformi, George Nodza, Abdulwakil Olawale Saba, Edward Entalai Besi and Rusea Go</i>	175
Effects of Temperature on Growth and Biochemical Composition of Arctic <i>Pseudanabaena</i> sp. and Tropical <i>Synechococcus</i> sp. <i>Nurul Farhanah Azlee, Azmir Hamidi, Zoya Khan, Faradina Merican, Jerzy Smykla, Siti Aisyah Alias and Wan Maznah Wan Omar</i>	201
Heavy Metals Assessment in Selected Leafy Vegetables from Selangor, Malaysia <i>Sian Nee See, Mohd Sabri Pak Dek, Maimunah Sanny, Radhiah Shukri and Nurul Shazini Ramli</i>	215
<i>Review Article</i>	
Effects of Different Extraction Methods on Yield, Polyunsaturated Fatty Acids, Antioxidants, and Stability Improvement of Chia Seed Oil: A Review <i>Izzreen Ishak, Ranil Coorey, Maaruf Abd Ghani, Chin Ping Tan, Nazamid Saari and Norhayati Hussain</i>	237

# Pertanika Journal of Tropical Agricultural Science

## Vol. 48 (1) Jan. 2025

### Content

Foreword <i>Chief Executive Editor</i>	i
Principal Component Analysis of Physicochemical Parameters and Microstructure Characteristics of Wampee Fruit Affected by Storage Temperatures <i>Hai Wang, Feilong Yin, Shurou Chen, Ting Wei, Ziyi Qin, Jing Li, Xia Li, Xinhong Dong and Hock Eng Khoo</i>	1
Morphological Sex Determination of East Asian Barn Swallows ( <i>Hirundo rustica</i> ) in Tropical Wintering Region <i>Nor Adibah Ismail, Ummi Nur Syaftiqah Daud, Noor Fatimah Najihah Arazmi, Nurfatin Batrisyia Md Ali, Shukor Md Nor and Mohammad Saiful Mansor</i>	19
A Comprehensive Method to Generating and Identifying Transgenic Tobacco Lines with a Single Transgene Integration Locus for Functional Analysis <i>Mohamad Shafek Hilman, Omar Nawawi, Mohd Farhan Azhari, Tianqi Bai, Cuixian Zhang, Mohd Puad Abdullah, Mat Yunus Abdul Masani and Chong Yu Lok Yusuf</i>	31
Microalgae as Potential Antioxidants: Assessment of Antioxidant Capacities in Microalgae from Selected Regions of Peninsular Malaysia <i>Noor Amanina Awang, Malinna Jusoh, Nor Faizura Said, Norhayati Yusuf, Mohd Nizam Lani and Fauziah Tufail Ahmad</i>	59
Low-sodium Chaya Leaf Seasoning Powder with Potassium Chloride Substitution: Nutritional, Antioxidant, and Microbial Quality Assessment <i>Theeraphol Senphan, Kotchaporn Puangtong, Benyapa Namdamrassiri, Chodsana Sriket, Md. Sazedul Hoque, Supatra Karnjanapratum and Patcharaporn Narkthewan</i>	77
Nanoemulsion and Topical Cream for Delivery of Tocotrienol-rich fraction, Ascorbyl Tetraisopalmitate, and Carotenes: Formulation and <i>in vitro</i> Release <i>Yee-Lin Gan, Chin Ping Tan, Cheah Yoke Kqueen, Hidayah Ariffin, Helmi Wasoh and Oi Ming Lai</i>	91



Pertanika Editorial Office, Journal Division,  
Putra Science Park,  
1st Floor, IDEA Tower II,  
UPM-MTDC Center,  
Universiti Putra Malaysia,  
43400 UPM Serdang,  
Selangor Darul Ehsan  
Malaysia

<http://www.pertanika.upm.edu.my>  
Email: [executive\\_editor.pertanika@upm.edu.my](mailto:executive_editor.pertanika@upm.edu.my)  
Tel. No.: +603- 9769 1622

PENERBIT  
**UPM**  
UNIVERSITI PUTRA MALAYSIA  
PRESS

<http://www.penerbit.upm.edu.my>  
Email: [penerbit@upm.edu.my](mailto:penerbit@upm.edu.my)  
Tel. No.: +603- 9769 8851

